

UNIVERSITA' DEGLI STUDI DI MILANO

Department of Pharmaceutical Sciences

Doctoral Program in Pharmaceutical Sciences – XXXI Cycle



**Subtype-selective Neuronal Nicotinic
Acetylcholine Receptor Agonists and
Antagonists**

CHIM/08 – Medicinal Chemistry

PhD thesis of Francesco BAVO

Reg. Number: R11276

Supervisor: Dr. Cristiano BOLCHI

Co-Supervisor: Prof. Marco PALLAVICINI

PhD Coordinator: Prof. Giancarlo ALDINI

Academic Year 2017-2018

Preface

This dissertation entitled “Subtype-selective Neuronal Nicotinic Acetylcholine Receptor Agonists and Antagonists” describes the research performed as part of the PhD program of Pharmaceutical Sciences at the Department of Pharmaceutical Sciences at the University of Milan from October 2015 to September 2018, that resulted in three publications. In addition to the PhD project, some time was dedicated to green chemistry topics, which are not included in this thesis, but resulted in three publications. The chemistry experimental work was performed at the department of Pharmaceutical Sciences, University of Milan, and was supervised by Researcher Dr. Cristiano Bolchi and Full Professor Marco Pallavicini as Principal Scientist.

The time period from March 2017 to August 2017 was spent at the department of Drug Design and Pharmacology, University of Copenhagen, under the supervision of Professor Bente Frølund and Dr. Kasper Harpsøe. The computational work conducted during this period is not included as an integrated part of this thesis. Some of the work performed at University of Copenhagen is described in the article published in *Journal of Medicinal Chemistry*.

The PhD program was financed by The University of Milan.

The title of the thesis is based on the research conducted at University of Milan. Figures, schemes, tables, and references are numbered consecutively through the text. Final compounds already described in literature are identified by roman progressive numbers; unreported final compounds and intermediate chemical compounds are identified by Arabic progressive numbers.

Publication list

The PhD study resulted in the following publications:

- Bavo, F.; Pucci, S.; Fasoli, F.; Lammi, C.; Moretti, M.; Mucchietto, V.; Lattuada, D.; Viani, P.; De Palma, C.; Budriesi, R.; Corradini, I.; Dowell, C.; McIntosh, J.M.; Clementi, F.; Bolchi, C.; Gotti, C.; Pallavicini, M. Potent anti-glioblastoma agents by hybridizing the onium-alkyloxy-stilbene based structures of an $\alpha 7$ -, $\alpha 9$ -nAChR antagonist and of a pro-oxidant mitocan. *J. Med. Chem.*, **2018**, doi: 10.1021/acs.jmedchem.8b01052.
- Bolchi, C.; Bavo, F.; Fumagalli, L.; Gotti, C.; Fasoli, F.; Moretti, M.; Pallavicini, M. Novel 5-Substituted 3-Hydroxyphenyl and 3-Nitrophenyl Ethers of S-Prolinol as $\alpha 4\beta 2$ -Nicotinic Acetylcholine Receptor Ligands. *Bioorganic Med. Chem. Lett.* **2016**, *26* (23), 5613–5617.
- Bolchi, C.; Bavo, F.; Gotti, C.; Fumagalli, L.; Fasoli, F.; Binda, M.; Mucchietto, V.; Sciaccaluga, M.; Plutino, S.; Fucile, S.; et al. From Pyrrolidinyl-Benzodioxane to Pyrrolidinyl-Pyridodioxanes, or from Unselective Antagonism to Selective Partial Agonism at $\alpha 4\beta 2$ Nicotinic Acetylcholine Receptor. *Eur. J. Med. Chem.* **2017**, *125*, 1132–1144.
- Krall, J.; Jensen, C. H.; Bavo, F.; Falk-Petersen, C. B.; Haugaard, A. S.; Vogensen, S. B.; Tian, Y.; Nittegaard-Nielsen, M.; Sigurdardóttir, S. B.; Kehler, J.; et al. Molecular Hybridization of Potent and Selective γ -Hydroxybutyric Acid (GHB) Ligands: Design, Synthesis, Binding Studies, and Molecular Modeling of Novel 3-Hydroxycyclopent-1-Enecarboxylic Acid (HOCPCA) and Trans - γ -Hydroxycrotonic Acid (T-HCA) Anal. *J. Med. Chem.* **2017**, *60*, 9022–9039.
- Bolchi, C.; Bavo, F.; Regazzoni, L.; Pallavicini, M. Preparation of Enantiopure Methionine, Arginine, Tryptophan, and Proline Benzyl Esters in Green Ethers by Fischer–Speier Reaction. *Amino Acids* **2018**, *50* (9), 1261–1268.
- Bolchi, C.; Bavo, F.; Pallavicini, M. Phase Diagrams to Evaluate the Opportunity for Enantiomeric Enrichment of Some Nonracemic Mixtures of Amino Acid Benzyl Esters by Crystallization as *p*-Toluenesulfonate Salts. *Org. Process Res. Dev.* **2017**, *21*, 1752–1757.
- Bolchi, C.; Bavo, F.; Pallavicini, M. Preparation and Unequivocal Identification of the Regioisomers of Nitrocatechol Monobenzyl Ether. *Synth. Commun.* **2017**, *47* (16), 1507–1513.

- Bolchi, C.; Bavo, F.; Pallavicini, M. One-Step Preparation of Enantiopure L- or D-Amino Acid Benzyl Esters Avoiding the Use of Banned Solvents. *Amino Acids* **2017**, *49* (5), 965–974.
- Fumagalli, L.; Bolchi, C.; Bavo, F.; Pallavicini, M. Crystallization-Based Resolution of 1,4-Benzodioxane-2-Carboxylic Acid Enantiomers via Diastereomeric 1-Phenylethylamides. *Tetrahedron Lett.* **2016**, *57* (18), 2009–2011.

Abstract

This PhD thesis focuses on two specific targets, belonging to the same receptor class of Nicotinic Acetylcholine Receptors (nAChRs): the $\alpha 4\beta 2$ subtype and the $\alpha 7$ subtype. This elaborate is divided in two parts. The aim of the first part is the design and synthesis of $\alpha 4\beta 2$ selective partial agonists as potential smoking-cessation agents. The aim of the second part is the design and synthesis of $\alpha 7$ antagonists with mitocan properties as antitumoral agents.

Part 1.

In the first project, a series of 3-nitrophenyl ethers and 3-hydroxyphenyl ethers of (*S*)-*N*-methylprolinol bearing bulky and lipophilic substituents at the C5 were designed, synthesized and assayed as putative selective $\alpha 4\beta 2$ ligands. Two of them, 5-substituted with a 6-hydroxy-1-hexynyl, had high $\alpha 4\beta 2$ affinity and increased $\alpha 4\beta 2/\alpha 3\beta 4$ selectivity when compared with the correspondent unsubstituted parent compounds.

In the second project, each -CH= of the unselective antagonist (*S,R*)-*N*-methyl-2-pyrrolidinyl-1,4-benzodioxane and of its epimer at the benzodioxane stereocenter, was replaced by a nitrogen. The resulting four diastereomeric pairs of pyrrolidinyl-pyridodioxanes, also designed as the product of rigidification of the flexible scaffolds of pyridyl ethers of *N*-methyl prolinol, were studied for their nicotinic affinity at the $\alpha 4\beta 2$ and $\alpha 3\beta 4$. The isosteric -CH= to N substitution was detrimental for all the compounds, with the only exception of *N*-Methyl-pyrrolidinyl 5-pyridodioxane, with the nitrogen at position 5. Indeed, this ligand had similar affinity to its benzodioxane parent compound, but it had high $\alpha 4\beta 2/\alpha 3\beta 4$ selectivity and it was shown to be a selective partial agonist.

In the third project, the unselective antagonist (*S,R*)-*N*-methyl-2-pyrrolidinyl-1,4-benzodioxane and of its epimer at the benzodioxane stereocenter were substituted at position 5 of the benzodioxane moiety, to explore the possibility of introducing selectivity and/or partial agonist as previously done with -CH= to N replacement. Among the synthesized compounds, (*S,S*)-*N*-Methyl-pyrrolidinyl-5-amino-benzodioxane had slightly improved affinity at the $\alpha 4\beta 2$ affinity and highly enhanced $\alpha 4\beta 2/\alpha 3\beta 4$ selectivity than the unsubstituted parent compound, and it was shown to be a very potent partial agonist.

In the fourth project, we applied computational techniques to support the interpretation of the biological results regarding *N*-Methyl-pyrrolidinyl 5-substituted benzodioxanes and pyridodioxanes. From these findings, we suggested that partial agonism and $\alpha 4\beta 2/\alpha 3\beta 4$ selectivity could be achieved when the benzodioxane scaffold is appropriately substituted with

an HBA/HBD system, that can displace a water molecule from a small and hydrophilic subpocket of the binding site.

Part 2.

Adenocarcinoma and glioblastoma cell lines express $\alpha 7$ and $\alpha 9$ - $\alpha 10$ nAChRs, whose activation promotes tumor cells growth. On these cells, the triethylammoniummethyl ether of 4-stilbenol **MG624**, a known selective antagonist of $\alpha 7$ and $\alpha 9$ - $\alpha 10$ nAChRs, has antiproliferative activity. The structural analogy of **MG624** with the mitocan **RDM-4'BTPI**, triphenylphosphoniumbutyl ether of pterostilbene, suggested us that molecular hybridization among their three substructures might result in novel antitumour agents with higher potency and selectivity. We found that replacement of ethylene with butylene in the triethylammonium derivatives results in more potent and selective toxicity towards adenocarcinoma and glioblastoma cells, which was paralleled by increased $\alpha 7$ and $\alpha 9$ - $\alpha 10$ nAChR antagonism and improved ability of reducing mitochondrial ATP production. Further elongation to octylene (**26**) provided a compound with 40-fold and 10-fold increased antiglioblastoma and antiadenocarcinoma activity respectively, when compared to **MG624**. Elongation of the alkylene linker was greatly advantageous also for the triphenylphosphonium derivatives. **RDM-4'BTPI** did not acquire, as expectable, antinicotinic activity by hybridization with **MG624** stilbene scaffold, but it was surpassed in glioblastoma cell viability reduction by its stilbene analogues with > 4C alkylene linker. In particular, the analogue with decylene between stilbenoxyl and triphenylphosphonium head (**24**) was ten-fold and two-fold more potent than **RDM-4'BTPI** in reducing glioblastoma cell viability and in increasing ROS production respectively. Overall, the ammonium compound **26** reached antiproliferative activities at glioblastoma and adenocarcinoma cells in the same range of the phosphonium **24**, but showed good selectivity against neuroblastoma and healthy mouse astrocytes.

Abbreviations and acronyms

α -Bgtx	α -Bungarotoxin
A549	Cell line of adenocarcinomic human alveolar basal epithelial cells
ACh	Acetylcholine
AChBP	Acetylcholine Binding Protein
AChE	Acetylcholine esterase
ACN	Acetonitrile
AcOH	Acetic Acid
ADHD	Attention Deficit Hyperactivity Disorder
Aq.	Aqueous
ArIB	α 7-specific antagonist α -Conotoxin
BBB	Blood Brain Barrier
bFGF	basic Fibroblast Grow Factor
Bn	Benzyl
Boc	<i>tert</i> -Butoxycarbonyl
Bu	Butyl
Cbz	Carboxybenzyl
ChAT	Choline Acetyltransferase
CHRNA7	Gene that encodes for neuronal acetylcholine receptor subunit alpha-7
CHRNA9	Gene that encodes for neuronal acetylcholine receptor subunit alpha-9
ChT	Choline Transporter
CI	Confidence Interval
CoA	Coenzyme A
CPu	Caudate nucleus-Putamen
CryoEM	Cryo Electron Microscopy

CTD	C-Terminal Domain
CV%	Coefficient of Variation Percentage
DA	Dopamine
DCM	Dichloromethane
DEAD	Diethyl Azodicarboxylate
DIAD	Diisopropyl Azodicarboxylate
DIPEA	N,N-Diisopropylethylamine
DME	Dimethoxyethane
DMSO	Dimethylsulphoxide
DOM	Direct <i>-orto</i> methallation
EC ₅₀	The molar concentration of an agonist that produces 50% of the maximal possible effect of an agonist
ECD	Extracellular Domain
EMA	European Medicines Agency
Epi	Epibatidine
ERK1	Extracellular signal-regulated kinase 1: protein-serine/threonine kinase or mitogen activated kinase
ERK2	Extracellular signal-regulated kinase 2: protein-serine/threonine kinase or mitogen activated kinase
Et	Ethyl
FACS	Fluorescence-activated cell sorting
FDA	US Food and Drug Administration
FOS	Transcription Factor
GABA	γ -aminobutyric acid
GABA-A	γ -aminobutyric acid receptor A

GABA-C	γ -aminobutyric acid receptor C
5-HT ₃	Serotonin receptor 3
GH4C1	rat anterior pituitary cell line
GID	unselective α -Conotoxin (antagonist at the $\alpha 4\beta 2$, $\alpha 3\beta 4$ and $\alpha 7$ subtype)
GPCR	G-Protein Coupled Receptor
h	hour
H1975	Human non-small-cell lung cancer cell line
HBA	Hydrogen Bond Acceptor
HBD	Hydrogen Bond Donor
HEK 243	Human Embryonic Kidney 243 cell line
HepG2	Human Caucasian hepatocyte carcinoma cell line
HPLC	High Performance Liquid Chromatography
HS	High Sensitive
<i>i</i> -Bu	<i>iso</i> -butyl
IC ₅₀	The molar concentration of an antagonist that inhibits 50% of the maximal possible effect of an agonist.
ICD	Intracellular Domain
I _{max}	Maximal current elicited by the agonist used as a control in an electrophysiologic assay.
JUN	Transcription Factor
K _i	The equilibrium dissociation constant of a ligand determined in inhibition studies
LBD	Ligand Binding Domain
LGIC	Ligand-Gated Ion Channel
LS	Low Sensitive

mAChR	Muscle Acetylcholine Receptor
mCPBA	<i>meta</i> -chloroperbenzoic acid
MEM	2-Methoxyethoxymethyl
MeOH	Methanol
Me	Methyl
Min	Minutes
MLA	Methyllycaconitine
MoA	Mechanism of Action
Ms	Mesyl
MTS	(3-(4,5-dimethylthiazol-2-yl)-5-(3-carboxymethoxyphenyl)-2-(4-sulfophenyl)-2H-tetrazolium)
MTS assay	Assay that uses MTS to assess metabolic activity
MW	Microwave irradiation
MWC	Monod-Wyman-Changeux
MYC	Transcription factor
N.D.	Not Detectable
NAc	Nucleus Accumbens
nAChR	Nicotinic Acetylcholine Receptors
NIH	National Institute of Health
NMDA	N-Methyl-D-Aspartate
NMR	Nuclear Magnetic Resonance
NNK	Nikotine-derived Nitrosamine Ketone
NNN	N-Nitroso Nornicotine
NRT	Nicotine Replacement Therapy
NSCLC	Non-Small-Cell Lung Carcinoma

NTD	N-Terminal Domain
OT	Olfactory Tubercle
pAKT	Phosphorylated AKT
PAM	Positive Allosteric Modulator
PDB-ID	Protein DataBank IDentifier
pERK	Phosphorylated ERK
Pg	Protecting Group
Ph	Phenyl
pic-BH3	Picoline-borane
PKC	Protein Kinase C
pLGIC	Pentameric Ligand-Gated Ion Channel
PNS	Peripheral Nervous System
Pr	Propyl
RAF1	Serine/Threonine kinase, Proto-oncogene
RFU	Reference Fluorescence Units
RgIA4	α 9-specific antagonist α -Conotoxin
ROS	Reactive Oxygen Species
Rt	Room Temperature
SAR	Structure-Activity Relationship
Sat.	Saturated
SCLC	Small-Cell Lung Carcinoma
SEM	Standard Error of Mean
SH-SY5Y	Human Neuroblastoma cell line
siRNA	Small Interference RNA

SN	Substantia Nigra
<i>t</i> -Bu	<i>tert</i> -butyl
Td	triplet of doublets
TEA	Triethylamine
TFA	Trifluoroacetic Acid
THF	Tetrahydrofuran
TM	Trans Membrane
TMD	Trans Membrane Domain
TNF- α	Tumor Necrosis Factor α
TPP+	Triphenyl Phosphonium Cation
Tr	Trytyl
U87MG	Uppsala-87 Malignant Glioma, human primary glioblastoma cell line
VAcHT	Vesicular Acetylcholine Transporter
VdW	Van der Waals
VEGF	Vascular Endothelial Grow Factor
VTA	Ventral Tegmental Area
WHO	World Health Organization

The 3-letter and 1-letter IUPAC nomenclature are used for the 21 proteinogenic amino acids.

Table of contents

Nicotinic acetylcholine receptors (nAChRs).....	4
General structure and function	4
Classification	6
Electrophysiology.....	8
Part 1: $\alpha 4\beta 2$ nAChRs.....	10
1.1 Introduction	10
1.1.1 $\alpha 4\beta 2$ Architecture and electrophysiology.....	10
1.1.2 Orthosteric binding site ^{19,20}	13
1.1.3 $\alpha 4\beta 2$ Functions	14
1.1.4 $\alpha 4\beta 2$ and nicotine	14
1.2 $\alpha 4\beta 2$ Ligands and selectivity.....	17
1.2.1 $\alpha 4\beta 2$ Full agonists	18
1.2.2 $\alpha 4\beta 2$ Partial agonists	19
1.2.3 $\alpha 4\beta 2$ Antagonists.....	21
1.3 State of the art.....	22
1.4 Outlook.....	30
1.5 Novel 5-substituted 3-hydroxyphenyl and 3-nitrophenyl ethers of (<i>S</i>)-prolinol as $\alpha 4\beta 2$ -nicotinic acetylcholine receptor ligands ⁷⁷	31
1.5.1 Introduction and aim.....	31
1.5.2 Synthetic schemes	32
1.5.3 Biology	34
1.5.4 Results and discussion.....	34
1.6 Synthesis of N-methyl-pyrrolidinyl-pyridodioxanes designed as isosteres of N-methyl-pyrrolidinyl-benzodioxanes ⁷⁸	38
1.6.1 Introduction and aim.....	38
1.6.2 Synthetic schemes	39

1.6.3 Biology	46
1.6.4 Results and discussion	47
1.7 Synthesis of N-Methyl-pyrrolidinyl-5-substituted-benzodioxanes	51
1.7.1 Introduction and aim.....	51
1.7.2 Synthetic schemes	52
1.7.3 Biology	58
1.7.4 Results and discussion	58
1.8 Computer-aided SAR interpretation	63
1.8.1 Introduction and aim.....	63
1.8.2 Computational methods	63
1.8.3 Results and discussion	64
Part 2: $\alpha 7$ nAChRs.....	70
2.1 Introduction	70
2.1.1 $\alpha 7$ Architecture	70
2.1.2 Orthosteric binding site	72
2.1.3 Allosteric binding site.....	75
2.1.4 Electrophysiology	76
2.1.5 $\alpha 7$ Functions	79
2.1.6 $\alpha 7$ nAChR and cancer.....	79
2.2 $\alpha 7$ Orthosteric ligands and selectivity	83
2.2.1 $\alpha 7$ Full agonists.....	83
2.2.2 $\alpha 7$ Partial agonists.....	84
2.2.3 $\alpha 7$ Antagonists	84
2.3 State of the art.....	85
2.4 Potent anti-glioblastoma agents by hybridizing the oniumalkoxy-stilbene based structures of an $\alpha 7/\alpha 9$ -nAChR antagonist and of a pro-oxidant mitocan.....	89
2.4.1 Aim	89

2.4.2 Synthetic schemes	91
2.4.3 Biology	92
2.4.4 Results and discussion	93
Concluding remarks and future perspectives.....	102
Part 1: $\alpha 4\beta 2$ nAChRs partial agonists	102
Mutational studies	102
<i>In-vivo</i> activity.....	102
Part 2: $\alpha 7$ and $\alpha 9/\alpha 9\alpha 10$ nAChRs antagonists.....	103
SAR investigation.....	103
Intracellular mechanism of actions.....	103
In-vivo activity	103
Experimental section	104
Part 1: $\alpha 4\beta 2$ nAChRs.....	105
Part 2: $\alpha 7$ nAChRs.....	253
Bibliography	302

Nicotinic acetylcholine receptors (nAChRs)

General structure and function

Acetylcholine (ACh), one of the most important neurotransmitters both in the central nervous system (CNS) and in the peripheral nervous system (PNS), exerts its physiological effects by acting on two classes of receptors: muscarinic acetylcholine receptors (mAChRs) and nicotinic acetylcholine receptors (nAChRs), whose most known exogenous agonists are muscarine and nicotine, respectively (*Figure 1*).

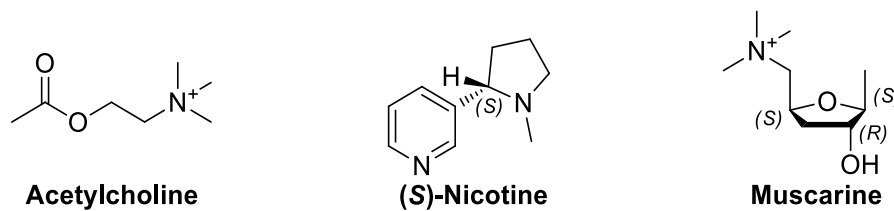


Figure 1: the endogenous neurotransmitter acetylcholine, the exogenous nAChR agonist (S)-Nicotine and mAChRs agonist Muscarine

mAChRs are seven-transmembrane domain receptors (7TM) and belong to the G-coupled receptors superfamily (GPCRs), whose activation, upon neurotransmitter binding, consists in an intracellular G-protein mediated metabotropic response.¹

Oppositely, nAChRs are ligand-gated ion channels (LGICs), and are therefore integral transmembrane proteins containing a pore that allows a regulated ion flux. Pore opening and, consequently, channel gating is triggered by a neurotransmitter (or, more broadly speaking, by an agonist).²

Specifically, nAChRs are homo- or heteropentameric ion channels (pLGICs), composed by 5 identical or different subunits surrounding a central and axial aqueous pore, permeable to mono- and/or divalent- cations. Each subunit is a polypeptide of approximately 500 amino acids, that begins with a short C-terminal extracellular domain (CTD), crosses the membrane 4 times with helical transmembrane domains (TMD), and ends in a long N-terminal extracellular domain (NTD). The NTD contains a loop of approximately 13 amino acids, constrained by a disulphide bridge between two cysteines, whose integrity is crucial for the architecture and function of the channel (Cys-loop receptors).³

The orthosteric binding site is located in the ligand binding domain (LBD), contained in the extracellular domain, at the interface between two adjacent subunits, provided that they have the appropriate architecture to correctly form it.

Upon agonist binding at the orthosteric site, the channel opens and cations such as Na^+ , Ca^{2+} and K^+ flux according to their electrochemical gradient (Na^+ and Ca^{2+} inward, K^+ outward), causing net membrane depolarization (*Figure 2*). The physiological consequences depend on their localization. Originally, nAChRs have been classified according to their tissue distribution in muscle nAChRs and neuronal nAChRs. The coordinated activation of postsynaptic neuronal nAChRs can elicit an action potential, while presynaptic neuronal nAChRs have a crucial role in regulating neurotransmitter release.^{3,4} Activation of muscle nAChRs in the neuromuscular junction allows muscle contraction.

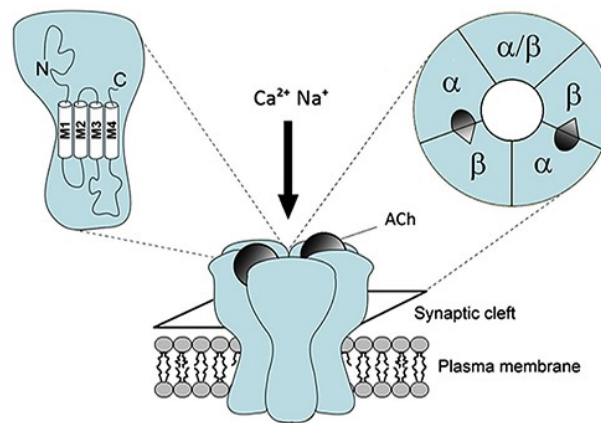


Figure 2: schematic representation of an $\alpha\beta$ nAChR. Acetylcholine binds at the two $\alpha\beta$ interfaces. Adapted from Zoli et al.⁴

Nicotinic receptor-mediated synaptic transmission plays pivotal roles both in the CNS and in the PNS, by regulating fast synaptic transmission, by controlling the release of other neurotransmitters and by influencing cell excitability. As the nicotinic cholinergic system is involved in various cognitive and behavioral functions, it is often impaired in CNS associated pathological conditions, like epilepsy, anxiety, depression, pain, neurodegenerative disorders such as Alzheimer and Parkinson, alcohol addiction and nicotine addiction.⁵

Recently, neuronal nicotinic receptors have been also found in non-neuronal tissues, like glial cells, endothelial cells, immune system cells, lung epithelia, mesenchymal cells and cancer cells where they are involved in cell-cell signaling, cell differentiation, cell proliferation and in inflammatory responses.⁶

Classification

Several classifications and nomenclatures of nAChRs, based both on classical pharmacological approaches and on phylogenetic approaches, have been proposed overtime.

In 1949 Barlow, Ing, Paton and Zaimis pharmacologically distinguished muscle type nicotinic receptors, located in the neuromuscular junctions, from neuronal types, originally found in the autonomic ganglia and later identified in the nervous system, on the basis of the more effective antagonism of decamethonium (C10) than hexamethonium (C6) in blocking muscle nAChRs, compared to the more effective antagonism of hexamethonium (C6) at the ganglionic nAChRs.^{7,8} (*Figure 3*)

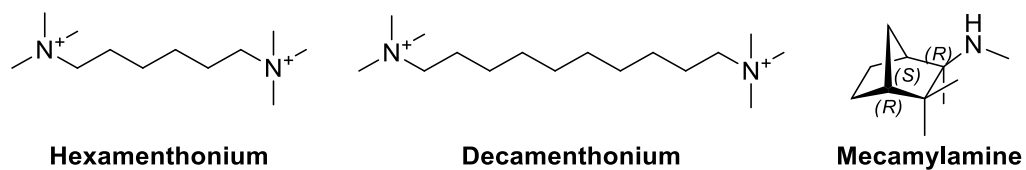


Figure 3: non-competitive nAChRs antagonists, originally used to classify nicotinic receptors.

Structurally, nAChRs are combination of 5 identical or different subunits among 16 subunits described in humans to date. Depending on how subunits assemble, they can form many different homo- or heteropentamers. These subunits, namely α (α 1-7, α 9-10), β (β 1-4), γ , δ and ϵ , have been originally divided into α , containing a disulphide bridge between two adjacent cysteines in the extracellular domain, and non- α . 5 Subunits (α 1, β 1, γ , δ and ϵ) assemble to form muscle nAChRs, while 11 (α 2-7, α 9-10 and β 2-4) compose neuronal nAChRs.⁹

Extraordinary subtype diversity is thus generated by the huge amount of possible combinations between subunits (*Figure 4*). The resulting homomeric or heteromeric receptor subtypes can have even profound differences in receptor pharmacology and channel function, even if structurally similar.¹⁰

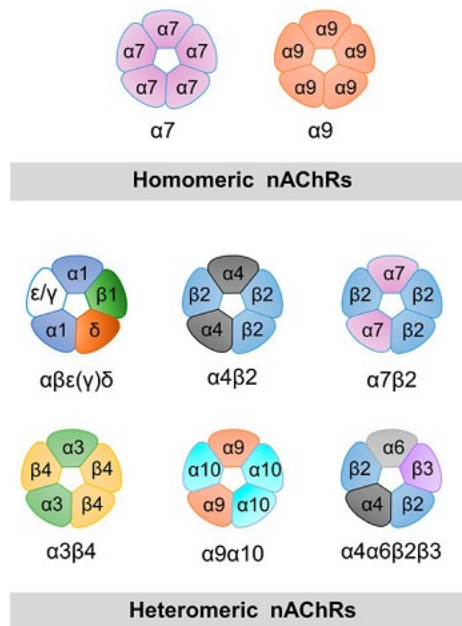


Figure 4: examples of homomeric and heteromeric nAChRs. Adapted from Bouzat et al.¹⁰

Moreover, nAChRs can be classified according to their sensitivity to the natural neurotoxic peptide α -bungarotoxin (α -Bgtx): those that bind α -Bgtx with high affinity and have low affinity for (*S*)-nicotine (homomeric $\alpha7$ and $\alpha9$; heteromeric $\alpha9\alpha10$) and those that do not, but that have high affinity to nicotine (heteromeric, combinations of $\alpha2$ -6 and $\beta2$ -4).^{11,12}

The protein sequences, the correspondent genes, and further specific information on their domains, their functions, annotations etc. can be easily retrieved from the online database Uniprot.¹³

Electrophysiology

Upon binding of an agonist in the orthosteric binding pocket, such as acetylcholine or nicotine, a conformational change of the receptor occurs and the channel pore opens, allowing a net influx of cations. Continuous or repeated exposure to agonists induces loss of functional response of nAChRs. This intriguing phenomenon, called desensitization,¹⁴ was investigated since 1957, when Katz and Thesleff provided a first comprehensive description of desensitization of muscle nAChRs, based on kinetics analysis.¹⁵ According to this two-state model, the ligand-free nAChRs are an equilibrium between resting and activatable state (R) and a desensitized non-conductive state (D). As relatively high concentrations of agonist are required to open the channel, the R conformation was considered to have low agonist affinity. Oppositely, as very low concentrations of agonist induce desensitization, D was considered a high affinity conformation. When even low agonist concentrations are incubated with the receptor, the agonist readily binds the pre-existing desensitized state due to its higher affinity, shifting the equilibrium toward the agonist-bound desensitized conformation (AD), turning R conformations to D conformations to restore the equilibrium (*Figure 5A*).

Later, this model was extended and refined until the complete cyclical model Monod-Wyman-Changeux (MWC) was proposed in 1984.^{16,17} The MWC model considers all the possible transitions between the resting state (R), the opened and activated state (A), an intermediate desensitized state (I, that occurs after short exposures and has faster recovery times) and a desensitized state (D) (*Figure 5B*).

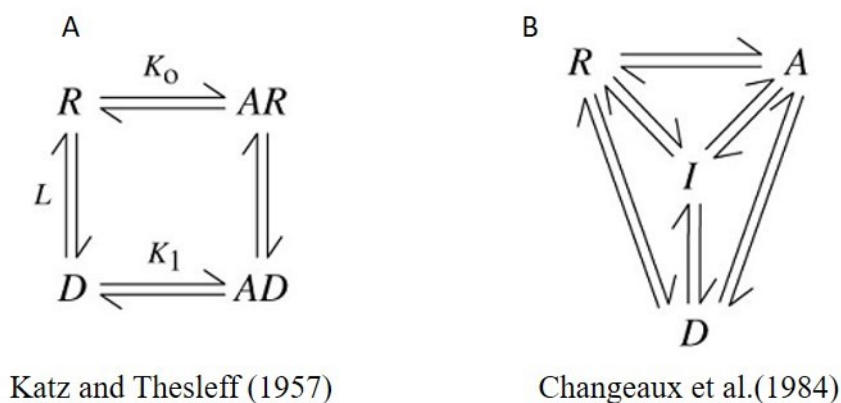


Figure 5: A) Kats and Thesleff kinetic model; B) MWC kinetic model. Adapted from Quick and Lester¹⁴.

The transition between a ligand-bound conductive conformation to a ligand-bound non-conductive desensitized conformation occurs due to a structural reorganization of the channel, during which some amino acids move and close into a gate that prevent the ion flux.

Even though desensitization is a shared feature among the nicotinic receptors, kinetic properties and electrophysiology markedly vary from subtype to subtype. Currently, detailed information about desensitization of specific nAChR subtypes are available, thanks to the development of specific techniques to investigate this phenomenon.

Part 1: $\alpha 4\beta 2$ nAChRs

1.1 Introduction

The most abundant nAChR subtypes in the CNS are the homopentameric $\alpha 7$ and the heteropentameric $\alpha 4\beta 2^*$ (the * mark is used to account for an accessory subunit, the $\alpha 5$ subunit in 20% of cases, forming $(\alpha 4)_2(\beta 2)_2\alpha 5$ subtypes). The $\alpha 3\beta 4^*$ subtype is highly expressed in the autonomic ganglia, in the adrenal medulla and in special subsets of neurons in the medial habenula, dorsal medulla, pineal gland, nucleus interperpendicularis and retina.^{5,12}

The $\alpha 4\beta 2$ usually assembles with two stoichiometries ($2\alpha:3\beta$ or $3\alpha:2\beta$), both functional but with different distributions, biophysical and pharmacological properties. For instance, $(\alpha 4)_2(\beta 2)_3$ has been demonstrated to have 100 folds higher affinity for both nicotine and acetylcholine, lower single channel conductance and calcium permeability (high sensitivity, HS) than the $(\alpha 4)_3(\beta 2)_2$ stoichiometry (low sensitivity, LS).¹⁸⁻²¹

1.1.1 $\alpha 4\beta 2$ Architecture and electrophysiology

Nicotinic receptors have always been considered good prototypes of pLGICs. The first structural information on the shape and overall architecture of nAChRs came from electron microscopy studies reported by Unwin in the '80s and '90s (resolution ranged from 30 Å in 1984²², to 9 Å in 1993²³ to 4.6 Å in 1999²⁴). These were performed on postsynaptic membranes taken from electric organs of electric rays (species *Torpedo Marmorata*), which contains nAChRs. Further detailed structural information about their three-dimensional architectures came, starting from 2001, from the X-Ray models of some snail proteins, the Acetylcholine Binding Proteins (AChBPs), which are secreted by molluscan glial cells (i.e. *Lymnaea Stagnalis* or *Alypsia Californica*) to modulate ACh-mediated synaptic transmission.²⁵ AChBPs are water-soluble homologs of the extracellular domain of nicotinic receptors, with which they share high sequence similarity.²⁶ As water-soluble proteins are much easier to be crystallized than transmembrane proteins, their X-Ray 3D structures have been widely used as surrogate models or as templates for homology modelling to study not only nicotinic receptors, but also other less similar pLGICs, like GABA-A, GABA-C, 5-HT₃ and Glycine receptors.

Obviously, even if the architecture of the ligand binding domain of nicotinic receptors is well represented by AChBPs, the sequences of specific subtypes deviate from the sequences of the molluscan surrogates. Moreover, since AChBPs aren't transmembrane proteins, they completely lack TM domains and they are consequently unable to mimic the physiological processes of channel gating and how ligand binding induces and/or influences it.

Despite the huge improvements of homology modelling and other computational techniques, a 3D X-Ray model of a native nicotinic receptor was highly recommended and sought.

The goal was achieved in 2016, when the first X-Ray structure of the full-length native nicotinic $\alpha 4\beta 2$ receptor was reported by Hibbs ($2\alpha:3\beta$ stoichiometry).²⁰

The $\alpha 4\beta 2$ receptor, co-crystallized with nicotine and a cholesterol analogue at 3.9 Å resolution, is made of five subunits pseudo-symmetrically arranged around a central channel axis, in an overall cylindrical-like shape (*Figure 6A*). As mentioned above, each subunit comprises a large extracellular N-terminal domain, followed by three α -helices which cross the membrane (M1-M3) and further continue in an intracellular MX helix connected to another transmembrane α -helix (M4) facing the channel pore, and a short extracellular C-terminal domain.

If looked from the side, three main portions are easily distinguished: the large extracellular domain (ECD), containing the ligand binding domain (LBD), the transmembrane region (TM) and the intracellular domain (ICD). In the ECD, each subunit contains an α -helix followed by 10 strands wrapped inward to form a sandwich.

The cation permeable pore, easily observable from a top viewpoint of the X-Ray structure, is lined by the M4 helix in the TM region (*Figure 6B*). The channel shows a constriction point of 3.8 Å diameter close to the cytosol, formed by glutamate side chains at the -1' position of the M2 helices, which are faced on the pore. The diameter of the resulting gate is smaller than the minimum consensus diameter of approximately 6.8 Å that would allow the movement of the smallest ion (Na^+) at least partially hydrated. This structural analysis, together with other functional analysis, were used by the authors to state that the X-Ray structure represent a non-conductive desensitized conformation.

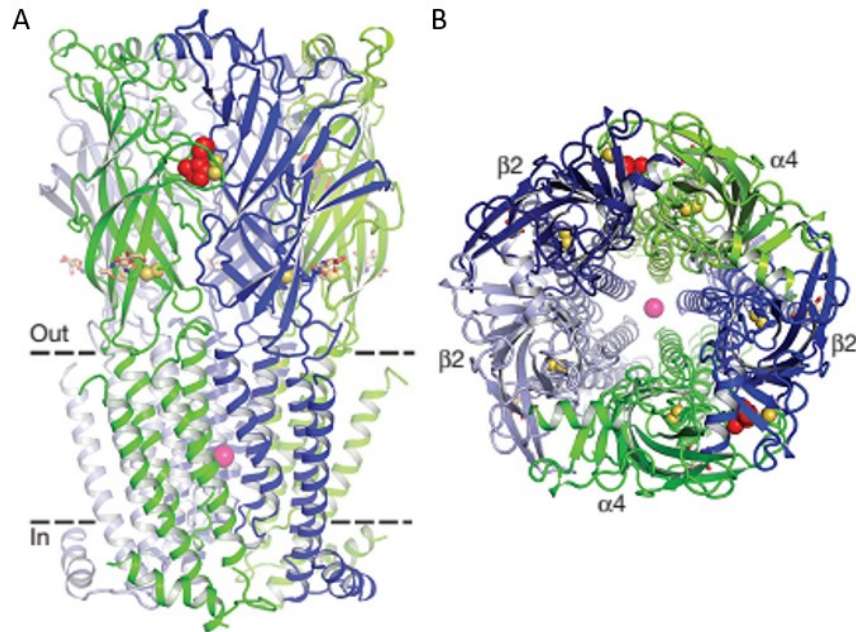


Figure 6: A) Side view and B) axial view of the X-Ray 3D structure of the $(\alpha 4)_2(\beta 2)_3$ co-crystallized with nicotine (red) and with a cholesterol analogue (not shown). Na^+ is shown in pink. Adapted from Morales-Perez et al.²⁰

Cationic permeability is controlled by the electrostatic properties of the channel: the surface of the extracellular vestibule of the pore is strongly electronegative, but becomes more neutral proceeding down into the pore until its extracellular end. Afterward, the electronegativity increases reaching its maximum at the desensitization gate, formed by 5 glutamate residues. This trend probably allows the vestibule to accumulate cations and then to funnel them into the pore (Figure 7A).

In 2018, the same authors reported the Cryo Electron Microscopy (CryoEM) structures of the two different stoichiometries of the $\alpha 4\beta 2$ subtypes together with specific antibody fragments and nicotine providing deep insights into principles underlying subunits assembly and differences in permeation properties between the $(\alpha 4)_2(\beta 2)_3$ and the $(\alpha 4)_3(\beta 2)_2$ subtypes.¹⁹

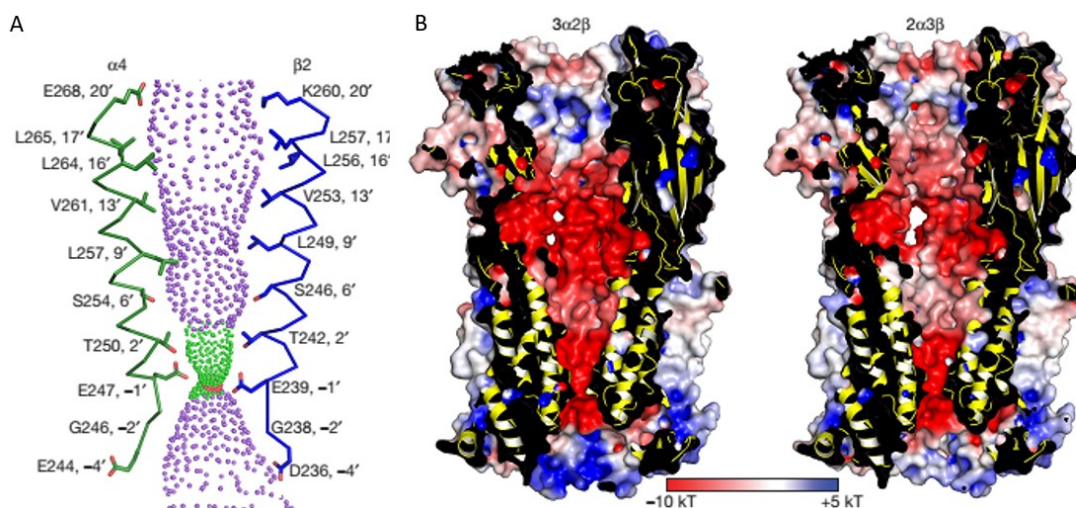


Figure 7: A) Representation of the pore diameter of the $3\alpha:2\beta$ assembly: purple spheres indicate pore diameter over 5.6 \AA , green between 2.8 and 5.6 \AA and red less than 2.8 \AA . B) cutaway of the $\alpha4\beta2$ subtype in both stoichiometries ($3\alpha:2\beta$ on the left side and $2\alpha:3\beta$ on the right side). The permeation pathway is colored by electrostatic potential. Adapted from Walsh et al.¹⁹

1.1.2 Orthosteric binding site^{19,20}

In the $2\alpha:3\beta$ stoichiometry, the $\alpha4$ and $\beta2$ subunits are ordered as $\alpha\text{-}\beta\text{-}\beta\text{-}\alpha\text{-}\beta$, forming two $\alpha\beta$, two $\beta\alpha$ and one $\beta\beta$ interfaces. Nicotine, acetylcholine and other orthosteric ligands bind only at the $\alpha\beta$ interfaces, in the classical neurotransmitter orthosteric binding site. The binding pocket is lined by the $\alpha4$ subunit ((+) side) and by the $\beta2$ subunit ((-) side). Both sides contribute with three loops to the construction of the binding site: A, B and C loops from the (+) side ($\alpha4$) and D, E and F from the (-) side ($\beta2$).

Nicotine is located within a tightly packed so-called “aromatic box”, paved by tyrosine Y100 ($\alpha4$ subunit, loop A) and by tryptophan W57 ($\beta2$ subunit, $\beta2$ strand, loop D). The back walls are formed by leucine L121 ($\beta2$ subunit, $\beta6$ strand, loop E) and by tryptophan W156 ($\beta2$ subunit, $\beta2$ strand, loop D), while the front wall is defined by the flexible loop C ($\alpha4$ subunit), tightly packed over the ligand, with its vicinal cysteines C199 and C200 linked with a disulphide bond and tyrosines Y197 and Y204 (Figure 8A).

Nicotine is embedded within the binding site due to several interactions: in addition to the hydrophobic and aromatic interactions with the aromatic box, its positively charged pyrrolidine nitrogen, protonated at physiological pH, is well placed to interact with a π -cation interaction with W156 and to form a hydrogen bond to the backbone carbonyl of the same residue.

As suggested by the authors, nicotine doesn't bind to $\beta\alpha$ or $\beta\beta$ interfaces ($\beta2$ as the (+) side), because of a profound reorganization of the binding site: the small-sized G154 of the $\alpha4$ subunit

is substituted by the long-chain R149 of $\beta 2$. The side chain of R149 extends in the binding pocket and its guanidinium group remains trapped in a π -cation sustained sandwich between Y196 (correspondent to Y197 of $\alpha 4$) and Y95 (correspondent to Y100 in $\alpha 4$), twisting away the crucial residue of W151 from the pocket and preventing access to the ligand (*Figure 8B and 8C*).

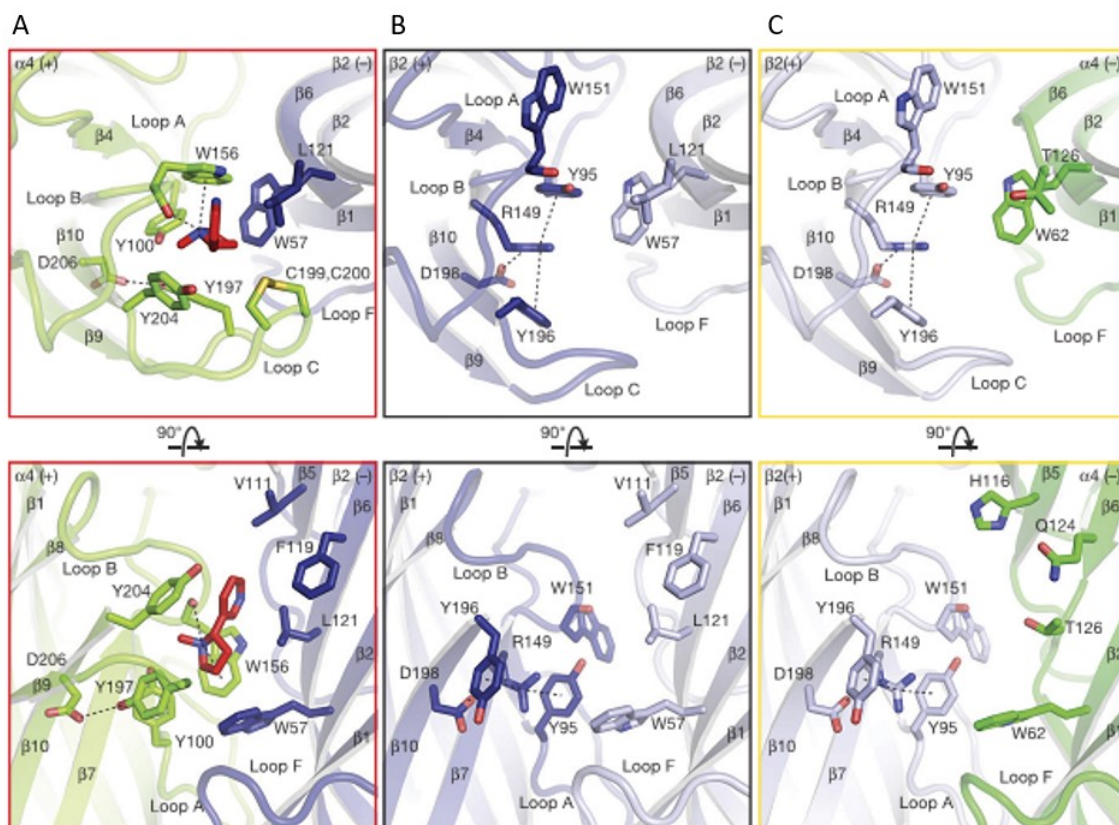


Figure 8: A) Nicotine bound at the $\alpha 4 \beta 2$ interface. B) Nicotine doesn't bind to the $\beta 2 \beta 2$ and C) to the $\beta 2 \alpha 4$ interface. Adapted from Morales-Perez et al.²⁰

1.1.3 $\alpha 4 \beta 2$ Functions

nAChRs $\alpha 4 \beta 2^*$ are the most prevalent CNS subtypes and are implicated in a wide range of physiological functions, including learning, memory, mood, cognition.²⁷⁻³⁰ Consequently, they are also involved in pathological conditions, like epilepsy, neurodegenerative disorders such as Parkinson and Alzheimer, depression, schizophrenia, drug abuse and nicotine addiction.³¹⁻³³

1.1.4 $\alpha 4 \beta 2$ and nicotine

Nicotine, a major component of tobacco, is the most known and very abused exogenous nicotinic agonist. It exerts its behavioral effects by interacting with nAChRs both in the CNS and in the PNS, and after chronic exposure it modulates and alters several neural pathways involved in learning, memory and other cognitive functions.³⁴

Importantly, nicotine causes a strong psychological addiction. According to the 2018 NIH report on “Tobacco, nicotine and e-cigarettes”, approximately 20% of the population smokes cigarettes and every year about half of them tries to quit permanently. Yet, only 6% can quit within a year.³⁵

The majority of the population assumes nicotine through cigarette smoke; the combustion of tobacco produces more than 7000 chemicals and many of them are carcinogenic.³⁶ Nicotine itself has been demonstrated to promote hyperproliferation of carcinoma cells.³⁷

The pharmacokinetic properties of nicotine, combined with the inhalator “route of administration” are perfect match to quickly deliver high amounts of nicotine in the brain. Due to pulmonary absorption, nicotine rapidly reaches high blood concentrations and easily crosses the blood-brain barrier (BBB) thanks to its lipophilicity. Once in the brain (within 10 seconds from the inhalation), 20-100 nM of nicotine is enough to activate and desensitize nAChRs. Particularly, nicotine activates the postsynaptic high affinity $\alpha 4\beta 2^*$ nAChRs located in dopaminergic and GABAergic neurons of the midbrain dopamine area or mesostriatal dopamine pathway and enhances firing of dopaminergic neurons and release of dopamine in the areas where the terminals are located. The mesostriatal dopamine pathway includes the ventral mesolimbic pathway, which has cell bodies in the ventral tegmental area (VTA) and terminals in the nucleus accumbens (NAc) and olfactory tubercle (OT) and the dorsal nigrostriatal pathway, which has cell bodies in the substantia nigra (SN) and terminals in the caudate-putamen (CPu) (*Figure 9*). These circuits are deeply involved in reward systems: release of dopamine in the NAc regulates motivation and desire for reward stimuli. The addictive properties of nicotine are mainly due to activation of $\beta 2^*$ receptors in the VTA and the consequent dopamine release in NAc.^{9,38}

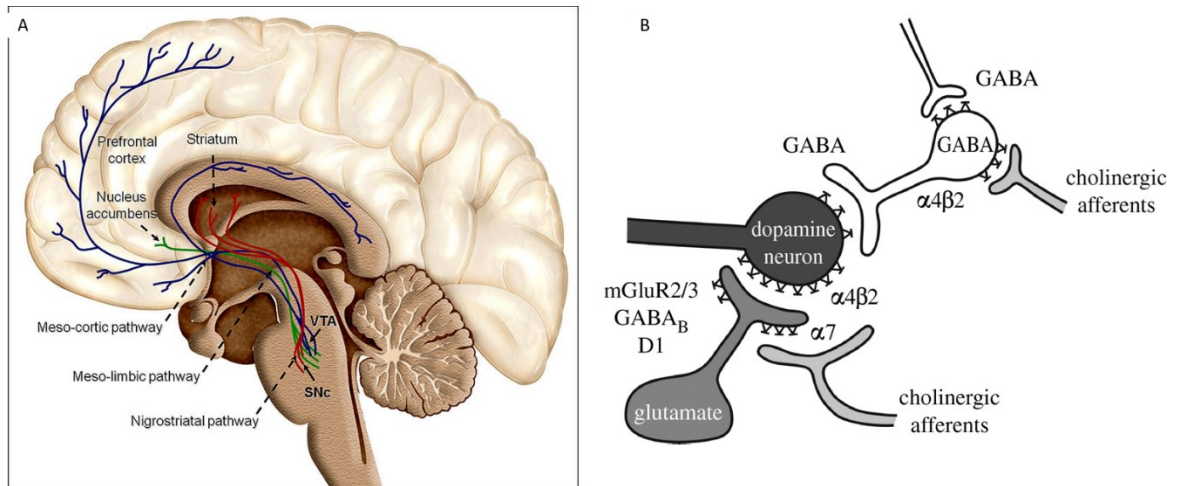


Figure 9: A) Mesostriatal dopamine pathways: mesolimbic pathway (green), dorsal nigrostriatal pathway (red). B) Nicotinic regulation of dopaminergic neurons in the VTA. Adapted from Markou.³⁸

In the midbrain, nicotine also acts on presynaptic $\alpha 7$ receptors located on glutamatergic terminus, stimulating the release of glutamate, an excitatory neurotransmitter that in turn stimulates dopamine firing.

Depolarization and firing of DA neurons also helps to relieve the divalent cation block of NMDA receptors enabling them to participate in long-term synaptic potentiation of glutamatergic afferents onto midbrain dopamine neurons.⁹

Moreover, after an initial activation of the $\alpha 4\beta 2^*$ in the VTA, the same receptors significantly desensitize, preventing the activation of the GABAergic neurons that normally inhibit DA firing.

Nicotine addiction is a severe issue for both individuals and society: according to the WHO every year more than 7 million people die for direct consume of tobacco, while around almost 900,000 die for second-hand smoke. Moreover, the NIH has estimated an overall cost of smoking of around 300 billion of \$ per year, which include 150 billion \$ for direct medical care of adults and 150 billion of \$ for lost productivity due to premature deaths.³⁵

1.2 $\alpha 4\beta 2$ Ligands and selectivity

During the last decades, due to their widespread distribution in the CNS and their involvements in numerous pathological conditions, $\alpha 4\beta 2$ nAChRs have been considered promising therapeutic targets for the treatment of CNS disorders like neurodegenerative conditions, pain, cognitive dysfunctions, alcohol dependence, anxiety and nicotine dependence.^{33,39–42}

The high variety of existing nicotinic subtypes, the crucial functions in which they are involved and the structural similarities of their binding sites make selectivity over off-target subtypes a central but very challenging goal in new ligands development.

In our specific case, selectivity on $\alpha 4\beta 2$ subtype over $\alpha 7$ (the other major subtype in the CNS) and $\alpha 3\beta 4$ (more abundant in the PNS) can be achieved both by designing ligands that do bind only to the $\alpha 4\beta 2$ subtype or by exploiting functional differences in electrophysiology at different subtypes (i.e. partial agonist with high potency at the $\alpha 4\beta 2$, but low potency at the $\alpha 3\beta 4$).

Depending on their electrophysiological effects, nicotinic orthosteric ligands can be functionally classified in full agonists, partial agonists, antagonists, inverse agonists and desensitizing agonists.

A very attractive category is represented by selective $\alpha 4\beta 2^*$ partial agonists, which have been studied up to clinical trials as novel antidepressant, for Alzheimer disease and for nicotine addiction. Especially for the last indication, $\alpha 4\beta 2$ partial agonists are recommended: the two mechanisms underlying smoking cessation are a “nicotine-like” agonist activity, that reduces craving by mimicking nicotine at a smoother extent during a quit attempt, followed by a “nicotine-blocking” antagonist activity that, competing for the $\alpha 4\beta 2$ with the inhaled nicotine, reduces the reinforcement mechanisms detailed in paragraph 1.1.4.⁴³

This dual agonist-antagonist mechanism was initially proposed by Rose and Levin in 1991, who suggested to combine a nicotine replacement therapy (NRT) with the non-competitive antagonist mecamylamine (*Figure 10*).⁴⁴ As the results of a small clinical trials were positive, several efforts have been done to gather the two effects in a single drug, such as a partial agonist.

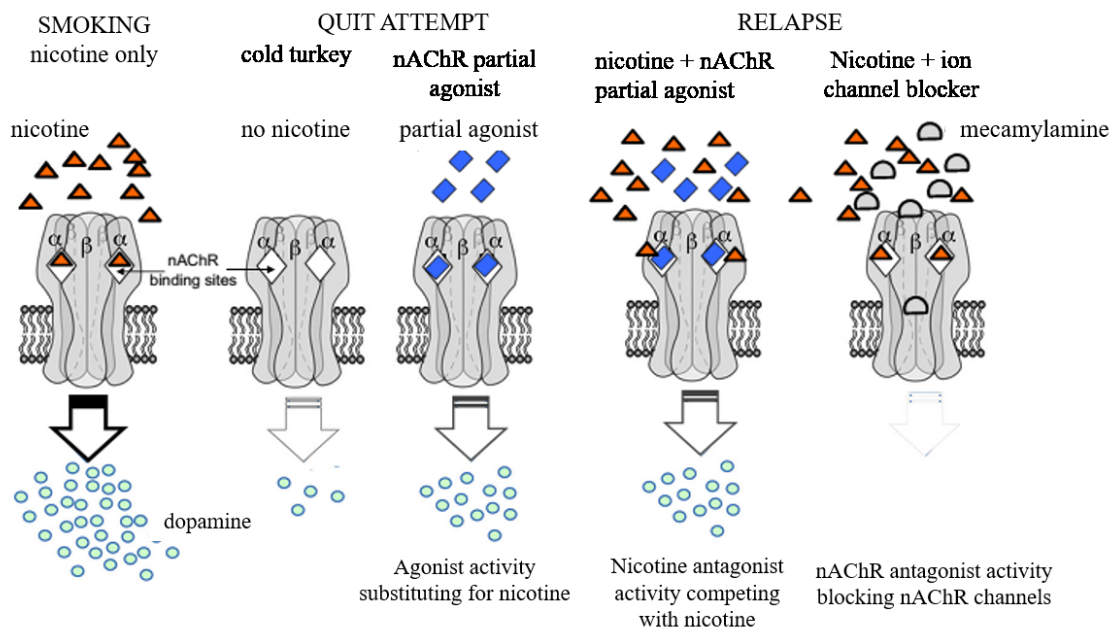


Figure 10: schematic representation of the effect of nicotine while smoking, of a nAChR partial agonist during a quit attempt and during relapse. Adapted from Rollema et al.⁴³

Moreover, desensitization induced by agonists contributes to reducing the effect of nicotine during a relapse, because the receptors are in a desensitized state due to prior occupancy by the nicotinic agonist and therefore they can't be activated by inhaled nicotine.

These are the rationales why the $\alpha 4\beta 2$ partial agonist Varenicline tartrate has been approved from the FDA and EMA in 2006 with the commercial name of Champix® or Chantix® as a tobacco use cessation agent.

1.2.1 $\alpha 4\beta 2$ Full agonists

Acetylcholine is the major neurotransmitter at neuromuscular junctions, autonomic ganglia, parasympathetic effector junctions, a subset of sympathetic junctions and many parts of the CNS. It is synthesized in cholinergic neurons by the enzyme choline acetyltransferase (ChAT) starting from choline and acetyl-CoA and it is then transported into storage vesicles by the vesicular ACh/H⁺ antiporter (VAChT), driven by a proton-pumping ATPase. In response to membrane depolarization, vesicles are fused with the membrane of the synaptic terminals and ACh is released in the synaptic cleft (or neuromuscular junction), where it exerts its physiological effects by binding and activating nAChRs and mAChRs located both on the presynaptic and on the postsynaptic membranes. ACh is then hydrolyzed in choline and acetate by the enzymes acetylcholine esterase (AChE) and choline is reuptaken into cells either by a ubiquitous low-affinity choline uptake system or with a cholinergic neuronal specific high-affinity choline symporter ACh/Na⁺ (ChT). Acetylcholine is a non-selective full agonist of

nicotinic receptors and it is used as a term of comparison for other ligands. It is used in therapy only for some ophthalmic applications.²⁷

Nicotine is an exogenous ligand, regularly assumed by cigarette smokers (and other tobacco products users). It is a competitive full agonist at all the nAChRs, but preferentially binds the heteromeric $\alpha 4\beta 2^*$ and other heteromeric combinations of $\alpha 2-6$ and $\beta 2-4$ (α -Bgtx insensitive) rather than to homomeric $\alpha 7$ and heteromeric $\alpha 9\alpha 10$ (α -Bgtx sensitive) receptors.

Epibatidine (*Figure 12*) was isolated in 1974 by Daly from the skin of the Ecuadorean frog *Epipdobates Tricolor*, whose extract was known to have very potent analgesic properties. Its structural determination was hampered by the low availability of the purified alkaloid and it was first reported in 1992. The year after, the research group of Corey, at the University of Harvard, reported the synthesis of both enantiomers of epibatidine and of some analogues and offered them to Daly for biological evaluations. Epibatidine is a non-selective full agonist with high affinity and high potency at the $\alpha 4\beta 2$ and $\alpha 3\beta 4$ and, with lower potency, at the $\alpha 7$ and muscle subtypes.^{45,46}

1.2.2 $\alpha 4\beta 2$ Partial agonists

Cytisine (*Figure 12*) is a natural alkaloid contained in some plants of the genera such as *Laburnum* or *Cytisus* of the family *Fabaceae* and it is extracted from the seeds of *Cytisus Laburnum*. It is a partial agonist at the $\alpha 4\beta 2$ subtype but a full agonist at the $\alpha 7$ and $\alpha 3\beta 4$ subtypes. Historically, it has been used as a smoking cessation agent since 1964 in Eastern Europe with the brand name of Tabex®, but insufficient preclinical and clinical studies on its safety and efficacy precluded its approval by FDA or EMA. However, some recent studies indicated that cytisine is more efficacious than nicotine replacement therapy in smoking cessation.^{43,47–50}

Recently, in 2018, a direct method via direct C-H functionalization of cytisine by Ir-catalyzed borylation to obtain analogues with $\alpha 4\beta 2$ partial agonism activity has been reported by Gallagher et al.⁵¹ In this work, the core structure of cytisine was decorated with various substituents at position C10 with the aim to preserve $\alpha 4\beta 2$ affinity and partial agonism, but to enhance selectivity against the $\alpha 7$ and $\alpha 3\beta 4$ subtypes. The C10-substituted variants of cytisine (i.e. **10-ethylcytisine**) displayed high affinity for the $\alpha 4\beta 2$ subtype, with preference for the $(\alpha 4)_2(\beta 2)_3$ stoichiometry and partial agonist activity. Additionally, they could not bind and/or activate the $\alpha 7$ subtype at therapeutically meaningful concentrations and they were weak partial agonists at the $\alpha 3\beta 4$ subtype with low affinity. Docking studies at the $\alpha 4\beta 2$, $\alpha 3\beta 4$ and $\alpha 7$

subtypes suggested similar binding poses at all the subtypes for the C10-substituted analogues of cytosine and cytosine itself, driven by a combination of cation- π interaction and H-bonding between the protonated secondary amine N and some residues of the α subunit. The pyridone carbonyl oxygen of cytosine or of its analogues pointed toward a small hydrophilic pocket lined by the amidic backbone of Leu 121, by the carbonyl backbone of Asn 109 and by the side chain of Ser 108 ($\alpha 4\beta 2$) or the correspondent threonine at the other subtypes ($\alpha 3\beta 4$ and $\alpha 7$), with the space for bridging a water molecule. The most different interactions between the ligands and the three subtypes considered were observed in proximity of position C10, investigated in this study. C10 was close to the hydrophobic residue located at position 111, which was the relatively small valine in the $\alpha 4\beta 2$, while the bulkier isoleucine and leucine respectively in the $\alpha 3\beta 4$ and in the $\alpha 7$ subtype. The authors suggested that selectivity of the bulkier C10-substituted analogues of cytosine could be related to their sterically disfavored interactions with the more hindered residues of the $\alpha 3\beta 4$ and of the $\alpha 7$ subtypes (*Figure 11*).

Therefore, the high selectivity of C10-substituted analogues of cytosine at the $\alpha 4\beta 2$ subtype versus the two major off-targets in smoking cessation ($\alpha 7$ and $\alpha 3\beta 4$ subtype) makes these compounds the ideal lead candidates for further modifications.

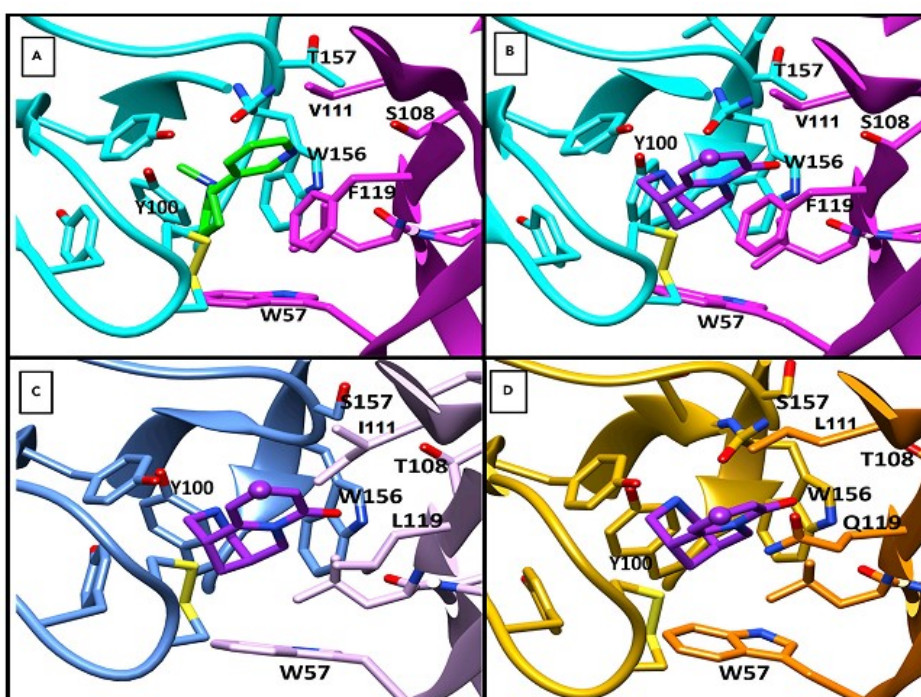


Figure 11: A) Nicotine bound at the $\alpha 4\beta 2$ binding site. B) Cytosine bound at the $\alpha 4\beta 2$, at the C) $\alpha 3\beta 4$ and at the D) $\alpha 7$ binding sites. Position 10 is represented with a purple sphere. Adapted from Campello et al.⁵¹

Varenicline (Figure 12) was developed by Pfizer as a cytosine analogue and was approved by the regulatory authorities in 2006 for smoking cessation with the commercial name of Chantix® (USA) or Champix® (EU, Canada). Varenicline is a high affinity partial agonist of the $\alpha 4\beta 2$ subtype but, as cytosine, it is also active on $\alpha 3\beta 4$, $\alpha 3\beta 2$ and $\alpha 6$ subtypes. Moreover, it is a full agonist at the $\alpha 7$ subtype.⁵²⁻⁵⁴

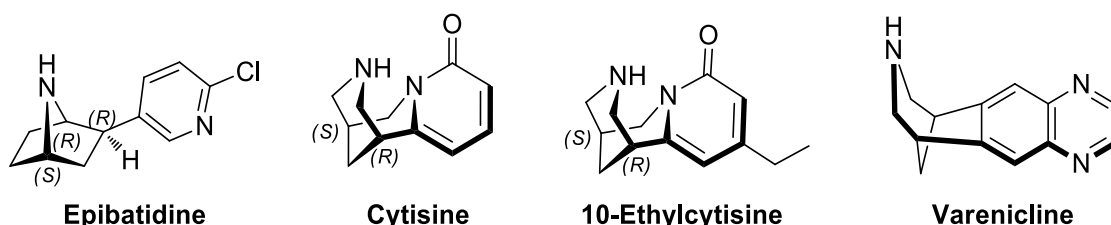


Figure 12: non-selective full agonist epibatidine; non-selective partial agonists cytosine and varenicline; selective partial agonist 10-Ethylcytosine.

1.2.3 $\alpha 4\beta 2$ Antagonists

α -Conotoxins are competitive nicotinic acetylcholine receptor antagonists and belong to a group of neurotoxic peptides (conotoxins) isolated from the venom of the predatory sea snails of the genus *Conus*. Even if more selective at the $\alpha 3\beta 4$ and at the $\alpha 7$ subtype, α -conotoxin GID showed high affinity toward the $\alpha 4\beta 2$ subtype and was used as scaffold for the design and synthesis of moderately more selective analogues.⁵⁵

Peptides or high molecular weight molecules such as conotoxins have been used to investigate nicotinic receptors pharmacology *in-vitro*, but they would encounter several pharmacokinetics problems into *in-vivo* studies or for potential therapeutic applications. For this reason, several selective small molecules acting as competitive antagonists have been developed.⁵⁶⁻⁵⁸

1.3 State of the art

In 1996, Abreo reported a series of 3-pyridyl ethers with nano- or subnanomolar affinity for the $\alpha 4\beta 2$ subtype, measured as [^3H]-(-)-cytisine displacement from whole rat brain, among which compounds **A-84543** and **A-85380** stood out as potent $\alpha 4\beta 2$ full agonists.⁵⁹ However, although **A-84543** was shown to be moderately selective in the $^{86}\text{Rb}^+$ efflux assay at the $\alpha 4\beta 2$ subtype against the ganglionic $\alpha 3\beta 4$ subtype, several efforts have been done to obtain analogues with improved binding and functional selectivity.⁶⁰⁻⁶²

The same year Elliot from the Abbot laboratories described the affinities of some analogues of **A-84543** and **A-85380** where the pyridine ring was bioisosterically replaced by aryl moieties, among which compound (*S*)-**I** and (*S*)-**II**, which showed good, albeit decreased, binding affinity when compared to their pyridyl ether progenitors (*Figure 13*).⁶³

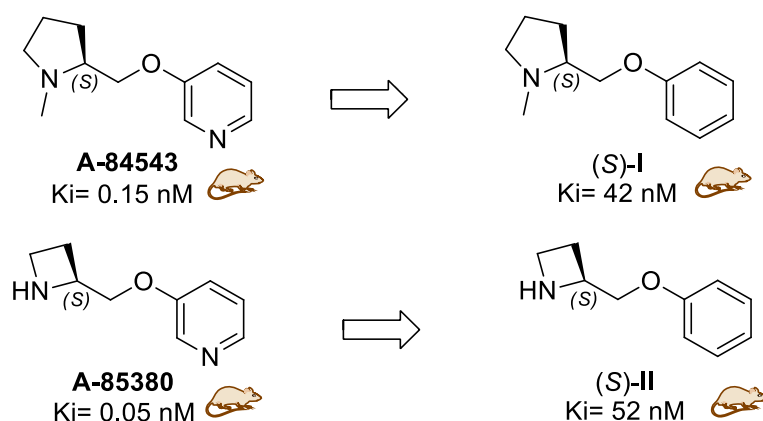


Figure 13: Phenyl ether analogues (S)-I and (S)-II (right) of the pyridyl ethers A-84543 and A-85480 (left). Binding affinities were measured as displacement of [^3H]-cytisine from whole rat brain preparations (rat symbol).⁶⁴

In 2005 a series of 5-substituted analogues of **A-84543** like (*S*)-**III** were reported by Kozikowski, who demonstrated that selectivity over rat $\alpha 3\beta 4$ could be improved by introducing differently elongated hydrophobic groups such as 5-hexynyl, obtaining further improvements when these linkers were terminally OH substituted.⁶¹ The year after, the same research group synthesized and pharmacologically characterized Sazetidine-A (**Saz-A**) (*Figure 14*) as a selective $\alpha 4\beta 2$ ligand (both at rat and human receptors), with the particular capability of desensitizing the channel without activating it in a $^{86}\text{Rb}^+$ -based assay (silent desensitizer).⁶⁵ However, since this result was not coherent with the *in-vitro* dopamine release assays, more detailed investigations were performed demonstrating that **Saz-A** had different functional activities at the two $\alpha 4\beta 2$ stoichiometries: it was a full agonist at the human high affinity $(\alpha 4)_2(\beta 2)_3$ stoichiometry, while a low efficacy partial agonist (6%) at the human $(\alpha 4)_3(\beta 2)_2$

stoichiometry.⁶⁶ **Saz-A** showed promising results as antidepressant and was demonstrated to decrease alcohol intake and nicotine self-administration and to improve performances in tests of attention in an animal model.^{67–71}

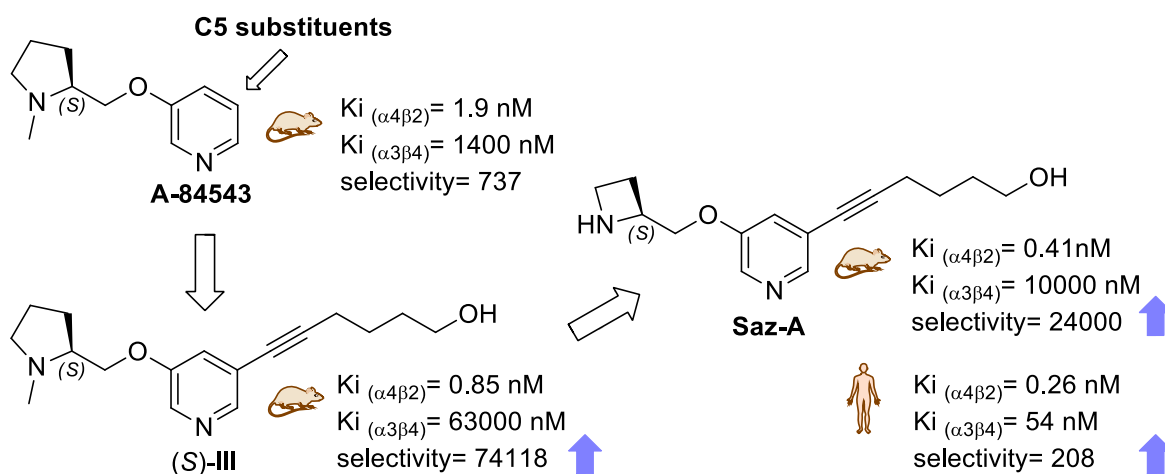


Figure 14: Design of **Saz-A**, a selective $\alpha 4\beta 2$ partial agonist. $\alpha 4\beta 2$ and $\alpha 3\beta 4$ binding affinities were measured as displacement of [^3H]-epibatidine from heteroexpressed rat $\alpha 4\beta 2$ and $\alpha 3\beta 4$ receptors (**A-84543**, **(S)-III** and **Saz-A**, rat symbol)⁶¹ or human $\alpha 4\beta 2$ and $\alpha 3\beta 4$ receptors (**Saz-A**, human symbols).^{65,66} Whereas **Saz-A** affinity for rat and human $\alpha 4\beta 2$ receptors is similar, **Saz-A** is much more affinitive for human $\alpha 3\beta 4$ than for rat $\alpha 3\beta 4$ receptors.

The same year, the synthesis of two rigidified analogues of **(S)-I**, namely N-methyl-2-(2-pyrrolidinyl)benzodioxanes **(S,R)-IV** and **(R,S)-IV** was carried out by Pallavicini et al. and was later extended to all the 4 possible stereoisomers in 2009, therefore including **(S,S)-IV** and **(R,R)-IV** (Figure 15).^{72,73} These compounds contain two stereocenters in close proximity to the pyrrolidine nitrogen, connected by the only rotatable bond of the molecule (pyrrolidine-benzodioxane). The more favored molecule conformations of the 4 isomers will strongly depend on the absolute configurations of the two vicinal stereocenters. As expectable from the comparison with other nicotinoids, only the two constrained N-Me-pyrrolidinyl-benzodioxanes that maintained the absolute configuration “S” at the pyrrolidine stereocenter **(S,S)-IV** and **(S,R)-IV** retained $\alpha 4\beta 2$ affinity and moderate selectivity against the $\alpha 7$, with a lower K_i value for **(S,R)-IV**. The very same N-des-methylated analogues showed micromolar affinity values and weren’t further considered by the research group.

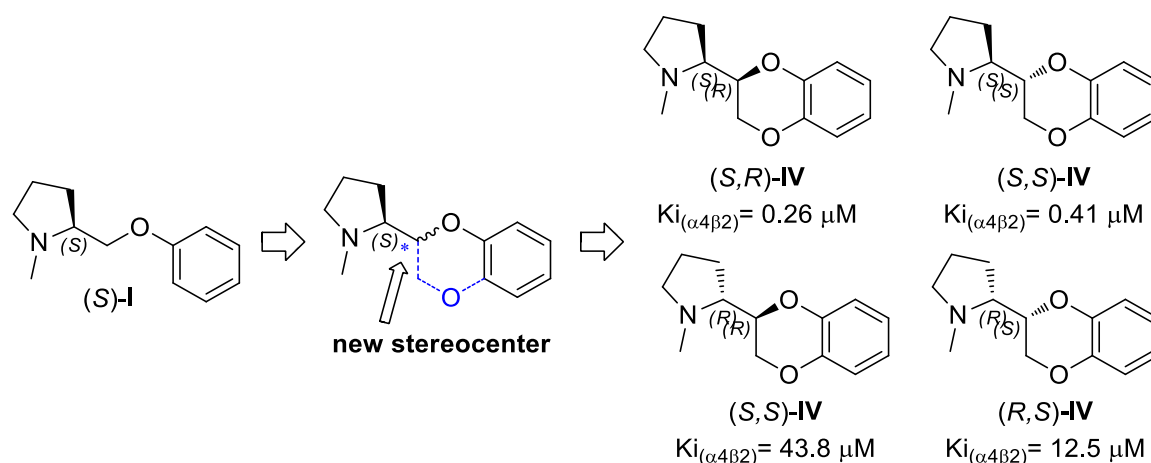


Figure 15: Design of *N*-Me-pyrrolidinyl-benzodioxanes as selective $\alpha 4\beta 2$ ligands. Only **(S,R)-IV** and **(S,S)-IV** have sub-micromolar affinities.

The rigid benzodioxane scaffold of **(S,R)-IV** represented an optimal platform to probe the features of receptor binding pocket and to identify additional pharmacophoric elements: substituents at the aromatic ring in such a constrained structure are placed in well-defined region of the 3D space if the binding mode is conserved. Intrigued by this opportunity and inspired by the known SAR studies on the phenyl- and pyridyl- ethers of prolinol (**(S)-I** and **A-84543**), according to which substitutions at the *meta*-position to their methylenoxy linker are the most beneficial for affinity and selectivity, the research group synthesized a series of 7-substituted analogues of **(SR)-IV**. The 7- position was chosen because it corresponded to the 5- position of **A-84543**.⁷⁴ Among the series, compound **(S,R)-IVa**, stood out as a $\alpha 4\beta 2$ and $\alpha 6\beta 2^*$ selective high affinity ligand, with partial agonist activity (51%) in the dopamine release assay from striatal slices (*Figure 16*). Since $\alpha 4\beta 2$ and $\alpha 6\beta 2^*$ subtypes approximately equally contribute to nicotine-induced striatal DA release, DA release induced by **(S,R)-IVa** in presence of a specific $\alpha 6\beta 2^*$ blocker (α -conotoxin α MII) was evaluated. This assay confirmed that **(S,R)-IVa** acted as a partial agonist at both subtypes. Later, in 2015, **(S,R)-IVa** was shown to be approximately 50 folds more potent as a partial agonist at the human $\alpha 4\beta 2$ subtype rather than at the human $\alpha 3\beta 4$ subtype in eliciting currents in electrophysiological assays.⁷⁵ These results together revealed that **(S,R)-IVa** had a similar, but more selective, nicotinoid profile to varenicline (non-selective $\alpha 4\beta 2$ partial agonist, 49% efficacy), the only approved drug up to now for nicotine addiction acting on nAChRs.

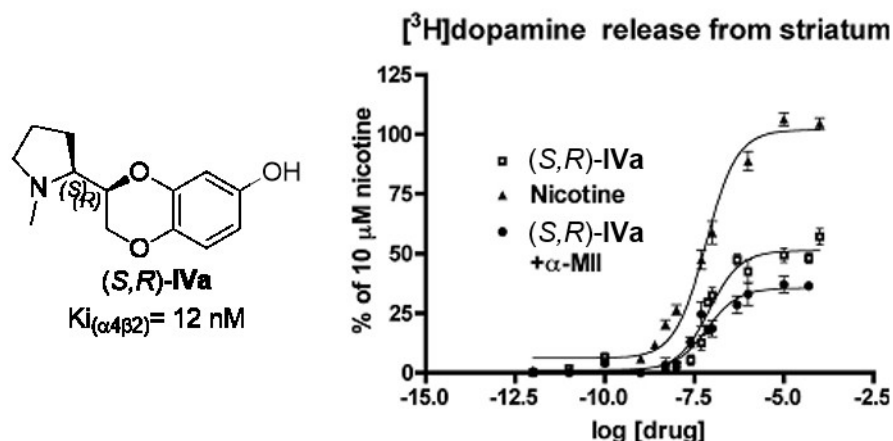


Figure 16: (S,R)-IVa acts as a partial agonist at the $\alpha4\beta2$ and $\alpha6\beta2$ subtypes: concentration-response curves of agonist-induced [³H]DA release from rat striatal slices. The slices were preloaded with 100 nM [³H]DA and exposed to the indicated concentration of nicotine, (S,R)-IVa alone, or in the presence of 100 nM α MII. Results were normalized and expressed as a percentage of 10 μ M nicotine-induced release. The data points represent the mean SEM of 3-4 separate experiments performed in triplicate.

Interestingly, all the other 7-substitutions of the benzodioxane scaffold were quite detrimental for $\alpha4\beta2$ affinity, indicating strict structural requirements for binding that region of the binding pocket (Figure 17). However, compounds with poor $\alpha4\beta2$ affinities provided valuable information for SAR analysis: neither small-sized apolar substituents ((S,R)-IVb - methyl), medium or bulky lipophilic or aromatic substituents ((S,R)-IVc - bromine, (S,R)-IVd - phenyl) nor bulkier but polar ones ((S,R)-IVe - hydroxymethyl, (S,R)-IVf - acetyl, (S,R)-IVg - methoxy) were tolerated, thus suggesting the existence of a small and hydrophilic non-conserved subpocket that can be reached only through an hydroxyl group.

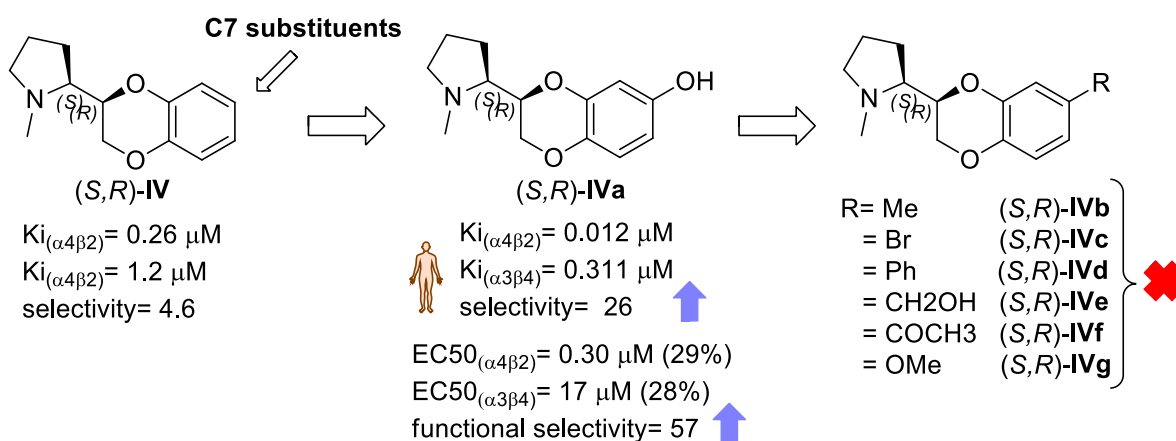


Figure 17: design of 7-substituted N-methyl-pyrrolidinyl-benzodioxanes as $\alpha4\beta2$ partial agonists. (S,R)-IVa is a partial agonist with high $\alpha4\beta2$ affinity. $\alpha4\beta2$ and $\alpha3\beta4$ affinities were measured as displacement of [³H]-epibatidine respectively from rat brain membranes and heterologously expressed human $\alpha3\beta4$ receptors (human symbol).⁷⁵ Every other 7-substitution substantially decreases $\alpha4\beta2$ affinity. EC₅₀ values relate to electrophysiological assays performed on human $\alpha4\beta2$ or $\alpha3\beta4$ subtypes.⁷⁵

In 2013, Brown et. al, aiming at potent and selective $\alpha 4\beta 2$ desensitizing agents with enhanced physicochemical properties (BBB permeability) in respect of those of **Saz-A**, synthesized three series of **Saz-A** analogues (*Figure 18*).⁷⁶ Among these, they identified compound **VMY-2-95** as the most promising candidate as a therapeutic agent for smoking cessation, due to its better brain tissue distribution, high selectivity over more than 40 CNS receptors, including $\alpha 3\beta 4$, $\alpha 7$ and 5-HT₃, high potency associated with low efficacy (30%), high desensitizing capability and effectiveness in reducing self-administration of nicotine in animal models.

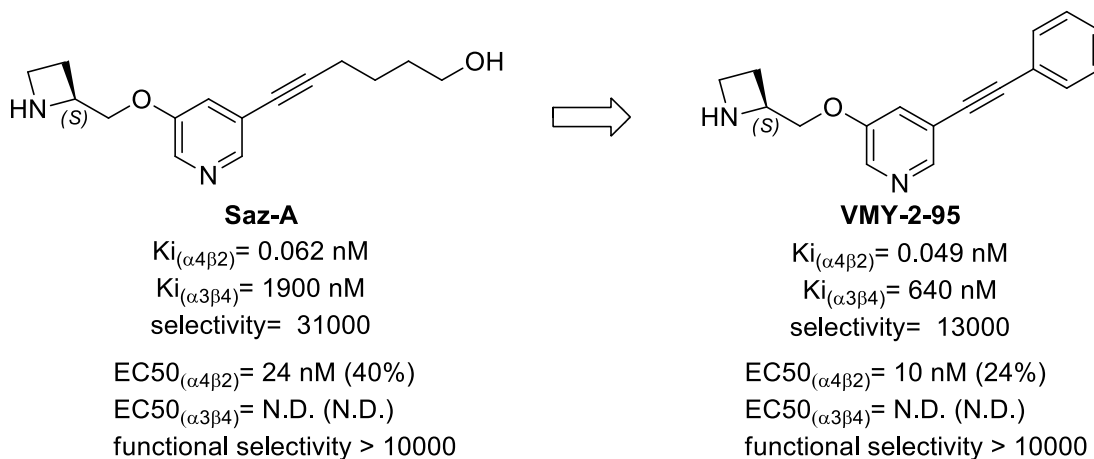


Figure 18: design of VMY-2-95 as an analogue of Saz-A with improved BBB permeability.

Although several 5-substituted analogues of the pyridyl- and phenyl-ethers of N-methyl prolinol (**A-84543** and (*S*)-**I**) have been studied (**Saz-A**, **VMY-2-95** and others), the effect of hydroxylation at that position had never been reported. Prompted by the considerable enhancement of $\alpha 4\beta 2$ affinity obtained by introducing an hydroxyl group at the 7 position of the benzodioxane scaffold of (*S,R*)-**IV** and by the functional $\alpha 4\beta 2/\alpha 3\beta 4$ selectivity of the resulting compound (*S,R*)-**IVa**, the research group of professor Pallavicini, which I joined for my master thesis and later for my PhD, investigated the effect of the same substituent (OH) when introduced in the correspondent *meta*-position of **A-84543** and (*S*)-**I**. The resulting compounds, namely (*S*)-**V** and (*S*)-**VI**, were shown to be highly potent $\alpha 4\beta 2$ full agonists, but only (*S*)-**V** showed functional selectivity. Compound (*S*)-**VI** can also be considered as a flexible analogue of the selective $\alpha 4\beta 2$ and $\alpha 6\beta 2$ partial agonist (*S,R*)-**IVa**, obtained by deconstruction of its benzodioxane moiety (*Figure 19* and *Figure 20*).⁷⁵

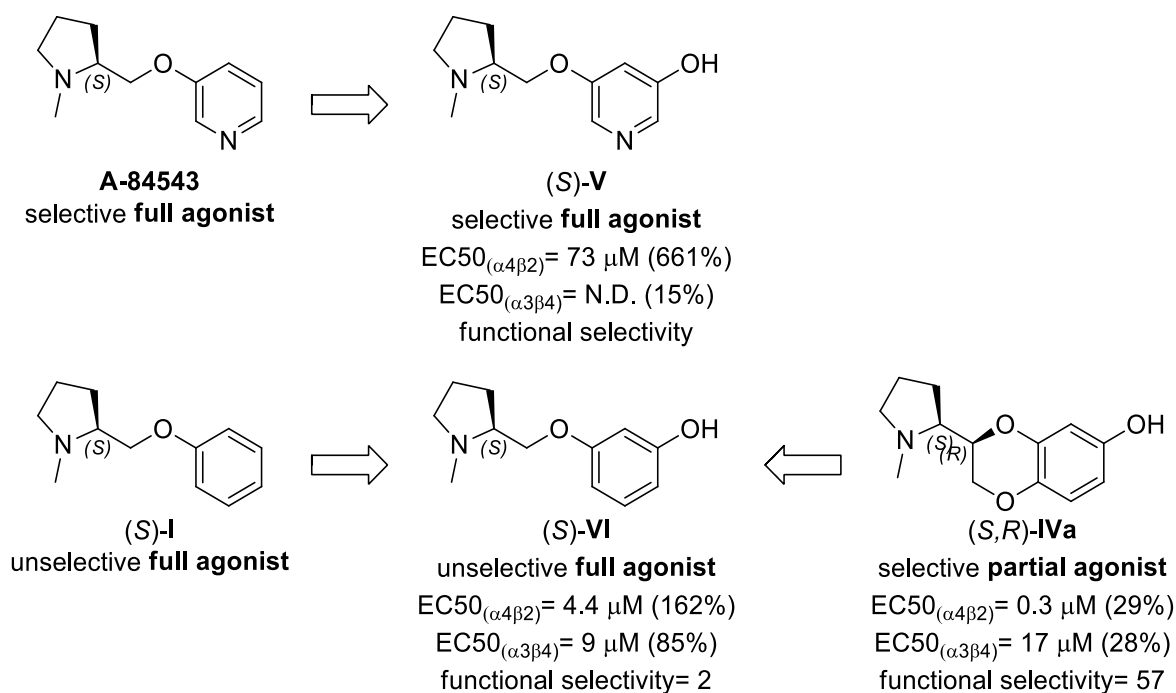


Figure 19: design of the selective full agonist (S)-V and of the unselective full agonist (S)-VI as analogues of A-84543 and of (S)-I.

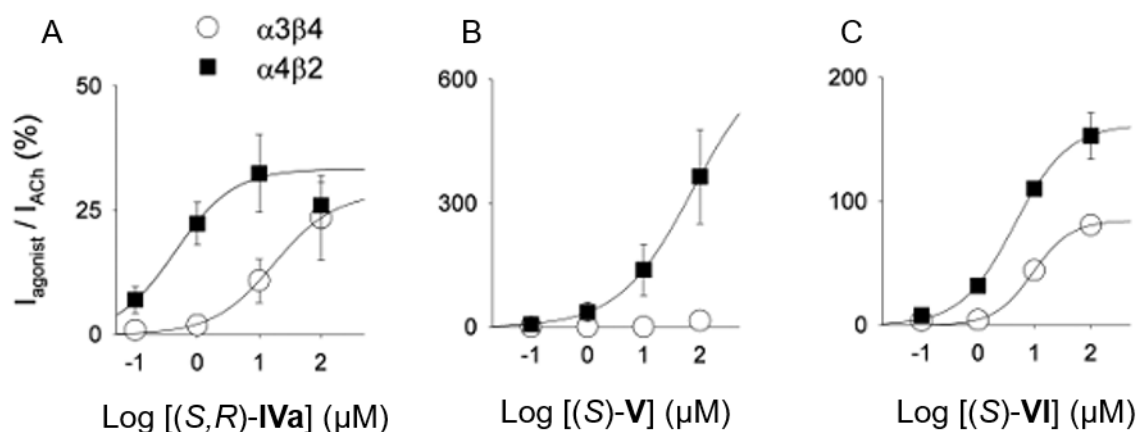


Figure 20: agonist effect of (S,R)-IVa, (S)-V and (S)-VI on transfected human $\alpha_4\beta_2$ and $\alpha_3\beta_4$ subtypes. The activation responses are normalized to the maximal response to 1 mM ACh.

Comparison between partial agonism of the rigid compound (S,R)-IVa and full agonism of the flexible (S)-VI suggested that conformational constrain could play a role in functional activity. For this reason, a series of semi-rigid analogues of both A-84543 and (S)-VI (for instance (S)-VII and (S)-VIII) was synthesized, assessed for $\alpha_4\beta_2$, $\alpha_3\beta_4$, α_7 affinities⁷⁵ (data not shown) and some selected compounds were tested in electrophysiological assays for $\alpha_4\beta_2$ and $\alpha_3\beta_4$ activities (Figure 21). The results confirmed that the extended conformation imposed by a semi-rigid or a rigid structure is correlated with partial agonism activity, whereas flexibility and

“compressibility” of the oxymethylene bridge between the aromatic ring and the pyrrolidine residue is associated with full agonism.

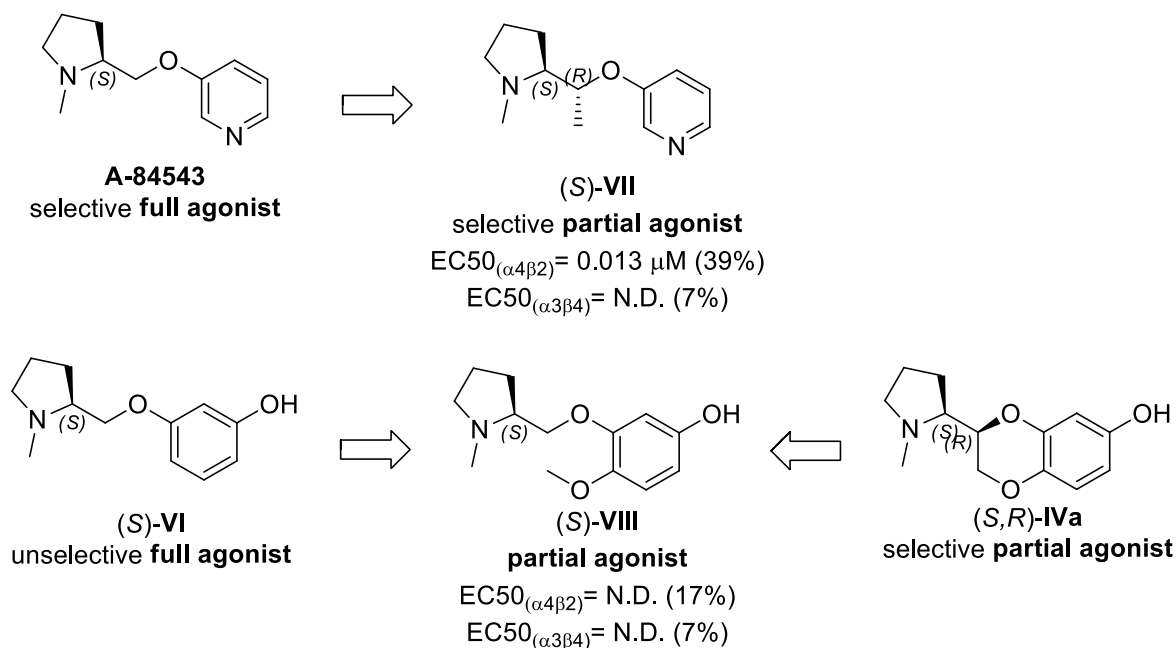


Figure 21: design of the partial agonists (S)-VII and (S)-VIII as semi-rigid analogues of A-84543, (S)-VI and (S,R)-IVa.

Docking studies at a homology model of the $\alpha_4\beta_2$ binding site suggested that the partial agonist activity and selectivity could be achieved due to additional interactions between the 7-hydroxy of (S,R)-IVa or the *meta*-hydroxy or *meta*-basic nitrogen of its semirigid analogues (S)-VII and (S)-VIII and a non-conserved small hydrophilic pocket within the β_2 subunit (Figure 22).

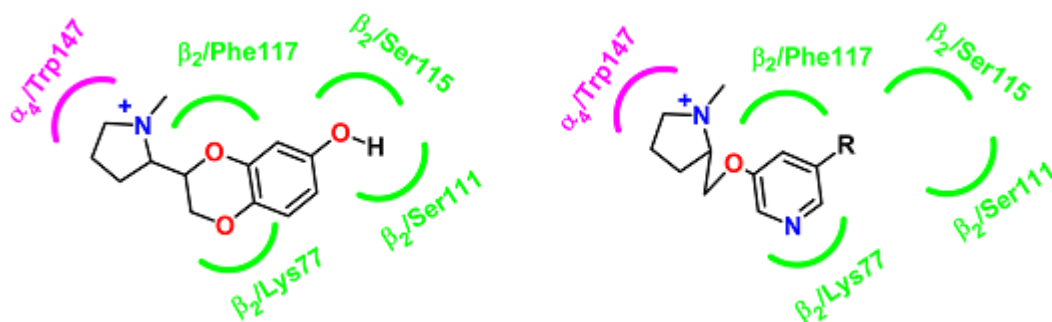


Figure 22: hypothetical binding modes at the $\alpha_4\beta_2$ subtype suggested by docking of rigid and semi-rigid ligands (left) and flexible ligands (right).

According to this model, rigid and semirigid ligands fit the pocket into an extended conformation imposed by their structural constraints, which moves the aromatic ring of the benzodioxane moiety away from the aromatic residue of phenylalanine of the binding site, but places the terminal hydroxyl pendant within a small and hydrophilic non-conserved binding pocket.

Contrariwise, flexible ligands fold into a compressed conformation and place their aromatic rings so that to maintain a π - π interaction with the residue of phenylalanine, but do not reach the above mentioned additional pocket.

1.4 Outlook

In this framework, the goals of this part of my project were the:

- synthesis of novel 5-substituted 3-hydroxyphenyl and 3-nitrophenyl ethers of (*S*)-prolinol as $\alpha 4\beta 2$ -nicotinic acetylcholine receptor ligands⁷⁷
- synthesis of N-methyl-pyrrolidinyl-pyridodioxanes designed as isosteres of N-methyl-pyrrolidinyl-benzodioxanes⁷⁸
- synthesis of N-methyl-pyrrolidinyl-5-substituted-benzodioxanes
- computer-aided SARs interpretation

1.5 Novel 5-substituted 3-hydroxyphenyl and 3-nitrophenyl ethers of (*S*)-prolinol as $\alpha 4\beta 2$ -nicotinic acetylcholine receptor ligands⁷⁷

1.5.1 Introduction and aim

As discussed in the previous chapter 1.3, N-Me-prolinol pyridyl ether **A-84543** and its azetidinyll analogue **A-85380** were reported at the end of the nineties as potent $\alpha 4\beta 2$ full agonists with selectivity over $\alpha 7$ and muscle-type nAChRs.⁵⁹ Later, selectivity over the ganglionic $\alpha 3\beta 4$ subtype was achieved by Kozikowski and Brown in Sazetidine-A and VMY-2-95, by introducing sterically bulky substituents at the 5-position of the pyridyl ether scaffolds.^{65,76} Since my research group had already discovered that replacement of the pyridyl ring of **A-84543** with a *meta*-hydroxyphenyl in compound (*S*)-**VI** resulted in comparable affinity, but lower selectivity, we aimed at understanding whether we could restore selectivity over the $\alpha 3\beta 4$ subtype by introducing sterically bulky substituents at the 5-position of compound (*S*)-**VI**.⁷⁵

We selected, as *meta*-substituents, 6-hydroxy-1-hexynyl, conferring high $\alpha 4\beta 2$ vs $\alpha 3\beta 4$ selectivity in **Saz-A**, and bromine and phenyl, which were reported to preserve high affinity at the $\alpha 4\beta 2$ when linked to C5 of **A-84543**.^{61,79} Additionally, we enclosed into this series also *p*-hydroxyphenyl, with the hypothesis that a terminal hydroxyl group could reinforce the interactions of the *meta*-substituent, like in **Saz-A** and in (*S,R*)-**IVa** (Figure 23).

Overall, compounds (*S*)-**1a**, (*S*)-**1b**, (*S*)-**1c** and (*S*)-**1d** were synthesized.

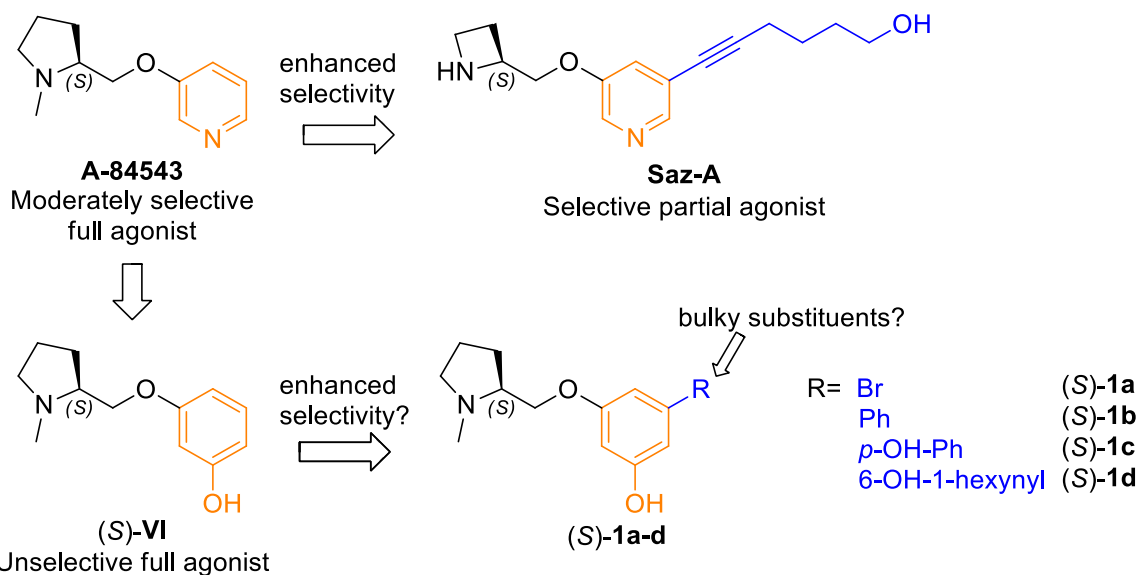


Figure 23: design of flexible $\alpha 4\beta 2$ selective ligands (*S*)-**1a-d** as 5-substituted analogues of (*S*)-**IV**.

Moreover, since often pyridyl rings can be bioisosterically replaced by nitrophenyl, we decided to include in our research compound (*S*)-**IX**, whose $\alpha 4\beta 2$ affinity had already been reported 20 years ago,⁸⁰ and its 5-substituted analogues (*S*)-**2a**, (*S*)-**2b**, (*S*)-**2c** and (*S*)-**2d** (Figure 24).

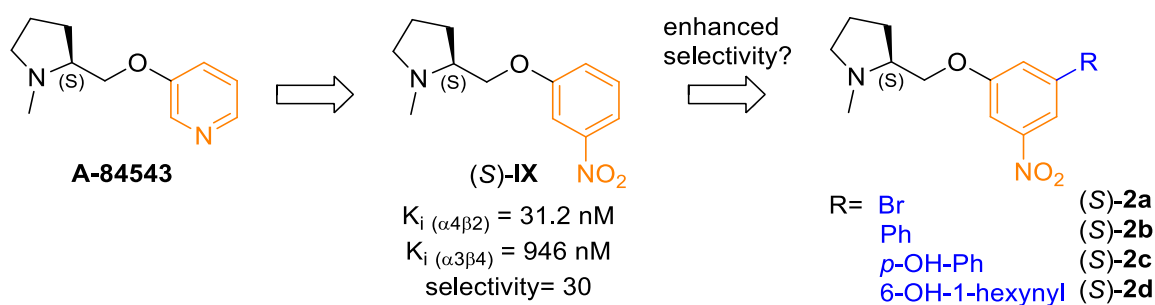


Figure 24: design of flexible $\alpha 4\beta 2$ selective ligands (*S*)-**2a-d** as 5-substituted analogues of (*S*)-**IX**, a putative bioisoster of **A-84543**.

As a term of comparison for (*S*)-**VI**, (*S*)-**1d** and (*S*)-**2d**, we also synthesized compounds (*S*)-**3** and (*S*)-**4** (Figure 25).

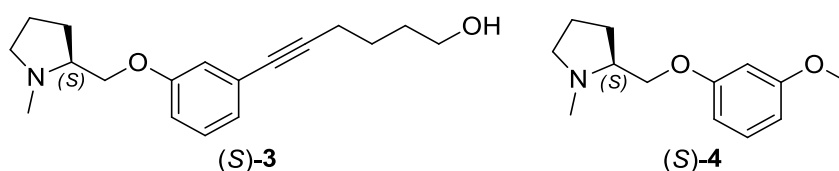


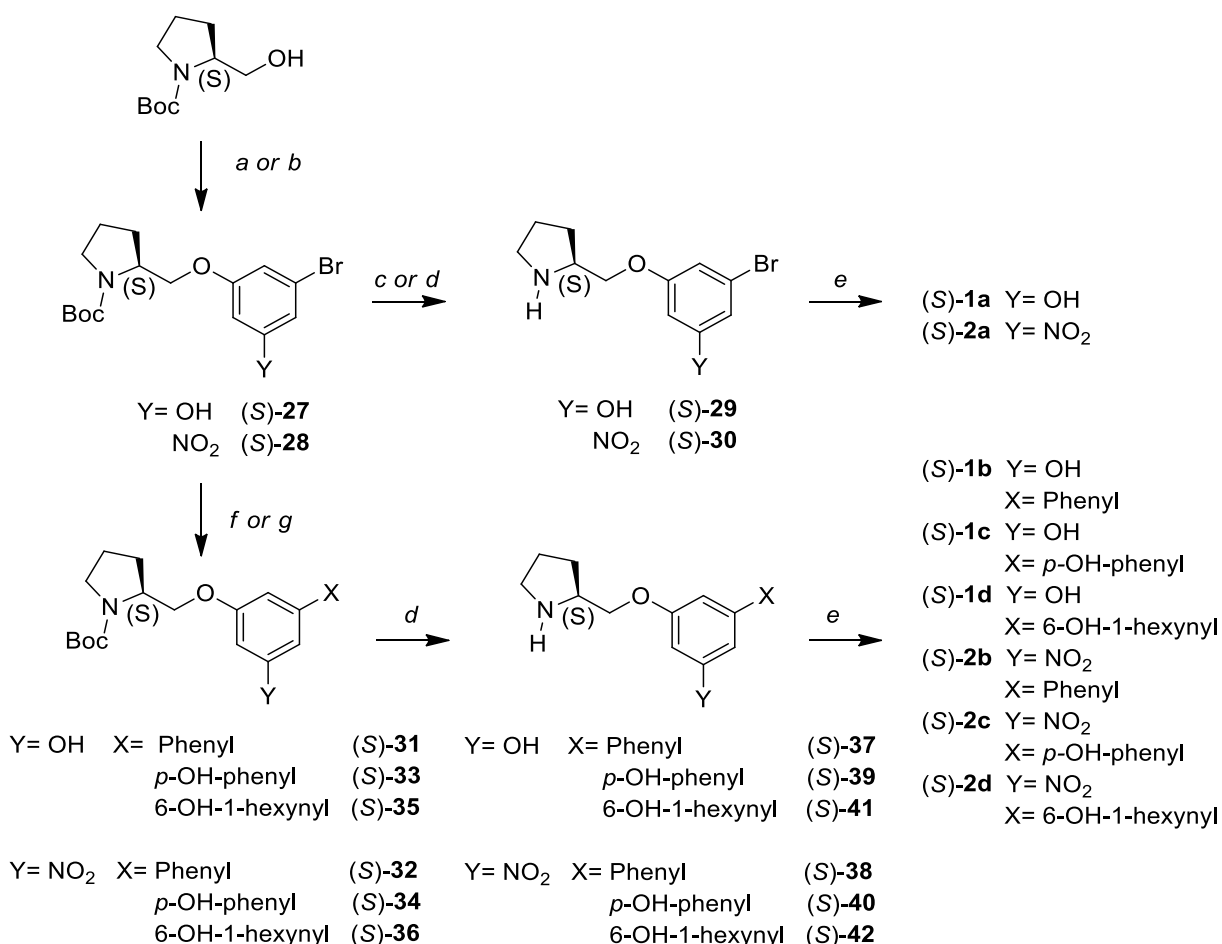
Figure 25: design of flexible $\alpha 4\beta 2$ selective ligands (*S*)-**3** and (*S*)-**4** as *meta*-substituted analogues of (*S*)-**I**.

Based on our previous hypothesis of different binding modes between rigid/semirigid compounds (partial agonists) and their flexible analogues (full agonists), we expected compounds (*S*)-**1a-d** and (*S*)-**2a-d** to bind similarly to **A-84543**. If so, the introduction of the listed substituents at the 5-position of the *meta*-hydroxyphenyl ether and *meta*-nitrophenyl ether scaffolds should result in parallel shifts in affinity and in selectivity when compared to the 5-substituted pyridyl ether, confirming a bioisosteric relationship between these three scaffolds and providing new analogues with good $\alpha 4\beta 2$ affinity and selectivity.

1.5.2 Synthetic schemes

Commercial N-Boc protected (*S*)-prolinol (Sigma Aldrich) was coupled by Mitsunobu reaction either with the commercial 3-hydroxy-5-bromophenol or 3-bromo-5-nitrophenol, to obtain respectively intermediates (*S*)-**27** and (*S*)-**28**, which were directly deprotected to (*S*)-**29** and (*S*)-**30** respectively with TFA and HCl and then N-methylated with formaldehyde and picoline borane to obtain the final compounds (*S*)-**1a** and (*S*)-**2a**.

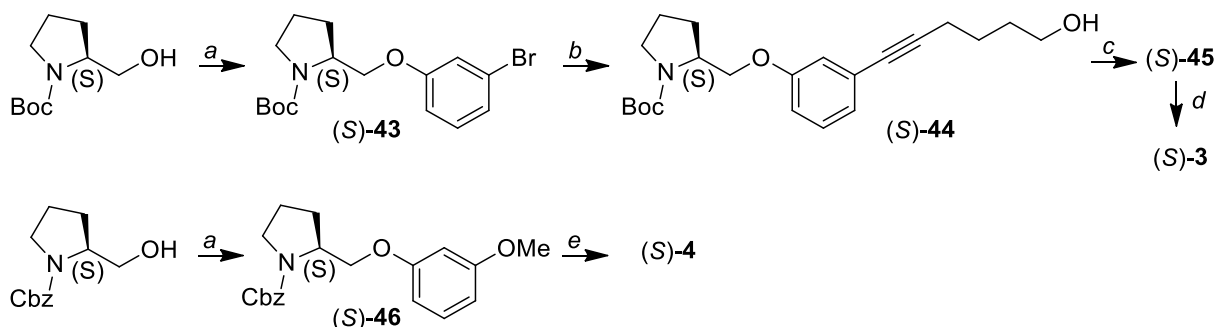
Intermediates (S)-27 and (S)-28 were coupled in a Suzuki reaction with phenylboronic acid to afford (S)-31 and (S)-32, and with 4-hydroxyphenylboronic acid to give (S)-33 and (S)-34, or reacted with 5-hexyn-1-ol in a Sonogashira coupling to obtain intermediates (S)-35 and (S)-36. Subsequently they were N-Boc deprotected with methanolic HCl to (S)-37-42 and N-methylated with formaldehyde and picoline borane to obtain the final compounds (S)-1b-d and (S)-2b-d (Scheme 1).



Scheme 1: Reagents and conditions. (a) 3-Hydroxy-5-bromophenol, PPh₃, DIAD, THF, 130 °C, 30 min, microwave, 34% ((S)-27); (b) 3-Bromo-5-nitrophenol, PPh₃, DIAD, THF, reflux, 12 h, 85% ((S)-28); (c) TFA, DCM, room temperature, 2 h, 80% ((S)-29); (d) Methanolic 1.25N HCl, room temperature, 12 h, 42% ((S)-30), 100% ((S)-37), 96% ((S)-39), 80% ((S)-41), 78% ((S)-38), 81% ((S)-40) and 95% ((S)-42); (e) 37% CH₂O, CH₃COOH, pic-BH₃, CH₃OH, room temperature, 4 h, 75% ((S)-1a), 80% ((S)-1b), 51% ((S)-1c), 87% ((S)-1d), 98% ((S)-2a), 86% ((S)-2b), 80% ((S)-2d), and 79% ((S)-2c); (f) Pd(PPh₃)₄, toluene, 2M aqueous Na₂CO₃, XB(OH)₂, ethanol, reflux, 12 h, 75% ((S)-31), 97% ((S)-33), 93% ((S)-32) and 63% ((S)-34); (g) Pd(PPh₃)₄, CuBr, 5-hexyn-1-ol, TEA, reflux, 12 h, 80% ((S)-35) and 61% ((S)-36).

The reference compound (S)-3 was synthesized following the same procedure used for the synthesis of (S)-1d and (S)-2d, but using 3-bromophenol in the first Mitsunobu coupling step. Similarly, the reference compound (S)-4 was synthesized starting from (S)-N-Cbz-prolinol and

3-methoxyphenol according to the same procedure used for the synthesis of (*S*)-**1a** and (*S*)-**2a** (Scheme 2).



Scheme 2: (a) 3-Bromophenol or 3-methoxyphenol, PPh_3 , DIAD, THF, reflux, 12 h, 48% ((*S*)-**28**); (b) $Pd(PPh_3)_4$, CuBr, 5-hexyn-1-ol, TEA, reflux, 12 h, 79%; (c) Methanolic 1.25N HCl, room temperature, 12 h, 71%; (d) 37% CH_2O , CH_3COOH , pic-BH₃, CH_3OH , room temperature, 4 h, 98%; (e) $LiAlH_4$, THF, reflux, 90 min, 67%.

1.5.3 Biology

We evaluated the binding affinity of (*S*)-**1a-d** and (*S*)-**2a-d**, (*S*)-**3** and (*S*)-**4** towards the $\alpha 4\beta 2$ nAChR present on rat cerebral cortex membranes and towards the human $\alpha 3\beta 4$ nAChR transiently transfected on HEK 243 cells according to a previously described experimental protocol.⁷⁵ The $\alpha 4\beta 2$ and $\alpha 3\beta 4$ nAChRs were labelled by [³H]-epibatidine and the binding affinities (K_i) of the compounds were determined with competition binding experiments. The results are listed on Table 1 together with the affinities of (*S*)-**IX** and nicotine, used as controls, and with those previously reported for the hydroxyphenyl ether (*S*)-**VI**.⁷⁵

1.5.4 Results and discussion

As shown in Table 1, our lead compounds 3-hydroxyphenyl ether (*S*)-**VI** and 3-nitrophenyl ether (*S*)-**IX** had high affinity at the $\alpha 4\beta 2$ subtype (1.1 and 31 nM respectively), higher than that determined for the unsubstituted phenyl ether progenitor (*S*)-**I** determined in 1995 by Elliot using [³H]-cytisine (42 nM). Therefore, the introduction of OH or NO₂ at the 3-position of the phenyl ether is beneficial for $\alpha 4\beta 2$ affinity and results in a *m*-hydroxylated ligand (*S*)-**VI**, with affinity in the same rank of the reference compound **A-84543** (1.9 nM) and in a ligand, (*S*)-**IX**, with intermediate affinity between (*S*)-**I** (42 nM) and **A-84543**. The importance of *m*-OH is further confirmed by the drop of $\alpha 4\beta 2$ affinity when methylated to compound (*S*)-**4** or removed from compound (*S*)-**1d** to (*S*)-**3**. Furthermore, (*S*)-**VI** and (*S*)-**IX** show moderate $\alpha 4\beta 2$ vs $\alpha 3\beta 4$ selectivity.

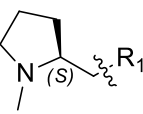
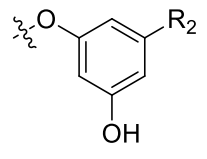
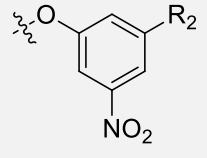
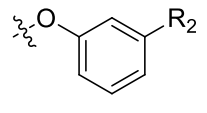
 R₁= R₂=		Compound	$\alpha 4\beta 2$ nAChR [³ H]-Epi (nM)	$\alpha 3\beta 4$ nAChR [³ H]-Epi (nM)	Selectivity Ki $\alpha 3\beta 4/\alpha 4\beta 2$
	H	(<i>S</i>)- VI	1.1 (29) ^a	74 (100) ^a	67
	Br	(<i>S</i>)- 1a	186 (25)	147 (30)	0.8
	Ph	(<i>S</i>)- 1b	528 (32)	200 (28)	0.4
	<i>p</i>-OH-Ph	(<i>S</i>)- 1c	3.8 (47)	30 (53)	8
	6-OH-1-hexynyl	(<i>S</i>)- 1d	23.7 (21)	3100 (34)	131
	H	(<i>S</i>)- IX ^b	31.2 (32)	946 (33)	30
	Br	(<i>S</i>)- 2a	55 (26)	415 (49)	8
	Ph	(<i>S</i>)- 2b	330 (45)	947 (38)	3
	<i>p</i>-OH-Ph	(<i>S</i>)- 2c	12 (43)	122 (41)	10
	6-OH-hexynyl	(<i>S</i>)- 2d	14.2 (31)	1200 (32)	85
	6-OH-hexynyl	(<i>S</i>)- 3	4400 (32)	8300 (44)	2
	OMe	(<i>S</i>)- 4	600 (32)	4500 (41)	7
		(<i>S</i>)-Nicotine	4 (18)	261 (30)	65

Table 1: Compounds (*S*)-**1a-d**, (*S*)-**IX**, (*S*)-**2a-d**, (*S*)-**3**, (*S*)-**4** and (*S*)-nicotine: affinity for native $\alpha 4\beta 2$ nAChR, present in rat brain membranes, labelled by [³H]-epibatidine, and for heterologously expressed human $\alpha 3\beta 4$ nAChR, labelled by [³H]-epibatidine and affinity ratios. The numbers in brackets are the % coefficient of variation (CV%).⁷⁵ ^aAffinity data for (*S*)-**VI** from literature.⁸¹ ^bAs the nicotinic affinity data reported in literature⁸⁰ of (*S*)-**IX** was not coherent with the rest of the dataset and the $\alpha 3\beta 4$ affinity had never been reported, (*S*)-**IX** was included in the current binding assays.

To probe whether bulky substituents at the 5-position of our scaffolds (*S*)-**VI** and (*S*)-**IX** would have led to the same effects observed in **A-84543**, we introduced the same substituents (Br, Ph, 4-hydroxyphenyl and 6-hydroxy-1-hexynyl) in the *meta*- positions of (*S*)-**VI** and (*S*)-**IX**. Interestingly, parallel trends of affinity were found between the two series: 1) *meta*-bromination ((*S*)-**1a** (*S*)-**2a**) and, to a greater extent, *meta*-phenylation ((*S*)-**1b** (*S*)-**2b**) lowered the $\alpha 4\beta 2$ affinity and canceled $\alpha 4\beta 2/\alpha 3\beta 4$ selectivity; 2) the *meta*-4-hydroxyphenyl substituted analogues (*S*)-**1c** and (*S*)-**2c** had the highest affinities in the series (3 and 12 nM respectively) but modest selectivity, highlighting the importance of a distal hydroxyl group for affinity, that

could enhance $\alpha 4\beta 2$ affinity up to 139 times when compared to the phenyl analogues; 3) both the meta-6-hydroxy-1-hexynyl substituted derivatives (*S*-**1d** and (*S*-**2d** showed respectively 24 and 14 nM affinities and significantly higher $\alpha 4\beta 2/\alpha 3\beta 4$ selectivity than the respective parent compounds (*S*-**VI** and (*S*-**IX**).

Proven the parallelism between the two series of compounds, we aimed to reveal the scaffold-dependent similarities/differences among each series of 5-substituted ligands. The comparison could only be drawn for the 5-(6-hydroxy-1-hexynyl) substituted analogues of the three scaffolds, namely (*S*-**1d**, (*S*-**2d** and (*S*-**III**, because the 5-(4-hydroxyphenyl)-substituted analogue of **A-84543** was not reported and the binding data for 5-bromo and 5-phenyl analogues were limited to $\alpha 4\beta 2$ affinity and not directly comparable to the K_i of **A-84543** (Figure 26).

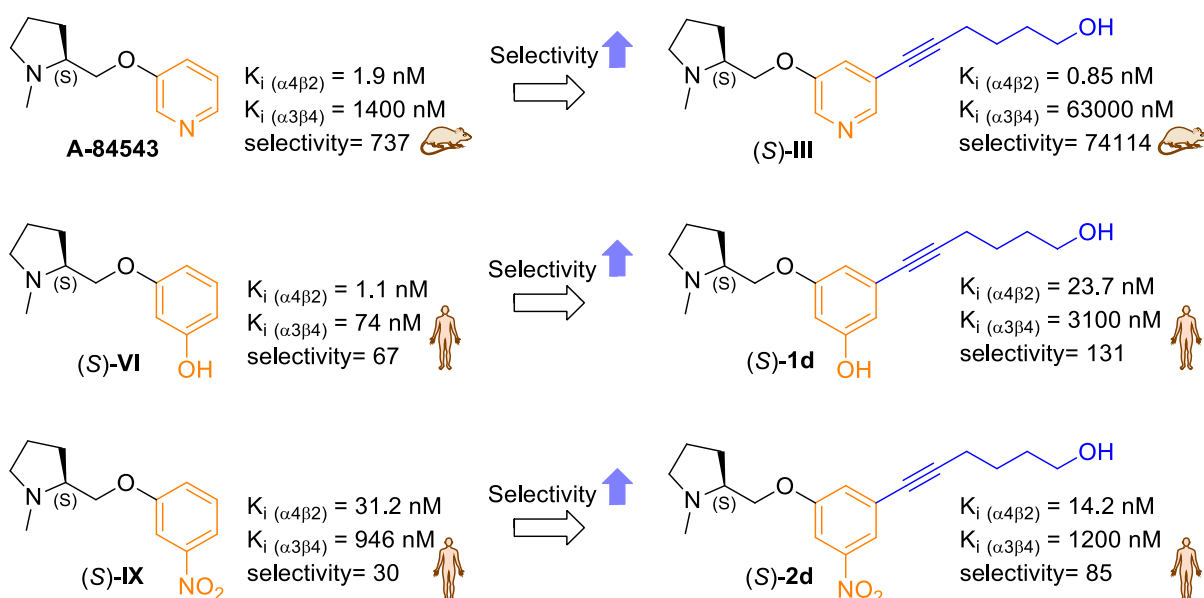


Figure 26: parallel shifts in $\alpha 4\beta 2$ affinities and selectivities among the series of 5-(6-hydroxy-1-hexynyl) substituted analogues. $\alpha 4\beta 2$ and $\alpha 3\beta 4$ affinities of **A-84543** and (*S*-**III**) were measured as displacement of [3 H]-epibatidine from heterologously expressed rat $\alpha 4\beta 2$ and $\alpha 3\beta 4$ receptors (rat symbols).⁶¹ $\alpha 4\beta 2$ and $\alpha 3\beta 4$ affinities of (*S*-**VI**, (*S*-**1d**, (*S*-**IX** and (*S*-**2d** were measured as displacement of [3 H]-epibatidine respectively from rat brain membranes and heterologously expressed human $\alpha 3\beta 4$ receptors (human symbols).⁷⁷

Compound (*S*-**III**, when compared to **A-84543**, maintained high $\alpha 4\beta 2$ affinity (0.85 nM) and had enhanced $\alpha 4\beta 2/\alpha 3\beta 4$ selectivity, like (*S*-**1d** and (*S*-**2d** when compared to their parental compounds (*S*-**VI** and (*S*-**IX**. The 5-(6-hydroxy-1-hexynyl) substitution similarly affects the nicotinic profiles of all the three scaffolds containing, respectively, a pyridyl, a meta-hydroxyphenyl and a meta-nitrophenyl moiety, suggesting common binding modes at the $\alpha 4\beta 2$ and a bioisosteric relationship for **A-84543**, (*S*-**VI** and (*S*-**IX**.

As previously proposed and discussed by Pethukov, selectivity on $\alpha 4\beta 2$ over $\alpha 3\beta 4$ can be obtained with a long and flexible alkynyl substituent at C5 of **A-84543** thanks to different interactions with non-conserved $\beta 2$ or $\beta 4$ residues located relatively far away from the charged pyrrolidine nitrogen.⁸² Such different interactions would influence the positioning of the pyrrolidine N⁺ within the aromatic box of the binding site, resulting in favored interactions to an α -conserved Trp in the $\alpha 4\beta 2$, but not in the $\alpha 3\beta 4$.

On the basis of the bioisosteric relationship between **A-84543**, (*S*)-**VI** and (*S*)-**IX**, we suggested that these binding modes and SARs formulated for (*S*)-**III**, could also be extended to (*S*)-**1d** and (*S*)-**2d**, which are in fact new potent and selective $\alpha 4\beta 2$ ligands.

1.6 Synthesis of N-methyl-pyrrolidinyl-pyridodioxanes designed as isosteres of N-methyl-pyrrolidinyl-benzodioxanes⁷⁸

1.6.1 Introduction and aim

I collaborated to the synthesis of the *SR* and *SS* diastereomers of three regioisomers N-Me-pyrrolidinyl-pyridodioxanes **5**, **6** and **7**, designed together with **8** as possible bioisosteres of N-Me-pyrrolidinyl-benzodioxanes (*S,R*)-**IV** and (*S,S*)-**IV** and as rigid analogues of compounds A-84543, (*S*)-**X** and (*S*)-**XI** (*Figure 27*).

Our interest in the challenging synthesis of pyrrolidinyl-pyridodioxanes was stimulated by the universally recognized isosteric relationship between pyridine and benzene. In our case, we already knew that phenyl and *meta*-pyridyl ethers of prolinol had similar nicotinic profiles, albeit **A-84543** was a more potent and selective agonist at the $\alpha 4\beta 2$ subtype than (*S*)-**I**.^{59,63}

Despite the similar activities of the flexible progenitors, we expected different nicotinic profiles by the replacement, one by one, of each of the four benzodioxane CH with a nitrogen. Indeed, many hints suggested that the position of the nitrogen in the pyridodioxane scaffold would have had a great impact on the nicotinic profile: 1) the different affinities of the regioisomers **A-84543**, (*S*)-**X** and (*S*)-**XI**;^{83,84} 2) the differences in affinity between the N-methyl-pyrrolidinyl-benzofurane (*S*)-**XII** and the regioisomers of its furopyridine analogues (*S*)-**XIII**, (*S*)-**XIV**, (*S*)-**XV** and (*S*)-**XVI**^{85,86} and 3) the known involvement of the aromatic system in π - π and HBA interactions, which are both strongly conditioned by the positioning of a heteroatom in the system.⁸⁷

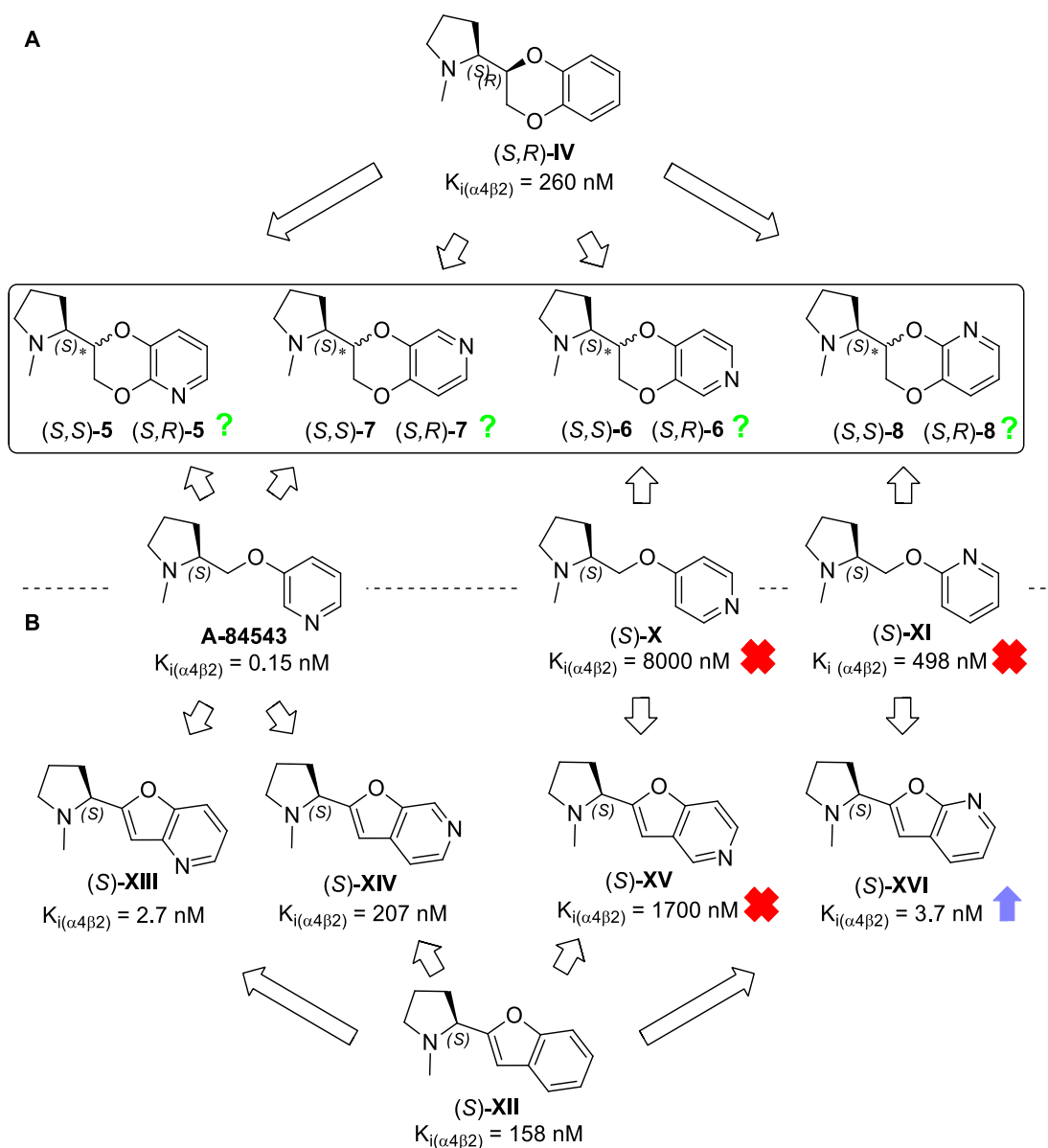


Figure 27: design of (S,S)- and (S,R)-N-methyl-pyrrolidinyl pyridodioxanes 5,6,7 and 8 as rigid analogues of A-84543, (S)-X and (S)-XI and as potential bioisosters of IV and comparison with their N-methyl-pyrrolidinyl-fuopyridines analogue (S)-XIII, (S)-XIV, (S)-XV and (S)-XVI.

According to the known SARs of the flexible pyridylether scaffold of A-84543 and of the rigid benzodioxane scaffold of (S,R)-IV, we expected compound (S,R)-7 to have hybrid characteristics between A-84543 and (S,R)-IVa: the pyridine nitrogen at position 7, ideally superimposable with the pyridine nitrogen of A-84543, might effectively replace the hydroxyl pendent of (S,R)-IVa. As a term of comparison, we evaluated the electrophysiological functional activity of the “naked” benzodioxane with SR absolute configuration (S,R)-IV.

1.6.2 Synthetic schemes

The retrosynthetic analysis of the 4 regioisomers of the pyrrolidinyl-pyridodioxane identified as crucial intermediates the correspondent N-protected-pyridyl ethers reported in Figure 28,

formally obtained by coupling the phenolic function of appropriate chlorinated 3-hydroxypyridine to the primary hydroxyl or to the secondary hydroxyl group derived from N-protected-2-bromoacetylpyrrolidine. Specifically, **8** and **5** could be obtained starting from 2-chloro-3-hydroxypyridine, connected respectively to the primary and secondary alcohol, while **6** and **7** starting from 3-hydroxy-4-chloropyridine, coupled respectively with the primary and secondary hydroxyl groups.

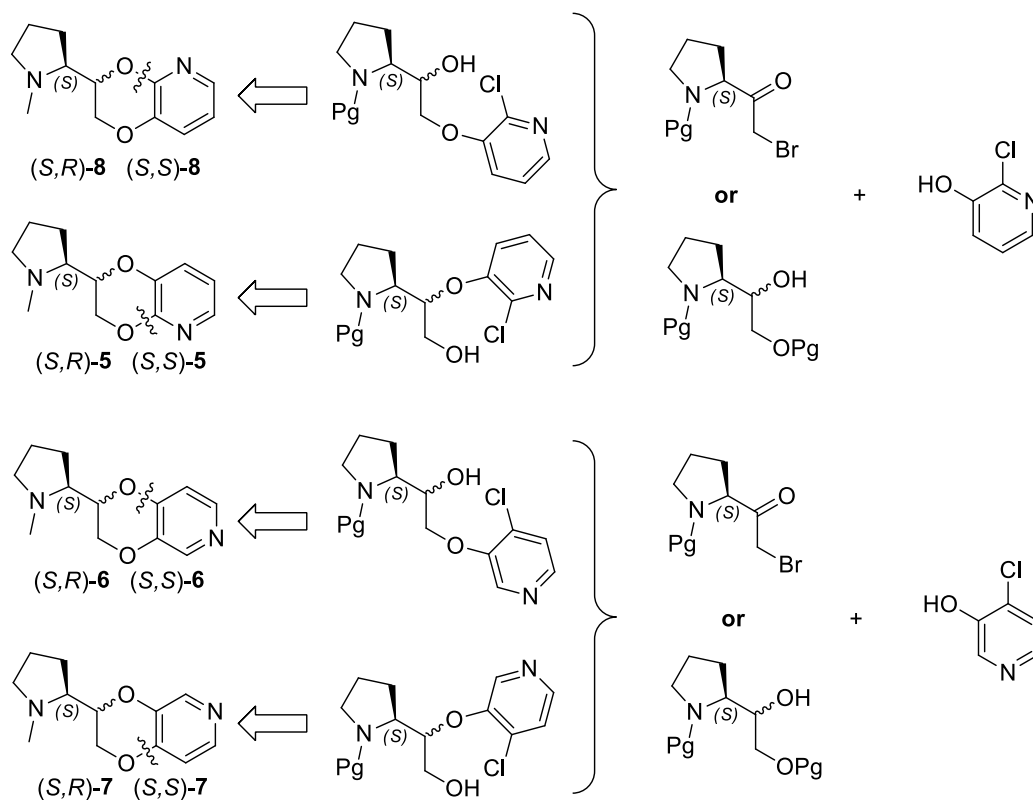
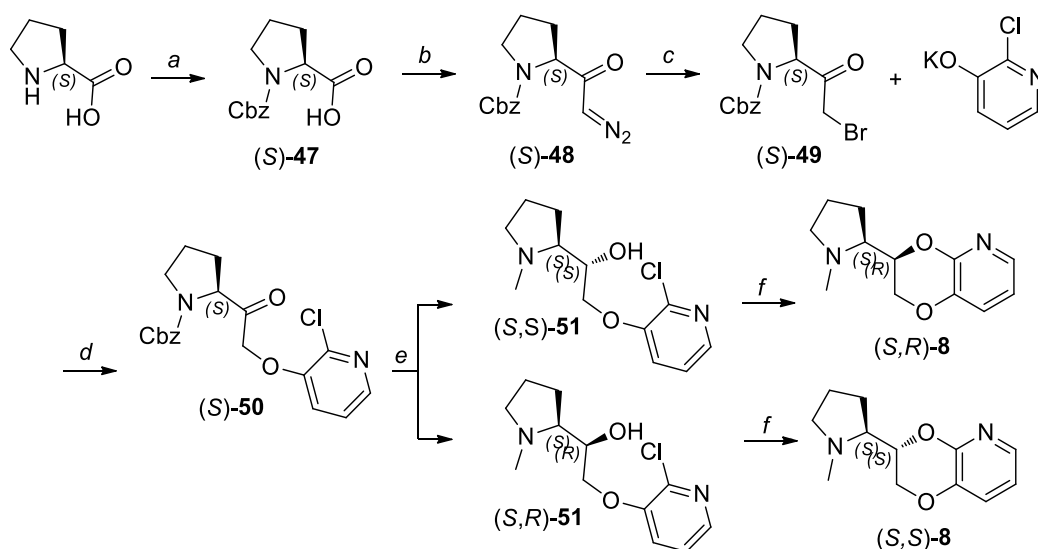


Figure 28: retrosynthetic analysis of N-methyl-pyrrolidinyl-pyridodioxanes (S,S)- and (S,R)-5-8.

According to this retrosynthetic analysis, the syntheses of compounds (S,R)- and (S,S)-**8** had already been reported by a former PhD student and is summarized in *Scheme 3*.

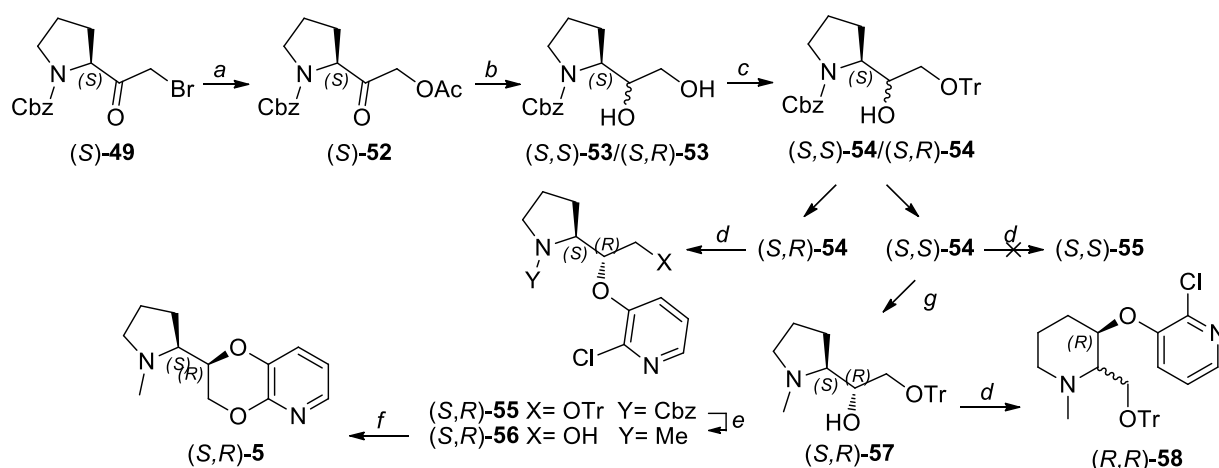


*Scheme 3: Reagents and conditions (a) (S)-Proline, NaOH 2M, Cbz-Cl, 3h, rt, 90%; (b) TEA, *i*-BuOCOCl, Et₂O, -15°C, 1h then CH₂N₂, 0 °C overnight, 89%; (c) HBr/H₂O, Et₂O, 25°C, 1h, 85%; (d) acetone, rt, 16 h, 81%; (e) LiAlH₄, THF, rt, 3 h and then purification through column chromatography 26% ((S,S)-51) and 43% ((S,R)-51); (f) NaH, DME, 120 °C, 1 h, MW, 28% ((S,R)-8) and 30% ((S,S)-8).*

Initially, a similar strategy was planned also for compounds **5**: the bromine of intermediate (S)-**49** was displaced by potassium acetate affording (S)-**52**, that was reduced by treatment with NaBH₄ providing the diastereomeric mixture of the N-protected diols (S,S)- and (S,R)-**53**. Upon protection of the primary alcohol with trityl chloride followed by purification through flash chromatography to the single diastereomers (S,S)- and (S,R)-**54**, the etherification of the secondary alcohol by Mitsunobu reaction instead of the primary alcohol with the same 2-chloro-3-hydroxypyridine mentioned above, should have afforded two intermediates, namely (S,R)-**55** and (S,S)-**55** that, after deprotection and cyclization, would have afforded compounds (S,R)- and (S,S)-**5** (*Scheme 4*).

The diastereomer (S,R)-**55** was obtained by Mitsunobu reaction with trimethylphosphine and DEAD by using microwave irradiation and was further deprotected by reduction with LiAlH₄ followed by hydrolysis in acidic conditions, providing intermediate (S,R)-**56**, that was then cyclized to the final compound (S,R)-**5** by treatment with NaH in DME.

Unfortunately, any attempt to introduce the pyridyl moiety by Mitsunobu reaction on the secondary alcohol of (S,R)-**54**, in the presence of the protecting groups N-Cbz and O-trytyl, was unsuccessful, due to steric reasons. The same reaction, performed on the reduced N-Me analogue (S,R)-**57**, lead to introduction of the pyridyl moiety accompanied by a aziridine-mediated ring-expansion of the pyrrolidine ring to obtain the byproduct (S,R)-**58**.



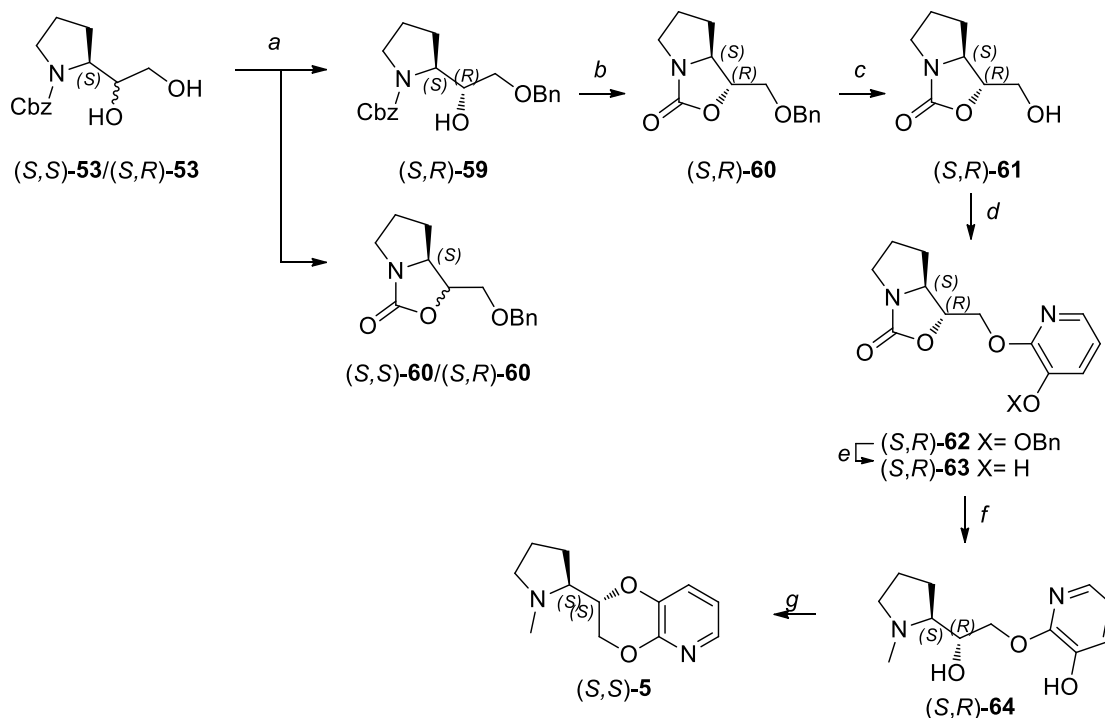
Scheme 4: Reagents and conditions. (a) CH₃COOK, DMSO, rt, 2 h, 98%; (b) NaBH₄, THF, rt, 2 h and then CH₃ONa, MeOH, rt, 1 h 97%; (c) TrCl, TEA, DME, reflux, 4h and then purification through flash chromatography 46% ((S,R)-54) and 34% ((S,S)-54); (d) 2-chloro-3-hydroxypyridine, (Me)₃P, DEAD, THF, 140 °C, 15 min, MW, 43% ((S,R)-55), 0% ((S,S)-55), 75% ((R,R)-58); (e) LiAlH₄, THF, reflux, 3 h and then HCl 1 M, rt, 1 h, 68%; (f) NaH, DME, reflux, 16 h, 75%; (g) CH₂O, H₂, Pd/C, MeOH, RT 12h, 90%.

This synthetic route was unsuccessful for the synthesis of diastereomer (S,S)-5. To overcome this issue, we designed a new synthetic strategy, based on the bicyclic oxazolidinone intermediate **60**, that could be obtained starting from the diastereomeric mixture of N-Cbz-protected diol (S,S)-53/(S,R)-53 by benzylation of the primary alcohol with dibutyltin oxide, accompanied by transcarbamoylation, providing the desired bicycle. The resulting oxazolidinone was synthetically very useful, because it trapped the secondary alcohol into the bicyclic moiety, leaving the benzylated primary hydroxyl free to be modified (*Scheme 5*).

Procedurally, the benzylation reaction of the diastereomeric mixture of (S,S)-53/(S,R)-53 with dibutyltin oxide, partially protected (S,R)-53 into the benzylated opened (S,R)-59 and partially transformed it to the bicyclic oxazolidinone (S,R)-60, while it completely converted (S,S)-53 into the bicyclic intermediate (S,S)-60 by transcarbamoylation. Overall, after chromatography separation, a mixture of the two O-Benzylated cyclic carbamates (S,R)-60/(S,S)-60 was isolated, while only one diastereomer, (S,R)-59, was obtained in the opened form benzylated at the primary alcohol.

The latter was cyclized to (S,R)-60 by treatment with NaH and, after debenylation to (S,R)-61 with H₂ on Pd/C, it was pyridylated with 3-benzyloxy-2-bromopyridine, affording (S,R)-62. The benzyloxy protecting group was removed by catalytic hydrogenation, providing (S,R)-63 and the cyclic carbamate was reduced with LiAlH₄ obtaining (S,R)-64, which was in turn

internally cyclized by Mitsunobu reaction between the two OH groups, affording the final compound (*S,S*)-**5**.



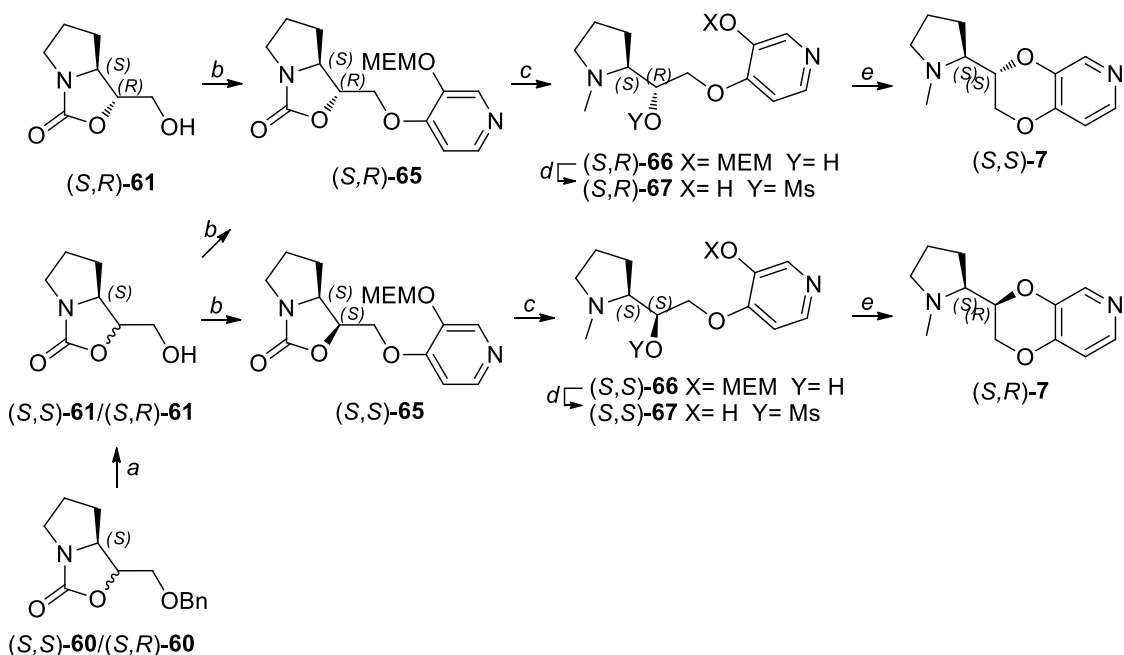
*Scheme 5: Reagents and conditions. (a) Bu_2SnO , toluene, reflux, 5 h and then $BnBr$, TBAI, reflux, 16 h, 37% (*S,R*)-**59**, 46% (*S,S*)-**60**/*(S,R)*-**60**; (b) NaH , DMF, rt, 3 h, 59%; (c) H_2 , Pd/C, MeOH, rt, 16 h, 97%; (d) 3-benzyloxy-2-bromopyridine, NaH , DMF, 80 °C, 4 h, 34%; (e) H_2 , Pd/C, EtOH, rt, 2 h, 99%; (f) $LiAlH_4$, THF, rt, 3 h, 77%; (g) $(Ph)_3P$, DIAD, THF, 120 °C, 15 min, MW, 54%.*

A similar synthetic scheme was applied for the synthesis of (*S,S*) and (*S,R*)-**7**, by coupling the bicyclic carbamate **61** with 4-hydroxy-3-[(2-methoxyethoxy)methoxy]pyridine **72** (*Scheme 6*).

(*S,R*)-**61** had already been isolated as a single diastereomer as described above and was thus coupled by Mitsunobu reaction with 4-hydroxy-3-[(2-methoxyethoxy)methoxy]pyridine, providing (*S,R*)-**65**. Differently, the pure (*S,S*) diastereomer of **61** was not available. Therefore, the diastereomeric mixture of its benzylated precursor (*S,S*)-**60**/*(S,R)*-**60** was debenzylated by catalytic hydrogenation, providing the mixture (*S,S*)-**61**/*(S,R)*-**61**, which was subsequently coupled with 4-hydroxy-3-[(2-methoxyethoxy)methoxy]pyridine **72** to obtain a mixture of (*S,S*)-**65**/*(S,R)*-**65**, whose purification through flash chromatography afforded the pure diastereomer (*S,S*)-**65**.

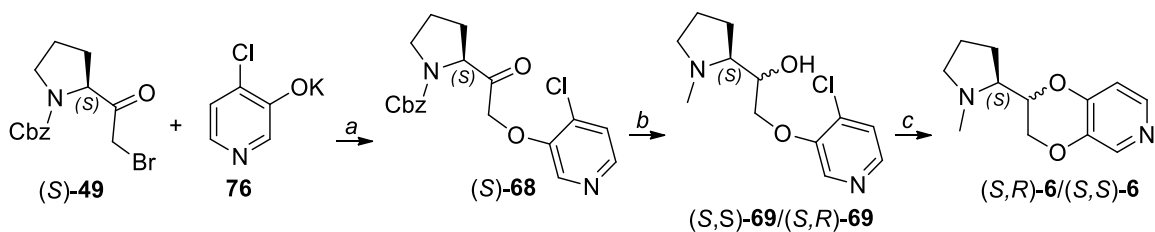
In both cases, the bicyclic oxazolidinone moieties of (*S,R*)-**65** and of (*S,S*)-**65** were reduced with $LiAlH_4$ providing (*S,R*)-**66** and (*S,S*)-**66**, whose secondary hydroxyl groups were activated by treatment with methanesulfonyl chloride and TEA in their mesylated analogues, which

were further deprotected with TFA to *(S,R)*-**67** and *(S,S)*-**67**, and, finally, internally cyclized to the final compounds *(S,S)*-**7** and *(S,R)*-**7** by treatment with K_2CO_3 in DME.



Scheme 6: Reagents and conditions. (a) H_2 , Pd/C, MeOH, rt, 16 h, 80%; (b) 4-hydroxy-3-(2-methoxyethoxy)methoxypyridine **72**, $(Ph)_3P$, DIAD, THF, reflux, 12 h, 80% (*(S,R)*-**65**) and 54% (*(S,S)*-**65**); (c) $LiAlH_4$, THF, rt, 3 h, 86% (*(S,R)*-**66**) and 95% (*(S,S)*-**66**); (d) MsCl, TEA, DCM, rt, 30 min and then TFA, DCM, rt, 3 h, 59% (*(S,R)*-**67**) and 40% (*(S,S)*-**67**); (e) K_2CO_3 , DME, reflux, 16 h, 46% (*(S,S)*-**7**) and 69% (*(S,R)*-**7**).

The two diastereomers of the last regioisomer *(S,R)*- and *(S,S)*-**6** were synthesized according to the procedure used for **8** (*Scheme 7*). *(S)*-N-Cbz-2-bromoacetylpyrrolidine was coupled with the potassium salt of 4-chloro-3-hydroxypyridine **76**, providing intermediate *(S)*-**68**, which was reduced by treatment with $NaBH_4$ to the diastereomeric mixture of secondary alcohols *(S,S)*-**69**/*(S,R)*-**69**. Cyclization with NaH in DME provided the final compounds as diastereomeric mixture *(S,R)*-**6**/*(S,S)*-**6** in a 60:40 ratio (determined by NMR).



Scheme 7: Reagents and conditions. (a) Acetone, rt, 5 h, 48%; (b) $LiAlH_4$, THF, rt, 3 h, 60%; (c) NaH, DMF, reflux, 16 h, 35%.

The absolute configuration of the pyrrolidine stereocenter is *S* in all the final compounds and the intermediates and it is indicated first in their chemical names when there are two

stereocenters, while that of the second stereocenter, namely that formed in the course of the synthesis and corresponding to dioxane C(2) in the final compounds, is either *R* or *S* and was assigned to the separated diastereomers of the final compounds and, retrospectively, to the same carbon of the respective precursors with the aid of ^1H NMR and conformational analysis as previously reported for the benzodioxane analogues and the prolinol phenyl ethers.^{72,74,75}

Briefly, we assigned *R* configuration to the pyridodioxane methine, when ^1H NMR spectrum showed that its proton was anti-disposed to the adjacent methine proton, because such a disposition is conformationally disfavored when the dioxane methine has *S* configuration. The anti disposition was revealed by the td (triplet of doublets) pattern of the dioxane methine signal resulting from the coupling with pyrrolidine methine proton and one of the two dioxane methylene protons with a similar large *J*, as shown in the ^1H NMR spectra of (*S,R*)-**7** reported in the Experimental Section and in its magnification in *Figure 29A*.

However, such an approach could not be extended to the diastereomers of **5** because of signals overlapping. Therefore, we relied on the ^1H NMR analysis of an (*S,S*)-**5** precursor, namely (*S,R*)-**60** (*Scheme 5*). In this precursor, where the two adjacent methine stereocenters are enclosed into a rigid bicyclic structure, the O-adjacent methine has its proton anti-disposed to the proton of the N-adjacent *S* stereocenter and therefore its configuration has to be *R*. The anti-disposition was revealed by the dt (doublet of triplets) pattern of its signal resulting from the coupling to the N-adjacent methine proton with a large *J* and to the exocyclic methylene protons with little lower, nearly equal coupling constants (see the ^1H NMR spectrum of (*S,R*)-**60** in the Experimental section and its magnification in *Figure 29B*).

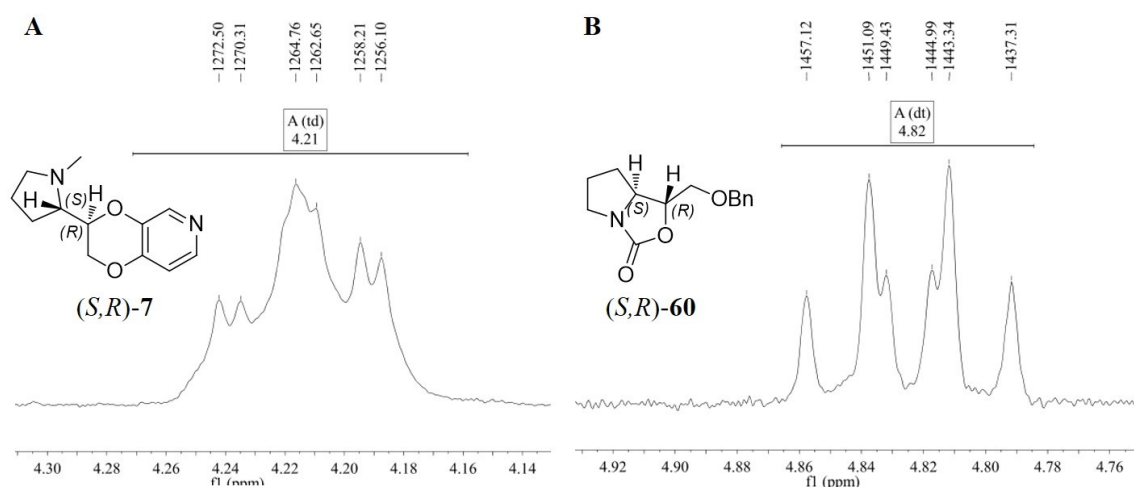
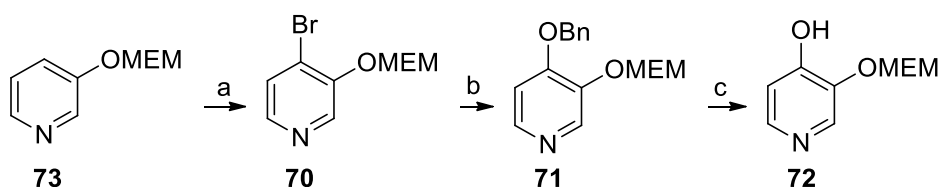


*Figure 29: magnification of the ^1H -NMR spectrum A) focused on the triplet of doublets (td) of the dioxane methine hydrogen of (*S,R*)-**7**; B) focused on the doublet of triplets (dt) of the O-adjacent methine hydrogen of (*S,R*)-**60**.*

As shown in *Scheme 5*, the absolute configuration of (*S,R*)-**60** is correlated not only to that of (*S,S*)-**5**, but also to that of (*S,S*)-**7** and this is congruent to the configuration assignment previously made to the other diastereomer of **8**.

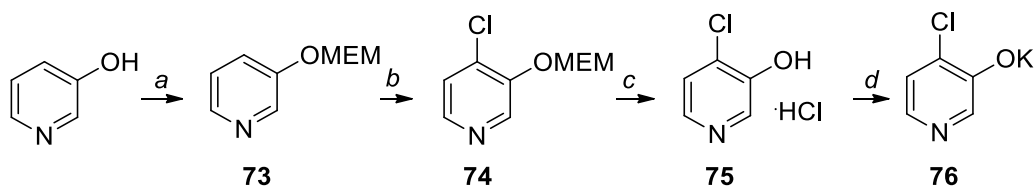
The enantiomeric excesses of key intermediates (*S*)-**50**, (*S*)-**52** and (*S*)-**68**, that could in principle undergo racemization on the chiral center due to the enhanced acidity of the α -methine H were assessed by chiral HPLC and were demonstrated to be higher than 99%.

The pyridylating agent **72** for the synthesis of **7** was synthesized starting from 3-(2-methoxyethoxy)pyridine **73**. Para-lithiation and lithium-bromine exchange afforded **70**, that was converted to **71** by nucleophilic displacement of bromine with benzylate. Further debenzylation provided **72** (*Scheme 8*).



Scheme 8: Reagents and conditions: (a) n-BuLi, THF, -78 °C, 1 h and then CBr₄, -90 °C, 1 h, 72%; (b) BnONa, DMSO, rt, 1h, 82%; (c) H₂, Pd/C 10%, MeOH, 1 h, 98%.

The potassium salt of 4-chloro-3-hydroxypyridine **76**, necessary for the synthesis of **6**, was obtained starting from 3-hydroxypyridine, that was O-protected with NaH and MEM-chloride (**73**) and subsequently chlorinated by direct ortho metalation (DOM) with *t*-BuLi and C₂Cl₆ providing **74**. Deprotection with hydrogen chloride (**75**) followed by treatment with KOH afforded the appropriate potassium phenate **76** (*Scheme 9*).



Scheme 9: Reagents and conditions. (a) NaH, MEM-Cl, DMF, 0°C, 3.5 h, 83%; (b) t-BuLi, C₂Cl₆, diethyl ether, -78°C and then rt, 1 h, 90%; (c) HCl, MeOH, rt, 16 h, 90%; (d) KOH, MeOH, rt, 10 min, 95%.

1.6.3 Biology

Compounds (*S,S*)- and (*S,R*)-**5-8** were assayed for binding affinity on native rat $\alpha 4\beta 2^*$ nAChR present on rat cerebral cortex membranes and on human $\alpha 3\beta 4$ nAChR transiently transfected into HEK 243 cells according to a previously described experimental protocol.^{74,75,88}

The $\alpha 4\beta 2$ and $\alpha 3\beta 4$ nAChRs were labeled by [^3H]-epibatidine ([^3H]-Epi) and the binding affinities (K_i) of the compounds were determined with competition binding experiments; the results are listed in *Table 2*. As controls in each experiment, we determined the affinity of (*S*)-(-)-nicotine for the two subtypes. As a reference, binding affinities of (*S,S*)- and (*S,R*)-**IV** at both subtypes were reported.

Electrophysiological functional assays for $\alpha 4\beta 2$ and $\alpha 3\beta 4$ nAChRs were performed on (*S,R*)-**IV** and on (*S,R*)-**5**. Data were collected via whole-cell patch clamp electrophysiology with GH4C1 cell line cells transiently expressing human $\alpha 4\beta 2$ and $\alpha 3\beta 4$ subtypes.

1.6.4 Results and discussion

The binding studies indicated that (*S,R*)-**5** was the compound with the highest $\alpha 4\beta 2$ affinity and highest $\alpha 4\beta 2/\alpha 3\beta 4$ selectivity, due to a much lower affinity towards the $\alpha 3\beta 4$ subtype, while its diastereomer (*S,S*)-**5** and all the other regioisomers showed supramicromolar $\alpha 4\beta 2$ binding affinities.

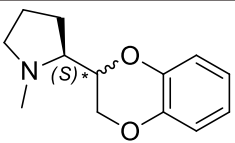
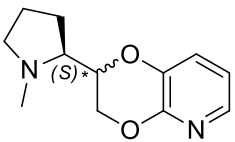
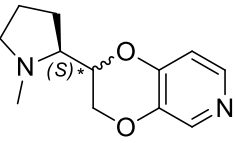
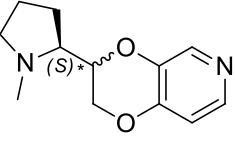
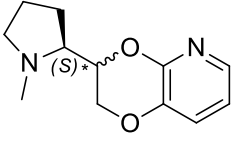
	Compound	$\alpha 4\beta 2$ nAChR [^3H]-Epi (μM)	$\alpha 3\beta 4$ nAChR [^3H]-Epi (μM)
	(S)-Nicotine	0.004	0.261
	(S,R)-IV	0.26 (32) ^a	1.2 (20)
	(S,S)-IV	0.47 (30) ^a	8.2 (25)
	(S,R)-5	0.41 (20)	16.2 (35)
	(S,S)-5	30.4 (34)	22 (22)
	(S,R)-6+(S,S)-6	2.5 (30)	12.3 (37)
	(S,R)-7	1.64 (19)	5.8 (27)
	(S,S)-7	3.6 (16)	8.9 (31)
	(S,R)-8	43 (29)	-
	(S,R)-8	30 (23)	-

Table 2: compounds (S,R)- and (S,S)-5-8, nicotine and (S,R)- and (S,S)-IV: affinity for native $\alpha 4\beta 2$ nAChR, present in rat brain membranes, labelled by [^3H]-epibatidine, and for heterologously expressed

human $\alpha 3\beta 4$ nAChR, labelled by [3 H]-epibatidine and affinity ratios. The numbers in brackets are the % coefficient of variation (CV%).⁷⁵ ^a $\alpha 4\beta 2$ affinity data from literature⁷³.

Particularly, when we compared the moderate affinities of the parent compounds (*S,R*)-**IV** and of its epimer (*S,S*)-**IV** with the modest supramicromolar or high micromolar affinities of their pyridodioxane analogues (*S,S*)-**5**, (*S,R*)-**6**, (*S,S*)-**6**, (*S,R*)-**7**, (*S,S*)-**7**, (*S,R*)-**8** and (*S,S*)-**8** and with the moderate $\alpha 4\beta 2$ affinity of (*S,R*)-**5**, we could conclude that the replacement of an aromatic CH with a nitrogen was invariably deleterious for affinity with the only exception of (*S,R*)-**5**. Quite surprisingly, an opposite trend was normally observed for other nicotinoids, like the pairs nicotine/nornicotine or **A-85453**/*(S)*-**I**, where the nitrogen-containing one had higher affinity, attributed to the presence of a HBA system (*Figure 30*).

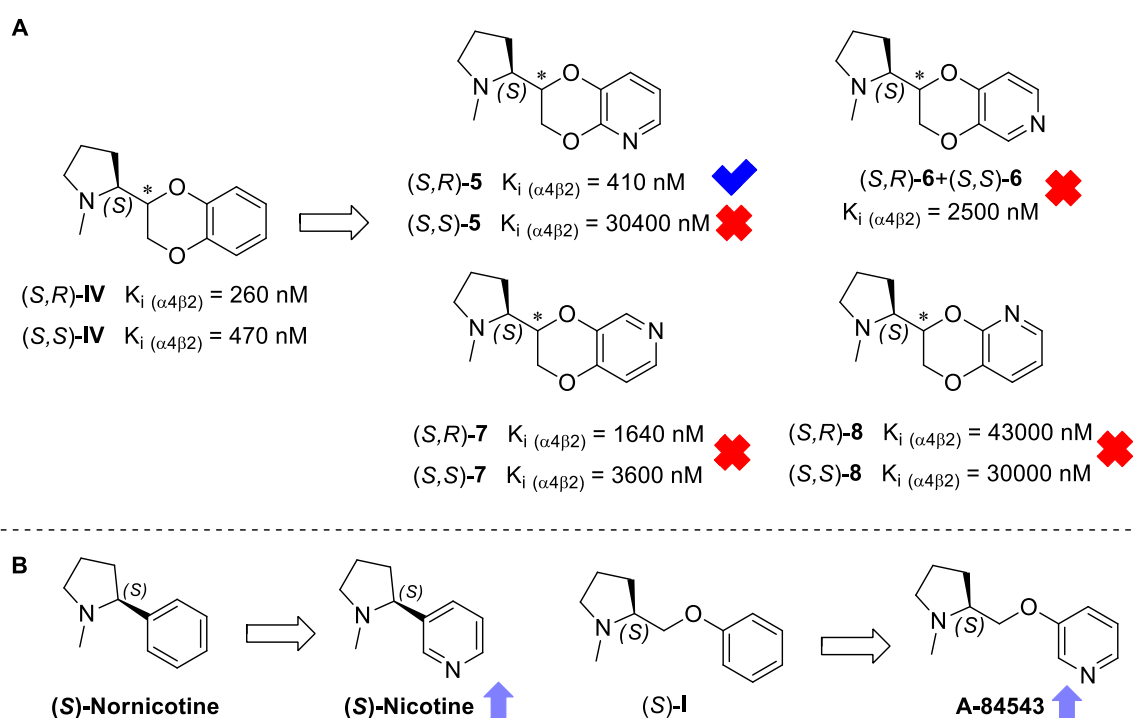


Figure 30: divergent effect of CH → N replacement in A) rigid ligands and B) flexible ligands.

However, this divergent trend in affinity can be explained if we consider the different SARs for flexible and rigid compounds, already reported for the effect of *meta*-hydroxylation of prolinol phenyl ethers and of the 7-hydroxylation of pyrrolidinyl benzodioxanes.

Whereas flexible ligands like **A-84543** and, in a lesser extent, nicotine, can orient their pyridyl ring to place the nitrogen in the appropriate position to interact as an HBA with the binding site, rigid and bulky ligands like N-Me-pyrrolidinyl-pyridodioxanes are conformationally constrained and forcedly place the aromatic nitrogen in regions of the binding site which do not necessarily correspond to the ideal position of the HBA system.

Indeed, if we compare the pairs **A-84543**/*(S)*-**I**, we see that replacement of the pyridine nitrogen with a -CH= results in approximately 300-fold drop of affinity, consistent with a HBA loss. On the other hand, if the nitrogen is repositioned, instead of being replaced with a -CH=, a further drop in affinity is observed, obtaining analogues *(S)*-**X** and *(S)*-**XI** with 10000 or 1000-lower affinities than **A-84543**, indicating a simultaneous loss of the HBA system and a weakening of π - π interactions.

Oppositely, the removal of the aromatic nitrogen of *(S,R)*-**5** to *(S,R)*-**IV** didn't decrease affinity, but slightly increased it, suggesting that the nitrogen, in that position, is not involved in specific interactions beneficial for affinity when compared to *(S,R)*-**IV**. However, its repositioning in the cycle or the inversion at the pyridodioxane stereocenter is detrimental for $\alpha 4\beta 2$ affinity. Together, these evidences, stress the different binding modes and the different roles of the pyridyl nitrogen between flexible and rigid ligands.

In order to determine the effects of *(S,R)*-**5** on $\alpha 4\beta 2$, and $\alpha 3\beta 4$ nAChRs, in vitro, data were collected via whole-cell patch clamp electrophysiology with GH4C1 cell line cells transiently expressing human $\alpha 4\beta 2$ and $\alpha 3\beta 4$ subtypes. Compound *(S,R)*-**5** did not have any activity at the $\alpha 3\beta 4$ subtype, but it was a partial agonist at the $\alpha 4\beta 2$ with an I_{max} of 24.2% of that elicited by 1 mM ACh with an effective concentration (EC_{50}) of 10.1 μM (Figure 31). As term of comparison, *(S,R)*-**IV** was also assayed and, surprisingly, it was found to be a competitive antagonist with similar potencies at either the $\alpha 4\beta 2$ (IC_{50} = 5.36 μM) and the $\alpha 3\beta 4$ (IC_{50} = 2.78 μM) subtypes.

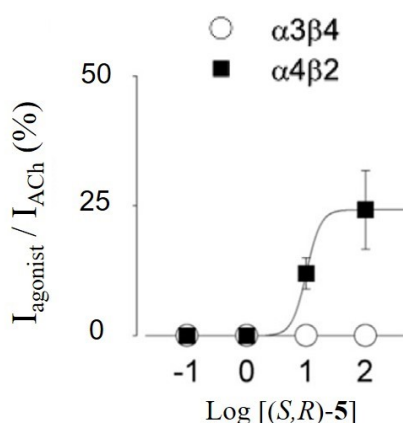


Figure 31: partial agonist activity of *(S,R)*-**5** on transfected human $\alpha 4\beta 2$ and $\alpha 3\beta 4$ subtypes. The activation responses are normalized to the maximal response to 1 mM ACh.

Overall, these findings confirmed our expectations: the four diastereomeric pairs of regioisomeric N-Methyl-pyrrolidiny-pyridodioxanes exhibited very different binding affinities

and selectivities depending on the position of the nitrogen. Only compound (*S,R*)-**5**, where the CH in position 5 of the benzodioxane scaffold was replaced by nitrogen, showed submicromolar affinity and good selectivity. Moreover, the electrophysiological assays highlighted that 5CH in place of N converted the antagonism activity of (*S,R*)-**IV** into a $\alpha 4\beta 2$ selective partial agonist, thus exerting a pivotal role in receptor activation.

This result, together with the $\alpha 4\beta 2$ partial selective agonism of (*S,R*)-**IVa** (retested 29%), suggested that the naked and rigid antagonist (*S,R*)-**IV** can be turned into a selective partial agonist by decorating it with an OH group at the 7 position or by replacing the CH in position 5 with a nitrogen.

1.7 Synthesis of N-Methyl-pyrrolidinyl-5-substituted-benzodioxanes

1.7.1 Introduction and aim

As detailed in chapter 1.3, substitution at position 7 of the benzodioxane moiety of **IV** with a small and polar hydroxyl group lead to great enhancement of $\alpha 4\beta 2$ affinity and $\alpha 4\beta 2$ vs $\alpha 3\beta 4$ functional selectivity in (S,R) -**IVa**. On the other hand, replacement of CH at position 7 with N resulting in the pyridodioxane (S,R) -**7** markedly reduced affinity, whereas CH replacement at position 5 with N provided a ligand, (S,R) -**5**, with similar affinity to the benzodioxane parental compound and with high $\alpha 4\beta 2$ vs $\alpha 3\beta 4$ selectivity.

These results prompted us to investigate the effect of the substitution at position 5 of the benzodioxane scaffold of **IV**. Therefore we synthesized the N-methyl-pyrrolidinyl 5-substituted benzodioxanes (S,R) - and (S,S) -**9a-d**, which we expected to have interesting biological profiles as those of **5** (Figure 32)

Moreover, compounds **9a-d** were compared to the correspondent 7-substituted analogues **IVa**, **10**, **11** and **IVd**. Compounds **10** and **11** were synthesized and characterized previously (unpublished data). Nitro-substituted (S,R) -**10** and (S,S) -**10** had modest micromolar affinities at the $\alpha 4\beta 2$ subtype, while, in line with our previous findings, the introduction of a relatively small and polar amino substituent provided (S,R) -**11**, with 27 nM affinity at the $\alpha 4\beta 2$ subtype and (S,S) -**11**, with 144 nM affinity. However, differently from (S,R) -**IVa**, (S,R) -**11** was not selective versus the $\alpha 3\beta 4$ subtype.

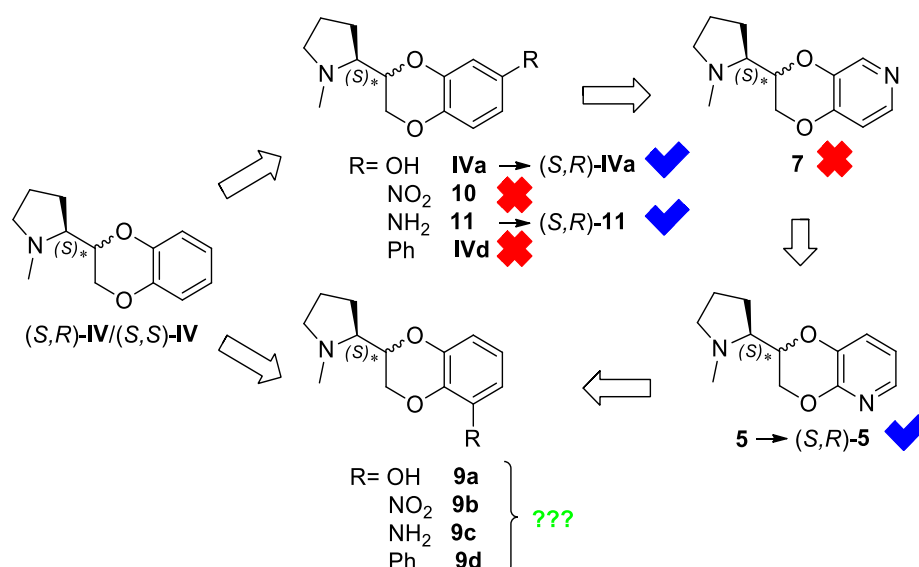
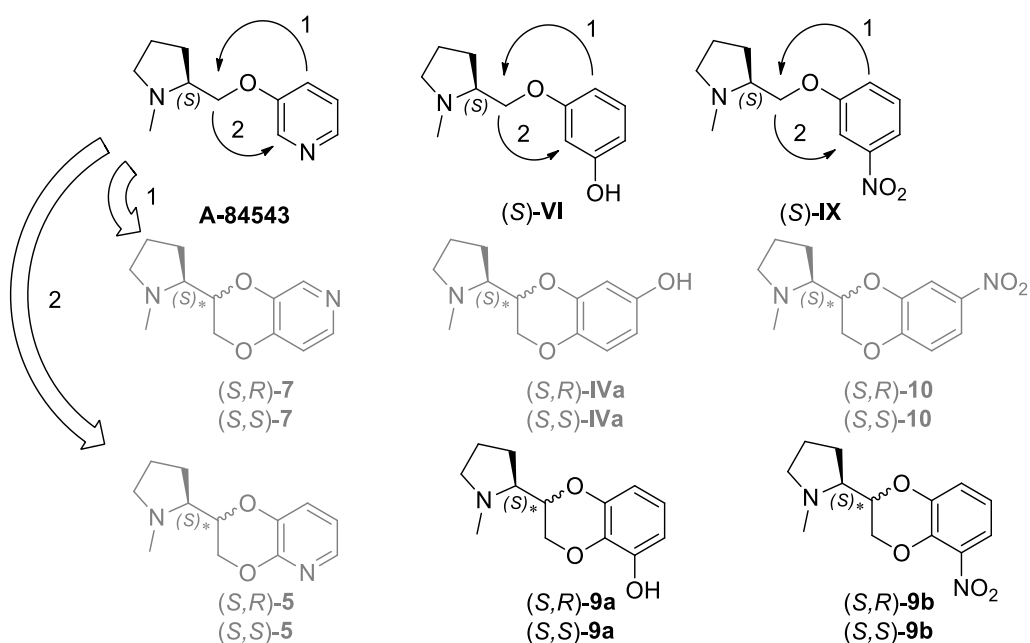


Figure 32: design of 5-substituted benzodioxanes (S,R) - and (S,S) -**9a-d** as analogues of **IV** and **5**

Compounds **5**, **9a** and **9b** could also be considered as the result of conformational constriction of the flexible bioisosteric ligands **A-84543**, (*S*)-**VI** and (*S*)-**IX**.⁷⁷ Ideally, the rigidification of such flexible compounds respectively into a pyridodioxane or into a substituted benzodioxane moiety, could result into two series of correspondent regioisomers in both diastereomeric pairs depending on where the nitrogen or the substituent was constrained. As illustrated in *Figure 33*, the first approach constrained the substituent or the nitrogen in position 7 affording compounds **7**, **IVa** and **10**, while the second approach blocked it in position 5, providing compounds **5**, **9a** and **9b**.



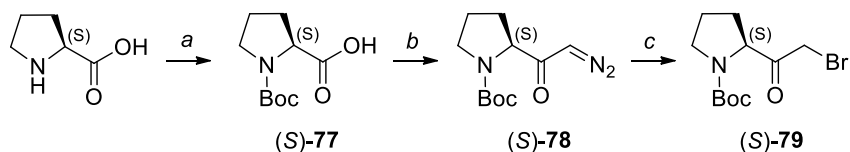
*Figure 33: design of 5-substituted benzodioxanes (*S,R*)- and (*S,S*)-**9a,b** as constrained analogues of (*S*)-**VI** and of (*S*)-**IX**.*

Since we already demonstrated similar binding modes for the *meta*-pyridyl, the *meta*-hydroxyphenyl and *meta*-nitrophenyl ethers of *N*-methyl-prolinol parental compounds,⁷⁷ we also aimed at understanding whether the same rationales could be applied to their conformational constrained analogues with a pyridodioxane or substituted benzodioxane moiety.

1.7.2 Synthetic schemes

A key intermediate for the synthesis of compounds (*S,S*)- and (*S,R*)-**9a-d** was (*S*)-*N*-Boc-2-bromoacetylpyrrolidine (*S*)-**79**. The commercially available (*S*)-Proline was *N*-protected by treatment with Boc₂O providing (*S*)-**77**. The carboxylic group of (*S*)-**77** was activated as a mixed anhydride with isobutylchloroformate and converted to the correspondent diazoketone

(*S*)-**78** by treatment with diazomethane that was further reacted with aqueous HBr to obtain the α -bromoketone (*S*)-**79** (Scheme 10).

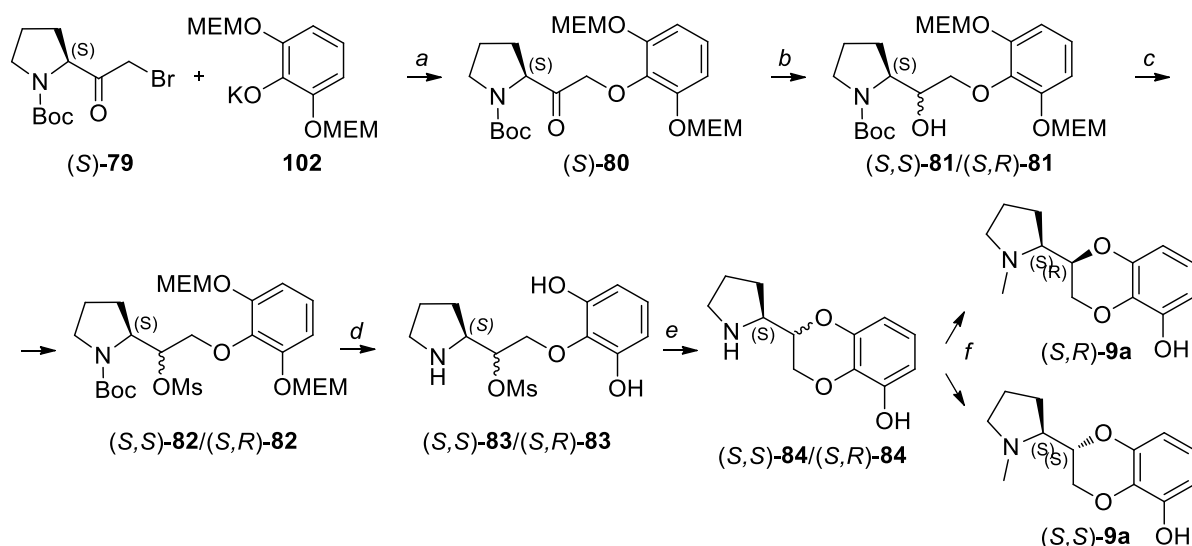


Scheme 10: Reagents and conditions. (a) NaOH, Boc₂O, rt, 5 h, 95%; (b) TEA, *i*-BuOCOCl, Et₂O, -15°C, 1h. CH₂N₂, 0 °C and then overnight at 25 °C, 78%; (c) HBr/H₂O, Et₂O, 25°C, 1h, 71%.

The core reaction of all the synthetic routes described below was the nucleophilic displacement of the bromine of the bromoketone (*S*)-**79** with the potassium salt of an appropriate substituted phenol, exemplified by potassium 2,6-bis((2-methoxyethoxy)methoxy)phenolate **102** for the synthesis of (*S*)-**80**, an intermediate of the synthetic scheme to afford (*S,R*)- and (*S,S*)-**9a**.

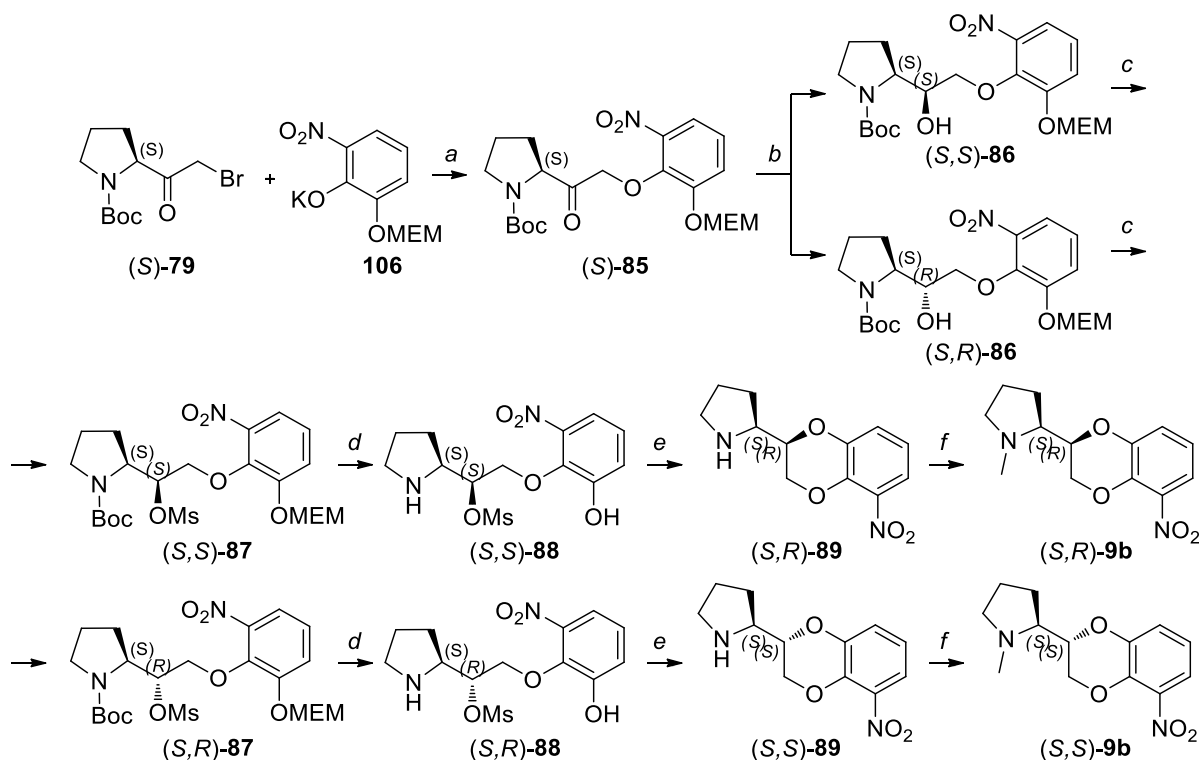
The stereochemistry of this reaction, and of the corresponding reactions in the following schemes, was investigated through chiral HPLC, because the acidity of the methinic hydrogen could drive racemization of the chiral center through an enolization process, depending on the reaction conditions. Therefore, we developed chiral HPLC methods to evaluate the enantiomeric excesses of the coupled ketones, and we identified the most convenient reaction conditions to avoid racemization for each intermediate. To assess enantiomeric excesses, the syntheses of both the enantiomeric forms of the ketone intermediates were necessary. The *R* enantiomers of each coupled ketone were obtained following the same reaction schemes used to synthesize the *S* enantiomers, but starting from (*R*)-proline instead of (*S*)-proline.

Compounds (*S,S*)- and (*S,R*)-**9a** were obtained starting from the nucleophilic substitution between the bromo ketone (*S*)-**79** and potassium 2,6-bis((2-methoxyethoxy)methoxy)phenolate **102** in acetone overnight at room temperature, which provided intermediate (*S*)-**77**. The ketone functionality was reduced with NaBH₄ to provide a diastereomeric mixture of (*S,S*)-**81**/*(S,R)*-**81**, which couldn't be separated by flash chromatography due to too similar retention times in all the eluents tested. The mixture was treated with methansulphonylchloride and TEA, providing (*S,S*)-**82**/*(S,R)*-**82**, whose Boc- and MEM- protecting groups were removed by treatment with HCl affording (*S,S*)-**83**/*(S,R)*-**83**. The intermediates were cyclized by treatment with K₂CO₃ in DME/DMF, to give the benzodioxanes (*S,S*)-**84**/*(S,R)*-**84**, which were methylated to the final compounds (*S,S*)-**9a**/*(S,R)*-**9a** with formaldehyde and picoline borane. Upon chromatography separation, the single diastereomers (*S,S*)-**9a** and (*S,R*)-**9a** were obtained (Scheme 11).



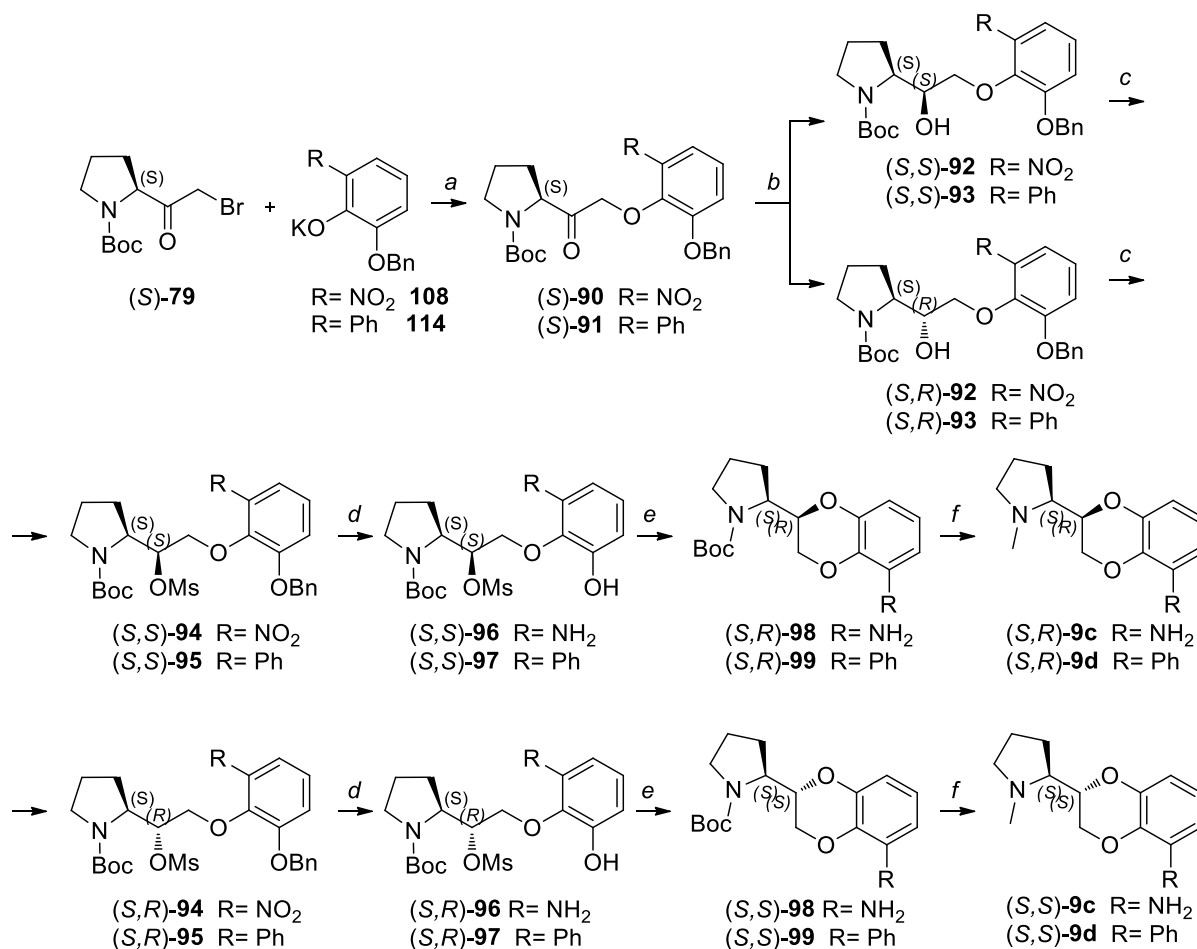
Scheme 11: Reagents and conditions. (a) Acetone, rt, overnight, 77%; (b) NaBH₄, THF anidro, rt, 3h, 97%; (c) DCM, TEA, MsCl, rt, 2h, 54%; (d) HCl/MeOH (1.25 M), rt, 2h, 99%; (e) K₂CO₃, DME, DMF, reflux, 3h, 25%; (f) MeOH, CH₃COOH, HCOH/H₂O 37%, pic-BH₃, rt, 3h, HCl/H₂O (1M), 30 min and then purification through flash chromatography, 46% (S,S) -9a, 36% (S,R) -9a.

Compounds (S,S) - and (S,R) -9b were obtained starting from the nucleophilic substitution between the bromo ketone (S) -79 and potassium 2-((2-methoxyethoxy)-methoxy)-6-nitrophenolate 106 in acetone overnight at room temperature, which provided intermediate (S) -85. The ketone functionality was reduced with NaBH₄, providing a mixture of diastereomers which were separated by chromatography in the single diastereomers (S,S) -86 and (S,R) -86. The secondary hydroxyl groups were mesylated with methansulphonyl chloride and TEA to give (S,S) -87 and (S,R) -87 which were in turn deprotected with HCl to (S,S) -88 and (S,R) -88, cyclized to (S,S) -89 and (S,R) -89 in K₂CO₃ and DME and then methylated to the final compounds (S,S) -9b and (S,R) -9b with formaldehyde and picoline-borane (*Scheme 12*).



Scheme 12: Reagents and conditions. (a) Acetone, 25 °C, overnight, 42%; (b) NaBH₄, THF, 25 °C, 3 h, 80% and then purification through flash chromatography 72% ((S,S)-86) and 28% ((S,R)-28); (c) TEA, MsCl, DCM, 25 °C, 1h, 58% ((S,S)-87), 66% ((S,R)-87); (d) HCl/dioxane 4M, MeOH, 25 °C, 2h; (e) K₂CO₃, DME, reflux, 5h, 87% (S,R)-89; 80% ((S,S)-89); (f) CH₂O, Pic-BH₃, AcOH, MeOH, 25 °C, 3h, 25% ((S,R)-9b) and 81% ((S,S)-9b).

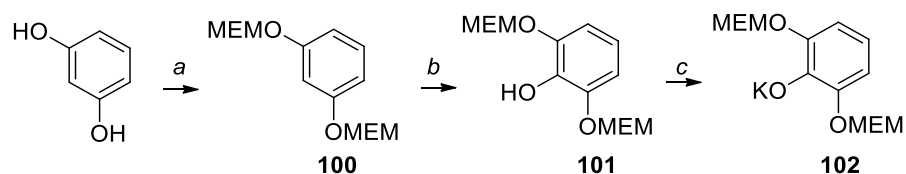
Compounds (S,S)- and (S,R)-9c,d were synthesized according to a similar synthetic scheme, starting from nucleophilic substitution in acetone at room temperature overnight between (S)-79 and potassium 2-benzyloxy-6-nitrophenolate 93 for the synthesis of 9c, or potassium 2-benzyloxy-6-phenylphenolate 114 for 9d. The ketone functionalities of the resulting intermediates, respectively (S)-90 and (S)-91 were reduced with NaBH₄, providing a mixture of diastereomers which were separated by chromatography in the single diastereomers, respectively the pair (S,S)-92 and (S,R)-92 and the pair (S,S)-93 and (S,R)-93. The secondary hydroxyl groups were mesylated with methanesulphonyl chloride and TEA to give the pair (S,S)-94 and (S,R)-94 and the pair (S,S)-95 and (S,R)-95, which were in turn hydrogenated under catalytic conditions. In these conditions debenzylation occurred in both cases, but the nitro groups of intermediates 94 were reduced to amino groups. Overall, hydrogenation of (S,S)-94 and (S,R)-94 provided (S,S)-96 and (S,R)-96, while debenzylation of (S,S)-95 and (S,R)-95 afforded (S,S)-97 and (S,R)-97. Upon cyclization with K₂CO₃ in DME to give (S,S)- and (S,R)-98 and (S,S)- and (S,R)-99, the final compounds (S,R)- and (S,S)-9c, and (S,R)- and (S,S)-9d, respectively 5-amino and 5-phenyl substituted benzodioxanes were obtained by reduction of the N-carbamate with LiAlH₄ (Scheme 13).



Scheme 13: Reagents and conditions. (a) Acetone, 25 °C, overnight, 81% ((S)-90), 1.5 h, 30%, ((S)-91); (b) NaBH₄, THF, 25 °C, 3 h, 75% and then purification through flash chromatography, 26% ((S,S)-92) and 74% ((S,R)-92), -10 °C, 2 h, 80% and then purification through flash chromatography, 62% ((S,R)-93) and 24% ((S,S)-93); (c) TEA, Ms-Cl, DCM, 25 °C, 2h, 86% ((S,S)-94), 59% ((S,R)-94), 42% ((S,R)-94) and 46% ((S,S)-94); (d) H₂, Pd/C 5%, MeOH, 25 °C, 6h, 73% ((S,S)-96), 82% ((S,R)-96), 48 h, 77% ((S,R)-97) and 91% ((S,S)-97); (e) K₂CO₃, DME, reflux, 7h, 78% ((S,R)-98), 84% ((S,S)-98), 5h, 49% ((S,S)-99) and 34% ((S,R)-99); (f) LiAlH₄, THF dry, reflux, 4h, 100% ((S,R)-9c), 83% ((S,S)-9c), 39% ((S,S)-9d) and 85% ((S,R)-9d).

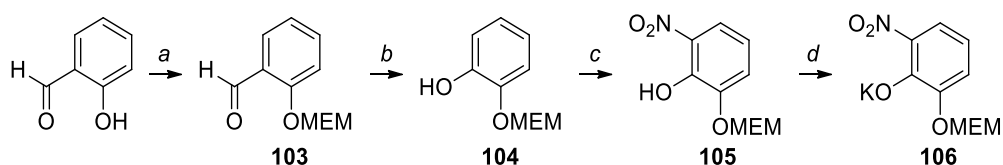
Absolute configuration of the pyrrolidine stereocenter was *S* in all the final compounds, while the absolute configuration of the benzodioxane stereocenter was assigned to the single diastereomers of the final compounds and then retrospectively assigned to their precursors, as described in paragraph 1.5.2.

Potassium 2,6-bis((2-methoxyethoxy)methoxy)phenolate **102** was synthesized starting from resorcinol, which was protected at its phenolic groups by treatment with MEM-Cl and TEA, obtaining **100**. The latter was lithiated by DOM by treatment with *n*-BuLi and oxidized with Oxone®, affording **101**, which was converted into its potassium salt by treatment with KOH in methanol (*Scheme 14*).



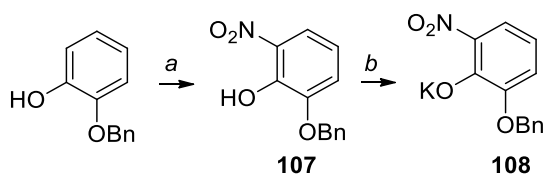
*Scheme 14: Reagents and conditions. (a) MEM-Cl, DIPEA, DCM, rt, overnight, 46%; (b) THF dry, *n*-BuLi, 1h, B(OMe)₃, 30 min, NaHCO₃ 20% in aqueous acetone, Oxone®, 5 min, NaHSO₃, 65%; (c) KOH/MeOH (1M), rt, 15 min, 95%.*

Potassium 2-((2-methoxyethoxy)-methoxy)-6-nitrophenolate **106** was synthesized reacting the commercially available 2-hydroxybenzaldehyde with MEM-Cl and N,N-diisopropylamine, obtaining the intermediate **103**, which was converted into its correspondent phenolic analogue **104** through a Baeyer-Villiger reaction with mCPBA followed by hydrolysis. Nitration at its *o*-position by treatment with CeNH₄(NO₃)₂ in ACN followed by chromatography purification afforded the phenol **105**, that was converted into its correspondent potassium salt **106** by treatment with KOH 1M in methanol (*Scheme 15*).



Scheme 15: reagents and conditions. (a) DIPEA, MEM-Cl, DCM, 25 °C, overnight, 87%; (b) mCPBA, DCM, 25 °C, 48 h and then KOH 2M, MeOH, 25 °C, 5h, 56%; (c) CAN, acetonitrile, 10 °C, 3h, 40%; (d) KOH 1M, MeOH, 25 °C, 15 min, 100%.

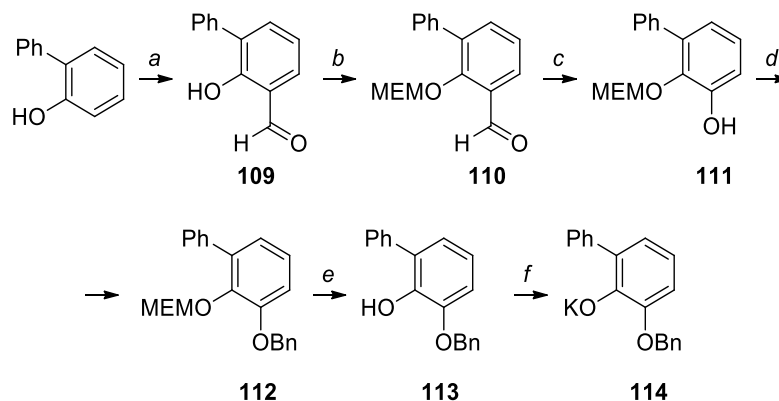
Potassium 2-benzyloxy-6-nitrophenolate **108** was obtained from commercial 2-benzyloxyphenol, that was nitrated with CAN to **107** that, after chromatography purification, was converted into its correspondent potassium phenate **108** (*Scheme 16*).



Scheme 16: reagents and conditions. (a) CAN, acetonitrile, 10 °C, 3h, 58%; (d) KOH 1M, MeOH, 25 °C, 15 min, 92%.

Potassium 2-benzyloxy-6-phenylphenolate **114** was obtained starting from commercial 2-phenylphenol, that was carbonylated to compound **109** with paraformaldehyde, MgCl₂ and TEA. The phenolic function was protected by treatment with MEM-Cl, providing intermediate **110**, that was converted in compound **111** by Baeyer Villiger reaction with *m*-MCPA followed by hydrolysis in basic conditions. The free phenolic function was benzylated with benzyl

bromide in intermediate **112**, that was deprotected in acidic conditions to **113**. The potassium salt **114** was obtained by treatment with KOH in methanol (*Scheme 17*).



Scheme 17: reagents and conditions. (a) MgCl₂, TEA, dry THF, paraformaldehyde, reflux, 3 h, 88%; (b) NaH, dry THF, MEM-Cl, rt, overnight, 71%; (c) m-CPBA, EtOAc, 72 h and then MeOH, NaOH 2.5M, 2h, rt, 73%; (d) K₂CO₃, DMF, BnBr, 50 °C, 1.5 h, 78%; (e) HCl 37%, MeOH, 60 °C, 1 h, 96%; (f) MeOH, KOH 1M, 30 mins, rt, 91%.

1.7.3 Biology

Binding assays were performed on compounds (*S,R*)- and (*S,S*)-**9a-d** as described in paragraph 1.6.3 and the results are reported in *Table 3*, together with those of compounds (*S,S*)- and (*S,R*)-**IV** reported as reference.

Electrophysiological functional activity was assessed for (*S,S*)-**9c** according to the methods previously described, and it was compared with the electrophysiological activities of (*S,R*)-**IV**, (*S,R*)-**IVa** and (*S,R*)-**5**.

1.7.4 Results and discussion

Among the series of 7-substituted benzodioxanes, the (*S,R*)- diastereomers of compounds with a HBA/HBD group such as a hydroxyl or an amine, namely (*S,R*)-**IVa** and (*S,R*)-**11**, had the highest affinities at the $\alpha 4\beta 2$ subtype (respectively 12 and 27 nM). Differently, nitro-substituted benzodioxanes (*S,R*)-**10** and (*S,S*)-**10** and phenyl-substituted benzodioxanes (*S,R*)-**IVb** and (*S,S*)-**IVb** had modest micromolar affinities.

As the 5-substituted benzodioxanes could be formally considered as analogues of the moderate affinitive $\alpha 4\beta 2$ ligand (*S,R*)-**5**, we expected them to have similar biological profiles to that of (*S,R*)-**5**.

As shown in *Table 3*, the introduction of relatively small substituents at position 5 of the benzodioxane scaffold did not have great impact on binding affinity at the $\alpha 4\beta 2$ subtype when compared to the unsubstituted benzodioxane (*S,R*)-**IV**. In fact, compounds (*S,R*)-**9a**, (*S,S*)-**9b**

and (*S,S*)-**9c** had K_i values respectively of 549 nM, 335 nM and 131 nM, similar to those of (*S,R*)- and (*S,S*)-**IV**. Also the introduction of a bulkier phenyl group in (*S,R*)-**9d** was tolerated, although with a slightly higher K_i value.

Interestingly, we observed an inverse stereospecificity of binding between 7-substituted and 5-substituted benzodioxanes: (*S,R*)-configuration was required to achieve high affinity in the 7-substituted benzodioxanes (*S,R*)-**IVa** and (*S,R*)-**11**, while (*S,S*)- configuration was needed for the 5-substituted benzodioxanes exhibiting the highest affinities, namely those bearing NO_2 (**9b**) and NH_2 (**9c**).

Even though this divergent trend couldn't be easily explained by classical SAR, we speculated that the combination of the absolute stereochemistry and of the positioning of the substituents could result in a 3D conformation that oriented the ligands to place similar functional groups in the same region of the binding site (see chapter 1.8).

When (*S,R*)-**IVa** was first reported, our group attributed its enhanced $\alpha 4\beta 2$ affinity and its $\alpha 4\beta 2$ vs $\alpha 3\beta 4$ selectivity to some additional interactions between its hydroxyl group and a small, hydrophilic and non-conserved binding pocket located in the $\beta 2$ subunit.⁷⁴ In line with it, the amino analogue (*S,R*)-**11**, that could in principle interact with the same region, had high affinity $\alpha 4\beta 2$, but was found to be non-selective, making the interpretation of the binding data even more complicated. Instead, compounds (*S,S*)-**9b,c** were $\alpha 4\beta 2$ vs $\alpha 3\beta 4$ selective, achieving 100 fold selectivity for (*S,S*)-**9c**.

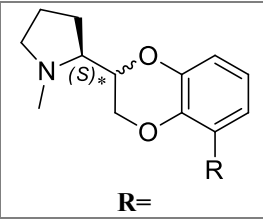
 R=	Compound	$\alpha 4\beta 2$ nAChR [^3H]-Epi (μM)	$\alpha 3\beta 4$ nAChR [^3H]-Epi (μM)	Selectivity Ki $\alpha 3\beta 4/\alpha 4\beta 2$
H	(<i>S,R</i>)-IV	260 ^a	1200 ^a	4.6
H	(<i>S,S</i>)-IV	470 ^a	8200 ^a	17.4
OH	(<i>S,R</i>)-9a	549	3900	7.1
OH	(<i>S,S</i>)-9a	1710	100000	58
NO₂	(<i>S,R</i>)-9b	12200	1080	0.09
NO₂	(<i>S,S</i>)-9b	335	6700	20
NH₂	(<i>S,R</i>)-9c	7100	3900	0.55
NH₂	(<i>S,S</i>)-9c	131	13000	99
Ph	(<i>S,R</i>)-9d	636	2660	4.18
Ph	(<i>S,S</i>)-9d	7300	5280	0.72

Table 3: compounds (*S,R*)- and (*S,S*)-**9a-d**, compared with (*S,R*)- and (*S,S*)-**IV**⁷⁴: affinity for native $\alpha 4\beta 2$ nAChR, present in rat brain membranes, labelled by [^3H]-epibatidine, and for heterologously expressed human $\alpha 3\beta 4$ nAChR, labelled by [^3H]-epibatidine and affinity ratios. ^aBinding affinity data from literature.^{73,89}

When the naked benzodioxane moiety of (*S,R*)-**IV** was decorated with a small and hydrophilic substituent, such as hydroxyl or amino group, the affinity increased or, at least, it was not significantly decreased regardless its 5- or 7 positioning, but depending on the absolute configuration at the chiral center.

These results also suggested divergent structural requirements for 5- and 7- substituted benzodioxanes, proving that the bioisosteric relationship between flexible *meta*-hydroxyphenyl, *meta*-nitrophenyl and *meta*-pyridyl ethers is not preserved into their products of rigidification.

Compound (*S,S*)-**9c** was assayed for its electrophysiological activity at the $\alpha 4\beta 2$ and at the $\alpha 3\beta 4$ subtype and it was found to be an $\alpha 4\beta 2$ partial agonist with a bimodal dose-response curve, that could only be interpreted as the combination of different activities at the two stoichiometries of the $\alpha 4\beta 2$ subtype (Figure 34). Particularly, the lower EC₅₀ was calculated to be 4.98 nM with

a maximal response of 20%, while the higher EC₅₀ was 8.7 μM with a maximal response of 60%. From the curve we observed that, overall, when (S,S)-**9c** was administered at a concentration of 100 μM, it elicited a total current equal to 60% of that evoked by acetylcholine at 1 mM.

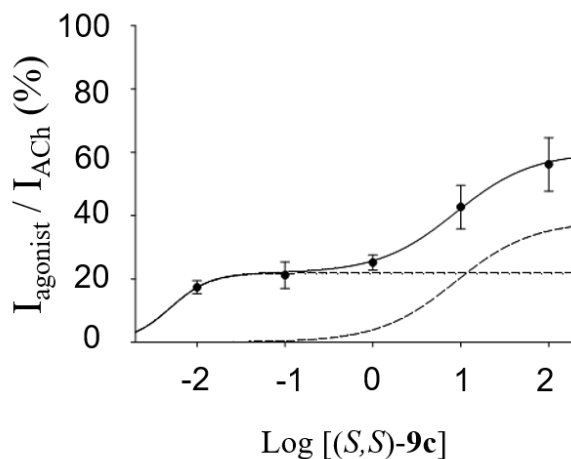


Figure 34: partial agonist activity of (S,S)-**9c** on transfected human $\alpha 4\beta 2$ subtypes. The activation responses are normalized to the maximal response to 1 mM ACh. Data can be only fitted as the sum of two sigmoidal dose-response curves, suggesting two different activities at the two $\alpha 4\beta 2$ stoichiometries.

When compared with the partial agonist (S,R)-**IVa**, the ligand with highest affinity in the series, and with the pyridodioxane (S,R)-**5**, (S,S)-**9c** was found to be the most efficacious at the $\alpha 4\beta 2$, with a maximal response (60%) almost twice the efficacy of (S,R)-**IVa** (29%) and of (S,R)-**5** (24.1%). Even though a direct comparison between the two potencies couldn't be drawn due to the bimodal sigmoidal curve of (S,S)-**9c**, the administration of even low concentrations of (S,S)-**9c** (such as 100 nM) elicited approximately 20% of the total current, because the first curve has already reached the plateau due to its extremely high potency of 4.9 nM at one stoichiometry. Differently, the same concentration of (S,R)-**IVa** or of (S,R)-**5** evoked respectively only 7% and 0% of the maximal response induced by ACh 1 mM, because of their lower potency of 0.3 μM for (S,R)-**IVa**, and of 10.1 μM for (S,R)-**5** (Figure 35).

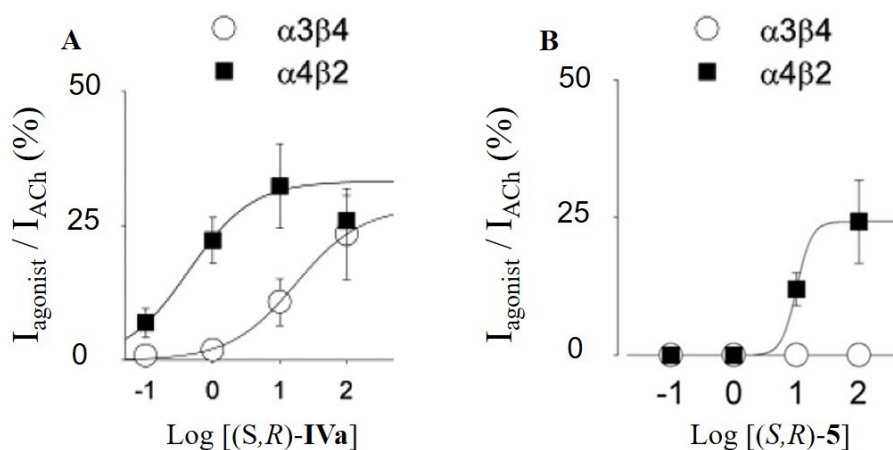


Figure 35: partial agonist activities of (S,R)-IVa and (S,R)-5 on transfected human $\alpha 4\beta 2$ and $\alpha 3\beta 4$ subtypes. The activation responses are normalized to the maximal response to 1 mM of ACh.

Furthermore, (S,R)-9c was found to be a very weak antagonist of the $\alpha 3\beta 4$ subtype, with an IC_{50} of 54.6 μM , thus having a very high $\alpha 4\beta 2/\alpha 3\beta 4$ selectivity, much higher than that of (S,R)-IVa.

Since binding and functional data alone could not fully explain the SARs of these constrained nicotinoids, we applied some computational tools to support their interpretation, which will be discussed in the following chapter.

1.8 Computer-aided SAR interpretation

1.8.1 Introduction and aim

The complexity of the SARs of our constrained nicotinoids, together with the high number of pharmacological data, prompted us to use a 3D model of the target to understand structural details of the binding modes and of the interactions between the $\alpha 4\beta 2$ receptor and the rigid N-methyl-pyrrolidinyl- benzodioxanes, -pyridodioxanes and substituted -benzodioxanes.

Aiming at unrevealing the key elements that drive binding and to obtain some hints about $\alpha 4\beta 2/\alpha 3\beta 4$ selectivity and functional activity, we performed docking studies of our ligands in an adapted binding site of the high affinity $\alpha 4\beta 2$ nAChR subtype.

1.8.2 Computational methods

As described in paragraph 1.1.1, in 2016 a full-length X-Ray 3D model of the $\alpha 4\beta 2$ subtype in the stoichiometry $2\alpha:3\beta$ stoichiometry was reported with a resolution of 3.9 Å.²⁰

Unfortunately, when in 2018 the cryoEM models of the two stoichiometries of $\alpha 4\beta 2$ were reported, our modelling studies had already been completed on the basis of the X-Ray structure.¹⁹ However, a punctual comparison showed that the X-Ray (5KXI) and the CryoEM (6CNJ) structures were very similar. To confirm the findings hereby reported, based on the X-Ray structure, we performed a preliminary docking study on the binding site derived from the CryoEM model, obtaining comparable results.

Ligand preparation

Both (*S,R*)- and (*S,S*)- diastereomers of compounds **IV**, **IVa**, **10**, **11**, **IVd**, **5**, **7**, and **9a-d** were built with the 2D sketch editor of Maestro (Schrödinger Release 2017-3: Schrodinger, LCC, New York, NY, 2017) and assigned ionization state with LigPrep (Schrödinger Release 2017-3: Schrodinger, LCC, New York, NY, 2017) using default settings.

Protein preparation

The ligand binding domain of the $\alpha 4\beta 2$ was refined starting from the X-Ray structure of the full-length $\alpha 4\beta 2$ receptor (5KXI). The pdb structure and the electron density maps of 5KXI were retrieved from the online database RSCB and the ligand binding domain was carefully inspected with Maestro. The $\alpha 4\beta 2$ dimer, containing nicotine in the binding site, at the interface between the two subunits, was extracted from 5KXI and preprocessed, optimized and minimized with the Protein Preparation Wizard with default settings (Schrödinger Release 2017-3: Schrodinger, LCC, New York, NY, 2017).

Although the presence of a water molecule in the $\alpha 4\beta 2$ binding site has been observed in X-Ray crystal structures of AChBPs, neither the X-Ray structure of 5KXI nor the cryoEM structure of 6CNJ showed it, probably due to too low resolution. Therefore, the water-containing X-Ray structure of the homologous AChBP from *Lymnaea Stagnalis* (1UW6) was superimposed to the $\alpha 4\beta 2$ structure.⁹⁰ Its water molecule was extracted from the AChBP binding site and merged with one duplicate of the prepared $\alpha 4\beta 2$ dimer. The resulting water-containing dimer was preprocessed with the Protein Preparation Wizard with default settings.

Overall, two models of binding pocket were obtained: a water-free model and a water-containing model.

Binding pocket analysis and docking

Binding pockets analyses were performed using Sitemap (Schrödinger Release 2017-3: Schrodinger, LCC, New York, NY, 2017) centered on the ligand, with default settings.

Next, the bulkiest compound with highest $\alpha 4\beta 2$ affinity of the series, namely *(S,R)*-**IVa**, was docked in the water-free binding site using the Induced Fit Protocol (Schrödinger Release 2017-3: Schrodinger, LCC, New York, NY, 2017) to adapt the receptor binding pocket to the shape and size of our rigid nicotinoids. The docking center was defined by the present ligand (nicotine), scaling was set to 0.8 to avoid profound deformation of the binding site, rescoring was performed with Glide-XP (Schrödinger Release 2017-3: Schrodinger, LCC, New York, NY, 2017) and otherwise default settings were used.

The complex $\alpha 4\beta 2$ /*(S,R)*-**IVa** with the highest Glide XP Score was selected as adapted complex and all the prepared compounds were docked within the binding site with Glide XP with the grid centered on the ligand and otherwise using default settings.

The same compounds were also docked in the binding site of the water-containing model with GlideXP and otherwise using default settings.

1.8.3 Results and discussion

Binding pocket analysis of the X-Ray crystal structure 5KXI confirmed that probably a water molecule is included in the binding pocket but is not visible in the X-Ray structure due to low resolution. If the water molecule contained in the correspondent 3D position of the homologous *Lymnaea Stagnalis* AChBP (*Ls*-AChBP) 1UW6 is incorporated in the $\alpha 4\beta 2$ binding site, it seems to play a pivotal role in binding: it bridges the pyridine nitrogen of nicotine with a small

hydrophilic pocket of the minus $\beta 2$ side, hydrogen-bonding the -NH backbone of Leu 121, the -CO backbone of Asn 109 and the hydroxylated side chain of Ser 108.

The role of two of these amino acids was investigated in 2010 by Dougherty et al., who proved through mutational studies that a water molecule bridges the pyridine nitrogen to the backbone amidic -NH of Leu 121 in the $\beta 2$ subunit ($\beta 2L119$ according to Dougherty's numbering) with an H-bond in the $\alpha 4\beta 2$ subtype.⁹¹ The role of the carbonyl of amino acid Asn 109 ($\beta 2N109$ according to Dougherty's numbering) couldn't be elucidated due to technical reasons. The third amino acid, Ser 108, was not considered by the authors in the mutational study because in the AChBPs sequences (the most similar proteins to the $\alpha 4\beta 2$ receptor available at that time) it was formally replaced by a glutamine and in the AChBP X-Ray structure the orientation of the entire loop was bent by a proline residue that immediately precedes glutamine (*Figure 36*).

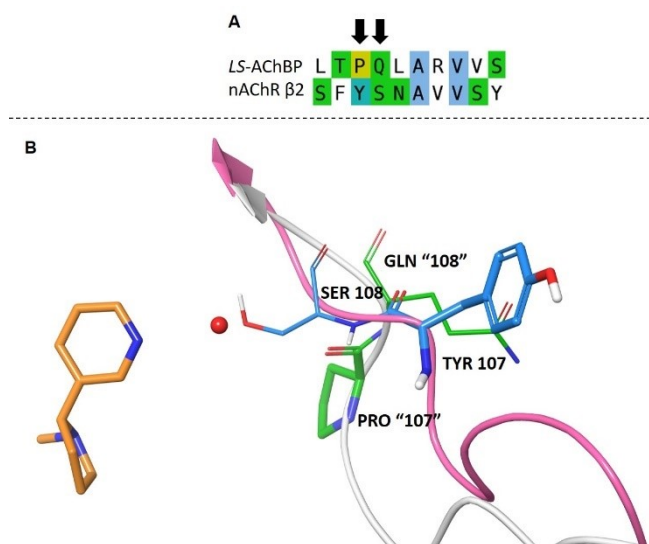
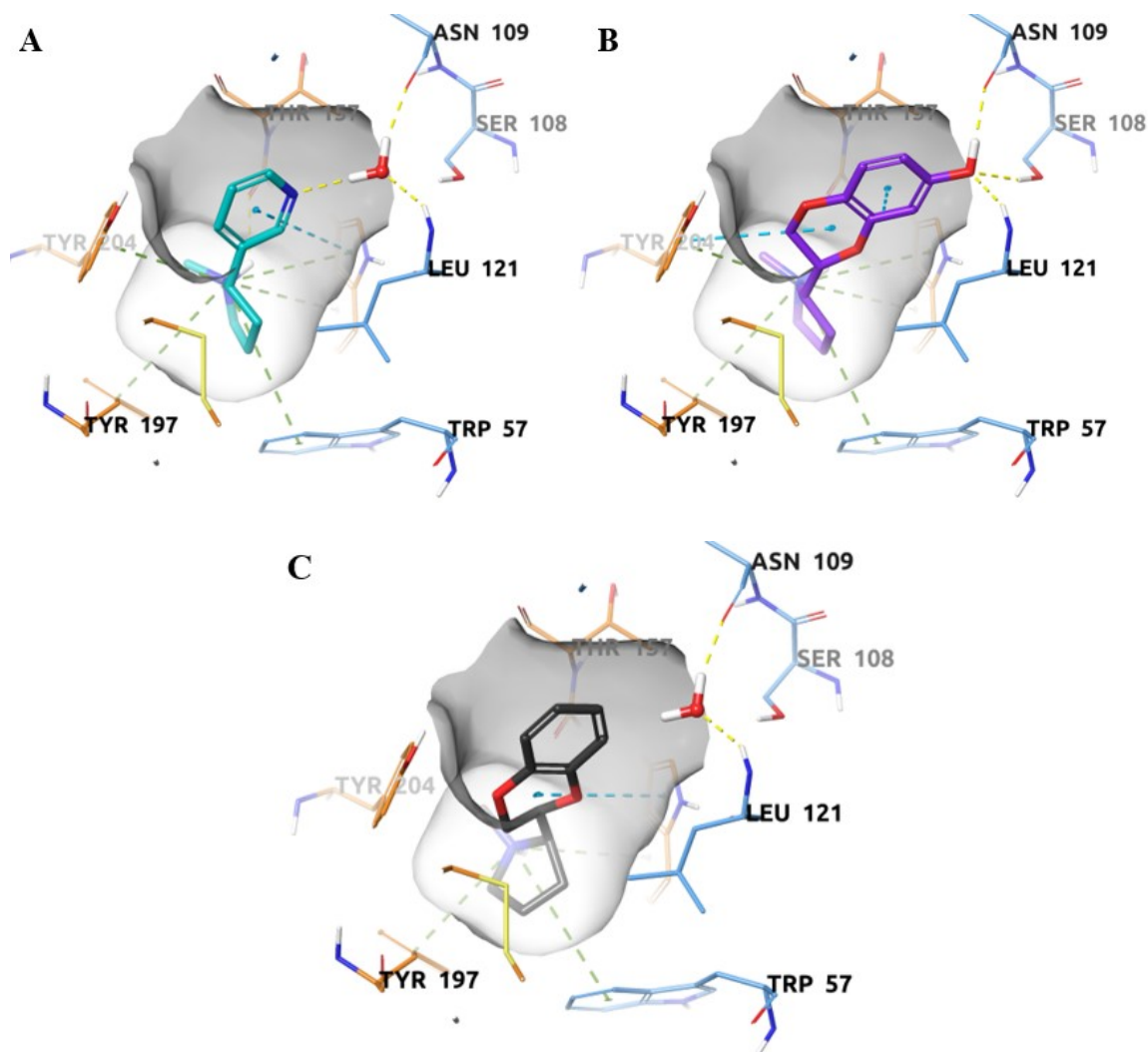


Figure 36: A) extract of the sequence alignment between Ls-AChBP and nAChR $\beta 2$; major differences are indicated by black arrows (Pro "107" vs Tyr107 and Gln "108" vs Ser108). B) 3D alignment between the loop of interest of Ls-AChBP and nAChR $\beta 2$. In Ls-AChBP, Pro 107 bends the entire loop and moves Gln 108 out from the binding site. In the $\beta 2$ subunit, Pro 107 is replaced by Tyr 107, that does not twist the loop and orients the side chain of the Ser 108 toward a water molecule in the binding site.

When (*S,R*)-**IVa** was docked within the water-free $\alpha 4\beta 2$ binding pocket to adapt it to the size and shape of our ligands, it assumed a conformation that maintained all the principal interactions of nicotine and surprisingly placed its hydroxyl group in the same small hydrophilic pocket mentioned just above. Indeed, if we compare the binding poses of (*S,R*)-**IVa** in the water-free receptor and nicotine in the water-adapted receptor, we observe a perfect overlay between the hydroxyl group of (*S,R*)-**IVa** and water (*Figure 37A* and *37B*).

These two premises alone suggested a reasonable explanation of the 20 folds higher affinity of *(S,R)*-**IVa** compared to its non-hydroxylated precursor *(S,R)*-**IV**: whereas the “naked” benzodioxane is not able to displace water from the binding site, *(S,R)*-**IVa** kicks out water and replaces it with its hydroxyl group, that interacts with the side chain of Ser 108 and the backbone carbonyl of Gln 109 and NH Leu 121. Indeed, the unsubstituted benzodioxane *(S,R)*-**IV**, lacking of any small and polar substituent, fitted the water-containing binding site with a docking pose quite different from that of *(S,R)*-**IV**, suggesting that the driving force for binding with high affinity to the $\alpha 4\beta 2$ subtype in this series of rigid ligands is displacement of water accompanied by a new network of H-bond interactions (*Figure 37C*).



*Figure 37: A) nicotine bound at the water-containing $\alpha 4\beta 2$ binding site. B) *(S,R)*-**IVa** binds maintaining comparable interactions to nicotine, displaces water and fits the small hydrophilic pocket with its 7-OH substituent. C) *(S,R)*-**IV** can't displace water and assumes a different orientation in the binding site.*

Normally, if water molecules are located in hydrophobic regions of the binding pocket, their displacement by lipophilic groups strongly enhance affinity, due both to additional Van Der

Waals interactions and to an entropic contribution driven by the release of an ordered and “trapped” water molecule to the disordered bulk of the aqueous environment. In our case, displacement of the water molecule from a small hydrophilic pocket was more challenging and could be only achieved if driven by comparable interactions that could compensate the enthalpic loss, such as H-bonds between the hydroxyl group of (*S,R*)-**IVa** and the residues of the hydrophilic pocket.⁹²

Moreover, interactions with this small hydrophilic binding pocket seemed to be involved in receptor activation: whereas (*S,R*)-**IV** is an antagonist, (*S,R*)-**IVa** is a partial agonist. A similar hypothesis had already been advanced and investigated by Dougherty et al., who observed lower potency for nicotine when the hydrogen bonding donor feature of the amidic NH of Leu 121 was impaired (β 2L119 according to Dougherty’s numbering). Thus, we are currently designing a mutational study where we will investigate the role of the interaction between (*S,R*)-**IVa** and Ser 108, the residue that was not included in Dougherty’s investigation. According to our design of experiments, Ser108 will be mutated to hydrophobic amino acids and binding affinities and electrophysiological functional activities of (*S,R*)-**IV** and (*S,R*)-**IVa** will be assayed.

Afterwards, all the 5-substituted benzodioxanes were docked in the water-free binding site and very interestingly, diastereomers with (*S,S*)- absolute configuration, except for the bulky (*S,S*)-**9d**, fitted it maintaining similar interactions to those of (*S,R*)-**IV**, but also interacted through H-bonding with their 5-substituent with the hydrophilic pocket lined by Gln 107, Ser 108 and Leu 121, similarly to (*S,R*)-**IVa**. In order to reach these residues with the 5-substituent, the core benzodioxane moiety had to be twisted of approximately 180° (*Figure 38A*). Oppositely, the (*S,R*)-diastereomers were predicted to place their 5-substituents far from this pocket, with a docking pose almost superimposable with that of (*S,R*)-**IV** (*Figure 38B*).

These findings, in line with the binding assays, suggested that water displacement, accompanied by additional interactions to the small hydrophilic binding pocket at the β 2 subunit could be so important that, when a suitable H-bond partner is introduced in the 5 position, the ligand reorients itself to place the 5-substituent in the additional pocket, resulting in a conformational twist of the benzodioxane moiety to keep the pyrrolidine nitrogen within the aromatic box.

Additionally, N-methyl-pyrrolidinyl-pyridodioxanes (*S,R*)- and (*S,S*)-**5-8** were docked and, among them, compound (*S,R*)-**5** was predicted to hydrogen-bond the water molecule that

bridges it with an H-bond network with Leu 121 and Asn 109, in a similar way to nicotine (Figure 38C).

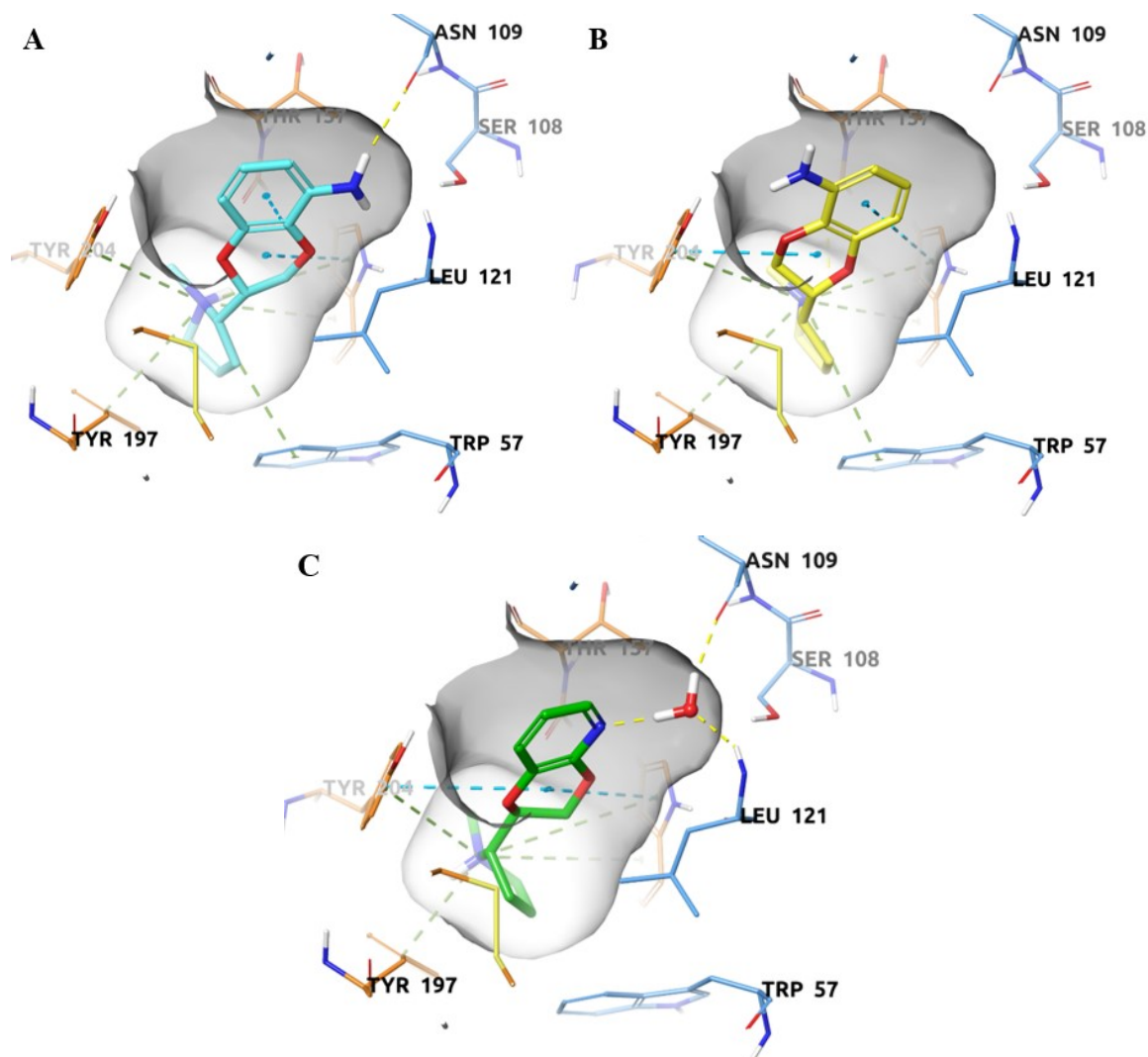


Figure 38: A) *(S,S)*-9c twists its core benzodioxane scaffold to place the 5-amino substituent in the small hydrophilic cavity. B) *(S,R)*-9c places its 5-amino substituent far from the hydrophilic cavity. C) *(S,R)*-5 indirectly binds Asn 109 and Leu 121 by H-bonding a water molecule that bridges it with the hydrophilic pocket.

The results of this docking study prompted us to hypothesize a reasonable explanation for the differences in the electrophysiological activities of *(S,R)*-IV, *(S,R)*-IVa, *(S,R)*-5 and *(S,S)*-9c.

The antagonists *(S,R)*-IV did not have any hydrophilic substituent that could neither drive the expulsion of water from the binding site nor interact with it, while the partial agonists *(S,R)*-IVa, *(S,R)*-5 and *(S,S)*-9c directly or indirectly interacted, with different extent, with at least one residue among Leu 121, Asn 109 and Ser 108, suggesting that this additional interactions could be responsible for channel activation. As introduced in the previous paragraph, this

hypothesis will be further explored by coupling mutational experiments on Ser 108 with electrophysiological assays.

Part 2: $\alpha 7$ nAChRs

2.1 Introduction

$\alpha 7$ Subunits usually assemble into homopentamers, but in heterologous systems they also form functional heteropentameric channels with other nicotinic subunits, like $\alpha 5$, $\beta 2$ and $\beta 3$, among which the $\alpha 7\beta 2$ heteromeric subtype has been found in rat and human basal forebrain cholinergic neurons.^{5,93}

The $\alpha 7$ -containing receptors are largely expressed in the brain, with particularly high abundance in the cortex, hippocampus, hypothalamus and some brain stem nuclei. Lower levels can be found in thalamic regions and basal ganglia.^{6,12}

Upon agonist binding, the $\alpha 7$ subtype undergoes rapid activation, followed by quick desensitization, and mediates a brief influx of positive cations (Na^+ and Ca^{2+}) and an efflux of K^+ . It is localized on presynaptic membranes, where it is involved in the control of neurotransmitter release (e.g. glutamate or noradrenaline) and on postsynaptic membranes, where it cooperates to the fast synaptic transmission and it can have long-term effects on metabolic pathways and gene-expression, due to its high calcium permeability.⁹⁴

Even if, historically, the neuronal nicotinic receptors have been thought to be expressed only on neuronal cells within the nervous system, the $\alpha 7$ subtype has also been found in non-excitabile cells such as the pulmonary epithelial cells, astrocytes, glial cells, endothelial cells and many tumoural cells, where they mediate pro-proliferative, survival and anti-inflammatory signalling.⁶

2.1.1 $\alpha 7$ Architecture

The overall architecture of nAChRs is shared among all the subtypes: the homomeric $\alpha 7$ subtype is a pentameric structure formed by 5 identical $\alpha 7$ subunits (encoded by the CHRNA7 gene) pseudo-symmetrically arranged around a central aqueous pore.¹³ Each monomer contains a long and folded extracellular N-terminal domain (NTD), three alpha-helices which span the cell membrane (TM1-3) connected with a short intracellular loop to the subsequent transmembrane alpha-helix (TM4) and a short extracellular C-terminal domain (CTD).³ The extracellular domain (ECD) contains 5 identical binding sites at each $\alpha 7/\alpha 7$ interface (LBD), while the transmembrane region (TM) and the intracellular domain (ICD) are involved in the channel gating (*Figure 39*).

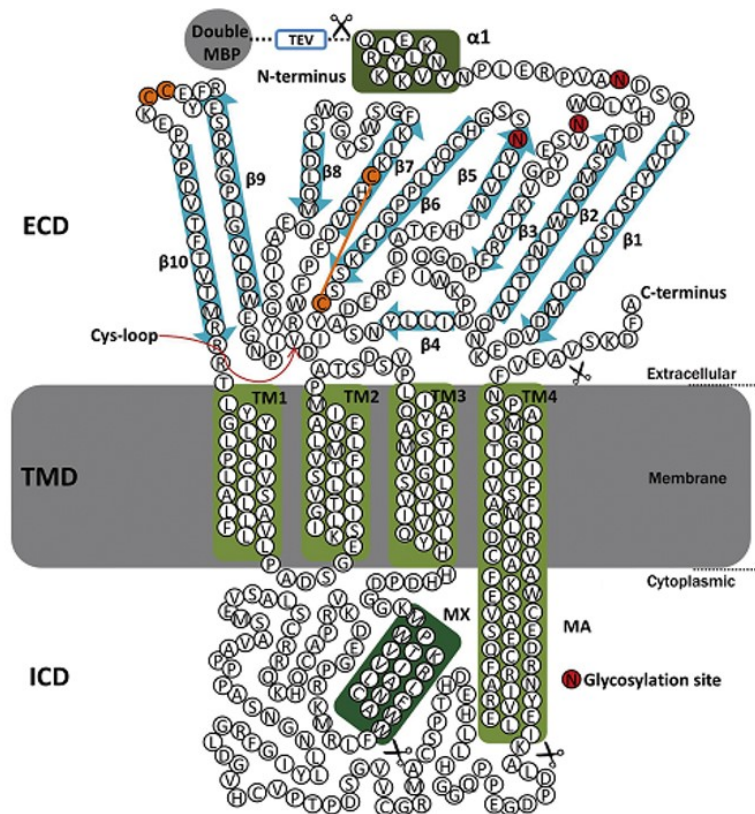


Figure 39: Schematic representations of $\alpha 7$ nAChR: topological structure showing the primary sequence and the organization in three domains (ECD, TMD and ICD). Adapted from Cheng *et al.*⁹⁵

To date, no X-Ray or CryoEM 3D models of the $\alpha 7$ nAChR are available. The early structural information about the architecture of the extracellular domain of the $\alpha 7$ subtype have been obtained by combining the 3D X-Ray structures of the homologous proteins AChBPs with homology modelling techniques and sequence analysis.

Later, in 2011, Chen *et al.* published the crystal structure of the ECD of the receptor chimera between the human $\alpha 7$ nAChR and the homologous AChBP of *Lymnaea Stagnalis* (*Ls-AChBP*), either bound to the agonist epibatidine and in its *apo* form (Figure 40 and Figure 42).⁹⁶ Although still non-identical to the native human $\alpha 7$ ECD and lacking the TMD and ICD, these two structures were a more realistic model of the extracellular domain of the $\alpha 7$ nAChRs.

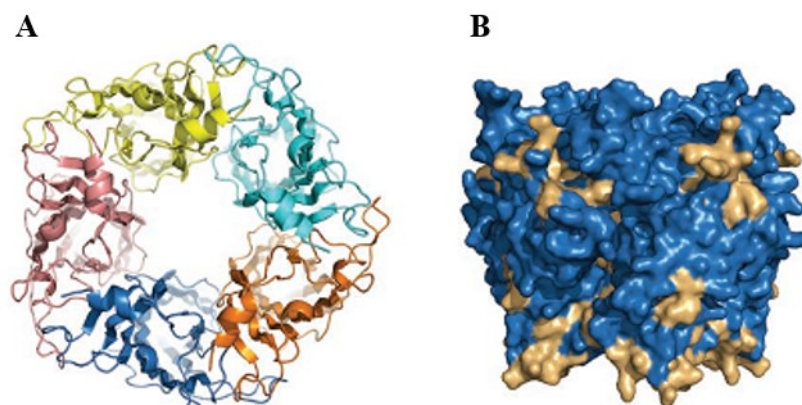


Figure 40: A) Top view of the pentameric $\alpha 7$ -AChBP chimera; each subunit is shown in a different color. B) Surface representation showing $\alpha 7$ residues (blue) and AChBP residues area (beige) on the $\alpha 7$ -AChBP chimera. Adapted from Li et al.⁹⁶

In 2013, the same authors reported on the RCSB database the X-Ray structure of the same chimera co-crystallized with the $\alpha 7$ antagonist a-bungarotoxin (PDB ID: 4HQP), deepening the knowledge about the binding site and its interactions with agonists and antagonists.

Further structural information on the ligand binding domain and the first insights on the potential localization of allosteric binding sites were provided by Ulens et al. in 2015, who reported a X-Ray structure of an $\alpha 7$ -AChBP chimera co-crystallized with lobeline either alone or together with 5 different allosteric fragments.⁹⁷

In the meantime, the structures of the TM domain of the $\alpha 7$ nAChRs were determined by NMR⁹⁸ and the full-length structures of some LGIC (i.e. Glutamate-gated chloride channel from *C. Elegans*,⁹⁹ $\beta 3$ GABA-A¹⁰⁰ and $\alpha 4\beta 2$ nAChR²⁰) structurally similar to the $\alpha 7$ subtype were resolved by X-Ray crystallography.

2.1.2 Orthosteric binding site

As the orthosteric $\alpha 7$ binding pockets are located in the ECD at each $\alpha 7/\alpha 7$ interface, 5 identical binding sites exist. However, occupancy of only one binding site is required for activation. Each binding cavity is lined by two adjacent $\alpha 7$ subunits, which simultaneously contribute either as the principal side (or (+) side) or as the complementary side ((-) side). The principal side contributes to the binding pocket with three strands connected by the same number of loops (loops A – C), while the complementary subunits lines the binding pocket with three loops (loops D – F) (Figure 41).

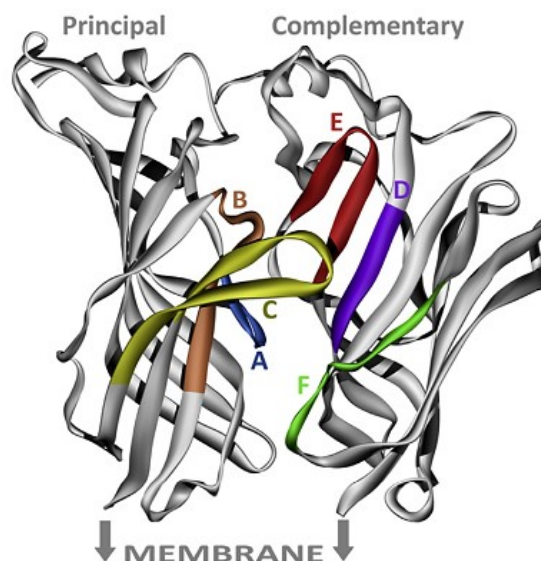


Figure 41: cartoon showing a ribbon representation of an $\alpha 7\alpha 7$ dimer. The loops that line the binding site are colored. Adapted from Thompson et al.¹⁰¹

The analysis of the epibatidine-bound $\alpha 7$ -AChBP X-Ray crystal structure reported by Chen in 2011 provided interesting insights on the structural features of the $\alpha 7$ binding site.⁹⁶

The crystal structure revealed that the azabicyclo moiety of the agonist epibatidine was accommodated into the aromatic cage formed by residues of Tyr 91 from loop A, Trp 145 from loop B, Tyr 184 and Tyr 191 from loop C and Trp 53 from loop D (according to the author's numbering).

The basic nitrogen of epibatidine is protonated at physiological pH and the resulting positively charged ammonium group interacts with the indole ring of Trp145 through a π -cation interaction and through hydrogen bonds with the backbone carbonyl group of the same amino acid and the hydroxyl of Tyr 91. Extensive Van Der Waals contacts between the aliphatic portions of the ligand and Tyr184, Cys186, Cys 187 and Trp145 further stabilize the complex. Additionally, one of the electropositive carbons directly connected to the cationic nitrogen, is near to the aromatic ring of Tyr191. The chloropyridine ring stacks edge-to-face against the indole ring of Trp145 and makes Van Der Waals contact with Thr146, Leu104, Leu106 and Gln114. The chlorine atom has been suggested to stabilize the complex by halogen-bonding Gln114 and Leu104. Trp53 doesn't directly interact with epibatidine, but keeps Trp145 in lieu by mean of face-to-edge π - π stacking (Figure 42A).

In 2017, a mutational study performed by Ruepp et. al. demonstrated that almost all the residues mentioned above were important for epibatidine binding at the $\alpha 7$ nAChRs.¹⁰¹ Differently from

the interaction information obtained from the co-crystals between epibatidine and AChBP or $\alpha 7$ -AChBP chimera, these experiments aimed to clearly determine which amino acids were involved in epibatidine binding at human $\alpha 7$ nAChRs. Its binding affinity was 1) impaired with the mutations C186A or C187A; 2) completely abolished by W53C, Y91C, N104C, W145C, Y184C and Y191C; 3) enhanced by Q114C and S144C and 4) unaffected by the substitutions Q55C, L106C, L116C, T146C, D140C and S162C.

Chen also reported the X-Ray crystal structure of the Apo form of the $\alpha 7$ -AChBP and compared it with the epibatidine-bound $\alpha 7$ -AChBP (Epi). Substantial differences were observed between the conformations of loops C. In the Epi structure it was tightly closed on the ligand in all the subunits, while in the Apo structure the loop C assumed a range of opened conformations (*Figure 42*). Loop C was stabilized to an even more open conformation when $\alpha 7$ -AChBP is bound to a classical antagonist, like methyllicaconitine.¹⁰²

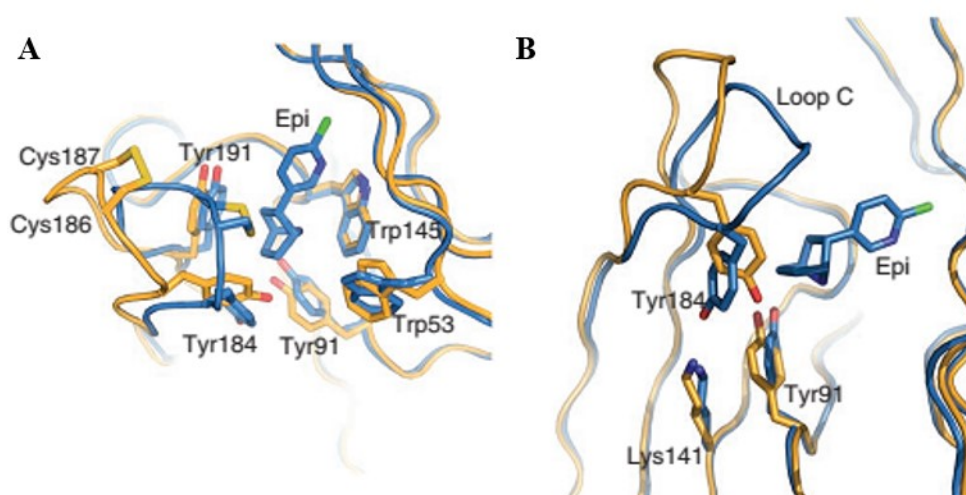


Figure 42: overlay of the ligand-binding site between the Apo (gold) and Epi (blue) structures. A) Top view (B) Side view. Adapted from Li et al.⁹⁶

These evidences strengthened the well-established hypothesis that associates closed conformations of loop C with agonist-induced activated (A) or desensitized (D) states and open conformations with Apo or antagonists-stabilized resting conformations (R).¹⁰³

Later, in 2015, Ulens et. al. resolved the X-Ray crystal structures of an $\alpha 7$ -AChBP chimera co-crystallized with lobeline, a ligand of the $\alpha 7$ subtype. Although lobeline, due to its size, binds differently to the pocket when compared to epibatidine, the main interaction is maintained: the positively charged ammonium group is lodged within the aromatic box at a suitable distance for π -cation interactions with the side chain of Trp145. The authors took advantage of the good resolution of co-crystals $\alpha 7$ /AChBP-lobeline to perform a fragment-library screening coupled

with X-Ray analysis to identify potential allosteric binding site. In addition to three putative allosteric binding sites, the authors identified an additional subpocket of the orthosteric binding site (*Figure 43*).

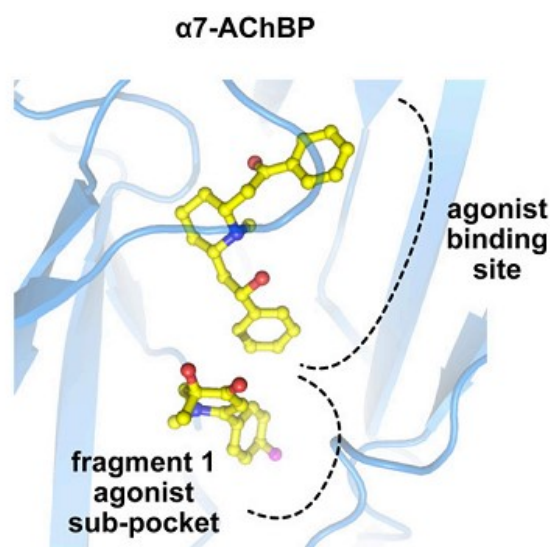


Figure 43: X-Ray co-crystal structure of the chimera $\alpha 7$ /AChBP with lobeline and fragment 1.

2.1.3 Allosteric binding site

Allosteric modulators indirectly influence the effect of an orthosteric ligand, by binding to a distinct site from the orthosteric. Positive allosteric modulators (PAMs) increase the agonist activity, negative allosteric modulators (NAMs) decrease the agonist activity, while silent or null allosteric modulators (SAMs) compete for the allosteric binding site without affecting the orthosteric agonist activity. More accurately, allosteric modulation was defined by Ulens as “the process that modifies the energetic barriers between the resting and activated state and that is caused by binding of a molecule at a site that is different from the orthosteric binding”.⁹⁷

$\alpha 7$ nAChRs PAMs have been widely studied overtime. Initial works in this area were performed by Bertrand et al. in 1998 and by Sher et al. in 2002, who respectively identified Invermectin and 5-hydroxyindole as $\alpha 7$ PAM.^{104,105} Nowadays, positive allosteric modulators can be classified into type I PAM and type II PAM. Type I PAMs, such as invermectin and 5-hydroxyindole, enhance agonist-evoked peak currents without delaying receptor desensitization. Contrariwise, type II PAMs like PNU-120596, the first $\alpha 7$ -selective to be disclosed, increase the agonist response, decrease receptor desensitization and also reactivate desensitized receptors (*Figure 44*).^{106,107}

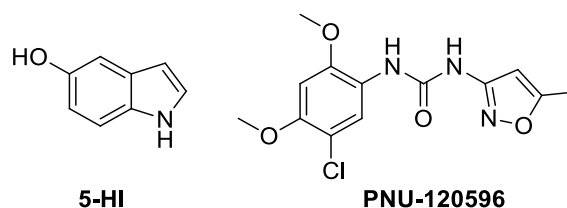


Figure 44: examples of positive allosteric modulators 5-HI (PAM-I) and PNU-120596 (PAM-II).

$\alpha 7$ nAChR PAMs arouse great interest for potential therapeutic applications in the fields of neurodegenerative disorders and neuroinflammation, and at least one $\alpha 7$ nAChR modulator has been tested in clinical trials.^{108,109}

Although the exact localization of the allosteric binding sites has not been clarified, type-I PAM are expected to bind at a site in the extracellular domain, while type-II PAM have been suggested to bind in the transmembrane domain.¹¹⁰ In 2015 Ulens et. al. co-crystallized an $\alpha 7$ -AChBP chimera with lobeline and 5 different allosteric fragments, identifying 3 different potential binding sites in the ECD, among which one could correspond to the PAM-I binding site.⁹⁷

In 2018, Arias et al. performed an *in-silico* study, where they used docking and molecular dynamics to identify and study the binding sites of PAM-I and PAM-II. Interestingly, PAM-II were predicted to interact with a binding pocket at the ECD-TM interface, while PAM-I with the ECD domain.¹⁰⁷

2.1.4 Electrophysiology

The $\alpha 7$ subtype has been widely studied for its unique electrophysiological properties, which make $\alpha 7$ nAChRs pharmacology very complex. Whereas the other major central nAChR subtype, the $\alpha 4\beta 2$, has slow activation and desensitization kinetics and low calcium permeability, the $\alpha 7$ subtype is rapidly activated upon agonist binding and desensitize immediately afterwards (submillisecond time scale) (Figure 45).^{10,111} Due to its high calcium permeability, this brief elapse of time is enough to guarantee an intense influx of calcium, which is involved in facilitation of neurotransmitter release from presynaptic terminals, depolarization of post-synaptic membranes and initiation of Ca^{2+} -triggered intracellular processes.

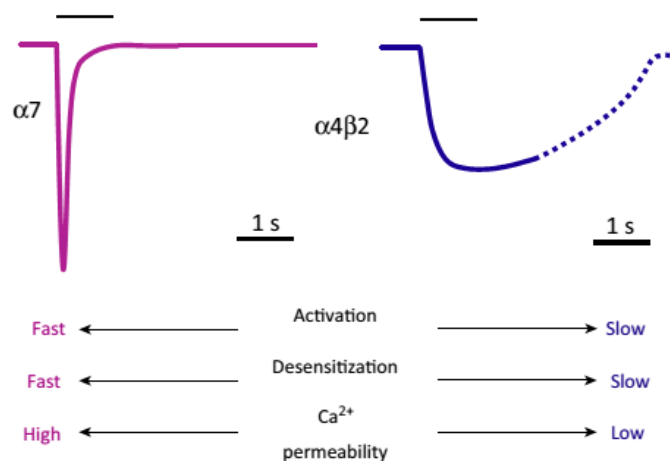


Figure 45: schematic representation of basic functional and pharmacological properties of the $\alpha 7$ and $\alpha 4\beta 2$ nAChR subtypes. Adapted from Dineley et al.¹¹²

The MWC model, described in the general introduction, had been implemented by Papke to account for the new insights on the peculiar pharmacology of the $\alpha 7$ nAChR.^{113–115} When no ligands are applied, this receptor can interconvert between four main states: resting or closed (C), activated and opened (O*), intermediate desensitized (D_i) and desensitized (D_s) non-conductive states (Figure 46A). Without any ligand, the most stable conformation is the non-conducting closed state C. As a high energy barrier has to be overcome to reach the opened state O*, the receptor spontaneously opens with low probability, as demonstrated by single-channel experimental data.^{111,116} After opening, the receptor rapidly converts to a more stable desensitized state (D_i or D_s) and then relaxes back to the resting conformation. Upon binding of an efficacious agonist, the energy landscape is perturbed and both the energy barriers to reach the O* state and the energy of the desensitized states (D_i and D_s) are reduced (Figure 46B). Consequently, the agonist-bound channel either converts into the O* state and then quickly falls into a more stable desensitized conformation (D_s or D_i) or directly desensitizes. Due to its fast desensitization kinetics, the receptor remains opened for very short times, and it mediates very fast inward currents. Since the energy barriers to convert back from the desensitized states (D_i and D_s) to the closed state (C) are quite high, the process is slow. When desensitized, the receptor can't be activated by agonists.

In 2013, Papke et al. identified a new pharmacological class of $\alpha 7$ nAChR ligands, named silent agonists, which bind to the orthosteric binding site but have little or no efficacy in eliciting the current.¹¹⁷ Even if in classical electrophysiologic studies they appear as very low efficacy partial agonists or antagonists, when they are co-applied with a type-II PAM, they produce marked channel activation. According to Papke's kinetic model, silent agonists alone modify the energy

landscape of the $\alpha 7$ by increasing the energy of the O^* state (Figure 46C). Consequently, the transition $C \rightarrow O^*$ is no longer accessible due to a too high energy barrier, while the transitions $C \rightarrow D_i$ or D_s are energetically favored, meaning that the receptor directly converts from a closed non-conducting conformation to a desensitized non-conducting conformation, without transiting from the opened conductive state. Thus, silent agonists are thought to bind with high affinity to a desensitized state.

Type-II PAMs alone increase the energy of the D_i state and reduce the energy of D_s , but they don't modify the energy of O^* and therefore they don't affect channel opening. Moreover, a new high energy opened state O' is virtually accessible, but the energy barrier is too high to be reached (Figure 46D). However, when a PAM-II is coapplied with an agonist (Figure 46E) or with a silent agonist (Figure 46F) the energy of O' is lowered, so that the transition $D_s \rightarrow O'$ is allowed. This model explains why the co-application of a silent agonist, that desensitizes the receptor, with a type-II PAM, produces channel opening and current influx.

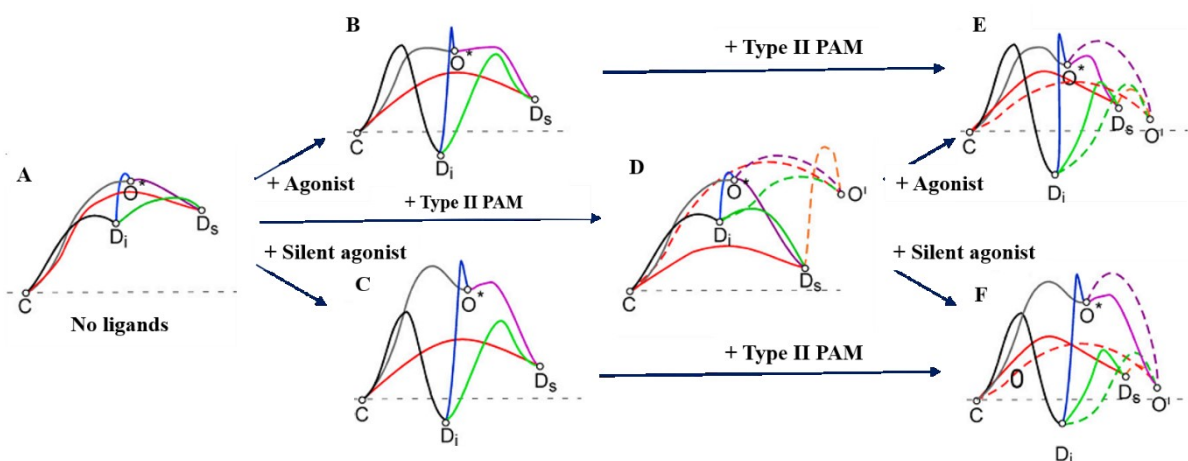


Figure 46: Hypothetical energy landscapes of the conformational states of the $\alpha 7$ nAChRs A) without any ligand or when bound to B) an efficacious agonist; C) a silent agonist; D) a PAM-II alone; E) a PAM-II and an efficacious agonist; F) a PAM-II and a silent agonist. Adapted from Papke et al.¹¹⁵

In 2017, Cottone et. al. constructed a full-length homology model of the $\alpha 7$ receptor and performed molecular dynamics simulations of the receptor complexed with the agonist epibatidine without any constrains, starting from an opened conformation previously described.^{99,103,118} Interestingly, after a few ns, they observed that the pore was collapsed to a very low hydrated conformation, claimed to be a non-conductive conformation. Furthermore, in the time scale of the simulation, the LBD-TMD interface underwent conformational changes that could be associated with an $O^* \rightarrow D$ transition.

2.1.5 $\alpha 7$ Functions

$\alpha 7$ nAChRs are widely expressed in the CNS where they play crucial roles in several physiological processes, such as cognition, learning, attention and memory. Consequently, they are also involved in many pathological conditions, like Alzheimer disease, Parkinson disease, schizophrenia, ADHD, and autism spectrum disorder.^{112,119}

In addition to the pivotal role in the brain, the $\alpha 7$ subtype is also expressed in non-excitabile cells like airway epithelial cells, endothelial cells, pancreatic cells, glial cells, lymphocytes, bone marrow cells, monocytes, macrophages and microglia and several tumoral cells. It is involved in other biological processes, among which cell-cell signalling, regulation of cell survival and of cell death and it is implicated in many pathological conditions, like cancer progression, uncontrolled angiogenesis, inflammation and pain.⁶

For instance, the autonomous nervous system regulates cytokine production by the immune system through an ensemble of neural circuits called “cholinergic anti-inflammatory pathway”. Activation of the $\alpha 7$ subtype reduces the production of pro-inflammatory cytokines like tumour-necrosis factor (TNF- α) or interleukin-1.¹²⁰

2.1.6 $\alpha 7$ nAChR and cancer

Nicotine, the primary addictive component of tobacco, was reported to participate in cancer promotion and progression: it promotes cancer cells survival, proliferation, angiogenesis, tumour dissemination, invasion and angiogenesis through the activation of nAChRs.^{121,122} Cigarette smoking is the predominant risk factor for lung cancer and it has also been related to other types of cancers, such as pancreatic cancer and gastric cancer.^{121,123} During combustion, nicotine is partially decomposed to the carcinogenic nitrosamines NNK (4-(methylnitrosamino)-1-(3-pyridyl)-1-butanone), agonist at the $\alpha 7$ nAChRs and NNN (N-nitrosornicotine), agonist at the heteromeric $\alpha\beta$ nAChRs (*Figure 47*). These highly reactive compounds and their metabolites form toxic adducts with DNA nucleotides, causing deleterious mutations to oncogenes or tumour suppressor genes.

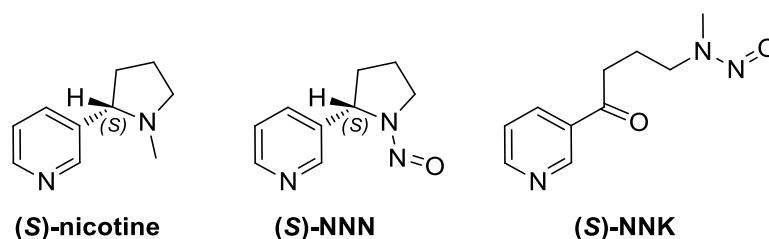


Figure 47: main components of cigarette smoke: (S)-nicotine and its combustion byproducts (S)-NNN and (S)-NNK.

Lung cancers, the leading cause of cancer-related deaths worldwide, are classified in small-cell lung cancers (SCLCs), which account for 20% of all lung cancer cases, and in non-small cell lung cancers (NSCLCs), which account for 80% of all lung cancer cases.^{124,125} NSCLCs are further divided into three subtypes: squamous-cell carcinoma (SCC-L), adenocarcinoma and large-cells carcinoma. The main subtype that mediates the proliferative and angiogenic effects of nicotine in lung cancer cells is the $\alpha 7$ subtype.³⁷

The expression of $\alpha 7$ and of $\alpha 9$ - $\alpha 10$ nicotinic receptors is upregulated in human SCC-L cell lines (NSLCLCs) and in animal models, with expression levels that can vary depending on the specific cell line. In 2018, Gotti et al. demonstrated that nicotine or the selective $\alpha 7$ agonist ICH3¹²⁶ increased cell proliferation and viability of adenocarcinoma cell lines expressing high level of $\alpha 7$ and $\alpha 9$ - $\alpha 10$ nAChR subtypes (A549), while nicotine hadn't any effect on proliferation and viability on adenocarcinoma cell lines expressing none or low levels of the $\alpha 7$ or $\alpha 9$ - $\alpha 10$ subtypes (H1975) (Figure 48A). After nicotine administration, the amount of activated pERK and pAkt, two activated proliferative kinases, were increased in A549 cells, but not in H1975 cells (Figure 48B). Together, these results confirm that nicotine activates and induces the expression of some specific nAChR subtypes, whose activation drives hyperproliferation of adenocarcinoma cells through enhancement of intracellular proliferative pathways of pERK and pAKT.³⁷

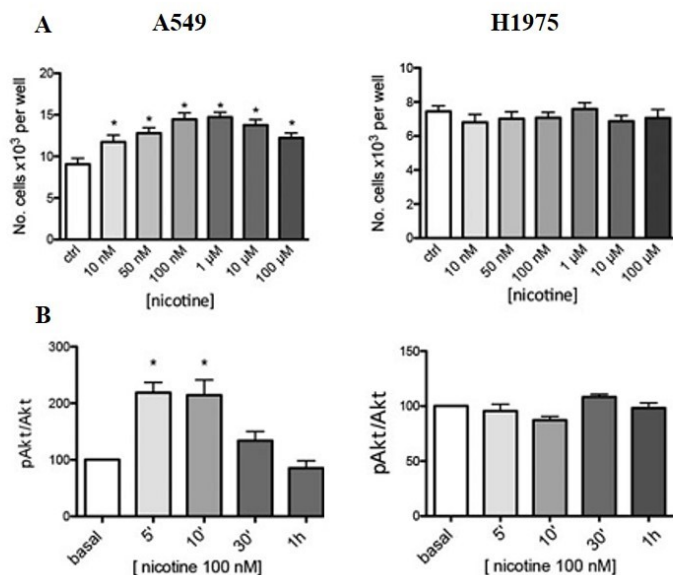


Figure 48: nicotine A) induces hyperproliferation and B) activates the pAkt/Akt pathway of $\alpha 7$ and $\alpha 9$ - $\alpha 10$ containing tumoral cells (A549), but not of tumoral cells with no $\alpha 7$ and low levels of $\alpha 9$ - $\alpha 10$ (H1975).

Further studies using either siRNAs or specific $\alpha 7$ and $\alpha 9$ - $\alpha 10$ antagonists demonstrated that both receptors, the $\alpha 7$ and the $\alpha 9/\alpha 10$ subtype are responsible for nicotine-induced hyperproliferation of A549 cells. When A549 were treated with the specific antagonists methyllycaconitine (MLA) or α -bungarotoxin (α -Bgtx), both nicotine-induced hyperproliferation and nicotine-induced activation of pERK and pAKT were reverted (*Figure 49A* and *49B*). Similarly, but to a lesser extent, administration of $\alpha 7$ selective or $\alpha 9$ selective peptidic antagonists (respectively the α -conotoxins ArIB and RgIA4) reduced nicotine-induced hyperproliferation (*Figure 49C* and *Figure 49D*) and pERK and pAKT activation. The same effect was observed by knock-down experiments with $\alpha 7$ or $\alpha 9$ siRNAs.³⁷

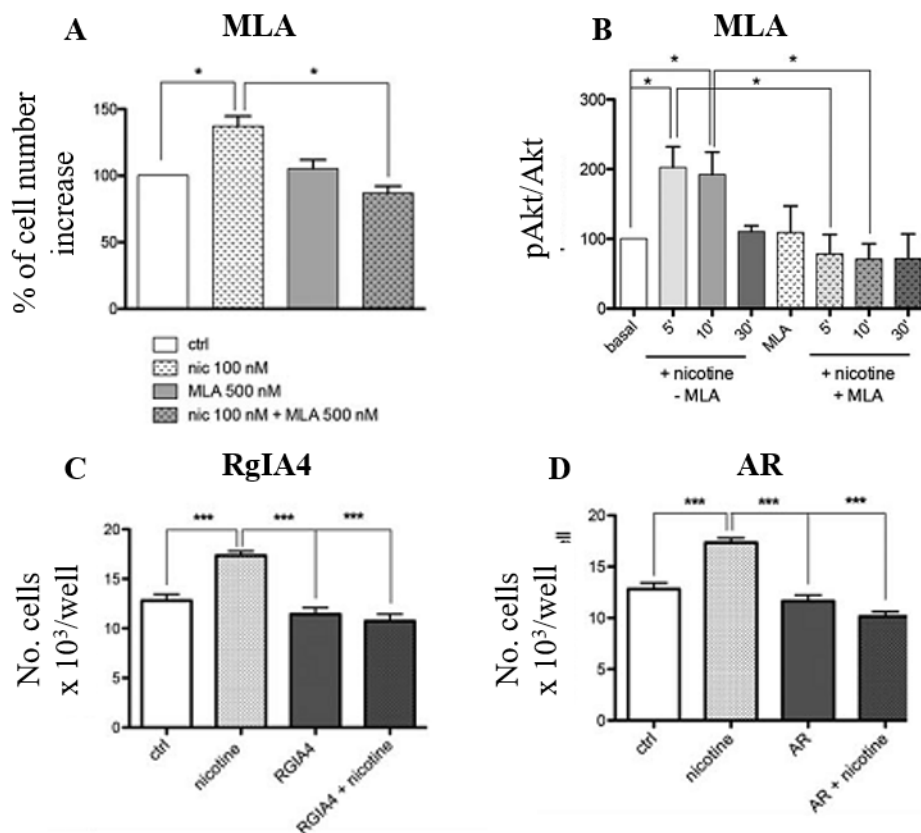


Figure 49: antiproliferative effect on A549 cells pre-treated with nicotine of A) the $\alpha 7$ and $\alpha 9$ antagonist MLA; C) the selective $\alpha 9$ antagonist RgIA4 and of D) the selective $\alpha 7$ antagonist ArIB; B) MLA reduce the activation of the nicotine-induced pAkt/Akt pathway. Adapted from Mucchietto et al.³⁷

Nicotine- or NNK-stimulated hyperproliferation of SCLC cells *in-vitro* has been related to the activation of $\alpha 7$ nAChRs, via activation of many pro-proliferative intracellular mediators like PKC (protein kinase C), RAF1 (serine/threonine kinase), ERK1 and ERK2 (mitogen activated kinases) and the transcription factors FOS, JUN and MYC. The same cascade enhances production and/or release of the growth factors for SCLCs like serotonin, mammalian

bombesins, bradykinin, vasopressin, neurotensin and proangiogenic factors like vascular endothelial growth factor (VEGF) and basic fibroblast growth factor (bFGF).¹²⁷

nAChRs have been also found to be involved in promotion and progression of other types of cancer, such as pancreatic cancer, glioma and glioblastoma (unpublished data).^{128,129}

2.2 $\alpha 7$ Orthosteric ligands and selectivity

Since a high number of nicotinic acetylcholine receptor subtypes can be obtained by combining different subunits, selectivity on a certain subtype over off-target subtypes is a crucial requirement to achieve a desired pharmacological effect. The two subtypes that are usually considered for this purpose are the heteropentameric $\alpha 4\beta 2$, the major subtype in the CNS, and the $\alpha 3\beta 4$, mainly expressed in autonomic ganglia.

Despite the huge amount of information that have been collected for the $\alpha 7$ nAChR, the structural and functional details of other homopentameric nAChRs have not been deeply explored yet. Particularly, the $\alpha 9$ subtype, formed by 5 identically $\alpha 9$ subunits (encoded by the gene *CHRNA9*¹³) shares high sequence similarity with the $\alpha 7$ subtype. Even if the X-Ray 3D structure of an $\alpha 9$ monomer co-crystallized with the unspecific antagonists MLA and α -Bgtx has been reported, the dimer, containing the entirety of the binding site has never been described.

Probably due to high similarity between the two subtypes, many ligands targeting the $\alpha 7$ subtype, like the antagonists MLA or α -Bgtx, are not selective versus the $\alpha 9$ subtype. Subtype-selectivity between the $\alpha 7$ and $\alpha 9$ is therefore desirable.

The $\alpha 9$ subtype also coassembles with the $\alpha 10$ subunit forming the heteromeric $\alpha 9\alpha 10$ subtype. As it is quite complicated to express them in heterologous systems, the study of human $\alpha 9$ subtypes is very limited. $\alpha 9$ nAChRs are expressed in both the inner and outer hair cells of the adult cochlea, where they are involved in its function, but they are also expressed in a wide variety of non-neuronal tissues, ranging from immune cells to carcinomas.

2.2.1 $\alpha 7$ Full agonists

Acetylcholine, **nicotine** and **epibatidine** have already been discussed in paragraph number 1.2.1.

Anabaseine (*Figure 50*) is an alkaloid produced by *Aphaenogaster* ants and by ribbon worms *Nemertea*. It is structurally similar to nicotine and it is a full agonist for the $\alpha 7$ subtype, with higher affinity than nicotine, and a partial agonist at the $\alpha 4\beta 2$ subtype with lower affinity than nicotine. Anabaseine has been used as a scaffold for the design and synthesis of “functionally” selective $\alpha 7$ agonists, like GTS-21, described in the paragraph 2.2.2. These ligands bound to both subtypes, but elicited functional responses only at the $\alpha 7$ subtype, meaning that they had agonist activity at the $\alpha 7$ receptor, but antagonist activity at the $\alpha 4\beta 2$.¹³⁰

AR-R17779 (Figure 50) is a constrained analogue of acetylcholine with a spirooxazolidinone structure and was reported in 2000 as the first “affinity” selective $\alpha 7$ full agonist without any non-competitive antagonist activity.¹³¹ Prior to AR-R17779, some $\alpha 7$ agonists, derived from anabaseine (i.e. GTS-21, described below), were described as “functionally” selective on the $\alpha 7$ subtype over the $\alpha 4\beta 2$, but they all had high affinity to the $\alpha 4\beta 2$ subtype, at which they had antagonist effect.

2.2.2 $\alpha 7$ Partial agonists

GTS-21 (Figure 50). Several analogues of anabaseine were designed to obtain selective $\alpha 7$ agonists. Among these, compound GTS-21, also known as DMBX-A was reported in 1996 to bind both to the $\alpha 7$ and to the $\alpha 4\beta 2$ subtypes with affinity.^{130,132} However, it was shown to be a partial agonist at the $\alpha 7$ subtype, while it had antagonist activity at the $\alpha 4\beta 2$ subtype. Although this “functional” selectivity is normally not ideal for therapeutic application, GTS-21 has been studied in multiple Phase I studies and in Phase I/II studies for schizophrenia and Alzheimer disease.²⁷

ICH-3 (Figure 50). In 2011, De Micheli et al. reported the synthesis of a series of $\alpha 7$ ligands based on the structure of AR-R17779, among which compound ICH-3 stood out as a potent and selective $\alpha 7$ partial agonist, which was later investigated for its potential anti-inflammatory properties.¹²⁶

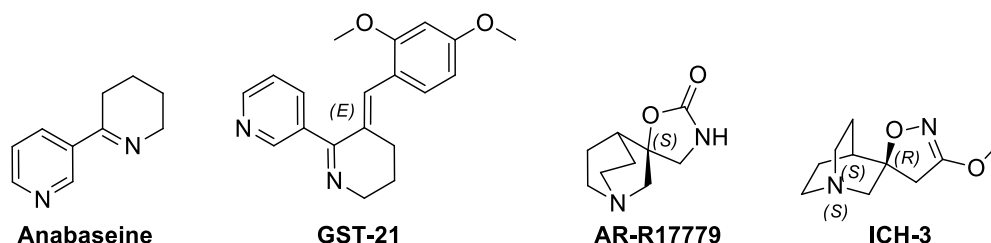


Figure 50: non-selective full agonist anabaseine; $\alpha 7$ functionally selective partial agonist **GST-21**; $\alpha 7$ “affinity” selective full agonist **AR-R17779** and selective $\alpha 7$ partial agonist **ICH-3**.

2.2.3 $\alpha 7$ Antagonists

α -Conotoxins have been already introduced in paragraph 1.2.3. They are competitive nAChRs antagonists isolated from the venom of sea snails of the genus *Conus*. α -Conotoxin ArIB is a selective antagonist for the rat and human $\alpha 7$ subtype, able to block acetylcholine-evoked currents in *Xenopus Oocytes* expressing the human $\alpha 7$ nAChRs and the choline- or AR-R17779-evoked currents in SH-SY5Y cells, potentiated by the type II PAM PNU-120596. Although ArIB has been widely used as a pharmacological tool for investigation of the $\alpha 7$ pharmacology and functions, its peptidic nature and huge size hamper its utility as a potential drug. Conotoxin

RgIA4 is a other interesting selective conotoxin, which has been specifically designed to be selective at the human $\alpha 9$ -containing receptors.^{133–135}

α -Bungarotoxin is a peptidic $\alpha 7$ antagonist and it was first isolated from the venom of the Taiwanese banded krait snake (*Bungarus Multicinctus*) in 1971.¹³⁶ It binds with high affinity and with slow off- kinetics to the muscle nAChRs at the neuromuscular junctions, causing paralysis, respiratory failure and, ultimately, death. It also has antagonist activity at the homomeric $\alpha 9$ and $\alpha 7$ subtypes and it is therefore often used as a pharmacological tool to study these receptors.

Methyllicaconitine (MLA) is a diterpene alkaloid isolated from many species of the *genus Delphinium*, plants commonly referred to as “larkspur”. At the neuromuscular junction it blocks the $\alpha 3\beta 4$ nAChR with high affinity, causing curare-like effects, while in the CNS it antagonizes both the $\alpha 4\beta 2$ and the $\alpha 7$ subtypes. MLA has been widely used as pharmacological tool and tested for different applications, such as neurological disorders and nicotine addiction.

2.3 State of the art

In 1953 Cavallini et al. reported the synthesis of the oxystilbene compound **MG624**, formally obtained by arylation of the hydroxyl group of triethylcholine, as a molecule with ganglioplegic activity (*Figure 51*).¹³⁷

In 1998 Clementi et al. pharmacologically characterized compound **MG624** as a high affinity ligand at the chick $\alpha 7$ containing receptors, selective against the $\beta 2$ - containing and $\beta 4$ -containing subtypes.¹³⁸ The year after, Gotti et al. demonstrated that **MG624** inhibited ACh-evoked currents in oocyte-expressed chick $\alpha 7$ with an IC_{50} of 109 nM, while it had supramicromolar IC_{50} s at the $\alpha 4\beta 2$ and at the muscle $\alpha 1\beta 1\gamma\delta$ subtypes. The possibility of a direct channel blockage was excluded both by competition binding experiments at the orthosteric binding site and by finding that the block of **MG624** was not voltage dependent.¹³⁹

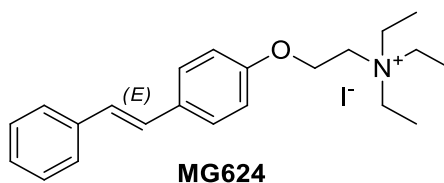


*Figure 51: high affinity $\alpha 7$ orthosteric ligand with moderate selectivity and $\alpha 7$ antagonism activity **MG624**.*

Recently, as detailed in paragraph 2.1.5, the activation of the $\alpha 7$ and $\alpha 9$ - $\alpha 10$ nAChRs has been related to cancer promotion and progression and therefore molecules like **MG624**, able to prevent or block their activation, could be promising antitumoral candidates.

In 2018, Gotti et al. found that **MG624**, able to block acetylcholine-elicited currents both at the $\alpha 7$ and at the $\alpha 9$ - $\alpha 10$ subtype by binding at the orthosteric binding sites, not only reverted the hyperproliferation induced by nicotine in a similar way to the $\alpha 7$ or $\alpha 9$ - $\alpha 10$ selective toxins ArIB or RgIA4 or to the use of siRNAs, but also had a dose-dependent cytotoxic effect on adenocarcinoma cells (*Figure 52*).³⁷

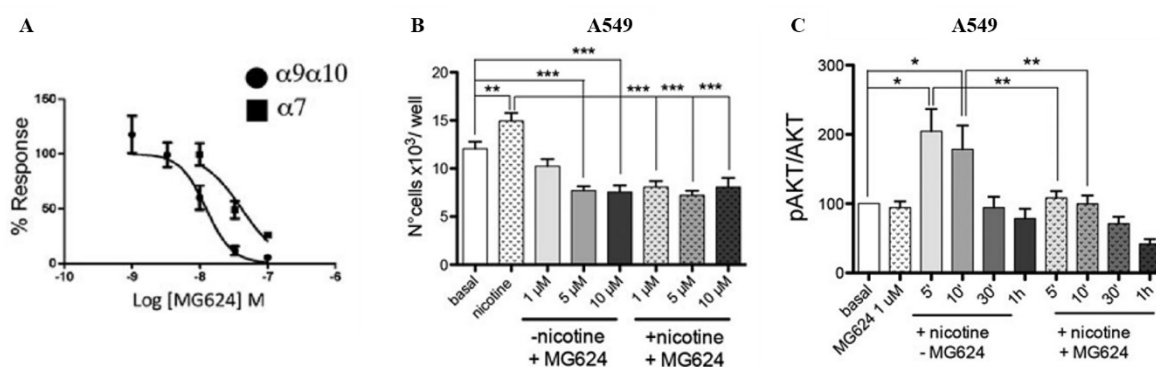


Figure 52: A) MG624 blocks ACh elicited currents in transfected Xenopus oocytes expressing $\alpha 9$ - $\alpha 10$ and $\alpha 7$ subunits; B) MG624 decreases A549 proliferation; C) MG624 blocks the nicotine-induced activation of the p-Akt pathway.

In 2008, Paradisi et al. combined the structures of the polyphenol resveratrol with the triphenylphosphonium cation (TPP⁺) by connecting them with a 4 carbons long linker, into compound **XVII** that structurally resembles **MG624** (*Figure 53*).¹⁴⁰ Polyphenols like resveratrol can act both as pro-oxidants or anti-oxidants depending on the redox potential of the polyphenol and on the molecular environment of the subcellular compartment where they are localized within cells. As the anti-proliferative and pro-apoptotic effects of resveratrol had already been reported and associated with the production of ROS in the mitochondria, the authors intended to boost the antiproliferative action by targeting the resveratrol-containing molecule to the mitochondria.¹⁴¹⁻¹⁴⁴ TPP⁺ is a membrane permeable lipophilic cation that drives the accumulation of **XVII** in subcellular compartments held at a negative voltage, like the mitochondrial matrix.¹⁴⁵ Selectivity over non-tumoral cells can be achieved because of the higher transmembrane potential of tumoral cells than that of healthy cells.¹⁴⁶ As expected, **XVII** was shown to have mitochondrial tropism and antitumoral activity on rapid-growth cell types.

Later, in 2014, Biasutto et al. demonstrated that compound **XVII** and its methylated analogue **RDM-4'BTPI**, with higher antitumoral activity, killed fast-growing cancer cells through a necrosis mechanism.¹⁴⁷ Upon accumulation in the mitochondria, they enhanced production of reactive oxygen species (especially superoxide anion, then converted to H₂O₂), causing cellular damage and membrane depolarization and therefore acting as mitocans. The same year, Biasutto et al. further studied the mechanism of cytotoxicity of these mitochondriotropic resveratrol derivatives and discovered that **RDM-4'BTPI** was a strong inhibitor of the complex I and III of the respiratory chain.¹⁴⁸ These protein complexes are known to be the major sources of ROS in healthy and untreated mitochondria as byproducts of the respiratory chain and it is plausible that their inhibition could lead to favour this side reaction. Moreover, **RDM-4'BTPI** was also found to be an inhibitor of the F₀F₁ ATP synthase, perhaps through a proton slipping (decoupling) mechanism. Similarly to **RDM-4'BTPI**, the mitochondrially targeted derivative of vitamin E (VE) analogous α -tocopheryl succinate, MitoVES (or MitoVE₁₁S, *Figure 53*), was reported to be inhibit mitochondrial respiratory complex II (CII) leading to ROS generation and cell death induction with IC₅₀ values for apoptosis in various malignant cell lines mainly ranging between 0.5 and 3 μ M.¹⁴⁹

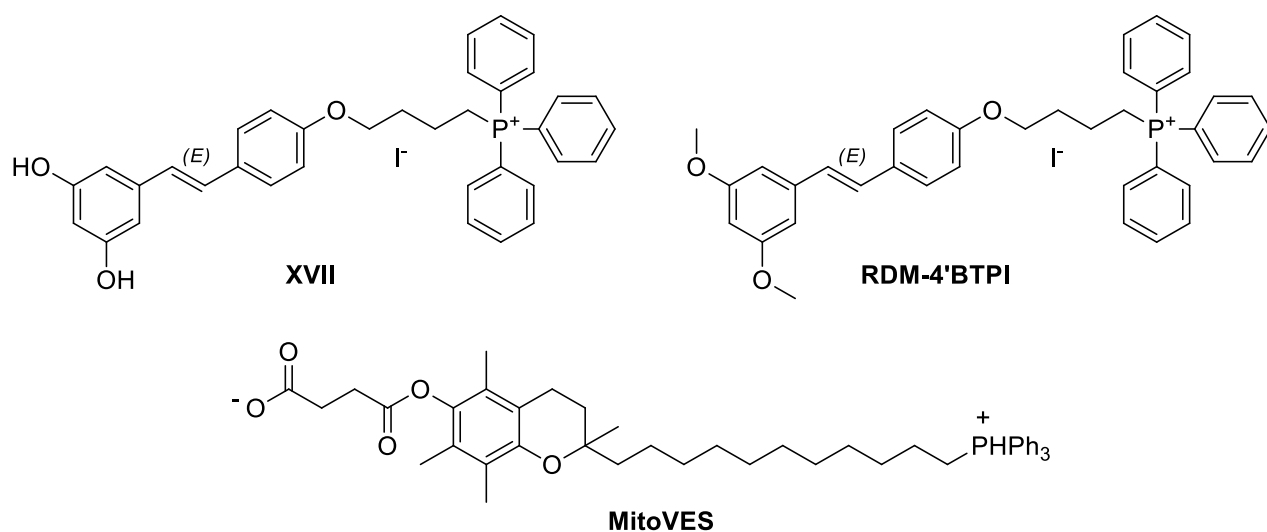


Figure 53: mitochondriotropic compounds XVII and RDM-4'BTPI and MitoVES with antitumoral activity.

Preliminary results (unpublished data) showed that both **MG624** and **RDM-4'BTPI** had respectively micro- and submicromolar antitumoral activity on adenocarcinoma (A549) and malignant glioma (U87MG) cell lines. Additionally, **RDM-4'BTPI** also reduced cell viability of neuroblastoma cell lines (SH-SY5Y).

The two reference molecules share some common structural features: 1) they both have a permanently charged cationic head, that is a triethylammonium moiety in **MG624** and triphenylphosphonium moiety in **RDM-4'BTPI**; 2) they both share a stilbenolic core, “naked” in **MG624** and “decorated” with two *meta*-methoxy substituents (pterostilbene) in **RDM-4'BTPI**; 3) the aromatic moiety and the permanently charged cationic head are connected through a flexible alkyl linker, which is an ethyl linker (2 carbons) for **MG624**, while it is a butyl linker (4 carbons) for **RDM-4'BTPI**.

2.4 Potent anti-glioblastoma agents by hybridizing the oniumalkyloxy-stilbene based structures of an $\alpha 7/\alpha 9$ -nAChR antagonist and of a pro-oxidant mitocan

2.4.1 Aim

As detailed in chapter 2.3, the antitumoral activity of **MG624** had been related to $\alpha 7$ and $\alpha 9$ - $\alpha 10$ antagonism, while compound **RDM-4'BTPI** was described by its inventors as a mitocan.^{37,147} Given the antitumoral activities of **MG624** and of **RDM-4'BTPI** and their structural similarities, our first goal was to understand whether the two molecules could share some mechanism of actions (MoAs). Then, aiming at elucidating to what extent each substructure (onium head/stilbene scaffold/interposed alkylene linker) would address toward one MoA or the other, we designed a series of hybrids (*Figure 54*) between the three constitutive portions of **RDM-4'BTPI** (pterostilbene residue, triphenylphosphonium head and 4 carbons linker) and of **MG624** (stilbenoxy residue, triethylammonium head and 2 carbons linker). Moreover, this design strategy could provide some hybrids where the two MoAs are partially merged, obtaining antitumoral compounds with a hybrid pharmacological profile. In principle, this systematic hybridization panel should provide 8 compounds: **MG624**, **12**, **13**, **14**, **15**, **16**, **17**, **RDM-4'BTPI**, but the triphenylphosphonium compounds with 2 carbons long linker **12** and **14** couldn't be enclosed in this investigation because ready decomposition to stilbenol and pterostilbene, respectively, and vinyl-triphenylphosphonium precluded their isolation and characterization.

The compounds were assayed for their binding affinities at the $\alpha 7$ subtype, for their ability to block ACh-evoked currents in *Xenopus Oocytes* expressing human $\alpha 7$ and $\alpha 9$ - $\alpha 10$ receptors, for their anti-proliferative activity on different tumor cells expressing $\alpha 7$ and/or $\alpha 9$ - $\alpha 10$ nAChRs, for mitochondrial ROS production and for ATP production impairment.

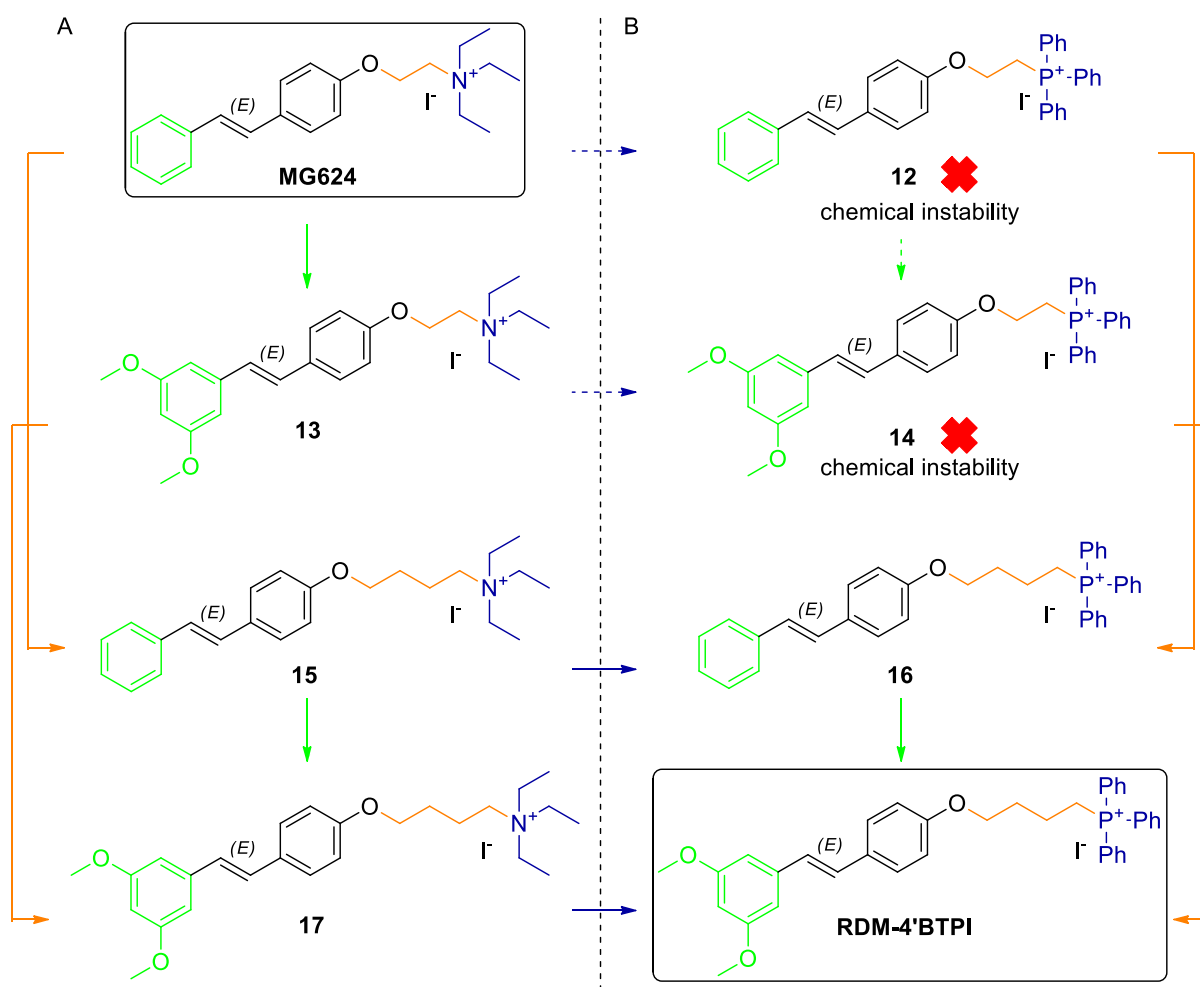


Figure 54: design of a series of hybrid compounds between the $\alpha 7$ and $\alpha 9$ - $\alpha 10$ antagonist **MG624** and the mitocan **RDM-4'BTPI**.

Furthermore, we were particularly interested in the elongation of the alkylene linker, a structural modification expected to be relevant to both nicotinic antagonism, for the increase of steric encumbrance, and cytotoxic pro-oxidant activity. Useful information would have been gained from $\alpha 7$ and $\alpha 9$ - $\alpha 10$ nAChR antagonism comparison between **13** and its two-carbon-elongated analogue **17** and between **MG624** and the elongated **15**, **25** and **26** analogues, while a further elongation of the butylene linker of the phosphonium derivatives was strongly suggested by evidences from the literature. In fact, **RDM-4'BTPI** has been suggested to act as mitoVE₁₁S, whose activity has been reported to be diminished by shortening its eleven-carbon long linker.¹⁴⁹ Consistently with such a trend, elongation of the short 4 C linker of **16**, the stilbene analogue of **RDM-4'BTPI**, could be beneficial. Therefore, we extended the series of compounds to be investigated over the stilbenoxyalkyl triphenylphosphonium iodides **18** and **19-24** having alkylene linkers of increasing length (Figure 55).

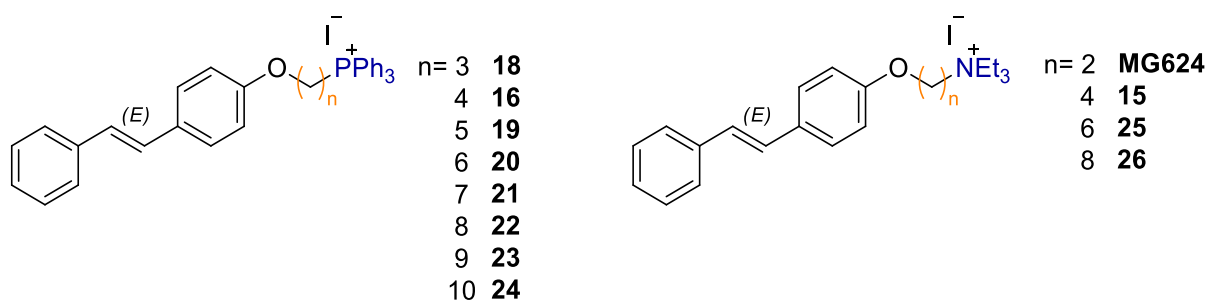


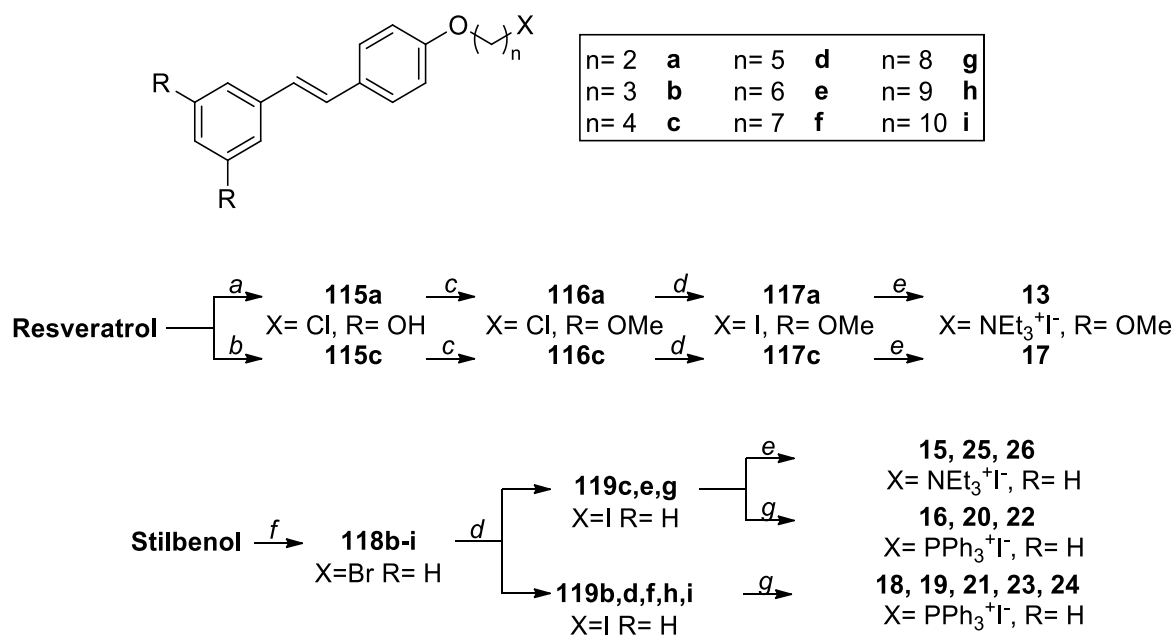
Figure 55: design of elongated analogues of compound **16** and of **MG624**.

2.4.2 Synthetic schemes

The target ammonium compounds **13** and **17** were synthesized starting from commercial resveratrol, while ammonium and phosphonium compounds **15**, **25**, **26**, **16** and **18-24** were from commercial 4-(*E*)-stilbenol (*Scheme 18*).

Alkylation of resveratrol with 1-bromo-2-chloroethane and 1-bromo-4-chlorobutane afforded, respectively, the intermediates **115a** and **115c**, whose free phenolic functions were methylated to obtain the O-chloroalkyl pterostilbene intermediates **116a** and **116c**. These were converted into the corresponding iodoalkyl analogues **117a** and **117c** by Finkelstein reaction and then into the final triethylammonium derivatives **13** and **17** by treatment with triethylamine.

The ethers **15**, **25**, **26**, **16** and **18-24** with stilbene scaffold were synthesized by the same strategy but using α,ω -dibromoalkanes to O-alkylate 4-(*E*)-stilbenol. The resulting ω -bromoalkyl ethers **118b-i** were converted into the corresponding ω -iodoalkyl ethers **119b-i**. Reaction of **119c**, **119e** and **119g** with triethylamine and triphenylphosphine afforded **15**, **25**, **26** and **16**, **20**, **22** respectively, while reaction of **119b**, **119d**, **119f**, **119h** and **119i** with triphenylphosphine provided the corresponding triphenylphosphonium derivatives **18**, **19**, **21**, **23**, **24**. **MG624** and **RDM-4'BTPI** were synthesized as previously reported.^{138,147}



Scheme 18: reagents and conditions. (a) 1-bromo-2-chloroethane, K₂CO₃, DMF, 60 °C, overnight, 32% (115a); (b) 1-bromo-4-chlorobutane, K₂CO₃, DMF, 60 °C, overnight, 30% (115c); (c) MeI, CsCO₃, DMF, rt, overnight, 90% (116a), 63% (116c); (d) NaI sat. in acetone, reflux, overnight, 97% (117a), 96% (117c), 98% (119b), 99% (119c), 100% (119d), 100% (119e), 100% (119f), 99% (119g), 100% (119h), 100% (119i); (e) NEt₃, toluene, reflux, 5 h, 89% (15), 92% (25), 92% (26), 81% (13), 75% (17); (f) NaOH, DMSO, rt, 3h, dibromopropane, 52% (118b) or dibromobutane, 37% (118c) or dibromopentane, 28% (118d) or dibromohexane, 40% (118e) or dibromoheptane, 41% (118f) or dibromooctane, 45% (118g) or dibromononane, 84% (118h) or dibromodecane, 37% (118i); (g) PPh₃, neat, 100 °C, 3 h, 72% (18), 80% (16), 92% (19), 89% (20), 89% (21), 86% (22), 81% (23), 87% (24).

2.4.3 Biology

Antiproliferative activity. Nine compounds, namely the three phosphoniums **RDM-4'BTPI**, **16** and **24** and all the six ammoniums **MG624**, **15**, **25**, **26** and **13**, **17**, were tested for their cytotoxic/cytostatic action using the MTS assay on U87MG glioblastoma, A549 adenocarcinoma and SH-SY5Y neuroblastoma cell lines (*Table 4*). The most interesting compounds were also tested using the same assay on normal mouse astrocytes. All the other phosphonium compounds, namely **18-23**, were assayed for their cytotoxic/cytostatic action on A549 and U87MG cell lines (*Table 5*). All of the tumor and control astrocytes were incubated with increasing concentrations of the compounds for 72 h and their activity was tested taking the absorbance of the control cells (not treated with compounds) as 100%. The dose–response curves were fitted by non-linear regression analysis and the concentration that blocked 50% of the viability (IC₅₀) was determined.

Binding affinities. The binding affinity of the synthesized compounds for the human α4β2 or α7 subtypes expressed in heterologous cells respectively labelled by [³H]-Epibatidine or [¹²⁵I]-

α -Bungarotoxin was assayed with competition binding experiments and the results were reported in *Table 4* and in *Table 5*.

In vitro functional activity. Inhibition of respectively 200 μ M or 10 μ M ACh-evoked currents in *Xenopus Oocytes* expressing human $\alpha 7$ and $\alpha 9$ - $\alpha 10$ nAChRs was tested for all the triethylammonium compounds **MG624**, **15**, **25**, **26**, **13**, **17** and for the triphenylphosphonium **RDM-4'BTPI**, according to the method previously used for **MG624** (*Table 4*).³⁷

HepG2 cells permeation. The ability of **MG624** to permeate HepG2 cells was evaluated exploiting their natural fluorescence. **MG624** fluoresces at 350 nm after excitation at 260 nm. **MG624** was administered in different concentrations (1, 10, 50, 100 μ M) to cells and fluorescence (RFU 350/620 nm) was measured after 1, 6 and 24 hours. A blank sample was included as reference (vehicle alone, DMSO), and its fluorescence (background signal) was subtracted from each normalized signal. The same assay was repeated at the single concentration of 1 μ M with compounds **15**, **26** and **22**. Cells treated with 100 μ M of **MG624** for 24 h were lysed and the cell lysates were analyzed by mass spectrometry, with the aim of finding fragments coming from **MG624** (*Figure 56*).

ROS production. We verified the effects of 1 h exposure of U87MG cells to the phosphonium and ammonium compounds on the ROS production as monitored by FACS experiments using the fluorescence indicator MitoSOX®. (*Figure 57* and *Table 5*).

ATP production. The ability of **MG624**, of **RDM-4'BTPI**, of the four hybrids (**15**, **16**, **13** and **17**) and of **24** to interfere with ATP production after incubation with U87MG cells in culture for 1 or 72 h was determined. The concentrations tested were those determined by the MTS assay and in the range of the IC₅₀ values (*Figure 58*).

2.4.4 Results and discussion

Antiproliferative activity. As shown in *Table 4*, at all the three tumoural cell lines tested, linker length elongation from **MG624** and **13** respectively to **15** and **17**, produced from slight (for glioblastoma U87MG and adenocarcinoma A549) to moderate (neuroblastoma SH-SY5Y) potency increase. Against adenocarcinoma A549 and neuroblastoma SH-SY5Y, the elongated ammonium compounds **15** and **17** were less potent (higher IC₅₀ values, in the range of 3-30 μ M) than the correspondent phosphonium compounds **16** and **RDM-4'BTPI** (IC₅₀ in the range 0.3-3 μ M), but they were similarly potent at glioblastoma cell lines U87MG.

Although phosphonium compounds were generally more potent than ammonium compounds, they revealed to be similarly potent against all the tumoral cell lines tested and against non-tumoral cells (astrocytes) (IC₅₀ in the range 0.5-3 μM). On the other hand, ammonium compounds, still active against U87MG and A549 cells, were less potent on SH-SY5Y or on control astrocytes cells (in the range of 10-30 μM).

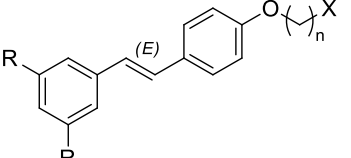
				<u>Viability</u> U87MG IC ₅₀ , μM 72h	<u>Viability</u> A549 IC ₅₀ , μM 72h	<u>Viability</u> SH-SY5Y IC ₅₀ , μM 72h	<u>Viability</u> Astrocytes IC ₅₀ , μM 72h	Affinity α7 K _i , nM	α7 IC ₅₀ nM	α9-α10 IC ₅₀ , nM
R=	n=	X=	Cpd							
H	2	NEt ₃ ⁺	MG624	4.4	4.7	>100	47	104	41	10
OMe	2	NEt ₃ ⁺	13	5.3	12	>100	23	189	47	17.2
H	4	NEt ₃ ⁺	15	1.8	3.5	31	20	186	6.5	5
OMe	4	NEt ₃ ⁺	17	0.57	3.3	11	22	305	24.3	11.9
H	4	PPh ₃ ⁺	16	0.64	0.42	3.0	0.4	1638	Not done	Not done
OMe	4	PPh ₃ ⁺	RDM-4'BTPI	0.86	0.26	0.55	1.0	1826	>10000	>10000
H	10	PPh ₃ ⁺	24	0.06	0.10	0.21	0.6	1930	Not done	Not done
H	6	NEt ₃ ⁺	25	3.9	3.6	30	5.8	465	12.3	4.8
H	8	NEt ₃ ⁺	26	0.11	0.49	10	2.0	164	92	6.6

Table 4: MG624, RDM-4'BTPI, their structural hybrids (13, 15, 16, 17) and the elongated analogues 24, 25 and 26: antiproliferative activity at glioblastoma U87MG, at adenocarcinoma A549, at neuroblastoma SH-SY5Y, at normal mouse astrocytes cell lines, α7 binding affinity, α7 and α9-α10 antagonism.

In both ammonium and phosphonium series, the maximum potencies corresponded to the maximum linker length, eight and ten methylenes respectively, converging on similar ≤ 100 nM U87MG and A549 cytotoxicities. Table 5 reports the cytotoxic/cytostatic action of all the phosphonium compounds on U87MG glioblastoma and A549 cell lines. The potency of the compounds almost monotonically increases along with the length of the alkylene linker from >1 μ M (**18**) to ≤ 100 nM IC_{50} values (**24**).

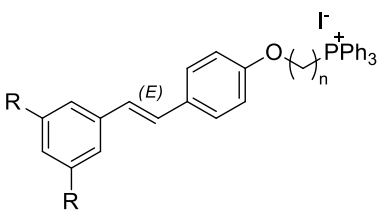
			Viability U87MG IC_{50} , μ M 72h	Viability A549 IC_{50} , μ M 72h	Affinity $\alpha 7$ receptors K_i , nM	% ROS production over 0.05 mM Antimycin A
R=	n=	Compound				
OMe	4	RDM-4'BTPI	0.86	0.26	1826	16.3
H	3	18	1.4	1.	984	21
H	4	16	0.64	0.42	1638	1.5
H	5	19	0.67	0.3	2800	20
H	6	20	0.38	0.15	559	27.3
H	7	21	0.36	0.1	617	39.5
H	8	22	0.07	0.26	909	46.3
H	9	23	0.09	0.11	1288	56.3
H	10	24	0.06	0.10	1930	58.2

Table 5: Phosphonium compounds **RDM-4'BTPI**, **16** and **18-24**: antiproliferative activity at U87MG and at A549 cells, binding affinity at the $\alpha 7$ nAChR accompanied by their confidence intervals (CI), %ROS production induced by administration of 500 nM of each compound compared with ROS production induced by 0.05 mM of Antimycin A.

Binding affinities. As the antiproliferative activity of **MG624** had already been related to its $\alpha 7$ and/or $\alpha 9$ - $\alpha 10$ nicotinic activity,³⁷ binding affinity at $\alpha 7$ subtype was determined for all the reported compounds.

The six compounds with ammonium head had similar $\alpha 7$ affinities, ranging between 100 and 500 nM K_i , whereas all the phosphonium compounds had much lower $\alpha 7$ affinities, approximately 6-10 times less than that of **MG624** (see Table 4 and Table 5). Phosphonium

compounds were expected to be poor binders at the nAChRs, because they lacked of the important pharmacophoric element of the positively charged ammonium group.

When tested on the $\alpha 4\beta 2$ subtypes, all the ammonium compounds showed very similar low affinities ($K_i > 3 \mu\text{M}$) (data not shown).

As single modifications, the linker elongation (compound **15**) and the 3',5'-dimethoxy substitution (compound **13**) only slightly diminished the high $\alpha 7$ nicotinic affinity of **MG624** ($0.104 \mu\text{M } K_i$), but, together, they led to a greater decrease (compound **17**, $0.3 \mu\text{M } K_i$). Further linker elongation to six and eight carbons was accomplished in the stilbene-ammonium series, providing **25**, with a decreased $\alpha 7$ nicotinic affinity ($0.465 \mu\text{M } K_i$), and **26**, that had an $\alpha 7$ affinity ($0.164 \mu\text{M } K_i$) similar to that of **MG624**.

After investigating the antiproliferative activity of the six hybrids on various tumor cells, we investigated whether the mechanisms of action underlying their antitumor activity were similar to that of **MG624** (reported as a $\alpha 7$ and $\alpha 9$ antagonist), to that of **RDM-4'BTPI** (reported as a mitocan), or they had hybrid mechanisms, by considering their nAChR activity and two intracellular parameters: the increase in mitochondrial ROS generation and the decrease in ATP production.

Antagonist activities. The six compounds with ammonium head inhibited $10 \mu\text{M}$ or $200 \mu\text{M}$ ACh-induced currents in oocytes expressing the human $\alpha 9\alpha 10$ and $\alpha 7$ subtypes with IC_{50} values $< 100 \text{ nM}$ (*Table 4*). Increasing the linker length from **MG624** to **15**, **25** and **26** sensibly increased antagonist potency against both subtypes except for **26**, whose $\alpha 7$ IC_{50} remained, however, sub- 100 nM .

We also tested the possible antagonist activity of the low affinity binder **RDM-4'BTPI** on nicotinic subtypes; the IC_{50} was greater than $10 \mu\text{M}$ at $\alpha 7$ and $\alpha 9\alpha 10$ subtypes, confirming that phosphonium compounds were not active on nAChRs and meaning that their antitumoural activity has to be related to a different MoA.

Overall, similar trends observed for $\alpha 7$ affinity were observed for $\alpha 7$ and $\alpha 9\text{-}\alpha 10$ antagonism: 1) the 3',5'-dimethoxy substitution from **MG624** to **13** was irrelevant both for $\alpha 7$ and $\alpha 9\text{-}\alpha 10$ IC_{50} s; 2) the elongation of the linker from 2 carbons to 4 carbons was beneficial both for **15** and for **17**. Further elongation in the StN series to **25** (6 carbons) and to **26** (8 carbons) confirmed the $\alpha 9\text{-}\alpha 10$ sub- 10 nM potency achieved by **15** and, though not ameliorative, the considerable sub- 100 nM potency of **MG624** at the $\alpha 7$ subtype. Overall, as shown in *Table 1*, elongation of

the ethylene linker in the ammonium compounds resulted in generally higher antagonist activities at the two nicotinic receptors with non-negligible $\alpha 9$ - $\alpha 10$ vs $\alpha 7$ selectivity in the case of **26**.

As all the ammonium compounds are active in blocking ACh-induced currents mediated by $\alpha 7$ and $\alpha 9$ subtypes, their moderate to high antitumoral activities could be correlated to their nicotinic activity.

Cell permeation. Prior to determine whether **MG624**, the structural hybrids between **MG624** and **RDM-4'BTPI** and their elongated derivatives could at least partially impair the mitochondrial functionality as mitocans in a similar way to **RDM-4'BTPI**, their cell membrane permeability had to be ascertained. Whereas the triphenylphosphonium moiety is known to confer mitochondrial tropism to molecules due to its lipophilicity and positive charge,¹⁴⁵ cell permeation of triethylammonium-containing molecule had to be investigated.

Our findings clearly indicated that **MG624** is taken up by HepG2 cells with a concentration and time response trend (*Figure 56A*). Mass spectrometry analysis confirmed **MG624** intake from HepG2 cells when they were incubated for 24 h with 100 μ M of **MG624**. The MS/MS fragmentation pattern of the cell lysate and the observed product ions are completely assigned to the product ions generated during the fragmentation. In the MS/MS spectrum the base peak at m/z 222.9 corresponds to the loss of the styrene moiety. This experiment clearly showed that **MG624** permeates the cell membrane and therefore satisfies the first requirement necessary to be classified as a mitocan.

Cell membrane permeability was also tested for the elongated compounds **15**, **26** and its phosphonium analogue **22**. Prior to evaluate their permeability, the compounds were assessed for their fluorescence properties and they were found to emit at 350 nM upon irradiation at 260 nM with the same magnitude of **MG624**. Interestingly, they were all found to permeate the cell membrane when administered at 1 μ M with a time dependent trend (*Figure 56B*).

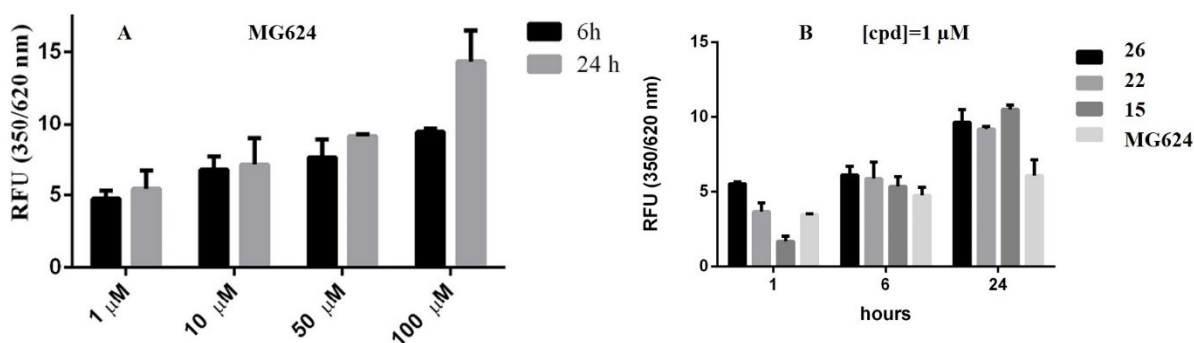


Figure 56: A) concentration- and time-dependent HepG4 cell membranes permeation of **MG624**; B) time-dependent HepG4 cell membranes permeation of 1 μ M of compounds **26**, **22**, **15**, **MG624**.

ROS production. The first intracellular parameter that we examined was ROS production in the mitochondria. Mitocans like **RDM-4'BTPI** are driven toward the mitochondrial matrix (negative relative voltage) due to their quaternary but lipophilic onium group, where they impair mitochondrial functionality by interacting with the respiratory processes. Particularly, **RDM-4'BTPI** has been shown to enhance ROS production by inhibiting the complex I and III.¹⁴⁸

Aiming to understand whether **MG624**, the hybrids between **MG624** and **RDM-4'BTPI** and their elongated analogues, could enhance ROS production in the mitochondria, we measured mitochondrial ROS production in U87MG cells upon administration of the compounds at a concentration similar to the EC₅₀ in the MTS assay.

None of the triethylammonium compounds increased ROS production, while all the triphenylphosphoniums **RDM-4'BTPI**, **16** and **18-24** enhanced ROS production in a dose-dependent manner, with potency increasing accordingly to the alkylene linker length (*Figure 57* and *Table 5*). Therefore, phosphonium compounds permeate the cell membranes and are driven toward the mitochondria, where they increase ROS production (acting as mitocans), while ammonium compounds, according to this assay, permeate the cell membrane but appear not to enhance ROS production. On the other hand, phosphonium compounds have only modest affinity and no antagonist activity at the α 7 and α 9 subtype, while ammonium compounds potently block ACh-induced currents mediated by the α 7 and α 9 subtype.

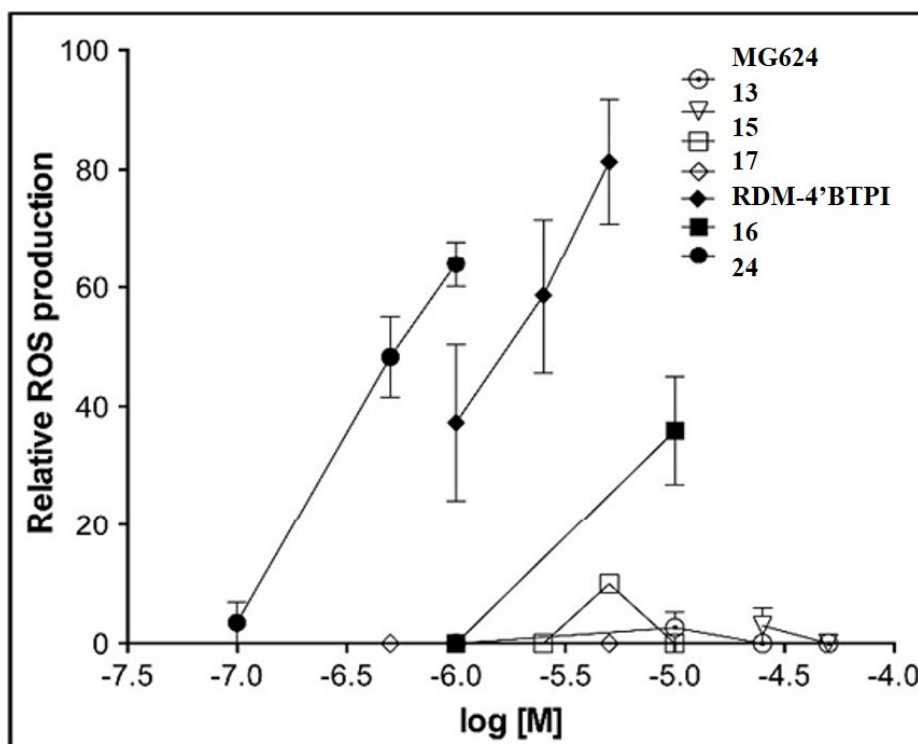


Figure 57: phosphonium compounds **RDM-4'BTPI**, **16** and **24** increase mitochondrial ROS production in a concentration-dependent manner, while the ammonium compounds **MG624**, **13**, **15** and **17** do not enhance ROS production. The compounds were tested at concentrations in the range of their EC_{50} .

According to these results, the antitumoural activity appear to be related to a mitocan-like mechanism for phosphonium compounds, while to nicotinic antagonism for ammonium compounds. However, among other cytotoxic effects, the mitocan **RDM-4'BTPI** has been reported to impair ATP production, probably by decoupling the respiratory chain from the F_0F_1 ATPase. Consequently, enhancement of ROS production alone can't be used to claim to clearly distinct MoAs of the structural hybrids between **MG624** and **RDM-4'BTPI**.

ATP production. The second intracellular parameter we examined was the decrease in ATP production, which is indicative of dysregulated mitochondrial function and antitumor activity.¹⁵⁰ Tumor cells have to upregulate their inefficient glycolytic ATP production in order to satisfy their energy requirements and preventing mitochondrial ATP production has a highly toxic and antiproliferative effect. There was a reduction in the ATP production in glioblastoma cells, as early as one hour after the administration of **RDM-4'BTPI** and **15** (Figure 58A), whereas ATP was reduced only after 72 hours in the case of the other three ammonium derivatives, **MG624**, **13** and **17** (Figure 58B). Phosphonium **16**, unlike its 3',5'-dimethoxy substituted analogue **RDM-4'BTPI**, did not affect ATP production. Of note removal of the two methoxyls is not necessarily detrimental for such an activity considering that **24**, the elongated

analogue of **16**, is a potent inhibitor of ATP production though devoid of these substituents at the distal phenyl ring.

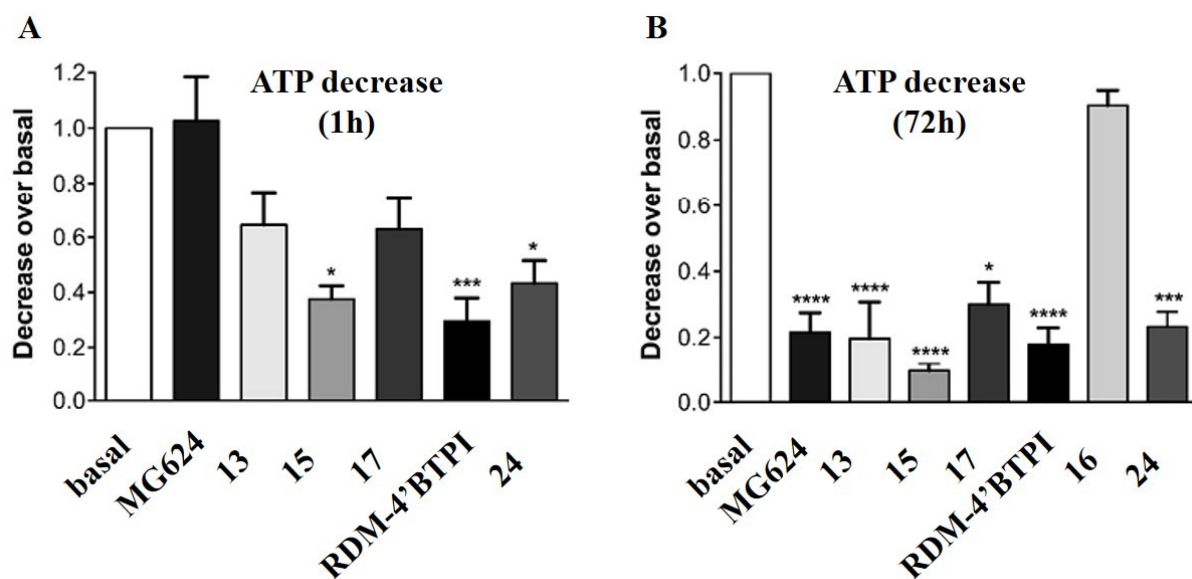


Figure 58: decrease of ATP production in glioblastoma cells after A) 1 hour or B) 72 hours of incubation with **MG624**, **RDM-4'BTPI**, their structural hybrids and **24**. **16** didn't reduce ATP production after 72 hours and was further excluded by the assay at 1 hour.

Overall, the results of these experiments indicate that the mechanism of action underlying the antitumor activity of the triphenylphosphonium derivatives is the profound impairment of mitochondrial functions, as revealed by the immediate and conspicuous increase in ROS production and decrease in ATP production and by their quite indistinct cytotoxicity. On the other hand, the antitumor activity of the triethylammonium derivatives seems to be mainly connected to their interactions with $\alpha 7$ and $\alpha 9$ - $\alpha 10$ nAChRs. However, it cannot be excluded that, after entering cells, the triethylammonium derivatives, interfere with mitochondria function albeit less potently than the phosphonium analogues possibly due to a lower level of mitochondriotropism. This may be why, with the exception of **15**, our triethylammonium derivatives decreased ATP production, only after 72 hours, and induced no immediate increase in ROS production.

As expected, elongation of the alkylene linker in the phosphonium series, importantly ameliorated antitumoural activity at glioblastoma U87MG and adenocarcinoma A549 cell lines, reaching, on glioblastoma cell lines, an IC_{50} of $0.06 \mu M$ for **24**, the longest in the series, due to enhanced mitocans properties, as shown by ROS production increase. However, as exemplified by **24**, phosphonium compounds were also cytotoxic/cytostatic at neuroblastoma cell lines SH-

SY5Y and at normal mouse astrocytes and therefore they were not selective against specific tumoural cell lines or against non-tumoral cells.

Similarly, elongation of the alkylene linker in the ammonium series markedly enhanced antitumoural activity, reaching in **26**, the longest term in the series, IC₅₀ of 0.11 μM on glioblastoma cells. For the ammonium compounds, the antitumoural activity coincided with high capacity of blocking ACh-induced currents in *Xenopus Oocytes* expressing α7 and α9α10 nAChRs, with IC₅₀s in the range of 10-100 nM. Differently from the phosphonium series, ammonium compounds had cytotoxic/cytostatic effects on glioblastoma U87MG and on adenocarcinoma A549 cells, while they were less toxic at neuroblastoma SH-SY5Y and at normal mouse astrocytes. **26**, the compound with highest antiproliferative activity, was also a very potent and moderately selective α9α10 antagonist.

Concluding remarks and future perspectives

Development of new subtype-selective nAChR ligands with different pharmacological profiles will certainly enable further understanding of the molecular mechanisms underlying many pathologies, such as nicotine addiction and glioblastoma. The new ligands presented in this dissertation provide a new platform for the design and development of other novel $\alpha 4\beta 2$ -selective partial agonists as smoking cessation agents and of $\alpha 7$ - and/or $\alpha 9/\alpha 9\alpha 10$ -selective antagonists as antiglioblastoma/anticarcinoma agents.

Part 1: $\alpha 4\beta 2$ nAChRs partial agonists

Mutational studies

New $\alpha 4\beta 2$ weak partial agonists could be designed starting from the scaffolds of *(S,R)*-**IV**, *(S,R)*-**IVa**, *(S,R)*-**5** and *(S,S)*-**9c**, upon clarification of the role played by the residue Ser108 in binding affinity and in receptor activation. Indeed, as introduced in paragraph 1.8, the side chain of Ser108 ($\beta 2$ subunit) seems to be 1) involved in binding the water molecule that bridges either *(S)*-nicotine or *(S,R)*-**5** with the receptors; 2) involved in binding directly the hydroxyl appendage of *(S,R)*-**IVa** or the amino group of *(S,R)*-**9c**; 3) not involved in binding the naked benzodioxane moiety of *(S,R)*-**IV**. As all the rigid ligands predicted to interact with such a residue are partial agonists, while *(S,R)*-**IV** is an antagonist, this interaction could also be involved in receptor activation. If so, novel partial agonists targeting specifically that residue could be designed. To shed light on this pocket, we are currently designing a mutational study where we will replace Ser108 with apolar residues (i.e. Phe, Leu, Ala). We will then reveal the role of Ser108 by evaluation of binding affinity and electrophysiological activity of *(S,R)*-**IV** and at least one partial agonist (i.e. *(S,R)*-**IVa**, or *(S,R)*-**5** or *(S,S)*-**9c**) at the wild type and mutated receptors.

In-vivo activity

Although the pharmacological profile of *(S,R)*-**IVa** and of *(S,S)*-**9c** is promisingly similar to that of the clinically approved Varenicline, no *in-vivo* data on *(S,R)*-**IVa** and on *(S,S)*-**9c** are currently available. Upon investigation of the ADMET profiles *in-silico* and *in-vitro*, a behavioural study on animal models (i.e. *Zebrafish*) could be performed with the most interesting compounds, to probe whether they could be relevant in nicotine addiction or in cognitive deficits.

Part 2: $\alpha 7$ and $\alpha 9/\alpha 9\alpha 10$ nAChRs antagonists

SAR investigation

The $\alpha 7$ and $\alpha 9/\alpha 9\alpha 10$ nAChRs antagonists reported in this dissertation will provide an optimal platform for further investigation of the structure activity relationships. Particularly, the structural requirements to diversificate between $\alpha 7$ -selectivity (vs $\alpha 9/\alpha 9\alpha 10$) and $\alpha 9/\alpha 9\alpha 10$ -selectivity (vs $\alpha 7$) should be identified. Compound **26** is moderately selective for the $\alpha 9/\alpha 9\alpha 10$ and could therefore represent a new lead compound for the development of $\alpha 9/\alpha 9\alpha 10$ -selective antagonists. The SAR analysis could be systematically performed on the three moieties of the chosen lead compound (i.e. **MG624**, **15** or **26**): 1) development of analogues bearing charged ammonium heads with diverse linear or cyclic alkyl substituents, to probe the size of the cavity where the positive nitrogen is lodged; 2) development of rigid analogues, where the flexible linker is constrained into a cyclic structure, to identify the binding conformation at both subtypes; 3) replacement of the stilbene or pterostilbene aromatic moieties with other scaffolds, to probe the role of geometry, planarity, lipophilicity and electronic properties. Furthermore, these modifications could be designed considering the optimization of physicochemical properties. Homology modelling of the $\alpha 7$ and $\alpha 9/\alpha 9\alpha 10$ subtype could support the SAR investigation.

Intracellular mechanism of actions

The structural hybrids between an $\alpha 7$ and $\alpha 9/\alpha 9\alpha 10$ antagonist and a mitocan developed in this thesis could be used to further investigate the MoAs underlying their antiglioblastoma and antiadenocarcinoma activities. Specifically, they could be exploited to support the identification of intracellular pathways which link the $\alpha 7$ and $\alpha 9/\alpha 9\alpha 10$ antagonist activity to the antiproliferative activity.

In-vivo activity

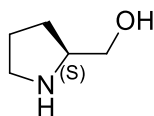
The antiproliferative activity of **24** and of **26** on glioblastoma and adenocarcinoma cell lines is very promising and **26** is not toxic on healthy astrocytes. However, ADMET profiles *in-silico* and *in-vitro*, should be performed with the aim of developing analogues with comparable antiglioblastoma and antiadenocarcinoma potencies but with pharmacokinetic profiles suitable for an *in-vivo* evaluation of efficacy and safety in animal models of glioblastoma and adenocarcinoma.

Experimental section

All chemicals and solvents were used as received from commercial sources or prepared as described in the literature. Flash chromatography purifications were performed using KP-Sil 32-63 μm 60 \AA cartridges. TLC analyses were carried out on alumina sheets precoated with silica gel 60 F254 and visualized with UV light; Rf values are given for guidance. ^1H and ^{13}C -NMR spectra were recorded at 300 and 75 MHz using an FT-NMR spectrometer. Chemical shifts are reported in ppm relative to residual solvent (CHCl_3 , MeOH or DMSO) as internal standard. Melting points were determined by Buchi Melting Point B-540 apparatus. Optical rotations were determined in a 1 dm cell of 1 mL capacity. Chiral HPLC analyses were performed using Hewlett Packard 1050 instrument. CHN, P and I elemental microanalysis were performed. Phosphorous was measured by ICP-AES (Inductively Coupled Plasma Atomic Emission Spectroscopy), upon microwave-assisted mineralization of the sample in HNO_3 . Iodine was measured by ionic chromatography, upon thermal decomposition at 1000 $^\circ\text{C}$. High Resolution Electrospray Mass Spectra of all the final compounds were acquired with Q-TOF Synapt G2 Si (WATERS).

Part 1: $\alpha 4\beta 2$ nAChRs

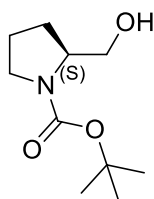
Synthesis of (*S*)-prolinol



Molecular Weight: 101.15

Procedure adapted from literature.¹⁵¹ Under nitrogen atmosphere, LiAlH₄ (2.96 g – 78.16 mmol) was suspended in 110 mL of anhydrous THF and refluxed for 15 minutes. The heating was suspended and the commercial (*S*)-proline (5 g – 43.42 mmol) was added stepwise, so that to maintain a boiling mixture. Afterward, the reaction was refluxed for 2 hours under vigorous stirring. After cooling to 40 °C, the mixture was treated with a 20% aqueous solution of KOH and filtered. The filtration cake was resuspended in fresh THF (40 ml), refluxed for 30 minutes and then filtered on a small pan of Celite®. The two filtrates were reunited, and the solvent was evaporated under vacuum to obtain the desired product as a dark yellow oil (3.8 g – 37.6 mmol, 87%). $[\alpha]_D^{25} = +31.70^\circ$ (*c*1, CHCl₃); literature¹⁵²: $[\alpha]_D^{25} = +35.6^\circ$ (*c*1, CHCl₃). ¹H-NMR (300 MHz, CDCl₃): δ 3.55 – 3.48 (m, 1H), 3.34 – 3.24 (m, 2H), 3.15 – 3.04 (bs, 2H), 2.96 – 2.82 (m, 2H), 1.86 – 1.66 (m, 3H), 1.45 – 1.34 (m, 1H).¹⁵³

Synthesis of (*S*)-*N*-*tert*-butoxycarbonyl-prolinol



Molecular Weight: 201.26

Procedure adapted from literature.¹⁵⁴ (*S*)-prolinol (4.21 g – 41.62 mmol) was dissolved in 42 ml of DCM and the resulting solution was cooled to 0 °C. Afterward, 6 ml of TEA (4.65 g – 45.82 mmol) and di-*tert*-butyl dicarbonate (10 g – 45.82 mmol) were added under vigorous stirring. The reaction mixture, warmed to room temperature, was vigorously stirred for 30 minutes. The suspension was diluted with 30 ml of DCM and then washed twice with a 1M aqueous solution of HCl. The organic phase was dried over anhydrous sodium sulphate, filtered and concentrated under vacuum affording a crude, that was purified by silica gel flash chromatography (Cyclohexane/Ethyl Acetate 75:25, R_f=0.4). The pure product was isolated as a white solid (6.28g – 31.22 mmol, 75%). TLC (Dichloromethane / Methanol 95:5 + 1% NH₃(30% in water); stained with KMnO₄): R_f= 0.7. **M.p.** = 56.0 °C; Literature¹⁵⁵: **M.p.** = 56.1 -

57.4 °C. $[\alpha]_D^{25} = -46.76^\circ$ (*c*1, CHCl₃); literature¹⁵⁶: $[\alpha]_D^{20} = -45.9^\circ$ (*c*1, CHCl₃). ¹H-NMR (300 MHz, CDCl₃): δ 3.97 (m, 1H), 3.65 – 3.53 (m, 2H), 3.49 – 3.40 (m, 1H), 3.34 – 3.26 (m, 1H), 3.01 (bs, 1H), 2.06 – 1.94 (m, 1H), 1.88 – 1.71 (m, 2H), 1.67 – 1.52 (m, 1H), 1.44 (s, 9H).¹⁵³

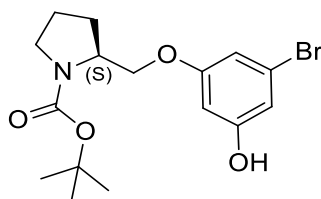
Synthesis of 3-hydroxy-5-bromophenol



Molecular Weight: 189.01

Procedure adapted from literature.¹⁵⁷ BBr₃ (65.5 mmol – 1M in hexane) was added dropwise under anhydrous atmosphere to a solution of 1-bromo-3,5-dimethoxybenzene (7 g – 32.25 mmol) in 23 ml of anhydrous DCM, previously cooled to -10 °C. The reaction mixture was stirred at room temperature for 12 hours. Afterwards, the mixture was cooled to -10° C and the excess of BBr₃ was quenched by adding dropwise 20 ml of methanol. The solvent was evaporated under vacuum and the resulting residue was diluted with ethyl acetate and washed with water. The organic phase was dried over anhydrous sodium sulphate, filtered and the solvent was removed by rotary evaporation. The resulting crude was purified by silica gel flash chromatography, affording the pure product as a pale green solid (3.96 g – 20.96 mmol, 65%). TLC (Cyclohexane / Ethyl Acetate 7:3, stained with Cerium Sulphate): **R_f** = 0.4. **M.p.** = 72.0 °C. ¹H-NMR (300 MHz, CD₃OD): δ 6.41 (d, *J* = 2.1 Hz, 2H); 6.19 (t, *J* = 2.1 Hz, 1H).¹⁵⁷

Synthesis of (*S*)-*N*-*tert*-butoxycarbonyl-2-[(3-hydroxy-5-bromo)phenoxy]methylpyrrolidine [(*S*)-27]

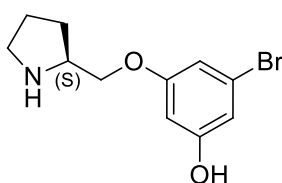


Molecular Weight: 372.25

3-hydroxy-5-bromo-phenol (705 mg – 3.73 mmol) and (*S*)-*N*-*tert*-butoxycarbonyl-prolinol (500 mg – 2.48 mmol), dissolved each in 2 ml of anhydrous THF, were added to a solution of triphenylphosphine (787 mg – 3.00 mmol) in 2 ml of anhydrous THF. The reaction mixture was cooled to -10°C and DIAD (0.60 mL – 3.00 mmol) was added dropwise, under vigorous stirring. The reaction mixture was refluxed for 12 hours. After cooling to room temperature, the mixture

was diluted with 10 mL of 1M aqueous solution of NaOH and extracted with DCM twice. The organic phase was dried over anhydrous sodium sulphate, filtrated and concentrated in vacuo to obtain a crude that was further purified through silica-gel flash column chromatography (gradient from cyclohexane to cyclohexane/ethyl acetate 9:1). The pure compound (*S*)-**27** was obtained as a white solid (317 mg – 0.85 mmol, 34%). **TLC** (Cyclohexane / Ethyl Acetate 9:1): **R_f** = 0.5. **M.p.** = 140.5 °C. **[α]_D²⁵** = -23.87° (*c*1, CHCl₃). **¹H-NMR** (300 MHz, CDCl₃): δ 6.60 (m, 2H), 6.38 (s, 1H), 4.10 – 4.02 (m, 2H), 3.77 (m, 1H), 3.37 (m, 2H), 2.00 – 1.83 (m, 4H), 1.48 (s, 9H).

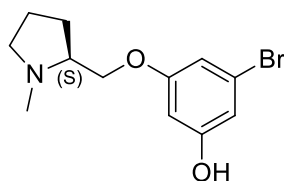
Synthesis of (*S*)-2-[(3-hydroxy-5-bromo)phenoxy]methylpyrrolidine [(*S*)-**29**]



Molecular Weight: 272.14

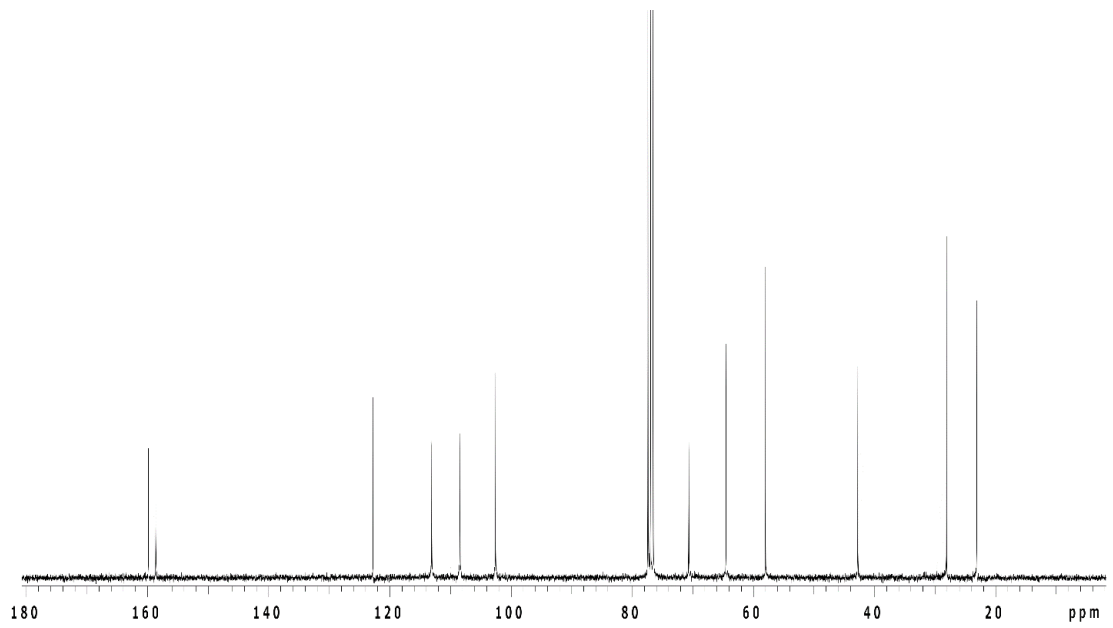
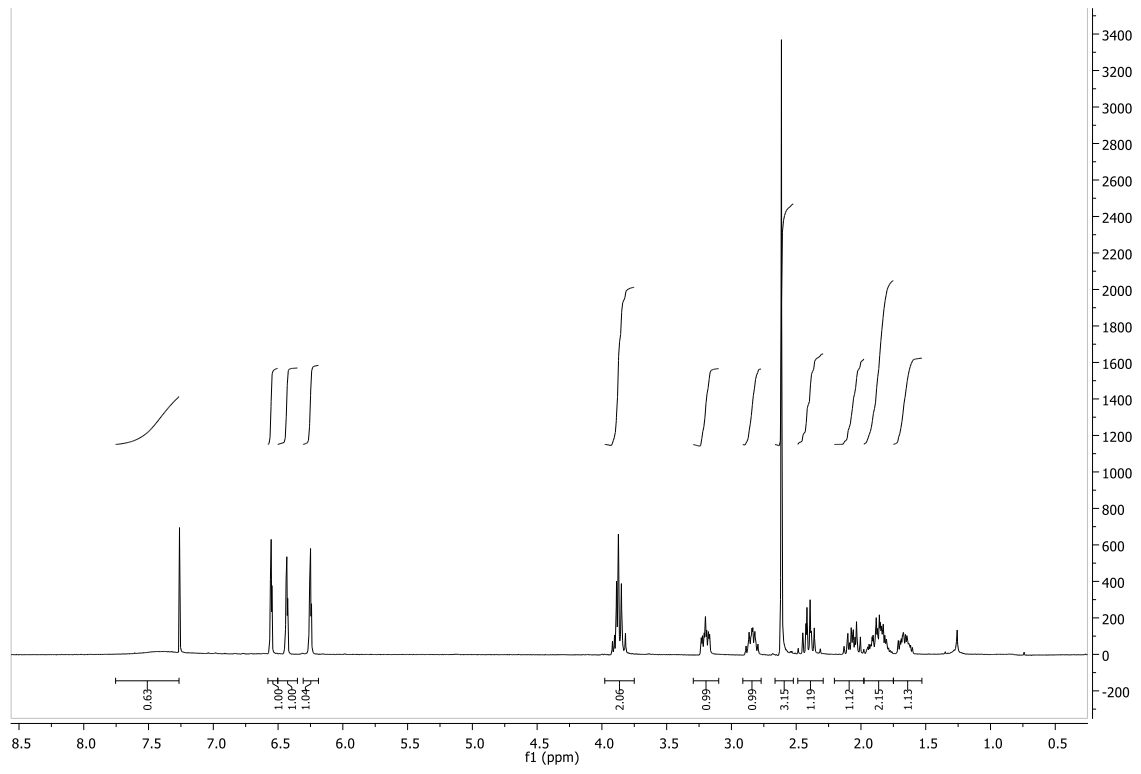
(*S*)-*N*-*tert*-butoxycarbonyl-2-[(3-hydroxy-5-bromo)phenoxy]methylpyrrolidine [(*S*)-**27**] (209 mg – 0.56 mmol) was dissolved in 5 ml of DCM and the resulting solution was cooled to 0 °C. Under vigorous stirring, TFA (1 ml) was added dropwise and the reaction mixture was stirred at room temperature for 2 hours. Afterward, the mixture was diluted with an aqueous solution of HCl 1M (8 ml) and washed with diethyl ether. The aqueous phase was cooled to 0 °C and the pH was adjusted to pH 12 by adding dropwise a solution of NaOH 1 M. After washing again with diethyl ether, the aqueous phase was cooled to 0 °C and acidified with acetic acid to reach pH 6/7 and extracted with ethyl acetate. The organic phase was dried over anhydrous sodium sulphate, filtered and evaporated in vacuo obtaining the desired product (*S*)-**29** as a white sticky solid (122 mg – 0.45 mmol, 80%). **TLC** (Dichloromethane / Methanol 95:5 + 0.3 % NH₃(30% in water)): **R_f** = 0.2. **[α]_D²⁵** = +9.07° (*c*1, MeOH). **¹H-NMR** (300 MHz, CD₃OD): δ 6.55 (m, 2H), 6.31 (m, 1H), 3.94 (m, 1H), 3.85 (m, 1H), 3.53 (m, 1H), 3.07 – 2.90 (m, 2H), 2.07 – 1.96 (m, 1H), 1.91 – 1.78 (m, 2H), 1.66 – 1.47 (m, 1H).

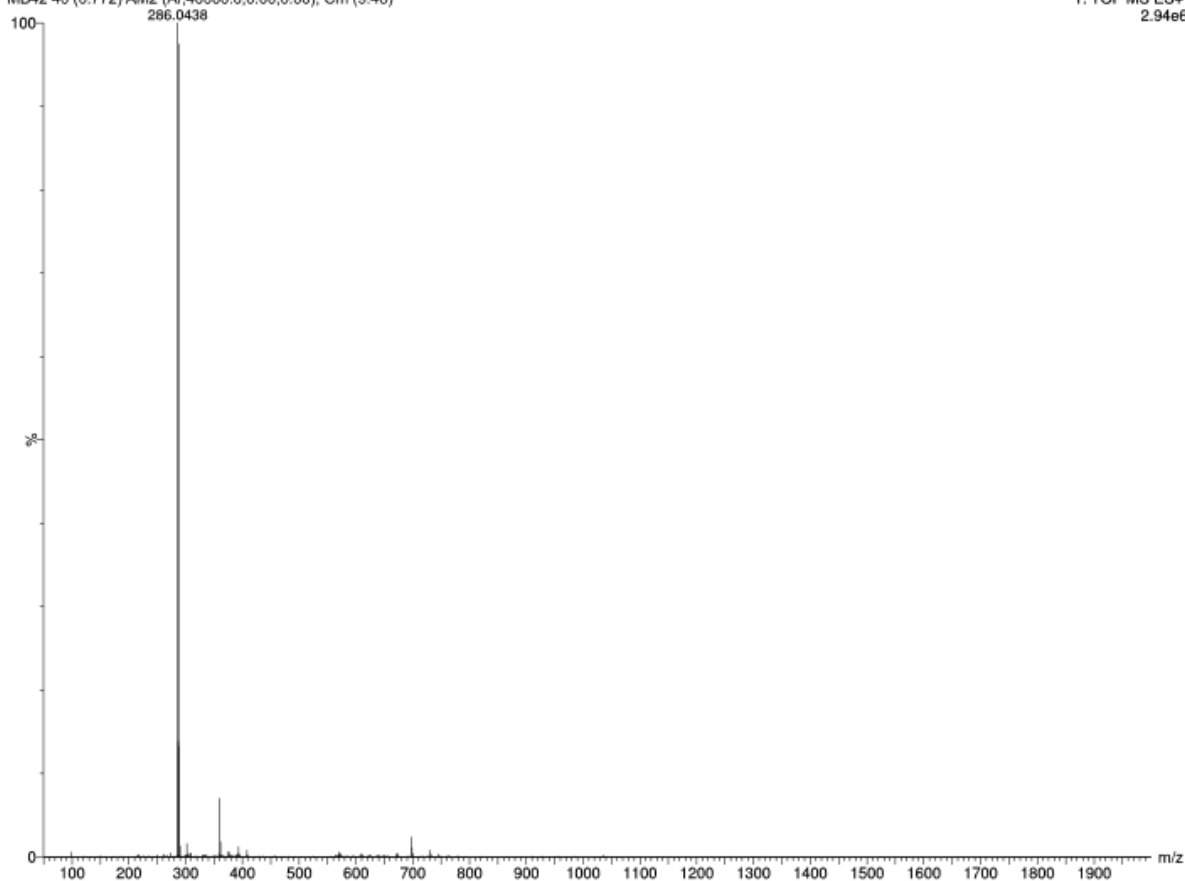
Synthesis of (*S*)-*N*-methyl-2-[(3-hydroxy-5-bromo)phenoxy]methylpyrrolidine [(*S*)-**1a**]



Molecular Weight: 286.16

Under vigorous stirring at 0 °C, an aqueous solution of formaldehyde (37% in water, 0.13 ml) was added dropwise to a solution of (*S*)-2-[(3-hydroxy-5-bromo)phenoxy]methylpyrrolidine [(*S*)-**29**] (120 mg – 0.44 mmol) in 8 ml of methanol and 160 µl of glacial acetic acid. Upon addition of 2-picolin borane (50 mg – 0.44 mmol), the mixture was reacted for 4 hours at room temperature. The solvent was evaporated in vacuo, the residue was diluted with 10 ml of a 1M HCl solution and stirred for 1 hour to quench the unreacted 2-picolin-borane. Then, the pH was adjusted to 8 by adding an aqueous solution of Na₂CO₃ 2M and the aqueous phase was extracted with ethyl acetate (3x30 ml). The organic phase was washed with brine, dried over sodium sulphate, filtered and evaporated in vacuo, providing a crude that was purified through silica gel flash chromatography. The pure compound (*S*)-**1a** was obtained as a yellow sticky solid (125 mg – 0.39 mmol, 75%). **TLC** (Dichloromethane / Methanol 98:2 + 1% NH₃(30% in water)): **R_f**= 0.2. **[α]_D²⁵** = -18.36° (*c*1, CH₃OH). **¹H-NMR** (300 MHz, CDCl₃): δ 6.56 (t, *J*= 1.9 Hz 1H), 6.47 (t, *J*= 1.9 Hz, 1H), 6.28 (t, *J*= 1.9 Hz, 1H), 4.00 – 3.81 (m, 2H), 3.21 – 3.14 (m, 1H), 2.86 – 2.79 (m, 1H), 2.60 (s, 3H), 2.42 – 2.31 (m, 1H), 2.12 – 2.00 (m, 1H), 1.93 – 1.89 (m, 2H), 1.82 – 1.61 (m, 1H). **¹³C-NMR** (75 MHz, CDCl₃): δ 159.9, 158.7, 122.8, 113.1, 108.4, 102.6, 70.7, 64.6, 58.0, 42.8, 28.2, 23.1. **HRMS (ESI⁺)**: calc. for C₁₂H₁₇NO₂⁷⁹Br: theor. 286.0443; found [M+H]⁺: 286.0438.





Elemental Composition Report

Single Mass Analysis

Tolerance = 5.0 PPM / DBE: min = -1.5, max = 200.0
 Element prediction: Off
 Number of isotope peaks used for i-FIT = 5

Monoisotopic Mass, Even Electron Ions

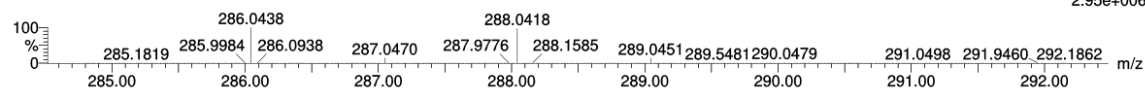
130 formula(e) evaluated with 1 results within limits (all results (up to 1000) for each mass)

Elements Used:

C: 12-12 H: 10-100 N: 0-5 O: 0-5 Na: 0-1 Br: 0-1

MB42 40 (0.772) AM2 (Ar,40000.0,0.00,0.00); Cm (9:48)

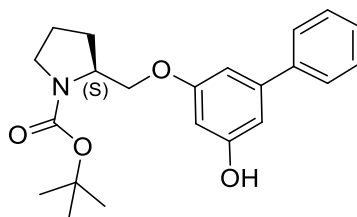
1: TOF MS ES+
2.95e+006



Minimum: -1.5
 Maximum: 0.5 5.0 200.0

Mass	Calc. Mass	mDa	PPM	DBE	i-FIT	Norm	Conf (%)	Formula
286.0438	286.0443	-0.5	-1.7	4.5	2371.1	n/a	n/a	C12 H17 N O2 Br

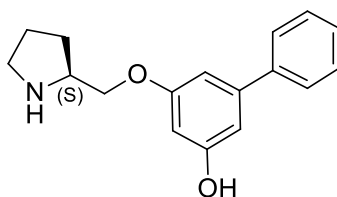
Synthesis of (*S*)-*N*-*tert*-butoxycarbonyl-2-[(3-hydroxy-5-phenyl)phenoxy]methylpyrrolidine [(*S*)-31]



Molecular Weight: 369.45

Under nitrogen atmosphere, tetrakis(triphenylphosphine)Pd(0) (30 mg – 0.026 mmol) was added to a solution of (*S*)-*N*-*tert*-butoxycarbonyl-2-[(3-hydroxy-5-bromo)phenoxy]methylpyrrolidine [(*S*)-27] (250 mg – 0.672 mmol) in 6 ml of toluene. Upon stirring for 10 minutes at room temperature, 2 ml of an aqueous solution of Na₂CO₃ 2M and a solution of *p*-hydroxyphenyl boronic acid (90 mg – 0.74 mmol) in ethanol (1.5 ml) were sequentially added. The mixture was refluxed for 12 hours. Afterward, the mixture was diluted with ethyl acetate (30 ml) and the organic phase was dried over anhydrous sodium sulphate, filtered and concentrated in vacuo, providing a crude that was purified through silica gel flash chromatography (cyclohexane/ethyl acetate 9:1). The pure product (*S*)-31 was obtained as a white sticky solid (185 mg – 0.50 mmol, 75%). TLC (Cyclohexane / Ethyl Acetate 8:2): R_f = 0.5. [α]_D²⁵ = -17.04 ° (c0.5, CHCl₃). ¹H-NMR (300 MHz, CDCl₃): δ 7.55 (d, *J* = 9.3 Hz, 2H), 7.42 – 7.31 (m, 3H), 6.68 (m, 2H), 6.54 (m, 1H), 6.27 (bs, 1H), 4.19 – 4.09 (m, 2H), 3.87 (m, 1H), 3.40 (m, 2H), 2.04 – 1.84 (m, 4H), 1.47 (s, 9H).

Synthesis of (*S*)-2-[(3-hydroxy-5-phenyl)phenoxy]methylpyrrolidine [(*S*)-37]

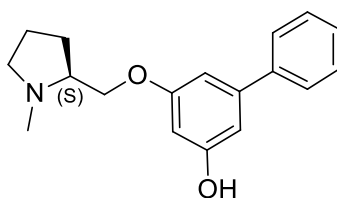


Molecular Weight: 269.34

(*S*)-*N*-*tert*-butoxycarbonyl-2-[(3-hydroxy-5-phenyl)phenoxy]methylpyrrolidine [(*S*)-31] (185 mg – 0.50 mmol) was dissolved in 2 ml of methanol and the solution was cooled to 0 °C. Upon dropwise addition of 2.5 ml of a 1.25 M methanolic solution of HCl under vigorous stirring, the reaction mixture was warmed to room temperature and reacted for 12 hours. Afterward, methanol was evaporated in vacuo, the residue was diluted with a 1 M aqueous solution of HCl

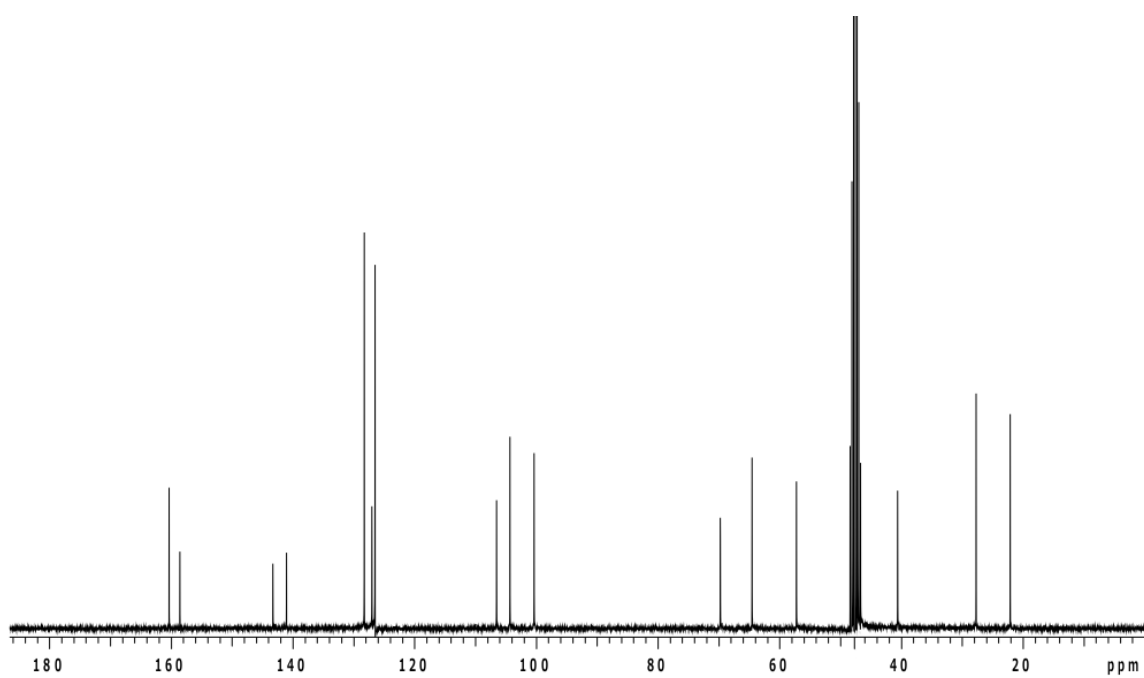
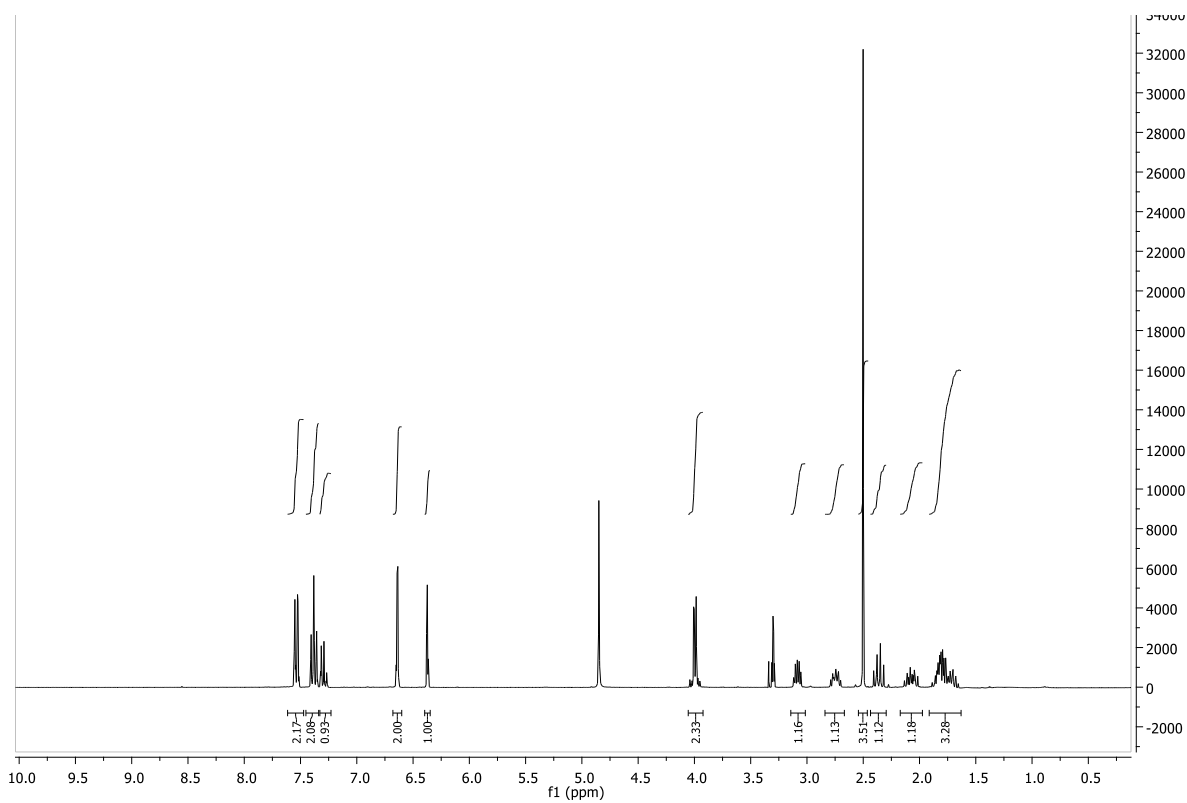
(5 ml) and washed with DCM. The aqueous phase was basified to pH 8 with NH_3 (30% in water) and extracted with ethyl acetate. The organic phase was dried over anhydrous sodium sulphate, filtrated and evaporated in vacuo, affording the pure product (*S*)-**37** as a yellow solid (135 mg – 0.50 mmol, 100%). **TLC** (Dichloromethane / Methanol 9:1 + 3% NH_3 (30% in water)): **Rf**= 0.25. $[\alpha]_{\text{D}}^{25} = +2.71^\circ$ (*c*0.5, CH_3OH). **$^1\text{H-NMR}$** (300 MHz, CD_3OD): δ 7.54 (d, *J*= 7.5 Hz, 2H), 7.37 (t, *J*= 7.5, 2H), 7.29 (t, *J*= 7.5 Hz, 1H), 6.64 (m, 2H), 6.38 (m, 1H), 4.02 (dd, *J*= 9.3, 4.5 Hz, 1H), 3.93 (dd, *J*= 9.3, 7.0 Hz, 1H), 3.57 – 3.48 (m, 1H), 3.07 – 2.90 (m, 2H), 2.08 – 1.91 (m, 1H), 1.90 – 1.80 (m, 2H), 1.67 – 1.57 (m, 1H).

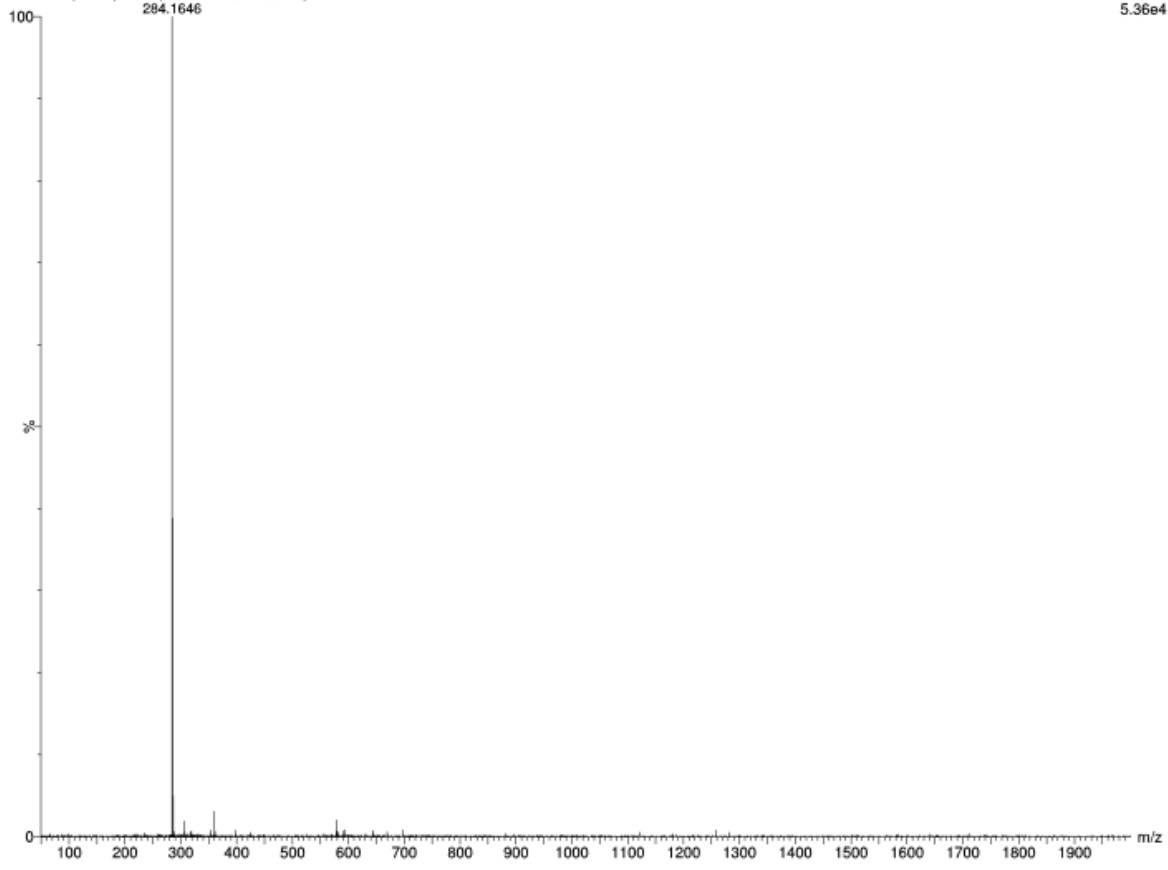
Synthesis of (*S*)-*N*-methyl-2-[(3-hydroxy-5-phenyl)phenoxy]methylpyrrolidine [(*S*)-**1b**]



Molecular Weight: 283.36

Under vigorous stirring at 0 °C, an aqueous solution of formaldehyde (37% in water, 0.15 ml) was added dropwise to a solution of (*S*)-2-[(3-hydroxy-5-phenyl)phenoxy]methylpyrrolidine (100 mg – 0.35 mmol) [(*S*)-**37**] in 3 ml of methanol and 60 μl of glacial acetic acid. Upon addition of 2-picolin borane (45 mg – 0.42 mmol), the mixture was reacted for 3 hours. Upon vacuo evaporation of methanol the residue is diluted with 5 ml of a 1M HCl solution and stirred for 1 hour to quench the unreacted 2-picolin-borane. Then, the pH was adjusted to 8 by adding an aqueous solution of Na_2CO_3 2M and the aqueous phase was extracted with ethyl acetate (3x30). The organic phase was washed with brine, dried over anhydrous sodium sulphate, filtered and evaporated in vacuo, obtaining a crude that was purified by silica gel flash chromatography (Dichloromethane / Methanol 9:1 + 3% NH_3 (30% in water)), affording the pure compound (*S*)-**1b** as a yellow sticky solid (80 mg – 0.28 mmol, 80%). **TLC** (Dichloromethane / Methanol 9:1 + 3% NH_3 (30% in water)): **Rf**= 0.45. $[\alpha]_{\text{D}}^{25} = -27.8^\circ$ (*c*0.5, CH_3OH). **$^1\text{H-NMR}$** (300 MHz, CD_3OD): δ 7.54 (d, *J*= 7.5 Hz, 2H), 7.39 (t, *J*= 7.5 Hz, 2H), 7.29 (t, *J*= 7.5 Hz, 1H), 6.63 (m, 2H), 6.38 (m, 1H), 4.01 (m, 2H), 3.12 – 3.07 (m, 1H), 2.76 – 2.73 (m, 1H), 2.42 (s, 3H), 2.40 – 2.33 (m, 1H), 2.13 – 2.07 (m, 1H), 1.88 – 1.70 (m, 3H). **$^{13}\text{C-NMR}$** (75 MHz, CD_3OD): δ 160.4, 158.6, 143.3, 141.1, 128.3, 127.0, 126.5, 106.6, 104.4, 100.4, 69.8, 64.6, 57.3, 40.6, 27.7, 22.1. **HRMS (ESI⁺)**: calc. for $\text{C}_{18}\text{H}_{22}\text{NO}_2$: theor. 284.1651; found $[\text{M}+\text{H}]^+$: 284.1646.





Elemental Composition Report

Single Mass Analysis

Tolerance = 5.0 PPM / DBE: min = -1.5, max = 200.0
 Element prediction: Off
 Number of isotope peaks used for i-FIT = 5

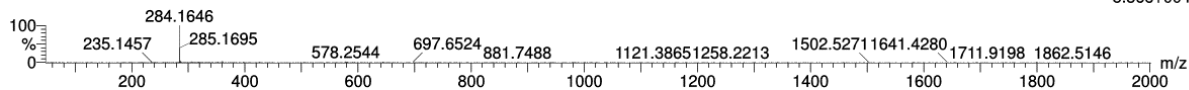
Monoisotopic Mass, Even Electron Ions

356 formula(e) evaluated with 1 results within limits (all results (up to 1000) for each mass)

Elements Used:

C: 18-18 H: 10-100 N: 0-20 O: 0-15 Na: 0-1

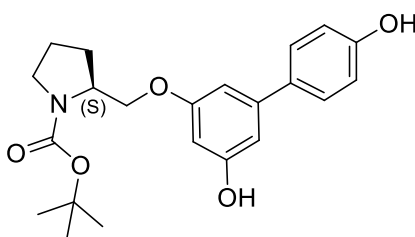
MB71 40 (0.772) AM2 (Ar,40000.0,0.00,0.00)



Minimum: -1.5
 Maximum: 0.5 5.0 200.0

Mass	Calc. Mass	mDa	PPM	DBE	i-FIT	Norm	Conf (%)	Formula
284.1646	284.1651	-0.5	-1.8	8.5	455.4	n/a	n/a	C18 H22 N O2

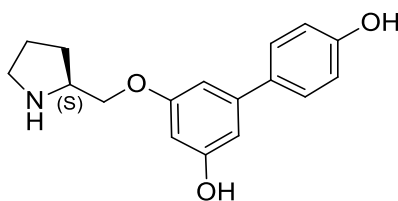
Synthesis of (*S*)-*N*-*tert*-butoxycarbonyl-2-[(3-hydroxy-5-(4-hydroxyphenyl))phenoxyethyl]pyrrolidine [(*S*)-**33**]



Molecular Weight: 385.45

Nitrogen was bubbled into a vigorously stirred solution (*S*)-*N*-*tert*-butoxycarbonyl-2-[(3-hydroxy-5-bromo)phenoxyethyl]pyrrolidine [(*S*)-**27**] (278 mg – 0.747 mmol) in 10 ml of toluene and tetrakis(triphenylphosphine)Pd (0) (27 mg – 0.023 mmol) was added. Nitrogen was flowed for 10 more minutes. Then, 2 ml of a 2M aqueous solution of Na₂CO₃ and 1 ml of ethanolic solution of 4-hydroxy-phenylboronic acid (114 mg – 0.827 mmol) were added. The reaction mixture was refluxed for 12 hours. After cooling to room temperature, the mixture was diluted with 30 ml of ethyl acetate and the organic phase and, upon anhydriification with sodium sulphate and filtration, was concentrated under vacuum. The crude was purified through silica gel flash chromatography (cyclohexane/ethyl acetate 6:4) and the pure product (*S*)-**33** was isolated as yellow oil (280 mg – 0.727 mmol, 97%). **TLC** (Cyclohexane / Ethyl Acetate 6:4): **R_f**= 0.28. **[α]_D²⁵** = -9.07° (*c*1, CH₃OH). **¹H-NMR** (300 MHz, CDCl₃): δ 7.36 (d, *J*= 8.2 Hz, 2H), 6.66 (m, 2H), 6.59 (d *J*= 8.2 Hz, 2H), 6.44 (m, 1H), 4.13 (m, 2H), 3.85 (m, 1H), 3.40 (m, 2H), 2.05 – 1.53 (m, 4H), 1.47 (s, 9H).

Synthesis of (*S*)-2-[(3-hydroxy-5-(4-hydroxyphenyl))phenoxyethyl]pyrrolidine [(*S*)-**39**]

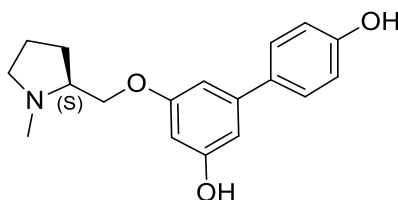


Molecular Weight: 285.34

(*S*)-*N*-*tert*-butoxycarbonyl-2-[(3-hydroxy-5-(4-hydroxyphenyl))phenoxyethyl]pyrrolidine [(*S*)-**33**] (280 mg – 0.727 mmol) was dissolved in 1 ml of methanol and the solution was cooled to 0 °C. Upon dropwise addition of 6 ml of a 1.25 M methanolic solution of HCl under vigorous stirring, the reaction mixture was warmed to room temperature and reacted for 12 hours.

Afterward, methanol was evaporated in vacuo, the residue was diluted with 5 ml of a 1M aqueous solution of HCl and washed with DCM twice. A solution of NH₃(30% in water) was added to the aqueous phase until pH 8 and the aqueous phase was extracted with ethyl acetate (3x30 ml). The organic phase was dried over anhydrous sodium sulphate, filtered and concentrated in vacuo, providing the pure compound (*S*)-**39** as a white sticky solid. (200 mg – 0.700 mmol, 96%). **TLC** (Dichloromethane / Methanol 9:1 + 2% NH₃(30% in water)): **R_f**= 0.17. **[α]_D²⁵** = +6.16° (*c*1, CH₃OH). **¹H-NMR** (300 MHz, CD₃OD): δ 7.39 (d, *J*= 8.5 Hz, 2H), 6.81 (d, *J*= 8.5 Hz, 2H), 6.58 (m, 2H), 6.30 (t, *J*= 2.3 Hz, 1H), 3.99 (dd, *J*= 4.7, 9.4 Hz, 1H), 3.90 (dd, *J*= 7.0, 9.4 Hz, 1H), 3.48 (m, 1H), 3.02 – 2.89 (m, 2H), 2.02 – 1.87 (m, 1H), 1.83 (m, 2H), 1.62 (m, 1H).

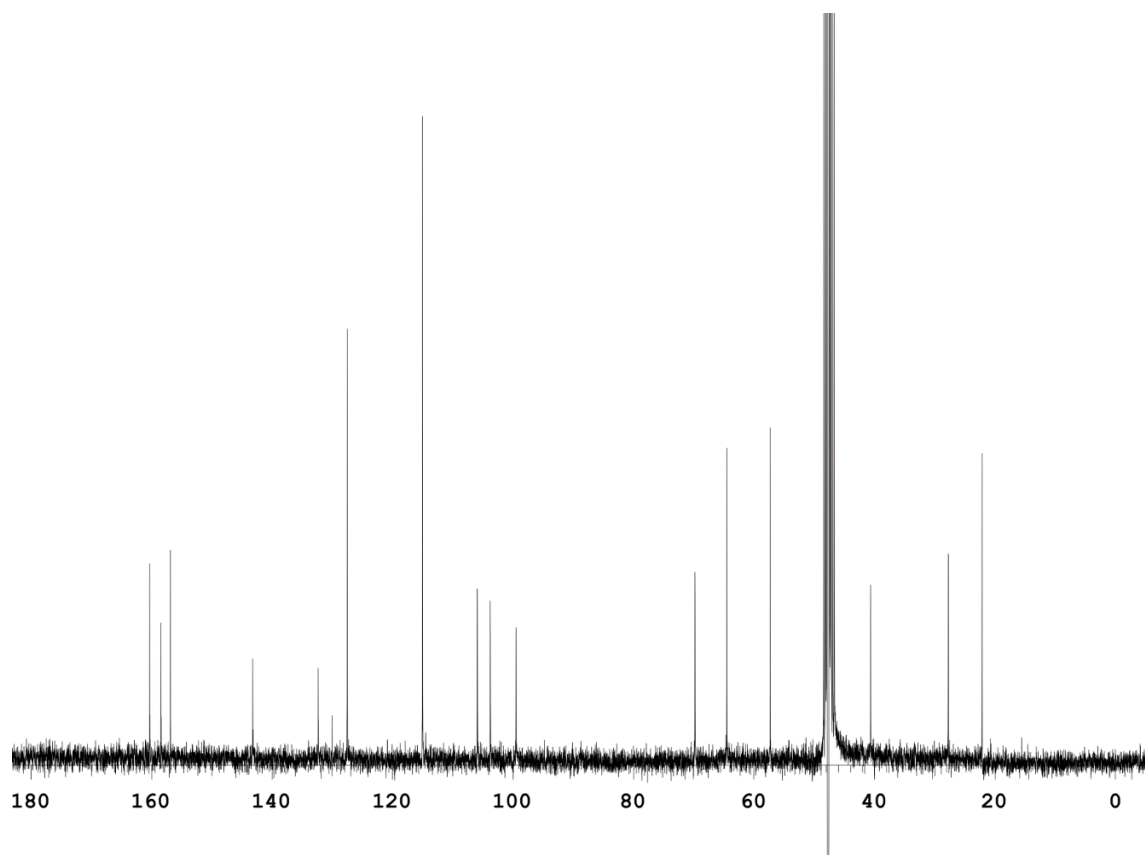
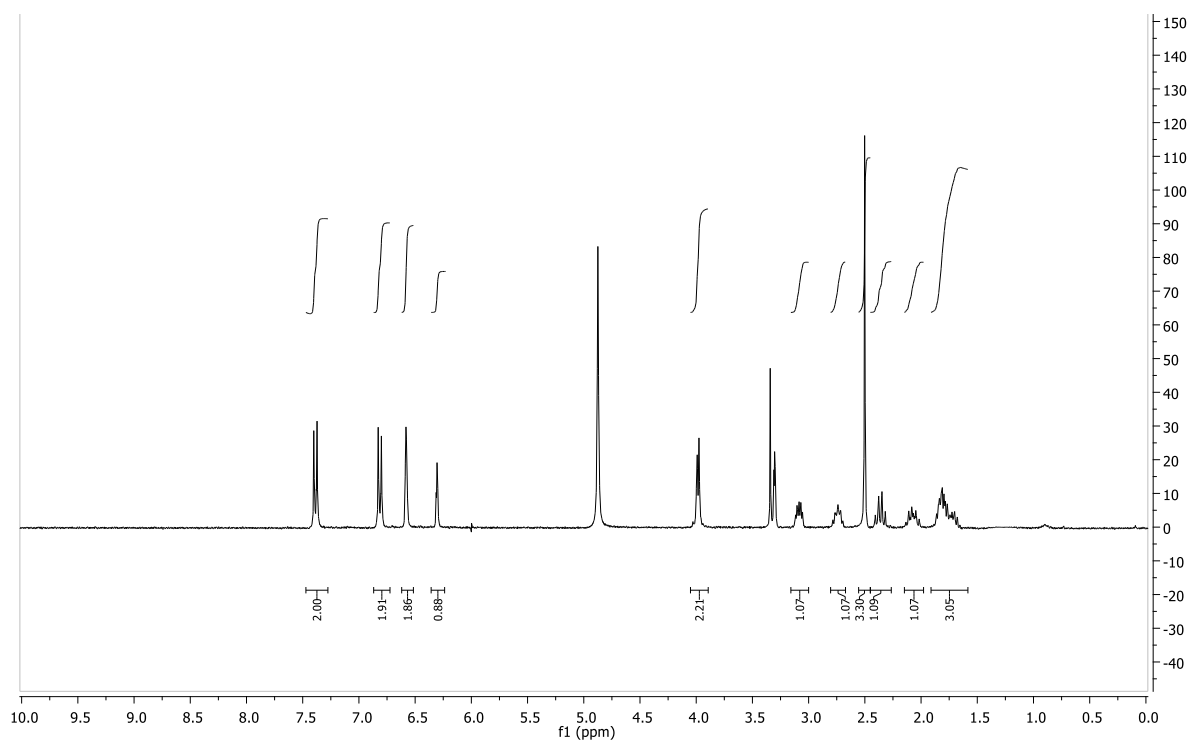
Synthesis of (*S*)-N-methyl-2-[(3-hydroxy-5-(4-hydroxyphenyl))phenoxyethyl]pyrrolidine [(*S*)-**1c**]

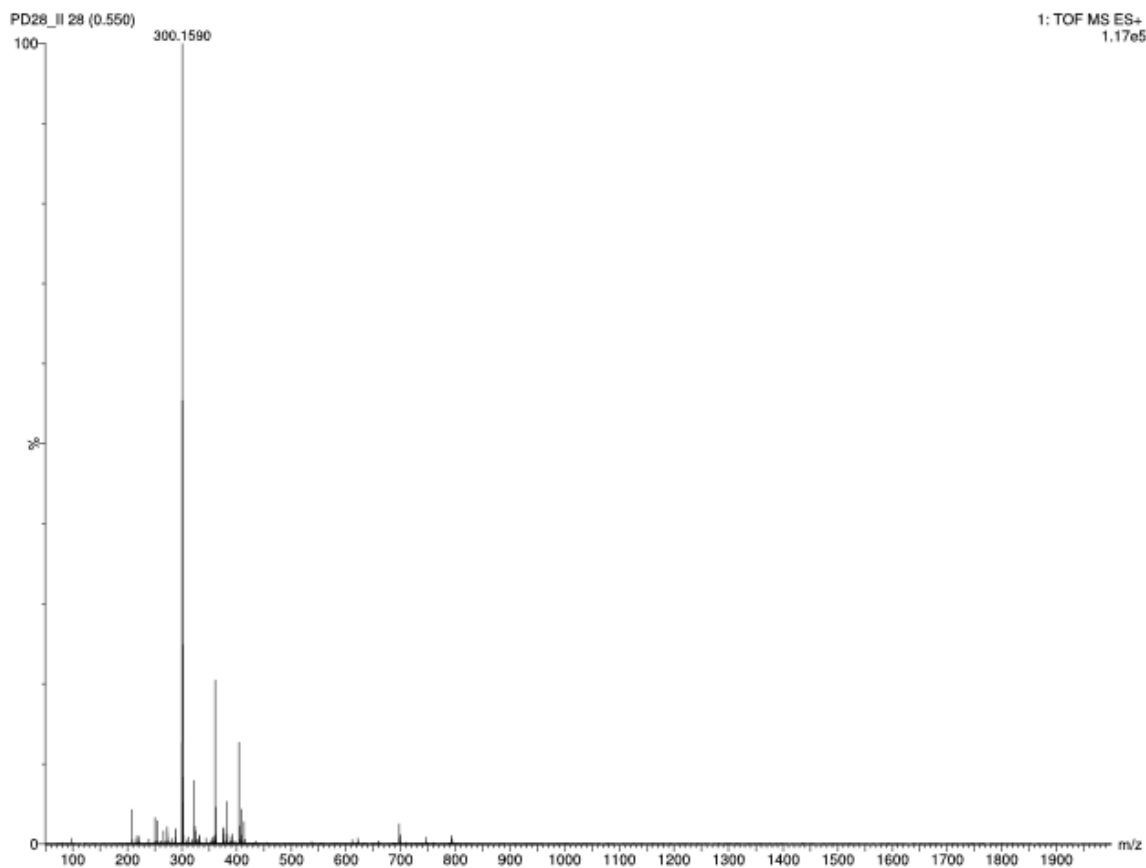


Molecular Weight: 299.36

Under vigorous stirring at 0 °C, an aqueous solution of formaldehyde (37% in water, 0.14 ml) was added dropwise to a solution of (*S*)-2-[(3-hydroxy-5-(4-hydroxyphenyl))phenoxyethyl]pyrrolidine [(*S*)-**39**] (110 mg – 0.386 mmol) in 3 ml of methanol and 80 μl of glacial acetic acid. Upon addition of 2-picolin borane (42 mg – 0.386 mmol), the mixture was reacted for 6 hours. Upon vacuo evaporation of methanol, the residue is diluted with 5 ml of a 1M HCl solution and stirred for 1 hour to quench the unreacted 2-picolin-borane. Then, the pH was adjusted to 8 by adding an aqueous solution of Na₂CO₃ 2M and the aqueous phase was extracted with ethyl acetate (3x30). The organic phase was washed with brine, dried over sodium sulphate, filtered and evaporated, obtaining a crude that was purified by silica gel flash chromatography (dichloromethane/methanol 90:10 + 2% NH₃(30% in water), affording the pure compound (*S*)-**1c** as a dark yellow oil (60 mg – 0.20 mmol, 51%). **TLC** (Dichloromethane / Methanol 9:1 + 2% NH₃(30% in water)): **R_f**= 0.3. **[α]_D²⁵** = -20.93° (*c*1, CH₃OH). **¹H-NMR** (300 MHz, CD₃OD): δ 7.39 (d, *J*= 8.6 Hz, 2H), 6.81 (d, *J*= 8.6 Hz, 2H), 6.58 (m, 2H), 6.30 (t, *J*= 1.8 Hz, 1H), 3.99 (m, 2H), 3.10 (m, 1H), 2.75 (m, 1H), 2.50 (s, 3H), 2.36 (m, 1H), 2.09 (m, 1H), 1.81 (m, 3H). **¹³C-NMR** (75 MHz, CD₃OD): δ 160.3, 158.4, 156.9, 143.2, 132.4, 130.0, 127.5, 115.0, 105.9, 103.8, 99.5, 69.8, 64.5, 57.3, 40.6, 27.8, 22.1. **HRMS (ESI⁺)**:

calc. for $C_{18}H_{22}NO_3$: theor. 300.1600; found $[M+H]^+$: 300.1593. **HRMS (ESI)**: calc. for $C_{18}H_{20}NO_3$: theor. 298.1443; found $[M-H]^-$: 298.1448.





Elemental Composition Report

Page 1

Single Mass Analysis

Tolerance = 5.0 PPM / DBE: min = -1.5, max = 200.0

Element prediction: Off

Number of isotope peaks used for i-FIT = 5

Monoisotopic Mass, Even Electron Ions

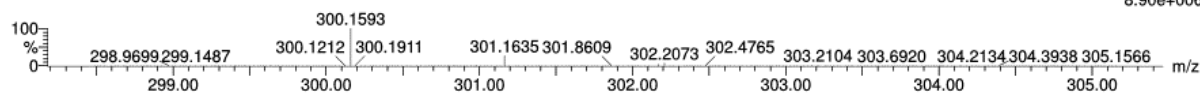
297 formula(e) evaluated with 1 results within limits (all results (up to 1000) for each mass)

Elements Used:

C: 10-30 H: 0-45 N: 0-10 O: 0-10

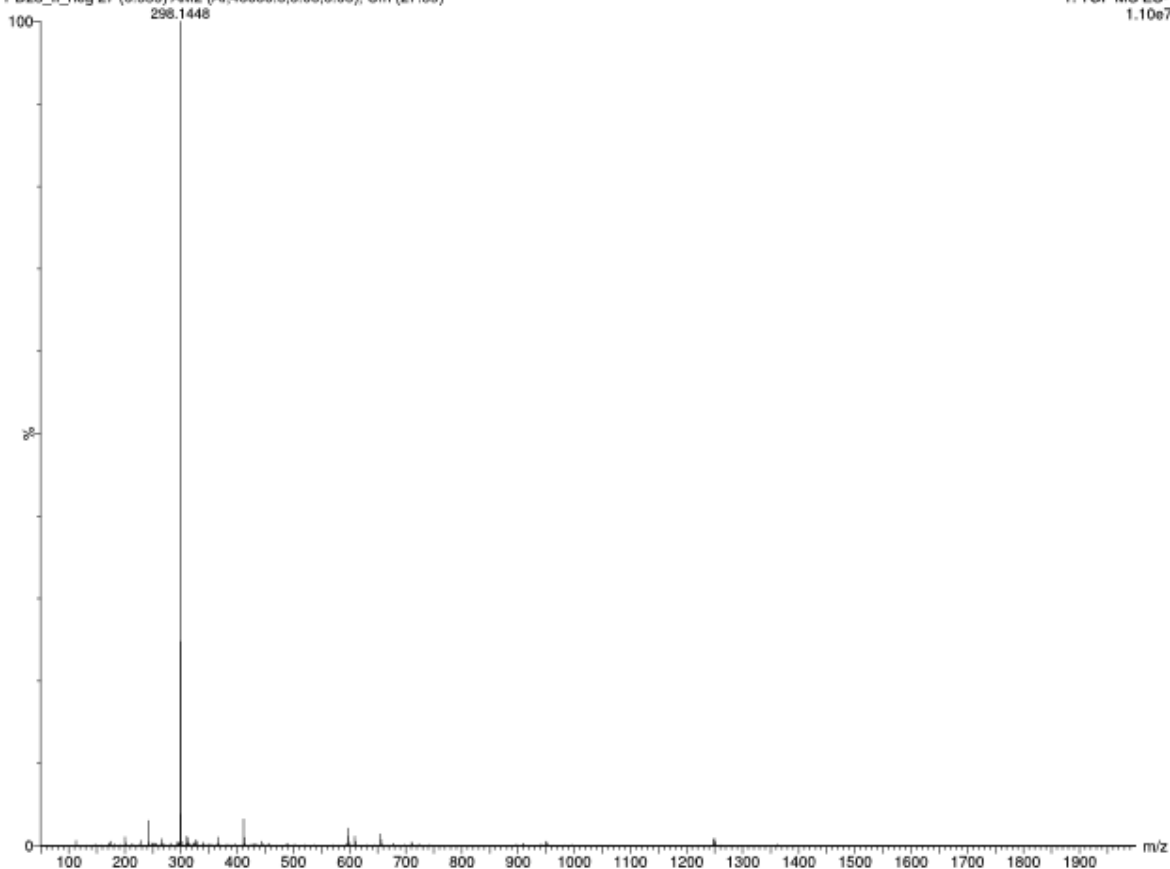
PD28_II 46 (0.874) AM2 (Ar,40000.0,0.00,0.00); Cm (30:46)

1: TOF MS ES+
8.90e+006



Minimum: -1.5
Maximum: 200.0

Mass	Calc. Mass	mDa	PPM	DBE	i-FIT	Norm	Conf (%)	Formula
300.1593	300.1600	-0.7	-2.3	8.5	2719.4	n/a	n/a	C18 H22 N O3



Elemental Composition Report

Single Mass Analysis

Tolerance = 5.0 PPM / DBE: min = -1.5, max = 200.0
 Element prediction: Off
 Number of isotope peaks used for i-FIT = 5

Monoisotopic Mass, Even Electron Ions

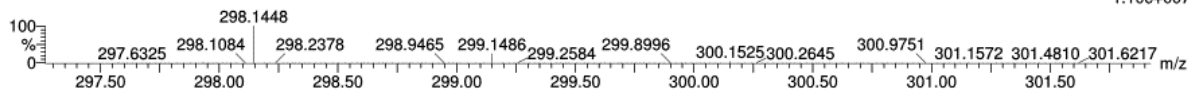
287 formula(e) evaluated with 1 results within limits (all results (up to 1000) for each mass)

Elements Used:

C: 10-30 H: 0-45 N: 0-10 O: 0-10

PD28_II_neg 27 (0.533) AM2 (Ar,40000.0,0.00,0.00); Cm (27:39)

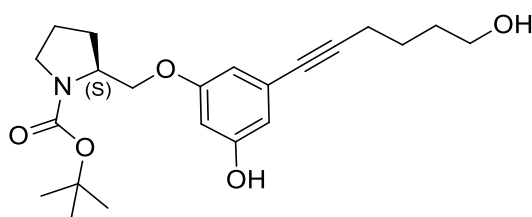
1: TOF MS ES-
1.10e+007



Minimum: -1.5
 Maximum: 0.5 5.0 200.0

Mass	Calc. Mass	mDa	PPM	DBE	i-FIT	Norm	Conf(%)	Formula
298.1448	298.1443	0.5	1.7	9.5	2051.4	n/a	n/a	C18 H20 N O3

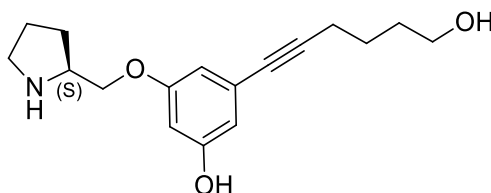
Synthesis of (*S*)-*N*-*tert*-butoxycarbonyl-2-[(3-hydroxy-5-(6-hydroxy-1-hexynyl))phenoxy]methyl]pyrrolidine [(*S*)-**35**]



Molecular Weight: 389.49

Under nitrogen atmosphere, CuBr (23 mg – 0.47 mmol) and tetrakis(triphenylphosphine)Pd(0) (32 mg – 0.03 mmol) were added to a solution of (*S*)-*N*-*tert*-butoxycarbonyl-2-[(3-hydroxy-5-bromo)phenoxy]methyl]pyrrolidine [(*S*)-**27**] (265 mg – 0.71 mmol) in 3 ml of triethylamine. Upon stirring for 30 minutes at room temperature, 5-hexyn-1-ol (140 mg – 1.42 mmol) was added and the mixture was refluxed for 12 hours. Afterward, the mixture was diluted with 10 ml of 1M aqueous HCl and extracted with ethyl acetate (3x30 ml). The organic phase was washed with brine (15 ml), dried over anhydrous sodium sulphate, filtered on diatomaceous earth and concentrated in vacuo, providing a crude that was purified through silica gel flash chromatography (cyclohexane/ethyl acetate 6:4). The pure product (*S*)-**35** was obtained as a colourless oil (220 mg – 0.57 mmol, 80%). TLC (Dichloromethane / Methanol 98:2): $R_f = 0.3$. $[\alpha]_D^{25} = -18.77^\circ$ (c_1 , CHCl₃). $^1\text{H-NMR}$ (300 MHz, CD₃OD) δ : 6.48 (m, 3H), 6.43 (bs, 1H, exchange with D₂O), 4.11 (m, 1H), 3.80 – 3.69 (m, 2H), 3.36 (m, 2H), 2.43 (m, 2H), 2.00 – 1.80 (m, 6H), 1.79 – 1.65 (m, 4H), 1.47 (s, 9H).

Synthesis of (*S*)-2-[(3-hydroxy-5-(6-hydroxy-1-hexynyl))phenoxy]methyl]pyrrolidine [(*S*)-**41**]

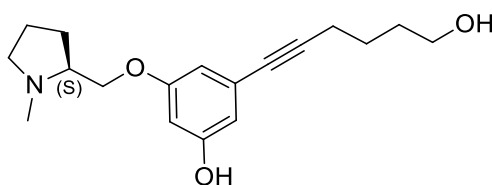


Molecular Weight: 289.37

(*S*)-*N*-*tert*-butoxycarbonyl-2-[(3-hydroxy-5-(6-hydroxy-1-hexynyl))phenoxy]methyl]pyrrolidine [(*S*)-**35**] (194 mg 0.50 mmol) was dissolved in 2 ml of methanol and the solution was cooled to 0 °C. Upon dropwise addition of 4 ml of a 1.25 M methanolic solution of HCl under vigorous stirring, the reaction mixture was warmed to room

temperature and reacted for 12 hours. Afterward, methanol was evaporated in vacuo, the residue was diluted with 10 ml of a 10% aqueous solution of NaHCO₃ and extracted with DCM. The organic phase was dried over anhydrous sodium sulphate, filtered and the solvent was evaporated in vacuo, affording a crude that was purified through silica gel flash chromatography (dichloromethane/methanol 9:1 + 3% NH₃(30% in water)). The pure product (*S*)-**41** was obtained as a brown sticky solid (115 mg – 0.40 mmol, 80%). **TLC** (Dichloromethane / Methanol 9:1 + 3% NH₃(30% in water)): **R_f**= 0.16. **[α]_D²⁵** = +6.3° (*c*1, CH₃OH). **¹H-NMR** (300 MHz, CD₃OD): δ 6.39 (m, 2H), 6.32 (t, *J*= 2.2 Hz, 1H), 3.91 (dd, *J*= 9.2, 4.8 Hz, 1H), 3.83 (dd, *J*= 9.2, 7.2 Hz, 1H), 3.60 (m, 2H), 3.46 (m, 1H), 3.07 – 2.80 (m, 2H), 2.40 (t, *J*= 6.6 Hz, 2H), 2.07 – 1.80 (m, 3H), 1.73 – 1.58 (m, 5H).

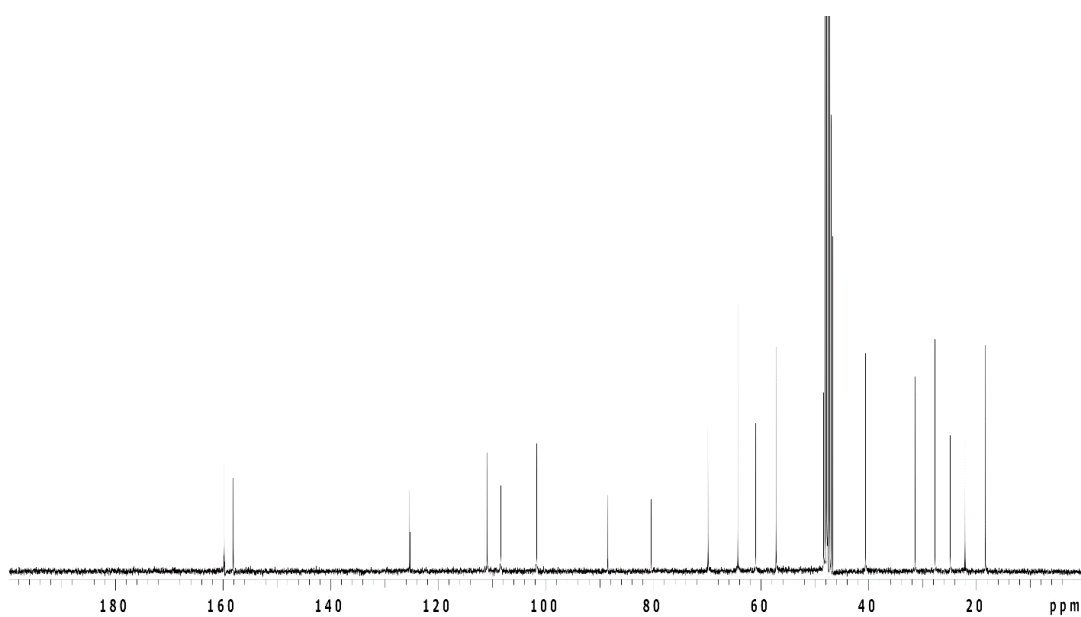
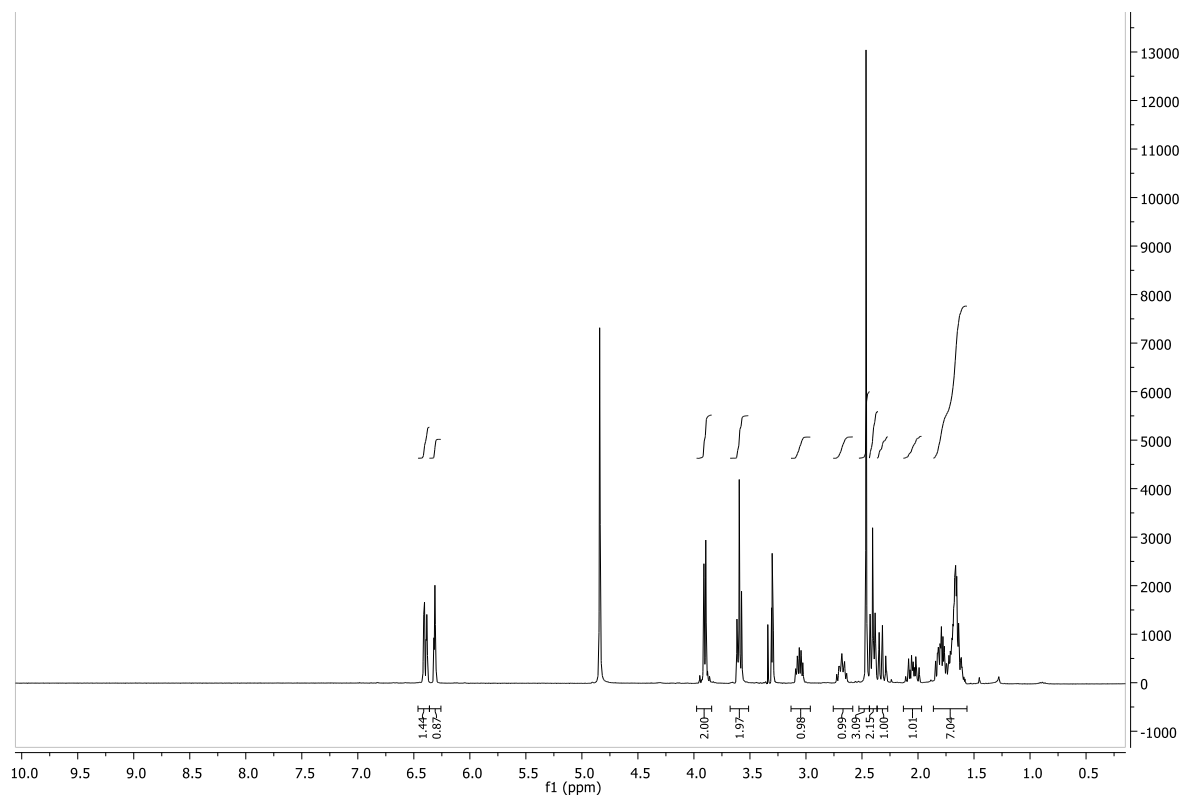
Synthesis of (*S*)-N-methyl-2-[(3-hydroxy-5-(6-hydroxy-1-hexynyl))phoxymethyl]pyrrolidine [(*S*)-**1d**]

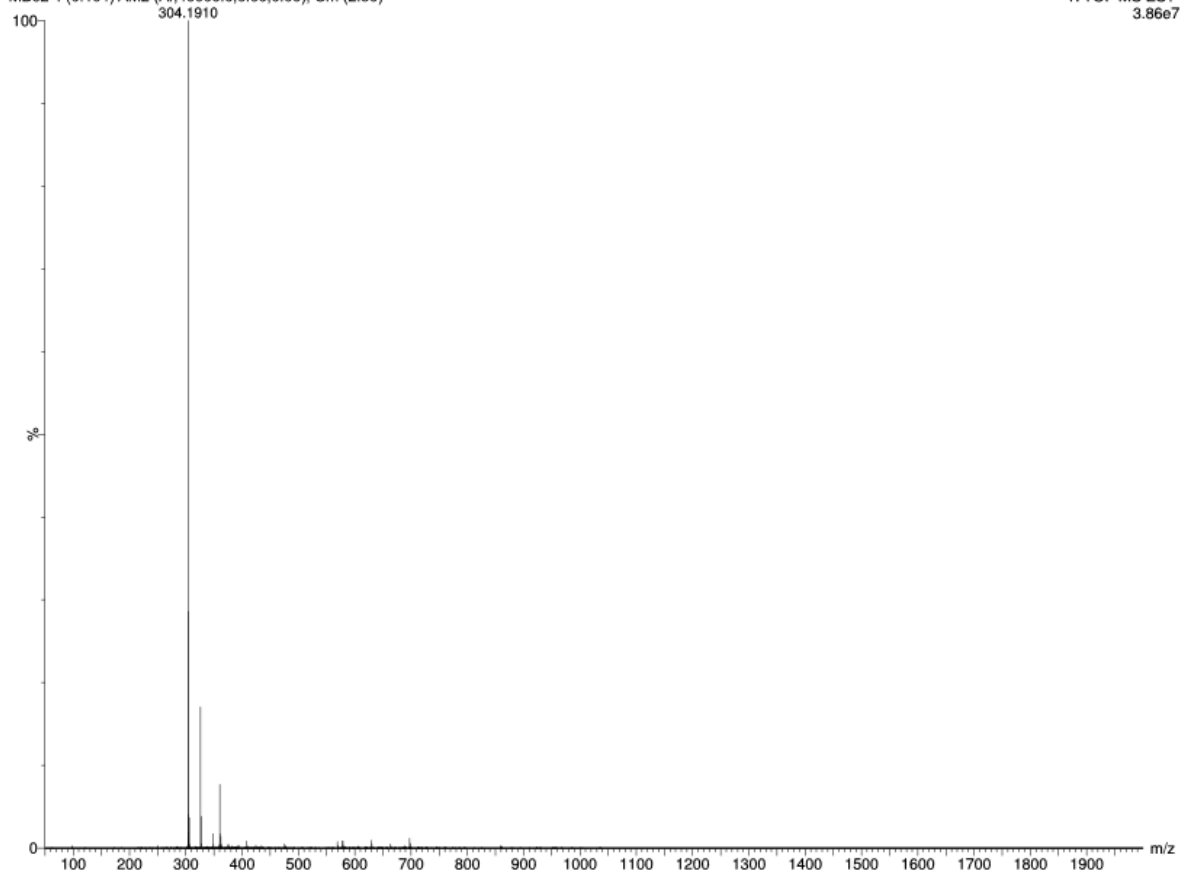


Molecular Weight: 303.40

Under vigorous stirring at 0 °C, an aqueous solution of formaldehyde (37% in water, 0.09 ml) was added dropwise to a solution of (*S*)-2-[(3-hydroxy-5-(6-hydroxy-1-hexynyl))phoxymethyl]pyrrolidine [(*S*)-**41**] (66 mg – 0.23 mmol) in 4 ml of methanol and 80 μl of glacial acetic acid. Upon addition of 2-picolin borane (24 mg – 0.23 mmol), the mixture was reacted for 2 hours. The solvent was evaporated in vacuo, the residue was diluted with 10 ml of a 1M HCl solution and stirred for 1 hour to quench the unreacted 2-picolin-borane. Then, the pH was adjusted to 8 by adding an aqueous solution of Na₂CO₃ 2M and the aqueous phase was extracted with ethyl acetate (3x30 ml). The organic phase was washed with brine, dried over anhydrous sodium sulphate, filtered and the solvent was evaporated in vacuo, providing a crude, that was further purified through silica-gel flash chromatography (gradient from dichloromethane to dichloromethane/methanol 9:1 + 10% NH₃(30% in water)). The pure compound (*S*)-**1d** was obtained as a yellow sticky solid (60 mg – 0.20 mmol, 87%). **TLC** (Dichloromethane / Methanol 9:1 + 3% NH₃(30% in water)): **R_f**= 0.4. **[α]_D²⁵** = -19.02° (*c*0.5, CH₃OH). **¹H-NMR** (300 MHz, CD₃OD): δ 6.39 (m, 2H), 6.31 (m, 1H), 3.90 (m, 2H), 3.60 (t, *J*= 6.4 Hz, 2H), 3.10 – 3.02 (m, 1H), 2.73 – 2.64 (m, 1H), 2.48 (s, 3H), 2.41 (t, *J*= 6.7 Hz, 2H),

2.31 (m, 1H), 2.09 – 1.99 (m, 1H), 1.84 – 1.61 (m, 7H). ^{13}C -NMR (75 MHz, CD_3OD): δ 159.8, 158.1, 125.3, 110.9, 108.4, 101.7, 88.5, 80.5, 69.7, 64.4, 61.1, 57.3, 40.6, 31.4, 27.7, 24.9, 22.1, 18.3. HRMS (ESI⁺): calc. for $\text{C}_{18}\text{H}_{26}\text{NO}_3$: theor. 304.1913; found $[\text{M}+\text{H}]^+$: 304.1910.





Elemental Composition Report

Single Mass Analysis

Tolerance = 5.0 PPM / DBE: min = -1.5, max = 200.0
 Element prediction: Off
 Number of isotope peaks used for i-FIT = 5

Monoisotopic Mass, Even Electron Ions

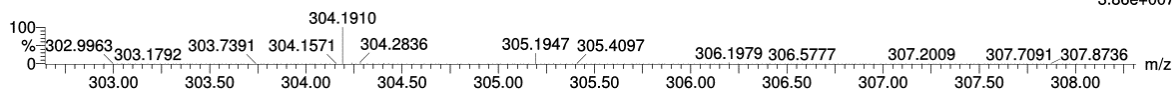
60 formula(e) evaluated with 1 results within limits (all results (up to 1000) for each mass)

Elements Used:

C: 18-18 H: 10-100 N: 0-5 O: 0-5 Na: 0-1

MB62 4 (0.104) AM2 (Ar,40000.0,0.00,0.00); Cm (2:50)

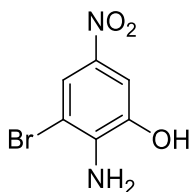
1: TOF MS ES+
3.86e+007



Minimum: -1.5
 Maximum: 0.5 5.0 200.0

Mass	Calc. Mass	Mass mDa	PPM	DBE	i-FIT	Norm	Conf (%)	Formula
304.1910	304.1913	-0.3	-1.0	6.5	2563.4	n/a	n/a	C18 H26 N O3

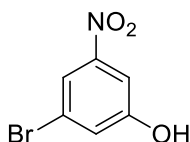
Synthesis of 2-amino-3-bromo-5-nitrophenol



Molecular Weight: 233.02

Procedure adapted from literature.¹⁵⁸ A solution of 2-amino-5-nitrophenol (500 mg – 3.24 mmol) in 40 ml of DCM and 20 ml of acetonitrile was cooled to -10 °C and vigorously stirred. Br₂ (0.29 ml – 5.64 mmol) was carefully added dropwise and the resulting mixture was warmed to 35 °C. After 12 hours, the reaction mixture was cooled to room temperature and the excess of Br₂ was quenched by adding a 10% aqueous solution of Na₂S₂O₅. The organic phase was dried over anhydrous sodium sulphate, filtered and concentrated in vacuo, providing a crude that was purified through silica gel flash chromatography (cyclohexane/ethyl acetate 7:3). The pure product was obtained as a red sticky solid (730 mg – 3.13 mmol, 97%). **TLC** (Cyclohexane / Ethyl Acetate 6:4): **R_f**= 0.37. **¹H-NMR** (300 MHz, DMSO): δ 10.65 (s, exchange with D₂O, 1H), 7.83 (s, 1H), 7.47 (s, 1H), 6.13 (bs, exchange with D₂O, 2H).^{159,160}

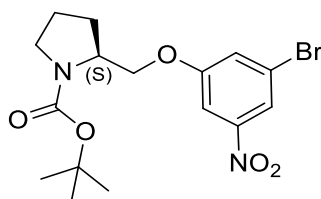
Synthesis of 3-bromo-5-nitrophenol



Molecular Weight: 218.00

Procedure adapted from literature.¹⁵⁸ Concentrated H₂SO₄ (2.18 ml, 96%) was carefully added dropwise to a solution of 2-amino-3-bromo-5-nitrophenol (2.62 g – 3.22 mmol) in 63 ml of ethanol, previously cooled to -10 °C. Upon heating to 55 °C, NaNO₂ (2.73 g – 39.56 mmol) was added. The resulting mixture was refluxed for 3 hours. Afterward, the mixture was cooled to room temperature and the solvent was evaporated in vacuo. The residue was diluted with ethyl acetate (15 ml) and washed with a 1M aqueous solution of NaOH (5 ml) and subsequently, with brine (5 ml). The organic phase was dried over sodium sulphate, filtrated and evaporated in vacuo, providing a crude that was purified through silica gel flash chromatography (cyclohexane/ethyl acetate 6:4). The pure product was obtained as a reddish sticky solid (1.8 g – 8.26 mmol, 74%). **TLC** (Cyclohexane / Ethyl Acetate 6:4): **R_f**= 0.45. **¹H-NMR** (300 MHz, DMSO): δ 10.92 (s, exchange with D₂O, 1H), 7.78 (s, 1H), 7.53 (s, 1H), 7.38 (s, 1H).¹⁶¹

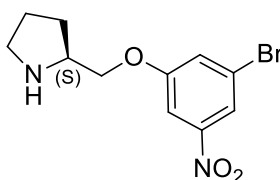
Synthesis of (*S*)-*N*-*tert*-butoxycarbonyl-2-[(3-bromo-5-nitro)phenoxy]methyl]pyrrolidine [(*S*)-28]



Molecular Weight: 401.25

3-bromo-5-nitrophenol (440 mg – 2.02 mmol) and (*S*)-*N*-*tert*-butoxycarbonyl-2-hydroxymethyl-pyrrolidine (403 mg – 2.00 mmol), dissolved each in 2 ml of anhydrous THF, were added to a solution of triphenylphosphine (630 mg – 2.40 mmol) in 2 ml of anhydrous THF. The reaction mixture was cooled to -10°C and DIAD (0.47 mL – 2.40 mmol) was added dropwise, under vigorous stirring. The reaction mixture was refluxed for 12 hours. After cooling to room temperature, the mixture was diluted with 10 mL of 1M aqueous solution of NaOH and extracted with DCM twice. The organic phase was dried over anhydrous sodium sulphate, filtrated and concentrated in vacuo to obtain a crude that was further purified through silica-gel flash column chromatography (gradient from cyclohexane to cyclohexane/ethyl acetate 9:1). The pure compound (*S*)-28 was obtained as a dark green oil (685 mg – 1.70 mmol, 85%). TLC (Cyclohexane / Ethyl Acetate 6:4; stained with cerium sulphate): **R_f** = 0.55. **[α]_D²⁵** = -64.71° (*c*1, CH₃OH). **¹H-NMR** (300 MHz, CD₃OD): δ 7.95 (s, 1H), 7.69 (s, 1H), 7.40 (s, 1H), 4.16 (m, 2H), 3.99 (m, 1H), 3.39 (m, 2H), 2.05 – 1.86 (m, 4H), 1.53 (s, 4.5H), 1.47 (s, 4.5H).

Synthesis of (*S*)-2-[(3-bromo-5-nitro)phenoxy]methyl]pyrrolidine [(*S*)-30]



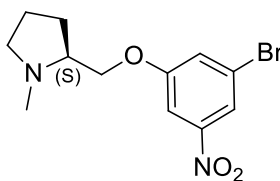
Molecular Weight: 301.14

(*S*)-*N*-*tert*-butoxycarbonyl-2-[(3-bromo-5-nitro)phenoxy]methyl]pyrrolidine [(*S*)-28] (385 mg – 0.96 mmol) was dissolved in 2 ml of methanol and the solution was cooled to 0 °C. Upon dropwise addition of 8 ml of a 1.25 M methanolic solution of HCl under vigorous stirring, the reaction mixture was warmed to room temperature and reacted for 12 hours. Afterward, methanol was evaporated in vacuo, the residue was diluted with 10 ml of a 10% aqueous

solution of NaHCO₃ and extracted with DCM. The organic phase was dried over sodium sulphate, filtrated and evaporated in vacuo, affording the pure product (*S*)-**30** as a yellow sticky solid (120 mg – 0.40 mmol, 42%). [α]_D²⁵ = +12.73° (*c*1, CH₃OH). ¹H-NMR (300 MHz, CD₃OD): δ 7.96 (t, *J*= 2.3 Hz, 1H), 7.77 (t, *J*= 2.3 Hz, 1H), 7.56 (t, *J*= 2.3 Hz, 1H), 4.08 (dd, *J*= 4.7, 9.4 Hz, 1H), 3.96 (dd, *J*= 7.0, 9.4 Hz, 1H), 3.56 – 3.30 (m, 1H), 3.02 – 2.88 (m, 2H), 2.06 – 1.88 (m, 1H), 1.87 – 1.78 (m, 2H), 1.65 – 1.54 (m, 1H).

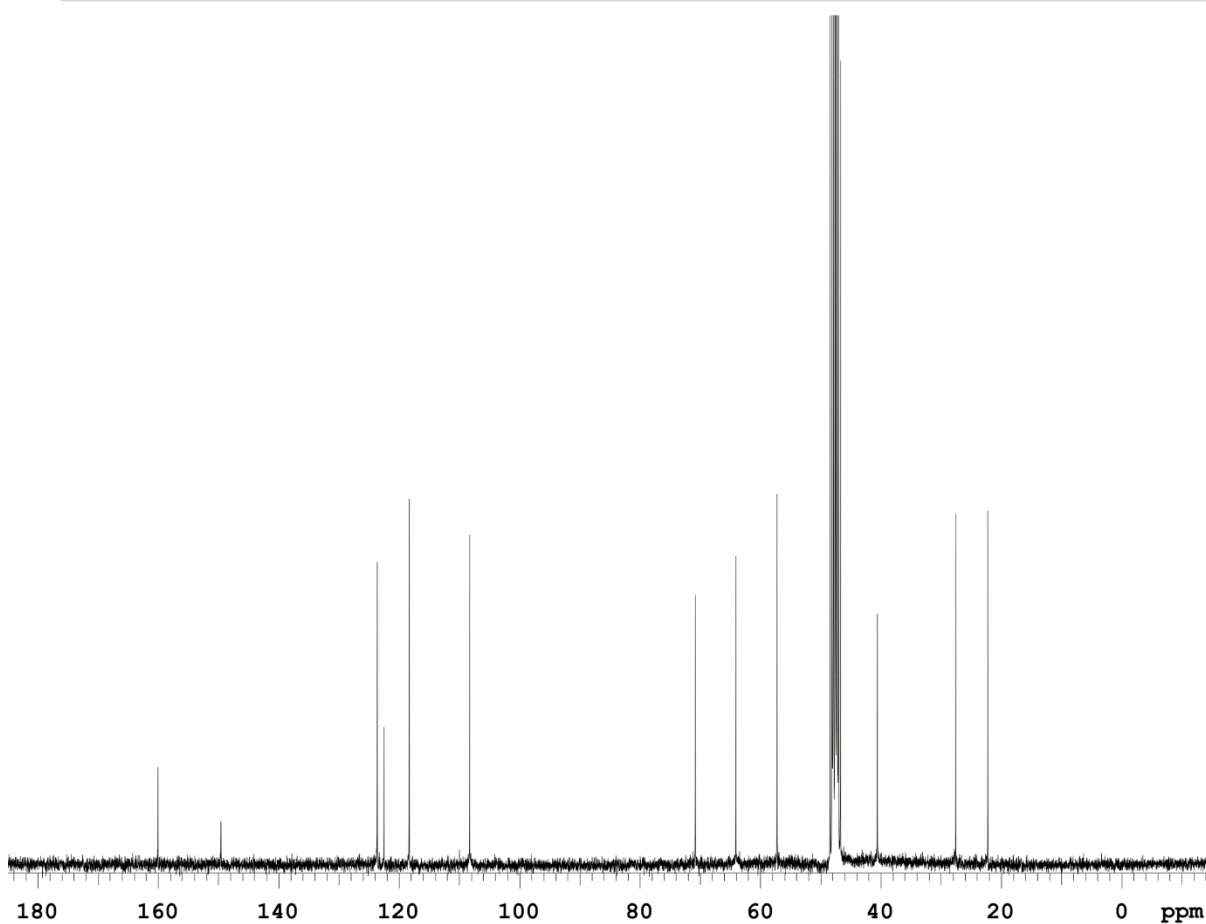
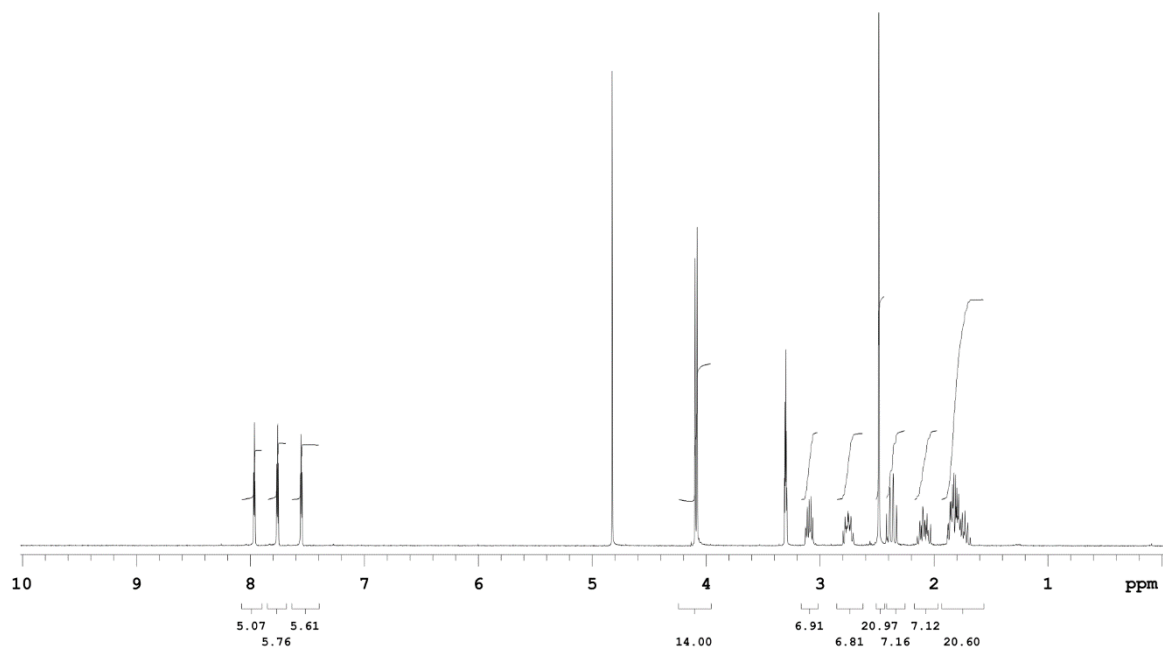
Synthesis of (*S*)-N-methyl-2-[(3-bromo-5-nitro)phoxymethyl]pyrrolidine

[(*S*)-**2a**]



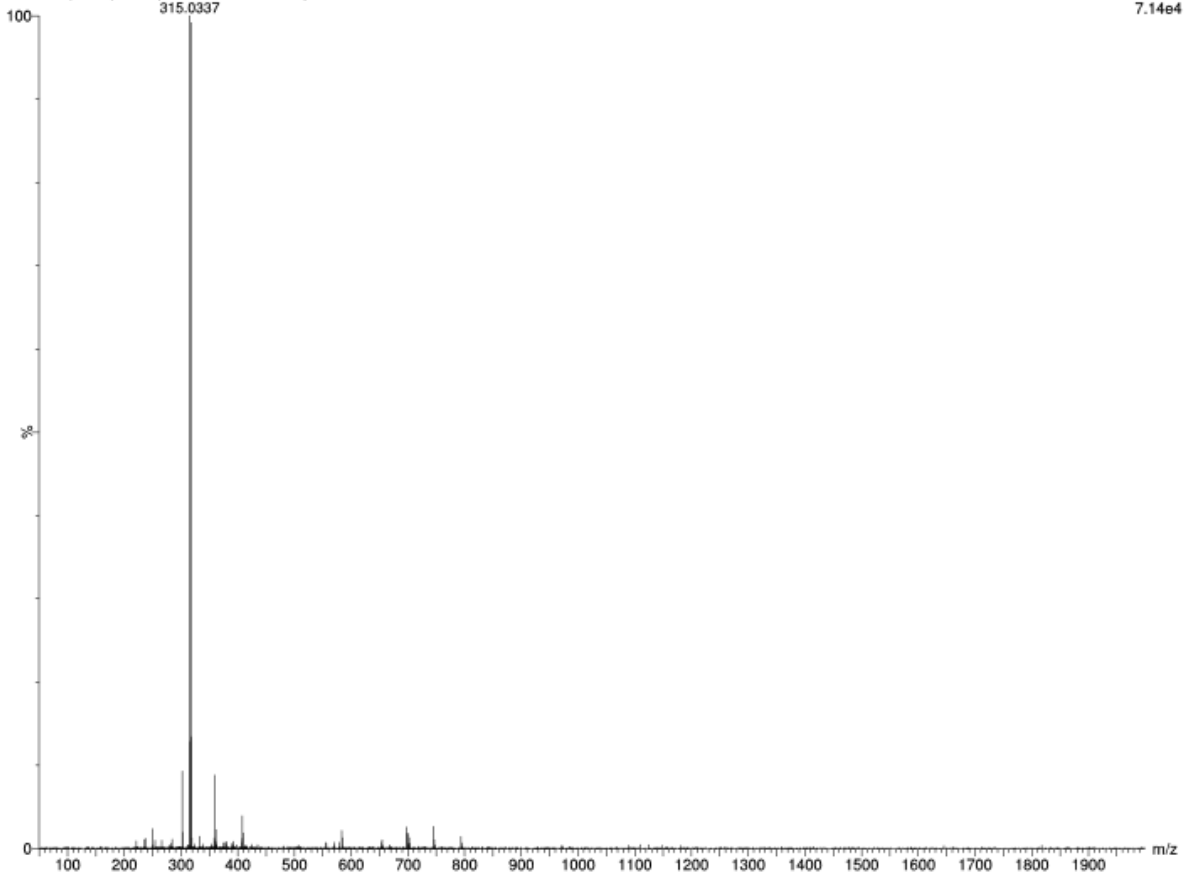
Molecular Weight: 315.16

Under vigorous stirring at 0 °C, an aqueous solution of formaldehyde (37% in water, 0.12 ml) was added dropwise to a solution of (*S*)-2-[(3-bromo-5-nitro)phoxymethyl]pyrrolidine [(*S*)-**30**] (117 mg – 0.40 mmol) in 4 ml of methanol and 80 μ l of glacial acetic acid. Upon addition of 2-picolin borane (43 mg – 0.40 mmol), the mixture was reacted for 3 hours. The solvent was evaporated in vacuo, the residue was diluted with 5 ml of a 1M HCl solution and stirred for 1 hour to quench the unreacted 2-picolin-borane. Then, the pH was adjusted to 8 by adding an aqueous solution of Na₂CO₃ 2M and the aqueous phase was extracted with ethyl acetate (3x30 ml). The organic phase was washed with brine, dried over sodium sulphate, filtered and evaporated in vacuo, providing the pure compound (*S*)-**2a** as a yellow sticky solid (125 mg – 0.39 mmol, 98%). TLC (Dichloromethane / Methanol 9:1 +2% NH₃(30% in water)): R_f= 0.71. [α]_D²⁵ = -6.67° (*c*1, CH₃OH). ¹H-NMR (300 MHz, CD₃OD): δ 7.96 (t, *J*= 1.8 Hz, 2H), 7.76 (t, *J*= 1.8 Hz, 1H), 7.55 (t, *J*= 1.8 Hz, 1H), 4.08 (d, *J*= 5.3 Hz, 2H), 3.12 – 3.06 (m, 1H), 2.80 – 2.71 (m, 1H), 2.49 (s, 3H), 2.42 – 2.33 (q, *J*= 9.4 Hz, 4H), 2.13 – 2.03 (m, 1H), 1.88 – 1.70 (m, 3H). ¹³C-NMR (75 MHz, CD₃OD): δ 160.1, 149.6, 123.7, 122.6, 118.4, 108.3, 70.9, 64.1, 57.2, 40.6, 27.6, 22.2. HRMS (ESI⁺): calc. for C₁₂H₁₆N₂O₃⁷⁹Br: theor. 315.0344; found [M+H]⁺: 315.0337.



PD36 27 (0.533) AM2 (Ar,40000.0,0.00,0.00)

1: TOF MS ES+
7.14e4



Elemental Composition Report

Single Mass Analysis

Tolerance = 5.0 PPM / DBE: min = -1.5, max = 200.0
 Element prediction: Off
 Number of isotope peaks used for i-FIT = 5

Monoisotopic Mass, Even Electron Ions

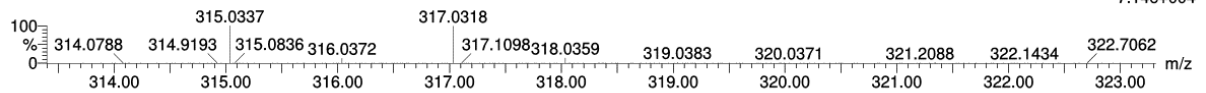
132 formula(e) evaluated with 1 results within limits (all results (up to 1000) for each mass)

Elements Used:

C: 12-12 H: 10-100 N: 0-5 O: 0-5 Na: 0-1 Br: 0-1

PD36 27 (0.533) AM2 (Ar,40000.0,0.00,0.00)

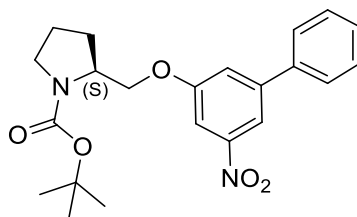
1: TOF MS ES+
7.14e+004



Minimum: -1.5
 Maximum: 0.5 5.0 200.0

Mass	Calc. Mass	mDa	PPM	DBE	i-FIT	Norm	Conf(%)	Formula
315.0337	315.0344	-0.7	-2.2	5.5	732.1	n/a	n/a	C12 H16 N2 O3 Br

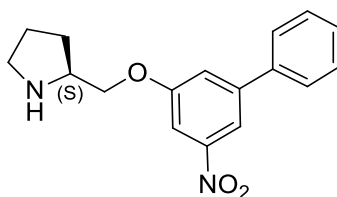
Synthesis of (*S*)-*N*-*tert*-butoxycarbonyl-2-[(3-nitro-5-phenyl)phenoxy]methyl]pyrrolidine [(*S*)-**32**]



Molecular Weight: 398.45

Under nitrogen atmosphere, tetrakis(triphenylphosphine)Pd(0) (52 mg – 0.045 mmol) was added to a solution of (*S*)-*N*-*tert*-butoxycarbonyl-2-[(3-bromo-5-nitro)phenoxy]methyl]pyrrolidine [(*S*)-**28**] (260 mg – 0.65 mmol) in 6 ml of toluene. Upon stirring for 10 minutes at room temperature, 1 ml of an aqueous solution of Na₂CO₃ 2M and a solution of *p*-hydroxyphenyl boronic acid (88 mg – 0.72 mmol) in ethanol (0.5 ml) were sequentially added. The mixture was refluxed for 12 hours. Afterward, the mixture was diluted with ethyl acetate (30 ml) and the organic phase was dried over anhydrous sodium sulphate, filtered and concentrated in vacuo, providing a crude that was purified through silica gel flash chromatography (gradient from cyclohexane/ethyl acetate 8:2 to 6:4). The pure product (*S*)-**32** was obtained as a yellow oil (241 mg – 0.60 mmol, 93%). TLC (Cyclohexane / Ethyl Acetate 6:4): R_f = 0.40. [α]_D²⁵ = -55.09° (c1, MeOH). ¹H NMR (300 MHz, CDCl₃): δ 8.05 (s, 1H), 7.71 (s, 1H), 7.67 – 7.58 (m, 2H), 7.53 – 7.37 (m, 4H), 4.31 – 4.11 (m, 2H), 4.10 – 3.92 (m, 1H), 3.50 – 3.32 (m, 2H), 2.15 – 1.82 (m, 4H), 1.47 (s, 9H).

Synthesis of (*S*)-2-[(3-nitro-5-phenyl)phenoxy]methyl]pyrrolidine [(*S*)-**38**]



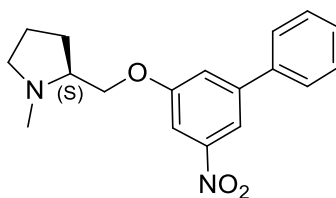
Molecular Weight: 298.34

(*S*)-*N*-*tert*-butoxycarbonyl-2-[(3-nitro-5-phenyl)phenoxy]methyl]pyrrolidine [(*S*)-**32**] (167 mg – 0.42 mmol) was dissolved in 5 ml of DCM and the resulting solution was cooled to 0 °C. Under vigorous stirring, TFA (0.5 ml) was added dropwise and the reaction mixture was stirred at room temperature for 3 hours. Afterward, the mixture was diluted with an aqueous solution of HCl 1M (8 ml) and washed with diethyl ether. The aqueous phase was cooled to 0 °C and

the pH was adjusted to pH 12 by adding dropwise a solution of NaOH 1 M. After washing again with diethyl ether, the aqueous phase was cooled to 0 °C and acidified with acetic acid to reach pH 6/7 and extracted with ethyl acetate. The organic phase was dried over anhydrous sodium sulphate, filtered and evaporated *in vacuo* obtaining the desired product (*S*)-**38** as yellow oil (97 mg – 0.33 mmol, 78%). **TLC** (Dichloromethane / Methanol 95:5 + 0.3 % NH₃(al 30% in acqua)): **Rf**= 0.23. **¹H NMR** (300 MHz, MeOD): δ 8.04 (s, 1H), 7.75 (s, 1H), 7.73 – 7.63 (m, 2H), 7.58 (s, 1H), 7.55 – 7.37 (m, 3H), 4.14 (dd, *J*= 9.4, 4.8 Hz, 1H), 4.04 (dd, *J*= 9.4, 7.0 Hz, 1H), 3.62 – 3.46 (m, 1H), 3.10 – 2.85 (m, 2H), 2.13 – 1.95 (m, 1H), 1.95 – 1.73 (m, 2H), 1.73 – 1.53 (m, 1H).

Synthesis of (*S*)-N-methyl-2-[(3-nitro-5-phenyl)phenoxy]methylpyrrolidine

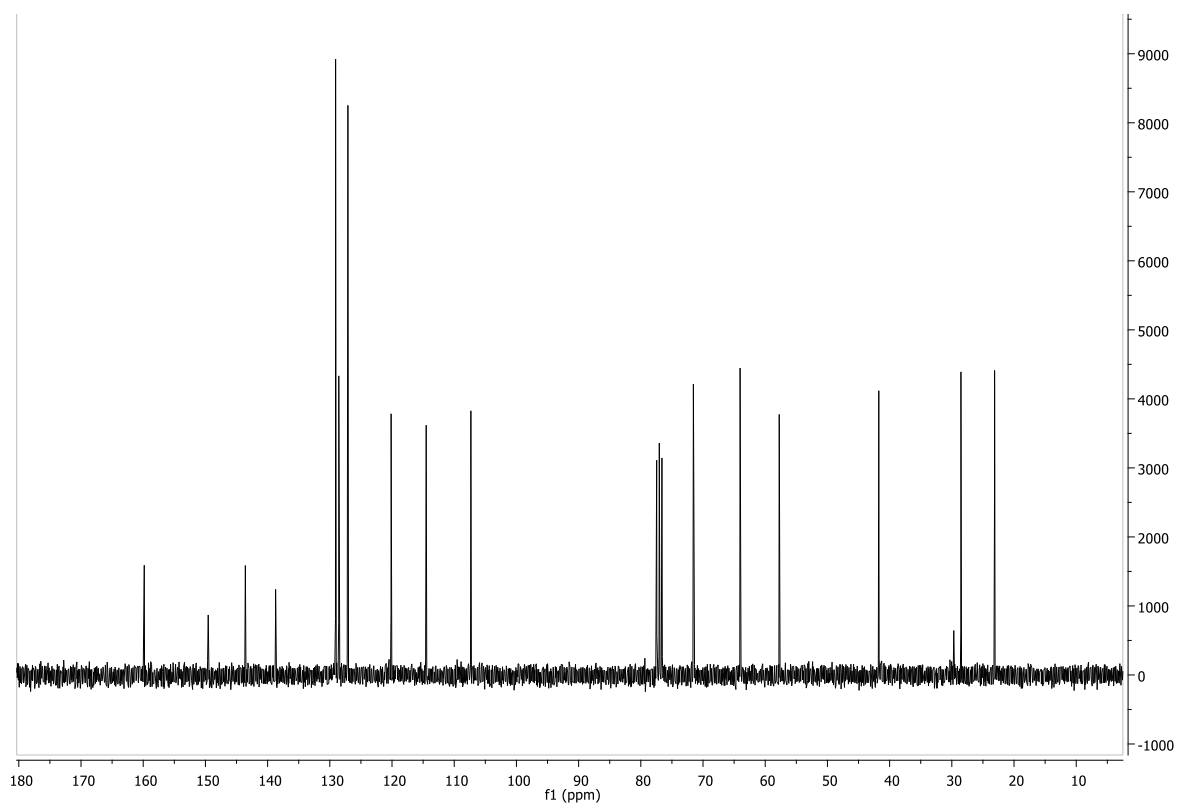
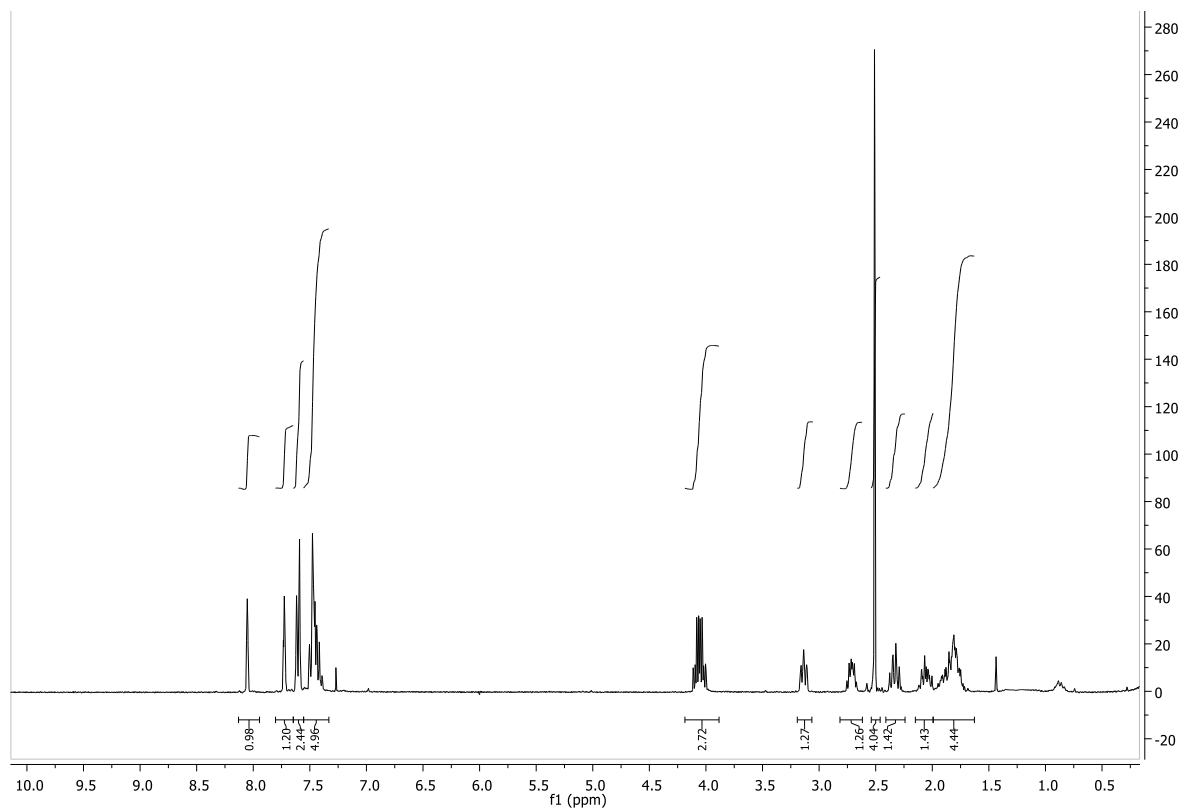
[(*S*)-2b]

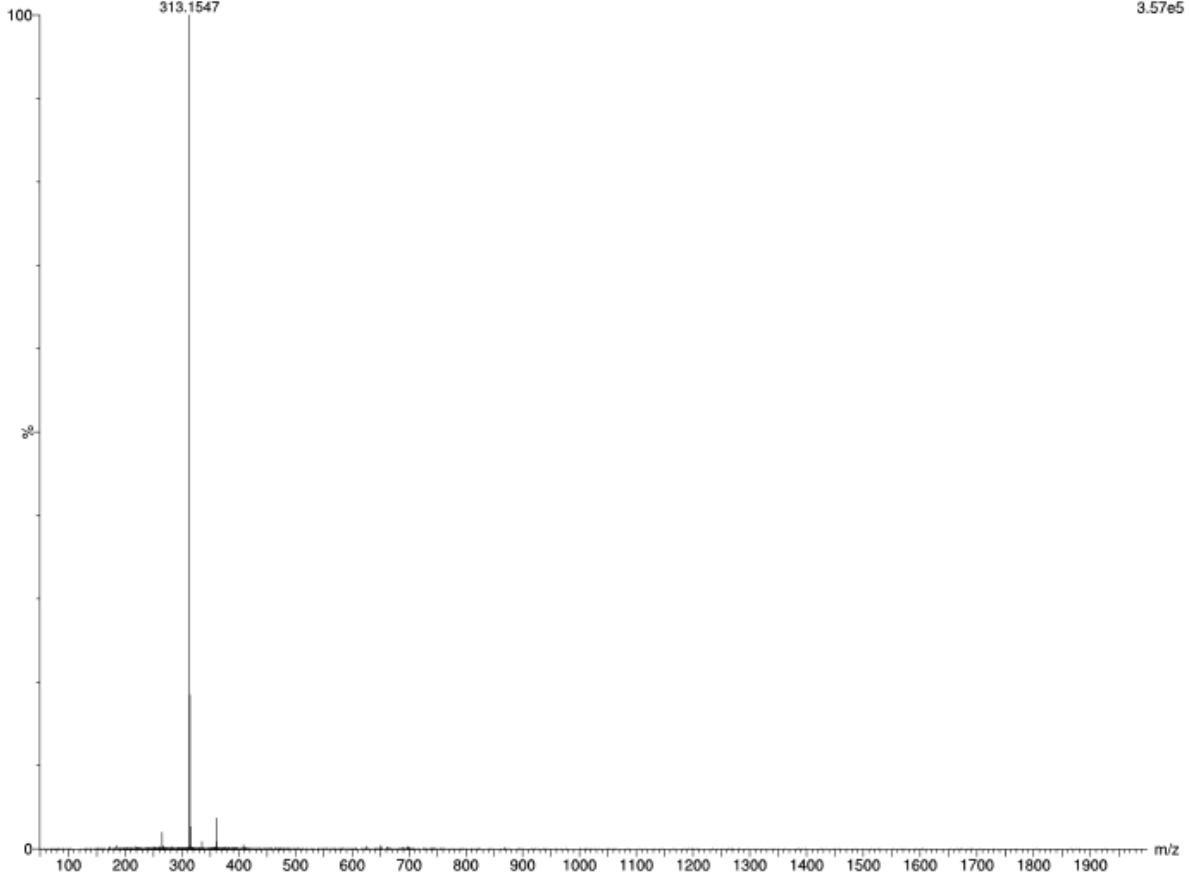


Molecular Weight: 312.36

Under vigorous stirring at 0 °C, an aqueous solution of formaldehyde (37% in water, 0.07 ml) was added dropwise to a solution of (*S*)-2-[(3-nitro-5-phenyl)phenoxy]methylpyrrolidine [(*S*)-**38**] (68 mg – 0.23 mmol) in 2 ml of methanol and 60 µl of glacial acetic acid. Upon addition of 2-picolin borane (25 mg – 0.23 mmol), the mixture was reacted for 3 hours. The solvent was evaporated *in vacuo*, the residue was diluted with 5 ml of a 1M HCl solution and stirred for 1 hour to quench the unreacted 2-picolin-borane. Then, the pH was adjusted to 8 by adding an aqueous solution of Na₂CO₃ 2M and the aqueous phase was extracted with ethyl acetate (3x30 ml). The organic phase was washed with brine, dried over sodium sulphate, filtered and evaporated *in vacuo*, providing a crude that was further purified through silica gel flash chromatography (dichloromethane/methanol 95:5). The pure compound (*S*)-**2b** was obtained as a yellow oil (40 mg – 0.13 mmol, 86%). **TLC** (Dichloromethane / Methanol 9:1 +2% NH₃(30% in water)): **Rf**= 0.24. **[α]_D²⁵** = –38.42° (*c*0.5, MeOH). **¹H NMR** (300 MHz, CDCl₃): δ 8.05 (m, 1H), 7.73 (t, *J*= 2.1 Hz, 1H), 7.61 (m, 2H), 7.52 – 7.33 (m, 4H), 4.09 (dd, *J*= 9.3, 5.3 Hz, 1H), 4.03 (dd, *J*= 9.3, 5.3 Hz, 1H), 3.14 (m, 1H), 2.81 – 2.61 (m, 1H), 2.51 (s, 3H), 2.39 – 2.25 (m, 1H), 2.13 – 1.97 (m, 1H), 1.97 – 1.69 (m, 3H). **¹³C NMR** (75 MHz, CDCl₃): δ 159.83, 149.55,

143.58, 138.72, 129.07, 128.56, 127.09, 120.15, 114.51, 107.32, 71.55, 64.04, 57.75, 41.75, 28.54, 23.13. **HRMS (ESI⁺)**: calc. for C₁₈H₂₁N₂O₃; theor. 313.1552; found [M+H]⁺: 313.1547.





Elemental Composition Report

Single Mass Analysis

Tolerance = 5.0 PPM / DBE: min = -1.5, max = 200.0
 Element prediction: Off
 Number of isotope peaks used for i-FIT = 5

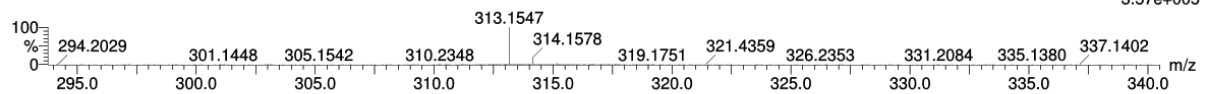
Monoisotopic Mass, Even Electron Ions

264 formula(e) evaluated with 1 results within limits (all results (up to 1000) for each mass)

Elements Used:

C: 18-18 H: 10-100 N: 0-5 O: 0-5 Na: 0-1 Cl: 0-3

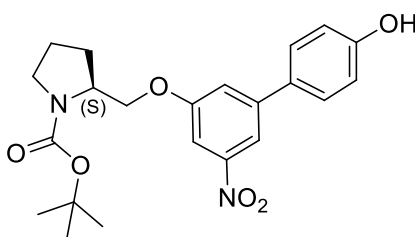
PD55 20 (0.394) AM2 (Ar,40000.0,0.00,0.00)



Minimum: -1.5
 Maximum: 0.5 5.0 200.0

Mass	Calc. Mass	mDa	PPM	DBE	i-FIT	Norm	Conf(%)	Formula
313.1547	313.1552	-0.5	-1.6	9.5	1280.0	n/a	n/a	C18 H21 N2 O3

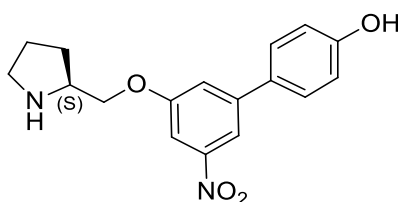
Synthesis of (*S*)-*N*-*tert*-butoxycarbonyl-2-[(3-nitro-5-(4-hydroxyphenyl)phenoxy)methyl]pyrrolidine [(*S*)-34]



Molecular Weight: 414.45

Under nitrogen atmosphere, tetrakis(triphenylphosphine)Pd(0) (164 mg – 0.14 mmol) was added to a solution of (*S*)-*N*-*tert*-butoxycarbonyl-2-[(3-bromo-5-nitro)phenoxy)methyl]pyrrolidine [(*S*)-28] (820 mg – 2 mmol) in 6 ml of toluene. Upon stirring for 10 minutes at room temperature, 3 ml of an aqueous solution of Na₂CO₃ 2M and a solution of *p*-hydroxyphenyl boronic acid (304 mg – 2.2 mmol) in ethanol (0.5 ml) were sequentially added. The mixture was refluxed for 12 hours. Afterward, the mixture was diluted with ethyl acetate (30 ml) and the organic phase was dried over anhydrous sodium sulphate, filtered and concentrated in vacuo, providing a crude that was purified through silica gel flash chromatography (gradient from cyclohexane to cyclohexane/ethyl acetate 8:2). The pure product (*S*)-34 was obtained as a yellow oil (522 mg – 1.26 mmol, 63%). TLC (Cyclohexane / Ethyl acetate 9:1): R_f = 0.38. [α]_D²⁵ = -55.27° (c1, MeOH). ¹H NMR (300 MHz, CDCl₃) δ 7.41 – 7.32 (m, 2H), 6.90 – 6.80 (m, 2H), 6.64 – 6.56 (m, 2H), 6.43 (s, 1H), 4.19 – 4.10 (m, 2H), 3.91 – 3.80 (m, 1H), 3.51 – 3.25 (m, 2H), 2.14 – 1.84 (m, 4H), 1.55 – 1.38 (m, 9H).

Synthesis of (*S*)-2-[(3-nitro-5-(4-hydroxyphenyl)phenoxy)methyl]pyrrolidine [(*S*)-40]

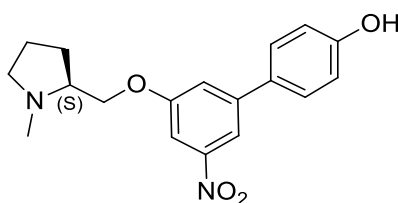


Molecular Weight: 314.34

(*S*)-*N*-*tert*-butoxycarbonyl-2-[(3-nitro-5-(4-hydroxyphenyl)phenoxy)methyl]pyrrolidine [(*S*)-34] (465 mg – 1.12 mmol) was dissolved in 13 ml of DCM and the resulting solution was cooled to 0 °C. Under vigorous stirring, TFA (2 ml) was added dropwise and the reaction mixture was stirred at room temperature for 3 hours. Afterward, the mixture was diluted with an aqueous

solution of HCl 1M (8 ml) and washed with diethyl ether. The aqueous phase was cooled to 0 °C and the pH was adjusted to pH 12 by adding dropwise a solution of NaOH 1 M. After washing again with diethyl ether, the aqueous phase was cooled to 0 °C and acidified with acetic acid to reach pH 6/7 and extracted with ethyl acetate. The organic phase was dried over anhydrous sodium sulphate, filtered and evaporated *in vacuo* obtaining the desired product (*S*)-**40** as a yellow oil (285 mg – 0.91 mmol, 81%). **TLC** (Dichloromethane / Methanol 95:5 + 0.3 % NH₃(30% in water)): **R_f**= 0.22. **¹H NMR** (300 MHz, DMSO-*d*₆): δ 9.80 (bs, 1H, exchange with D₂O), 7.96 – 7.88 (m, 1H), 7.66 – 7.50 (m, 4H), 6.86 (d, *J* = 8.2 Hz, 2H), 3.98 (d, *J* = 6.3 Hz, 2H), 3.48 – 3.35 (m, 1H), 2.88 – 2.75 (m, 2H), 1.93 – 1.77 (m, 1H), 1.77 – 1.55 (m, 2H), 1.55 – 1.38 (m, 1H).

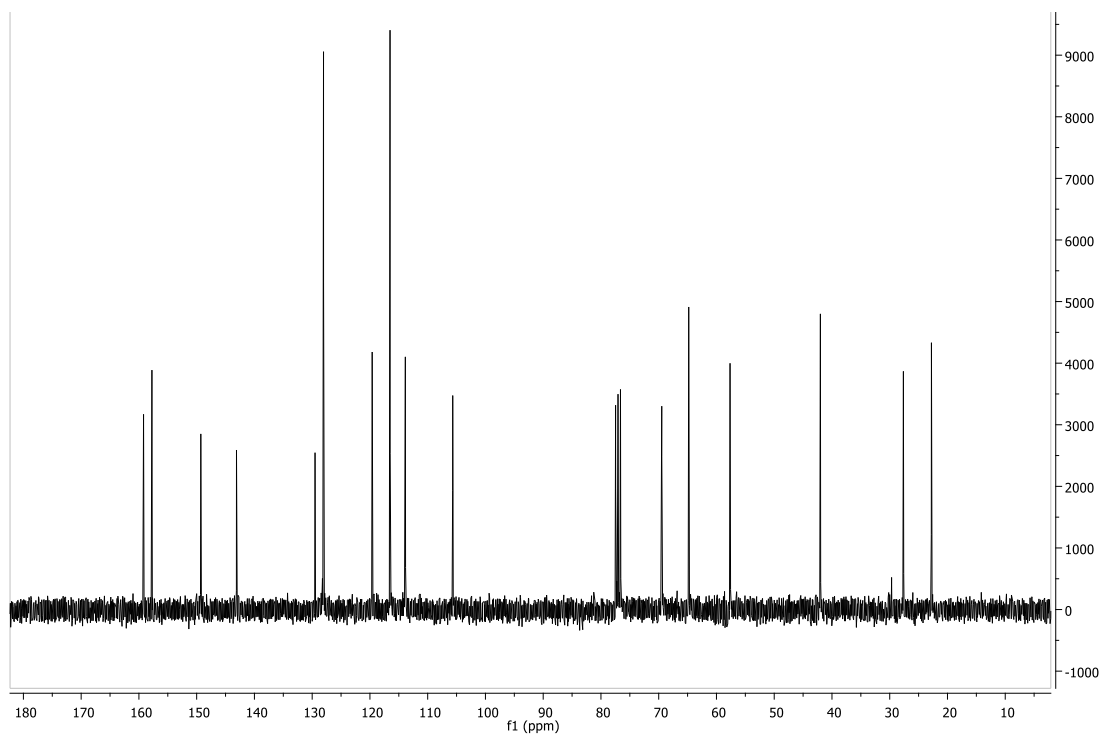
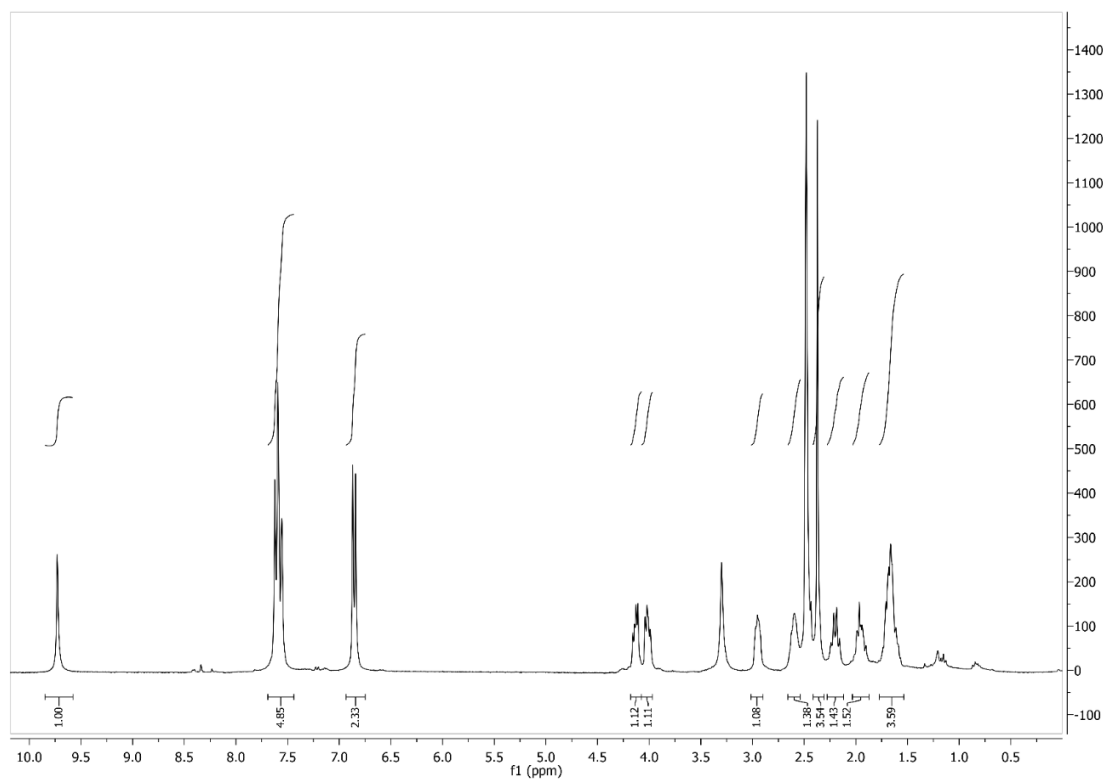
Synthesis of (*S*)-N-methyl-2-[(3-nitro-5-(4-hydroxyphenyl)phenoxy)methyl]pyrrolidine [(*S*)-**2c**]

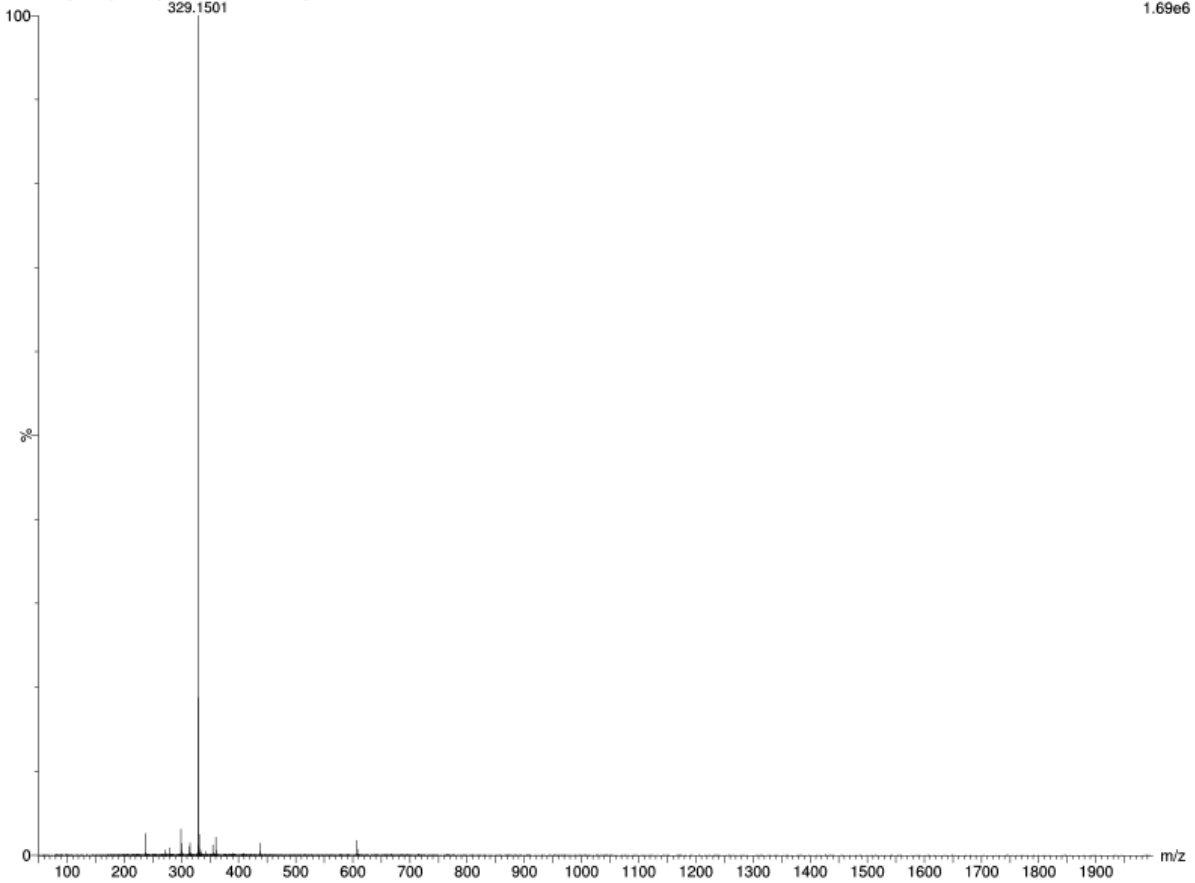


Molecular Weight: 328.36

Under vigorous stirring at 0 °C, an aqueous solution of formaldehyde (37% in water, 0.1 ml) was added dropwise to a solution of (*S*)-2-[(3-nitro-5-(4-hydroxyphenyl)phenoxy)methyl]pyrrolidine [(*S*)-**40**] (100 mg – 0.32 mmol) in 3 ml of DMF and 80 µl of glacial acetic acid. Upon addition of 2-picolin borane (34 mg – 0.32 mmol), the mixture was reacted for 3 hours. The solvent was evaporated *in vacuo*, the residue was diluted with 5 ml of a 1M HCl solution and stirred for 1 hour to quench the unreacted 2-picolin-borane. Then, the pH was adjusted to 8 by adding an aqueous solution of Na₂CO₃ 2M and the aqueous phase was extracted with ethyl acetate (3x30 ml). The organic phase was washed with brine, dried over sodium sulphate, filtered and evaporated *in vacuo*, providing a crude that was further purified through silica gel flash chromatography (dichloromethane/methanol 95:5 + 2% NH₃(30% in water)). The pure compound (*S*)-**2c** was obtained as a yellow solid (83 mg – 0.25 mmol, 79%). **TLC** (Dichloromethane / Methanol 95:5 +2% NH₃(30% in water)): **R_f**= 0.33. **M.p.**= 163.8 °C. **[α]_D²⁵** = -22.49° (*c*1, MeOH). **¹H NMR** (300 MHz, DMSO-*d*₆) δ 9.73 (s, exchange with D₂O, 1H), 7.71 – 7.48 (m, 5H), 6.86 (d, *J* = 8.3 Hz, 2H), 4.13 (dd, *J* = 9.6, 5.3 Hz, 1H), 4.01 (dd, *J* = 9.6, 5.8 Hz, 1H), 3.02 – 2.90 (m, 1H), 2.68 – 2.52 (m, 1H), 2.37 (s, 3H), 2.28 –

2.10 (m, 1H), 2.05 – 1.84 (m, 1H), 1.80 – 1.55 (m, 3H). ^{13}C NMR (75 MHz, CDCl_3): δ 159.20, 157.75, 149.28, 143.11, 129.50, 128.04, 119.61, 116.52, 113.88, 105.67, 69.48, 64.81, 57.65, 42.01, 27.64, 22.79. **HRMS (ESI $^+$)**: calc. for $\text{C}_{18}\text{H}_{21}\text{N}_2\text{O}_4$: theor. 329.1501; found $[\text{M}+\text{H}]^+$: 329.1501.





Elemental Composition Report

Single Mass Analysis

Tolerance = 5.0 PPM / DBE: min = -1.5, max = 200.0
 Element prediction: Off
 Number of isotope peaks used for i-FIT = 5

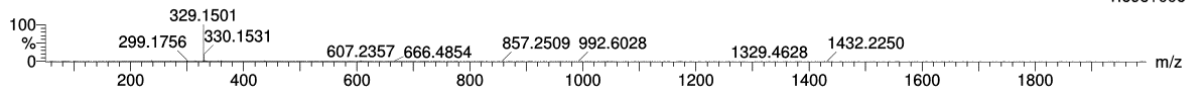
Monoisotopic Mass, Even Electron Ions

260 formula(e) evaluated with 1 results within limits (all results (up to 1000) for each mass)

Elements Used:

C: 18-18 H: 10-100 N: 0-5 O: 0-5 Na: 0-1 Cl: 0-3

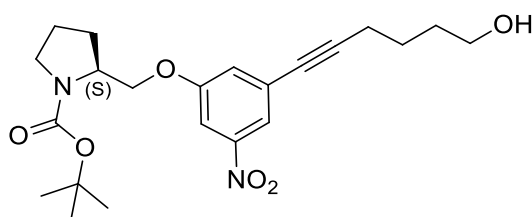
PD58 32 (0.617) AM2 (Ar,40000.0,0.00,0.00)



Minimum: -1.5
 Maximum: 0.5 5.0 200.0

Mass	Calc. Mass	mDa	PPM	DBE	i-FIT	Norm	Conf (%)	Formula
329.1501	329.1501	0.0	0.0	9.5	1969.0	n/a	n/a	C18 H21 N2 O4

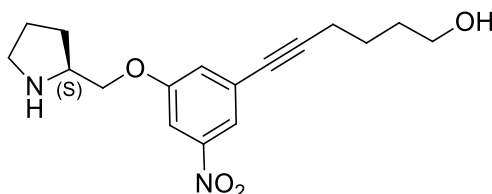
Synthesis of (*S*)-*N*-*tert*-butoxycarbonyl-2-[(3-nitro-5-(6-hydroxy-1-hexynyl))phenoxy]methyl]pyrrolidine [(*S*)-**36**]



Molecular Weight: 418.48

Under nitrogen atmosphere, CuBr (10 mg – 0.07 mmol) and tetrakis(triphenylphosphine)Pd(0) (41 mg – 0.035 mmol) were added to a solution of (*S*)-*N*-*tert*-butoxycarbonyl-2-[(3-bromo-5-nitro)phenoxy]methyl]pyrrolidine [(*S*)-**28**] (352 mg – 0.877 mmol) in 5 ml of triethylamine. Upon stirring for 30 minutes at room temperature, 5-hexyn-1-ol (172 mg – 1.75 mmol) was added and the mixture was refluxed for 12 hours. Afterward, the mixture was diluted with 10 ml of 1M aqueous HCl and extracted with ethyl acetate (3x30 ml). The organic phase was washed with brine (15 ml), dried over anhydrous sodium sulphate, filtered on diatomaceous earth and concentrated in vacuo, providing a crude that was purified through silica gel flash chromatography (dichloromethane/methanol 98:2). The pure product (*S*)-**36** was obtained as a yellow oil (265 mg – 0.533 mmol, 61%). TLC (Dichloromethane / Methanol 98:2): $R_f = 0.24$. $[\alpha]_D^{25} = -7.08^\circ$ (c_1 , CH₃OH) $^1\text{H-NMR}$ (300 MHz, CD₃OD): 7.81 (s, 1H), 7.26 (m, 2H), 4.15 (m, 2H), 3.97 (m, 1H), 3.71 (m, 2H), 3.38 (m, 2H), 2.47 (t, $J = 6.4$ Hz, 2H), 2.01 – 1.67 (m, 8H), 1.47 (s, 9H).

Synthesis of (*S*)-2-[(3-nitro-5-(6-hydroxy-1-hexynyl))phenoxy]methyl]pyrrolidine [(*S*)-**42**]

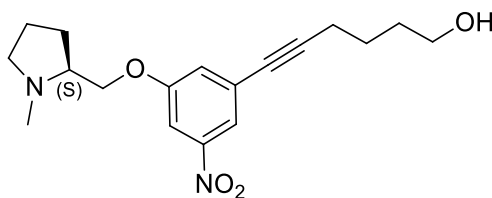


Molecular Weight: 318.37

(*S*)-*N*-*tert*-butoxycarbonyl-2-[(3-nitro-5-(6-hydroxy-1-hexynyl))phenoxy]methyl]pyrrolidine [(*S*)-**36**] (200 mg 0.40 mmol) was dissolved in 2 ml of methanol and the solution was cooled to 0 °C. Upon dropwise addition of 10 ml of a 1.25 M methanolic solution of HCl under vigorous stirring, the reaction mixture was warmed to room temperature and reacted for 12 hours.

Afterward, methanol was evaporated in vacuo, the residue was diluted with 10 ml of a 10% aqueous solution of NaHCO₃ and extracted with DCM. The organic phase was dried over sodium sulphate, filtrated and evaporated in vacuo, affording a crude that was purified through silica gel flash chromatography (from dichloromethane/methanol 98:2 to 9:1). The pure product (*S*)-**42** was obtained as a yellow-brown oil (150 mg – 0.38 mmol, 95%). TLC (Dichloromethane / Methanol 98:2 + 2% NH₃(30% in water)): **R_f** = 0.17. [α]_D²⁵ = +7.20° (c1, CH₃OH). ¹H-NMR (300 MHz, CD₃OD): δ 7.63 (s, 1H), 7.70 (s, 1H), 7.32 (s, 1H), 4.14 (dd, *J* = 9.6, 4.4 Hz, 1H), 4.03 (dd *J* = 9.6, 7.4 Hz, 1H), 3.62 (m, 3H), 3.04 (m, 2H), 2.48 (m, 2H), 2.03 (m, 1H), 1.87 (m, 2H), 1.70 – 1.63 (m, 5H).

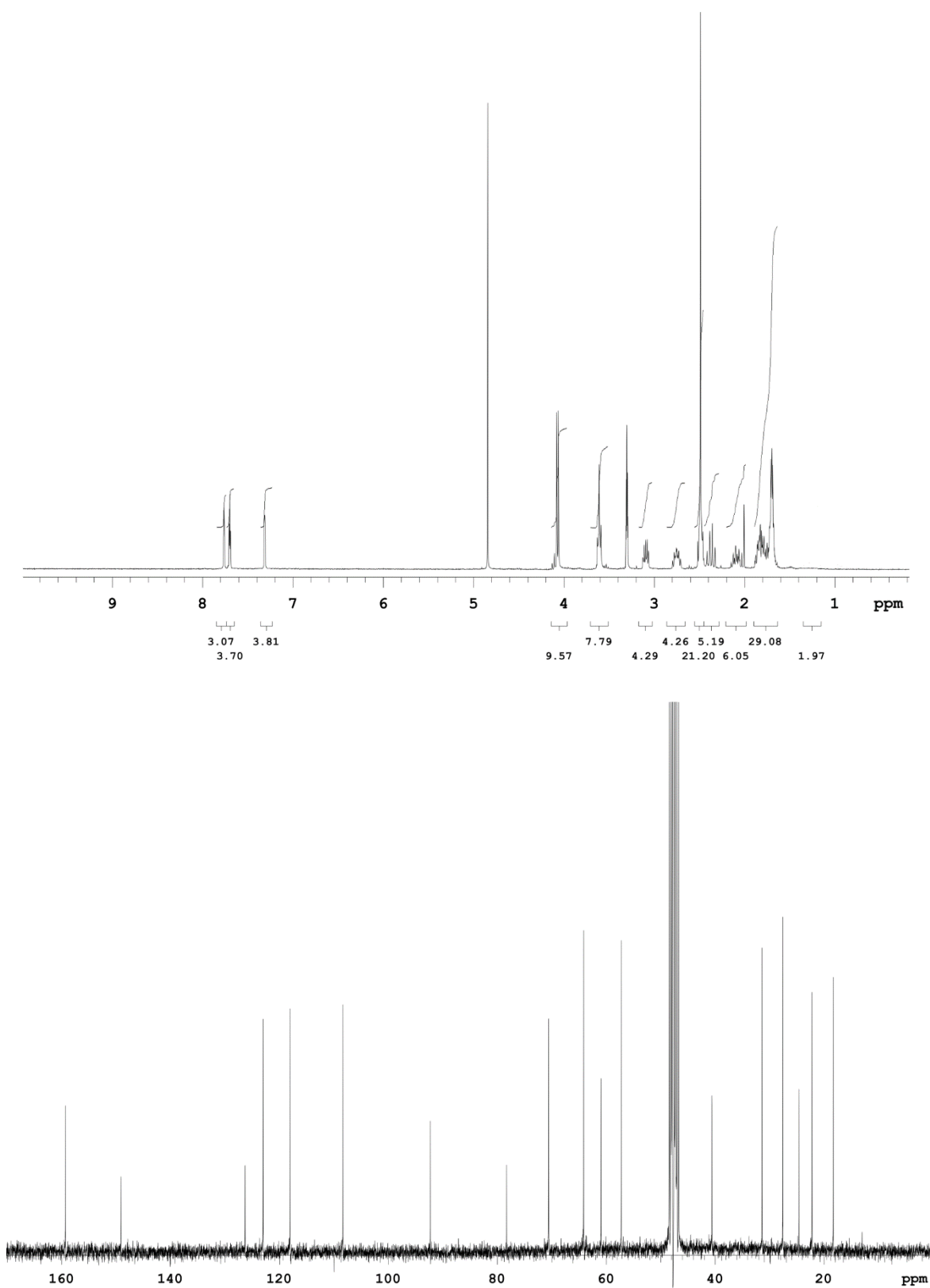
Synthesis of (*S*)-N-methyl-2-[(3-nitro-5-(6-hydroxy-1-hexynyl))phoxymethyl]pyrrolidine [(*S*)-**2d**]



Molecular Weight: 332.39

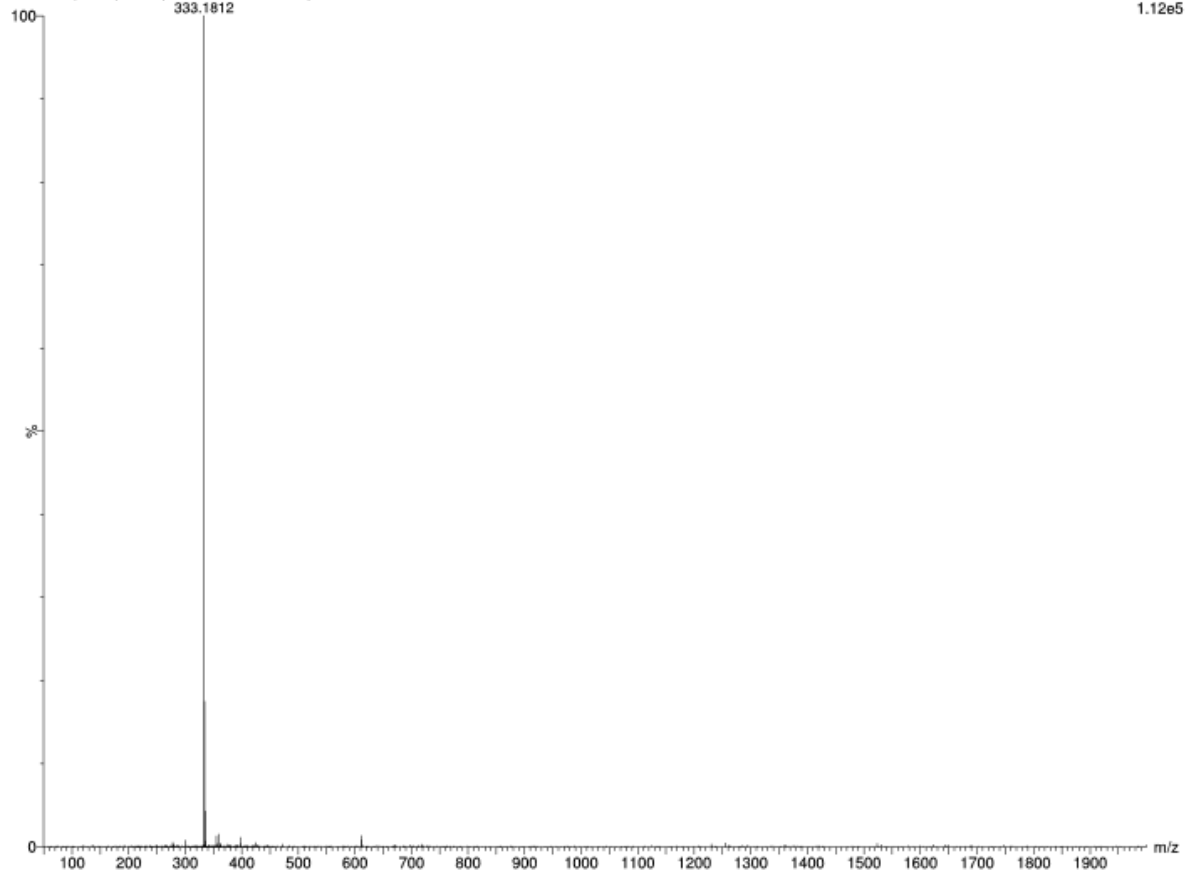
Under vigorous stirring at 0 °C, an aqueous solution of formaldehyde (37% in water, 0.06 ml) was added dropwise to a solution of (*S*)-2-[(3-nitro-5-(6-hydroxy-1-hexynyl))phoxymethyl]pyrrolidine [(*S*)-**42**] (68 mg – 0.17 mmol) in 4 ml of methanol and 80 μ l of glacial acetic acid. Upon addition of 2-picolin borane (18 mg – 0.17 mmol), the mixture was reacted for 6 hours. The solvent was evaporated in vacuo, the residue was diluted with 5 ml of a 1M HCl solution and stirred for 1 hour to quench the unreacted 2-picolin-borane. Then, the pH was adjusted to 8 by adding an aqueous solution of Na₂CO₃ 2M and the aqueous phase was extracted with ethyl acetate (3x30 ml). The organic phase was washed with brine, dried over sodium sulphate, filtered and evaporated in vacuo, providing a crude, that was further purified through silica-gel flash chromatography (gradient from dichloromethane to dichloromethane/methanol 9:1). The pure compound (*S*)-**2d** was obtained as a yellow oil (56 mg- 0.14 mmol, 80%). TLC (Dichloromethane / Methanol 9:1 +2% NH₃(30% in water)): **R_f** = 0.57. [α]_D²⁵ = +30.23° (c1, CH₃OH). ¹H-NMR (300 MHz, CD₃OD): δ 7.76 (s, 1H), 7.70 (s, 1H), 7.31 (s, 1H), 4.07 (d, *J* = 5.3 Hz, 2H), 3.61 (t, *J* = 6.4 Hz, 2H), 3.01 (m, 1H), 2.75 (m, 1H), 2.49 (m, 5H), 2.38 (m, 1H), 2.05 (m, 1H), 1.86 – 1.67 (m, 7H). ¹³C-NMR (75 MHz, CD₃OD): δ 159.3,

149.1, 126.3, 123.0, 118.0, 108.4, 92.3, 78.3, 70.6, 64.2, 61.0, 57.3, 40.6, 31.4, 27.6, 24.6, 22.2, 18.3. **HRMS (ESI⁺):** calc. for C₁₈H₂₅N₂O₄: theor. 333.1814; found [M+H]⁺: 333.1812.



PD45 27 (0.533) AM2 (Ar,40000.0,0.00,0.00)

1: TOF MS ES+
1.12e5



Elemental Composition Report

Single Mass Analysis

Tolerance = 5.0 PPM / DBE: min = -1.5, max = 200.0
 Element prediction: Off
 Number of isotope peaks used for i-FIT = 5

Monoisotopic Mass, Even Electron Ions

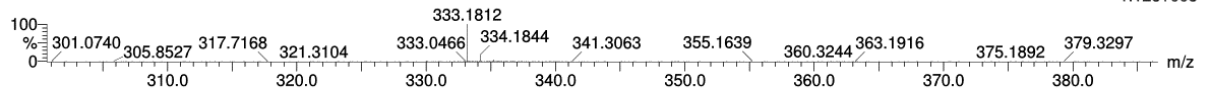
259 formula(e) evaluated with 1 results within limits (all results (up to 1000) for each mass)

Elements Used:

C: 18-18 H: 10-100 N: 0-5 O: 0-5 Na: 0-1 Cl: 0-3

PD45 27 (0.533) AM2 (Ar,40000.0,0.00,0.00)

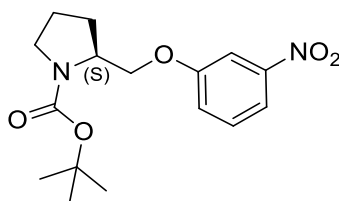
1: TOF MS ES+
1.12e+005



Minimum: -1.5
 Maximum: 0.5 5.0 200.0

Mass	Calc. Mass	mDa	PPM	DBE	i-FIT	Norm	Conf (%)	Formula
333.1812	333.1814	-0.2	-0.6	7.5	644.5	n/a	n/a	C18 H25 N2 O4

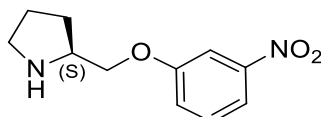
Synthesis of (*S*)-*N*-*tert*-butoxycarbonyl-2-(3-nitrophenoxy)methylpyrrolidine



Molecular Weight: 322.36

Procedure adapted from literature.¹⁶² 3-nitrophenol (209 mg – 1.50 mmol) and (*S*)-*N*-*tert*-butoxycarbonyl-2-hydroxymethyl-pyrrolidine (300 mg – 1.50 mmol), dissolved each in 2 ml of anhydrous THF, were added to a solution of triphenylphosphine (472 mg – 1.8 mmol) in 2 ml of anhydrous THF. The reaction mixture was cooled to -10°C and DIAD (0.35 mL – 1.80 mmol), was added dropwise, under vigorous stirring. The reaction mixture was refluxed for 12 hours. After cooling to room temperature, the mixture was diluted with 10 mL of 1M aqueous solution of NaOH and extracted with ethyl acetate twice (2x30 ml). The organic phase was dried over anhydrous sodium sulphate, filtrated and concentrated in vacuo to obtain a crude that was further purified through silica-gel flash column chromatography (gradient from cyclohexane/ethylacetate 9:1 to 6:4). The pure compound was obtained as a yellowish - brownish oil (400 mg – 1.24 mmol, 82%). **TLC** (Cyclohexane / Ethyl Acetate 6:4; stained with cerium sulphate): **R_f** = 0.46. **[α]_D²⁵** = -52.34° (*c*1, CH₃OH). **¹H-NMR** (300 MHz, CDCl₃): δ 7.78 (m, 2H), 7.42 (t, *J*= 8.2 Hz, 1H), 7.34 – 7.19 (m, 1H), 4.16 (m, 2H); 3.90 (m, 1H), 3.37 (m, 2H), 2.03 – 1.86 (m, 4H), 1.55 (s, 4.5H), 1.52 (s, 4.5H).

Synthesis of (*S*)-*N*-*tert*-butoxycarbonyl-2-(3-nitrophenoxy)methylpyrrolidine

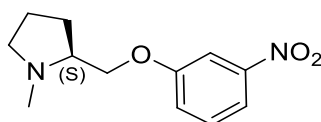


Molecular Weight: 222.24

(*S*)-*N*-*tert*-butoxycarbonyl-2-(3-nitrophenoxy)methylpyrrolidine (360 mg – 1.12 mmol) was dissolved in 2 ml of methanol and the solution was cooled to 0 °C. Upon dropwise addition of 8 ml of a 1.25 M methanolic solution of HCl under vigorous stirring, the reaction mixture was warmed to room temperature and reacted for 12 hours. Afterward, methanol was evaporated in

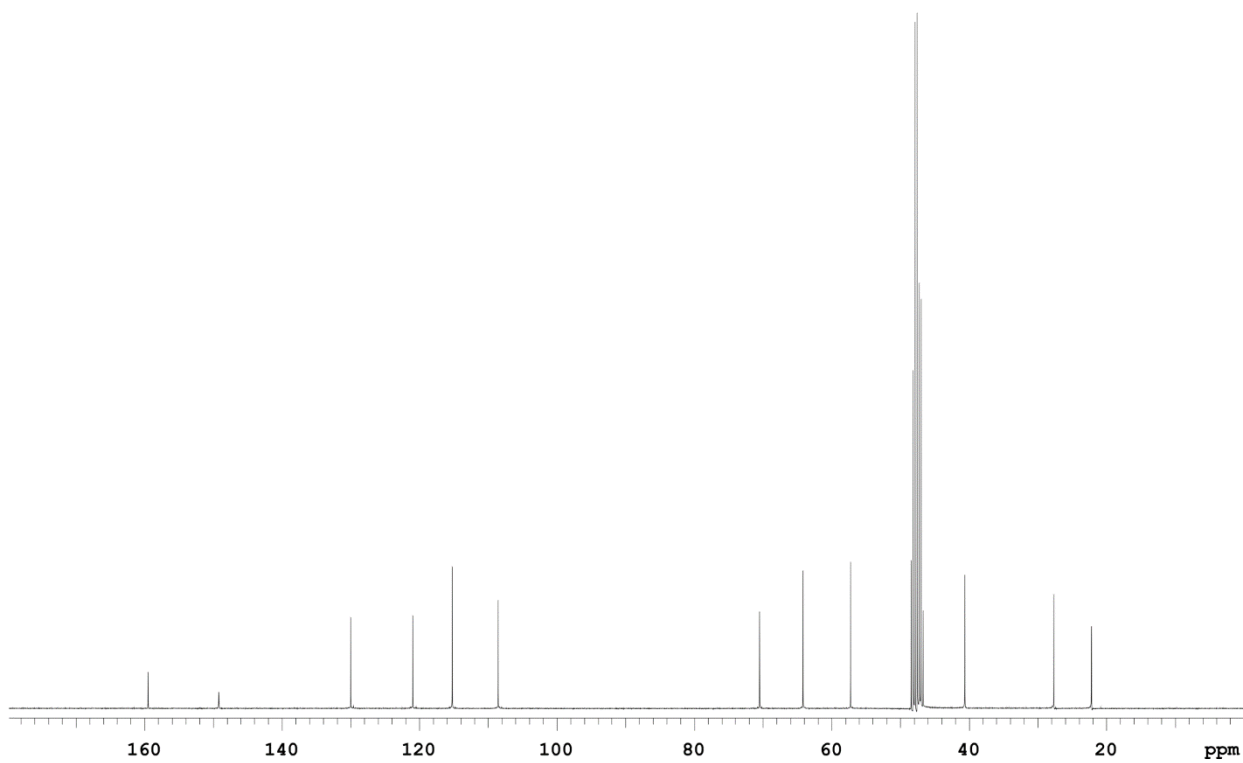
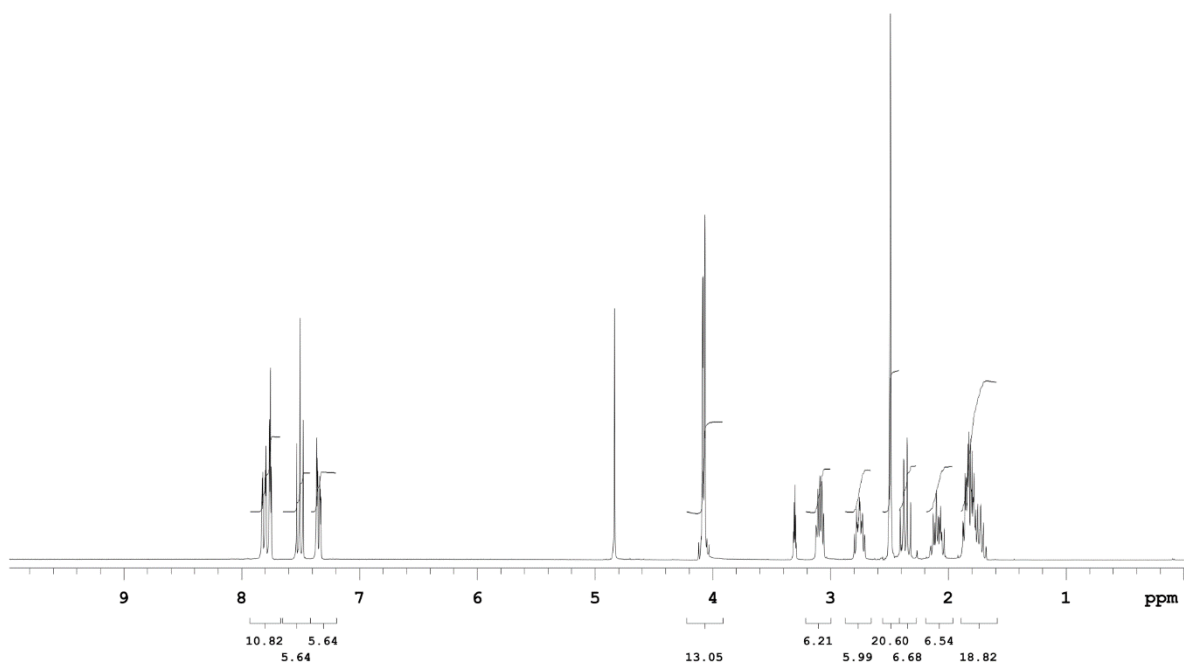
vacuo, the residue was diluted with 10 ml of a 10% aqueous solution of NaHCO₃ and extracted with DCM (3x30ml). The organic phase was dried over sodium sulphate, filtrated and evaporated in vacuo, affording the pure product as a brownish sticky solid (230 mg – 1.03 mmol, 100%). **TLC** (Dichloromethane / Methanol 9:1 + 2% NH₃(30% in water)): **R_f**= 0.5. **[α]_D²⁵** = +7.52 (c1, CHCl₃). **¹H-NMR** (300 MHz, CD₃OD): δ 7.82 (ddd, *J*= 8.2, 2.3, 0.9 Hz, 1H), 7.78 (t, *J*= 2.3 Hz, 1H), 7.51 (t, *J*= 8.2 Hz, 1H), 7.35 (ddd, *J*= 8.2, 2.3, 0.9 Hz, 1H), 4.10 (dd, *J*= 9.4, 4.7 Hz, 1H), 3.99 (dd, *J*= 9.4, 7.3 Hz, 1H), 3.55 (qd, *J*= 7.3, 4.7 Hz, 1H), 3.08 – 2.88 (m, 2H), 2.14 – 1.95 (m, 1H), 1.95 – 1.71 (m, 2H), 1.71 – 1.53 (m, 1H).

Synthesis of (*S*)-*N*-*tert*-butoxycarbonyl-2-(3-nitrophenoxy)methylpyrrolidine

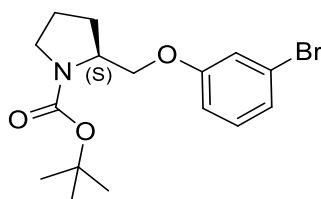


Molecular Weight: 236.27

Under vigorous stirring at 0 °C, an aqueous solution of formaldehyde (37% in water, 0.16 ml) was added dropwise to a solution of (*S*)-*N*-*tert*-butoxycarbonyl-2-(3-nitrophenoxy)methylpyrrolidine (120 mg – 0.540 mmol) in 3 ml of methanol and 80 μl of glacial acetic acid. Upon addition of 2-picolin borane (58 mg – 0.540 mmol), the mixture was reacted for 3 hours. The solvent was evaporated in vacuo, the residue was diluted with 5 ml of a 1M HCl solution and stirred for 1 hour to quench the unreacted 2-picolin-borane. Then, the pH was adjusted to 8 by adding an aqueous solution of Na₂CO₃ 2M and the aqueous phase was extracted with ethyl acetate (3x30 ml). The organic phase was washed with brine, dried over sodium sulphate, filtered and evaporated in vacuo, providing the pure compound as a yellow oil (125 mg – 0.53 mmol, 98%). **TLC** (Dichloromethane / Methanol 9:1 +2% NH₃(30% in water)): **R_f**= 0.64. **[α]_D²⁵** = -33.90° (c1, CH₃OH). **¹H-NMR** (300 MHz, CD₃OD): δ 7.82 (ddd, *J*= 8.2, 2.2, 0.9 Hz, 1H), 7.77 (t, *J*= 2.2 Hz, 1H), 7.51 (t, *J*= 8.2 Hz, 1H), 7.37 (ddd, *J*= 8.2, 2.2, 0.9 Hz, 1H), 4.08 (d, *J*= 5.6 Hz, 2H), 3.30 (m, 1H), 3.09 (m, 1H), 2.76 (m, 1H), 2.42 (s, 3H), 2.37 (q, *J*= 9.4 Hz, 1H), 2.04 – 2.13 (m, 1H), 1.88 – 1.70 (m, 3H). **¹³C-NMR** (75 MHz, CD₃OD): δ 159.5, 149.2, 130.0, 120.9, 115.3, 108.6, 70.5, 64.2, 57.3, 40.6, 27.7, 22.2.



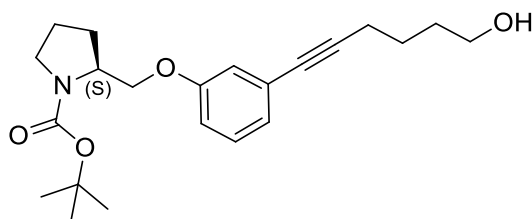
Synthesis of (*S*)-*N*-*tert*-butoxycarbonyl-2-(3-bromophenoxymethyl)pyrrolidine [(*S*)-43]



Molecular Weight: 356.25

3-bromophenol (429 mg – 2.48 mmol) and (*S*)-*N*-*tert*-butoxycarbonyl-2-hydroxymethylpyrrolidine (500 mg – 2.48 mmol) dissolved each in 2 ml of anhydrous THF, were added to a solution of triphenylphosphine (781 mg – 2.976 mmol) in 2 ml of anhydrous THF. The reaction mixture was cooled to -10°C and DIAD (0.60 mL – 2.976 mmol) was added dropwise, under vigorous stirring. The reaction mixture was refluxed for 12 hours. After cooling to room temperature, the mixture was diluted with 10 mL of 1M aqueous solution of NaOH and extracted with ethyl acetate (2x30 ml). The organic phase was dried over anhydrous sodium sulphate, filtrated and concentrated in vacuo to obtain a crude that was further purified through silica-gel flash column chromatography (gradient from cyclohexane/ethyl acetate 9:1 to 8:2). The pure compound (*S*)-43 was obtained as a yellow oil (420 mg – 1.18 mmol, 48%). TLC (Cyclohexane / Ethyl Acetate 8:2): $R_f = 0.44$. $[\alpha]_D^{25} = -42.44^{\circ}$ (c_1 , CHCl_3). $^1\text{H-NMR}$ (300 MHz, CDCl_3): δ 7.11 (m, 3H), 6.86 (d, $J = 8.2$ Hz, 1H), 4.10 (d, $J = 7.0$ Hz, 2H), 3.84 (m, 1H), 3.37 (m, 2H), 2.02 – 1.83 (m, 4H), 1.54 (s, 4.5H), 1.47 (s, 4.5H).¹⁶⁴

Synthesis of (*S*)-*N*-*tert*-butoxycarbonyl-2-[3-(6-hydroxy-1-hexynyl)phenoxy]methylpyrrolidine [(*S*)-44]

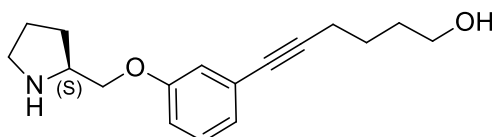


Molecular Weight: 373.49

Under nitrogen atmosphere, CuBr (13 mg – 0.09 mmol) and tetrakis(triphenylphosphine)Pd(0) (51 mg – 0.044 mmol) were added to a solution of (*S*)-*N*-*tert*-butoxycarbonyl-2-(3-bromophenoxymethyl)pyrrolidine [(*S*)-43] (400 mg – 1.12 mmol) in 3 ml of triethylamine. Upon stirring for 30 minutes at room temperature, 5-hexyn-1-ol (220 mg – 2.24 mmol) was

added and the mixture was refluxed for 12 hours. Afterward, the mixture was diluted with 10 ml of 1M aqueous HCl and extracted with ethyl acetate (3x30 ml). The organic phase was washed with brine (15 ml), dried over anhydrous sodium sulphate, filtered on diatomaceous earth and concentrated in vacuo, providing a crude that was purified through silica gel flash chromatography (dichloromethane/methanol 98:2). The pure product (*S*)-**43** was obtained as a yellow-brown oil (400 mg – 0.88 mmol, 79%). **TLC** (Dichloromethane / Methanol 95:5): **Rf**= 0.44. $[\alpha]_D^{25} = -22.68^\circ$ (*c*1, CH₃OH). **¹H-NMR** (300 MHz, CDCl₃): 7.16 (m, 1H), 6.96 (m, 2H), 6.86 (m, 1H), 4.10 (d, *J*= 7.6 Hz, 2H), 3.90 – 3.76 (m, 1H), 3.71 (t, *J*= 6.2 Hz, 2H), 3.38 (t, *J*= 6.1 Hz, 2H), 2.44 (t, *J*= 6.7 Hz, 2H), 2.01 – 1.69 (m, 8H), 1.62 – 1.44 (m, 9H).

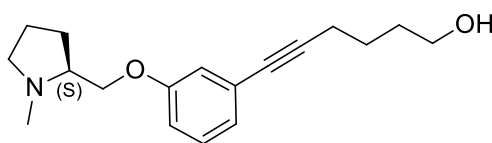
Synthesis of (*S*)-2-[3-(6-hydroxy-1-hexynyl)phenoxy]methylpyrrolidine [(*S*)-**45**]



Molecular Weight: 273.37

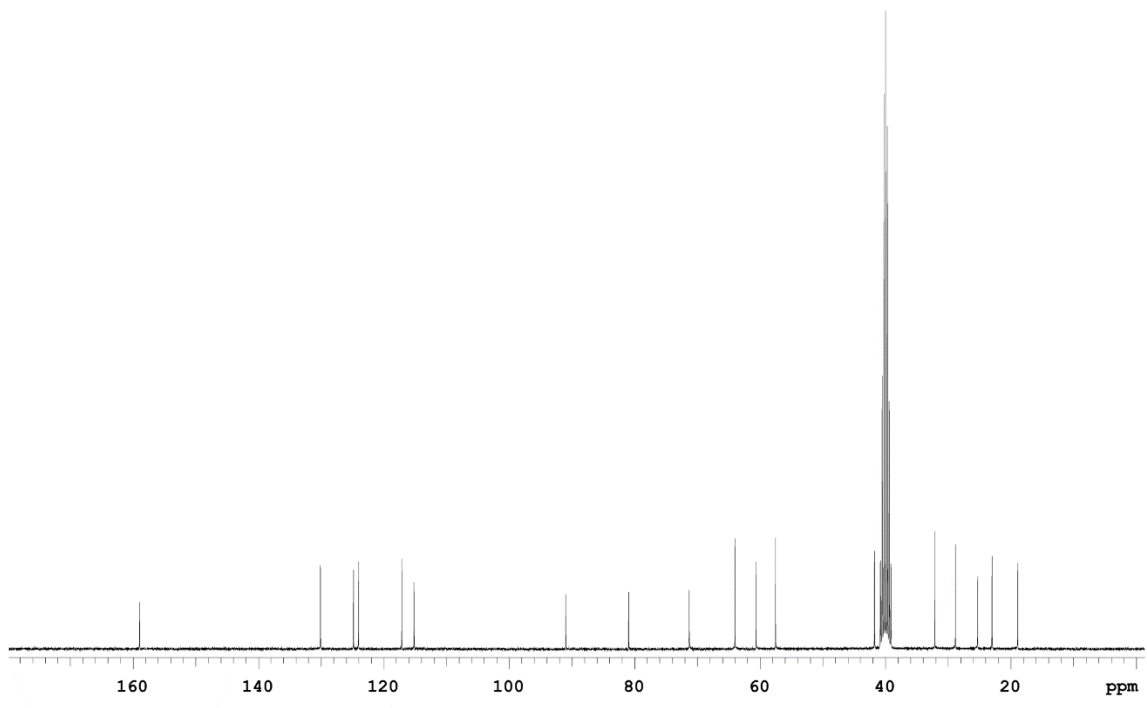
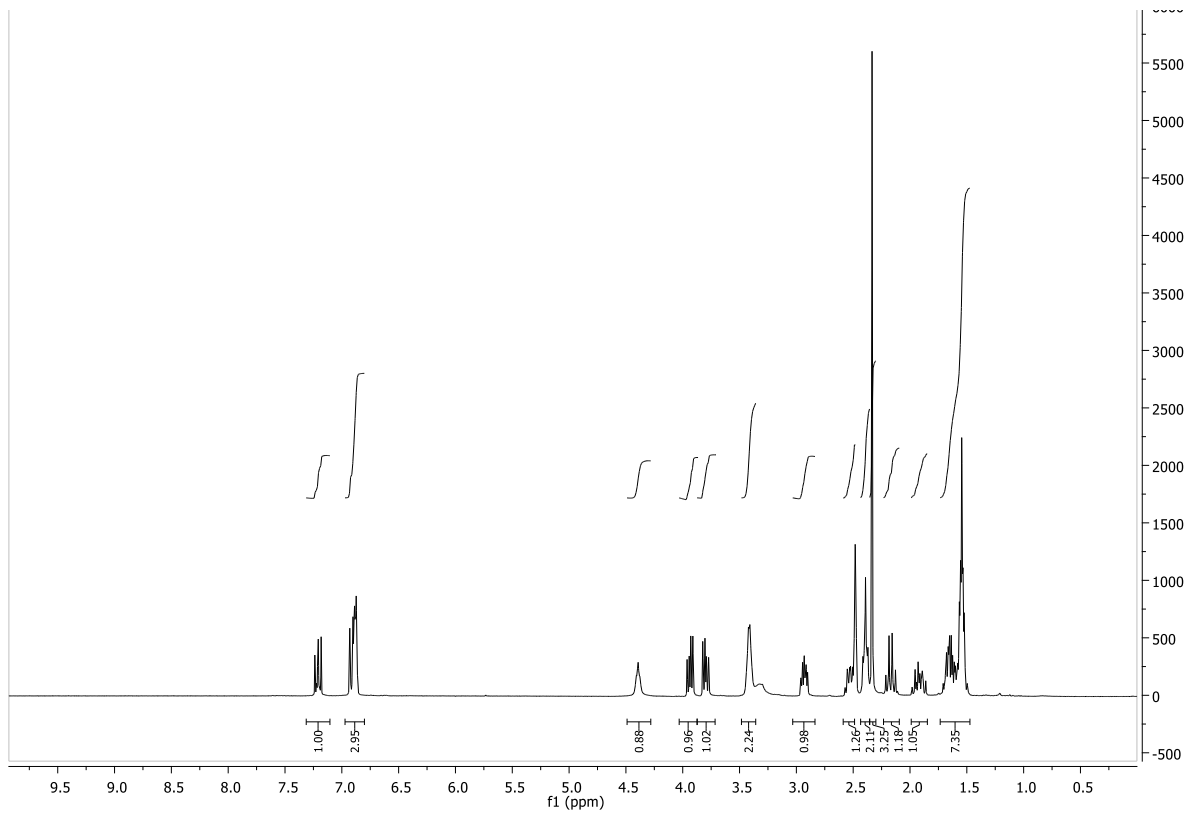
(*S*)-*N*-*tert*-butoxycarbonyl-2-[3-(6-hydroxy-1-hexynyl)phenoxy]methylpyrrolidine [(*S*)-**44**] (460 mg – 1.02 mmol) was dissolved in 2 ml of methanol and the solution was cooled to 0 °C. Upon dropwise addition of 10 ml of a 1.25 M methanolic solution of HCl under vigorous stirring, the reaction mixture was warmed to room temperature and reacted for 12 hours. Afterward, methanol was evaporated in vacuo, the residue was diluted with 10 ml of a 10% aqueous solution of NaHCO₃ and extracted with DCM (3x30ml). The organic phase was dried over sodium sulphate, filtrated and evaporated in vacuo, affording the pure product [(*S*)-**45**] as a brownish oil (255 mg – 0.72 mmol, 71%). **TLC** (Dichloromethane / Methanol 9:1 + 2% NH₃(30% in water)): **Rf**=0.38. $[\alpha]_D^{25} = +5.99^\circ$ (*c*1, CH₃OH). **¹H-NMR** (300 MHz, CD₃OD): δ 7.20 (t, *J*= 8.5 Hz, 1H), 6.95 (m, 2H), 6.82 (dd, *J*= 2.3, 8.5 Hz, 1H), 3.95 (dd, *J*= 9.4, 4.9 Hz, 1H), 3.86 (dd, *J*= 9.4, 7.0 Hz, 1H), 3.60 (t, *J*= 6.1 Hz, 2H), 3.52 – 3.37 (m, 1H), 3.06 – 2.82 (m, 2H), 2.43 (t, *J*= 6.6 Hz, 2H), 2.01 – 1.90 (m, 1H), 1.90 – 1.76 (m, 2H), 1.76 – 1.49 (m, 5H).

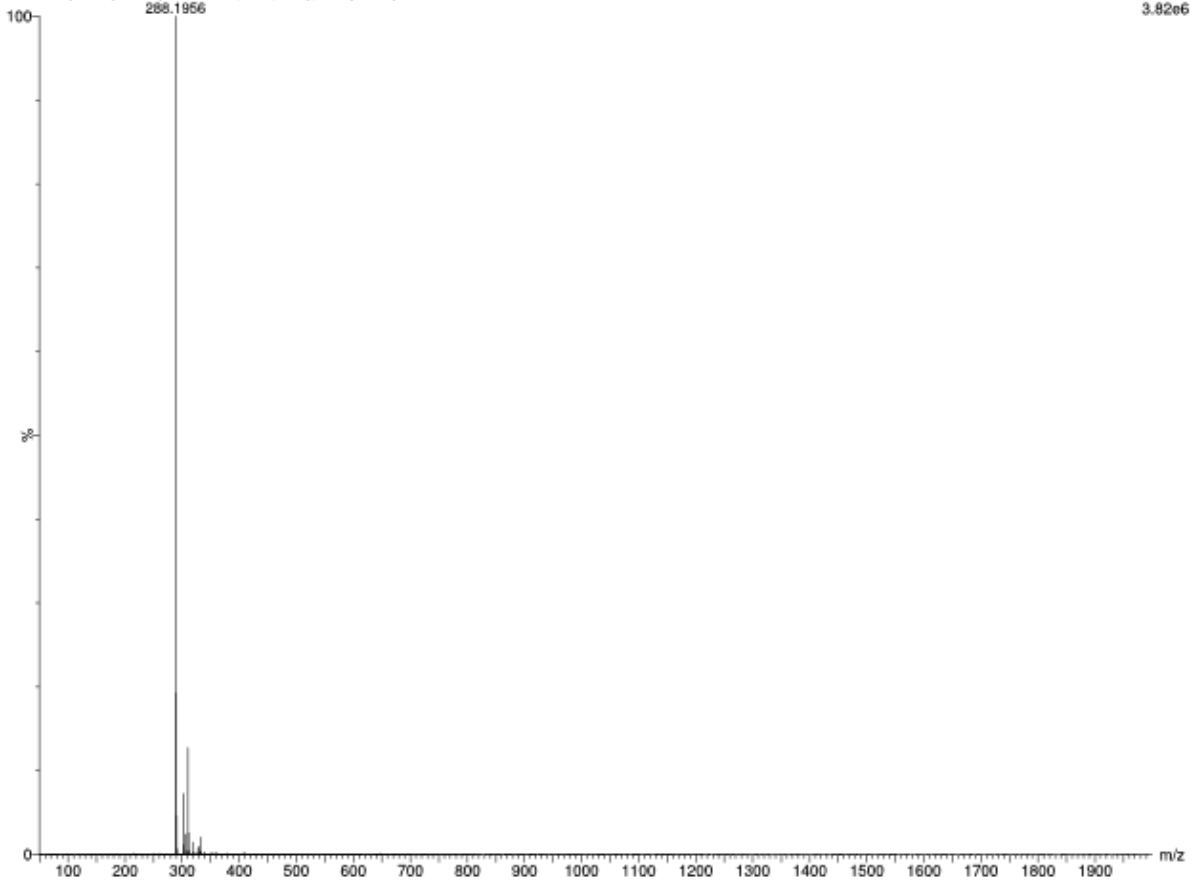
Synthesis of (*S*)-*N*-methyl-2-[3-(6-hydroxy-1-hexynyl)phenoxy]methylpyrrolidine [(*S*)-**3**]



Molecular Weight: 287.40

Under vigorous stirring at 0 °C, an aqueous solution of formaldehyde (37% in water, 0.22 ml) was added dropwise to a solution of (*S*)-2-[3-(6-hydroxy-1-hexynyl)phenoxy]methylpyrrolidine [(*S*)-**45**] (255 mg – 0.724 mmol) in 4 ml of methanol and 80 μ l of glacial acetic acid. Upon addition of 2-picolin borane (78 mg – 0.724 mmol), the mixture was reacted for 3 hours. The solvent was evaporated in vacuo, the residue was diluted with 5 ml of a 1M HCl solution and stirred for 1 hour to quench the unreacted 2-picolin-borane. Then, the pH was adjusted to 8 by adding an aqueous solution of Na₂CO₃ 2M and the aqueous phase was extracted with ethyl acetate (3x30 ml). The organic phase was washed with brine, dried over sodium sulphate, filtered and evaporated in vacuo, providing a crude that was further purified through silica gel flash chromatography (dichloromethane/methanol 9:1). The pure compound (*S*)-**3** was obtained as a yellow oil (205 mg- 0.56 mmol, 77%). **TLC** (Dichloromethane / Methanol 9:1 +2% NH₃(30% in water)): **R_f**= 0.24. **[α]_D²⁵** = -5.07° (*c*1, CHCl₃). **¹H-NMR** (300 MHz, DMSO-*d*6): δ 7.21 (m, 1H), 6.90 (m, 3H), 4.40 (m, exchange with D₂O, 1H), 3.94 (dd, *J*= 9.6, 5.3 Hz, 1H), 3.80 (dd, *J*= 9.6, 5.9 Hz, 1H), 3.42 (m, 2H), 2.94 (m, 1H), 2.59 – 2.50 (m, 1H), 2.39 (m, 2H), 2.33 (s, 3H), 2.17 (q, *J*= 8.6 Hz, 1H), 1.96 – 1.86 (m, 1H), 1.71 – 1.50 (m, 7H). **¹³C-NMR** (75 MHz, DMSO-*d*6): δ 158.9, 130.1, 124.8, 124.0, 117.1, 115.2, 91.0, 81.0, 71.3, 64.0, 60.6, 57.5, 41.8, 32.1, 28.9, 25.3, 23.0, 18.9. **HRMS (ESI⁺)**: calc. for C₁₈H₂₆NO₂: theor. 288.1964; found [M+H]⁺: 288.1956.





Elemental Composition Report

Single Mass Analysis

Tolerance = 5.0 PPM / DBE: min = -1.5, max = 200.0
 Element prediction: Off
 Number of isotope peaks used for i-FIT = 5

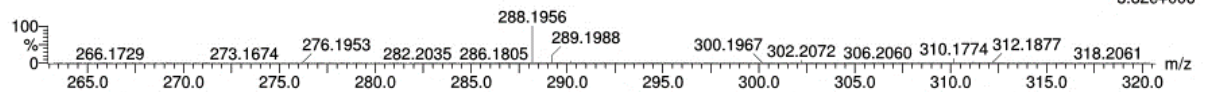
Monoisotopic Mass, Even Electron Ions

117 formula(e) evaluated with 1 results within limits (all results (up to 1000) for each mass)

Elements Used:

C: 18-18 H: 0-45 N: 0-10 O: 0-10

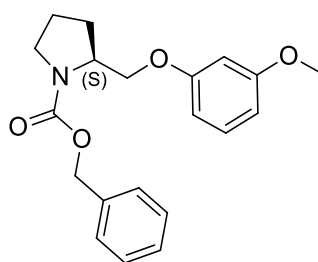
PD22 24 (0.462) AM2 (Ar,40000.0,0.00,0.00); Cm (15:41)



Minimum: -1.5
 Maximum: 0.5 5.0 200.0

Mass	Calc. Mass	mDa	PPM	DBE	i-FIT	Norm	Conf(%)	Formula
288.1956	288.1964	-0.8	-2.8	6.5	2460.9	n/a	n/a	C18 H26 N O2

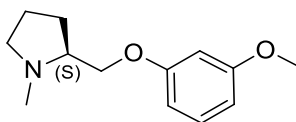
Synthesis of (*S*)-*N*-carbobenzyloxy-2-(3-methoxyphenoxy)methylpyrrolidine [(*S*)-46]



Molecular Weight: 341.40

3-methoxyphenol (521 mg – 4.2 mmol) and (*S*)-*N*-tert-butoxycarbonyl-2-hydroxymethylpyrrolidine (1 g – 4.2 mmol), dissolved each in 5 ml of anhydrous THF, were added to a solution of triphenylphosphine (1.3 g – 5.1 mmol) in 8 ml of anhydrous THF. The reaction mixture was cooled to -10°C and DIAD (0.83 mL – 5.1 mmol), in 2 ml of anhydrous THF, was added dropwise under vigorous stirring. The reaction mixture was refluxed for 12 hours. After cooling to room temperature, the mixture was diluted with 10 mL of 1M aqueous solution of NaOH and extracted with dichloromethane twice (2x30 ml). The organic phase was dried over anhydrous sodium sulphate, filtrated and the solvent was evaporated in vacuo to obtain a crude that was further purified through silica-gel flash column chromatography (gradient from cyclohexane/ethyl acetate 9:1 to 7:3). The pure compound (*S*)-46 was obtained as a pale yellow oil (901 mg – 2.63 mmol, 63%). TLC (Cyclohexane / Ethyl Acetate 7:3): $R_f = 0.7$. $[\alpha]_D^{25} = -45.22^\circ$ (*c*1, CHCl₃). ¹H-NMR (300 MHz, CDCl₃): δ 7.35 – 7.30 (m, 5H), 7.16 – 7.09 (m, 1H), 6.56 – 6.42 (m, 3H), 5.15 (s, 2H), 4.20 – 4.17 (m, 2H), 4.08 – 3.95 (m, 1H), 3.78 (s, 3H), 3.49 (m, 2H), 2.10 – 1.86 (m, 4H).

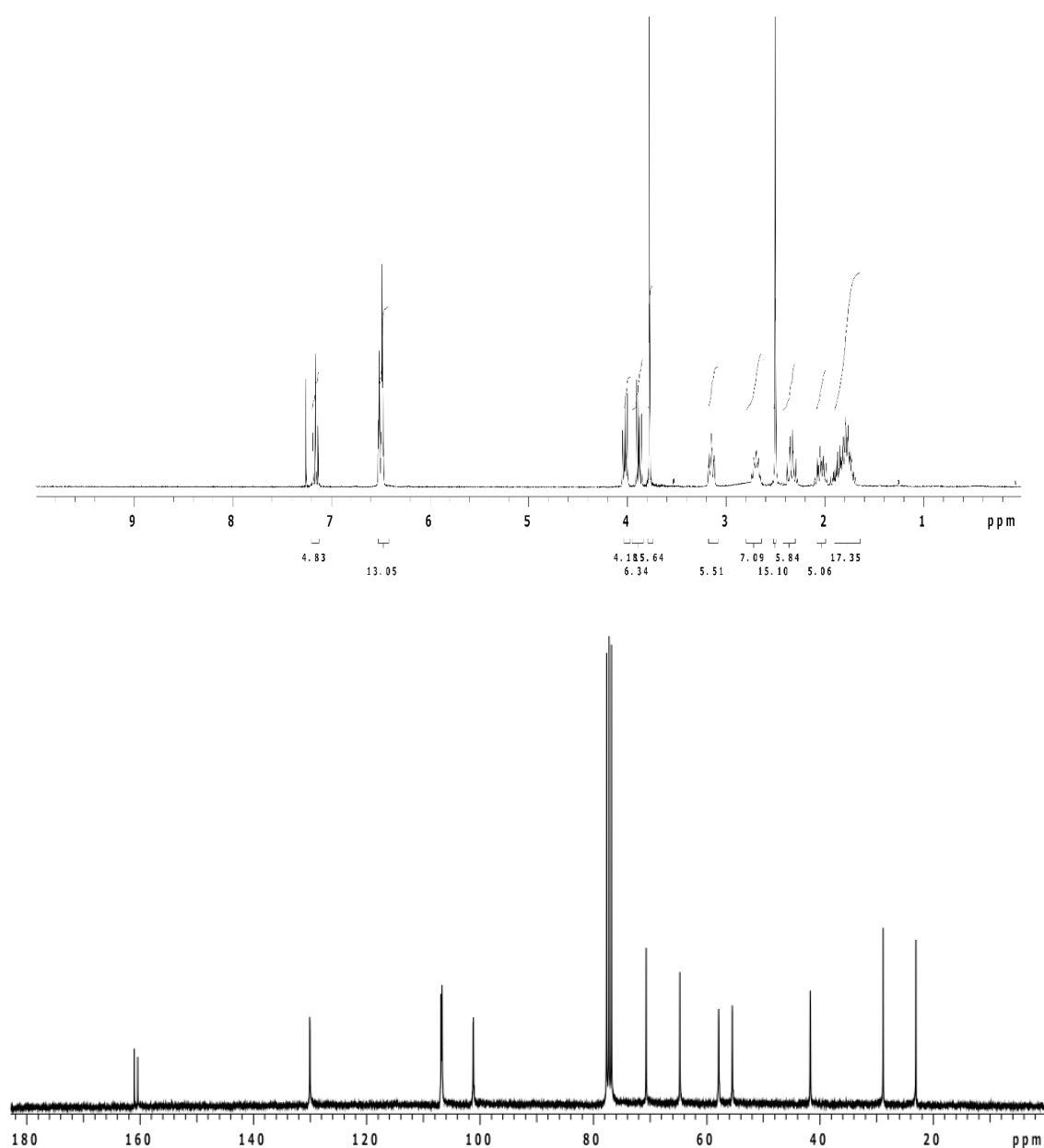
Synthesis of (*S*)-*N*-methyl-2-(3-methoxyphenoxy)methylpyrrolidine [(*S*)-4]

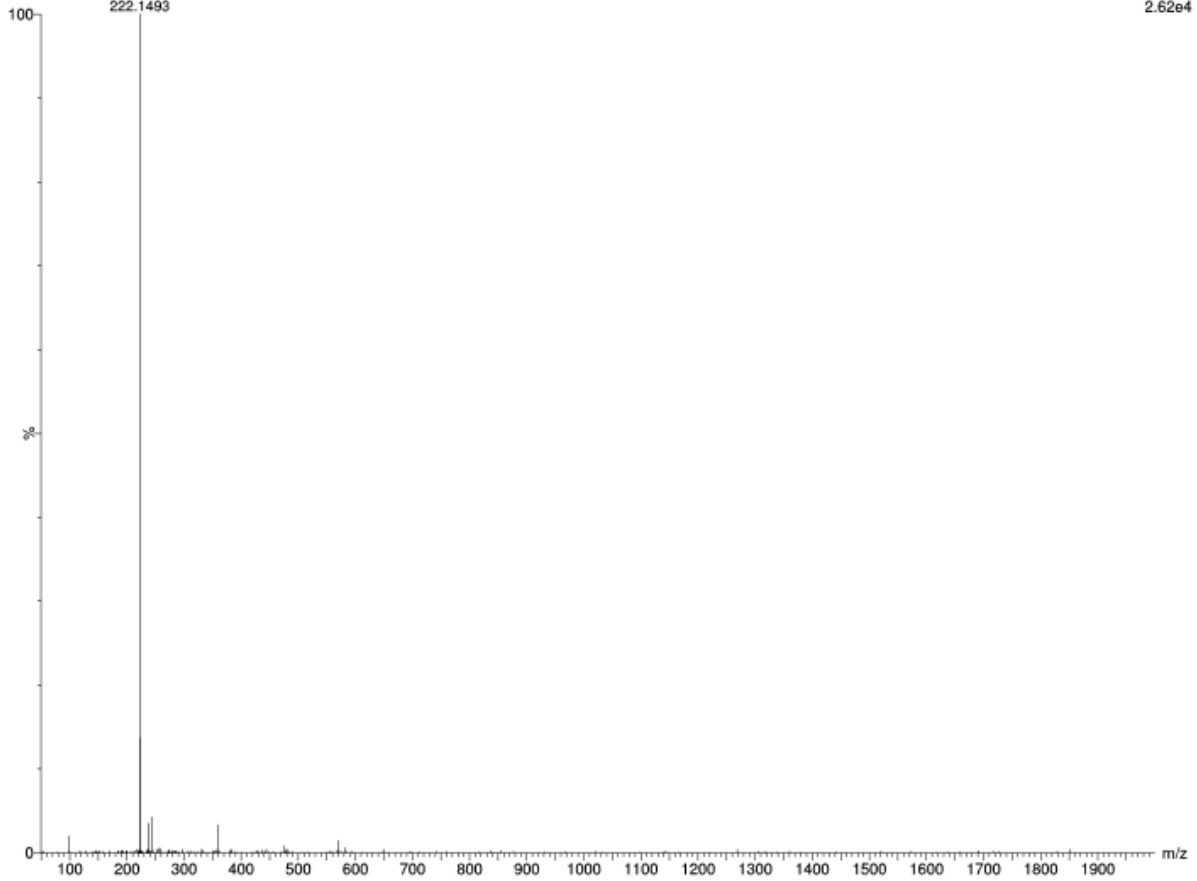


Molecular Weight: 221.30

Under inert atmosphere and at -10 °C, a solution of (*S*)-2-(3-methoxyphenoxy)methylpyrrolidine [(*S*)-47] (250 mg – 0.73 mmol) was added dropwise to a vigorously stirred suspension of LiAlH₄ (70 mg – 1.84 mmol) in THF (1 ml). The reaction mixture was stirred at room temperature for 90 minutes. Afterward, upon cooling to -10 °C, the excess of LiAlH₄ was quenched by dropwise addition of water. The crude was diluted with a

1M aqueous solution of HCl (10 ml) and washed with diethyl ether (2x5 ml) and DCM (5 ml). The aqueous phase was basified to pH 12 with an aqueous solution of NaOH and extracted with DCM (3x20 ml). the organic phase was dried over anhydrous sodium sulphate, filtered and evaporated in vacuo, providing the pure product (*S*)-**4** as a yellow oil (108 mg – 0.49 mmol, 67%). **TLC** (Ethyl Acetate + TEA 3%): **R_f**= 0.4. **[α]_D²⁵** = -52.67° (*c*1, CHCl₃). **¹H-NMR** (300 MHz, CDCl₃): δ 7.17 (t, *J*= 7.7 Hz, 1 H), 6.50 (m, 3H), 4.00 (dd, *J*= 9.3, 5.1 Hz, 1H), 3.87 (dd, *J*= 9.3, 6.0, 1H), 3.78 (s, 3H), 3.12 (m, 1H), 2.66 (m, 1H), 2.49 (s, 3H), 2.32 (m, 1H), 2.07 – 1.98 (m, 1H), 1.89 – 1.71 (m, 3H). **¹³C-NMR** (75 MHz, CDCl₃): δ 161.0, 160.4, 130.1, 106.9, 106.7, 101.2, 70.7, 64.7, 57.9, 55.5, 41.7, 28.9, 23.1. **HRMS (ESI⁺)**: calc. for C₁₅H₂₀NO₂: theor. 222.1494; found [M+H]⁺: 222.1493.





Elemental Composition Report

Single Mass Analysis

Tolerance = 5.0 PPM / DBE: min = -1.5, max = 200.0
 Element prediction: Off
 Number of isotope peaks used for i-FIT = 5

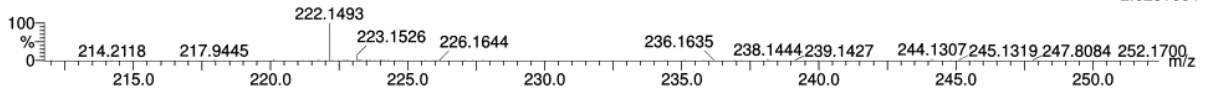
Monoisotopic Mass, Even Electron Ions

62 formula(e) evaluated with 1 results within limits (all results (up to 1000) for each mass)

Elements Used:

C: 13-13 H: 10-100 N: 0-5 O: 0-5 Na: 0-1

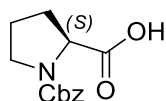
MB10 26 (0.496) AM2 (Ar,40000.0,0.00,0.00)



Minimum: -1.5
 Maximum: 0.5 5.0 200.0

Mass	Calc. Mass	mDa	PPM	DBE	i-FIT	Norm	Conf(%)	Formula
222.1493	222.1494	-0.1	-0.5	4.5	210.0	n/a	n/a	C13 H20 N O2

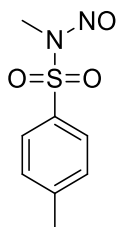
Synthesis of (*S*)-*N*-carbobenzyloxy-proline [(*S*)-47]



Molecular Weight: 249.26

Procedure adapted from literature.¹⁶⁵ A solution of (*S*)-proline (10.0 g – 86.8 mmol) in 40 ml of an aqueous solution of NaOH 2M was cooled to 0 °C and benzyloxycarbonyl chloride (Cbz-Cl) (17.5 ml – 116.4 mmol) was added in three sequential portions of 5.9 ml, each followed by an addition of 10 ml of NaOH 4 M. The reaction mixture was stirred for 3 hours. Afterward, the aqueous layer was washed with diethyl ether (30 ml) and, upon cooling to 0 °C, it was acidified to pH 2 and extracted with ethyl acetate. The organic phase was dried over anhydrous sodium sulphate, filtered and the solvent was evaporated in vacuo, providing the pure product (*S*)-47 as a white solid (19.5 g – 78.1 mmol, 90%). TLC (Dichloromethane / Methanol 9:1, stained with Blue Shift): **R_f**= 0.26. **M.p.**= 72.5 °C; literature¹⁶⁶: **M.p.** = 78 °C; literature¹⁶⁷: **M.p.** = 60 – 61 °C. **[α]_D²⁵** = -77.53° (*c*2, EtOH). **¹H-NMR** (300 MHz, CDCl₃): δ 9.20 (bs, 1H, exchange with D₂O), 7.33 – 7.26 (m, 5H), 5.20 – 5.00 (m, 2H), 4.30 (m, 1H), 3.60 – 3.40 (m, 2H), 2.25 – 1.75 (m, 4H).¹⁶⁸

Synthesis of *N*-methyl-*N*-nitrosotoluene-*p*-sulfonamide

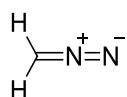


Molecular Weight: 214.24

A total amount of *p*-toluensulphonyl chloride of 100 g was divided in three portions of 59.5 g, 28.1 g and 12.5 g. An aqueous solution of methylamine (52.8 ml – 625 mmol) was mechanically stirred at room temperature and the first portion of *p*-toluensulphonyl chloride (59.4 g – 312 mmol) was added over 5 minutes. The reaction mixture is heated to 80-90 °C, high enough to melt the *p*-toluene-*N*-methylsulphonylamide intermediate and maintain it in the liquid phase, but not too high to avoid methylamine loss. After 5 minutes, the pH must be acid. A 50% m/V aqueous solution of NaOH was prepared (23.5 g – 587 mmol in 47 ml of H₂O) and was used in the following steps. Cautiously, the solution of NaOH (15.6 ml) was added, immediately followed by the addition of the second portion of *p*-toluene sulphonyl chloride (28.1 g – 147

mmol). Again, the pH was controlled to be acid. 7.8 ml of the same aqueous solution of NaOH were added, followed by the addition of the third portion of *p*-toluene sulphonyl chloride (12.5 g – 66 mmol). When the pH of the reaction mixture was acid, the spare solution of NaOH was added. If the aqueous phase was not basic, methylamine was added until basic pH. The mixture was stirred for further 15 minutes and was then poured, still hot, into a round-bottomed flask containing glacial acetic acid (470 ml). Glacial acetic acid (80 ml) was also used to carefully recover all the residues of the reaction mixture from the first flask. The mixture was cooled at 5 °C and a solution of NaNO₂ (39.1 g – 566 mmol) in 39 ml of water was added dropwise over 45 minutes. The mixture was stirred for further 15 minutes at 10 °C, diluted with water (155 + 125 ml) and filtered. The resulting solid was washed and filtered many times with water, until removal of whole glacial acetic acid. The resulting solid (103 g – 479 mmol, 91%) was dried over P₂O₅. **M.p.** = 58.0 °C. **¹H-NMR** (300 MHz, CDCl₃): δ 7.84 (m, 2H), 7.35 (m, 2H), 3.10 (s, 3H), 2.43 (s, 3H).

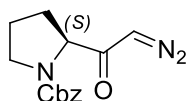
Synthesis of diazomethane



Molecular Weight: 42.04

A solution of KOH (12.0 g – 182 mmol) in water (19.2 ml) and ethanol (24 ml) was prepared in a round-bottom flask equipped with a Claisen condenser connected at the opposite end to a collecting round-bottom flask maintained at – 30 °C. The hydroethanolic solution was heated to 55-60 °C and a solution of N-methyl-N-nitroso-*p*-toluenesulphonamide (12 .0 g – 56 mmol) in diethyl ether (110 ml) was added dropwise, to a controlled rate equal to the distillation rate. Thus, the ethereal solution of diazomethane was distilled until the distilling fraction appeared colourless (diethyl ether alone), collected at – 30 °C and immediately used thereafter for the following reaction.

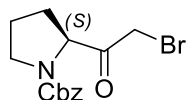
Synthesis of (*S*)-*N*-carbobenzyloxy-diazoproline [(*S*)-48]



Molecular Weight: 273.29

Procedure adapted from literature.¹⁶⁹ Under inert atmosphere, a suspension of (*S*)-*N*-carbobenzyloxy-proline [(*S*)-47] (6.0 g – 24 mmol) in anhydrous diethyl ether (50 ml) was cooled to -15 °C and triethylamine (3.36 ml – 24 mmol) was added dropwise. After 5 minutes, isobutylchloroformiate (3.12 ml – 24.1 mmol) was added dropwise, maintaining the temperature below -10 °C. After 20 minutes, upon formation of the mixed anhydride, controlled by TLC, the mixture was equilibrated to 0 °C and the solid was removed by filtration and washed with diethyl ether. The filtrate was cooled to 0 °C and, under inert atmosphere, an ethereal solution of diazomethane was carefully added dropwise over 45 minutes (approximately 75 mmol in 150 ml of diethyl ether). The reaction mixture was stirred vigorously at room temperature overnight. Afterward, the ethereal solution was washed first with a saturated solution of NaHCO₃ and then with water. The organic phase was dried over anhydrous sodium sulphate, filtrated and the solvent was evaporated in vacuo, affording a crude that was purified through silica gel flash chromatography (cyclohexane/ethyl acetate 7:3). The pure product (*S*)-48 was isolated as a yellow solid (5.8 g – 18 mmol, 75%). TLC (Cyclohexane / Ethyl Acetate 6:4; staining agent: Blue Shift): R_f= 0.40. M.p.= 64.6 °C; literature¹⁷⁰: 58 – 60 °C; literature¹⁷¹: 66 – 67 °C. [α]_D²⁵ = -147.32 (*c*1, CHCl₃); literature¹⁷¹: [α]_D²⁵ = -131.8 (*c*1.1, CHCl₃). The product shows the typical IR stretching band of CHN₂ at 2104 cm⁻¹. ¹H-NMR (300 MHz, CDCl₃): δ 7.40 – 7.26 (m, 5H), 5.46 – 5.25 (m, 1H), 5.20 – 5.00 (m, 2H), 4.38 – 4.25 (m, 1H), 3.60 – 3.40 (m, 2H), 2.25 – 1.75 (m, 4H).¹⁷⁰

Synthesis of (*S*)-*N*-carbobenzyloxy-2-bromoacetylpyrrolidine [(*S*)-49]

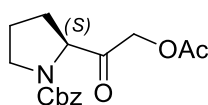


Molecular Weight: 326.19

Procedure adapted from literature.¹⁷² Upon cooling to -10 °C, aqueous HBr (2.68 ml – 53.32 mmol) was added dropwise to a solution of (*S*)-*N*-carbobenzyloxy-diazoproline [(*S*)-48] (4.0 g – 14.6 mmol) in diethyl ether (50 ml). The resulting mixture was warmed to room temperature and vigorously stirred for 1 hour. Afterward, the mixture is diluted with diethyl ether (40 ml)

and washed several times with a saturated solution of NaHCO₃ and then with water. The organic phase was dried over anhydrous sodium sulphate, filtered and the solvent was evaporated in vacuo providing the pure product [(*S*)-**49**] was isolated as a pale yellow oil (4.1 g – 12.6 mmol, 85%). **TLC** (Cyclohexane / Ethyl Acetate 6:4; stained with Blue Shift): **R_f**= 0.56. [α]_D²⁵ = -51.59° (*c*1, MeOH); literature¹⁷²: [α]_D²⁵ = -51° (*c*1, MeOH). **¹H-NMR** (300 MHz, CDCl₃): δ 7.36 – 7.25 (m, 5H), 5.18 – 5.02 (m, 2H), 4.64 – 4.50 (m, 1H), 4.15 (d, *J* = 12.9 Hz, 0.5H), 4.04 (d, *J* = 12.9 Hz, 0.5H), 3.80 (s, 1H), 3.63 – 3.52 (m, 2H), 2.26 – 2.18 (m, 1H), 2.07 – 1.88 (m, 3H).¹⁷²

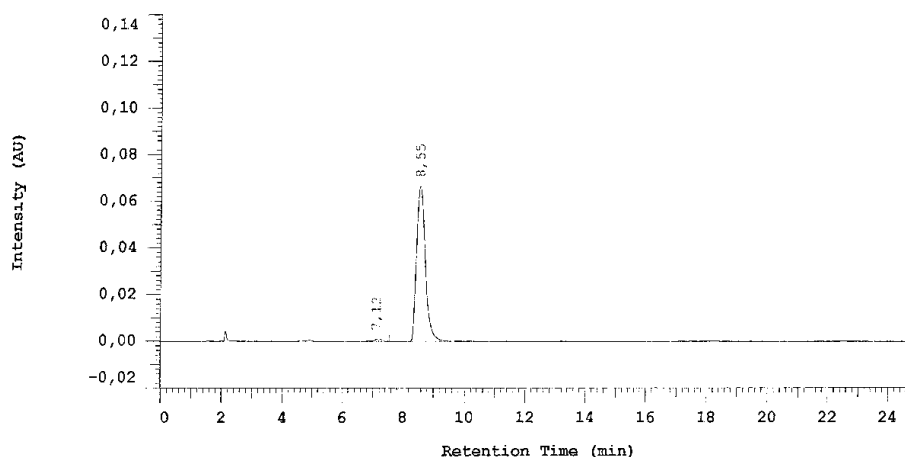
Synthesis of (*S*)-*N*-carbobenzyloxy-2-acetoxyacetylpyrrolidine [(*S*)-**52**]



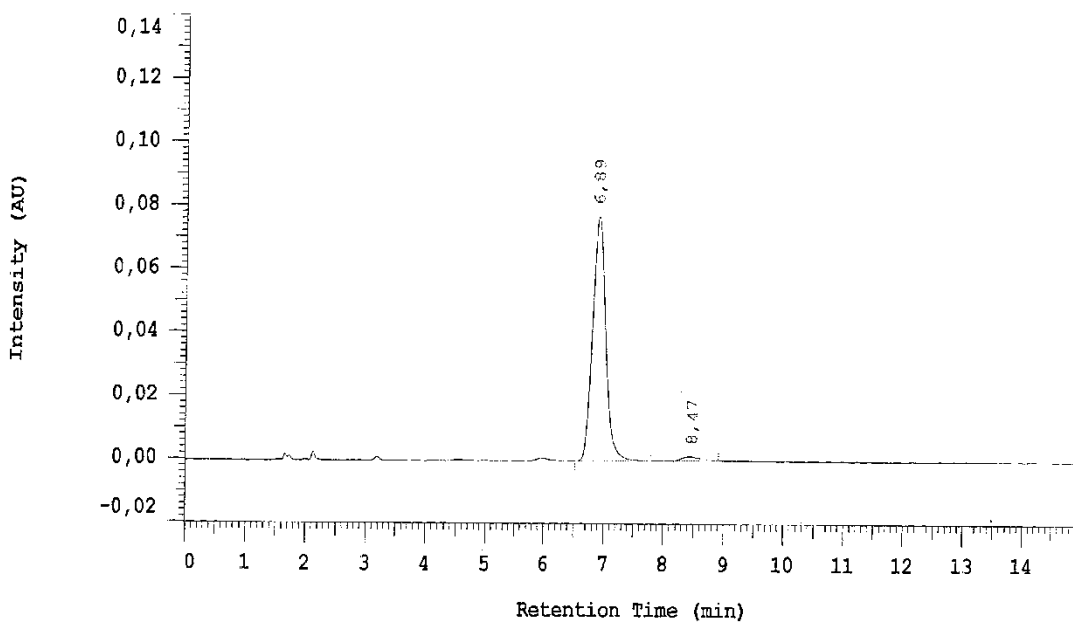
Molecular Weight: 305.33

(*S*)-*N*-carbobenzyloxy-2-bromoacetylpyrrolidine [(*S*)-**49**] (545 mg – 1.67 mmol) was added to a solution of KOAc (164 mg – 1.67 mmol) in 5 ml of DMSO. The resulting reaction mixture was stirred at room temperature for 1.5 hours. Afterward, the mixture was diluted with diethyl ether and washed sequentially with water and brine. The organic phase was dried over anhydrous sodium sulphate, filtered and the solvent was removed in vacuo, affording the pure product [(*S*)-**52**] as a colourless oil (499 mg – 1.64 mmol, 98%). The enantiomeric excess was assessed by chiral HPLC. [α]_D²⁵ = -79.4 (*c*1, CHCl₃). **¹H-NMR** (300 MHz, CDCl₃): δ 7.36 – 7.25 (m, 5H), 5.18 – 5.09 (m, 2H), 4.83 (s, 1.2H), 4.62 (s, 0.8H), 4.47 – 4.42 (m, 0.6H), 4.41 – 4.37 (m, 0.4H), 3.62 – 3.46 (m, 2H), 2.23 – 1.86 (m, 4H), 2.15 (s, 3H). **e.e. %** = 99.28% (Chiralcel OJ; hexane/isopropanol 9:1, 2 ml/min, λ =258 nm; **R_{tR}**= 6.85min, **R_{tS}**=8.52 min)

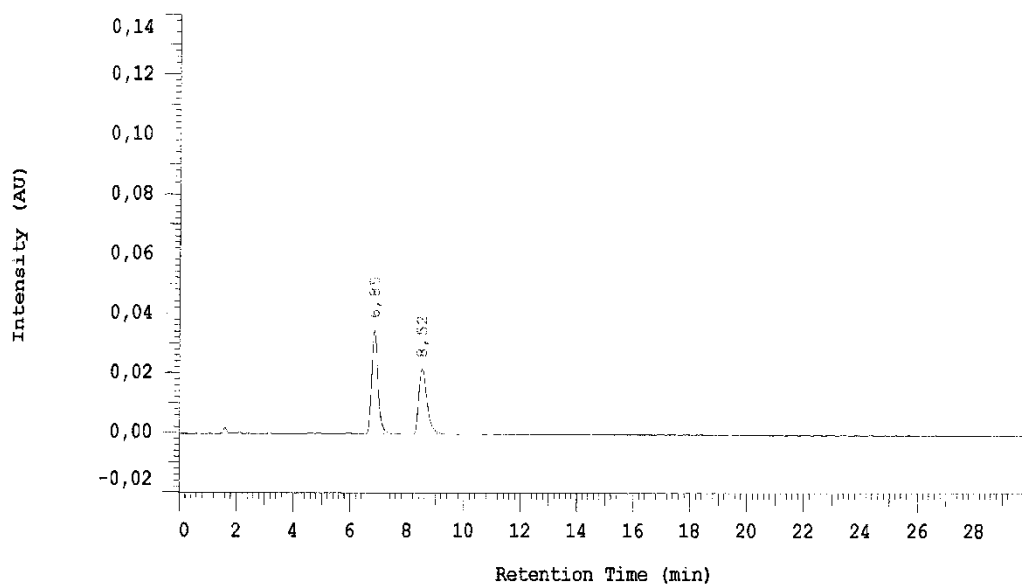
Chiral HPLC analysis: (*S*)-*N*-carbobenzyloxy-2-acetoxyacetylpyrrolidine



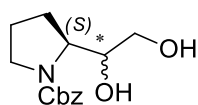
Chiral HPLC analysis: (R)-N-carbobenzyloxy-2-acetoxyacetylpyrrolidine



Chiral HPLC analysis: mixture of (S)- and (R)-N-carbobenzyloxy-2-acetoxyacetylpyrrolidine



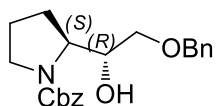
Synthesis of (*S,R*)/(*S,S*)-*N*-carbobenzyloxy-2-(1,2-dihydroxyethyl)pyrrolidine [(*S,S*)-53/(*S,R*)-53]



Molecular Weight: 264.30

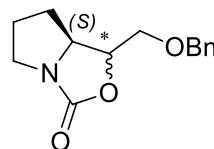
A solution of *N*-carbobenzyloxy-(*S*)-2-acetoxyacetylpyrrolidine [(*S*)-52] (505 mg, 1.65 mmol) in anhydrous THF (4 mL) was added dropwise to a suspension of NaBH₄ (66 mg – 1.4 mmol) in anhydrous THF (4 mL) at -10 °C. The reaction mixture was allowed to reach the room temperature and stirred for 3 h at this temperature. Afterwards, dichloromethane was added, and the organic phase was washed with water. The separated organic layer was dried over Na₂SO₄, filtered and concentrated in vacuo to provide a residue that was dissolved in methanol (20 mL). Sodium methoxide (88 mg, 1.63 mmol) was added to the resulting solution at -10 °C and the reaction mixture was stirred for 1 h. Dichloromethane was added, and the organic phase was washed with water, separated and filtered through a Celite® plug. The solvent was evaporated in vacuo to obtain a mixture of (*S,S*) and (*S,R*)-*N*-carbobenzyloxy-2-(1,2-dihydroxyethyl)pyrrolidine [(*S,S*)-53/(*S,R*)-53] as a light yellow oil (285 mg – 1.07 mmol, 97%). TLC (Cyclohexane / Ethyl Acetate 1:1): R_f = 0.21. ¹H NMR (CDCl₃) δ 7.38 – 7.25 (m, 5H), 5.15 (s, 2H), 4.08 – 3.89 (m, 1H), 3.66 – 3.50 (m, 3H), 3.45 – 3.30 (m, 2H), 3.05 (bs, 2H), 2.11 – 1.71 (m, 4H).¹⁷³

Synthesis of (*S,R*)-*N*-carbobenzyloxy-2-(1-hydroxy-2-benzyloxy)ethylpyrrolidine [(*S,R*)-59] and of (*S,S*)/(*S,R*)-1-(benzyloxymethyl)tetrahydro-1*H*,3*H*pyrrolo[1,2-*c*]oxazol-3-one [(*S,S*)-60/(*S,R*)-60]



(*S,R*)-59

Molecular Weight: 355.43

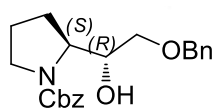


(*S,S*)-60/(*S,R*)-60

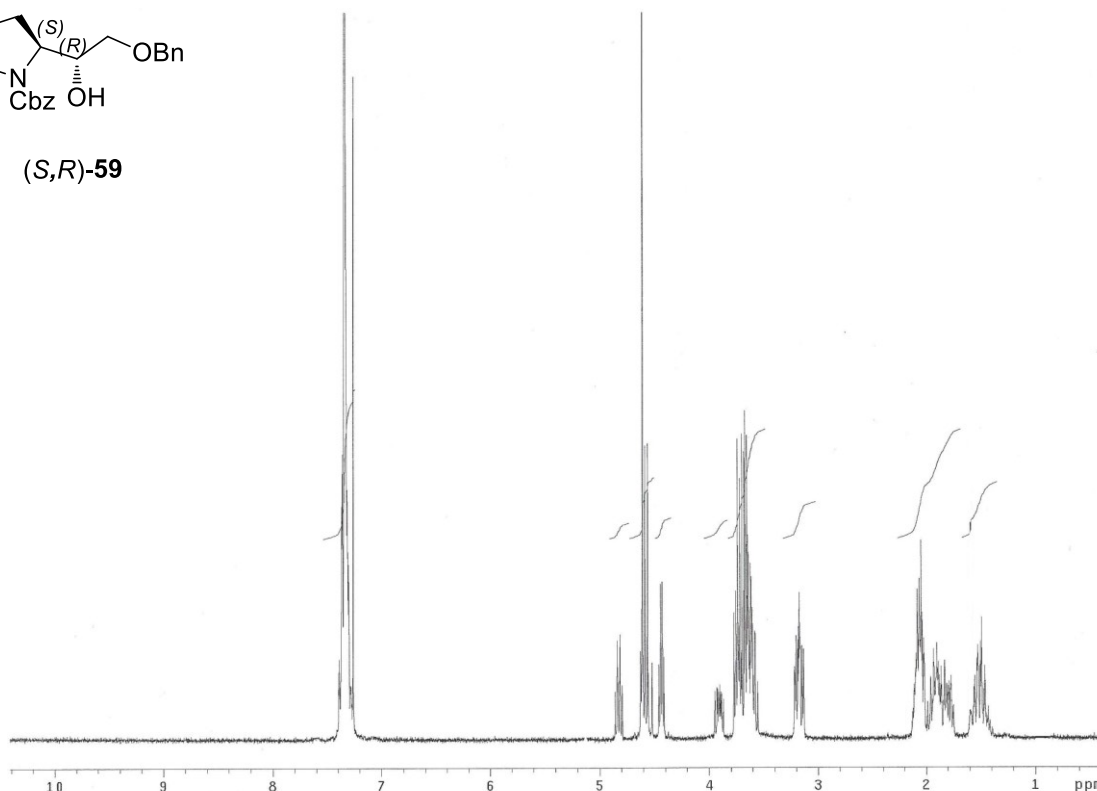
Molecular Weight: 246.28

(*S,S*)/(*S,R*)-*N*-carbobenzyloxy-2-(1,2-dihydroxyethyl)pyrrolidine [(*S,S*)-53/(*S,R*)-53] (500 mg – 1.88 mmol) was dissolved in anhydrous toluene (10 mL) and dibutyltin oxide (609 mg – 2.45 mmol) was added. The reaction mixture was refluxed for 5 h and water was azeotropically

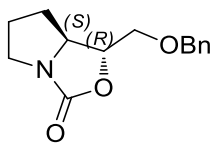
removed by dean-stark apparatus. Then benzyl bromide (0.25 mL – 2.07 mmol) and tetrabutylammonium iodide (35 mg) were added and the mixture was refluxed for additional 16 h. Afterward, the solvent was evaporated in vacuo and the resulting residue was purified by silica gel flash chromatography (cyclohexane/ethyl acetate 1:1). The pure product (*S,R*)-N-carbobenzyloxy-2-(1-hydroxy-2-benzyloxy)ethylpyrrolidine [(*S,R*)-**59**] was obtained as a yellow oil (250 mg – 0.70 mmol, 37%). **TLC** (Cyclohexane / Ethyl Acetate 1:1): **R_f**= 0.25. **[α]_D²⁵** = -24.0 (*c*1, CHCl₃). **¹H NMR** (300 MHz, CDCl₃): δ 7.46 – 7.26 (m, 10H), 5.16 – 5.09 (m, 2H), 4.60 – 4.38 (m, 2H), 4.10 – 3.85 (m, 2H), 3.60 – 3.32 (m, 4H), 2.15 – 1.82 (m, 4H) [figure in the next page]. The diastereoisomeric mixture of (*S,S*)/(*S,R*)-1-(benzyloxymethyl)tetrahydro-1H,3Hpyrrolo[1,2-*c*]oxazol-3-one [(*S,S*)-**60**]/[(*S,R*)-**59**] was obtained as an orange oil (198 mg – 0.80 mmol, 46%), in a 60:40 diastereoisomeric ratio. **TLC** (Cyclohexane / Ethyl Acetate 1:1): **R_f**= 0.30. **¹H NMR** (300 MHz, CDCl₃): δ 7.41 – 7.30 (m, 5H), 4.82 (dt, *J*= 7.7, 6.1 Hz, 0.4H), 4.52 – 4.65 (m, 2H), 4.41 – 4.45 (q, *J*= 5.2 Hz, 0.6H), 3.86 – 3.94 (m, 0.4H), 3.55 – 3.77 (m, 3.6H), 3.13 – 3.21 (m, 1H), 1.74 – 2.17 (m, 2.4H), 1.43 – 1.58 (m, 1.6H).



(*S,R*)-**59**

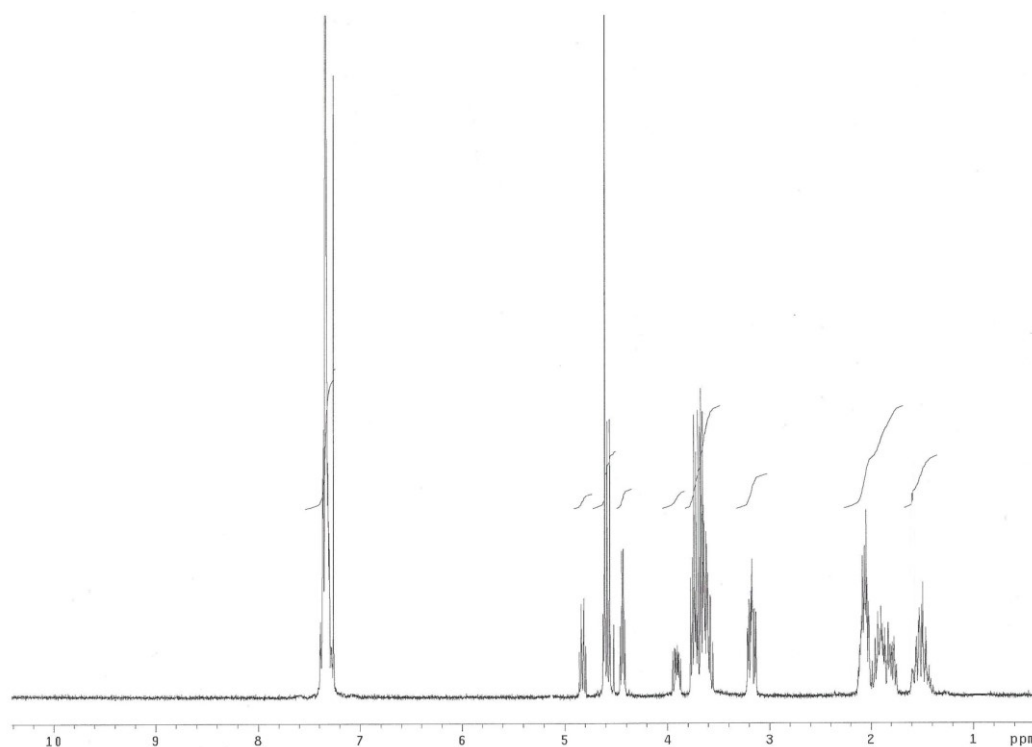


Synthesis of (*S,R*)-1-(Benzyloxymethyl)tetrahydro-1*H*,3*H*-pyrrolo[1,2-*c*]oxazol-3-one [(*S,R*)-**60**]

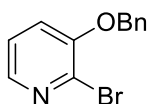


Molecular Weight: 247.29

A solution of (*S,R*)-*N*-carbobenzyloxy-2-(1-hydroxy-2-benzyloxy)ethylpyrrolidine [(*S,R*)-**59**] (1.5 g – 4.79 mmol) in anhydrous DMF (10 mL) was added dropwise to a suspension of NaH (115 mg – 4.79 mmol) in anhydrous DMF (5 mL) at -10 °C under inert atmosphere. The reaction was warmed to room temperature and stirred at the same temperature for 3 h. Upon addition of dichloromethane, the reaction mixture was washed with water. The organic layer was separated, dried over Na₂SO₄, filtered and evaporated in vacuo providing a residue that was further purified by silica gel flash chromatography (cyclohexane/ethyl acetate 4:6). The pure compound (*S,R*)-**60** was obtained as a yellow oil (699 mg – 2.83 mmol, 59%). **TLC** (Cyclohexane / Ethyl Acetate 4:6): **R_f** = 0.45. [α]_D²⁵ = -23.9 (*c*2, CHCl₃). **¹H NMR** (300 MHz, CDCl₃): δ 7.41 – 7.30 (m, 5H), 4.82 (dt, *J* = 7.7, 6.1 Hz, 1H), 4.57 (q, *J* = 11.8 Hz, 2H), 3.90 (ddd, *J* = 10.5, 7.7, 5.5 Hz, 1H), 3.76 – 3.54 (m, 3H), 3.20 – 3.12 (m, 1H), 2.18 – 1.75 (m, 3H), 1.60 – 1.43 (m, 1H). **¹³C NMR** (75 MHz, CDCl₃): δ 161.21, 137.60, 128.75, 128.21, 128.06, 74.68, 73.97, 68.51, 62.10, 45.72, 25.80, 25.26.



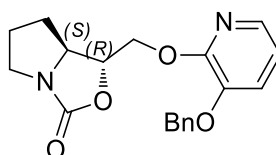
Synthesis of 3-benzyloxy-2-bromopyridine



Molecular Weight: 264.12

Procedure adapted from literature.¹⁷⁴ A solution of 3-hydroxy-2-bromopyridine (3 g – 17.24 mmol) in DMF (12 ml) was added dropwise to a suspension of K₂CO₃ (2.62 g – 18.96 mmol) in DMF (8 ml). Upon stirring for 10 minutes, benzyl bromide (2.25 ml – 18.96 mmol) was added dropwise. The reaction mixture was stirred overnight at room temperature. Afterward, the solvent was concentrated in vacuo, the residue was diluted with DCM and then washed with an aqueous solution of NaOH 10%. The organic phase was dried over anhydrous sodium sulphate, filtered and the solvent was removed in vacuo. The pure product (4 g – 15.17 mmol, 88%) was obtained as a light yellow oil. **TLC** (Cyclohexane / Ethyl Acetate 7:3): **R_f** = 0.38. **¹H-NMR** (300 MHz, CDCl₃): δ 7.99 (dd, *J* = 4.7, 1.7 Hz, 1H), 7.47 – 7.34 (m, 5H), 7.20 – 7.12 (m, 2H), 5.19 (s, 2H).¹⁷⁴

Synthesis of (*S,R*)-1-(3-benzyloxy-2-pyridyloxymethyl)tetrahydro-1H,3H-pyrrolo[1,2-c]oxazol-3-one [(*S,R*)-62]

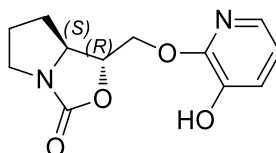


Molecular Weight: 340.37

A solution of (*S,R*)-1-(hydroxymethyl)tetrahydro-1H,3H-pyrrolo[1,2-c]oxazol-3-one [(*S,R*)-61] (950 mg – 6.04 mmol) in anhydrous DMF (4 mL) was added dropwise to a suspension of NaH (148 mg – 6.04 mmol) in anhydrous DMF (1 mL) at -10 °C. Upon addition of 2-bromo-3-benzyloxy-2-pyridine (1.6 g – 6.04 mmol) at the same temperature, the reaction mixture was stirred at 80 °C for 4 h. Afterwards the solvent was evaporated in vacuo to give a residue that was dissolved in diethyl ether and washed with water. The separated organic phase was dried over Na₂SO₄, filtered and concentrated under vacuum, affording a residue that was purified by silica gel flash chromatography (cyclohexane/ethyl acetate 1:1). The pure compound (*S,R*)-62 was obtained as a light oil (698 mg – 2.05 mmol, 34%). **TLC** (Cyclohexane / Ethyl Acetate 1:1): **R_f** = 0.40. **[α]_D²⁵** = -30.1 (*c* 1, CHCl₃). **¹H NMR** (300 MHz, CDCl₃): δ 7.70 (dd, *J* = 5.0, 1.4 Hz, 1H), 7.39 – 7.26 (m, 5H), 7.12 (dd, *J* = 7.7, 1.4 Hz, 1H), 6.84 (dd, *J* = 7.7, 5.0 Hz, 1H),

5.26 (dt, $J= 9.4, 5.0$ Hz, 1H), 5.12 (s, 2H), 4.61 (dd, $J= 10.5, 5.0$ Hz, 1H), 4.10 (pt, 1H), 3.78 – 3.70 (dt, $J= 9.9, 5.0$ Hz, 1H), 3.65 – 3.49 (m, 2H), 2.31 – 2.23 (m, 1H), 2.06 – 1.97 (m, 1H), 1.89 – 1.66 (m, 2H).

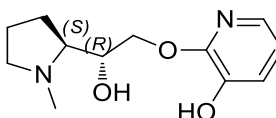
Synthesis of (*S,R*)-1-(3-hydroxy-2-pyridyloxymethyl)tetrahydro-1H,3H-pyrrolo[1,2-c]ossazol-3-one [(*S,R*)-63]



Molecular Weight: 250.25

A suspension of (*S,R*)-1-(3-benzyloxy-2-pyridyloxymethyl)tetrahydro-1H,3H-pyrrolo[1,2-c]ossazol-3-one [(*S,R*)-62] (260 mg – 0.76 mmol) and 10% Pd/C (26 mg) in ethanol (10 ml) was vigorously stirred under H₂ atmosphere for 2 hours. Afterward, the catalyst was removed by filtration on a Celite® pad and the solvent was evaporated in vacuo, affording the pure product (*S,R*)-63 as a white solid (188 mg – 0.75 mmol, 99%). TLC (Cyclohexane / Ethyl Acetate 2:8): R_f = 0.40. M.p. = 154.2 °C. $[\alpha]_{D}^{25} = -49.3$ (c0.5, EtOH). ¹H NMR (300 MHz, CDCl₃): δ 7.64 (dd, $J= 5.0, 1.4$ Hz, 1H), 7.17 (dd, $J= 7.7, 1.4$ Hz, 1H), 6.86 (dd, $J= 7.7, 5.0$ Hz, 1H), 6.12 (bs, 1H, exchange with D₂O), 5.30 (dt, $J= 9.1, 4.7$ Hz, 1H), 4.56 (dd, $J= 10.5, 4.7$ Hz, 1H), 4.10 (dd, $J= 10.5, 9.1$ Hz, 1H), 3.73 – 3.48 (m, 3H), 2.30 – 2.23 (m, 1H), 2.06 – 1.98 (m, 1H), 1.86 – 1.66 (m, 2H).

Synthesis of (*S,R*)-N-methyl-2-[2-(3-hydroxy-2-pyridyloxy)-1-hydroxyethyl]pyrrolidine [(*S,R*)-64]

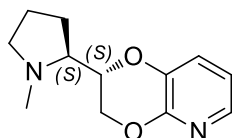


Molecular Weight: 238.28

A solution of (*S,R*)-1-(3-hydroxy-2-pyridyloxymethyl)tetrahydro-1H,3H-pyrrolo[1,2-c]ossazol-3-one [(*S,R*)-63] (200 mg – 0.8 mmol) in THF (4 mL) was added dropwise to a suspension of LiAlH₄ (92 mg – 2.40 mmol) in THF (4 mL) under inert atmosphere, at -10 °C. The reaction mixture was warmed to room temperature and stirred for 2 h. Upon cooling, dichloromethane and water were added. The resulting suspension was filtered through a Celite® plug and the filtrate was evaporated in vacuo providing a crude that was diluted with

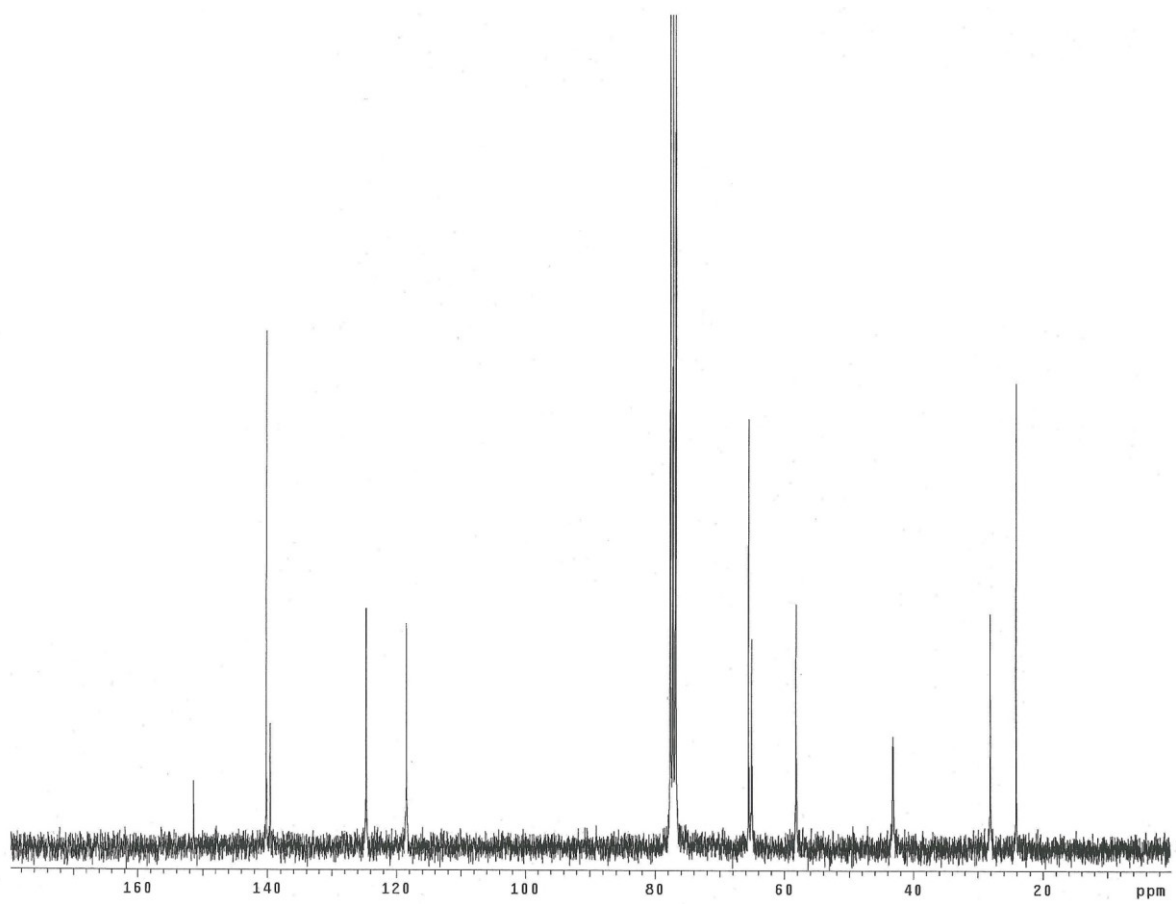
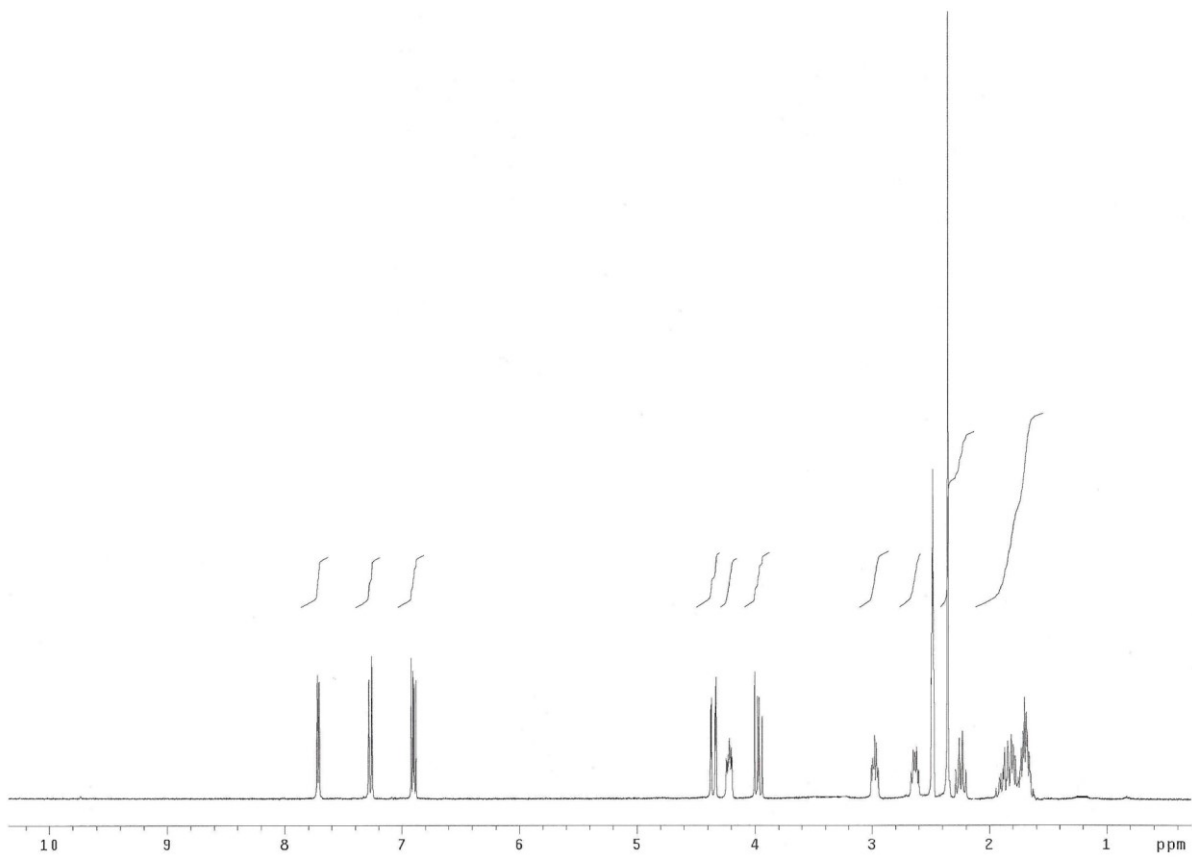
an aqueous solution of HCl 1M and washed with DCM. The aqueous phase was basified until pH=8 with a 30% solution of NH₃ in water and extracted with ethyl acetate. The organic phase was dried over anhydrous sodium sulphate, filtered and the solvent was removed in vacuo. The pure product (*S,R*)-**64** was isolated as a light yellow sticky solid (147 mg – 0.62 mmol, 77%). **TLC** (Dichloromethane / Methanol 9:1 + 0.5% NH₃(30% in water)): **Rf**= 0.35. **[α]_D²⁵** = -17.0 (c0.8, CHCl₃). **¹H NMR** (300 MHz, CDCl₃): δ 7.67 (dd, *J*= 4.7, 1.6 Hz, 1H), 7.21 (dd, *J*= 7.7, 1.6 Hz, 1H), 6.99 (dd, *J*= 7.7, 4.7 Hz, 1H), 5.60 (bs, 2H, exchange with D₂O), 4.10 (dt, *J*= 8.8, 2.2 Hz, 1H), 3.93 (dd, *J*= 11.8, 8.8 Hz, 1H), 3.66 (dd, *J*= 11.8, 2.2 Hz, 1H), 3.32 – 3.24 (m, 1H), 2.57 – 2.42 (m, 1H), 2.41 (s, 4H), 2.19 – 2.12 (m, 1H), 2.02 – 1.85 (m, 3H).

Synthesis of (*S,S*)-2-(*N*-Methyl-2-pyrrolidinyl)-2,3-dihydro-1,4-dioxino[2,3-*b*]pyridine [(*S,S*)-**5**]

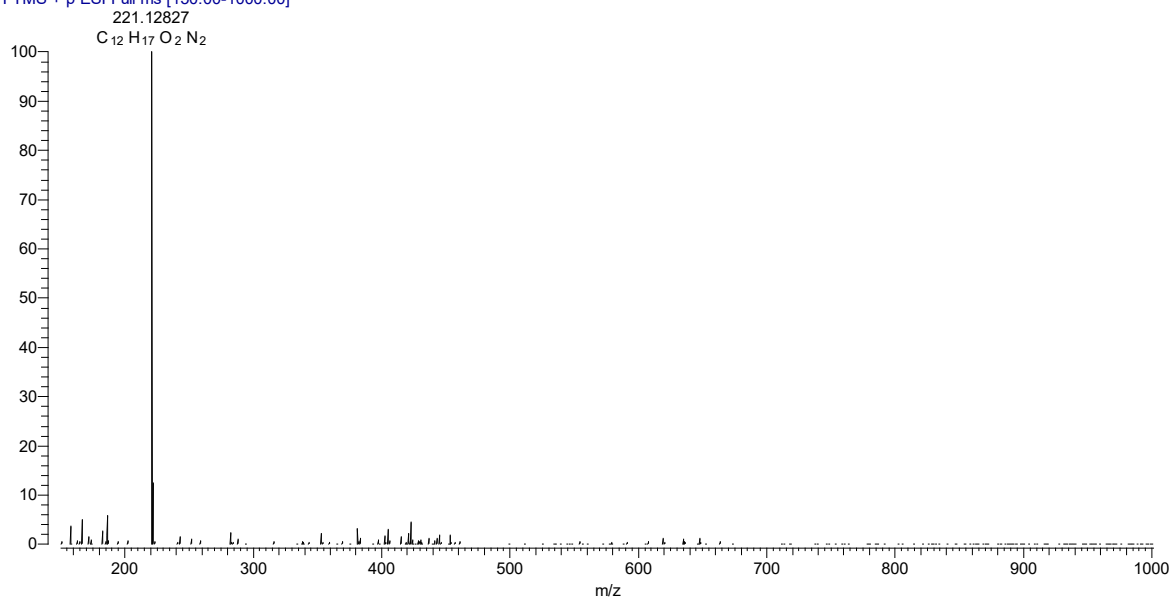


Molecular Weight: 220.27

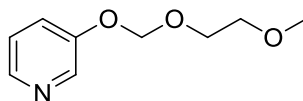
(*S,R*)-*N*-methyl-2-[2-(3-hydroxy-2-pyridyloxy)-1-hydroxyethyl]pyrrolidine [(*S,R*)-**64**] (150 mg – 0.63 mmol) was dissolved in anhydrous THF (2 mL) and triphenylphosphine (0.94 mmol) was added. The solution was cooled at -10 °C and diisopropyl azodicarboxylate (DIAD) (0.19 mL) was added. The reaction vessel was placed into a microwave reactor and irradiated at 120 °C for 15 min at 300 W. The solvent was removed under vacuum affording a residue that was purified by silica gel flash chromatography (dichloromethane/methanol 95:5 + 3% NH₃(30% in water)). The pure compound (*S,S*)-**5** was obtained as a light yellow oil (75 mg – 0.34 mmol, 54%). **TLC** (Dichloromethane / Methanol 95:5 + 3% NH₃(30% in water)): **Rf**= 0.15. **[α]_D²⁵** = -51.5 (c0.5, CHCl₃). **¹H NMR** (300 MHz, DMSO-*d*₆): δ 7.71 (dd, *J*= 4.7, 1.6 Hz, 1H), 7.27 (dd, *J*= 8.0, 1.6 Hz, 1H), 6.90 (dd, *J*= 8.0, 4.7 Hz, 1H), 4.34 (dd, *J*= 11.3, 2.2 Hz, 1H), 4.23 (ddd, *J*= 8.0, 4.7, 2.2 Hz, 1H), 3.96 (dd, *J*= 11.3, 8.0 Hz, 1H), 2.88 – 2.95 (m, 1H), 2.56 – 2.66 (m, 1H), 2.35 (s, 3H), 2.20 – 2.30 (m, 1H), 1.65 – 1.91 (m, 4H). **¹³C NMR** (75 MHz, CDCl₃): δ 151.38, 140.15, 139.56, 124.66, 118.40, 76.82, 65.53, 65.04, 58.16, 43.18, 28.09, 24.10. **Anal.** Calc. for C₁₂H₁₆N₂O₂: theor. C= 65.43; H= 7.32; N= 12.72; found C= 65.21; H= 7.34; N= 12.70. **HRMS (ESI⁺)**: calc. for C₁₂H₁₇N₂O₂: theor. 221.12845; found [M+H]⁺: 221.12827.



BC288 #1-10 RT: 0.02-0.27 AV: 10 NL: 4.59E7
T: FTMS + p ESI Full ms [150.00-1000.00]



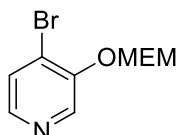
Synthesis of 3-((2-methoxyethoxy)methoxy)pyridine (**73**)



Molecular Weight: 183.20

Procedure adapted from literature.¹⁷⁵ Under inert atmosphere and at -10 °C, a solution of 3-hydroxypyridine (5.00 g – 52.58 mmol) in DMF (40 ml) was added dropwise to a suspension of NaH (1.5 g – 63.1 mmol) in DMF (10 ml). Upon stirring at -10 °C for 30 minutes, 2-methoxyethoxy-methylenchloride (7.85 g – 63.1 mmol) were added dropwise. The reaction mixture was equilibrated to 0 °C and stirred for 3.5 hours. Afterward, the mixture was concentrated in vacuo and the resulting residue was diluted with DCM and washed with a 10% aqueous solution of NaOH. The organic phase was dried over anhydrous sodium sulphate and the solvent was evaporated in vacuo. The pure product **73** was obtained as a yellow oil (9.2 g – 50.21 mmol, 95%). TLC (Cyclohexane / Ethyl acetate 3:7): **Rf**= 0.25. ¹H-NMR (300 MHz, CDCl₃): δ 8.38 (d, *J* = 2.7, 1H), 8.23 (dd, *J* = 5.0, 1.4 Hz, 1H), 7.37 (ddd, *J* = 8.5, 2.7, 1.4 Hz, 1H), 7.19 (ddd, *J* = 8.5, 5.0, 0.5 Hz, 1H), 5.26 (s, 2H), 3.82 – 3.75 (m, 2H), 3.56 – 3.47 (m, 2H), 3.33 (s, 3H).

Synthesis of 4-bromo-3-[(2-methoxyethoxy)methoxy]pyridine (**70**)

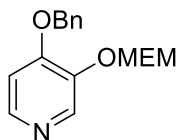


Molecular Weight: 262.10

Procedure adapted from literature.¹⁷⁶ A 2.7 M solution of n-BuLi in heptane (12.13 mL, 32.8 mmol) was added dropwise to a stirred solution of 3-((2-methoxyethoxy)methoxy)pyridine (**73**) (3.0 g – 16.4 mmol) in THF (60 mL) at -78 °C. After 1 h, the reaction mixture was cooled to -90 °C and a solution of tetrabromoethane (10.86 g – 32.8 mmol) in THF (15 mL) was added dropwise. Upon stirring at this temperature for further 1 h, water (20 mL) was added dropwise. The aqueous phase was extracted with ethyl acetate many times. The organic phases were combined, dried over anhydrous sodium sulphate, filtered and the solvent was evaporated in vacuo, and the resulting crude was purified by silica gel flash chromatography (Cyclohexane / Ethyl acetate 3:7). The pure product **70** was isolated as a yellow oil (3.1 g – 11.81 mmol, 72%). TLC(Cyclohexane / Ethyl acetate 3:7): **Rf**= 0.29. ¹H NMR (300 MHz, CDCl₃): δ 8.48 (s, 1H),

8.08 (d, $J= 5.2$ Hz, 1H), 7.48 (d, $J= 5.2$ Hz, 1H), 5.37 (s, 2H), 3.90 – 3.87 (m, 2H), 3.58 – 3.55 (m, 2H), 3.36 (s, 3H).

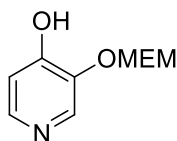
Synthesis of 4-benzyloxy-3-[(2-methoxyethoxy)methoxy]pyridine (**71**)



Molecular Weight: 289.33

Procedure adapted from literature.¹⁷⁷ Under nitrogen atmosphere, a solution of benzyl alcohol (3.55 mL – 34.4 mmol) in DMSO (5 mL) was added dropwise to a stirred suspension of NaH (1.37 g – 57.2 mmol) in DMSO (15 mL). The mixture was heated at 50 °C for 30 min and then cooled to 10 °C. Upon dropwise addition of a solution of 4-bromo-3-[(2-methoxyethoxy)methoxy]pyridine (**70**) (6.0 g – 22.9 mmol) in DMSO (40 mL), the temperature was increased to 20 °C and the whole reaction mixture was stirred at this temperature for 1 h. Afterward, diethyl ether and water were added. The organic phase was separated, washed with water, dried over anhydrous sodium sulphate, filtered and the solvent was evaporated in vacuo. The resulting crude was purified by silica gel flash chromatography (gradient from cyclohexane/ethyl acetate 3:7 to ethyl acetate). The pure product **71** was isolated as a yellow oil (5.4 g – 18.78 mmol, 82%). TLC (Cyclohexane / Ethyl acetate 3:7): **R_f**= 0.23. **¹H NMR** (300 MHz, CDCl₃) δ 8.38 (s, 1H), 8.17 (d, $J= 5.5$ Hz, 1H), 7.41 – 7.31 (m, 5H), 6.84 (d, $J= 5.5$ Hz, 1H), 5.29 (s, 2H), 5.16 (s, 2H), 3.88 – 3.86 (m, 2H), 3.55 – 3.52 (m, 2H), 3.39 (s, 3H).

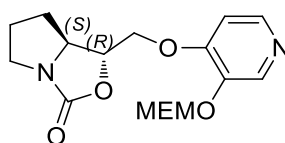
Synthesis of 4-hydroxy-3-[(2-methoxyethoxy)methoxy]pyridine (**72**)



Molecular Weight: 199.20

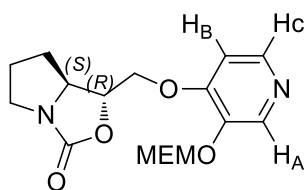
A mixture of 4-benzyloxy-3-[(2-methoxyethoxy)methoxy]pyridine (**71**) (5.2 g – 18.4 mmol) and 10% Pd/C (520 mg) in methanol (60 ml) was stirred under H₂ atmosphere for 1 h. Afterward, the catalyst was filtered off and the filtrate was concentrated in vacuo affording the product **72** as a white solid (3.57 g – 18.03 mmol, 98%). **M.p.**= 89.0 °C. TLC (Ethyl Acetate): **R_f**= 0.3. **¹H NMR** (300 MHz, CDCl₃) δ 7.89 (s, 1H), 7.69 (d, $J= 6.9$ Hz, 1H), 6.67 (d, $J= 6.9$ Hz, 1H), 5.24 (s, 2H), 3.86 – 3.81 (m, 2H), 3.58 – 3.48 (m, 2H), 3.35 (s, 3H).

Synthesis (*S,R*)-1-[3-(2-methoxyethoxy)methoxy-4-pyridyloxymethyl]tetrahydro-1*H*,3*H*-pyrrolo[1,2-*c*]oxazol-3-one [(*S,R*)-65]

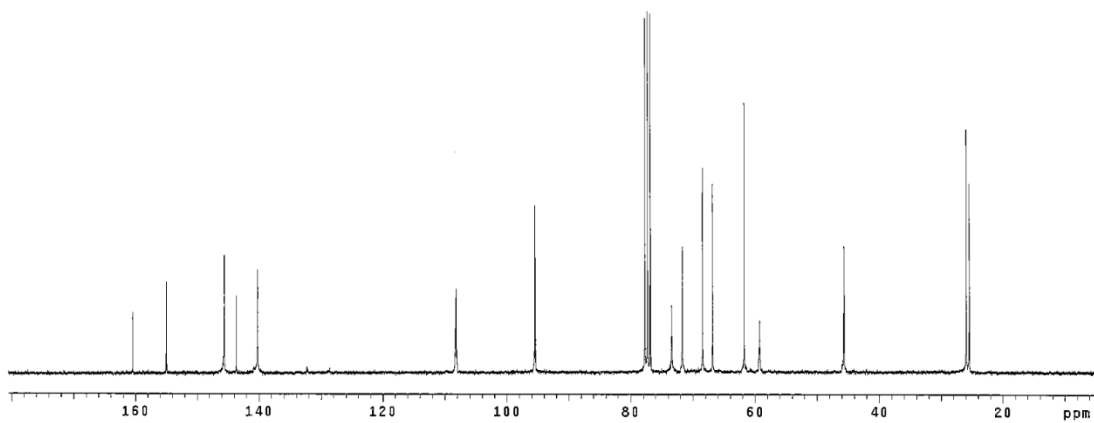
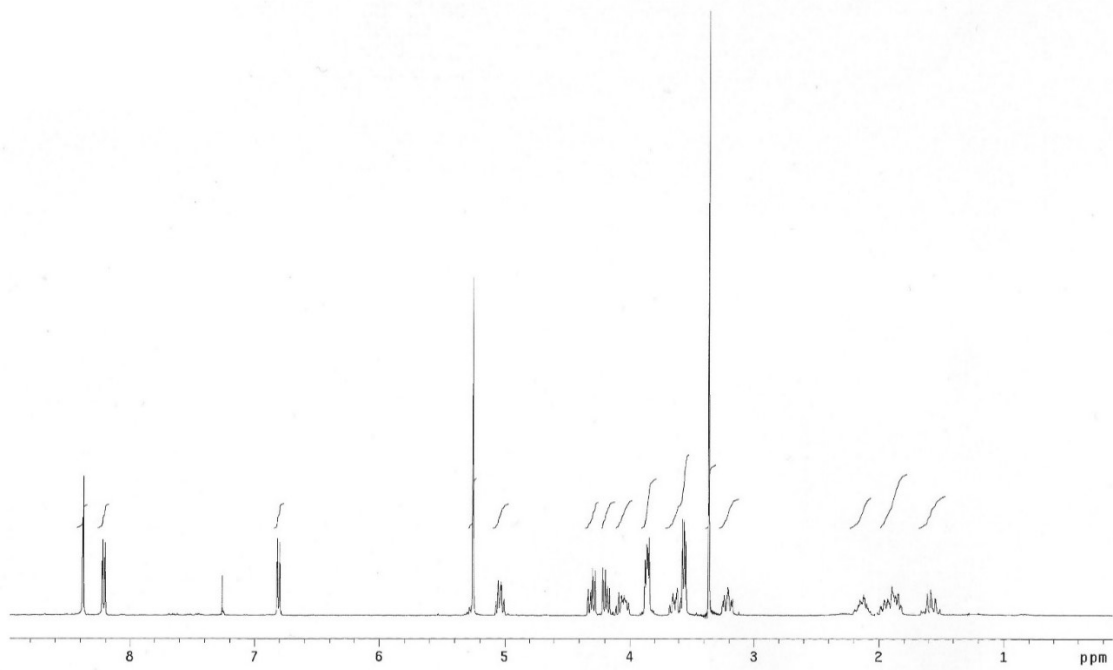


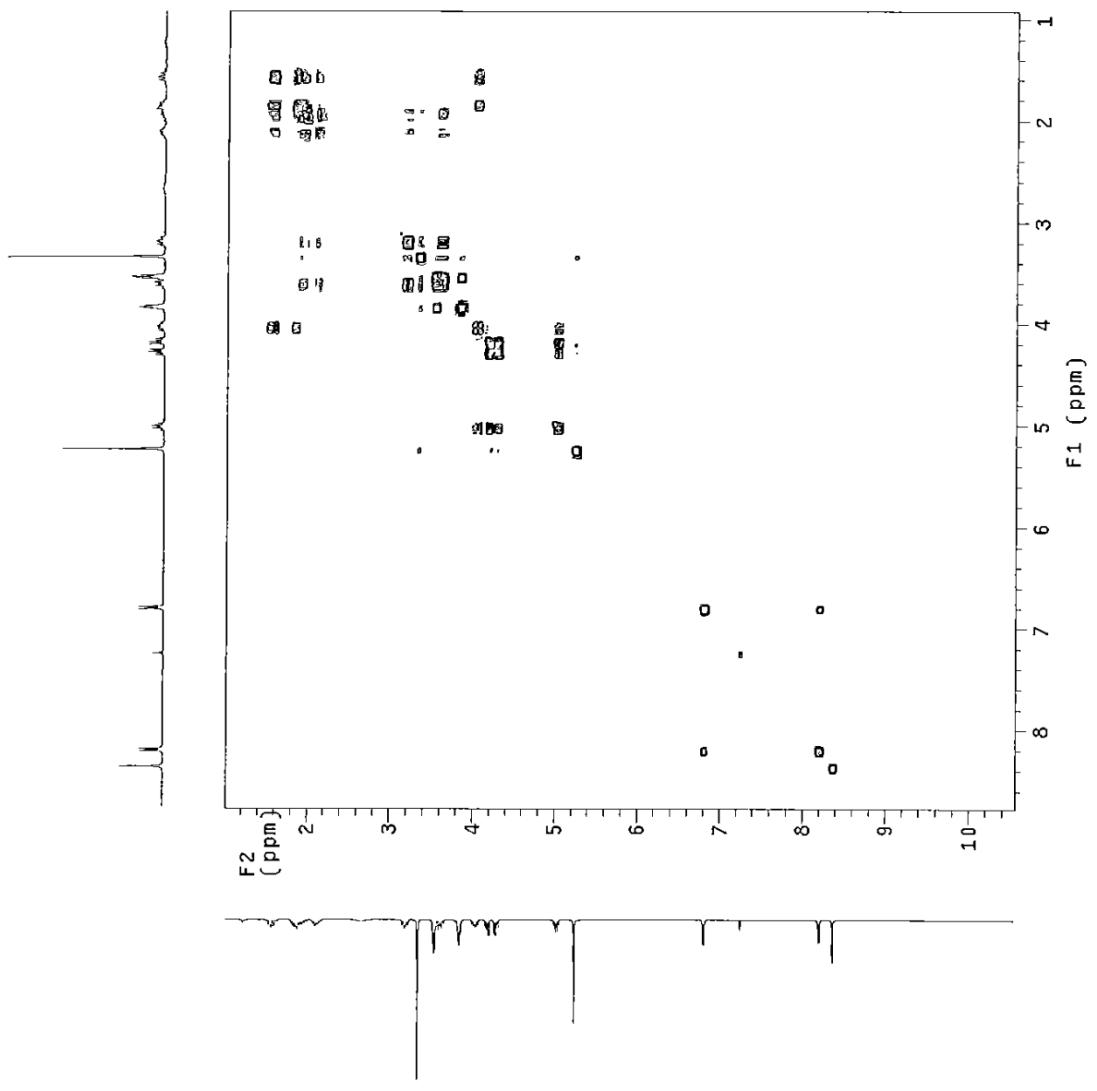
Molecular Weight: 338.36

4-hydroxy-3-(2-methoxyethoxy) methoxypyridine (**72**) (882 mg – 4.43 mmol) was dissolved in anhydrous THF (5 mL). Upon addition of triphenylphosphine (1.74 g – 6.65 mmol), the reaction mixture was cooled to -10 °C and a solution of (*S,R*)-1-(hydroxymethyl)tetrahydro-1*H*,3*H*-pyrrolo[1,2-*c*]oxazol-3-one [(*S,R*)-**61**] (696 mg – 4.43 mmol) in THF (5 mL) was added dropwise. Afterwards, diisopropyl azodicarboxylate (DIAD) (210 mg – 6.65 mmol) was added and the reaction mixture was refluxed for 12 h. Afterward, the solvent was evaporated in vacuo providing a residue that was purified by silica gel flash chromatography (dichloromethane/methanol 95:5). The pure compound (*S,R*)-**65** was obtained as an orange oil (1.2 g – 3.55 mmol, 80%). TLC (Dichloromethane / Methanol 95:5): $R_f = 0.31$. $[\alpha]_D^{25} = -7.6$ (c_1 , CHCl_3). $^1\text{H NMR}$ (300 MHz, CDCl_3): δ 8.37 (s, 1H, $\underline{\text{H}}_A$), 8.21 (d, $J = 5.5$ Hz, 1 H, $\underline{\text{H}}_C$), 6.81 (d, $J = 5.5$ Hz, 1H, $\underline{\text{H}}_B$), 5.25 (s, 2H, $\text{OCH}_2\text{O-MEM}$), 5.12 – 5.00 (m, 1H, $\text{C}^*\underline{\text{H}}\text{O}$), 4.35 – 4.22 (m, 1H, CH_2O), 4.25 – 4.11 (m, 1H, CH_2O), 4.15 – 4.00 (m, 1H, $\text{C}^*\underline{\text{H}}\text{N}$), 3.88 – 3.84 (m, 2H, $\text{CH}_2\text{OCH}_2\text{OPy-MEM}$), 3.67 – 3.58 (m, 1H, CH_2N), 3.57 – 3.53 (m, 2H, $\text{CH}_3\text{OCH}_2\text{-MEM}$), 3.35 (s, 3H, $\text{CH}_3\text{O-MEM}$), 3.24 – 3.16 (m, 1H, CH_2N), 2.17 – 2.09 (m, 1H, $\text{CH}_2\text{CH}_2\text{C}^*\text{HN}$), 1.98 – 1.82 (m, 2H, $\text{CH}_2\text{CH}_2\text{C}^*\text{HN}$), 1.61 – 1.54 (m, 1H, $\text{CH}_2\text{CH}_2\text{C}^*\text{HN}$).

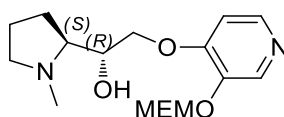


$^{13}\text{C NMR}$ (75 MHz, CDCl_3): δ 160.47, 155.02, 145.61, 143.61, 140.21, 108.20, 95.47, 73.46, 71.71, 68.44, 66.85, 61.77, 59.31, 46.67, 25.94, 25.44.

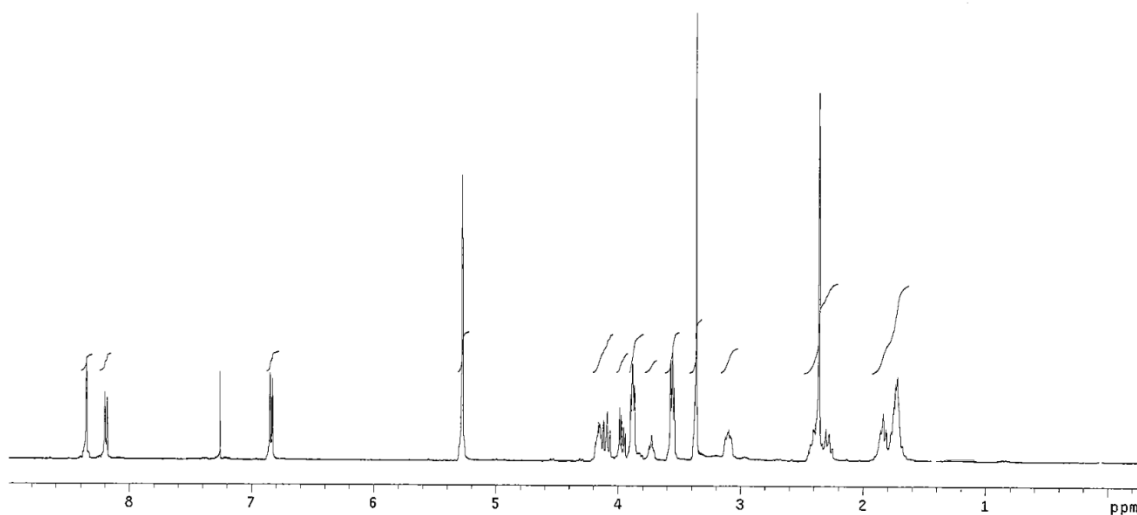




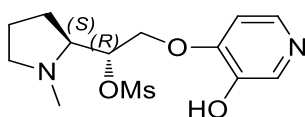
Synthesis of (*S,R*)-*N*-Methyl-2-[2-(3-(2-methoxyethoxy)methoxy)-4-pyridyloxy)-1-hydroxyethyl]pyrrolidine [(*S,R*)-66]



A solution of (*S,R*)-1-[3-(2-methoxyethoxy)methoxy-4-pyridyloxymethyl]tetrahydro-1*H*,3*H*-pyrrolo[1,2-*c*]oxazol-3-one [(*S,R*)-65] (1.1 g – 3.25 mmol) in THF (4 mL) was added dropwise to a suspension of LiAlH₄ (123 mg – 3.25 mmol) in THF (4 mL) under inert atmosphere, at -10 °C. The reaction mixture was warmed to room temperature and stirred for 2 h. Upon cooling, dichloromethane and water were added. The resulting suspension was filtered through a celite plug and the filtrate was evaporated in vacuo providing the pure compound (*S,R*)-66 as a light-yellow oil (910 mg – 2.79 mmol, 86%). TLC (Dichloromethane / Methanol 8:2 + 3% NH₃(30% in water)): R_f= 0.68. [α]_D²⁵ = -13.2 (*c*1, CHCl₃). ¹H NMR (300 MHz, CDCl₃): δ 8.35 (s, 1H), 8.19 (d, *J*= 5.5 Hz, 1H), 6.84 (d, *J*= 5.5 Hz, 1H), 5.27 (s, 2H), 4.18 – 4.06 (m, 2H), 3.97 – 3.88 (m, 1H), 3.87 – 3.82 (m, 2H), 3.57 – 3.52 (m, 2H), 3.38 (s, 3H), 3.19 – 3.08 (m, 1H), 2.46 – 2.33 (m, 1H), 2.37 (s, 3H), 2.44 – 2.25 (m, 1H), 1.85 – 1.68 (m, 4H).

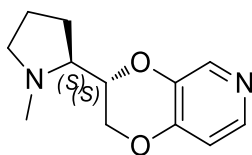


Synthesis of (*S,R*)-*N*-methyl-2-[2-(3-hydroxy-4-pyridyloxy)-1-mesyloxyethyl]pyrrolidine [(*S,R*)-67]



Mesyl chloride (0.08 mL – 0.810 mmol) was added to a solution of (*S,R*)-*N*-Methyl-2-[2-(3-(2-methoxyethoxy)methoxy-4-pyridyloxy)-1-hydroxyethyl]pyrrolidine [(*S,R*)-66] (1.00 g – 2.67 mmol) and triethylamine (0.085 mL – 0.810 mmol) in dichloromethane (5 mL) at -10 °C. Upon stirring for 30 min at room temperature, dichloromethane and 10% aqueous solution of NaHCO₃ were added. The organic phase was separated, dried over anhydrous sodium sulphate, and concentrated, affording a residue (1.00 g – 2.67 mmol) that was dissolved in dichloromethane (3 mL) and stirred with TFA at room temperature for 3 h. Afterwards, the solvent was evaporated in vacuo and the residue was purified by silica gel flash chromatography (dichloromethane/methanol 9:1 + 3%NH₃(30% in water)). The pure product (*S,R*)-67 was obtained as a pink sticky solid (500 mg – 1.58 mmol, 59%). TLC (Dichloromethane / Methanol 9:1 + 3% NH₃(30% in water)): R_f = 0.47. [α]_D²⁵ = +9.2 (c1, MeOH). ¹H NMR (CD₃OD): δ 7.97 (s, 1H), 7.93 (d, *J* = 5.7 Hz, 1H), 7.08 (d, *J* = 5.7 Hz, 1H), 4.71 (dd, *J* = 1.4, 11.0 Hz, 1H), 4.39 (dd, *J* = 2.4, 11.0 Hz, 1H), 4.22 – 4.14 (m, 1H), 3.32 (s, 3H), 3.18 – 3.10 (m, 1H), 2.51 – 2.40 (m, 1H), 2.41 (s, 3H), 2.39 – 2.28 (m, 1H), 1.84 – 1.75 (m, 4H).

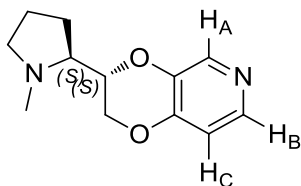
Synthesis of (*S,S*)-3-(*N*-methyl-2-pyrrolidinyl)-2,3-dihydro-1,4-dioxino[2,3-*c*]pyridine [(*S,S*)-7]



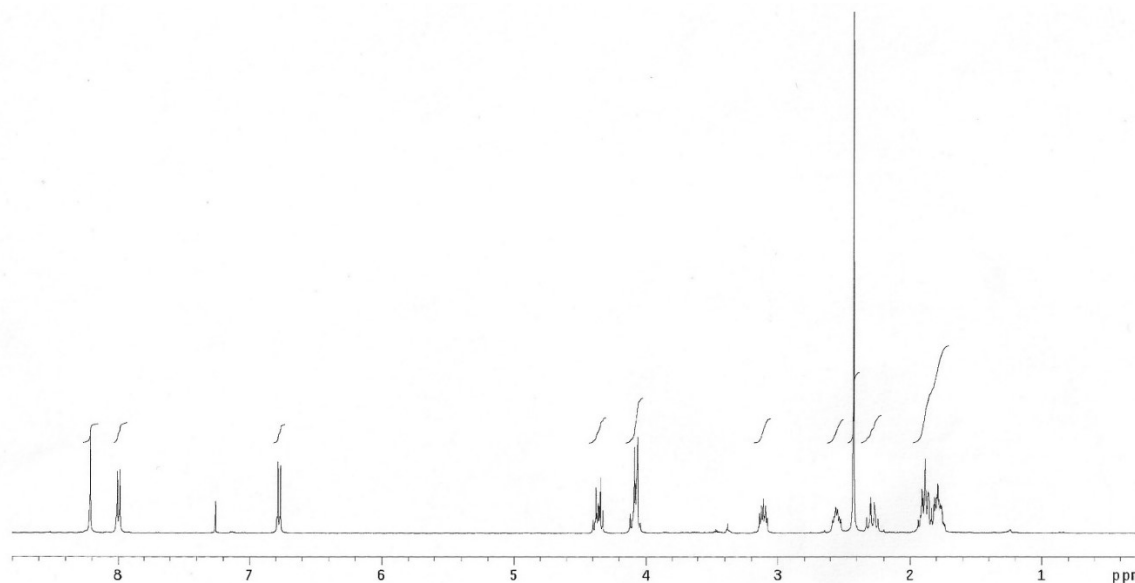
Molecular Weight: 220.27

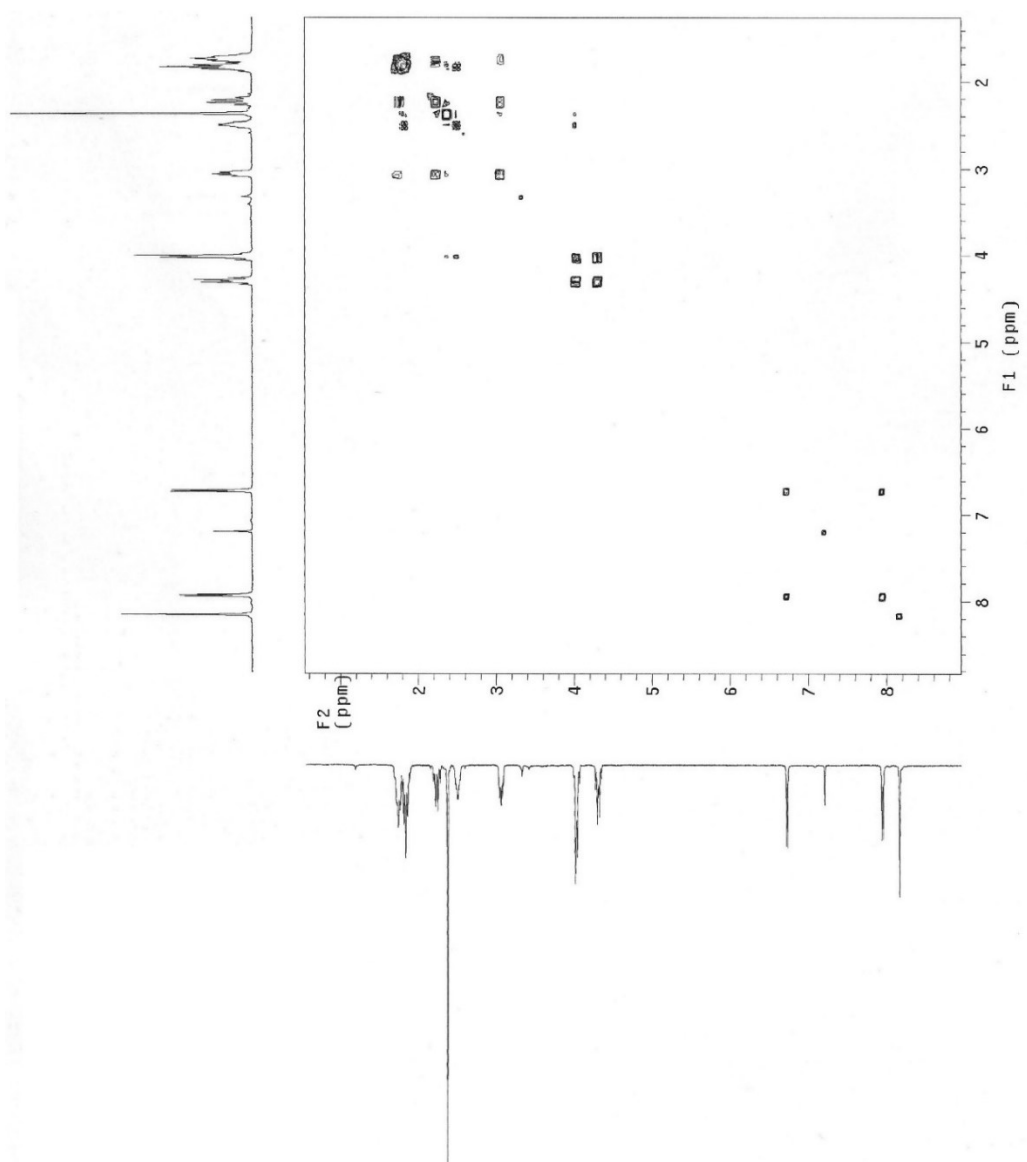
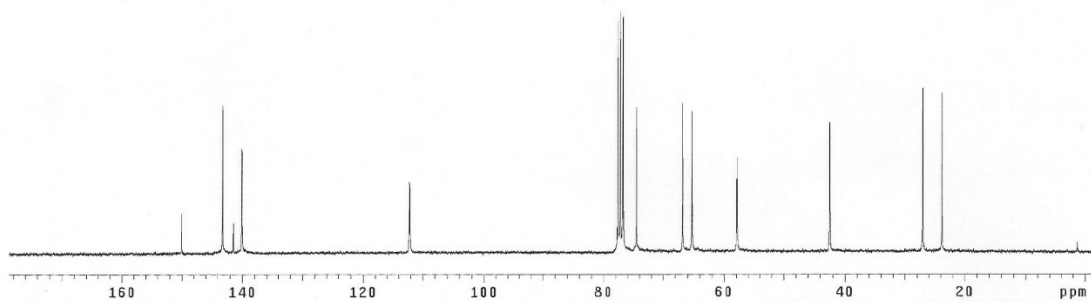
A solution of (*S,R*)-*N*-methyl-2-[2-(3-hydroxy-4-pyridyloxy)-1-mesyloxyethyl]pyrrolidine [(*S,R*)-67] (500 mg – 1.58 mmol) in dimethoxyethane (4 mL) was added to a suspension of potassium carbonate (642 mg – 4.64 mmol) in dimethoxyethane (1 mL) under inert atmosphere and the resulting mixture was refluxed for 16 h. Then, dichloromethane was added and the resulting mixture was washed with a 10% NaHCO₃ aqueous solution. The separated organic layer was dried over Na₂SO₄, filtered and evaporated in vacuo affording a crude that was

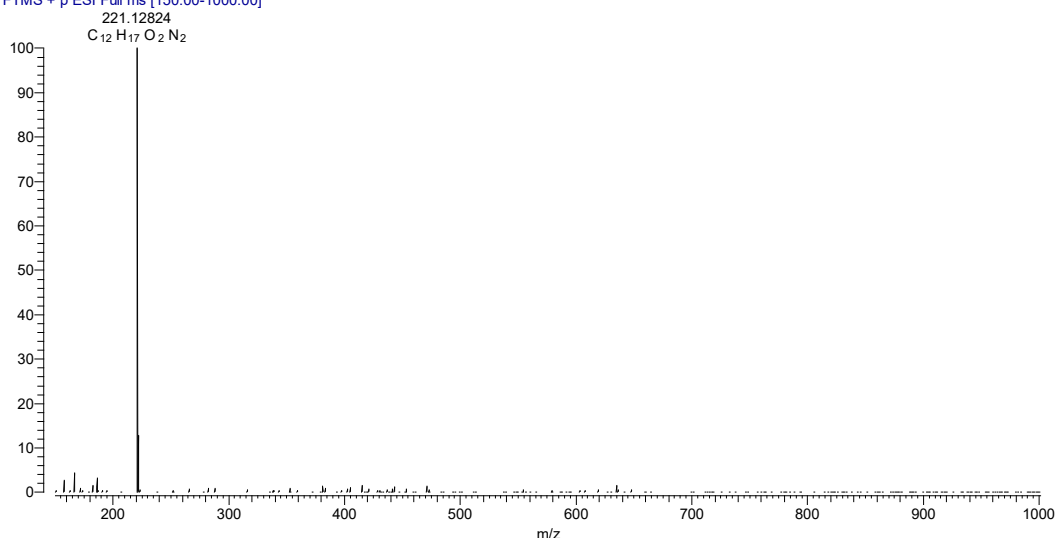
purified by silica gel flash chromatography (Dichloromethane / Methanol 9:1 + 3% NH₃(30% in water)). The pure compound (*S,S*)-7 was obtained as a white solid (160 mg – 0.73 mmol, 46%). **TLC** (Dichloromethane / Methanol 9:1 + 3% NH₃(30% in water)): **R_f**= 0.47. **M.p.**= 57.9 °C. **[α]_D²⁵** = -93.4 (*c*1, CHCl₃). **¹H NMR** (300 MHz, CDCl₃): δ 8.21 (s, 1H, H_A), 8.00 (d, *J*= 5.5 Hz, 1H, H_B), 6.78 (d, *J*= 5.5 Hz, 1H, H_C), 4.41 – 4.28 (m, 1H, CH₂O), 4.15 – 4.01 (m, 2H, CH₂O + C*HO), 3.14 – 3.08 (m, 1H, CH₂N), 2.61 – 2.51 (m, 1H, C*HN), 2.42 (s, 3H, CH₃N), 2.32 – 2.24 (m, 1H, CH₂N), 1.94 – 1.74 (m, 4H, CH₂CH₂C*HN).



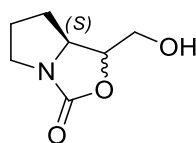
¹³C NMR (75 MHz, CDCl₃): δ 150.05, 143.29, 141.52, 140.06, 112.17, 74.58, 66.78, 65.28, 57.91, 42.49, 26.94, 23.75. **Anal.** Calc. for C₁₂H₁₆N₂O₂: theor. C= 65.43; H= 7.32; N= 12.72; found C= 65.32; H= 7.36; N= 12.69. **HRMS (ESI⁺)**: calc. for C₁₂H₁₇N₂O₂: theor. 221.12845; found [M+H]⁺: 221.12824.







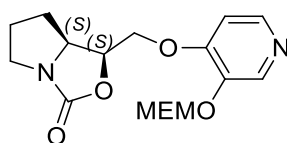
Synthesis of *(S,S)*/*(S,R)*-1-(hydroxymethyl)tetrahydro-1H,3H-pyrrolo[1,2-c]oxazol-3-one [*(S,S)*-61/*(S,R)*-61]



Molecular Weight: 157.17

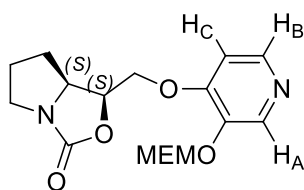
A suspension of *(S,S)*/*(S,R)*-1-(benzyloxymethyl)tetrahydro-1H, 3Hpyrrolo[1,2-c]oxazol-3-one [*(S,S)*-60/*(S,R)*-60] (2.37 g – 9.57 mmol) and 10% Pd/C (473 mg) in methanol (50 ml) was vigorously stirred under H_2 atmosphere for 8 hours. Afterward, the catalyst was removed by filtration on a Celite® pad and the solvent was evaporated in vacuo, affording the pure product *(S,S)*-61/*(S,R)*-61 as a yellow oil (1.2 g – 7.63 mmol, 80%). TLC (Ethyl Acetate): R_f = 0.3. 1H -NMR (300 MHz, $CDCl_3$): δ 4.73 – 4.67 (m, 0.2H), 4.38 – 4.33 (m, 0.8H), 3.95 – 3.81 (m, 0.6H), 3.78 – 3.67 (m, 2.4H), 3.57 – 3.47 (m, 1H), 3.40 – 3.08 (m, 3H, 1bs), 1.59 – 1.37 (m, 1H), 2.13 – 1.66 (m, 3H).

Synthesis of (*S,S*)-1-[3-(2-methoxyethoxy)methoxy-4-pyridyloxymethyl]tetrahydro-1*H*,3*H*-pyrrolo[1,2-*c*]oxazol-3-one [(*S,S*)-65**]**

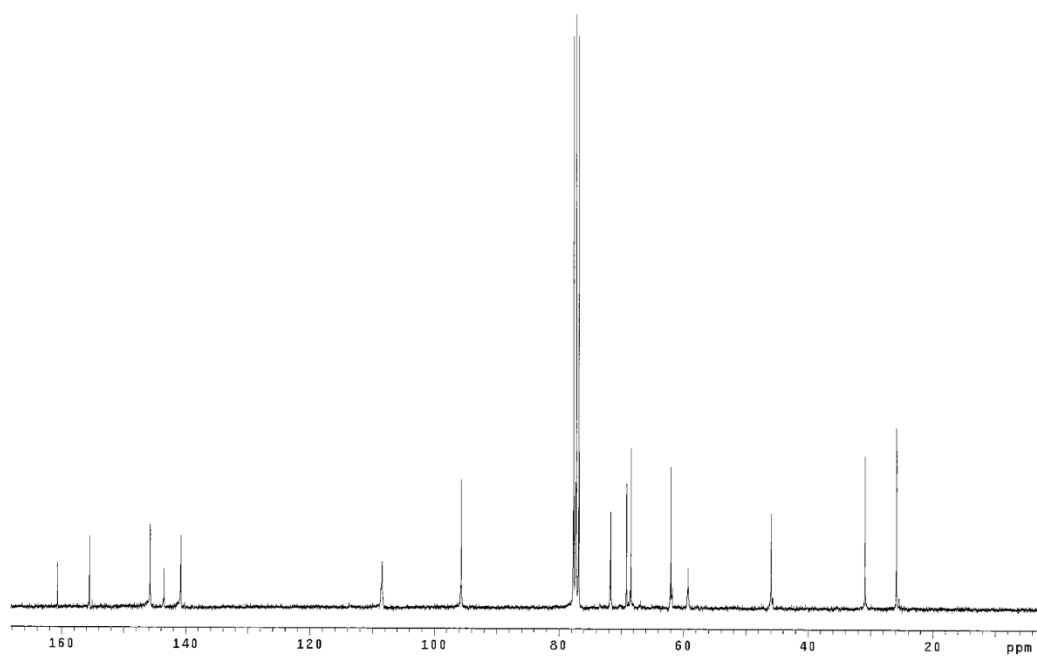
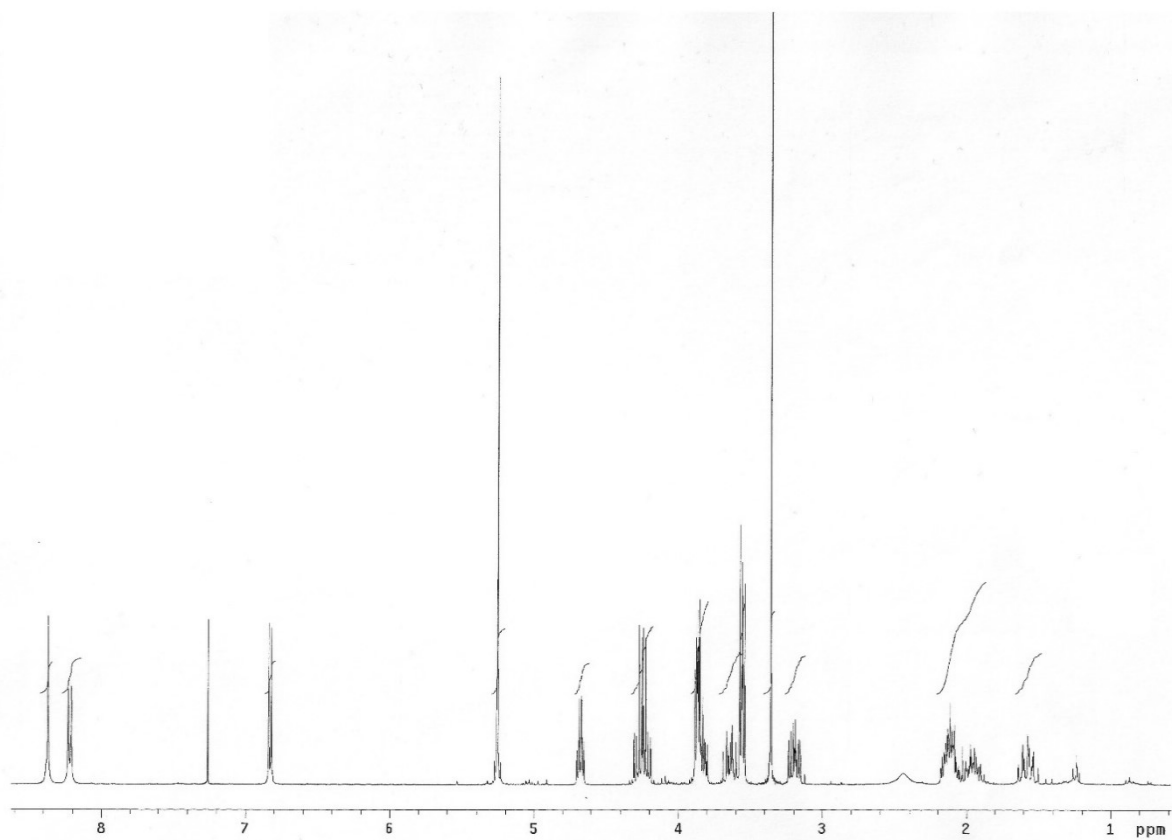


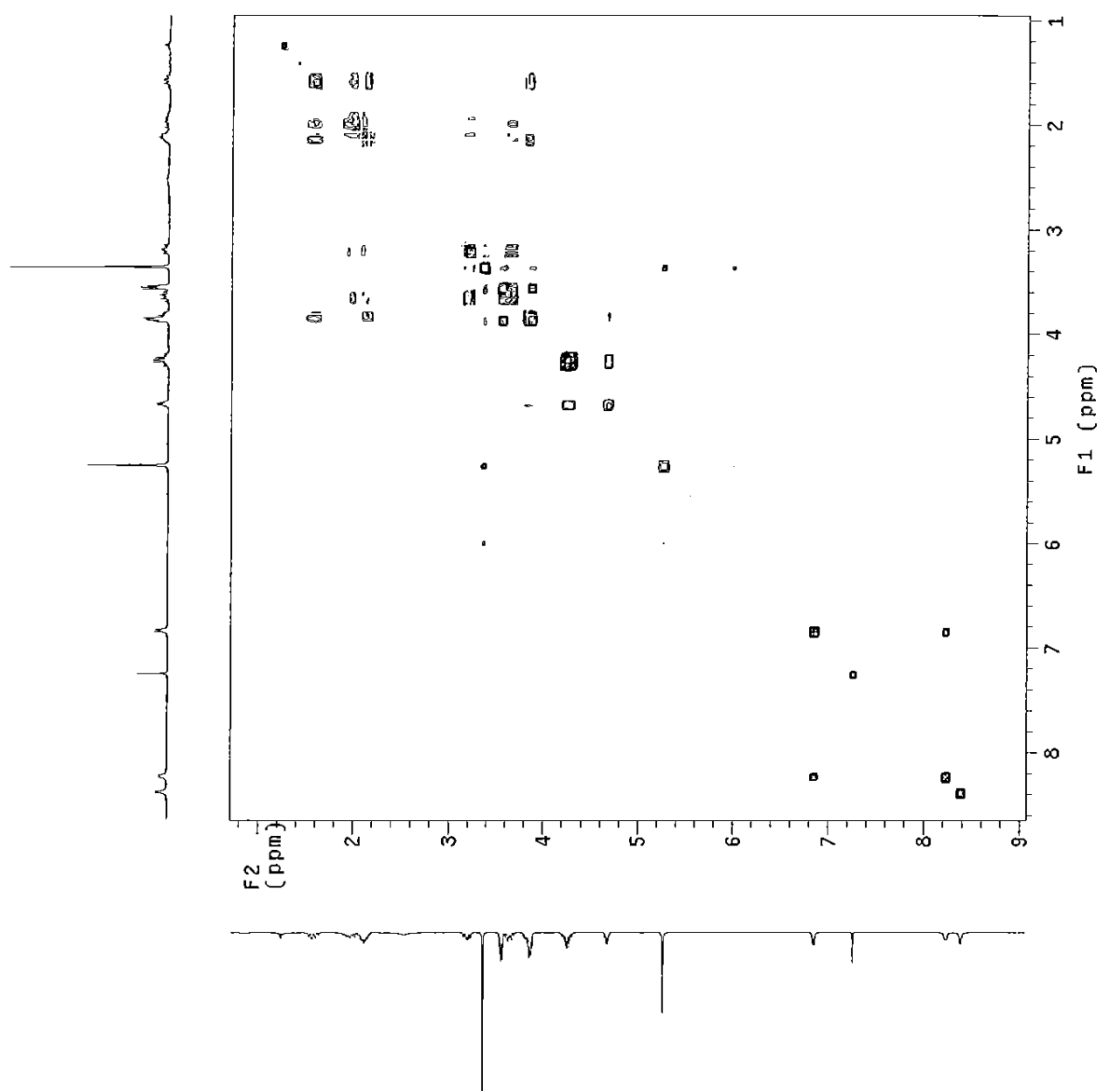
Molecular Weight: 338.36

4-hydroxy-3-(2-methoxyethoxy) methoxypyridine (**72**) (633 mg – 3.18 mmol) was dissolved in anhydrous THF (5 mL). Upon addition of triphenylphosphine (1.25 g – 4.77 mmol), the reaction mixture was cooled to -10 °C and a solution of the diastereoisomeric mixture of (*S,R*)/(*S,S*)-1-(hydroxymethyl)tetrahydro-1*H*,3*H*-pyrrolo[1,2-*c*]oxazol-3-one [(*S,S*)-**61**/*(S,R)*-**61**] (500 mg – 3.18 mmol) in THF (5 mL) was added dropwise. Afterwards, diisopropyl azodicarboxylate (DIAD) (151 mg – 4.77 mmol) was added and the reaction mixture was refluxed for 12 h. Afterwards, the solvent was evaporated in vacuo providing a residue that was purified by silica gel flash chromatography (dichloromethane/methanol 95:5). The pure compound (*S,S*)-**65** was obtained as a yellow oil (580 mg – 1.71 mmol, 54%). TLC (Dichloromethane / Methanol 95:5): *R_f* = 0.36. [α]_D²⁵ = -31.5 (*c*1, CHCl₃). ¹H NMR (300 MHz, CDCl₃): δ 8.37 (s, 1H, H_A), 8.22 (d, *J* = 5.5 Hz, 1H, H_B), 6.83 (d, *J* = 5.5 Hz, 1H, H_C), 5.23 (s, 2H, OCH₂O-MEM), 4.69 – 4.65 (m, 1H, C*H_O), 4.30 – 4.19 (m, 2H, CH₂O), 3.90 – 3.81 (m, 3H, C*H_N + CH₂OCH₂OPy-MEM), 3.67 – 3.59 (m, 1H, CH₂N), 3.59 – 3.54 (m, 2H, CH₃OCH₂-MEM), 3.36 (s, 3H, CH₃O-MEM), 3.23 – 3.16 (m, 1H, CH₂N), 2.18 – 1.87 (m, 3H, CH₂CH₂C*H_N), 1.63 – 1.50 (m, 1H, CH₂CH₂C*H_N).

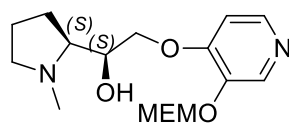


¹³C NMR (75 MHz, CDCl₃): δ 160.64, 155.48, 145.76, 143.55, 140.84, 108.46, 95.67, 76.84, 71.72, 69.14, 68.44, 61.99, 53.32, 45.96, 30.90, 25.89.





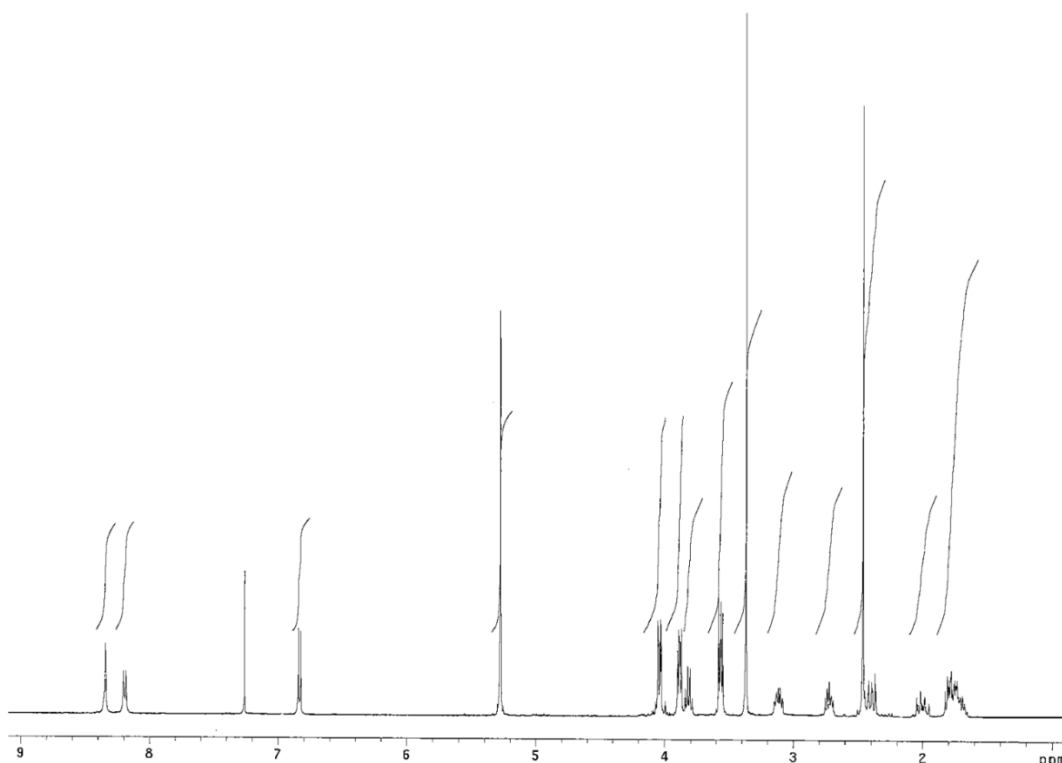
Synthesis of (*S,S*)-*N*-Methyl-2-[2-(3-(2-methoxyethoxy)methoxy-4-pyridyloxy)-1-hydroxyethyl]pyrrolidine [(*S,S*)-66]



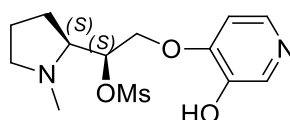
Molecular Weight: 326.39

A solution of (*S,S*)-1-[3-(2-methoxyethoxy)methoxy-4-pyridyloxymethyl]tetrahydro-1*H*,3*H*-pyrrolo[1,2-*c*]oxazol-3-one [(*S,S*)-65] (580 mg – 1.71 mmol) in THF (7 mL) was added dropwise to a suspension of LiAlH₄ (195 mg – 5.14 mmol) in THF (3 mL) under inert

atmosphere, at -10 °C. The reaction mixture was warmed to room temperature and stirred for 2 h. Upon cooling, dichloromethane and water were added. The resulting suspension was filtered through a celite plug and the filtrate was evaporated in vacuo providing the product (*S,S*)-**66** as a light yellow oil (523 mg – 1.62 mmol, 95%). **TLC** (Dichloromethane / Methanol 8:2 + 3% NH₃(30% in water)): **R_f**= 0.59. **[α]_D²⁵** = -18.0 (*c*1, CHCl₃). **¹H NMR** (300 MHz, CDCl₃): δ 8.34 (s, 1H), 8.19 (d, *J*= 5.5 Hz, 1H), 6.84 (d, *J*= 5.5 Hz, 1H), 5.27 (s, 2H), 4.06 – 3.99 (m, 2H), 3.90 – 3.87 (m, 2H), 3.84 – 3.78 (m, 1H), 3.60 – 3.54 (m, 2H), 3.36 (s, 3H), 3.14 – 3.08 (m, 1H), 2.75 – 2.69 (m, 1H), 2.50 (s, 3H), 2.46 – 2.38 (m, 1H), 2.26 – 1.95 (m, 1H), 1.83 – 1.37 (m, 3H).



Synthesis of (*S,S*)-*N*-Methyl-2-[2-(3-hydroxy-4-pyridyloxy)-1-mesyloxyethyl]pyrrolidine [(*S,S*)-**67**]

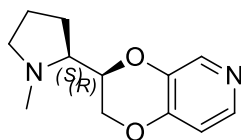


Molecular Weight: 316.37

Mesyloxy chloride (0.1 mL – 0.85 mmol) was added to a solution of (*S,S*)-*N*-Methyl-2-[2-(3-(2-methoxyethoxy)methoxy)-4-pyridyloxy]-1-hydroxyethyl]pyrrolidine [(*S,S*)-**66**] (230 mg – 0.71

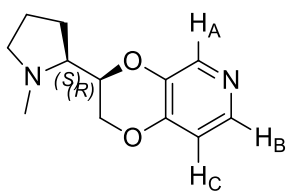
mmol) and triethylamine (0.09 ml – 0.85 mmol) in dichloromethane (5 mL) at -10 °C. Upon stirring for 30 min at room temperature, dichloromethane and 10% aqueous solution of NaHCO₃ were added. The organic phase was separated, dried over anhydrous sodium sulphate, and concentrated, affording a residue (180 mg) that was dissolved in dichloromethane (3 mL) and stirred with TFA (4.5 mmol) at room temperature for 3 h. Afterwards, the solvent was evaporated in vacuo and the residue was purified by silica gel flash chromatography (dichloromethane/methanol 9:1 + 3% NH₃(30% in water)). The pure product (*S,S*)-**67** was obtained as a yellow oil (56 mg – 0.18 mmol, 40%). **TLC** (Dichloromethane / Methanol 9:1 + 3% NH₃(30% in water)): **Rf**= 0.47. **[α]_D²⁵** = -33.2 (*c*1, MeOH). **¹H NMR** (300 MHz, CD₃OD): δ 7.92 – 7.90 (m, 2H), 7.04 (d, *J*= 3.0 Hz, 1H), 4.68 – 4.59 (m, 1H), 4.37 – 4.16 (m, 2H), 3.29 (s, 3H), 2.93 – 2.88 (m, 1H), 2.39 (s, 3H), 2.39 – 2.31 (m, 2H), 2.12 – 1.90 (m, 4H).

Synthesis of (*S,R*)-3-(*N*-Methyl-2-pyrrolidinyl)-2,3-dihydro-1,4-dioxino[2,3-*c*]pyridine [(*S,R*)-**7**]

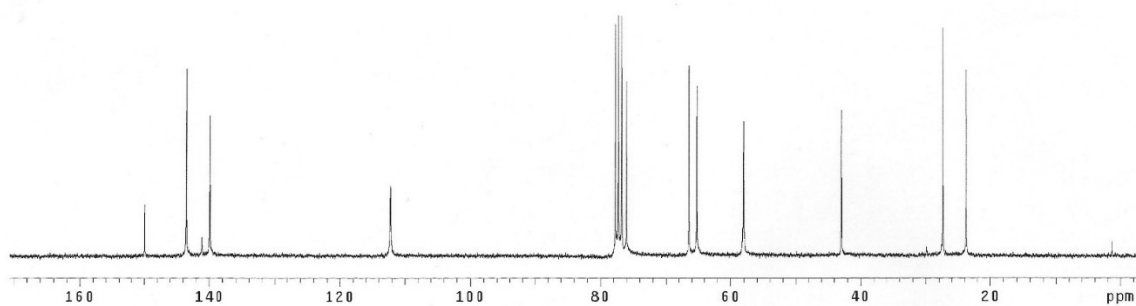
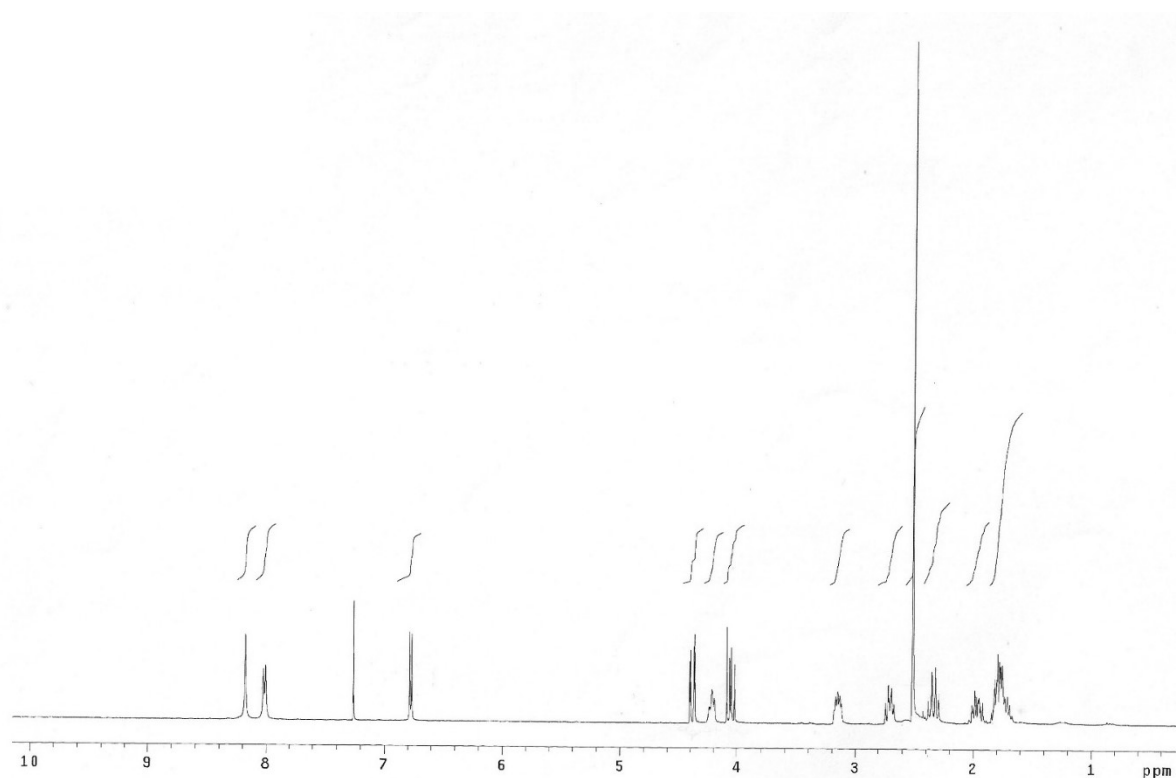


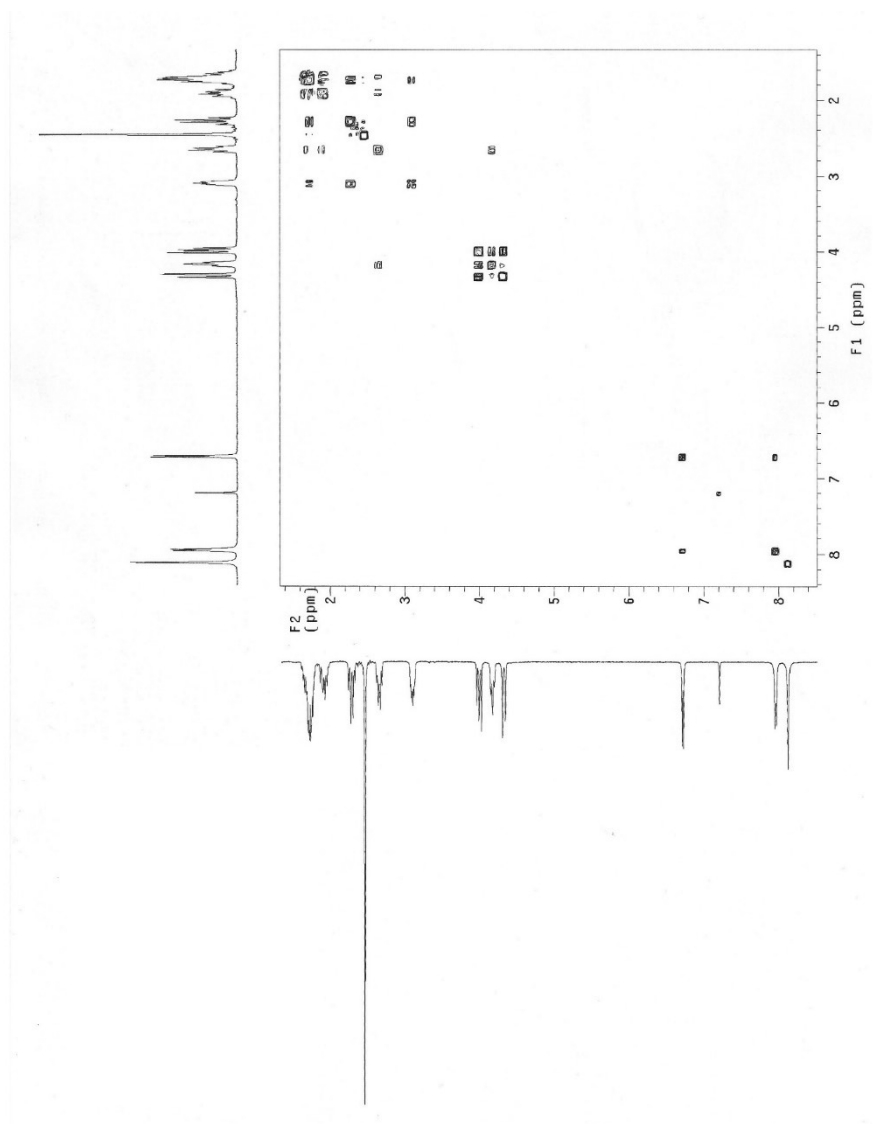
Molecular Weight: 220.27

A solution of (*S,S*)-*N*-Methyl-2-[2-(3-hydroxy-4-pyridyloxy)-1-mesyloxyethyl]pyrrolidine [(*S,S*)-**67**] (50 mg – 0.16 mmol) in dimethoxyethane (4 mL) was added to a suspension of potassium carbonate (65 mg – 0.47 mmol) in dimethoxyethane (1 mL) under inert atmosphere and the resulting mixture was refluxed for 16 h. Then, dichloromethane was added, and the resulting mixture was washed with a 10% NaHCO₃ aqueous solution. The organic layer was dried over Na₂SO₄, filtered and evaporated in vacuo affording a crude that was purified by silica gel flash chromatography (dichloromethane/methanol 9:1 + 3% NH₃(30% in water)). The pure compound (*S,R*)-**7** was obtained as a yellow oil (25 mg – 0.11 mmol, 69%). **TLC** (Dichloromethane / Methanol 9:1 + 3% NH₃(30% in water)): **Rf**= 0.39. **[α]_D²⁵** = +5.2 (*c*1, CHCl₃). **¹H NMR** (300 MHz, CDCl₃): δ 8.18 (s, 1H, H_A), 8.01 (d, *J*= 5.5 Hz, 1H, H_B), 6.78 (d, *J*= 5.5 Hz, 1H, H_C), 4.38 (dd, *J*= 11.6, 2.2 Hz, 1H, CH₂O), 4.21 (td, *J*= 7.7, 2.2 Hz, 1H, C*HO), 4.04 (dd, *J*= 11.6, 7.7 Hz, 1H, CH₂O), 3.16 – 3.11 (m, 1H, CH₂N), 2.73 – 2.66 (m, 1H, C*HN), 2.52 (s, 3H, CH₃N), 2.42 – 2.29 (m, 1H, CH₂N), 2.03 – 1.91 (m, 1H, CH₂CH₂C*HN), 1.84 – 1.67 (m, 3H, CH₂CH₂C*HN).



^{13}C NMR (75 MHz, CDCl_3): δ 149.96, 143.48, 141.18, 139.92, 112.20, 76.03, 66.47, 65.10, 58.01, 42.85, 27.39, 23.73. **Anal.** Calc. for $\text{C}_{12}\text{H}_{16}\text{N}_2\text{O}_2$: theor. C= 65.43; H= 7.32; N= 12.72; found C= 65.29; H= 7.35; N= 12.70. **HRMS (ESI⁺)**: calc. for $\text{C}_{12}\text{H}_{17}\text{N}_2\text{O}_2$: theor. 221.12845; found $[\text{M}+\text{H}]^+$: 221.12823.



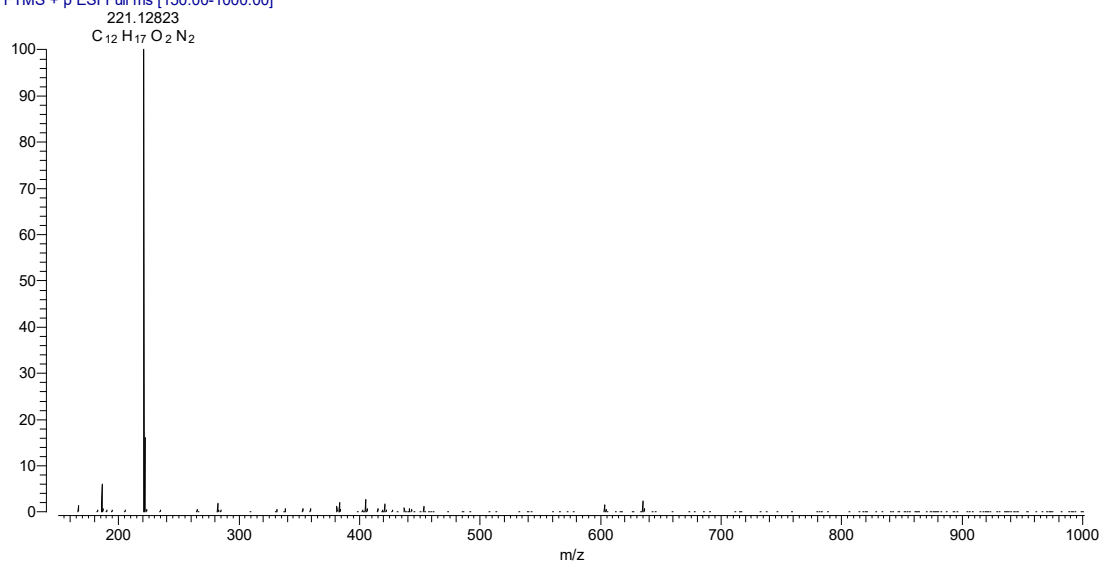


\\cubestation2\orbitrap\...DT96
1-500 in 0.1% HCOOH in H2O/CH3CN 50/50

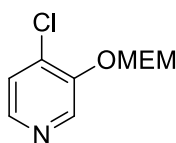
10/19/16 15:17:00

DT96 2 mg/mL IN CH3OH

DT96 #1-10 RT: 0.01-0.27 AV: 10 NL: 6.29E7
T: FTMS + p ESI Full ms [150.00-1000.00]



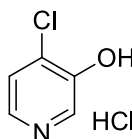
Synthesis of 4-Chloro-3-[(2-methoxyethoxy)methoxy]pyridine (**74**)



Molecular Weight: 217.65

Procedure adapted from literature.¹⁷⁵ Upon cooling to $-78\text{ }^{\circ}\text{C}$, a 1.7 M solution of tert-butyllithium in n-pentane (3.4 mL – 5.78 mmol) was added dropwise to a stirred solution of 3-[(2-Methoxyethoxy)methoxy]pyridine (**73**) (1 g – 5.46 mmol) in diethyl ether (40 mL). After 30 min, a solution of hexachloroethane (1.75 g – 6.55 mmol) in diethyl ether (5 mL) was added. After 30 min, temperature was increased to $20\text{ }^{\circ}\text{C}$ and the reaction mixture was further stirred for 1 h. Afterward, 10% aqueous NaHCO_3 was added. The organic phase was separated, washed with brine, dried over anhydrous sodium sulphate, filtered and evaporated in vacuo, affording a crude that was purified through silica gel flash chromatography (40-60 petroleum ether/acetone 8:2). The pure product **74** was isolated as a dark yellow oil (1.0 g – 4.91 mmol, 90%), which is stable if stored as a 50% v/v solution in MTBE at $-28\text{ }^{\circ}\text{C}$. **TLC** (Toluene / Ethyl Acetate 2:8): **Rf**= 0.30. **$^1\text{H NMR}$** (300 MHz, CDCl_3): δ 8.55 (s, 1H), 8.20 (d, J = 5.1 Hz, 1H), 7.34 (d, J = 5.1 Hz, 1H), 5.40 (s, 2H), 3.93 – 3.85 (m, 2H), 3.59 – 3.50 (m, 2H), 3.36 (s, 3H).

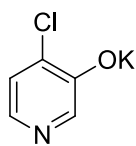
Synthesis of 4-Chloro-3-hydroxypyridine hydrochloride (**75**)



Molecular Weight: 166.01

Procedure adapted from literature.¹⁷⁸ Upon cooling to $-10\text{ }^{\circ}\text{C}$, a solution 1.25 M of methanolic HCl (9.2 mL – 11.5 mmol) was added dropwise to a stirred solution of 4-Chloro-3-[(2-methoxyethoxy)methoxy]pyridine (**74**) (500 mg – 2.3 mmol) in methanol (5 mL). After 1 h, the reaction mixture was warmed to $20\text{ }^{\circ}\text{C}$ was stirred for 16 h. Afterward, the solvent was evaporated in vacuo and the resulting crude product was crystallized in toluene, providing the pure product **75** as a white crystalline solid (342 mg – 2.07 mmol, 90%). **TLC** (40-60 $^{\circ}\text{C}$ Petroleum Ether / Acetone 6:4): **Rf**= 0.33. **M.p.**= $205.9\text{ }^{\circ}\text{C}$. **$^1\text{H NMR}$** (300 MHz, DMSO-d_6): δ 12.67 (bs, 2H), 8.52 (s, 1H), 8.30 (d, J = 5.9 Hz, 1H), 7.99 (d, J = 5.9 Hz, 1H).

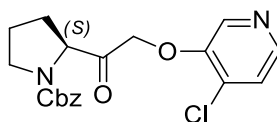
Synthesis of 4-chloro-3-hydroxypyridine potassium salt (**76**)



Molecular Weight: 167.63

Upon complete dissolution of compound 4-chloro-3-hydroxypyridine hydrochloride (**75**) (460 mg – 2.8 mmol) in the minimum volume possible of methanol, a 1N methanolic solution of KOH (5.3 ml – 5.3 mmol) was added dropwise. After 10 min, the mixture was cooled to 0 °C and the resulting suspension was filtered. The solid was dried in open air at room temperature, affording the product **76** as a beige powder (440 mg – 2.66 mmol, 95%). ¹H NMR (300 MHz, DMSO-d₆): δ 7.44 (s, 1H), 6.92 (d, *J*= 4.8 Hz, 1H), 6.81 (d, *J*= 4.8 Hz, 1H).

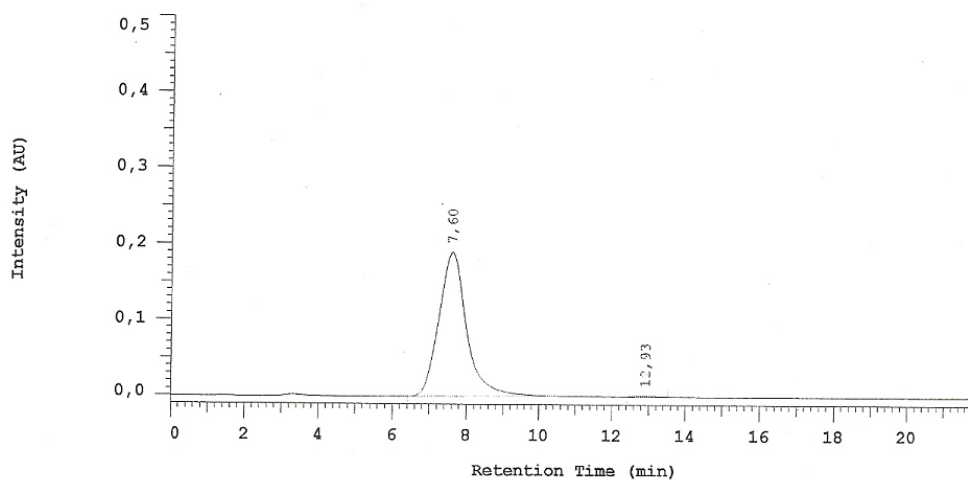
Synthesis of (*S*)-N-Cbz-2-[(4-chloro-3-pyridyloxy)acetyl]pyrrolidine [(*S*)-**68**]



Molecular Weight: 374.82

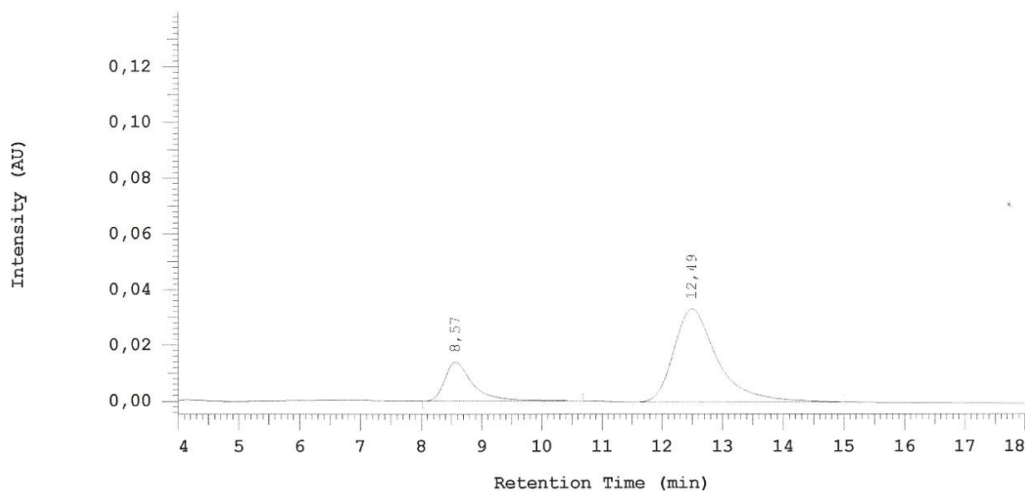
Under inert atmosphere and at -10 °C, a solution of 4-chloro-3-hydroxypyridine potassium salt (**76**) (470 mg – 2.82 mmol) in acetone (30 ml) was added dropwise to a solution of (*S*)-N-carbobenzyloxy-2-bromoacetylpyrrolidine [(*S*)-**49**] (1.09 g – 3.10 mmol) in acetone (10 ml). The reaction mixture was stirred for 5 hours at 15-20 °C. Afterward, the solvent was concentrated in vacuo, the residue was diluted in ethyl acetate and washed with an aqueous solution of NaOH 1 M and then with water. The organic phase was dried over anhydrous sodium sulphate and the solvent was removed in vacuo, providing a crude that was further purified through silica gel flash chromatography (gradient from cyclohexane/ethyl acetate 3:7 to 1:9). The pure product (*S*)-**68** was obtained as a dark yellow oil (510 mg – 1.36 mmol, 48%). The enantiomeric excess was evaluated by chiral HPLC analysis. TLC (Cyclohexane / Ethyl Acetate 2:8): *R_f*= 0.26. [α]_D²⁵ = -30.9 (*c*₁, CHCl₃). e.e. %= 99.50% (Chiracel OJ, hexane/EtOH 7:3, F= 1.5 ml/min, λ= 280 nm, *R_{tR}*= 12.93 min, *R_{tS}*= 7.60 min). ¹H NMR (300 MHz, DMSO-d₆, T= 100 °C): δ 8.27 (s, 1H), 8.16 (d, *J*= 5.0 Hz, 1H), 7.47 (d, *J*= 5.0 Hz, 1H), 7.35 – 7.26 (m, 5H), 5.13 (s, 2H), 5.07 (s, 2H), 4.64 – 4.56 (m, 1H), 3.49 – 3.40 (m, 2H), 2.31 – 2.10 (m, 1H), 2.04 – 1.85 (m, 3H).

Chiral HPLC analysis: (*S*)-*N*-carbobenzyloxy-2-[2'-(4-chloro-3-pyridiniloxy)acetyl]pyrrolidine



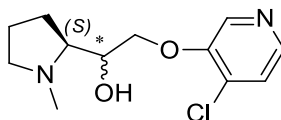
No.	RT	Area	Conc 1	BC
1	7,60	4914509	99,748	MC
2	12,93	12412	0,252	MC
		4926921	100,000	

Chiral HPLC analysis: diastereoisomeric mixture of (*S*)- and (*R*)-*N*-carbobenzyloxy-2-[2'-(4-chloro-3-pyridiniloxy)acetyl]pyrrolidine



No.	RT	Area	Conc 1	BC
1	8,57	219253	21,064	MC
2	12,49	821654	78,936	MC
		1040907	100,000	

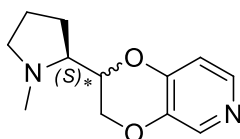
Synthesis of (*S,S*)/(*S,R*)-*N*-methyl-2-[1-hydroxy-2-(4-chloro-3-pyridyloxy)ethyl]pyrrolidine [(*S,S*)-69/(*S,R*)-69]



Molecular Weight: 255.72

Under a nitrogen atmosphere, at $-10\text{ }^{\circ}\text{C}$, a solution of (*S*)-*N*-Cbz-2-[(4-chloro-3-pyridyloxy)acetyl]pyrrolidine [(*S*)-68] (300 mg – 0.8 mmol) in anhydrous THF (10 ml) was added dropwise to a suspension of LiAlH_4 (91 mg – 2.4 mmol) in anhydrous THF (2 ml). The reaction mixture was refluxed for 3 hours under vigorous stirring. Afterward, the mixture was diluted with dichloromethane and the excess of LiAlH_4 was quenched by slowly adding water dropwise at $0\text{ }^{\circ}\text{C}$. The resulting suspension was filtered through Celite® and the solvent was concentrated in vacuo, affording a crude that was diluted with an aqueous solution of HCl 1 M and washed with diethyl ether. The aqueous phase was basified to pH 9 with an aqueous solution of NH_3 and extracted with ethyl acetate. The organic phase was dried over anhydrous sodium sulphate, filtered and the solvent was evaporated in vacuo, affording a crude that was purified through silica gel flash chromatography (dichloromethane/methanol 95:5 + 0.5% NH_3 (30% in water)) providing a diastereoisomeric mixture of (*S,S*)-69 and (*S,R*)-69 (123 mg – 0.48 mmol, 60%). TLC (Dichloromethane / Methanol 9:1 + 0.5% NH_3 (30% in water)): $\text{Rf}_1 = 0.27$, $\text{Rf}_2 = 0.18$. $^1\text{H NMR}$ (300 MHz, CDCl_3): δ 8.32 (s, 1H), 8.12 – 8.18 (m, 1H), 7.22 – 7.31 (m, 1H), 4.20 – 4.28 (m, 0.8H), 3.99 – 4.14 (m, 1.2H), 4.00 – 4.08 (m, 0.4H), 3.73 – 3.83 (m, 0.6H), 3.10 – 3.21 (m, 1H), 2.52 – 2.83 (m, 1H), 2.47 (s, 1.2H), 2.43 (s, 1.8H), 2.35 – 2.46 (m, 1H), 1.86 – 2.06 (m, 1H), 1.74 – 1.85 (m, 3H),

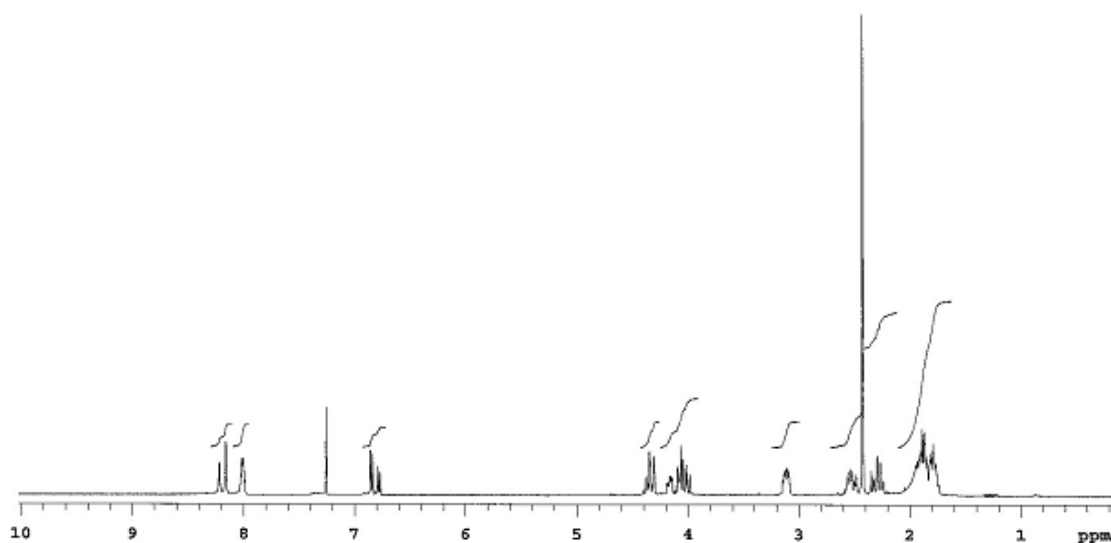
Synthesis of (*S,R*)/(*S,S*)-2-(*N*-Methyl-2-pyrrolidinyl)-2,3-dihydro-1,4-dioxino[2,3-*c*]pyridine [(*S,R*)-6/(*S,S*)-6]

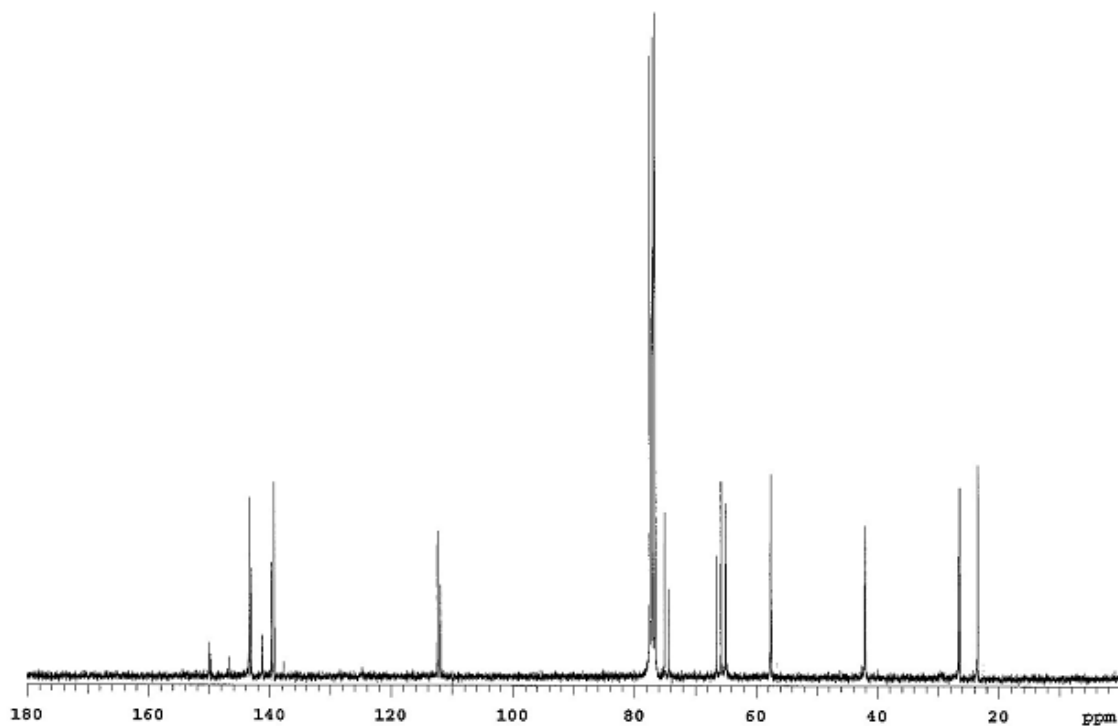


Molecular Weight: 219.26

Under inert atmosphere, a solution of the diastereoisomeric mixture of (*S,S*)/(*S,R*)-*N*-methyl-2-[1-hydroxy-2-(4-chloro-3-pyridyloxy)ethyl]pyrrolidine [(*S,S*)-69/(*S,R*)-69] (100 mg – 0.4 mmol) in DMF (2 ml) was added dropwise to a suspension of NaH (10 mg – 0.4 mmol) in DMF

(1 ml). The reaction mixture was refluxed overnight. Afterward, the mixture was cooled to room temperature, diluted with ethyl acetate and washed with an aqueous solution of NaOH 1M. The organic phase was dried over anhydrous sodium sulphate, filtered and the solvent was removed in vacuo, providing a crude that was purified through silica gel flash chromatography (dichloromethane/methanol 9:1 +0.5% NH₃(30% in water)). The diastereoisomeric mixture of (*S,R*)-**6**/*(S,S)*-**6** was obtained as a light yellow sticky solid (30 mg – 0.14 mmol, 35%). **TLC** (Dichloromethane / Methanol 9:1 + 2% NH₃(30% in water)): **R_{f1}**= 0.48, **R_{f2}**= 0.46. **¹H NMR** (300 MHz, CDCl₃): δ 8.22 (s, 0.4H), 8.18 (s, 0.6H), 8.08 – 7.99 (m, 1H), 6.83 (d, *J*= 5.3 Hz, 0.6H), 6.78 (d, *J*= 5.3 Hz, 0.4H), 4.41 – 4.43 (m, 1.6H), 4.22 – 4.16 (m, 0.4H), 4.12 – 3.98 (m, 1H), 3.18 – 3.08 (m, 1H), 2.60 – 2.45 (m 1H), 2.42 (s, 3H), 2.38 – 2.28 (m 1H), 1.98 – 1.78 (m, 4H). **¹³C NMR** (75 MHz, CDCl₃): δ 149.99, 149.82, 146.75, 143.38, 143.06, 141.25, 139.80, 139.3, 112.40, 111.94, 75.07, 74.27, 66.53, 65.76, 65.03, 64.97, 57.64, 57.55, 42.21, 42.08, 26.68, 26.48, 23.49. **Anal.** Calc. for C₁₂H₁₆N₂O₂: theor. C= 65.43; H= 7.32; N= 12.72; found C= 65.33; H= 7.39; N= 12.71. **HRMS (ESI⁺)**: calc. for C₁₂H₁₇N₂O₂: theor. 221.12845; found [M+H]⁺: 221.12825.



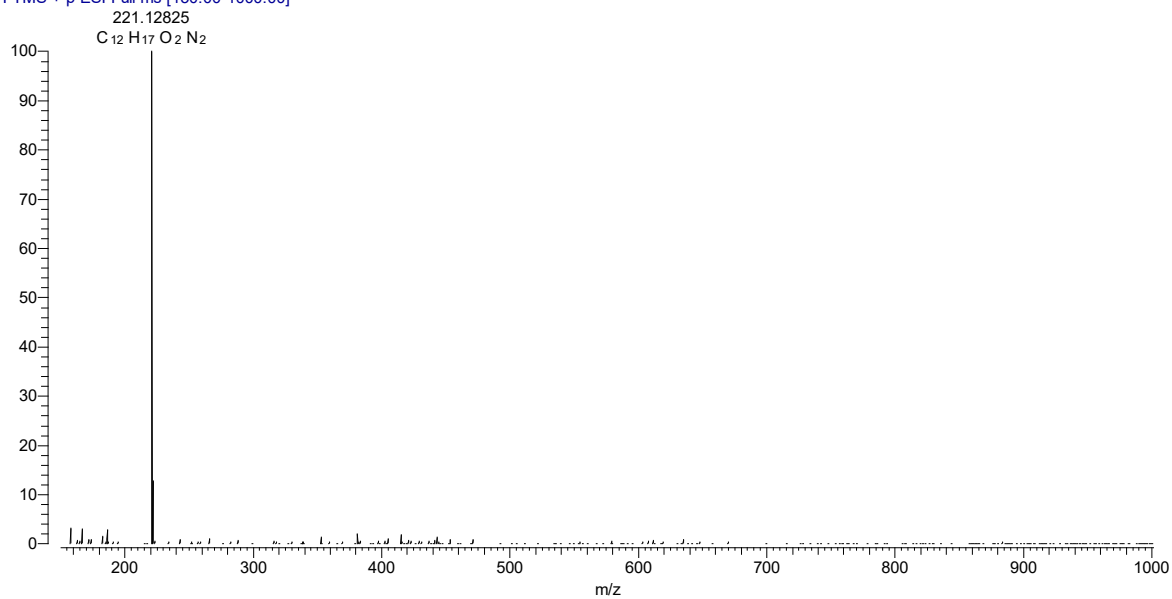


\\cubestation2\orbitrap\...SM53
1-500 in 0.1 % HCOOH in H2O/CH3CN 50/50

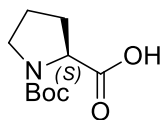
10/19/16 15:40:34

SM53 2 mg/mL IN CH3OH

SM53 #1-10 RT: 0.01-0.26 AV: 10 NL: 7.39E7
T: FTMS + p ESI Full ms [150.00-1000.00]



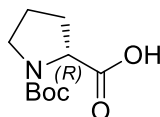
Synthesis of N-*tert*-butoxycarbonyl-(*S*)-proline [(*S*)-77]



Molecular Weight: 215.25

Procedure adapted from literature.¹⁷⁹ Upon addition of (*S*)-proline (10.0 g – 87 mmol) to a solution of NaOH (8.7 g – 218 mmol) in H₂O (65 ml), the solution was cooled to 10 °C and di-*tert*-butyl-dicarbonate (22.8 g – 104 mmol) was added in portions. The resulting suspension was warmed to room temperature and stirred for 5 hours. Afterward, diethyl ether was added and, upon phase separation, the aqueous phase was cooled to 0 °C, acidified to pH 2 and extracted with ethyl acetate. The organic phase was dried over anhydrous sodium sulphate and the solvent was evaporated in vacuo, affording a crude that was crystallized from diisopropyl ether and isopropanol. The pure compound (*S*)-77 was isolated as a white solid (17.8 g – 83 mmol, 95%). **M.p.** = 136.56 °C; literature¹⁸⁰: **M.p.** = 133 – 135 °C. $[\alpha]_D^{25} = -84.4^\circ$ (*c*1, CHCl₃); literature¹⁸¹: $[\alpha]_D^{25} = -54.5^\circ$ (*c*1, CHCl₃). **¹H-NMR** (300 MHz, CDCl₃): δ 10.48 (bs, 1H), 4.34 – 4.23 (m, 1H), 3.53 – 3.34 (m, 2H), 2.26 – 1.89 (m, 4H), 1.47 (s, 4H), 1.41 (s, 5H).¹⁸⁰

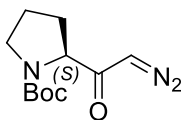
Synthesis of N-*tert*-butoxycarbonyl-(*R*)-proline [(*R*)-77]



Molecular Weight: 215.25

Procedure adapted from literature.¹⁷⁹ (*R*)-proline (10.0 g -87 mmol) was used to synthesize N-*tert*-butoxycarbonyl-(*R*)-proline, according to the procedure reported for the correspondent enantiomer (*S*). The pure product was obtained as a white solid (18.5 g – 86 mmol, 99%). **M.p.** = 136.92 °C; literature¹⁸²: **M.p.** = 132.6 – 135.2 °C. $[\alpha]_D^{25} = +84.2^\circ$ (*c*1, CHCl₃). **¹H-NMR** (300 MHz, CDCl₃): δ 10.48 (bs, 1H), 4.34 – 4.23 (m, 1H), 3.53 – 3.34 (m, 2H), 2.26 – 1.89 (m, 4H), 1.47 (s, 4H), 1.41 (s, 5H).¹⁸²

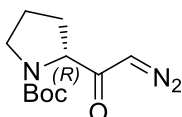
Synthesis of (*S*)-*N*-*tert*-butoxycarbonyl-diazoproline [(*S*)-78]



Molecular Weight: 239.27

Procedure adapted from literature.⁷³ Upon cooling to -15 °C, triethylamine (3.5 ml – 24 mmol) was added dropwise to a suspension of (*S*)-*N*-*tert*-butoxycarbonylproline [(*S*)-77] (5 g – 23 mmol) in anhydrous diethyl ether (40 ml). After 5 minutes, isobutylchloroformiate (3.2 ml – 24 mmol) was added dropwise, maintaining the temperature below -10 °C. After 20 minutes, upon formation of the mixed anhydride, controlled by TLC, the mixture was equilibrated to 0 °C and the solid was removed by filtration and washed with diethyl ether. The filtrate was cooled to 0 °C and, under inert atmosphere, an ethereal solution of diazomethane was carefully added dropwise over 45 minutes. The reaction mixture was stirred vigorously at room temperature overnight. Afterward, the ethereal solution was washed first with a saturated solution of NaHCO₃ and then with water. The organic phase was dried over anhydrous sodium sulphate, filtrated and the solvent was evaporated in vacuo, affording a crude that was purified through silica gel flash chromatography (cyclohexane/ethyl acetate 7:3). The pure product (*S*)-78 was isolated as a yellow solid (4.2 g – 18 mmol, 78%). TLC (Dichloromethane / Methanol 95:5; staining agent: Blue Shift): **Rf**= 0.57. TLC (Cyclohexane / Ethyl Acetate 7:3; staining agent: Blue Shift): **Rf**= 0.27. **M.p.**= 45 °C; literature⁷³: **M.p.** = 44 – 46 °C. **[α]_D²⁵** = -144.6 (*c*1, CHCl₃); literature¹⁸³: **[α]_D²⁵** = -145 (*c*1, CHCl₃). **¹H-NMR** (CDCl₃): δ 5.51 – 5.35 (m, 1H), 4.31 – 4.16 (m, 1H), 3.56-3.39 (m, 2H), 2.19-1.85 (m, 4H), 1.43 (s, 9H).¹⁸⁴

Synthesis of *N*-*tert*-butoxycarbonyl-(*R*)-diazoproline [(*R*)-78]¹

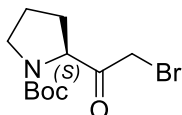


Molecular Weight: 239.27

Procedure adapted from literature.⁷³ *N*-*tert*-butoxycarbonyl-(*R*)-proline [(*R*)-77] (5.0 g – 20.9 mmol) was used to synthesize compound *N*-*tert*-butoxycarbonyl-(*R*)-diazoproline, according to the procedure reported for the correspondent enantiomer (*S*). The pure product [(*R*)-78] was obtained as a yellow solid (4.1 g – 17 mmol, 87%). TLC (Cyclohexane / Ethyl Acetate 7:3; stained with Blue Shift): **Rf**= 0.27. **M.p.**= 45 °C; literature⁷³: **M.p.** = 45 – 46 °C. **[α]_D²⁵** = +

141.8 (*c*1, CHCl₃); literature⁷³: $[\alpha]_D^{20} = +146$ (*c*1, CHCl₃). ¹H-NMR (CDCl₃): δ 5.51 – 5.35 (m, 1H), 4.31 – 4.16 (m, 1H), 3.56-3.39 (m, 2H), 2.19-1.85 (m, 4H), 1.43 (s, 9H).¹⁸³

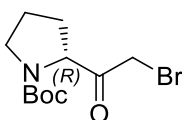
Synthesis of (*S*)-*N*-*tert*-butoxycarbonyl-2-bromoacetylpyrrolidine [(*S*)-79]



Molecular Weight: 292.17

Upon cooling to -10 °C, aqueous HBr (3.6 g – 21 mmol) was added dropwise to a solution of *N*-*tert*-butoxycarbonyl-(*S*)-diazoproline [(*S*)-78] (4.0 g – 17 mmol) in diethyl ether (80 ml). The resulting mixture was warmed to room temperature and vigorously stirred for 1 hour. Afterward, the mixture is diluted with diethyl ether (40 ml) and washed several times with a saturated solution of NaHCO₃ and then with water. The organic phase was dried over anhydrous sodium sulphate, filtered and the solvent was evaporated in vacuo, affording a crude that was purified through silica gel flash chromatography (cyclohexane/ethyl acetate 7:3). The pure product [(*S*)-79] was isolated as a pale yellow oil (3.53 g – 12 mmol, 71%). TLC (Cyclohexane/Ethyl Acetate 7:3; stained with Blue Shift): **R_f**= 0.50. $[\alpha]_D^{25} = -67.0$ (*c*1, Acetone); literature⁷³: $[\alpha]_D^{25} = -66.4$ (*c*1, Acetone). ¹H-NMR (300 MHz, CDCl₃): δ 4.55 – 4.45 (m, 1H), 4.17 – 4.02 (m, 2H), 3.56 – 3.41 (m, 2H), 2.29 – 2.12 (m, 1H), 2.05 – 1.87 (m, 3H), 1.44 (s, 4.5H), 1.41 (s, 4.5H).⁷³

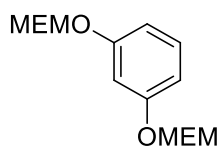
Synthesis of (*R*)-*N*-*tert*-butoxycarbonyl-2-bromoacetylpyrrolidine [(*R*)-79]



Molecular Weight: 292.17

N-*tert*-butoxycarbonyl-(*R*)-diazoproline [(*R*)-78] (4.0 g – 17 mmol) was used to synthesize compound *N*-*tert*-butoxycarbonyl-(*R*)-2-bromoacetylpyrrolidine, according to the procedure reported for the correspondent enantiomer (*S*). The pure product (*S*)-79 was obtained as a pale yellow oil (3.6 g – 12 mmol, 72%). TLC (Cyclohexane / Ethyl Acetate 7:3; stained with Blue Shift): **R_f**= 0.50. $[\alpha]_D^{25} = +66.4$ (*c*1, Acetone); literature⁷³: $[\alpha]_D^{25} = +66.4$ (*c*1, Acetone). ¹H-NMR (300 MHz, CDCl₃): δ 4.55 – 4.45 (m, 1H), 4.17 – 4.02 (m, 2H), 3.56 – 3.41 (m, 2H), 2.29 – 2.12 (m, 1H), 2.05 – 1.87 (m, 3H), 1.44 (s, 4.5H), 1.41 (s, 4.5H).⁷³

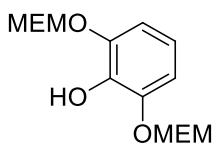
Synthesis of 1,3-bis[(2-methoxyethoxy)methoxy]benzene (**100**)



Molecular Weight: 286.32

Procedure adapted from literature.¹⁸⁵ Under a nitrogen atmosphere, at 0 °C, N,N-diisopropylamine (10.0 g – 80 mmol) was added to a solution of resorcinol (4.0 g – 36 mmol) in dichloromethane (20 ml). Upon stirring at 0 °C for 10 minutes, methoxyethoxymethylen chloride (10.0 g – 80 mmol) were added dropwise. The reaction mixture was warmed to room temperature and stirred overnight. Afterward, the mixture was diluted with dichloromethane and then sequentially washed with an aqueous solution of HCl 10% and an aqueous solution of NaOH 1M. The organic phase was dried over anhydrous sodium sulphate, filtrated and the solvent was evaporated in vacuo affording a crude that was purified through silica gel flash chromatography (cyclohexane/ethyl acetate 8:2). The pure product **100** was isolated as a pale yellow oil (4.7 g – 17 mmol, 46%). TLC (Cyclohexane / Ethyl Acetate 8:2; stained with Blue Shift): R_f= 0.26. ¹H-NMR (300 MHz, CDCl₃): 7.17 (t, *J*= 7.9 Hz, 1H), 6.75 – 6.70 (m, 3H), 5.24 (s, 4H), 3.83 – 3.80 (m, 4H), 3.57 – 3.54 (m, 4H), 3.39 – 3.36 (m, 6H).¹⁸⁶

Synthesis of 2,6-bis((2-methoxyethoxy)methoxy)phenol (**101**)

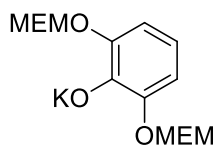


Molecular Weight: 302.32

Under a nitrogen atmosphere, at 0 °C, n-butyllithium 1.6 M in hexane (1.9 ml – 3.0 mmol) was carefully added dropwise to a solution of 1,3-bis[(2-methoxyethoxy)methoxy]benzene (**100**) (1.0 g – 3.6 mmol) in anhydrous THF (12 ml). Upon stirring for 1 hour at room temperature, the mixture was cooled to 0 °C and trimethyl borate (620 mg – 6 mmol) was added and the resulting solution was stirred for further 30 minutes. Then, the mixture was concentrated in vacuo and the residue was dissolved in a solution of NaHCO₃ (3.5 g) in aqueous acetone (water/acetone 8:2, 13 ml). Then, Oxone® (0.9 g – 6 mmol) was added and, upon stirring for 5 minutes, NaHSO₃ (0.5 g) was added. Afterward, the reaction mixture was extracted with ethyl acetate (2x20 ml). The organic phase was dried over anhydrous sodium sulphate, filtrated and evaporated in vacuo, affording a crude that was purified through silica gel flash chromatography

(cyclohexane/ethyl acetate 6:4). The pure product **101** was obtained as a pale yellow oil (0.7 g – 2.3 mmol, 65%). TLC (Cyclohexane / Ethyl Acetate 6:4): $R_f = 0.28$. $^1\text{H-NMR}$ (300 MHz, CDCl_3): δ 6.87 – 6.84 (m, 2H), 6.76 – 6.70 (m, 1H), 5.29 (s, 4H), 3.90 – 3.87 (m, 4H), 3.60 – 3.55 (m, 4H), 3.39 – 3.36 (m, 6H).

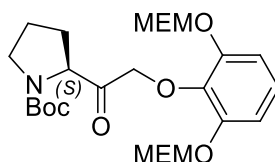
Synthesis of potassium 2,6-bis((2-methoxyethoxy)methoxy)phenolate (**102**)



Molecular Weight: 340.41

A solution of 2,6-bis((2-methoxyethoxy)methoxy)phenol (**101**) (2.80 g – 9 mmol) in methanol (20 ml) was vigorously stirred and cooled to 0 °C and a 1 M methanolic solution of KOH was added dropwise (8.3 ml – 8.3 mmol). After 15 minutes, the solvent is evaporated in vacuo providing the pure product as a viscous brown oil (3.0 g – 8.8 mmol, 98%). $^1\text{H-NMR}$ (300 MHz, CD_3OD): δ 6.74 – 6.71 (m, 2H), 6.71 – 6.34 (m, 1H), 5.19 (s, 4H), 3.87 – 3.83 (m, 4H), 3.58 – 3.55 (m, 4H), 3.36 – 3.29 (m, 6H).

Synthesis of (*S*)-*N*-*tert*-butoxycarbonyl-2-[2'-(2,6-bis((2-methoxyethoxy)methoxy)phenoxy)acetyl]pyrrolidine [(*S*)-**80**]

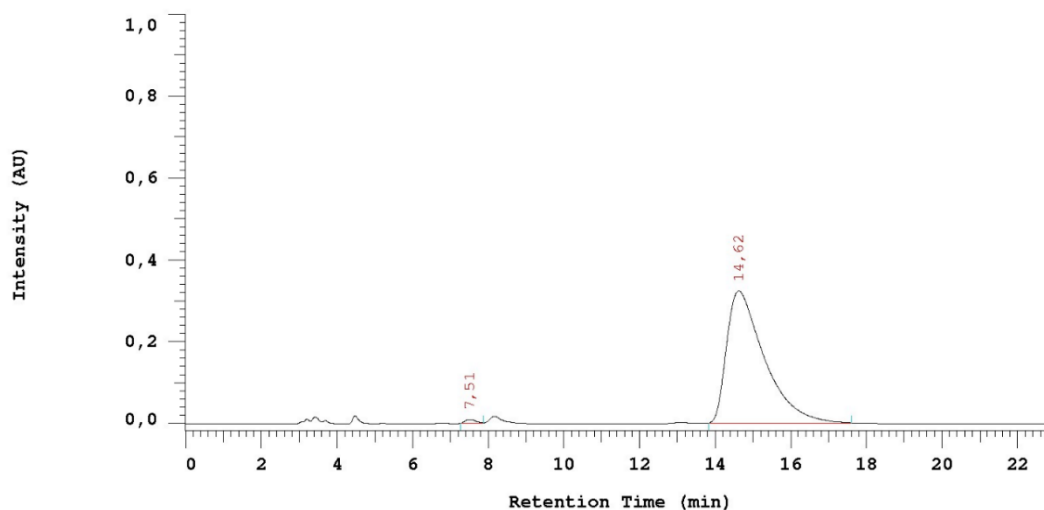


Molecular Weight: 513.58

Under a nitrogen atmosphere, at -10 °C, a solution of *N*-*tert*-butoxycarbonyl-(*S*)-2-bromoacetylpyrrolidine [(*S*)-**79**] (0.96 g – 3.3 mmol) in acetone (6 ml) was added to a solution of potassium 2,6-bis((2-methoxyethoxy)methoxy)phenolate (**102**) (0.86 g – 2.5 mmol) in acetone (5 ml). The resulting suspension was stirred overnight at room temperature. Afterward, the solvent was evaporated in vacuo and the resulting residue was diluted with ethyl acetate and washed with water. The organic phase was dried over anhydrous sodium sulphate, filtered and the solvent was evaporated in vacuo, affording a crude that was purified through silica gel flash chromatography (cyclohexane/ethyl acetate 7:3). The pure solid (*S*)-**80** was isolated as a pale yellow oil (1.0 g – 1.95 mmol, 77%). The enantiomeric excess was evaluated with chiral HPLC

analysis. TLC (Cyclohexane / Ethyl Acetate 6:4; stained with Blue Shift): **Rf**= 0.30. ¹H-NMR (300 MHz, CDCl₃): δ 6.99 – 6.90 (m, 1H), 6.89 – 6.83 (m, 2H), 5.27 (s, 4H), 4.71 – 4.66 (m, 2H), 3.84 – 3.81 (m, 5H), 3.56 – 3.53 (m, 6H), 3.36 (s, 6H), 2.38 – 1.98 (m, 4H), 1.42 (s, 9H).

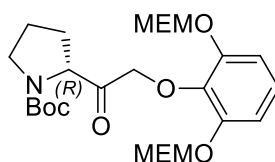
Chiral HPLC analysis: (*S*)-*N*-*tert*-butoxycarbonyl-2-[2'-(2,6-bis((2-methoxyethoxy)methoxy)phenoxy)acetyl]pyrrolidine



No.	RT	Area	Conc 1	BC
1	7, 51	80118	0, 713	MC
2	14, 62	11155987	99, 287	MC
		11236105	100, 000	

e.e. %= 98.6% (Column 5-Amycoat, n-hexane/ethanol 8:2, F= 1.0 ml/min, λ= 220 nm; R_T= 7.51 min, R_S= 14.62 min)

Synthesis of (*R*)-*N*-*tert*-butoxycarbonyl-2-[2'-(2,6-bis((2-methoxyethoxy)methoxy)phenoxy)acetyl]pyrrolidine [(*R*)-**80**]

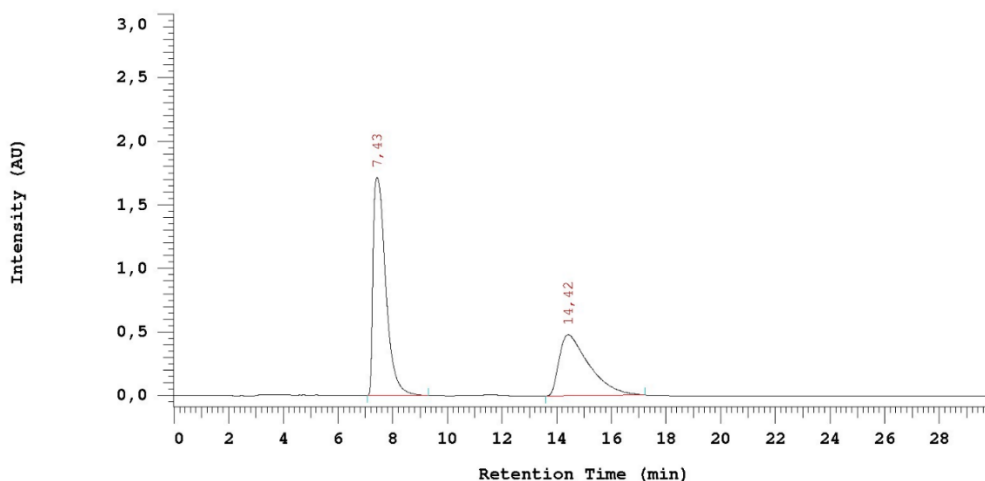


Molecular Weight: 513.58

Potassium 2,6-bis((2-methoxyethoxy)methoxy)phenolate **102** (98 mg – 0.3 mmol) and *N*-*tert*-butoxycarbonyl-(*R*)-2-bromoacetylpyrrolidine [(*R*)-**79**] (111 mg – 0.38 mmol) were used to synthesize compound (*R*)-**80**, according to the procedure reported for the correspondent enantiomer (*S*). The pure product (*R*)-**80** was obtained as a pale yellow oil (109 mg – 0.2 mmol,

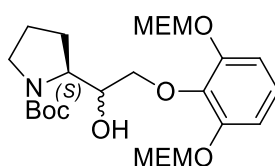
74%). ¹H-NMR (300 MHz, CDCl₃): δ 6.99 – 6.90 (m, 1H), 6.89 – 6.83 (m, 2H), 5.27 (s, 4H), 4.71 – 4.66 (m, 2H), 3.84 – 3.81 (m, 5H), 3.56 – 3.53 (m, 6H), 3.36 (s, 6H), 2.38 – 1.98 (m, 4H), 1.42 (s, 9H).

Chiral HPLC analysis: mixture of (*R*)- and (*S*)-*N*-*tert*-butoxycarbonyl-2-[2'-(2,6-bis((2-methoxyethoxy)methoxy)phenoxy)acetyl]pyrrolidine



No.	RT	Area	Conc 1	BC
1	7, 43	27665568	60, 289	MC
2	14, 42	18222916	39, 711	MC
		45888484	100, 000	

Synthesis of (*S,S*)/(*S,R*)-*N*-*tert*-butoxycarbonyl-2-[1'-hydroxy-2'-(2,6-bis((2-methoxyethoxy)methoxy)phenoxy)ethyl]pyrrolidine [(*S,S*)-81]/(*S,R*)-81]

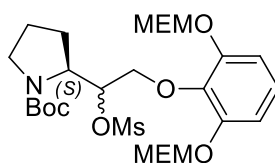


Molecular Weight: 515.59

Under a nitrogen atmosphere, at -10 °C, a solution of (*S*)-*N*-*tert*-butoxycarbonyl-2-[2'-(2,6-bis((2-methoxyethoxy)methoxy)phenoxy)acetyl]pyrrolidine [(*S*)-80] (2.5 g – 4.8 mmol) in 20 ml of anhydrous THF was added dropwise to a suspension of NaBH₄ (180 mg – 4.8 mmol) in 3 ml of anhydrous THF. Upon warming to room temperature, the reaction mixture was stirred for 3 hours. Afterward, the mixture was diluted with dichloromethane and washed with brine and then with water. The organic phase was dried over anhydrous sodium sulphate, filtered and the solvent was evaporated in vacuo. The resulting crude (2.4 g – 4.60 mmol, 97%) was a

diastereomeric mixture of (*S,S*)-**81** and (*S,R*)-**81**. The two diastereoisomers were separated at the last stage of the synthetic route and were further reacted as a diastereoisomeric mixture. TLC (Cyclohexane / Ethyl Acetate 6:4): **Rf**= 0.16. ¹H-NMR (300 MHz, CDCl₃): δ 6.95 – 6.85 (m, 3H), 5.29 (s, 4H), 4.27 – 4.23 (m, 1H), 4.12 (m, 1H), 3.92 (m, 2H), 3.86 – 3.82 (m, 4H), 3.78 – 3.72 (m, 2H), 3.57 – 3.54 (m, 4H), 3.36 (s, 6H), 2.00 – 1.9 (m, 2H), 1.87 – 1.79 (m, 2H), 1.42 (s, 9H).

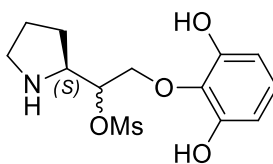
Synthesis of (*S,S*)/(*S,R*)-*N*-*tert*-butoxycarbonyl-2-[1'-mesyloxy-2'-(2,6-bis((2-methoxyethoxy)methoxy)phenoxy)ethyl]pyrrolidine [(*S,S*)-**82**/*(S,R)*-**82**]



Molecular Weight: 593.68

A solution of (*S,S*)/(*S,R*)-*N*-*tert*-butoxycarbonyl-2-[1'-hydroxy-2'-(2,6-bis((2-methoxyethoxy)methoxy)phenoxy)ethyl]pyrrolidine [(*S,S*)-**81**/*(S,R)*-**81**] (0.8 g – 1.5 mmol) in dichloromethane (8 ml) was cooled to -10 °C and triethylamine (0.26 ml – 180 mg – 1.80 mmol) was added. Upon stirring at that temperature for 10 minutes, methanesulphonylchloride (0.13 ml – 190 mg – 1.70 mmol) was added dropwise. The reaction mixture was warmed to room temperature and stirred for 1 hour. Afterward, the mixture was diluted with dichloromethane (30 ml) and washed with a 1M aqueous solution of HCl. The organic phase was dried over anhydrous sodium sulphate, filtered and the solvent was evaporated in vacuo, affording a crude that was purified through silica gel flash chromatography (cyclohexane/ethyl acetate 6:4). The diastereoisomeric mixture of (*S,S*)-**82** and (*S,R*)-**82** was isolated as pale yellow oil (460 mg – 0.80 mmol, 54%). TLC (Cyclohexane / Ethyl Acetate 6:4): **Rf**= 0.21. ¹H-NMR (300 MHz, CDCl₃): δ 6.99 – 6.89 (m, 1H), 6.86 – 6.82 (m, 2H), 5.27 (s, 4H), 4.21 – 4.11 (m, 1H), 4.12 – 3.97 (m, 3H), 3.86 – 3.82 (m, 4H), 3.59 – 3.51 (m, 6H), 3.37 (s, 6H), 3.22 (s, 1.5H), 3.18 (s, 1.5H), 2.10 – 1.9 (m, 2H), 1.83 – 1.79 (m, 2H), 1.42 (s, 9H).

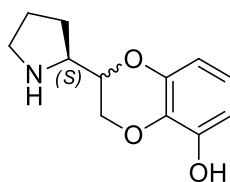
Synthesis of *(S,S)*/*(S,R)*-2-[1'-mesyloxy-2'-(2,6-dihydroxy)phenoxyethyl]pyrrolidine [*(S,S)*-83/*(S,R)*-83]



Molecular Weight: 317.36

Upon cooling to 0 °C, a 1.25 M solution of HCl in methanol (10 ml) were added to a solution of *(S,S)*/*(S,R)*-*N*-*tert*-butoxycarbonyl-2-[1'-mesyloxy-2'-(2,6-bis((2-methoxyethoxy)methoxy)phenoxy)ethyl]pyrrolidine [*(S,S)*-82/*(S,R)*-82] (1.0 g – 1.6 mmol) in methanol (10 ml). The reaction mixture was warmed to room temperature and stirred for 2 hours. Afterward, the solvent was evaporated in vacuo and the residue was diluted with a saturated aqueous solution of NaHCO₃ and extracted with ethyl acetate. The organic phase was dried over anhydrous sodium sulphate, filtered and the solvent was removed in vacuo, providing a crude diastereoisomeric mixture of *(S,S)*-83 and *(S,R)*-83 as a light yellow oil, which was directly used for the following reaction (507 mg – 1.6 mmol, 99%).

Synthesis of *(S,R)*/*(S,S)*-2-(2'-pyrrolidinyl)-5-hydroxy-1,4-benzodioxane [*(S,R)*-84/*(S,S)*-84]

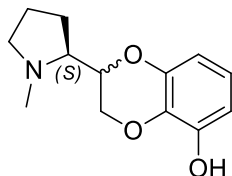


Molecular Weight: 221.25

Under nitrogen atmosphere, at 0 °C, a solution of *(S,S)*/*(S,R)*-2-[1'-mesyloxy-2'-(2,6-dihydroxy)phenoxyethyl]pyrrolidine [*(S,S)*-83/*(S,R)*-83] (730 mg – 2.3 mmol) in dimethoxyethane (15 ml) and dimethylformamide (10 ml) was added dropwise to a suspension of K₂CO₃ (625 mg – 4.5 mmol) in dimethoxyethane (15 ml). The reaction mixture was refluxed under vigorous stirring for 3 hours. Afterward, the solvent was concentrated in vacuo, the residue was diluted with diethyl ether and washed with brine. The organic phase was dried over anhydrous sodium sulphate, filtered and the solvent was evaporated in vacuo, affording a crude that was purified through silica gel flash chromatography (dichloromethane/methanol 97:3 + 1.5% NH₃(30% in water)). The pure diastereoisomeric mixture of *(S,R)*-84/*(S,S)*-84 was isolated as

a light yellow oil (133 mg – 0.6 mmol, 25%). **TLC** (Dichloromethane / Methanol 97:3 + 1.5% NH_3 (30% in water)): **Rf**= 0.20. **$^1\text{H-NMR}$** (300 MHz, CDCl_3): δ 6.57 (t, J = 8.2 Hz, 1H), 6.50 – 6.43 (m, 2H), 4.36 – 4.15 (m, 1H), 4.12 – 3.98 (m, 2H), 3.35 – 3.22 (m, 1H), 3.15 – 2.84 (m, 3H), 1.98 – 1.59 (m, 4H).

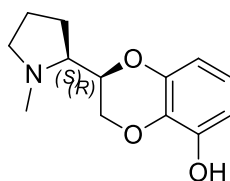
Synthesis of (*S,R*)/(*S,S*)-2-(*N*-methyl-2'-pyrrolidinyl)-5-hydroxy-1,4-benzodioxane [(*S,R*)-9a**/(*S,S*)-**9a**]**



Molecular Weight: 235.28

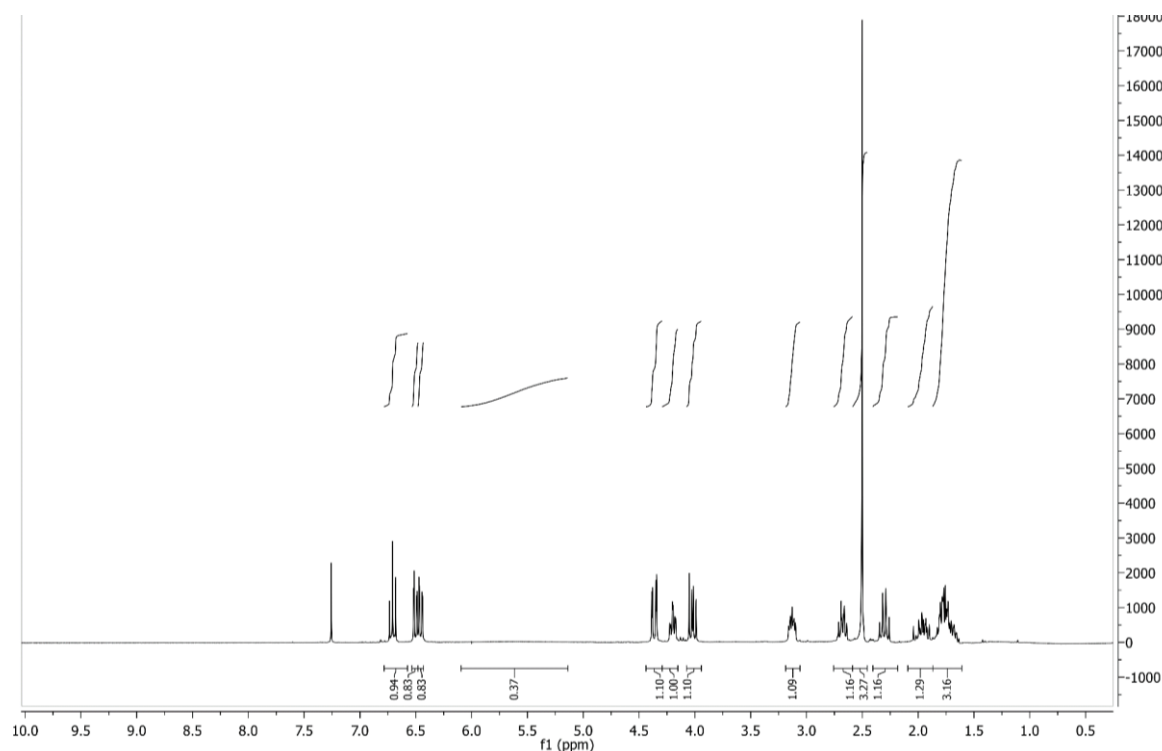
Under vigorous stirring at 0 °C, an aqueous solution of formaldehyde (37% in water, 0.20 ml – 69 mg – 2.3 mmol) was added dropwise to a solution of (*S,R*)/(*S,S*)-2-(2'-pyrrolidinyl)-5-hydroxy-1,4-benzodioxane [(*S,R*)-**84**/(*S,S*)-**84**] (51 mg – 0.23 mmol) in methanol (4 ml) and glacial acetic acid (0.02 ml) . Upon addition of 2-picolin borane (25 mg – 0.23 mmol), the mixture was warmed to room temperature and stirred for 3 hours. The solvent was evaporated in vacuo at 40 °C, the residue was diluted with 5 ml of a 1M HCl solution and stirred for 30 minutes to quench the unreacted 2-picolin-borane. Then, the aqueous solution was washed twice with diethyl ether. The aqueous phase was cooled to 0 °C, basified to pH 9 with NaHCO_3 and extracted with ethyl acetate. The organic phase was dried over anhydrous sodium sulphate, filtered and evaporated in vacuo, providing a diastereomeric mixture of (*S,R*)-**9a**/(*S,S*)-**9a** in a 44:56 ratio (43 mg – 0.18 mmol), that was further purified through silica gel flash column chromatography (dichloromethane/methanol 97:3 + 1.5% NH_3 (30% in water)). **TLC**= (Dichloromethane / Methanol 97:3 + 1.5% NH_3 (30% in water)): **Rf**₁= 0.37; **Rf**₂= 0.30.

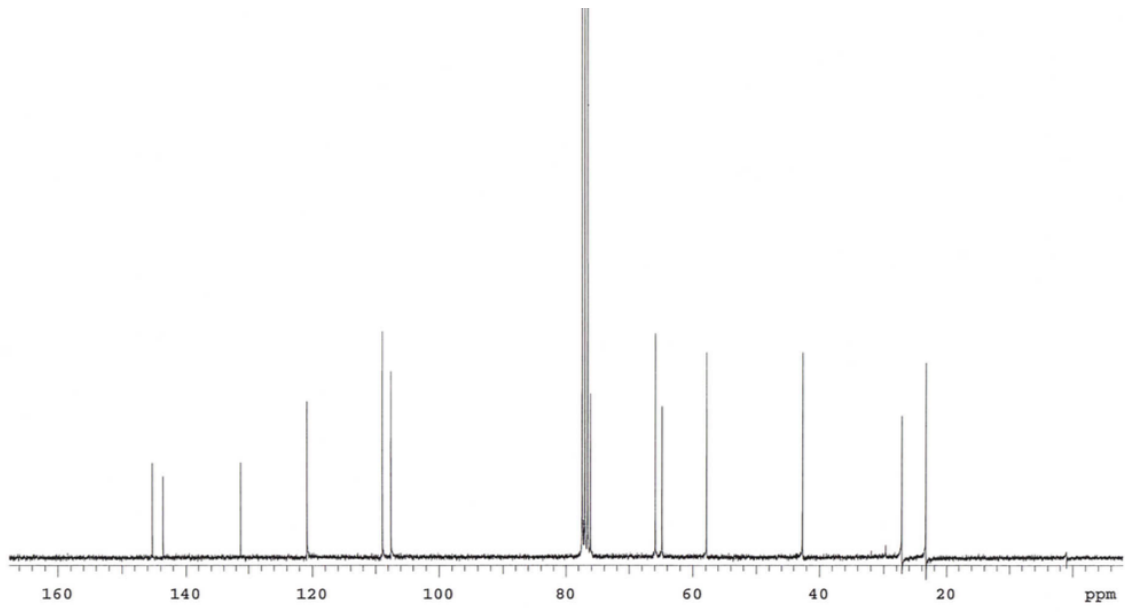
Synthesis of (*S,R*)-2-(*N*-methyl-2'-pyrrolidinyl)-5-hydroxy-1,4-benzodioxane [(*S,R*)-**9a**]



Molecular Weight: 235.28

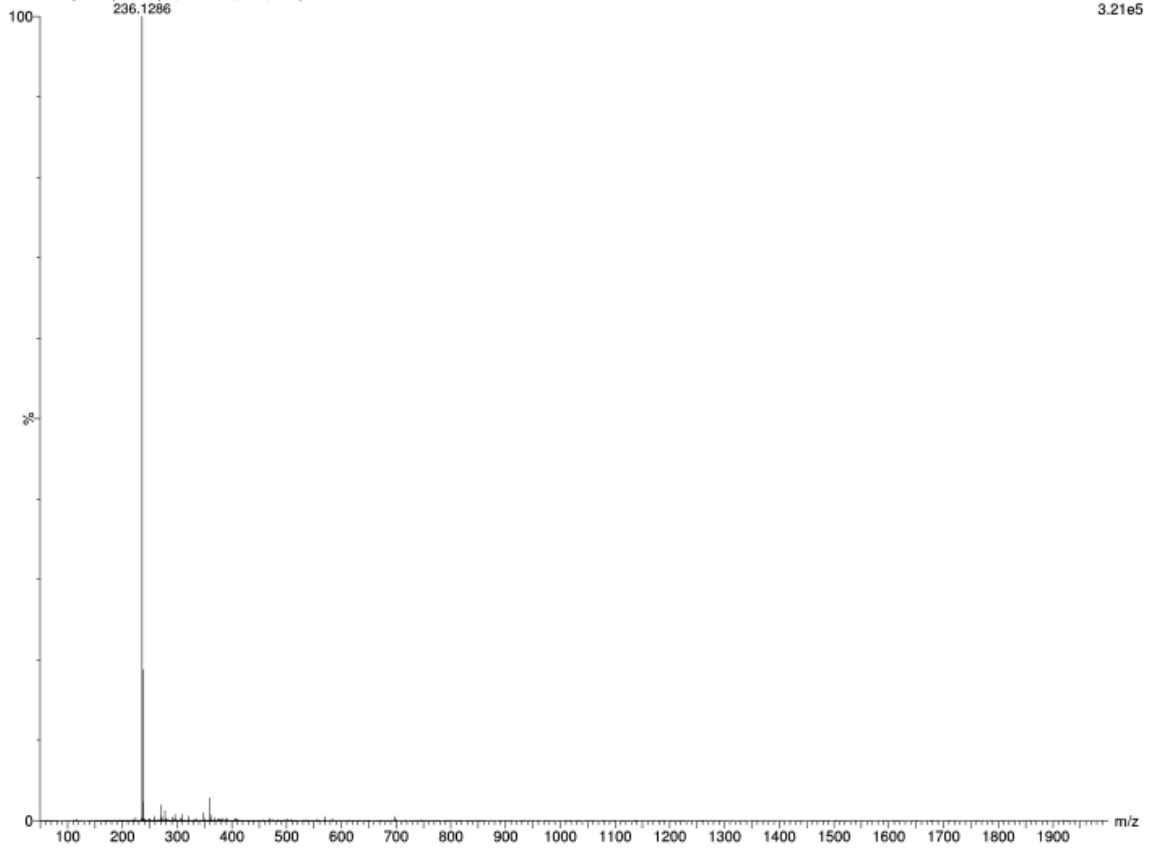
The pure (*S,R*) diastereoisomer (*S,R*)-**9a** was obtained as a white solid (15.4 mg – 0.065 mmol, 36%). **TLC**= (Dichloromethane / Methanol 97:3 + 1.5% NH₃(30% in water)): **R_{fSR}**= 0.30. **M.p.**= 105.2 °C. **[α]_D²⁵** = +5.97 (*c*1, MeOH). **¹H-NMR** (300 MHz, CDCl₃): δ 6.71 (t, *J*= 8.2 Hz, 1H), 6.50 (dd, *J*= 8.2, 1.4 Hz, 1H), 6.46 (dd, *J*= 8.2, 1.4 Hz, 1H), 5.56 (bs, 1H, exchange with D₂O), 4.36 (dd, *J*= 11.1, 2.1 Hz, 1H), 4.20 (td, *J*= 7.2, 2.1 Hz, 1H), 4.02 (dd, *J*= 11.1 Hz, 7.2 Hz, 1H), 3.12 (m, 1H), 2.67 (m, 1H), 2.50 (s, 3H), 2.30 (q, *J*= 8.7 Hz, 1H), 2.04 – 1.90 (m, 1H), 1.83 – 1.68 (m, 3H). **¹³C-NMR** (75 MHz, CDCl₃): δ 145.8, 143.9, 131.8, 121.3, 109.5, 107.9, 76.2, 66.1, 65.1, 57.9, 42.9, 27.1, 23.8. **HRMS (ESI⁺)**: calc. for C₁₃H₁₈NO₃: theor. 236.1287; found [M+H]⁺: 236.1286





MG61 41 (0.789) AM2 (Ar,40000.0,0.00,0.00)

1: TOF MS ES+
3.21e5



Single Mass Analysis

Tolerance = 5.0 PPM / DBE: min = -1.5, max = 200.0

Element prediction: Off

Number of isotope peaks used for i-FIT = 5

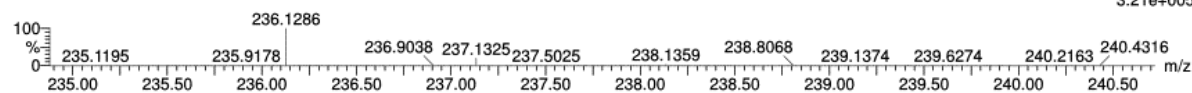
Monoisotopic Mass, Even Electron Ions

61 formula(e) evaluated with 1 results within limits (all results (up to 1000) for each mass)

Elements Used:

C: 13-13 H: 10-100 N: 0-5 O: 0-5 Na: 0-1

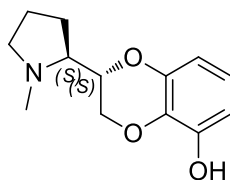
MG61 41 (0.789) AM2 (Ar,40000.0,0.00,0.00)

1: TOF MS ES+
3.21e+005

Minimum: -1.5
Maximum: 0.5 5.0 200.0

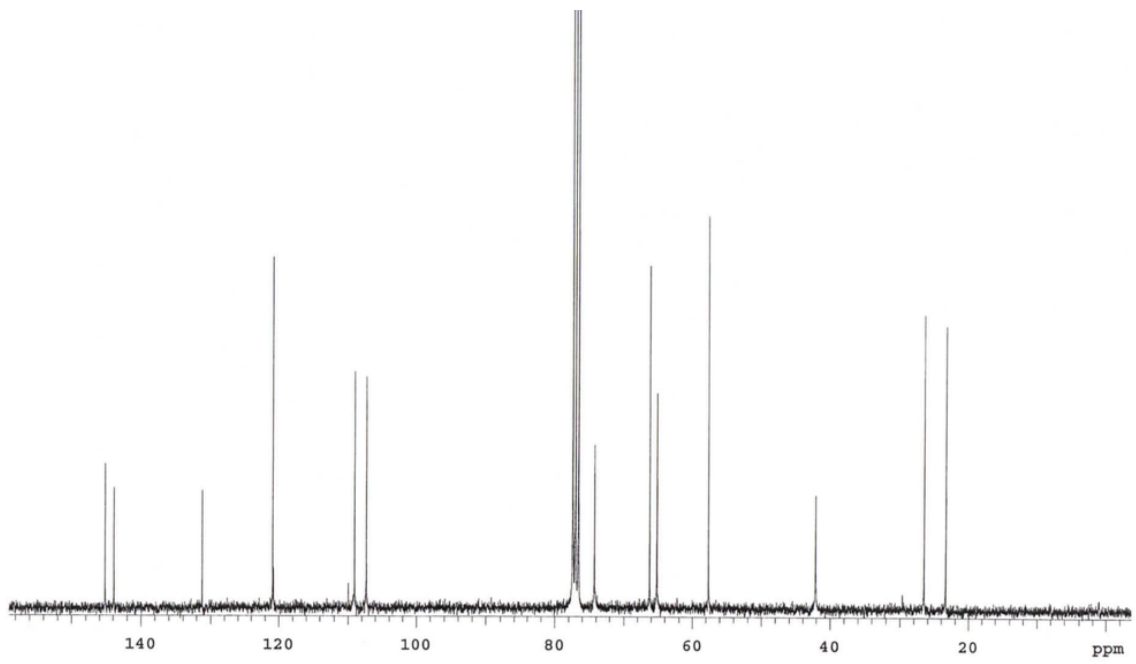
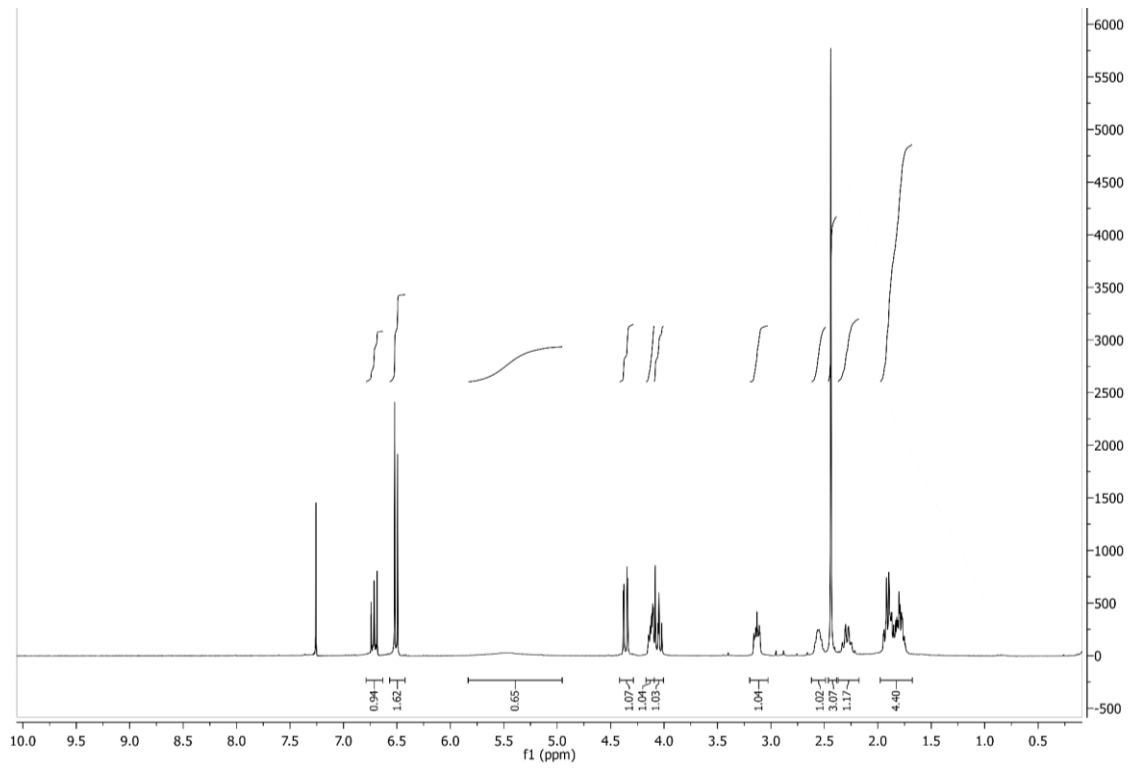
Mass	Calc. Mass	mDa	PPM	DBE	i-FIT	Norm	Conf(%)	Formula
236.1286	236.1287	-0.1	-0.4	5.5	1402.8	n/a	n/a	C13 H18 N O3

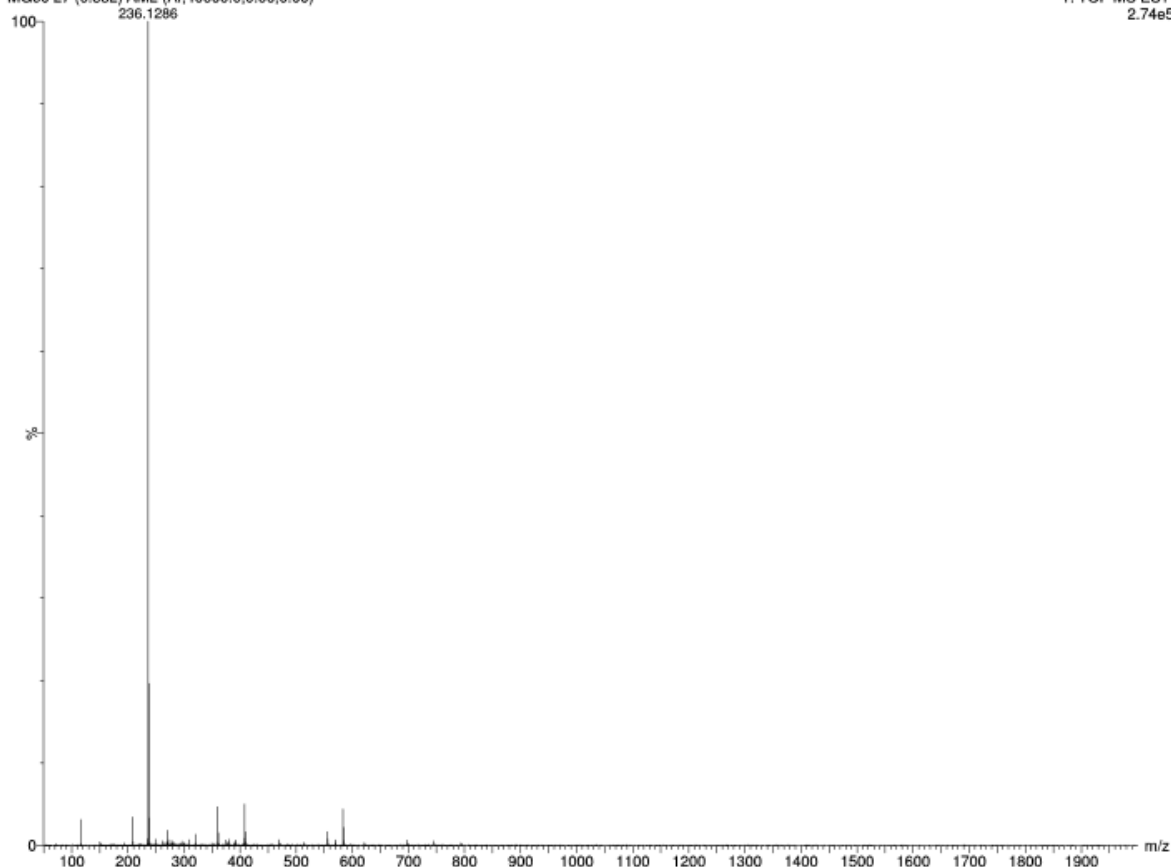
Synthesis of (*S,S*)-2-(*N*-methyl-2'-pyrrolidinyl)-5-hydroxy-1,4-benzodioxane [(*S,S*)-**9a**]



Molecular Weight: 235.28

The pure (*S,S*) diastereoismer (*S,S*)-**9a** was obtained as a white solid (19.6 mg – 0.08 mmol, 46%). **TLC**= (Dichloromethane / Methanol 97:3 + 1.5% NH₃(30% in water)): **R_f**= 0.37. **M.p.**= 130.3 °C. **[α]_D²⁵** = -57.15 (*c*₁, MeOH). **¹H-NMR** (300 MHz, CDCl₃): δ 6.71 (t, *J*= 8.3 Hz, 1H), 6.51 (d, *J*= 8.3, 2H), 5.50 (bs, 1H, exchange with D₂O), 4.36 (dd, *J*= 10.5, 1.4 Hz, 1H), 4.12 (m, 1H), 4.05 (dd, *J*= 10.5, 8.0, 1H), 3.13 (m, 1H), 2.56 (m, 1H), 2.44 (s, 3H), 2.37 – 2.18 (m, 1H), 1.95 – 1.75 (m, 4H). **¹³C-NMR** (75 MHz, CDCl₃): δ 145.5, 143.9, 131.4, 121.3, 109.1, 107.8, 74.1, 66.2, 64.6, 57.9, 42.8, 27.3, 23.7. **HRMS (ESI⁺)**: calc. for C₁₃H₁₈NO₃: theor. 236.1287; found [M+H]⁺: 236.1286.





Elemental Composition Report

Single Mass Analysis

Tolerance = 5.0 PPM / DBE: min = -1.5, max = 200.0
 Element prediction: Off
 Number of isotope peaks used for i-FIT = 5

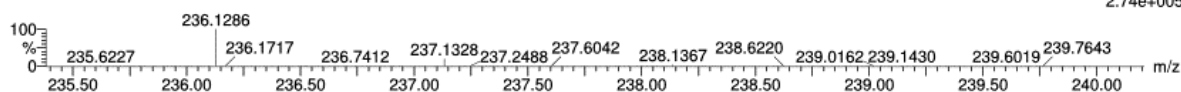
Monoisotopic Mass, Even Electron Ions

61 formula(e) evaluated with 1 results within limits (all results (up to 1000) for each mass)

Elements Used:

C: 13-13 H: 10-100 N: 0-5 O: 0-5 Na: 0-1

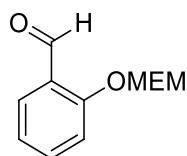
MG60 27 (0.532) AM2 (Ar,40000.0,0.00,0.00)



Minimum: -1.5
 Maximum: 0.5 5.0 200.0

Mass	Calc. Mass	mDa	PPM	DBE	i-FIT	Norm	Conf(%)	Formula
236.1286	236.1287	-0.1	-0.4	5.5	1280.9	n/a	n/a	C13 H18 N O3

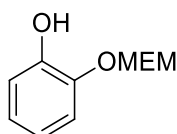
Synthesis of 2-((2-methoxyethoxy)methoxy)benzaldehyde (**103**)



Molecular Weight: 210.23

Procedure adapted from literature.¹⁸⁷ Under a nitrogen atmosphere, at 0 °C, *N,N*-diisopropylamine (9.97 ml – 7.40 g – 57.26 mmol) were added to a stirred solution of 2-hydroxybenzaldehyde (5 g – 40.9 mmol) in dichloromethane (100 ml). Upon stirring at 0 °C for 10 minutes, methoxyethoxymethylen chloride (5.60 ml – 6.11 g – 49.08 mmol) was added dropwise and the reaction mixture was warmed to room temperature and stirred overnight. Afterward, the reaction mixture was quenched with an aqueous saturated solution of NH_4Cl . Upon phase separation, the aqueous phase was extracted with dichloromethane (2x25 ml) and the organic phases were combined. The latter were subsequently washed with a saturated solution of NaHCO_3 (3x10 ml), a 1M aqueous solution of NaOH (2x10 ml) and brine (2x10 ml). The organic phase was dried over anhydrous sodium sulphate, filtered and the solvent was evaporated in vacuo, providing the pure product **103** as a light yellow oil (7.43 g – 35.85 mmol, 87%). **TLC** (Cyclohexane / Ethyl Acetate 7:3): **R_f**= 0.42. **¹H-NMR** (300 MHz, CDCl_3) δ 10.49 (s, 1H), 7.83 (dd, $J= 7.8$ Hz, $J= 1.8$ Hz, 1H), 7.53 (dt, $J= 8.0$ Hz, $J= 1.8$ Hz, 1H), 7.26 (m, 1H), 7.08 (dt, $J= 7.8$ Hz, $J= 0.8$ Hz, 1H), 5.40 (s, 2H), 3.87 (m, 2H), 3.56 (m, 2H), 3.37 (s, 3H).¹⁸⁸

Synthesis of 2-((2-methoxyethoxy)-methoxy)phenol (**104**)

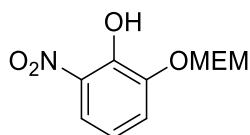


Molecular Weight: 198.22

Under a nitrogen atmosphere, *m*-chloro perbenzoic acid (8.49 g – 49.18 mmol) was added to a solution of 2-((2-methoxyethoxy)methoxy)benzaldehyde (**103**) (7.43 g – 35.38 mmol) in dichloromethane (30 ml). The resulting reaction mixture was stirred at room temperature for 48 hours. Afterward, the mixture was cooled to 0 °C, the suspension was filtered through Celite® and the white solid was removed. The filtrate was diluted with dichloromethane (20 ml) and washed with a saturated aqueous solution of $\text{Na}_2\text{S}_2\text{O}_3$ and then with brine. The organic phase was dried over anhydrous sodium sulphate, filtered and the solvent was evaporated in vacuo.

The resulting residue was suspended in a methanolic (31 ml) solution of KOH (3.10 g – 55.20 mmol) and the resulting reaction mixture was stirred for 5 hours at room temperature. Afterward, the mixture was concentrated in vacuo and the resulting residue was diluted with water (40 ml) and washed with diethyl ether (3x15 ml). Upon phase separation, the aqueous phase was acidified with formic acid until pH 5, extracted with ethyl acetate (3x15 ml) which was in turn washed with a saturated solution of NaHCO₃. The organic phase was dried over anhydrous sodium sulphate, filtrated and the solvent was evaporated in vacuo, providing the pure product **104** as a transparent light yellow oil (3.93 g – 19.86 mmol, 56%). TLC (Cyclohexane / Ethyl Acetate 7:3): R_f= 0.35. ¹H-NMR (300 MHz, CDCl₃): δ 7.05 (m, 1H), 6.94 (m, 2H), 6.81 (m, 1H), 6.35 (bs, 1H), 5.26 (s, 2H), 3.88 (m, 2H), 3.60 (m, 2H), 3.41 (s, 3H).

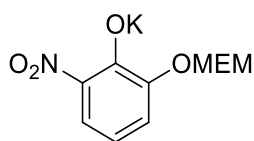
Synthesis of 2-((2-methoxyethoxy)-methoxy)-6-nitrophenol (**105**)



Molecular Weight: 243.21

A solution of 2-((2-methoxyethoxy)-methoxy)phenol (**104**) (3.93 g – 19.86 mmol) in acetonitrile (30 ml) was cooled to 10 °C and a solution of (NH₄)₂Ce(NO₃)₆ in acetonitrile (40 ml) was added dropwise. The reaction mixture was stirred at the same temperature for 3 hours. Afterward, the mixture was diluted with water and extracted with ethyl acetate. The organic phase was dried over anhydrous sodium sulphate, filtered and the solvent was evaporated in vacuo, affording a crude that was purified through silica gel flash chromatography (cyclohexane/ethyl acetate 8:2). The pure compound **105** was obtained as a bright yellow oil (1.92 g – 7.89 mmol, 40%). TLC (Cyclohexane / Ethyl Acetate 7:3): R_f= 0.33. ¹H-NMR (300 MHz, CDCl₃): δ 10.73 (bs, 1H), 7.78 (dd, *J*= 8.5 Hz, *J*= 1.5 Hz, 1H), 7.48 (dd, *J*= 8.5 Hz, *J*= 1.5 Hz, 1H), 6.90 (t, *J*= 8.5 Hz, 1H), 5.36 (s, 2H), 3.90 (m, 2H), 3.57 (m, 2H), 3.36 (s, 3H).

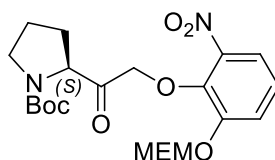
Synthesis of potassium 2-((2-methoxyethoxy)-methoxy)-6-nitrophenolate (106)



Molecular Weight: 281.30

A solution of 2-((2-methoxyethoxy)-methoxy)-6-nitrophenol (**105**) (1.92 g – 7.90 mmol) in methanol (20 ml) was vigorously stirred and cooled to 0 °C and a 1 M methanolic solution of KOH was added dropwise (7.10 ml – 7.10 mmol), forming an orange solution. After 15 minutes, the solvent is evaporated in vacuo providing the pure product as an orange solid (2.22 g – 7.90 mmol, 100%). **M.p.**= 197.6 °C. **¹H-NMR** (300 MHz, MeOD): δ 7.49 (dd, *J*= 7.0 Hz, *J*= 0.9 Hz, 1H), 7.00 (dd, *J*= 7.0 Hz, *J*= 0.9 Hz, 1H), 6.15 (t, *J*= 7.0 Hz, 1H), 5.20 (s, 2H), 3.83 (m, 2H), 3.56 (m, 2H), 3.29 (s, 3H).

Synthesis of (*S*)-*N*-*tert*-butoxycarbonyl-2-[2'-(2-(2-methoxyethoxymethoxy)-6-nitrophenoxy)acetyl]pyrrolidine [(*S*)-85]

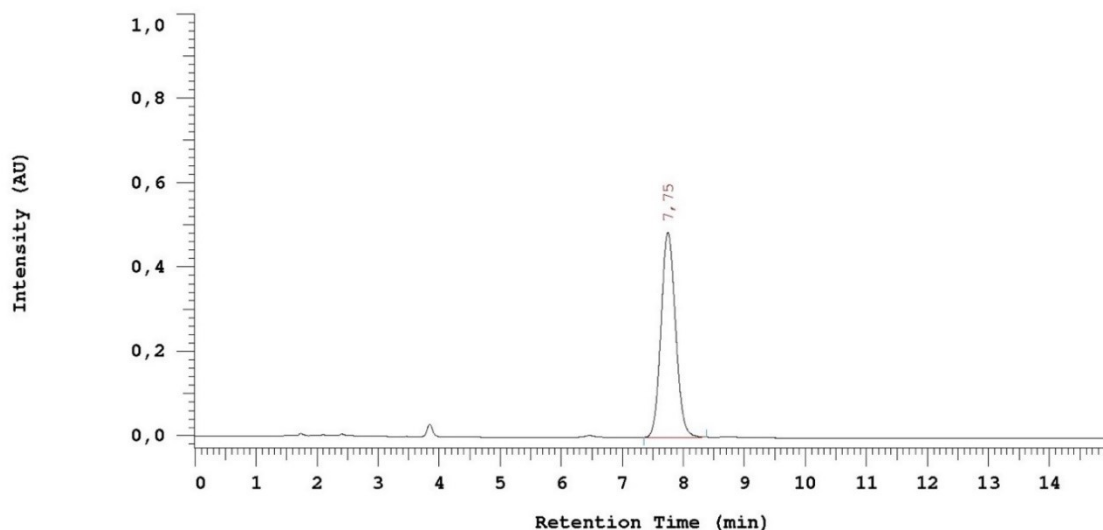


Molecular Weight: 454.47

Under a nitrogen atmosphere, at -10 °C, a solution of *N*-*tert*-butoxycarbonyl-(*S*)-2-bromoacetylpyrrolidine [(*S*)-79] (2.77 g – 9.50 mmol) in acetone (15 ml) was added to a solution of potassium 2-((2-methoxyethoxy)-methoxy)-6-nitrophenolate (**106**) (2.22 g – 7.90 mmol) in acetone (20 ml). The resulting suspension was stirred overnight at room temperature. Afterward, the solvent was evaporated in vacuo and the resulting residue was diluted with ethyl acetate and washed with water. The organic phase was dried over anhydrous sodium sulphate, filtered and the solvent was evaporated in vacuo, affording a crude that was purified through silica gel flash chromatography (cyclohexane/ethyl acetate 7:3). The pure product (*S*)-85 was isolated as a pale yellow oil (1.49 g – 3.28 mmol, 42%). The enantiomeric excess was evaluated with chiral HPLC analysis. **TLC** (Cyclohexane / Ethyl Acetate 1:1): **R_f**= 0.45. **[α]_D²⁵** = -12.30 (*c*1, MeOH). **¹H-NMR** (300 MHz, CDCl₃): δ 7.46 – 7.39 (m, 2H), 7.20 – 7.13 (m, 1H), 5.35 (s, 0.9H), 5.32 (s, 1.1H), 4.91 (s, 1.1H), 4.86 (s, 0.9H), 4.71 (m, 0.45H), 4.61 (m, 0.55H), 3.84 (m,

2H), 3.51 (m, 4H), 3.36 (s, 3H), 2.26 – 2.14 (m, 1H), 2.08 – 2.02 (m, 1H), 1.94 – 1.85 (m, 2H), 1.45 (s, 4.95H), 1.42 (s, 4.05H).

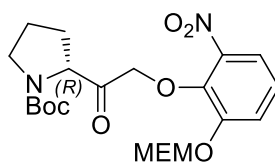
Chiral HPLC analysis: (*S*)-*N*-*tert*-butoxycarbonyl-2-[2'-(2-(2-methoxyethoxymethoxy)-6-nitrophenoxy)acetyl]pyrrolidine



No.	RT	Area	Conc 1	BC
1	7, 75	3977914	100, 000	MC
		3977914	100, 000	

e.e. %= 100% (Column Lux 3 μ Cellulose-2, n-hexane/ethanol 8:2, F= 1.0 ml/min, λ =276 nm (R_S= 7.75 min, R_T= 8.45 min)

Synthesis of (*R*)-*N*-*tert*-butoxycarbonyl-2-[2'-(2-(2-methoxyethoxymethoxy)-6-nitrophenoxy)acetyl]pyrrolidine [(*R*)-85]

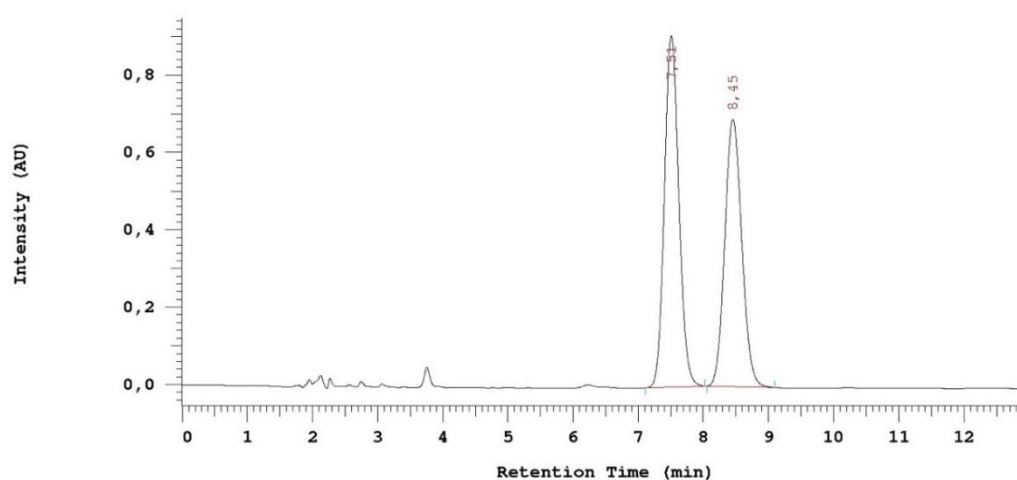


Molecular Weight: 454.47

(*R*)-*N*-*tert*-butoxycarbonyl-2-bromoacetylpyrrolidine [(*R*)-79] (220 mg – 0.75 mmol) and potassium 2-(2-methoxyethoxymethoxy)-6-nitrophenolate (**106**) (236 mg – 0.84 mmol) were coupled to synthesize compound (*R*)-85, according to the procedure reported for the correspondent enantiomer (*S*). The pure product (*R*)-85 was obtained as a pale yellow oil (90

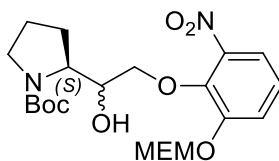
mg – 0.22 mmol, 30%). A mixture of (*S*)- and (*R*)- (*S*)-*N*-*tert*-butoxycarbonyl-2-[2'-(2-(2-methoxyethoxymethoxy)-6-nitrophenoxy)acetyl]pyrrolidine was analyzed by chiral HPLC to measure the retention times of the two enantiomers. **TLC** (Cyclohexane / Ethyl Acetate 1:1): **R_f**= 0.45. **[α]_D²⁵** = +11.92 (*c*1, MeOH). **¹H-NMR** (300 MHz, CDCl₃): δ 7.46 – 7.39 (m, 2H), 7.20 – 7.13 (m, 1H), 5.35 (s, 0.9H), 5.32 (s, 1.1H), 4.91 (s, 1.1H), 4.86 (s, 0.9H), 4.71 (m, 0.45H), 4.61 (m, 0.55H), 3.84 (m, 2H), 3.51 (m, 4H), 3.36 (s, 3H), 2.26 – 2.14 (m, 1H), 2.08 – 2.02 (m, 1H), 1.94 – 1.85 (m, 2H), 1.45 (s, 4.95H), 1.42 (s, 4.05H).

Chiral HPLC analysis: mixture of (*R*)- and (*S*)-*N*-*tert*-butoxycarbonyl-2-[2'-(2-(2-methoxyethoxymethoxy)-6-nitrophenoxy)acetyl]pyrrolidine



No.	RT	Area	Conc 1	BC
1	7,51	7041356	53,030	MC
2	8,45	6236730	46,970	MC
		13278086	100,000	

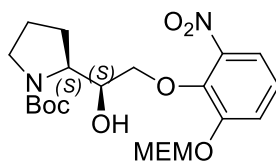
Synthesis of (*S,S*)/(*S,R*)-*N*-*tert*-butoxycarbonyl-2-[1'-hydroxy-2'-(2-(2-methoxyethoxymethoxy)-6-nitrophenoxy)ethyl]pyrrolidine [(*S,S*)-86**]/(*S,R*)-**86**]**



Molecular Weight: 456.49

Under a nitrogen atmosphere, at $-10\text{ }^{\circ}\text{C}$, a solution of (*S*)-*N*-*tert*-butoxycarbonyl-2-[2'-(2-(2-methoxyethoxymethoxy)-6-nitrophenoxy)acetyl]pyrrolidine [(*S*)-**85**] (1.19 g – 2.62 mmol) in 10 ml of anhydrous THF was added dropwise to a suspension of NaBH_4 (104.1 mg – 2.75 mmol) in 2 ml of anhydrous THF. Upon warming to room temperature, the reaction mixture was stirred for 3 hours. Afterward, the mixture was diluted with dichloromethane and washed with brine and then with water. The organic phase was dried over anhydrous sodium sulphate, filtered and the solvent was evaporated in vacuo. The resulting crude (958.6 mg – 2.10 mmol, 80%) was a diastereomeric mixture of (*S,S*)-**86**/*S,R*-**86**, in a 70:30 ratio. The diastereoisomers were separated through silica gel flash chromatography (cyclohexane/ethyl acetate 1:1). TLC (Cyclohexane / Ethyl Acetate 3:7): $R_{fSS} = 0.62$; $R_{fSR} = 0.57$.

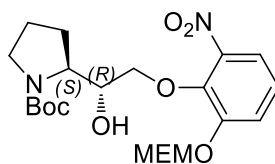
Synthesis of (*S,S*)-*N*-*tert*-butoxycarbonyl-2-[1'-hydroxy-2'-(2-(2-methoxyethoxymethoxy)-6-nitrophenoxy)ethyl]pyrrolidine [(*S,S*)-86**]**



Molecular Weight: 456.49

The pure (*S,S*) diastereoisomer (*S,S*)-**86** was obtained as a viscous yellow-ochre oil (680 mg – 1.49 mmol, 72%). $[\alpha]_{\text{D}}^{25} = -63.90$ (c_1 , MeOH). $^1\text{H-NMR}$ (300 MHz, CDCl_3): δ 7.43 – 7.36 (m, 2H), 7.10 (m, 1H), 5.34 (s, 2H), 4.33 (m, 1H), 4.15 – 4.08 (m, 2H), 3.88 – 3.85 (m, 3H), 3.57 – 3.54 (m, 2H), 3.54 – 3.40 (m, 1H), 3.37 (s, 3H), 3.37 – 3.30 (m, 1H), 2.00-1.89 (m, 3H), 1.83 – 1.79 (m, 1H), 1.45 (s, 9H).

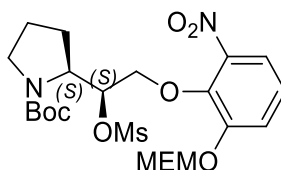
Synthesis of (*S,R*)-*N*-*tert*-butoxycarbonyl-2-[1'-hydroxy-2'-(2-(2-methoxyethoxymethoxy)-6-nitrophenoxy)ethyl]pyrrolidine [(*S,R*)-**86**]



Molecular Weight: 456.49

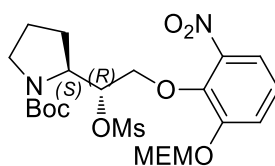
The pure (*S,R*) diastereoisomer (*S,R*)-**86** was obtained as a viscous yellow-ochre viscous oil (270 mg – 0.59 mmol, 28%). $[\alpha]_{\text{D}}^{25} = -19.65$ (*c*1, MeOH). $^1\text{H-NMR}$ (300 MHz, CDCl_3): δ 7.45 – 7.36 (m, 2H), 7.11 (t, $J = 8.0$ Hz, 1H), 5.34 (s, 2H), 4.34 (m, 1H), 4.12 – 4.02 (m, 2H), 3.87 – 3.84 (m, 3H), 3.57 – 3.54 (m, 3H), 3.44 (m, 1H), 3.37 (s, 3H), 2.10 (m, 1H), 1.97 – 1.79 (m, 3H), 1.45 (s, 9H).

Synthesis of (*S,S*)-*N*-*tert*-butoxycarbonyl-2-[1'-mesyloxy-2'-(2-(2-methoxyethoxymethoxy)-6-nitrophenoxy)ethyl]pyrrolidine [(*S,S*)-**87**]



A solution of (*S,S*)-*N*-*tert*-butoxycarbonyl-2-[1'-hydroxy-2'-(2-(2-methoxyethoxymethoxy)-6-nitrophenoxy)ethyl]pyrrolidine [(*S,S*)-**86**] (660 mg – 1.45 mmol) in dichloromethane (10 ml) was cooled to -10 °C and triethylamine (0.40 ml – 293 mg – 2.90 mmol) was added. Upon stirring at that temperature for 10 minutes, methanesulphonylchloride (0.22 ml – 332 mg – 2.90 mmol) were added dropwise. The reaction mixture was warmed to room temperature and stirred for 1 hour. Afterward, the mixture was diluted with dichloromethane (30 ml) and washed with a 1M aqueous solution of HCl. The organic phase was dried over anhydrous sodium sulphate, filtered and the solvent was evaporated in vacuo, affording a yellowish waxy crude that was purified through silica gel flash chromatography (cyclohexane/ethyl acetate 6:4). The pure product (*S,S*)-**87** was isolated as a white sticky solid (445 mg – 0.83 mmol, 58%). TLC (Toluene / Ethyl Acetate 1:1): $\text{Rf} = 0.62$. $[\alpha]_{\text{D}}^{25} = -31.77$ (*c*1, MeOH). $^1\text{H-NMR}$ (300 MHz, CDCl_3) δ 7.41 (m, 2H), 7.15 (m, 1H), 5.35 (s, 2H), 5.20 (m, 1H), 4.39 (m, 1H), 4.26 (m, 2H), 3.87 – 3.84 (m, 2H), 3.57 – 3.54 (m, 4H), 3.36 (s, 3H), 3.10 (s, 3H), 2.06 (m, 3H), 1.84 (m, 1H), 1.45 (s, 9H).

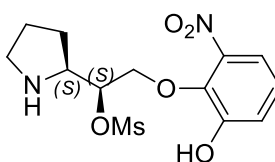
Synthesis of (*S,R*)-*N*-*tert*-butoxycarbonyl-2-[1'-mesyloxy-2'-(2-(2-methoxyethoxymethoxy)-6-nitrophenoxy)ethyl]pyrrolidine [(*S,R*)-**87**]



Molecular Weight: 534.58

A solution of (*S,R*)-*N*-*tert*-butoxycarbonyl-2-[1'-hydroxy-2'-(2-(2-methoxyethoxymethoxy)-6-nitrophenoxy)ethyl]pyrrolidine [(*S,R*)-**86**] (270 mg – 0.59 mmol) in dichloromethane (7 ml) was cooled to -10 °C and triethylamine (0.12 ml – 89.5 mg – 0.88 mmol) was added. Upon stirring at that temperature for 10 minutes, methanesulphonylchloride (0.07 ml – 101 mg – 0.88 mmol) were added dropwise. The reaction mixture was warmed to room temperature and stirred for 1 hour. Afterward, the mixture was diluted with dichloromethane (30 ml) and washed with a 1M aqueous solution of HCl. The organic phase was dried over anhydrous sodium sulphate, filtered and the solvent was evaporated in vacuo, affording a yellowish waxy crude that was purified through silica gel flash chromatography (cyclohexane/ethyl acetate 6:4). The pure product (*S,R*)-**87** was isolated as a yellow-ochre viscous oil (208 mg – 0.39 mmol, 66%). TLC (Toluene / Ethyl Acetate 7:3): $R_f = 0.45$. $[\alpha]_D^{25} = -20.81$ (c_1 , MeOH). $^1\text{H-NMR}$ (300 MHz, CDCl_3): δ 7.47 – 7.38 (m, 2H), 7.19 – 7.12 (m, 1H), 5.55 (m, 1H), 5.39 (s, 2H), 4.40 (m, 1H), 4.27 (m, 1H), 4.08 (m, 1H), 3.90 (m, 2H), 3.56 (m, 4H), 3.37 (s, 3H), 3.04 (s, 3H), 2.17 – 2.00 (m, 3H), 1.84 (m, 1H), 1.58 (s, 2.43H), 1.47 (6.57H).

Synthesis of (*S,S*)-2-[1'-mesyloxy-2'-(2-hydroxy-6-nitrophenoxy)ethyl]pyrrolidine [(*S,S*)-**88**]

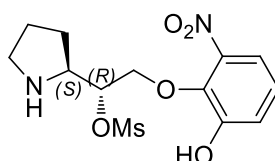


Molecular Weight: 346.36

Upon cooling to 0 °C, a 4 M solution of HCl in dioxane (4.15 ml) was added to a solution of (*S,S*)-*N*-*tert*-butoxycarbonyl-2-[1'-mesyloxy-2'-(2-(2-methoxyethoxymethoxy)-6-nitrophenoxy)ethyl]pyrrolidine (*S,S*)-**87** (445 mg – 0.83 mmol) in methanol (3 ml). The reaction mixture was warmed to room temperature and stirred for 2 hours. Afterward, the solvent was

evaporated in vacuo and the residue was diluted with a saturated aqueous solution of NaHCO_3 and extracted with ethyl acetate. The organic phase was dried over anhydrous sodium sulphate, filtered and the solvent was removed in vacuo, providing a crude product as a light yellow oil, which was directly used for the following reaction (330 mg – 0.95 mmol). TLC (Dichloromethane / Methanol 95:5 + 1% NH_3 (30% in water)): $R_f = 0.17$

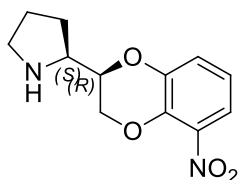
Synthesis of (*S,R*)-2-[1'-mesyloxy-2'-(2-hydroxy-6-nitrophenoxy)ethyl]pyrrolidine [(*S,R*)-88]



Molecular Weight: 346.36

Upon cooling to 0 °C, a 4 M solution of HCl in dioxane (1.0 ml) was added to a solution of (*S,R*)-*N*-*tert*-butoxycarbonyl-2-[1'-mesyloxy-2'-(2-(2-methoxyethoxymethoxy)-6-nitrophenoxy)ethyl]pyrrolidine [(*S,R*)-87] (208 mg – 0.39 mmol) in methanol (3 ml). The reaction mixture was warmed to room temperature and stirred for 2 hours. Afterward, the solvent was evaporated in vacuo and the residue was diluted with a saturated aqueous solution of NaHCO_3 and extracted with ethyl acetate. The organic phase was dried over anhydrous sodium sulphate, filtered and the solvent was removed in vacuo, providing a crude product as a viscous green oil, which was directly used for the following reaction (175 mg – 0.50 mmol). TLC (Dichloromethane / Methanol 95:5 + 1% NH_3 (30% in water)): $R_f = 0.15$.

Synthesis of (*S,R*)-2-(2'-pyrrolidinyl)-5-nitro-1,4-benzodioxane [(*S,R*)-89]

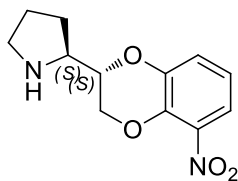


Molecular Weight: 250.25

Under nitrogen atmosphere, at 0 °C, a solution of (*S,S*)-2-[1'-mesyloxy-2'-(2-hydroxy-6-nitrophenoxy)ethyl]pyrrolidine [(*S,S*)-88] (330 mg – 0.95 mmol) in dimethoxyethane (5 ml) was added dropwise to a suspension of K_2CO_3 (236.36 – 1.90 mmol) in dimethoxyethane (3 ml). The reaction mixture was refluxed under vigorous stirring for 5 hours. Afterward, the solvent was concentrated in vacuo, the residue was diluted with dichloromethane and washed

with water and then brine. The organic phase was dried over anhydrous sodium sulphate, filtered and the solvent was evaporated in vacuo, affording a crude that was purified through silica gel flash chromatography (ethyl acetate+ 5% TEA). The pure product (*S,R*)-**89** was isolated as a dark yellow oil (207 mg – 0.83 mmol, 87%). **TLC** (Ethyl Acetate + 5% TEA): **Rf**= 0.40. $[\alpha]_{\text{D}}^{25} = -100.49$ (*c*1, MeOH). **¹H-NMR** (300 MHz, CDCl₃): δ 7.47 (dd, *J*= 8.2 Hz, *J*= 1.6 Hz, 1H), 7.11 (dd, *J*= 8.2 Hz, *J*= 1.6 Hz, 1H), 6.89 (t, *J*= 8.2 Hz, 1H), 4.54 – 4.50 (m, 1H), 4.20 – 4.04 (m, 2H), 3.35 (m, 1H), 2.53 (m, 2H), 2.04 – 1.78 (m, 4H).

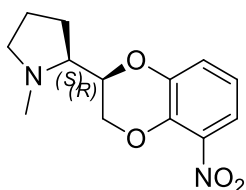
Synthesis of (*S,S*)-2-(2'-pyrrolidinyl)-5-nitro-1,4-benzodioxane [(*S,S*)-**89**]



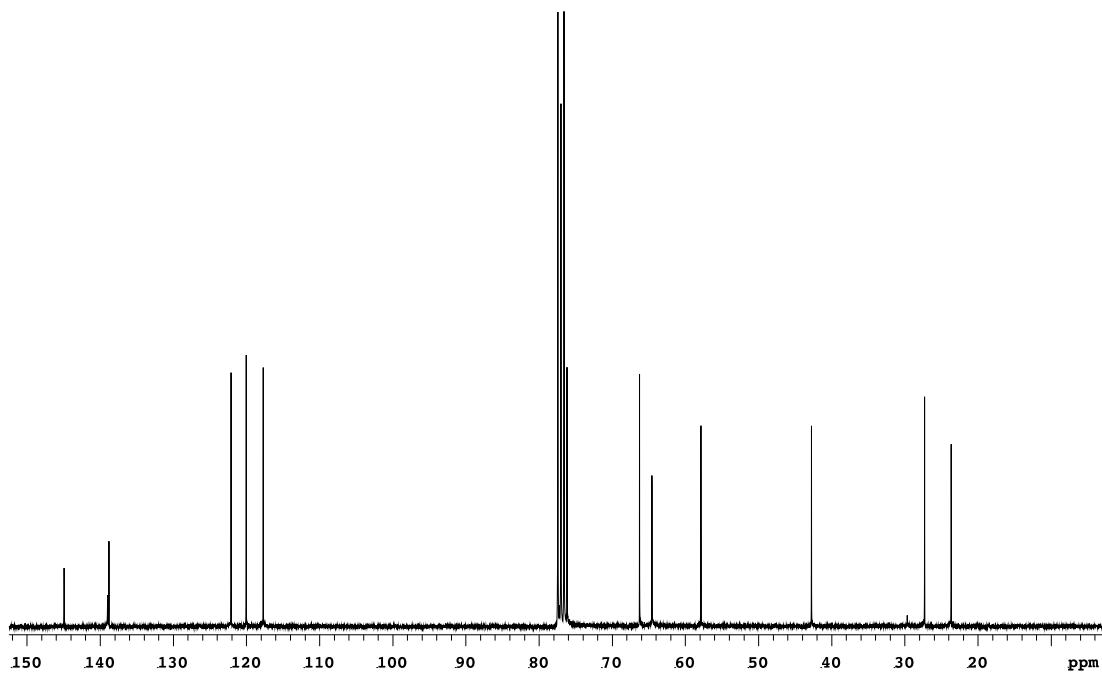
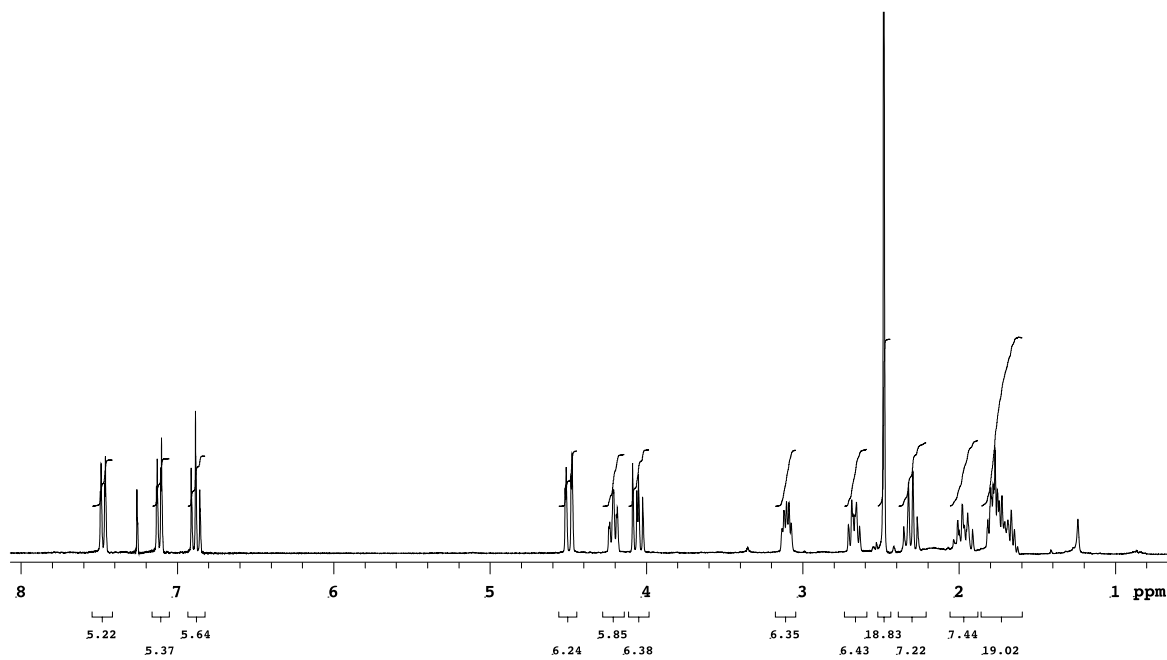
Molecular Weight: 250.25

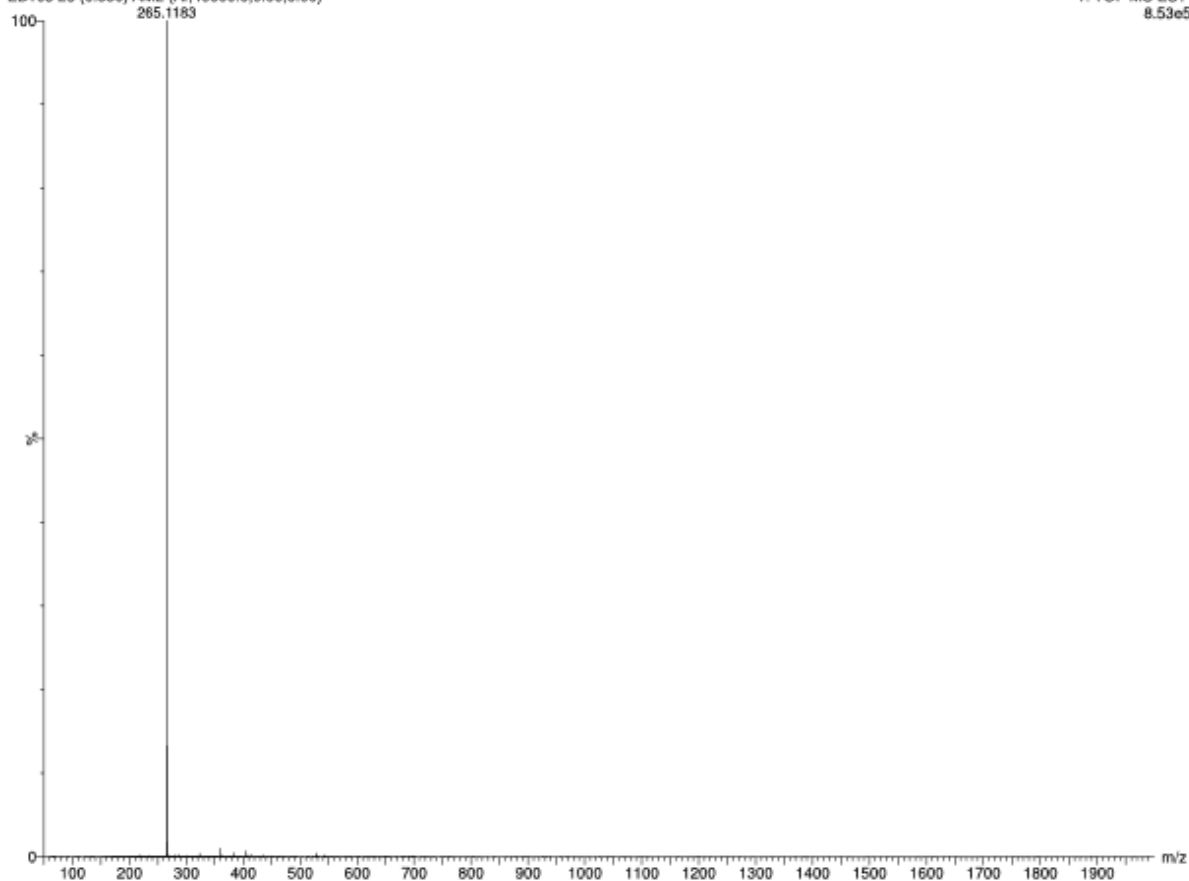
Under nitrogen atmosphere, at 0 °C, a solution of (*S,R*)-2-[1'-mesyloxy-2'-(2-hydroxy-6-nitrophenoxy)ethyl]pyrrolidine [(*S,R*)-**88**] (174 mg – 0.50 mmol) in dimethoxyethane (5 ml) was added dropwise to a suspension of K₂CO₃ (138.21 mg – 1.0 mmol) in dimethoxyethane (2 ml). The reaction mixture was refluxed under vigorous stirring for 5 hours. Afterward, the solvent was concentrated in vacuo, the residue was diluted with dichloromethane and washed with water and then brine. The organic phase was dried over anhydrous sodium sulphate, filtered and the solvent was evaporated in vacuo, affording a crude that was purified through silica gel flash chromatography (ethyl acetate+ 5% TEA). The pure product (*S,S*)-**89** was isolated as a yellow oil (100 mg – 0.40 mmol, 80%). **TLC** (Ethyl Acetate + 5% TEA): **Rf**= 0.42. $[\alpha]_{\text{D}}^{25} = -14.74$ (*c*1, MeOH). **¹H-NMR** (300 MHz, CDCl₃): δ 7.47 (dd, *J*= 8.2 Hz, *J*= 1.8 Hz, 1H), 7.10 (dd, *J*= 8.2 Hz, *J*= 1.8 Hz, 1H), 6.88 (t, *J*= 8.2 Hz, 1H), 4.52 (dd, *J*= 11.7 Hz, *J*= 2.3 Hz, 1H), 4.16 (dd, *J*= 11.7 Hz, *J*= 7.6 Hz, 1H), 4.02 (dt, *J*= 7.6 Hz, *J*= 2.3 Hz, 1H), 3.37 – 3.31 (m, 1H), 2.98 – 2.94 (m, 2H), 2.01 – 1.72 (m, 4H).

**Synthesis of (*S,R*)-2-(*N*-methyl-2'-pyrrolidinyl)-5-nitro-1,4-benzodioxane
[(*S,R*)-9b]**



Under vigorous stirring at 0 °C, an aqueous solution of formaldehyde (37% in water, 0.62 ml – 249 mg – 8.3 mmol) was added dropwise to a solution of (*S,R*)-2-(2'-pyrrolidinyl)-5-nitro-1,4-benzodioxane [(*S,R*)-89] (207 mg – 0.83 mmol) in methanol (10 ml) and glacial acetic acid (0.05 ml). Upon addition of 2-picolin borane (89 mg – 0.83 mmol), the mixture was warmed to room temperature and stirred for 3 hours. The solvent was evaporated in vacuo at 40 °C, the residue was diluted with 10 ml of a 1M HCl solution and stirred for 30 minutes to quench the unreacted 2-picolin-borane. Then, the aqueous solution was washed twice with diethyl ether. The aqueous phase was cooled to 0 °C, basified to pH 11 and extracted with ethyl acetate. The organic phase was dried over anhydrous sodium sulphate, filtered and evaporated in vacuo, providing a crude that was further purified through preparative TLC (ethyl acetate + 5% TEA). The pure compound (*S,R*)-9b was isolated as orange solid (50.0 mg- 0.19 mmol, 25%). **TLC** (Ethyl Acetate + 5% TEA): **R_f**= 0.64. **M.p.**= 77.0 °C. **[α]_D²⁵** = +40.39 (*c*1, MeOH). **¹H-NMR** (300 MHz, CDCl₃): δ 7.48 (dd, *J*= 8.3 Hz, *J*= 1.5 Hz, 1H), 7.12 (dd, *J*= 8.3 Hz, *J*= 1.5 Hz, 1H), 6.88 (t, *J*= 8.3 Hz, 1H), 4.50 (dd, *J*= 11.3 Hz, *J*= 2.1 Hz, 1H), 4.21 (dt, *J*= 8.0 Hz, *J*= 2.1 Hz, 1H), 4.06 (dd, *J*= 11.3 Hz, *J*= 8.0 Hz, 1H), 3.13 – 3.07 (m, 1H), 2.71 – 2.64 (m, 1H), 2.48 (s, 3H), 2.31 (q, *J*= 9.0 Hz, 1H), 2.01 – 1.91 (m, 1H), 1.82 – 1.65 (m, 3H). **¹³C-NMR** (300 MHz, CDCl₃): δ 144.93, 138.99, 138.80, 122.11, 120.03, 117.71, 76.19, 66.28, 64.58, 57.88, 42.77, 27.30, 23.67. **HRMS (ESI⁺)**: calc. for C₁₃H₁₇N₂O₄: theor. 265.1188; found [M+H]⁺: 265.1183.





Elemental Composition Report

Single Mass Analysis

Tolerance = 5.0 PPM / DBE: min = -1.5, max = 200.0
 Element prediction: Off
 Number of isotope peaks used for i-FIT = 5

Monoisotopic Mass, Even Electron Ions

62 formula(e) evaluated with 1 results within limits (all results (up to 1000) for each mass)

Elements Used:

C: 13-13 H: 10-100 N: 0-5 O: 0-5 Na: 0-1

EB103 28 (0.550) AM2 (Ar,40000.0,0.00,0.00)

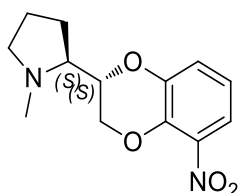
1: TOF MS ES+
8.53e+005



Minimum: -1.5
 Maximum: 0.5 5.0 200.0

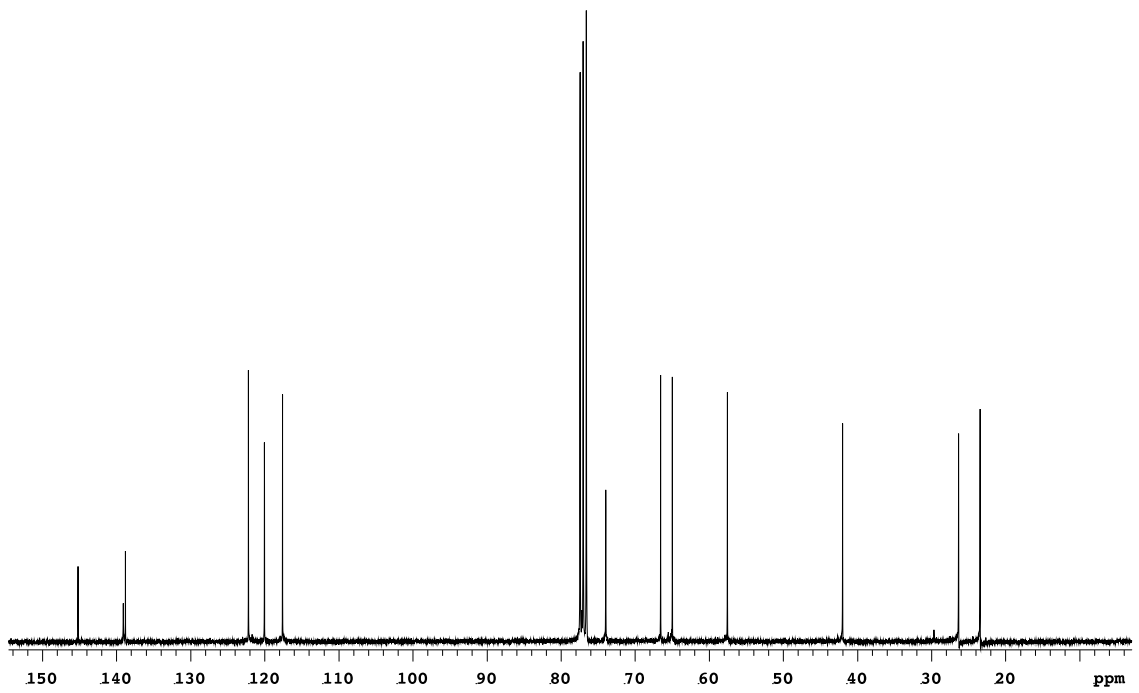
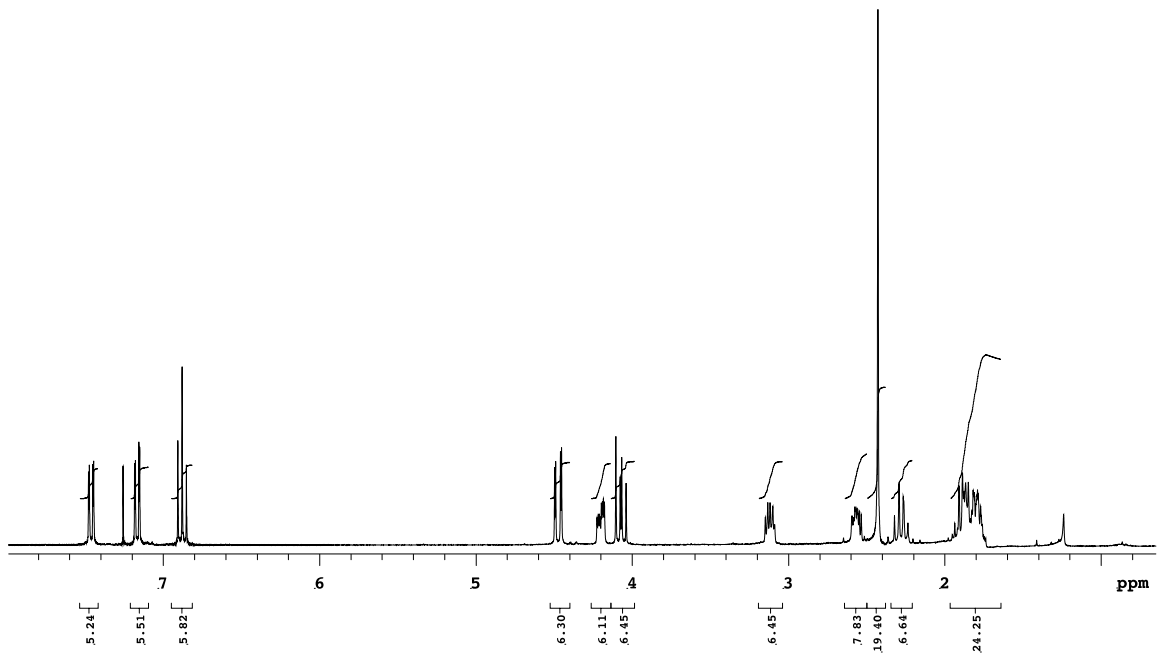
Mass	Calc. Mass	mDa	PPM	DBE	i-FIT	Norm	Conf (%)	Formula
265.1183	265.1188	-0.5	-1.9	6.5	1704.5	n/a	n/a	C13 H17 N2 O4

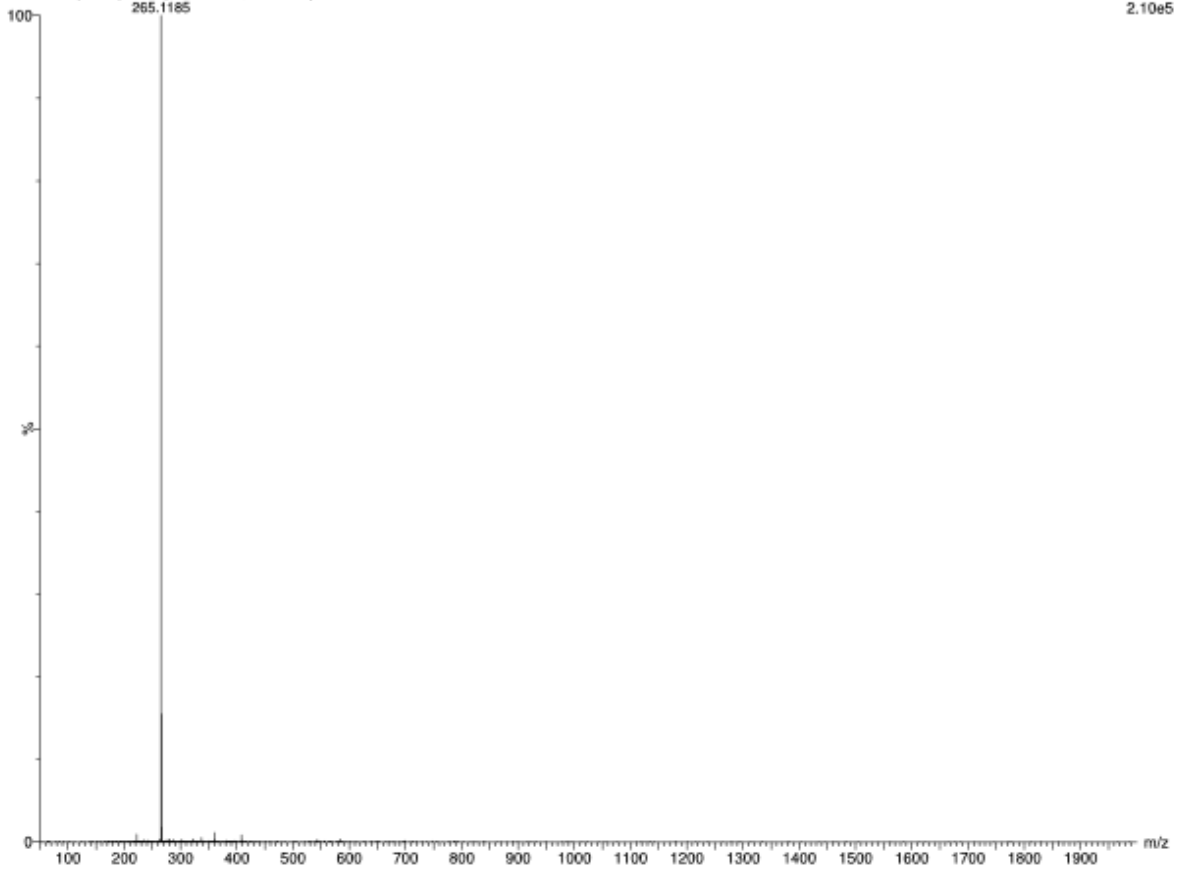
Synthesis of (*S,S*)-2-(*N*-methyl-2'-pyrrolidinyl)-5-nitro-1,4-benzodioxane [(*S,S*)-9b]



Molecular Weight: 264.28

Under vigorous stirring at 0 °C, an aqueous solution of formaldehyde (37% in water, 0.30 ml – 120 mg – 4.0 mmol) was added dropwise to a solution of (*S,S*)-2-(2'-pyrrolidinyl)-5-nitro-1,4-benzodioxane [(*S,R*)-89] (100 mg – 0.40 mmol) in methanol (5 ml) and glacial acetic acid (0.03 ml). Upon addition of 2-picolin borane (43 mg – 0.40 mmol), the mixture was warmed to room temperature and stirred for 3 hours. The solvent was evaporated in vacuo at 40 °C, the residue was diluted with 5 ml of a 1M HCl solution and stirred for 30 minutes to quench the unreacted 2-picolin-borane. Then, the aqueous solution was washed twice with diethyl ether. The aqueous phase was cooled to 0 °C, basified to pH 11 and extracted with ethyl acetate. The organic phase was dried over anhydrous sodium sulphate, filtered and evaporated in vacuo, providing a crude that was further purified through preparative TLC (ethyl acetate + 5% TEA). The pure compound (*S,S*)-9b was isolated as bright yellow oil (50.0 mg- 0.19 mmol, 81%). **TLC** (Ethyl Acetate + 5% TEA): **R_f**= 0.72. **[α]_D²⁵** = -90.12 (*c*1, MeOH). **¹H-NMR** (300 MHz, CDCl₃): δ 7.46 (dd, *J*= 8.3 Hz, *J*= 1.6 Hz, 1H), 7.17 (dd, *J*= 8.3 Hz, *J*= 1.6 Hz, 1H), 6.88 (t, *J*= 8.3 Hz, 1H), 4.47 (dd, *J*= 11.3 Hz, *J*= 2.0 Hz, 1H), 4.20 (ddd, *J*= 8.3 Hz, *J*= 3.9 Hz, *J*= 2.0 Hz, 1H), 4.07 (dd, *J*= 11.3 Hz, *J*= 8.3 Hz, 1H), 3.15 – 3.09 (m, 1H), 2.60 – 2.54 (m, 1H), 2.43 (s, 3H), 2.32 – 2.24 (m, 1H), 1.94 – 1.24 (m, 4H). **¹³C-NMR** (300 MHz, CDCl₃): δ 145.19, 139.09, 138.80, 122.20, 120.05, 117.59, 73.97, 66.57, 65.00, 57.56, 42.02, 26.36, 23.46. **HRMS (ESI⁺)**: calc. for C₁₃H₁₇N₂O₄: theor. 265.1188; found [M+H]⁺: 265.1185.





Elemental Composition Report

Single Mass Analysis

Tolerance = 5.0 PPM / DBE: min = -1.5, max = 200.0
 Element prediction: Off
 Number of isotope peaks used for i-FIT = 5

Monoisotopic Mass, Even Electron Ions

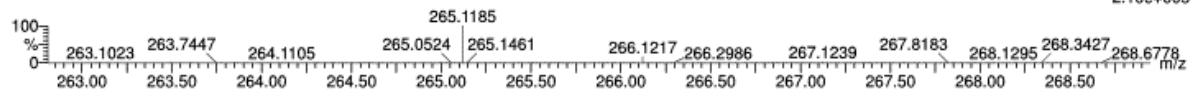
62 formula(e) evaluated with 1 results within limits (all results (up to 1000) for each mass)

Elements Used:

C: 13-13 H: 10-100 N: 0-5 O: 0-5 Na: 0-1

EB104 37 (0.702) AM2 (Ar,40000.0,0.00,0.00)

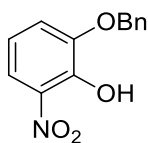
1: TOF MS ES+
2.10e+005



Minimum: -1.5
 Maximum: 0.5 5.0 200.0

Mass	Calc. Mass	mDa	PPM	DBE	i-FIT	Norm	Conf(%)	Formula
265.1185	265.1188	-0.3	-1.1	6.5	1013.1	n/a	n/a	C13 H17 N2 O4

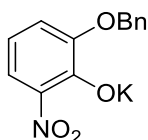
Synthesis of 2-benzyloxy-6-nitrophenol (**107**)



Molecular Weight: 245.23

Procedure adapted from literature.¹⁸⁹ A solution of 2-benzyloxyphenol (5 g – 25 mmol) in acetonitrile (40 ml) was cooled to -10 °C. Then, a solution of (NH₄)₂Ce(NO₃)₆ (10 g – 18.2 mmol) in acetonitrile (60 ml) was added dropwise. The reaction mixture was stirred for 3 hours at -10 °C. Afterward, the reaction was diluted with water and extracted three times with ethyl acetate. The combined organic phases were dried over anhydrous sodium sulphate, filtrated and the solvent was evaporated in vacuo. The resulting crude was purified through silica gel flash chromatography (cyclohexane/ethyl acetate 95:5). The pure product **107** was isolated as a bright yellow solid (3.56 g – 14.52 mmol, 58%). **TLC** (Cyclohexane / Ethyl Acetate 7:3): **R_f**= 0.65. **M.p.**= 97.7 °C. **¹H-NMR** (300 MHz, CDCl₃): δ 10.76 (bs, 1H), 7.71 (dd, *J*= 8.8 Hz, *J*= 1.7 Hz, 1H), 7.47 – 7.33 (m, 5H), 7.16 (dd, *J*= 8.8 Hz, *J*= 1.7 Hz, 1H), 6.85 (t, *J*= 8.8 Hz, 1H), 5.20 (s, 2H).

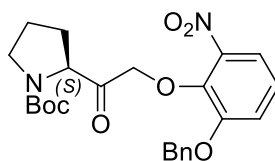
Synthesis of potassium 2-benzyloxy-6-nitrophenolate (**108**)



Molecular Weight: 283.32

A solution of 2-benzyloxy-6-nitrophenol (**107**) (2.8 g – 11.42 mmol) in methanol (30 ml) was vigorously stirred and cooled to 0 °C and a 1 M methanolic solution of KOH was added dropwise (17.13 ml – 17.13 mmol). After 15 minutes, the solid is filtered at 0 °C, washed with water and air-dried. The pure product **108** was isolated as a bright red solid (2.97 g – 10.49 mmol, 92%). **M.p.**= 114.7 °C. **¹H-NMR** (300 MHz, MeOD): δ 7.47 – 7.39 (m, 3H), 7.35 – 7.22 (m, 3H), 6.77 (dd, *J*= 7.7 Hz, *J*= 1.7 Hz, 1H), 6.18 (t, *J*= 7.7 Hz, 1H), 5.10 (s, 2H).

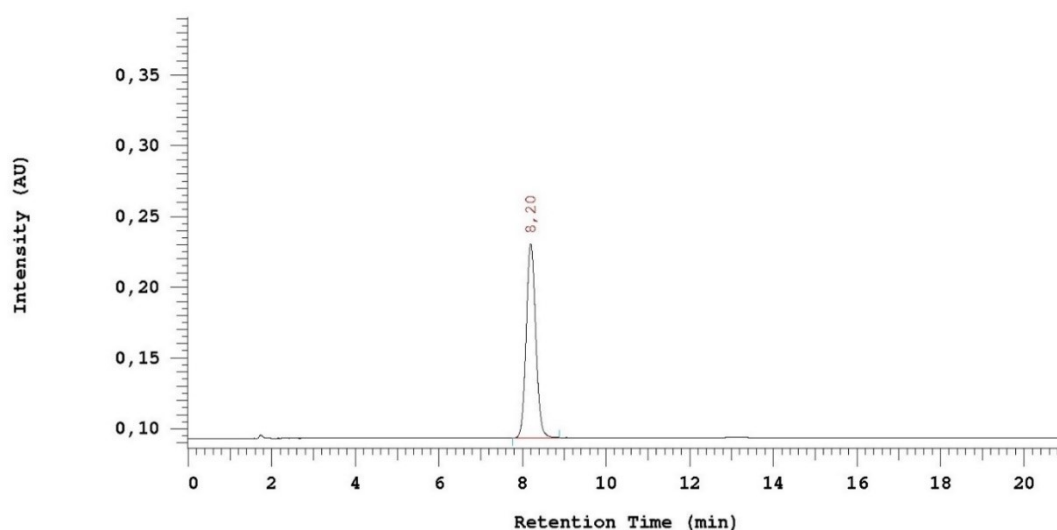
Synthesis of (*S*)-*N*-*tert*-butoxycarbonyl-2-[2'-(2-benzyloxy-6-nitrophenoxy)acetyl]pyrrolidine [(*S*)-**90**]



Molecular Weight: 456.49

Under a nitrogen atmosphere, at $-10\text{ }^{\circ}\text{C}$, a solution of *N*-*tert*-butoxycarbonyl-(*S*)-2-bromoacetylpyrrolidine [(*S*)-**79**] (2.76 g – 9.45 mmol) in acetone (15 ml) was added to a suspension of potassium 2-benzyloxy-6-nitrophenolate (**108**) (2.97 – 10.49 mmol) in acetone (20 ml). The resulting suspension was stirred overnight at room temperature. Afterward, the solvent was evaporated in vacuo and the resulting residue was diluted with ethyl acetate and washed with water. The organic phase was dried over anhydrous sodium sulphate, filtered and the solvent was evaporated in vacuo, affording a crude that was purified through silica gel flash chromatography (cyclohexane/ethyl acetate 8:2). The pure product (*S*)-**90** was isolated as a viscous yellow-ochre oil (3.49 g – 7.64 mmol, 81%). The enantiomeric excess was evaluated with chiral HPLC analysis. TLC (Cyclohexane / Ethyl Acetate 7:3): $R_f = 0.43$. $[\alpha]_D^{25} = -15.37$ (*c*1, MeOH). $^1\text{H-NMR}$ (300 MHz, CDCl_3): δ 7.38 – 7.31 (m, 6H), 7.20 – 7.09 (m, 2H), 5.17 (s, 0.66H), 5.12 (s, 1.34H), 4.95 (s, 0.66H), 4.86 (s, 1.34H), 4.61 (m, 0.33H), 4.52 (m, 0.67H), 3.47 – 3.36 (m, 2H), 2.13 – 2.04 (m, 1H), 1.82 – 1.69 (m, 3H), 1.44 (s, 3H), 1.37 (s, 6H).

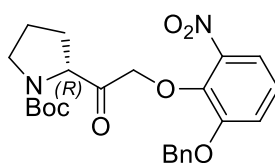
Chiral HPLC analysis: (*S*)-*N*-*tert*-butoxycarbonyl-2-[2'-(2-benzyloxy-6-nitrophenoxy)acetyl]pyrrolidine



No.	RT	Area	Conc 1	BC
1	8, 20	1073320	100, 000	MC
		1073320	100, 000	

e.e. %= 100% (Column Lux 3 μ Cellulose-2, n-hexane/ethanol 8:2, F= 1 ml/min, λ =276 nm (R_{tS}= 8.20 min, R_{tR}= 9.05 min)

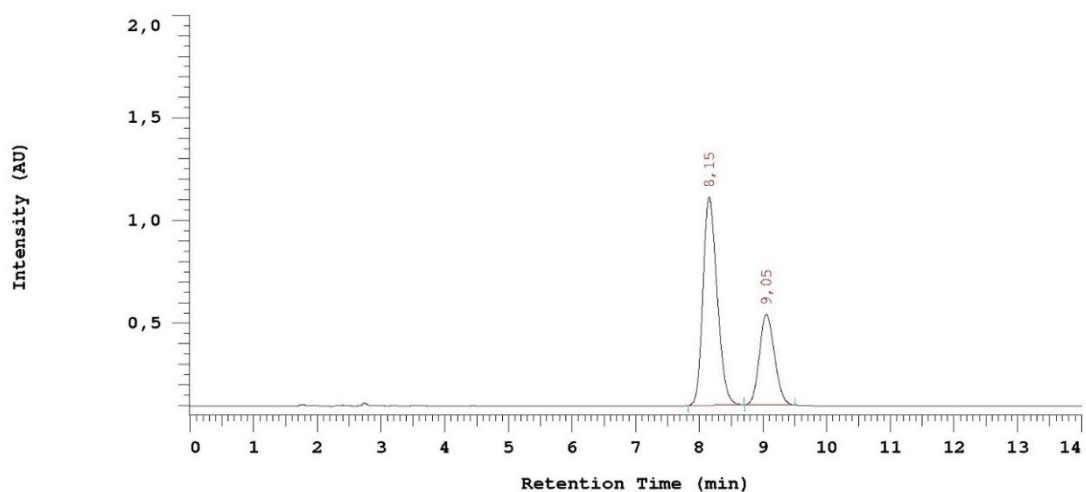
Synthesis of (*R*)-*N*-*tert*-butoxycarbonyl-2-[2'-(2-benzyloxy-6-nitrophenoxy)acetyl]pyrrolidine [(*R*)-**90**]



Molecular Weight: 456.49

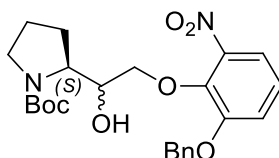
N-*tert*-butoxycarbonyl-(*R*)-2-bromoacetylpyrrolidine [(*R*)-**79**] (400 mg – 1.37 mmol) and potassium 2-benzyloxy-6-nitro-phenolate (**108**) (430 mg – 1.52 mmol) were coupled to synthesize compound (*R*)-**90**, according to the procedure reported for the correspondent enantiomer (*S*). The pure product (*R*)-**90** was obtained as a pale yellow oil (326 mg – 0.71 mmol, 47%). A mixture of (*S*)- and (*R*)-*N*-*tert*-butoxycarbonyl-2-[2'-(2-benzyloxy-6-nitrophenoxy)acetyl]pyrrolidine was analyzed by chiral HPLC to measure the retention times of the two enantiomers. TLC (Cyclohexane / Ethyl Acetate 7:3): R_f= 0.43. [α]_D²⁵ = +17.41 (*c*1, MeOH). ¹H-NMR (300 MHz, CDCl₃): δ 7.38 – 7.31 (m, 6H), 7.20 – 7.09 (m, 2H), 5.17 (s, 0.66H), 5.12 (s, 1.34H), 4.95 (s, 0.66H), 4.86 (s, 1.34H), 4.61 (m, 0.33H), 4.52 (m, 0.67H), 3.47 – 3.36 (m, 2H), 2.13 – 2.04 (m, 1H), 1.82 – 1.69 (m, 3H), 1.44 (s, 3H), 1.37 (s, 6H).

Chiral HPLC analysis: mixture of (*S*)- and (*R*)- *N*-*tert*-butoxycarbonyl-2-[2'-(2-benzyloxy-6-nitrophenoxy)acetyl]pyrrolidine



No.	RT	Area	Conc 1	BC
1	8,15	7921985	68,635	MC
2	9,05	3620176	31,365	MC
		11542161	100,000	

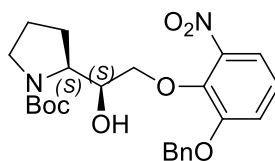
Synthesis of (*S,S*)/(*S,R*)-*N*-*tert*-butoxycarbonyl-2-[1'-hydroxy-2'-(2-benzyloxy-6-nitrophenoxy)ethyl]pyrrolidine [(*S,S*)-**92**/*(S,R)*-**92**]



Molecular Weight: 458.50

Under a nitrogen atmosphere, at $-10\text{ }^{\circ}\text{C}$, a solution of (*S*)-*N*-*tert*-butoxycarbonyl-2-[2'-(2-benzyloxy-6-nitrophenoxy)acetyl]pyrrolidine [(*S*)-**90**] (3.49 g – 7.64 mmol) in 30 ml of anhydrous THF was added dropwise to a suspension of NaBH_4 (300 mg – 8.02 mmol) in 5 ml of anhydrous THF. Upon warming to room temperature, the reaction mixture was stirred for 3 hours. Afterward, the mixture was diluted with dichloromethane and washed with brine and then with water. The organic phase was dried over anhydrous sodium sulphate, filtered and the solvent was evaporated in vacuo. The resulting crude (3.32 g – 7.25 mmol, 75%) was a diastereomeric mixture of (*S,S*)-**92** and (*S,R*)-**92**, in a 25:75 ratio. The diastereoisomers were separated through silica gel flash chromatography (cyclohexane/ethyl acetate 9:1). TLC (Cyclohexane / Ethyl Acetate 7:3): $\text{Rf}_{\text{SR}} = 0.51$; $\text{Rf}_{\text{SS}} = 0.42$.

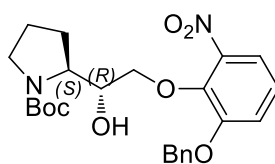
Synthesis of (*S,S*)-*N*-*tert*-butoxycarbonyl-2-[1'-hydroxy-2'-(2-benzyloxy-6-nitrophenoxy)ethyl]pyrrolidine [(*S,S*)-**92**]



Molecular Weight: 458.50

The pure (*S,S*) diastereoismer (*S,S*)-**92** was obtained as a viscous yellow oil (674 mg – 1.47 mmol, 26%). $[\alpha]_D^{25} = -42.56$ (*c*1, MeOH). $^1\text{H-NMR}$ (300 MHz, CDCl_3): δ 7.44 – 7.34 (m, 6H), 7.16 – 7.06 (m, 2H), 5.16 (s, 2H), 4.37 – 4.30 (m, 1H), 4.14 – 4.08 (m, 2H), 3.85 (m, 1H), 3.48 – 3.39 (m, 1H), 3.29 – 3.21 (m, 1H), 2.03 – 1.98 (m, 1H), 1.92 – 1.67 (m, 3H), 1.42 (s, 9H).

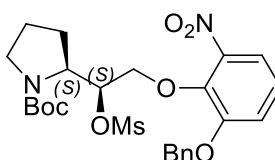
Synthesis of (*S,R*)-*N*-*tert*-butoxycarbonyl-2-[1'-hydroxy-2'-(2-benzyloxy-6-nitrophenoxy)ethyl]pyrrolidine [(*S,R*)-**92**]



Molecular Weight: 458.50

The pure (*S,R*) diastereoismer [(*S,R*)-**92**] was obtained as a viscous yellow oil (1.95 g – 4.26 mmol, 74%). $[\alpha]_D^{25} = -52.04$ (*c*1, MeOH). $^1\text{H-NMR}$ (300 MHz, CDCl_3): δ 7.46 – 7.35 (m, 6H), 7.16 – 7.05 (m, 2H), 5.16 (s, 2H), 4.36 (m, 1H), 4.14 (m, 1H), 4.02 (m, 1H), 3.92 (m, 1H), 3.45 (m, 1H), 3.28 (m, 1H), 1.93 – 1.80 (m, 3H), 1.78 – 1.72 (m, 1H), 1.44 (s, 9H).

Synthesis of (*S,S*)-*N*-*tert*-butoxycarbonyl-2-[1'-mesyloxy-2'-(2-benzyloxy-6-nitrophenoxy)ethyl]pyrrolidine [(*S,S*)-**94**]

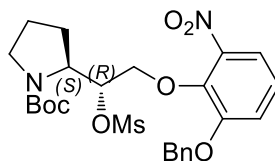


Molecular Weight: 536.59

A solution of (*S,S*)-*N*-*tert*-butoxycarbonyl-2-[1'-hydroxy-2'-(2-benzyloxy-6-nitrophenoxy)ethyl]pyrrolidine [(*S,S*)-**92**] (660 mg – 1.44 mmol) in dichloromethane (7 ml) was cooled to -10 °C and triethylamine (0.40 ml – 291.43 mg – 2.88 mmol) was added. Upon stirring

at that temperature for 10 minutes, methanesulphonylchloride (0.22 ml – 329.90 mg – 2.88 mmol) were added dropwise. The reaction mixture was warmed to room temperature and stirred for further 2 hours. Afterward, the mixture was diluted with dichloromethane (30 ml) and washed with a 1M aqueous solution of HCl. The organic phase was dried over anhydrous sodium sulphate, filtered and the solvent was evaporated in vacuo, affording a yellowish waxy crude that was purified through silica gel flash chromatography (toluene/ethyl acetate 9:1). The pure product (*S,S*)-**94** was isolated as a viscous yellow oil (665 mg – 1.24 mmol, 86%). **TLC** (Toluene / Ethyl Acetate 9:1): **R_f**= 0.31. **[α]_D²⁵** = -24.53 (*c*1, MeOH). **¹H-NMR** (300 MHz, CDCl₃): δ 7.44 – 7.34 (m, 6H), 7.22 – 7.13 (m, 2H), 5.33 (m, 1H), 5.16 (s, 2H), 4.41 (m, 1H), 4.01 (m, 1H), 3.47 – 3.30 (m, 3H), 2.94 (s, 3H), 2.02 – 1.84 (m, 3H), 1.78 – 1.74 (m, 1H), 1.45 (s, 9H).

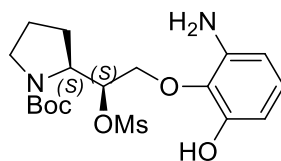
Synthesis of (*S,R*)-*N*-*tert*-butoxycarbonyl-2-[1'-mesyloxy-2'-(2-benzyloxy-6-nitrophenoxy)ethyl]pyrrolidine [(*S,R*)-**94**]



Molecular Weight: 536.59

A solution of (*S,R*)-*N*-*tert*-butoxycarbonyl-2-[1'-hydroxy-2'-(2-benzyloxy-6-nitrophenoxy)ethyl]pyrrolidine [(*S,R*)-**92**] (1.70 g – 3.71 mmol) in dichloromethane (20 ml) was cooled to -10 °C and triethylamine (0.93 ml – 675.95 mg – 6.68 mmol) was added. Upon stirring at that temperature for 10 minutes, methanesulphonylchloride (0.52 ml – 765.20 mg – 6.68 mmol) were added dropwise. The reaction mixture was warmed to room temperature and stirred for further 2 hours. Afterward, the mixture was diluted with dichloromethane (30 ml) and washed with a 1M aqueous solution of HCl. The organic phase was dried over anhydrous sodium sulphate, filtered and the solvent was evaporated in vacuo, affording a yellowish waxy crude that was purified through silica gel flash chromatography (cyclohexane/ethyl acetate 8:2). The pure product (*S,R*)-**94** was isolated as a viscous yellow oil (1.17 g – 2.18 mmol, 59%). **TLC** (Cyclohexane / Ethyl Acetate 7:3): **R_f**= 0.38. **[α]_D²⁵** = -46.47 (*c*1, MeOH). **¹H-NMR** (300 MHz, CDCl₃): δ 7.43 – 7.33 (m, 6H), 7.16 – 7.10 (m, 2H), 5.26 (m, 1H), 5.13 (s, 2H), 4.48 – 4.42 (m, 1H), 4.29 (m, 1H), 4.08 (m, 1H), 3.40 (m, 1H), 3.23 (m, 1H), 3.02 (s, 3H), 1.90 (m, 2H), 1.76 (m, 2H), 1.47 (s, 9H).

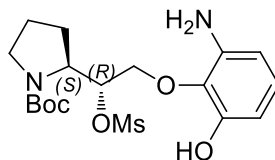
Synthesis of (*S,S*)-*N*-*tert*-butoxycarbonyl-2-[1'-mesyloxy-2'-(2-benzyloxy-6-aminophenoxy)ethyl]pyrrolidine [(*S,S*)-**96**]



Molecular Weight: 416.49

A suspension of (*S,S*)-*N*-*tert*-butoxycarbonyl-2-[1'-mesyloxy-2'-(2-benzyloxy-6-nitrophenoxy)ethyl]pyrrolidine [(*S,S*)-**94**] (616 mg – 1.15 mmol) and 5% Pd/C (123.2 mg) in methanol (10 ml) was vigorously stirred under H₂ atmosphere for 6 hours. Afterward, the catalyst was removed by filtration on a Celite® pad and the solvent was evaporated in vacuo, affording a crude that was purified through silica gel flash chromatography (cyclohexane/ethyl acetate 8:2). The pure product [(*S,S*)-**96**] was isolated as a pale yellow oil (350 mg – 0.84 mmol, 73%). **TLC** (Cyclohexane / Ethyl Acetate 1:1): **R_f**= 0.52. **[α]_D²⁵** = -37.35 (*c*1, MeOH). **¹H-NMR** (300 MHz, CDCl₃): δ 6.80 (t, *J*= 8.0 Hz, 1H), 6.38 (dd, *J*= 8.0 Hz, *J*= 1.7 Hz, 1H), 6.28 (dd, *J*= 8.0 Hz, *J*= 1.7 Hz, 1H), 4.95 (m, 1H), 4.45 (m, 1H), 4.07 (m, 2H), 3.43 (m, 1H), 3.28 (m, 1H), 3.15 (s, 3H), 2.10 – 2.00 (m, 1H), 1.99 – 1.85 (m, 3H), 1.45 (s, 9H).

Synthesis of (*S,R*)-*N*-*tert*-butoxycarbonyl-2-[1'-mesyloxy-2'-(2-benzyloxy-6-aminophenoxy)ethyl]pyrrolidine [(*S,R*)-**96**]

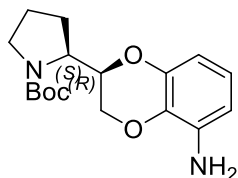


Molecular Weight: 416.49

A suspension of (*S,R*)-*N*-*tert*-butoxycarbonyl-2-[1'-mesyloxy-2'-(2-benzyloxy-6-nitrophenoxy)ethyl]pyrrolidine [(*S,R*)-**94**] (1.07 g – 2.0 mmol) and 5% Pd/C (214 mg) in methanol (20 ml) was vigorously stirred under H₂ atmosphere for 6 hours. Afterward, the catalyst was removed by filtration on a Celite® pad and the solvent was evaporated in vacuo, affording a crude that was purified through silica gel flash chromatography (cyclohexane/ethyl acetate 8:2). The pure product (*S,R*)-**96** was isolated as a white sticky solid (680 mg – 1.63 mmol, 82%). **TLC** (Cyclohexane / Ethyl Acetate 1:1): **R_f**= 0.58. **[α]_D²⁵** = -34.43 (*c*1, MeOH). **¹H-NMR** (300 MHz, CDCl₃): δ 6.80 (t, *J*= 8.0 Hz, 1H), 6.38 (dd, *J*= 8.0 Hz, *J*= 1.7 Hz, 1H),

6.30 (dd, $J= 8.0$ Hz, $J= 1.7$ Hz, 1H), 5.09 (m, 1H), 4.48 (m, 1H), 4.15 – 4.00 (m, 2H), 3.50 (m, 1H), 3.34 (m, 1H), 3.12 (s, 3H), 2.20 – 2.05 (m, 1H), 2.04 – 1.85 (m, 3H), 1.48 (s, 9H).

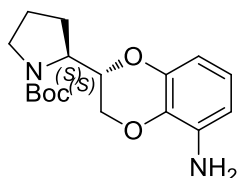
Synthesis of (*S,R*)-2-(*N*-*tert*-butoxycarbonyl-2'-pyrrolidinyl)-5-amino-1,4-benzodioxane [(*S,R*)-98]



Molecular Weight: 320.38

Under nitrogen atmosphere, a solution of (*S,S*)-*N*-*tert*-butoxycarbonyl-2-[1'-mesyloxy-2'-(2-benzyloxy-6-aminophenoxy)ethyl]pyrrolidine [(*S,S*)-96] (350 mg – 0.84 mmol) in dimethoxyethane (5 ml) was added dropwise to a suspension of K_2CO_3 (116.23 mg – 0.84 mmol) in dimethoxyethane (5 ml). The reaction mixture was refluxed under vigorous stirring for 7 hours. Afterward, the solvent was concentrated in vacuo, the residue was diluted with dichloromethane and washed with brine. The organic phase was dried over anhydrous sodium sulphate, filtered and the solvent was evaporated in vacuo, affording a crude that was purified through silica gel flash chromatography (cyclohexane/ethyl acetate 8:2). The pure product (*S,R*)-98 was isolated as a creamy-white sticky solid (210 mg – 0.65 mmol, 78%). TLC (Cyclohexane / Ethyl Acetate 1:1): $R_f= 0.73$. $[\alpha]_D^{25} = -7.84$ (c_1 , MeOH). 1H -NMR (300 MHz, $CDCl_3$): δ 6.69 (t, $J= 8.0$ Hz, 1H), 6.53 (dd, $J= 8.0$ Hz, $J= 1.7$ Hz, 1H), 6.44 (dd, $J= 8.0$ Hz, $J= 1.7$ Hz, 1H), 4.46 – 4.37 (m, 1H), 4.29 – 4.21 (m, 2H), 3.93 (m, 1H), 3.55 – 3.34 (m, 2H), 2.05 (m, 3H), 1.89 (m, 1H), 1.46 (s, 9H).

Synthesis of (*S,S*)-2-(*N*-*tert*-butoxycarbonyl-2'-pyrrolidinyl)-5-amino-1,4-benzodioxane [(*S,S*)-98]



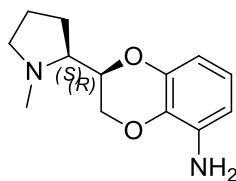
Molecular Weight: 320.38

Under nitrogen atmosphere, a solution of (*S,R*)-*N*-*tert*-butoxycarbonyl-2-[1'-mesyloxy-2'-(2-benzyloxy-6-aminophenoxy)ethyl]pyrrolidine [(*S,R*)-96] (680 mg – 1.63 mmol) in

dimethoxyethane (8 ml) was added dropwise to a suspension of K_2CO_3 (225.83 mg – 1.63 mmol) in dimethoxyethane (5 ml). The reaction mixture was refluxed under vigorous stirring for 7 hours. Afterward, the solvent was concentrated in vacuo, the residue was diluted with dichloromethane and washed with brine. The organic phase was dried over anhydrous sodium sulphate, filtered and the solvent was evaporated in vacuo, affording a crude that was purified through silica gel flash chromatography (cyclohexane/ethyl acetate 8:2). The pure product [(*S,S*)-**98**] was isolated as a white viscous oil (440 mg – 1.37 mmol, 84%). **TLC** (Cyclohexane / Ethyl Acetate 1:1): **R_f** = 0.78. $[\alpha]_D^{25} = -146.92$ (*c*1, MeOH). **¹H-NMR** (300 MHz, $CDCl_3$): δ 6.65 (t, *J* = 8.0 Hz, 1H), 6.36 (dd, *J* = 8.0 Hz, *J* = 1.4 Hz, 1H), 6.33 (dd, *J* = 8.0 Hz, *J* = 1.4 Hz, 1H), 4.36 (m, 1H), 4.08 (m, 1H), 3.97 (m, 2H), 3.49 (m, 1H), 3.38 (m, 1H), 2.21 (m, 1H), 2.02 – 1.91 (m, 3H), 1.48 (s, 9H).

Synthesis of (*S,R*)-2-(*N*-methyl-2'-pyrrolidinyl)-5-amino-1,4-benzodioxane

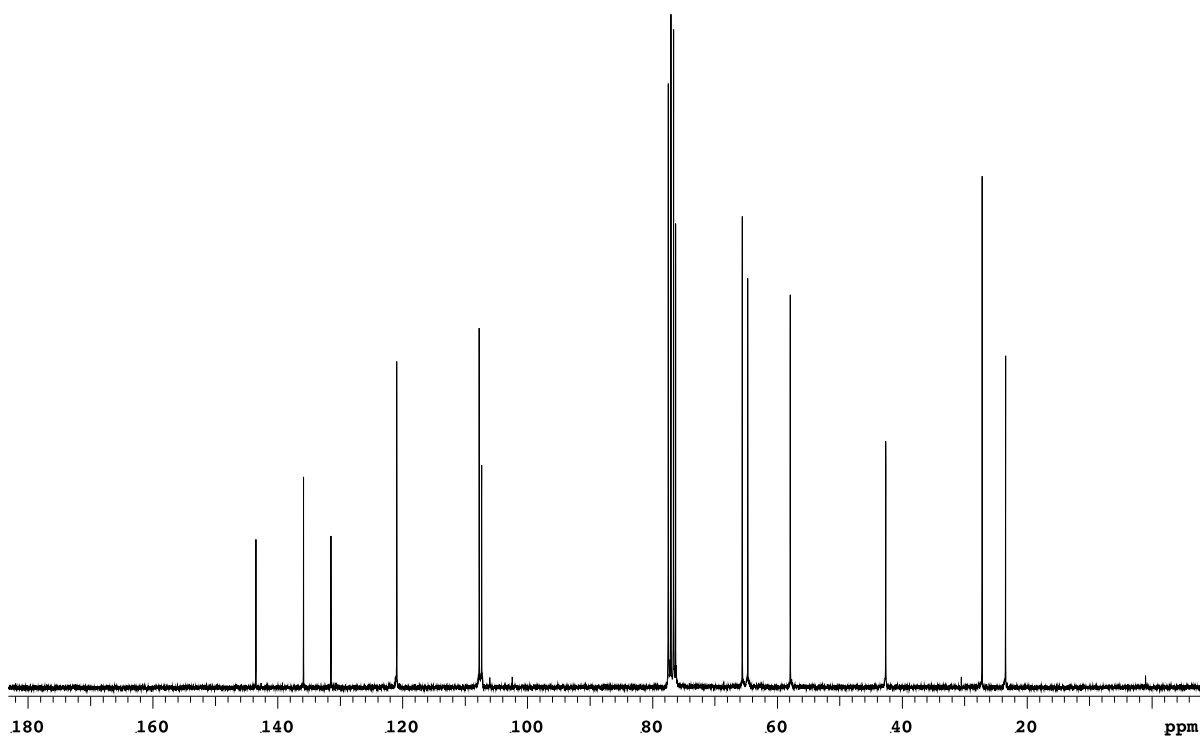
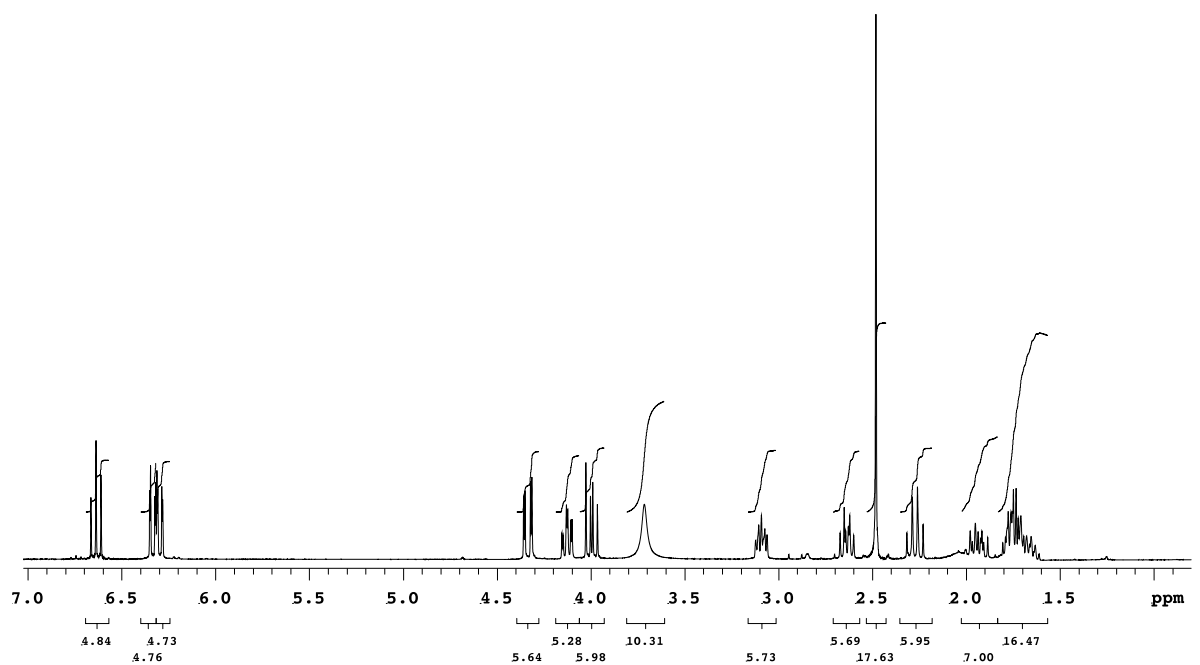
[(*S,R*)-**9c**]

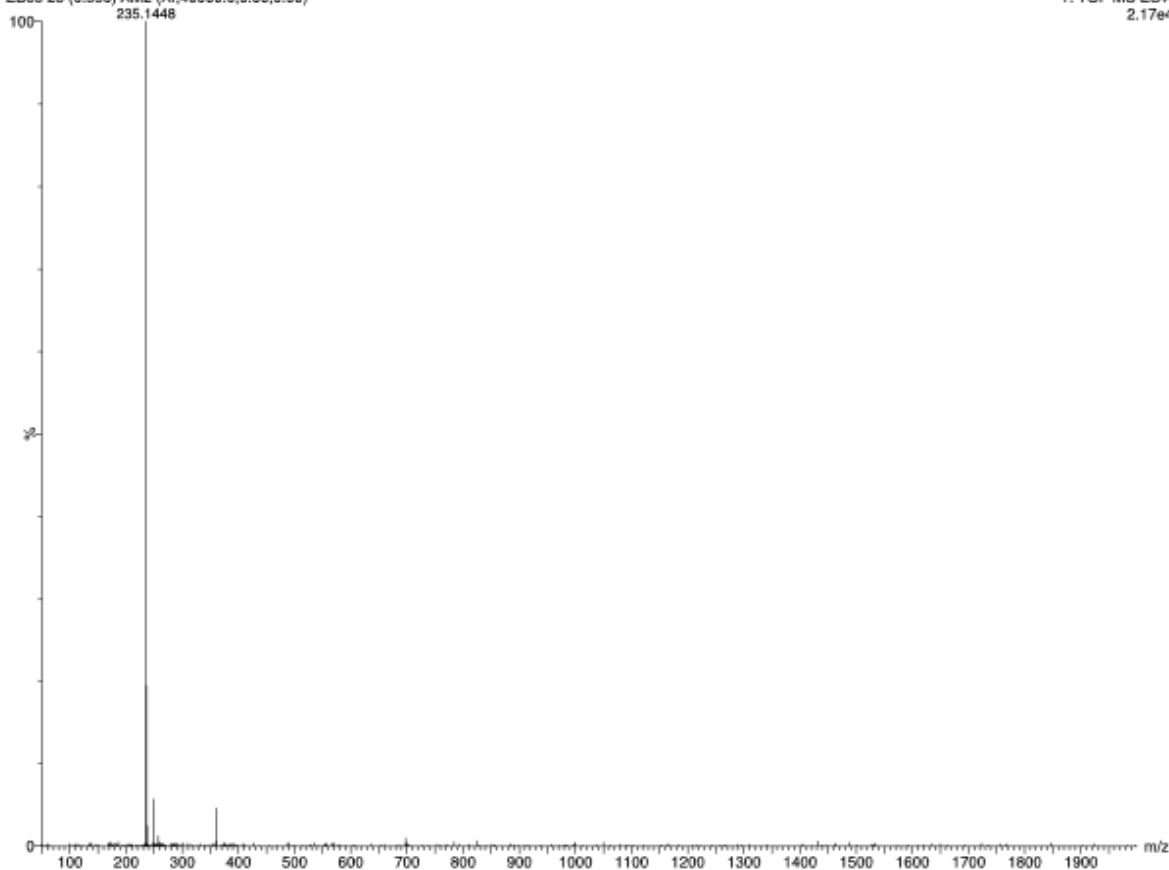


Molecular Weight: 234.29

Under a nitrogen atmosphere, at $-10\text{ }^\circ\text{C}$, a solution of (*S,R*)-2-(*N*-*tert*-butoxycarbonyl-2'-pyrrolidinyl)-5-amino-1,4-benzodioxane [(*S,R*)-**98**] (200 mg – 0.62 mmol) in anhydrous THF (5 ml) was added dropwise to a suspension of $LiAlH_4$ (70.6 mg – 1.86 mmol) in anhydrous THF (2 ml). The reaction mixture was refluxed for 4 hours under vigorous stirring. Afterward, the mixture was diluted with dichloromethane and the excess of $LiAlH_4$ was quenched by slowly adding water dropwise at $0\text{ }^\circ\text{C}$. The resulting suspension was filtered through celite and the solvent was concentrated in vacuo, affording a crude that was purified through silica gel flash chromatography (dichloromethane/methanol 95:5 + 0.5% NH_3 (30% in water)). The pure compound (*S,R*)-**9c** was isolated as a beige solid (145 mg – 0.62 mmol, 100%). **TLC** (Dichloromethane / Methanol 95:5 + 0.5% NH_3 (30% in water)): **R_f** = 0.23. **M.p.** = $59.1\text{ }^\circ\text{C}$. $[\alpha]_D^{25} = +26.86$ (*c*1, MeOH). **¹H-NMR** (300 MHz, $CDCl_3$): δ 6.64 (t, *J* = 7.8 Hz, 1H), 6.34 (dd, *J* = 7.8 Hz, *J* = 1.5 Hz, 1H), 6.30 (dd, *J* = 7.8 Hz, *J* = 1.5 Hz, 1H), 4.34 (dd, *J* = 11.1 Hz, *J* = 2.1 Hz, 1H), 4.13 (dt, *J* = 7.3 Hz, *J* = 2.1 Hz, 1H), 4.00 (dd, *J* = 11.1 Hz, *J* = 7.3 Hz, 1H), 3.72 (bs, 2H), 3.12 – 3.06 (m, 1H), 2.67 – 2.60 (m, 1H), 2.48 (s, 3H), 2.27 (q, *J* = 8.6 Hz, 1H), 2.00 – 1.89 (m, 1H),

1.81 – 1.61 (m, 3H). $^{13}\text{C-NMR}$ (300 MHz, CDCl_3): δ 143.50, 135.88, 131.48, 120.95, 107.74, 107.35, 76.29, 65.62, 64.74, 57.93, 42.65, 27.20, 23.44. **HRMS (ESI $^+$)**: calc. for $\text{C}_{13}\text{H}_{19}\text{N}_2\text{O}_2$: theor. 235.1447; found $[\text{M}+\text{H}]^+$: 235.1448.





Elemental Composition Report

Single Mass Analysis

Tolerance = 5.0 PPM / DBE: min = -1.5, max = 200.0

Element prediction: Off

Number of isotope peaks used for i-FIT = 5

Monoisotopic Mass, Even Electron Ions

61 formula(e) evaluated with 1 results within limits (all results (up to 1000) for each mass)

Elements Used:

C: 13-13 H: 10-100 N: 0-5 O: 0-5 Na: 0-1

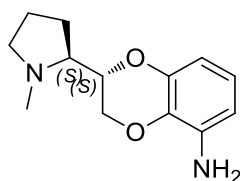
EB83 28 (0.550) AM2 (Ar,40000.0,0.00,0.00)



Minimum: -1.5
Maximum: 0.5 5.0 200.0

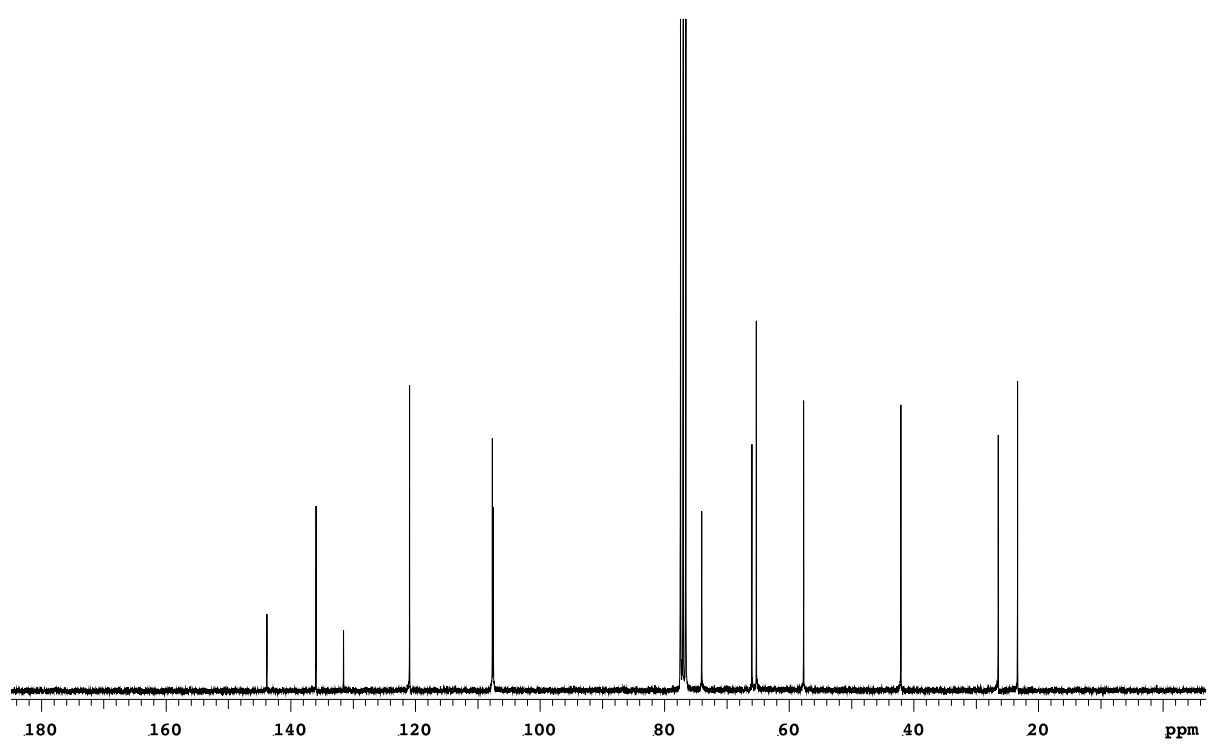
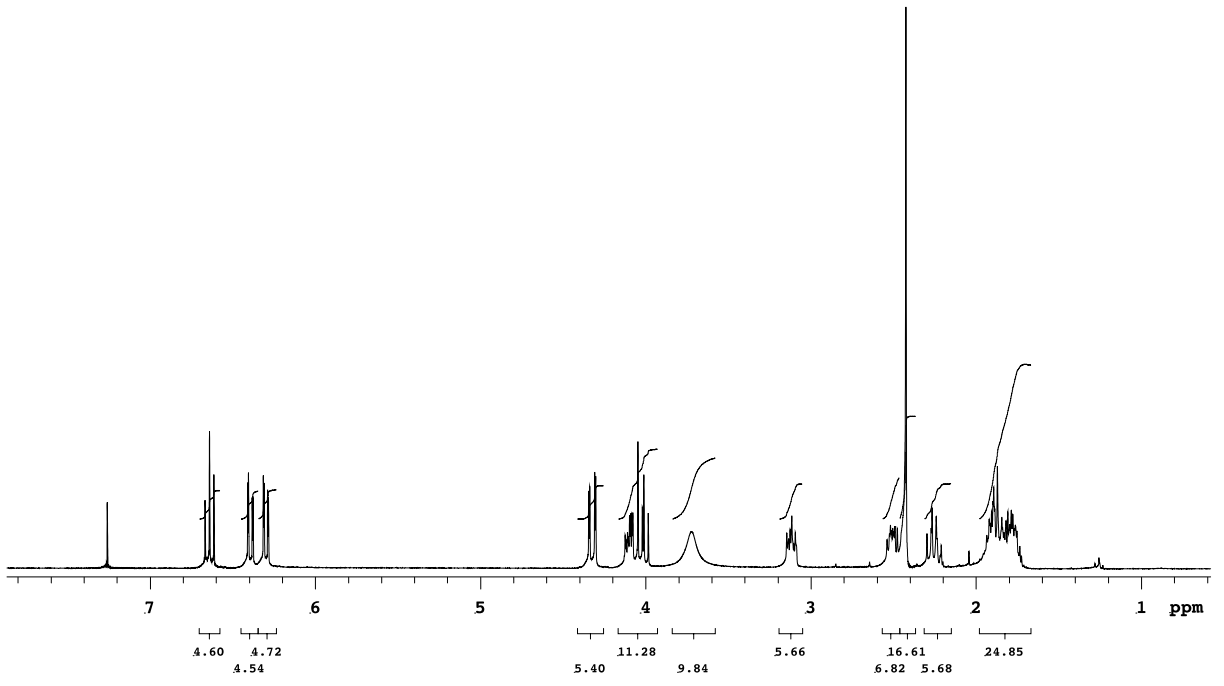
Mass	Calc. Mass	mDa	PPM	DBE	i-FIT	Norm	Conf (%)	Formula
235.1448	235.1447	0.1	0.4	5.5	209.9	n/a	n/a	C13 H19 N2 O2

Synthesis of (*S,S*)-2-(*N*-methyl-2'-pyrrolidinyl)-5-amino-1,4-benzodioxane [(*S,S*)-9c]



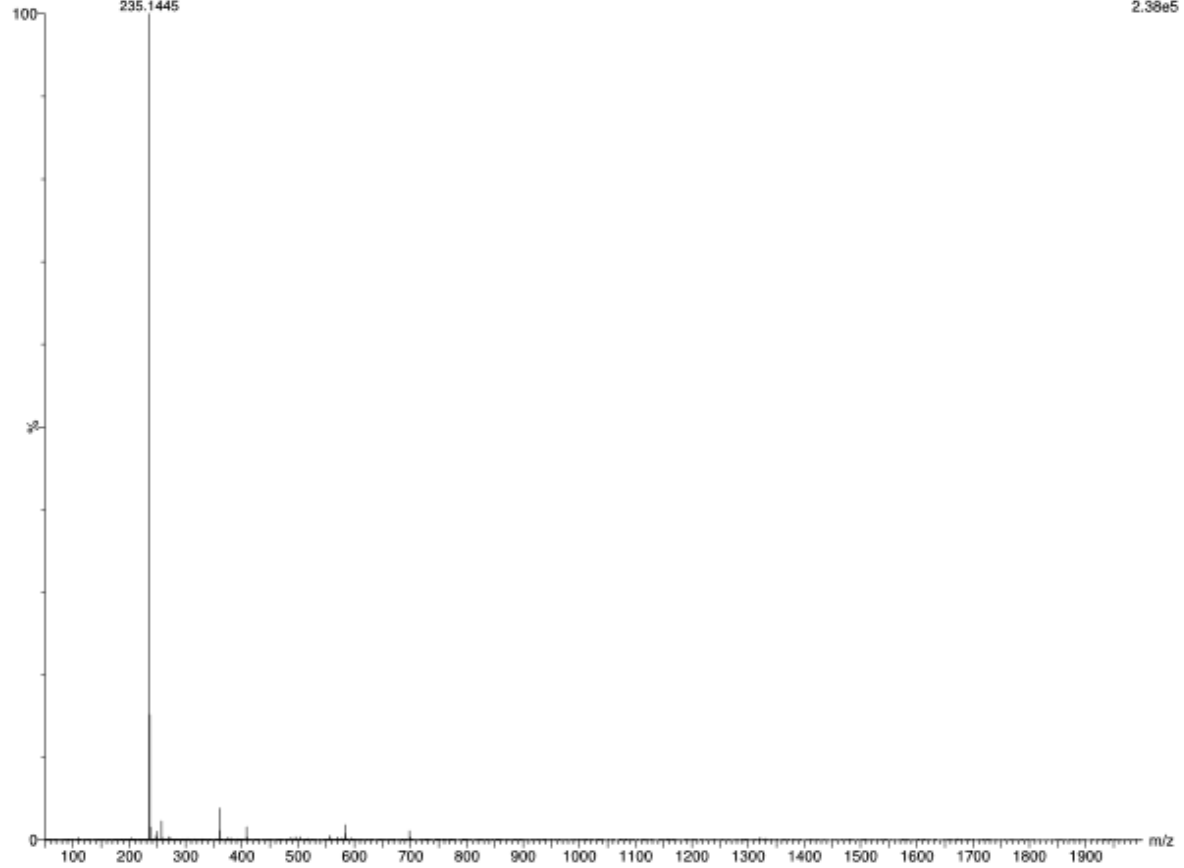
Molecular Weight: 234.29

Under a nitrogen atmosphere, at $-10\text{ }^{\circ}\text{C}$, a solution of (*S,S*)-2-(*N-tert*-butoxycarbonyl-2'-pyrrolidinyl)-5-amino-1,4-benzodioxane [(*S,S*)-98] (227 mg – 0.72 mmol) in anhydrous THF (5 ml) was added dropwise to a suspension of LiAlH_4 (82 mg – 2.13 mmol) in anhydrous THF (2 ml). The reaction mixture was refluxed for 4 hours under vigorous stirring. Afterward, the mixture was diluted with dichloromethane and the excess of LiAlH_4 was quenched by slowly adding water dropwise at $0\text{ }^{\circ}\text{C}$. The resulting suspension was filtered through celite and the solvent was concentrated in vacuo, affording a crude that was purified through silica gel flash chromatography (dichloromethane/methanol 95:5 + 0.5% NH_3 (30% in water)). The pure compound (*S,S*)-9c was isolated as a beige solid (140 mg – 0.60 mmol, 83%). **TLC** (Dichloromethane / Methanol 95:5 + 0.5% NH_3 (30% in water)): **R_f**= 0.25. **M.p.**= $104.45\text{ }^{\circ}\text{C}$. **[α]_D²⁵** = -127.83 (*c*1, MeOH). **¹H-NMR** (300 MHz, CDCl_3): δ 6.64 (t, J = 8.1 Hz, 1H), 6.39 (dd, J = 8.1 Hz, J = 1.5 Hz, 1H), 6.30 (dd, J = 8.1 Hz, J = 1.5 Hz, 1H), 4.32 (dd, J = 10.8 Hz, J = 1.8 Hz, 1H), 4.10 (ddd, J = 8.0 Hz, J = 4.2, J = 1.8 Hz, 1H), 4.02 (dd, J = 10.8 Hz, J = 8.0 Hz, 1H), 3.72 (bs, 2H), 3.15 – 3.10 (m, 1H), 2.54 – 2.48 (m, 1H), 2.43 (s, 3H), 2.30 – 2.21 (m, 1H), 1.94 – 1.74 (m, 4H). **¹³C-NMR** (300 MHz, CDCl_3): δ 143.82, 135.94, 131.53, 120.93, 107.65, 107.50, 74.07, 66.00, 65.29, 57.70, 42.10, 26.46, 23.37. **HRMS (ESI⁺)**: calc. for $\text{C}_{13}\text{H}_{19}\text{N}_2\text{O}_2$: theor. 235.1447; found $[\text{M}+\text{H}]^+$: 235.1445.



EB82 40 (0.772) AM2 (Ar,40000.0,0.00,0.00)

1: TOF MS ES+
2.38e5



Elemental Composition Report

Page 1

Single Mass Analysis

Tolerance = 5.0 PPM / DBE: min = -1.5, max = 200.0
 Element prediction: Off
 Number of isotope peaks used for i-FIT = 5

Monoisotopic Mass, Even Electron Ions

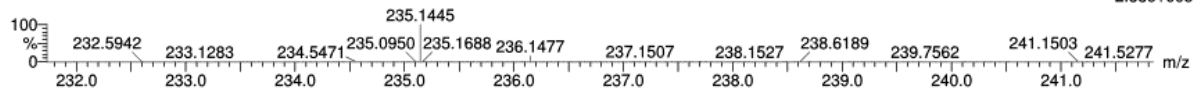
61 formula(e) evaluated with 1 results within limits (all results (up to 1000) for each mass)

Elements Used:

C: 13-13 H: 10-100 N: 0-5 O: 0-5 Na: 0-1

EB82 40 (0.772) AM2 (Ar,40000.0,0.00,0.00)

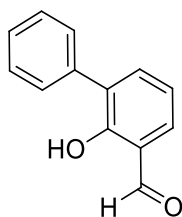
1: TOF MS ES+
2.38e+005



Minimum: -1.5
 Maximum: 0.5 5.0 200.0

Mass	Calc. Mass	mDa	PPM	DBE	i-FIT	Norm	Conf(%)	Formula
235.1445	235.1447	-0.2	-0.9	5.5	1204.2	n/a	n/a	C13 H19 N2 O2

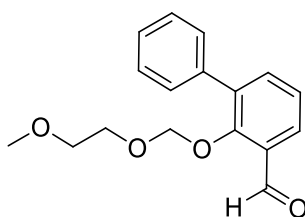
Synthesis of 2-hydroxy-3-phenylbenzaldehyde (**109**)



Molecular Weight: 198.22

Procedure adapted from literature.¹⁹⁰ Under inert atmosphere, a solution of 2-phenylphenol (3.4 g – 20.0 mmol), anhydrous triethylamine (10 ml) and anhydrous MgCl₂ (2.9 g – 30.0 mmol) in anhydrous THF (60 ml) was stirred for 20 minutes. Paraformaldehyde (4.0 g) was added in 8 portions (500 mg each) every 6 minutes and the reaction mixture was refluxed for 3 hours. Afterwards, upon cooling to room temperature, an aqueous solution 2M of HCl was added to reach pH 5 and the mixture was stirred for further 5 minutes. The product was extracted with ethyl acetate (3x40 ml) and the organic phase was washed with brine, dried over anhydrous sodium sulphate, filtered and the solvent was evaporated under vacuo, affording a crude that was purified through silica-gel flash chromatography (cyclohexane/ethyl acetate 9:1). The pure product **109** was isolated as a yellow solid (3.49 g – 17.6 mmol, 88%). TLC= (Cyclohexane / Ethyl Acetate 9:1): R_f= 0.41. M.p.= 44 °C; literature¹⁹⁰: M.p. = 45 °C. ¹H-NMR (300 MHz, CDCl₃) δ 11.54 (s, 1H), 9.97 (s, 1H, exchange with D₂O), 7.70 – 7.53 (m, 4H), 7.46 (m, 2H), 7.38 (m, 1H), 7.12 (t, *J* = 7.6 Hz, 1H).¹⁹⁰

Synthesis of 2-((2-methoxyethoxy)methoxy)-3-phenylbenzaldehyde (**110**)

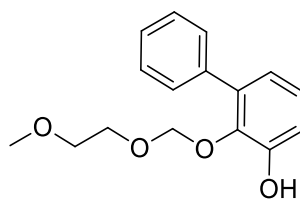


Molecular Weight: 286.32

Procedure adapted from literature.¹⁹¹ Under inert atmosphere at 0 °C, a solution of 2-hydroxy-3-phenylbenzaldehyde (**109**) (3.0 g – 15.1 mmol) in THF (10 ml) was added dropwise to a stirred suspension of NaH (399 mg – 16.6 mmol) in THF (40 ml) and the resulting mixture was stirred for 30 minutes. Upon dropwise addition of 2-methoxyethoxymethyl chloride (5.79 g – 5.31 ml – 46.5 mmol), the mixture was stirred overnight. Afterwards, the solvent was evaporated under vacuo, the residue was diluted with an aqueous solution 2M of KOH (50 ml)

and the product was extracted with diethyl ether. The organic phase was dried over anhydrous sodium sulphate, filtered and the solvent was removed under vacuo, affording a crude that was purified through silica gel flash chromatography (gradient cyclohexane/ethyl acetate from 9:1 to 7:3). The pure product **110** was obtained as a yellow oil (3.07 g – 10.72 mmol, 71%). **TLC**= (Cyclohexane / Ethyl Acetate 9:1): **Rf**= 0.18. **¹H-NMR** (300 MHz, CDCl₃): δ 10.49 (s, 1H), 7.87 (dd, *J*= 7.7, 1.8 Hz, 1H), 7.61 (dd, *J*= 7.5, 1.8 Hz, 1H), 7.58 – 7.50 (m, 2H), 7.50 – 7.28 (m, 4H), 4.81 (s, 2H), 3.56 (m, 2H), 3.35 (m, 2H), 3.29 (s, 3H).

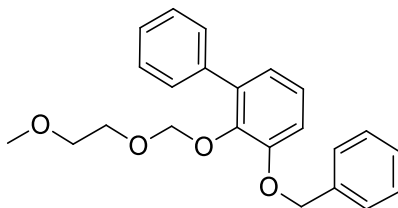
Synthesis of 2-((2-methoxyethoxy)methoxy)-3-phenylphenol (**111**)



Molecular Weight: 274.31

At 0 °C, *m*-CPBA (964 mg – 5.59 mmol) was added to a solution of 2-((2-methoxyethoxy)methoxy)-3-phenylbenzaldehyde (**110**) (640 mg – 2.24 mmol) in ethyl acetate (15 ml). The resulting mixture was stirred at room temperature for 72 hours. Afterwards, the solvent was evaporated under vacuo and the resulting crude was diluted in DCM (15 ml), washed with a saturated solution of NaHCO₃ (3x10 ml) and water (10 ml). The organic phase was dried over anhydrous sodium sulphate, filtered and the solvent was evaporated under vacuo. The resulting crude was dissolved in MeOH and a 2.5 M aqueous solution of NaOH was added. Upon stirring for 2 hours, methanol was removed under vacuo and the resulting aqueous residue was washed with diethyl ether. The aqueous phase was acidified to pH 5 with aqueous formic acid and the product was extracted with diethyl ether. The organic phase was dried over anhydrous sodium sulphate, filtered and the solvent was removed under vacuo, affording the pure product **111** as a brownish oil (450 mg – 1.64 mmol, 73%). **TLC**= (Cyclohexane / Ethyl Acetate 9:1): **Rf**= 0.19. **¹H-NMR** (300 MHz, CDCl₃) δ 7.56 (bs, 1H, exchange with D₂O), 7.54 – 7.47 (m, 2H), 7.40 (t, *J*= 7.6 Hz, 2H), 7.33 (m, 1H), 7.08 (dd, *J*= 8.1, 7.6 Hz, 1H), 6.97 (dd, *J*= 8.1, 1.7 Hz), 6.84 (dd, *J*= 7.6, 1.7 Hz, 1H), 4.71 (s, 2H), 3.81 (m, 2H), 3.58 (m, 2H), 3.44 (s, 3H).

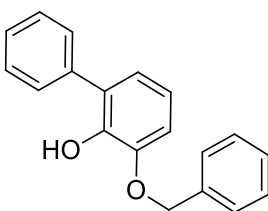
Synthesis of 2-((2-methoxyethoxy)methoxy)3-benzyloxy-biphenyl (**112**)



Molecular Weight: 364.43

A solution of 2-((2-methoxyethoxy)methoxy)-3-phenylphenol (**111**) (570 mg – 2.08 mmol) in DMF (10 ml) was added to a suspension of K_2CO_3 (574 mg – 4.16 mmol) in DMF (20 ml) and the resulting mixture was vigorously stirred for 20 minutes. Upon dropwise addition of benzyl bromide (462 mg – 0.32 ml – 2.7 mmol), the reaction mixture was warmed to 50 °C and stirred for 1.5 hours. Afterwards, the mixture was cooled to room temperature and the solvent was concentrated under vacuo. The resulting residue was diluted with diethyl ether and sequentially washed with brine, with an aqueous solution of NaOH 2.5 M (2x20 ml), with an aqueous solution of HCl 10% and then with water. The organic phase was dried over anhydrous sodium sulphate, filtered and the solvent was removed under vacuo, providing the pure compound **112** as an orange oil (590 mg – 1.62 mmol, 78%). TLC= (Cyclohexane / Ethyl Acetate 9:1): R_f = 0.29. 1H -NMR (300 MHz, $CDCl_3$): δ 7.58 – 7.50 (m, 2H), 7.49 – 7.27 (m, 8H), 7.13 – 7.05 (m, 1H), 7.00 – 6.93 (m, 2H), 5.13 (s, 2H), 4.99 (s, 2H), 3.23 – 3.16 (m, 5H), 3.14 – 3.05 (m, 2H).

Synthesis of 2-benzyloxy-6-phenylphenol (**113**)

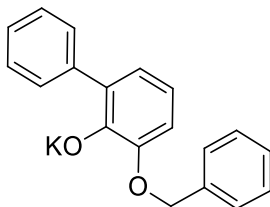


Molecular Weight: 276.33

A concentrated (37 %) aqueous solution of HCl (1 ml) was added dropwise to a solution of 2-((2-methoxyethoxy)methoxy)3-benzyloxy-biphenyl (**112**) (255 mg – 0.70 mmol) in methanol (50 ml). The resulting solution was vigorously stirred at 60 °C for 1 hour. Afterwards, the reaction mixture was cooled to room temperature and quenched by carefully adding dropwise a saturated aqueous solution of $NaHCO_3$. Methanol was removed in vacuo and the resulting aqueous phase was extracted with ethyl acetate. The organic phase was dried over anhydrous sodium sulphate, filtered and the solvent was evaporated under vacuo, providing the pure

product as a white solid (186 mg – 0.67 mmol, 96%). TLC= (Cyclohexane / Ethyl Acetate 9:1): R_f= 0.5. M.p.= 86 °C. ¹H-NMR (300 MHz, CDCl₃) δ 7.62 (m, 2H), 7.48 – 7.29 (m, 8H), 7.00 (dd, *J*= 5.2, 3.2 Hz, 1H), 6.95 – 6.84 (m, 2H), 5.93 (s, 1H, exchange with D₂O), 5.17 (s, 2H).

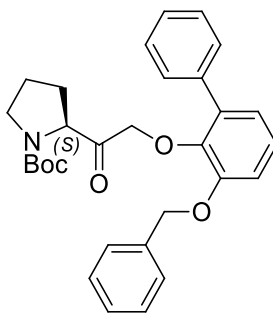
Synthesis of potassium 2-benzyloxy-6-phenylphenolate (**114**)



Molecular Weight: 314.42

A methanolic solution 1M of KOH (2.52 ml – 2.52 mmol) was added to a solution of 2-benzyloxy-6-phenylphenol (**113**) (735 mg – 2.66 mmol) in methanol (0.5 ml). Upon stirring for 30 minutes, the solvent was removed under vacuo and the residue was diluted with water. The resulting suspension was filtered and the pure product **114** was obtained as an grey solid (761 mg – 2.42 mmol, 91%). M.p.= 83 °C. ¹H-NMR (300 MHz, CDCl₃) δ 7.5 (d, *J*= 7.3 Hz, 2H), 7.47 – 7.26 (m, 8H), 6.98 (dd, *J*= 7.2, 1.5 Hz, 1H), 6.95 – 6.83 (m, 2H), 5.13 (s, 2H).

Synthesis of (*S*)-*N*-*tert*-butoxycarbonyl-2-[(2-benzyloxy-6-phenylphenoxy)acetyl]pyrrolidine [(*S*)-**91**]

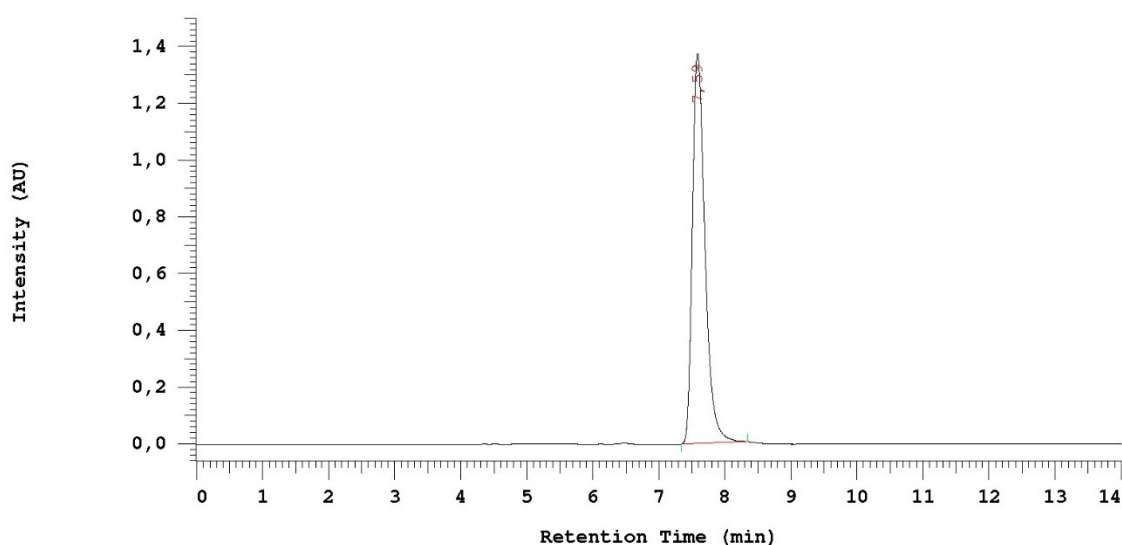


Molecular Weight: 487.59

Under a nitrogen atmosphere, at -10 °C, a solution of *N*-*tert*-butoxycarbonyl-(*S*)-2-bromoacetylpyrrolidine [(*S*)-**79**] (515 mg – 1.76 mmol) in acetone (5 ml) was added to a solution of potassium 2-benzyloxy-6-phenylphenolate **114** (530 mg – 1.69 mmol) in acetone (5 ml). The resulting suspension was stirred at room temperature for 1.5 hours. Afterward, the solvent was evaporated in vacuo and the resulting residue was diluted with DCM and washed with brine. The organic phase was dried over anhydrous sodium sulphate, filtered and the

solvent was evaporated in vacuo, affording a crude that was purified through silica gel flash chromatography (gradient from cyclohexane/ethyl acetate 9:1 to ethyl acetate). The pure product (*S*)-**91** was isolated as a pale yellow oil (1.49 g – 3.28 mmol, 30%). The enantiomeric excess was evaluated with chiral HPLC analysis. TLC (Dichloromethane / Toluene 9:1): **Rf**= 0.15. $[\alpha]_D^{25} = -5.88^\circ$ (*c*1, MeOH). $^1\text{H-NMR}$ (300 MHz, CDCl_3) δ 7.54 (d, $J = 7.1$ Hz, 2H), 7.48 – 7.28 (m, 8H), 7.23 – 7.04 (m, 1H), 6.99 (m, 2H), 5.12 (s, 2H), 4.50 (m, 1H), 4.39 (m, 2H), 3.35 (m, 2H), 1.99 – 1.67 (m, 4H), 1.23 (s, 9H).

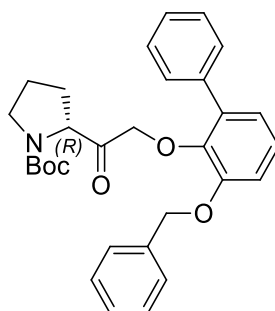
Chiral HPLC analysis: (*S*)-*N*-*tert*-butoxycarbonyl-2-[(2-benzyloxy-6-phenylphenoxy)acetyl]pyrrolidine



No.	RT	Area	Conc 1	BC
1	7,59	9025762	100,000	MC
		9025762	100,000	

e.e. % = 100% (Column Lux 3 μ Cellulose-1, n-hexane/ethanol 8:2, F= 0.5 ml/min, λ =276 nm (R_{tS}= 7.59 min, R_{tR}= 8.45 min)

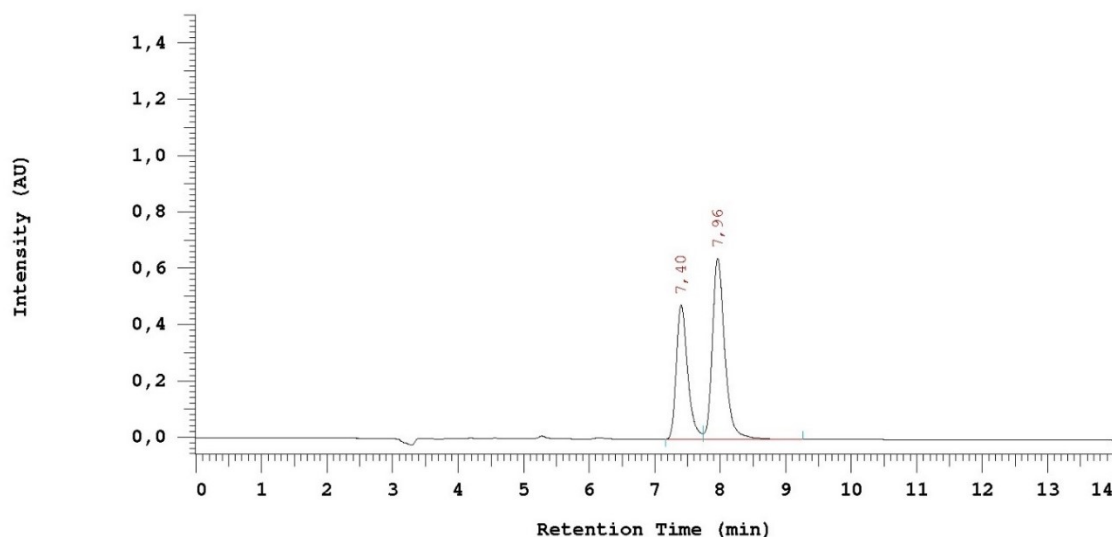
Synthesis of (*R*)-*N*-*tert*-butoxycarbonyl-2-[(2-benzyloxy-6-phenylphenoxy)acetyl]pyrrolidine [(*R*)-**91**]



Molecular Weight: 487.59

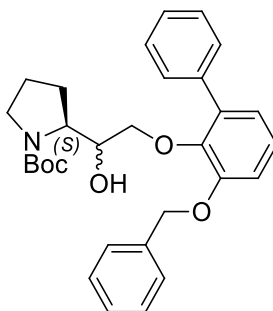
N-*tert*-butoxycarbonyl-(*R*)-2-bromoacetylpyrrolidine [(*S*)-**79**] (537 mg – 1.84 mmol) and potassium 2-benzyloxy-6-phenylphenolate (**114**) (550 mg – 1.75 mmol) were coupled to synthesize compound (*R*)-**91**, according to the procedure reported for the correspondent enantiomer (*S*). The pure product was obtained as a pale yellow oil (299 mg – 0.61 mmol, 35%). A mixture of (*S*)-**91** and (*R*)-**91** was analyzed by chiral HPLC to measure the retention times of the two enantiomers. TLC (Dichloromethane / Toluene 9:1): **Rf**= 0.15. ¹H-NMR (300 MHz, CDCl₃) δ 7.54 (d, *J* = 7.1 Hz, 2H), 7.48 – 7.28 (m, 8H), 7.23 – 7.04 (m, 1H), 6.99 (m, 2H), 5.12 (s, 2H), 4.50 (m, 1H), 4.39 (m, 2H), 3.35 (m, 2H), 1.99 – 1.67 (m, 4H), 1.23 (s, 9H).

Chiral HPLC analysis: mixture of (*R*)- and (*S*)-*N*-*tert*-butoxycarbonyl-2-[(2-benzyloxy-6-phenylphenoxy)acetyl]pyrrolidine



No .	RT	Area	Conc 1	BC
1	7,40	2835925	40,132	MC
2	7,96	4230539	59,868	MC
		7066464	100,000	

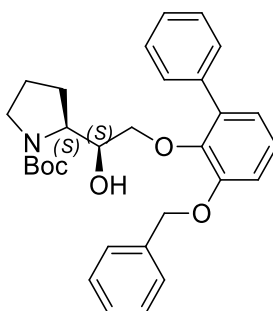
Synthesis of (*S,S*)/(*S,R*)-*N*-*tert*-butoxycarbonyl-2-[1'-hydroxy-2'-(2-benzyloxy-6-phenylphenoxy)ethyl]pyrrolidine [(*S,S*)-93**]/(*S,R*)-**93**]**



Molecular Weight: 489.60

Under a nitrogen atmosphere, at -10 °C, a solution of (*S*)-*N*-*tert*-butoxycarbonyl-2-[(2-benzyloxy-6-phenylphenoxy)acetyl]pyrrolidine [(*S*)-**91**] (1.48 g – 3.04 mmol) in 9 ml of anhydrous THF was added dropwise to a suspension of NaBH₄ (209 mg – 8.71 mmol) in 6 ml of anhydrous THF. The reaction was stirred for 2 hours at -10 °C. Afterwards, the mixture was diluted with dichloromethane and washed with an aqueous solution of HCl 1 M and then with water. The organic phase was dried over anhydrous sodium sulphate, filtered and the solvent was evaporated in vacuo. The resulting crude (1.31g – 2.68 mmol, 80%) was a diastereomeric mixture of (*S,S*)-**93** and (*S,R*)-**93**, in a 60:40 ratio. The diastereoisomers were separated through silica gel flash chromatography (toluene/ethyl acetate 8:2). TLC (Toluene / Ethyl Acetate 9:1): **R_{fSR}**= 0.45; **R_{fSS}**= 0.33.

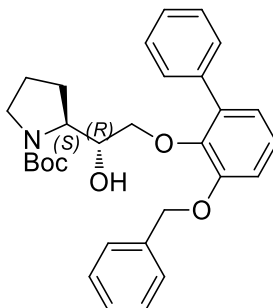
Synthesis of (*S,S*)-*N*-*tert*-butoxycarbonyl-2-[1'-hydroxy-2'-(2-benzyloxy-6-phenylphenoxy)ethyl]pyrrolidine [(*S,S*)-**93**]



Molecular Weight: 489.60

The pure (*S,S*) diastereoisomer (*S,S*)-**93** was obtained as a white sticky solid (360 mg – 0.74 mmol, 24%). $[\alpha]_D^{25} = -22.06$ (*c*1, CHCl₃). ¹H-NMR (300 MHz, CDCl₃): δ 7.54 (d, *J*= 7.9 Hz, 2H), 7.50 – 7.27 (m, 8H), 7.07 (m, 1H), 7.02 – 6.89 (m, 2H), 5.16 (s, 2H), 3.72 (m, 2H), 3.65 – 3.41 (m, 2H), 3.27 (m, 1H), 3.13 (m, 1H), 1.73 – 1.50 (m, 4H), 1.30 (s, 9H).

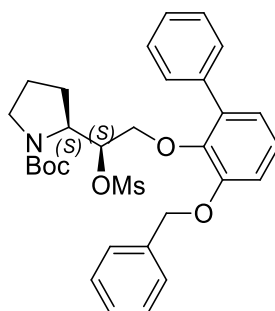
Synthesis of (*S,R*)-*N*-*tert*-butoxycarbonyl-2-[1'-hydroxy-2'-(2-benzyloxy-6-phenylphenoxy)ethyl]pyrrolidine [(*S,R*)-**93**]



Molecular Weight: 489.60

The pure (*S,R*) diastereoisomer (*S,R*)-**93** was obtained as a colourless oil (915 mg – 1.87 mmol, 62%). $[\alpha]_D^{25} = -20.62$ (*c*1, CHCl₃). ¹H-NMR (300 MHz, CDCl₃) δ 7.57 – 7.53 (m, 2H), 7.48 (m, 2H), 7.45 – 7.29 (m, 6H), 7.09 (dd, *J*= 8.5, 7.3 Hz, 1H), 6.99 – 6.94 (m, 2H), 5.15 (s, 2H), 3.83 (m, 2H), 3.61 (m, 2H), 3.31 (m, 1H), 3.12 (m, 1H), 1.95 – 1.55 (m, 4H), 1.36 (s, 9H).

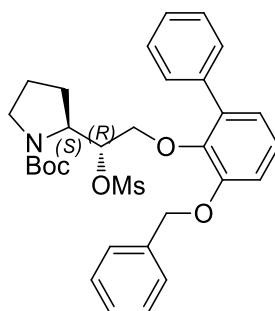
Synthesis of (*S,S*)-*N*-*tert*-butoxycarbonyl-2-[1'-mesyloxy-2'-(2-benzyloxy-6-phenylphenoxy)ethyl]pyrrolidine [(*S,S*)-**95**]



Molecular Weight: 567.69

Under inert atmosphere, a solution of (*S,S*)-*N*-*tert*-butoxycarbonyl-2-[1'-hydroxy-2'-(2-benzyloxy-6-phenylphenoxy)ethyl]pyrrolidine [(*S,S*)-**93**] (320 mg – 0.65 mmol) in dichloromethane (7 ml) was cooled to 0 °C and triethylamine (0.2 ml – 145 mg – 1.43 mmol) was added. Upon stirring at that temperature for 10 minutes, methanesulphonylchloride (0.1 ml – 148 mg – 1.29 mmol) was added dropwise. The reaction mixture was warmed to room temperature and stirred for further 2 hours. Afterward, the mixture was diluted with dichloromethane (30 ml) and washed with a 1M aqueous solution of HCl. The organic phase was dried over anhydrous sodium sulphate, filtered and the solvent was evaporated in vacuo, affording a yellowish waxy crude that was purified through silica gel flash chromatography (gradient from toluene to toluene/ethyl acetate 9:1). The pure product (*S,S*)-**95** was isolated as a viscous yellow oil (170 mg – 0.30 mmol, 46%). **TLC** (Toluene / Ethyl Acetate 9:1): **R_f**= 0.41. **[α]_D²⁵** = -44.81 (*c*0.5, CHCl₃). **¹H-NMR** (300 MHz, CDCl₃) δ 7.41 (m, 10H), 7.10 (m, 1H), 6.97 (m, 2H), 5.12 (s, 2H), 5.08 – 4.95 (m, 1H), 4.14 – 4.02 (m, 1H), 3.78 (m, 2H), 3.27 (m, 1H), 3.14 (m, 1H), 2.74 (s, 1.5H), 2.67 (s, 1.5H), 1.94 – 1.73 (m, 2H), 1.73 – 1.55 (m, 2H), 1.44 (s, 9H).

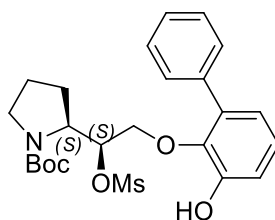
Synthesis of (*S,R*)-*N*-*tert*-butoxycarbonyl-2-[1'-mesyloxy-2'-(2-benzyloxy-6-phenylphenoxy)ethyl]pyrrolidine [(*S,R*)-95]



Molecular Weight: 567.69

Under inert atmosphere, a solution of (*S,R*)-*N*-*tert*-butoxycarbonyl-2-[1'-hydroxy-2'-(2-benzyloxy-6-phenylphenoxy)ethyl]pyrrolidine [(*S,R*)-93] (605 mg – 1.24 mmol) in dichloromethane (10 ml) was cooled to 0 °C and triethylamine (0.38 ml – 276 mg – 2.73 mmol) was added. Upon stirring at that temperature for 10 minutes, methanesulphonylchloride (0.21 ml – 310 mg – 2.71 mmol) was added dropwise. The reaction mixture was warmed to room temperature and stirred for further 2 hours. Afterward, the mixture was diluted with dichloromethane (30 ml) and washed with a 1M aqueous solution of HCl. The organic phase was dried over anhydrous sodium sulphate, filtered and the solvent was evaporated in vacuo, affording a yellowish waxy crude that was purified through silica gel flash chromatography (gradient from toluene to toluene/ethyl acetate 9:1). The pure product (*S,R*)-95 was isolated as a viscous yellow oil (296 mg – 0.52 mmol, 42%). TLC (Toluene / Ethyl Acetate 9:1): **R_f** = 0.39. **[α]_D²⁵** = -15.10 (*c*0.5, CHCl₃). **¹H-NMR** (300 MHz, CDCl₃): δ 7.58 – 7.29 (m, 10H), 7.14 – 7.05 (m, 1H), 6.97 (m, 2H), 5.12 (s, 2H), 4.86 (m, 1H), 4.14 (m, 1H), 3.92 (m, 2H), 3.50 – 3.01 (m, 2H), 2.77 (s, 2H, rotamers), 2.70 (s, 1H, rotamer), 2.01 – 1.68 (m, 4H), 1.38 (s, 9H).

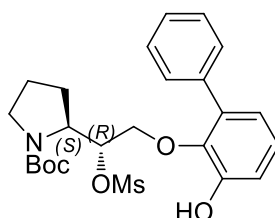
Synthesis of (*S,S*)-*N*-*tert*-butoxycarbonyl-2-[1'-mesyloxy-2'-(2-hydroxy-6-phenylphenoxy)ethyl]pyrrolidine [(*S,S*)-**97**]



Molecular Weight: 477.57

A suspension of (*S,S*)-*N*-*tert*-butoxycarbonyl-2-[1'-mesyloxy-2'-(2-benzyloxy-6-phenylphenoxy)ethyl]pyrrolidine [(*S,S*)-**95**] (200 mg – 0.35 mmol) and 5% Pd/C (60 mg) in methanol (10 ml) was vigorously stirred under H₂ atmosphere for 48 hours. Afterward, the catalyst was removed by filtration on a Celite® pad and the solvent was evaporated in vacuo, affording a crude that was partially purified through silica gel flash chromatography (toluene/ethyl acetate 9:1). The product (*S,S*)-**97** was isolated as an oil (154 mg – 0.32 mmol, 91%) and was further used as a crude for the next step. **TLC** (Toluene / Ethyl Acetate 9:1): **R_f**= 0.13

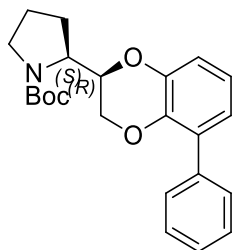
Synthesis of (*S,R*)-*N*-*tert*-butoxycarbonyl-2-[1'-mesyloxy-2'-(2-hydroxy-6-phenylphenoxy)ethyl]pyrrolidine [(*S,R*)-**97**]



Molecular Weight: 477.57

A suspension of (*S,R*)-*N*-*tert*-butoxycarbonyl-2-[1'-mesyloxy-2'-(2-benzyloxy-6-phenylphenoxy)ethyl]pyrrolidine [(*S,R*)-**95**] (390 mg – 0.69 mmol) and 5% Pd/C (80 mg) in methanol (10 ml) was vigorously stirred under H₂ atmosphere for 48 hours. Afterward, the catalyst was removed by filtration on a Celite® pad and the solvent was evaporated in vacuo, affording a crude that was partially purified through silica gel flash chromatography (toluene/ethyl acetate 9:1). The product (*S,R*)-**97** was isolated as a brown oil (254 mg – 0.53 mmol, 77%) and further used as a crude for the next step. **TLC** (Toluene / Ethyl Acetate 9:1): **R_f**= 0.37.

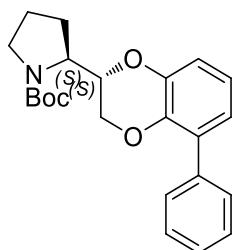
Synthesis of (*S,R*)-2-(*N*-*tert*-butoxycarbonyl-2'-pyrrolidinyl)-5-phenyl-1,4-benzodioxane [(*S,R*)-99]



Molecular Weight: 381.46

Under nitrogen atmosphere, at 0 °C, a solution of (*S,S*)-*N*-*tert*-butoxycarbonyl-2-[1'-mesyloxy-2'-(2-hydroxy-6-phenylphenoxy)ethyl]pyrrolidine [(*S,S*)-97] (154 mg – 0.32 mmol) in dimethoxyethane (10 ml) was added dropwise to a suspension of K₂CO₃ (53 mg – 0.38 mmol) in dimethoxyethane (5 ml). The reaction mixture was refluxed under vigorous stirring for 5 hours. Afterwards, the solvent was concentrated in vacuo, the residue was diluted with dichloromethane and washed with water and then brine. The organic phase was dried over anhydrous sodium sulphate, filtered and the solvent was evaporated in vacuo, affording a crude that was purified through silica gel flash chromatography (gradient toluene/ethyl acetate from 9:1 to 1:1). The pure product (*S,R*)-99 was isolated as a brown oil (42 mg – 0.11 mmol, 34%). TLC (Toluene / Ethyl Acetate 9:1): R_f = 0.50. [α]_D²⁵ = +5.86 ° (c0.5, MeOH). ¹H-NMR (300 MHz, CDCl₃): δ 7.56 – 7.51 (m, 2H), 7.41 (t, *J* = 7.3 Hz, 2H), 7.34 (m, 1H), 6.92 – 6.86 (m, 3H), 4.27 (m, 3H), 3.91 (m, 1H), 3.63 – 3.29 (m, 2H), 2.18 – 2.03 (m, 3H), 1.97 – 1.83 (m, 1H), 1.44 (s, 9H).

Synthesis of (*S,S*)-2-(*N*-*tert*-butoxycarbonyl-2'-pyrrolidinyl)-5-phenyl-1,4-benzodioxane [(*S,S*)-99]

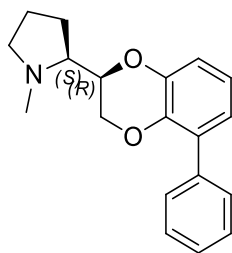


Molecular Weight: 381.46

Under nitrogen atmosphere, at 0 °C, a solution of (*S,R*)-*N*-*tert*-butoxycarbonyl-2-[1'-mesyloxy-2'-(2-hydroxy-6-phenylphenoxy)ethyl]pyrrolidine [(*S,R*)-97] (240 mg – 0.50 mmol) in

dimethoxyethane (10 ml) was added dropwise to a suspension of K_2CO_3 (83 mg – 0.60 mmol) in dimethoxyethane (5 ml). The reaction mixture was refluxed under vigorous stirring for 5 hours. Afterwards, the solvent was concentrated in vacuo, the residue was diluted with dichloromethane and washed with water and then brine. The organic phase was dried over anhydrous sodium sulphate, filtered and the solvent was evaporated in vacuo, affording a crude that was purified through silica gel flash chromatography (gradient toluene/ethyl acetate from 9:1 to 1:1). The pure product (*S,S*)-**99** was isolated as a white oil (93 mg – 0.25 mmol, 49%). **TLC** (Toluene / Ethyl Acetate 9:1): **R_f**= 0.44. $[\alpha]_D^{25} = -88.37$ (*c*0.5, MeOH). **¹H-NMR** (300 MHz, $CDCl_3$) δ 7.53 (d, *J* = 7.2 Hz, 2H), 7.41 (t, *J* = 7.2 Hz, 2H), 7.37 – 7.30 (m, 1H), 6.93 – 6.87 (m, 3H), 4.35 (dd, *J* = 11.4, 1.7 Hz, 1H), 4.12 (m, 1H), 4.03 – 3.86 (m, 2H), 3.43 – 3.31 (m, 2H), 2.31 – 2.21 (m, 1H), 2.02 – 1.85 (m, 3H), 1.45 (s, 9H).

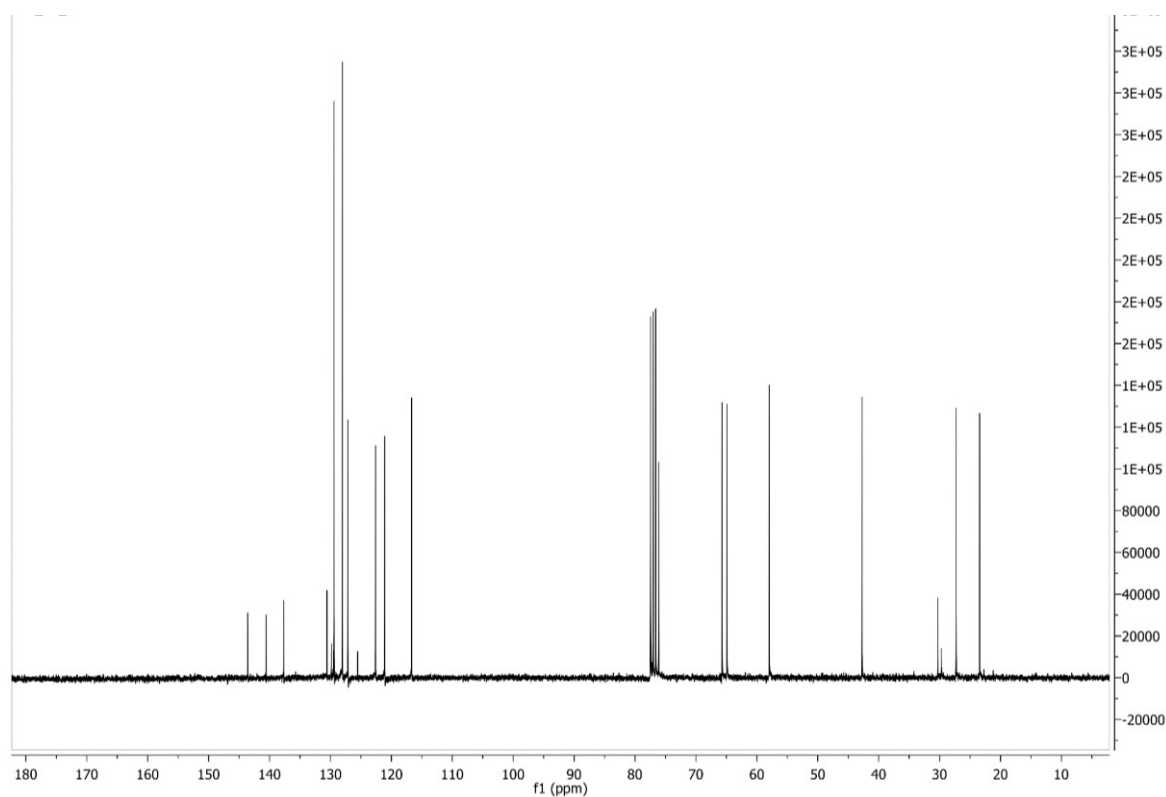
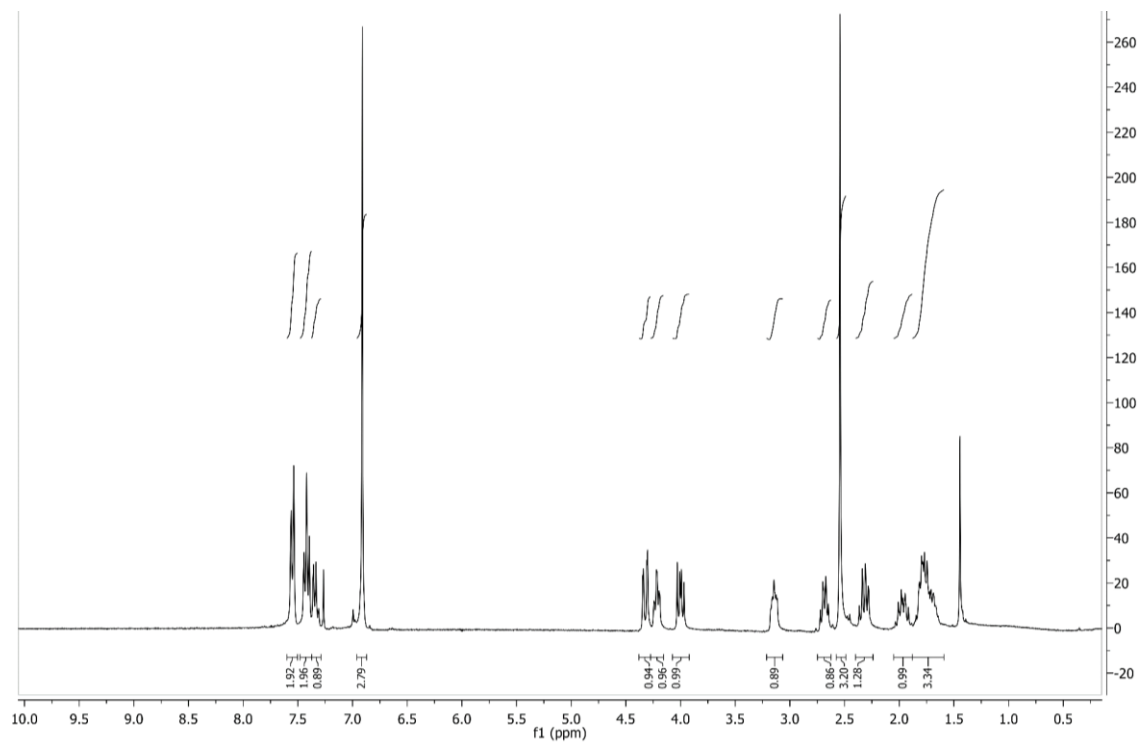
Synthesis of (*S,R*)-2-(*N*-methyl-2'-pyrrolidinyl)-5-phenyl-1,4-benzodioxane [(*S,R*)-**9d**]

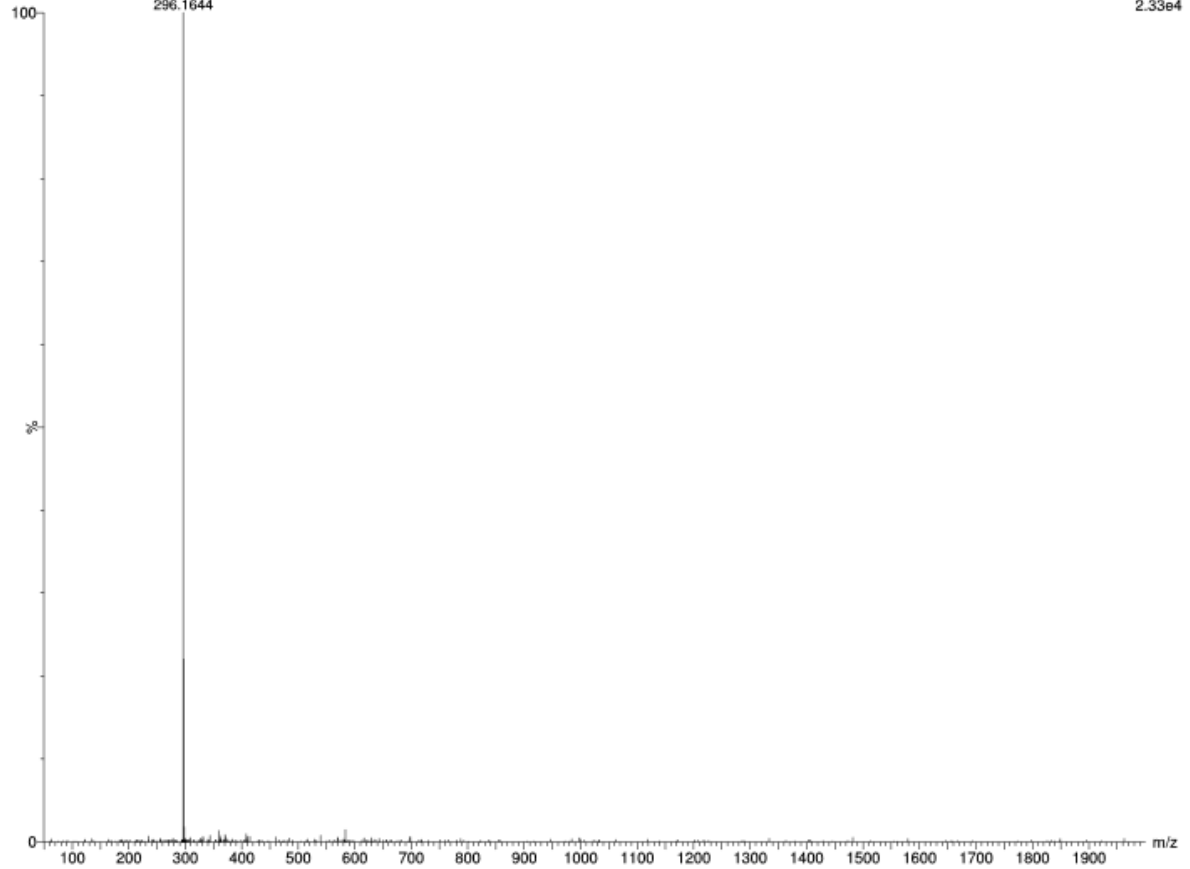


Molecular Weight: 295.38

Under a nitrogen atmosphere, at -10 °C, a solution of (*S,R*)-2-(*N*-*tert*-butoxycarbonyl-2'-pyrrolidinyl)-5-phenyl-1,4-benzodioxane [(*S,R*)-**99**] (42 mg – 0.11 mmol) in anhydrous THF (2 ml) was added dropwise to a suspension of $LiAlH_4$ (60 mg – 1.58 mmol) in anhydrous THF (3 ml). The reaction mixture was refluxed for 2 hours under vigorous stirring. Afterward, the mixture was diluted with dichloromethane and the excess of $LiAlH_4$ was quenched by slowly adding water dropwise at 0 °C. The resulting suspension was filtered through Celite® and the solvent was concentrated in vacuo, affording the pure compound (*S,R*)-**9d** as a white oil (28 mg – 0.09 mmol, 85%). **TLC** (Toluene / Ethyl Acetate 9:1 + 0.5% TEA): **R_f**= 0.26. $[\alpha]_D^{25} = +14.12$ ° (*c*0.5, $CHCl_3$). **¹H-NMR** (300 MHz, $CDCl_3$): δ 7.55 (d, *J* = 7.3 Hz, 2H), 7.42 (t, *J* = 7.3 Hz, 2H), 7.33 (t, *J* = 7.3 Hz, 1H), 6.96 – 6.87 (m, 3H), 4.32 (dd, *J* = 11.2, 1.8 Hz, 1H), 4.22 (td, *J* = 7.2, 1.8 Hz, 1H), 4.00 (dd, *J* = 11.2, 7.2 Hz, 1H), 3.21 – 3.07 (m, 1H), 2.68 (m, 1H), 2.54 (s, 3H), 2.32 (m, 1H), 2.05 – 1.88 (m, 1H), 1.88 – 1.59 (m, 3H). **¹³C-NMR** (75 MHz, $CDCl_3$): δ 143.58, 140.56, 137.66, 130.57, 129.83, 129.41, 128.02, 127.11, 125.53, 122.58, 121.09,

116.67, 76.12, 65.70, 64.88, 57.94, 42.72, 30.31, 29.71, 27.30, 23.42. **HRMS (ESI⁺)**: calc. for C₁₉H₂₂NO₂: theor. 296.1651; found [M+H]⁺: 296.1645.





Elemental Composition Report

Single Mass Analysis

Tolerance = 5.0 PPM / DBE: min = -1.5, max = 200.0
 Element prediction: Off
 Number of isotope peaks used for i-FIT = 5

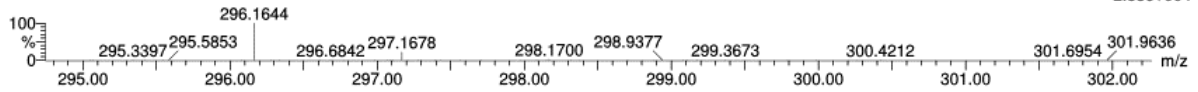
Monoisotopic Mass, Even Electron Ions

62 formula(e) evaluated with 1 results within limits (all results (up to 1000) for each mass)

Elements Used:

C: 19-19 H: 10-100 N: 0-5 O: 0-5 Na: 0-1

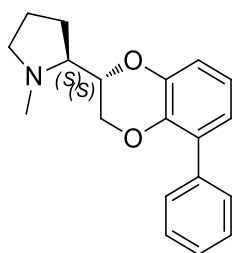
RF85 35 (0.668) AM2 (Ar,40000.0,0.00,0.00)



Minimum: -1.5
 Maximum: 0.5 5.0 200.0

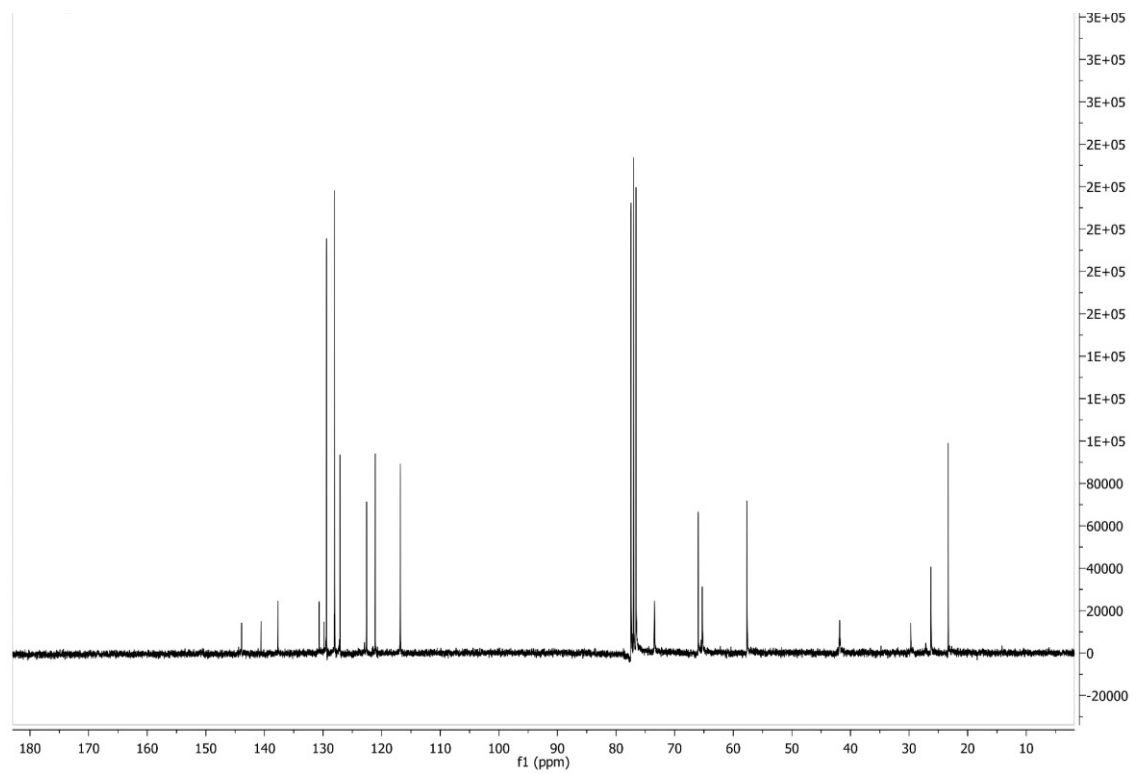
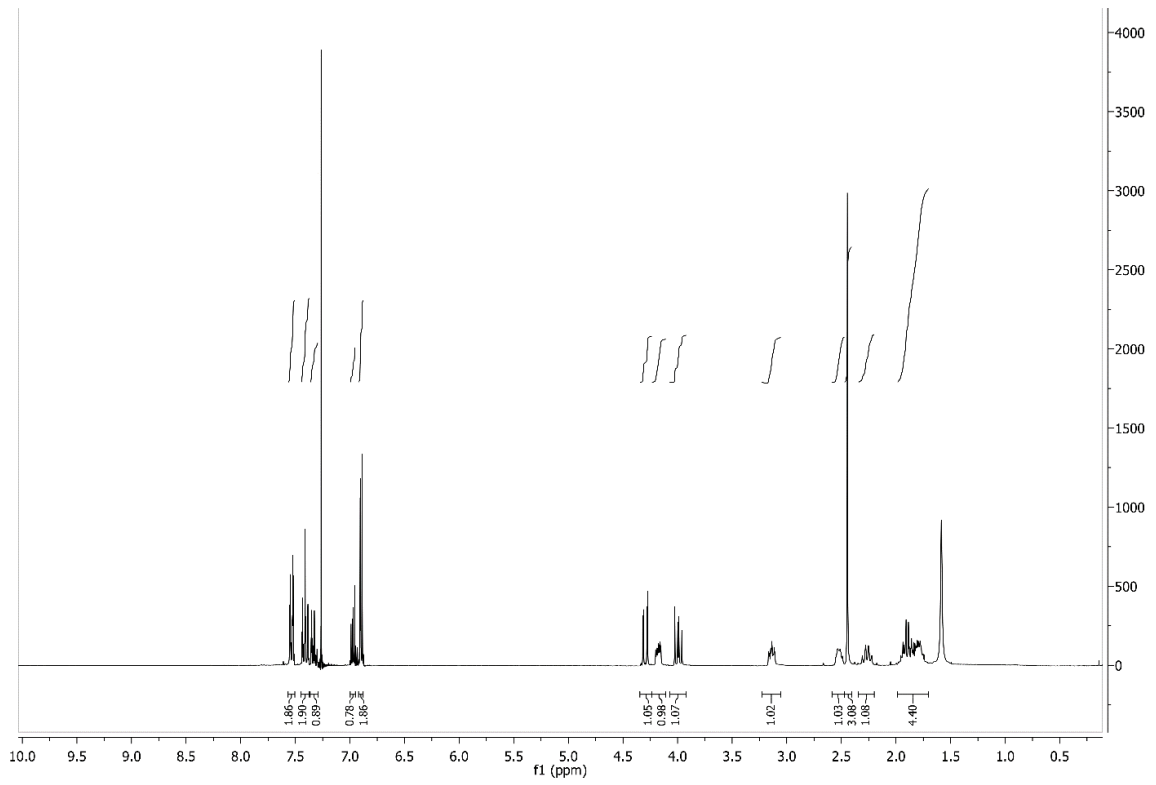
Mass	Calc. Mass	mDa	PPM	DBE	i-FIT	Norm	Conf (%)	Formula
296.1644	296.1651	-0.7	-2.4	9.5	206.9	n/a	n/a	C19 H22 N O2

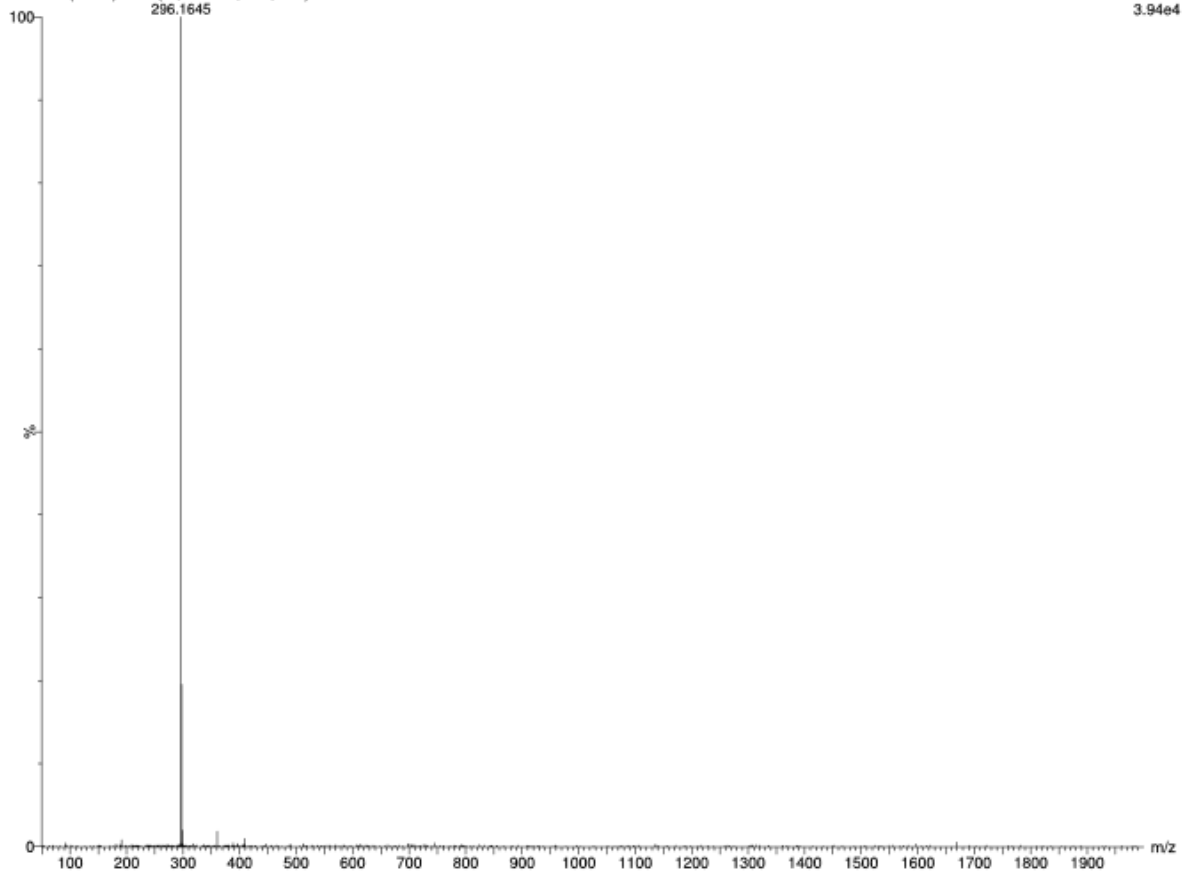
Synthesis of (*S,S*)-2-(*N*-methyl-2'-pyrrolidinyl)-5-phenyl-1,4-benzodioxane [(*S,S*)-9d]



Molecular Weight: 295.38

Under a nitrogen atmosphere, at $-10\text{ }^{\circ}\text{C}$, a solution of (*S,S*)-2-(*N-tert*-butoxycarbonyl-2'-pyrrolidinyl)-5-phenyl-1,4-benzodioxane [(*S,S*)-99] (90 mg – 0.26 mmol) in anhydrous THF (2 ml) was added dropwise to a suspension of LiAlH_4 (44 mg – 1.15 mmol) in anhydrous THF (3 ml). The reaction mixture was refluxed for 2 hours under vigorous stirring. Afterward, the mixture was diluted with dichloromethane and the excess of LiAlH_4 was quenched by slowly adding water dropwise at $0\text{ }^{\circ}\text{C}$. The resulting suspension was filtered through Celite® and the solvent was concentrated in vacuo, affording a crude that was purified through silica gel flash chromatography (toluene/ethyl acetate 9:1 + 0.5% TEA). The pure compound (*S,S*)-9d was isolated as a brownish oil (33 mg – 0.11 mmol, 39%). **TLC** (Toluene / Ethyl Acetate 9:1 + 0.5% TEA): **R_f** = 0.3. **[α]_D²⁵** = -64.74 ° (*c*0.5, CHCl_3). **¹H-NMR** (300 MHz, CDCl_3): δ 7.57 – 7.50 (m, 2H), 7.45 – 7.37 (m, 2H), 7.32 (t, *J* = 7.3 Hz, 1H), 6.97 (dd, *J* = 5.7, 4.2 Hz, 1H), 6.90 (d, *J* = 5.7 Hz, 1H), 6.89 (d, *J* = 4.2 Hz, 1H), 4.30 (dd, *J* = 11.2, 2.2 Hz, 1H), 4.18 (ddd, *J* = 8.0, 4.1, 2.2 Hz, 1H), 3.99 (dd, *J* = 11.2, 8.0 Hz, 1H), 3.23 – 3.05 (m, 1H), 2.59 – 2.47 (m, 1H), 2.45 (s, 3H), 2.26 (q, *J* = 8.4 Hz, 1H), 1.99 – 1.70 (m, 4H). **¹³C-NMR** (75 MHz, CDCl_3): δ 143.89, 140.58, 137.69, 130.67, 129.83, 129.40, 128.01, 127.11, 122.57, 121.09, 116.81, 73.45, 65.99, 65.28, 57.64, 41.86, 29.71, 26.26, 23.33. **HRMS (ESI⁺)**: calc. for $\text{C}_{19}\text{H}_{22}\text{NO}_2$: theor. 296.1651; found $[\text{M}+\text{H}]^+$: 296.1645.





Elemental Composition Report

Single Mass Analysis

Tolerance = 5.0 PPM / DBE: min = -1.5, max = 200.0
 Element prediction: Off
 Number of isotope peaks used for i-FIT = 5

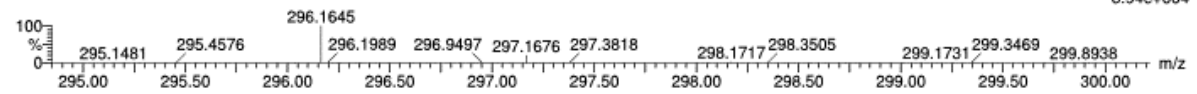
Monoisotopic Mass, Even Electron Ions

62 formula(e) evaluated with 1 results within limits (all results (up to 1000) for each mass)

Elements Used:

C: 19-19 H: 10-100 N: 0-5 O: 0-5 Na: 0-1

RF84 28 (0.549) AM2 (Ar,40000.0,0.00,0.00)

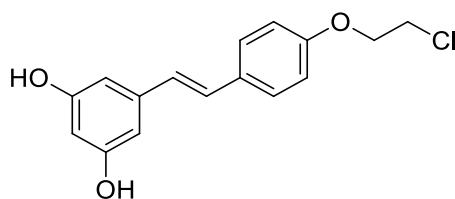


Minimum: -1.5
 Maximum: 0.5 5.0 200.0

Mass	Calc. Mass	mDa	PPM	DBE	i-FIT	Norm	Conf(%)	Formula
296.1645	296.1651	-0.6	-2.0	9.5	348.5	n/a	n/a	C19 H22 N O2

Part 2: $\alpha 7$ nAChRs

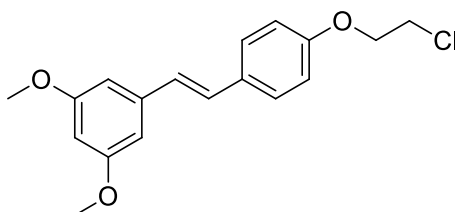
Synthesis of (*E*)-3,5-dihydroxy-4'-(2-chloroethoxy)stilbene (**115a**)



Molecular Weight: 290.74

Procedure adapted from literature.¹⁴⁰ K₂CO₃ (152 mg – 1.1 mmol) was added to a solution of resveratrol (228 mg – 1 mmol) in 1.2 ml of anhydrous DMF. After stirring for 20 minutes, 1-bromo-2-chloroethane (215 mg – 1.5 mmol) was added dropwise and the reaction was stirred overnight at 60 °C. After an HCl/AcOEt extraction, the organic phase was dried over NaSO₄, filtered and evaporated under vacuum. The crude was then purified by flash column chromatography (gradient dichloromethane/ethyl acetate from 9:1 to 8:2), affording the desired intermediate **115a** as a brownish solid (93 mg – 0.32 mmol, 32%). TLC (Dichloromethane / Ethyl Acetate 9:1): R_f = 0.22. M.p. = 161 °C. ¹H NMR (300 MHz, DMSO): δ 9.20 – 9.13 (s, 2H, exchange with D₂O), 7.49 (d, *J* = 8.8 Hz, 2H), 7.02 – 6.81 (m, 4H), 6.38 (d, *J* = 2.2 Hz, 2H), 6.10 (t, *J* = 2.2 Hz, 1H), 4.29 – 4.20 (m, 2H), 3.97 – 3.87 (m, 2H).

Synthesis of (*E*)-3,5-dimethoxy-4'-(2-chloroethoxy)stilbene (**116a**)

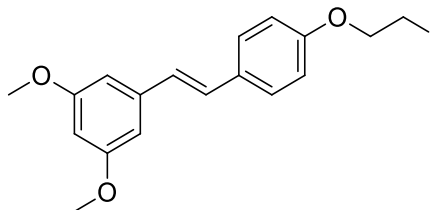


Molecular Weight: 318.79

Cs₂CO₃ (717 mg – 2.2 mmol) was added to a stirred solution of (*E*)-3,5-dihydroxy-4'-(2-chloroethoxy)stilbene (**115a**) (290 mg – 1 mmol) in anhydrous DMF (1.5 ml). The resultant mixture was stirred for 20 minutes. Afterward, MeI (312 mg – 2.2 mmol) was added dropwise and the reaction mixture was stirred overnight at room temperature. After HCl/EtOAc extraction, the organic phase was dried over NaSO₄, filtered and concentrated under vacuum. The crude residue was then purified by flash column chromatography (cyclohexane/ethyl acetate 9:1), affording the desired intermediate **116a** as a white solid (287 mg – 0.9 mmol, 90%). TLC (Cyclohexane / Ethyl acetate 9:1): R_f = 0.37. M.p. = 87 °C. ¹H NMR (300 MHz,

CDCl₃): δ 7.44 (d, J = 8.7 Hz, 2H), 7.03 (d, J = 16.3 Hz, 1H), 6.96 – 6.85 (m, 3H), 6.64 (d, J = 2.2 Hz, 2H), 6.37 (t, J = 2.2 Hz, 1H), 4.25 (t, J = 5.9 Hz, 2H), 3.85 – 3.79 (m, 8H).

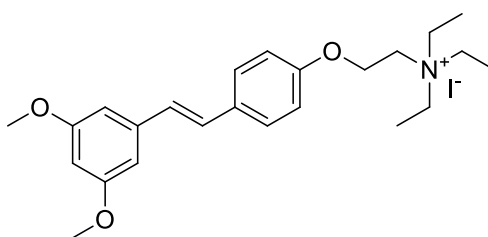
Synthesis of (*E*)-3,5-dimethoxy-4'-(2-iodoethoxy)stilbene (**117a**)



Molecular Weight: 410.25

Procedure adapted from Literature.¹⁴⁰ Intermediate (*E*)-3,5-dimethoxy-4'-(2-chloroethoxy)stilbene (**116a**) (319 mg – 1 mmol) was dissolved in a saturated solution of NaI in acetone (10 ml), which was then refluxed overnight. After concentrating under vacuum, the residue was diluted with diethyl ether and subsequently washed with 10% aqueous Na₂S₂O₅ and then with brine. The organic phase was dried over Na₂SO₄, filtered, and the solvent was evaporated under vacuum to give the desired intermediate **117a** as a white solid (398 mg – 0.97 mmol, 97%). TLC (Cyclohexane / Ethyl acetate 9:1): R_f = 0.43. M.p. = 83 °C. ¹H NMR (300 MHz, CDCl₃): δ 7.44 (d, J = 8.8 Hz, 2H), 7.03 (d, J = 16.3 Hz, 1H), 6.91 (m 3H), 6.64 (d, J = 2.2 Hz, 2H), 6.38 (t, J = 2.2 Hz, 1H), 4.27 (t, J = 6.9 Hz, 2H), 3.82 (s, 6H), 3.45 – 3.39 (t, J = 6.9 Hz, 2H).

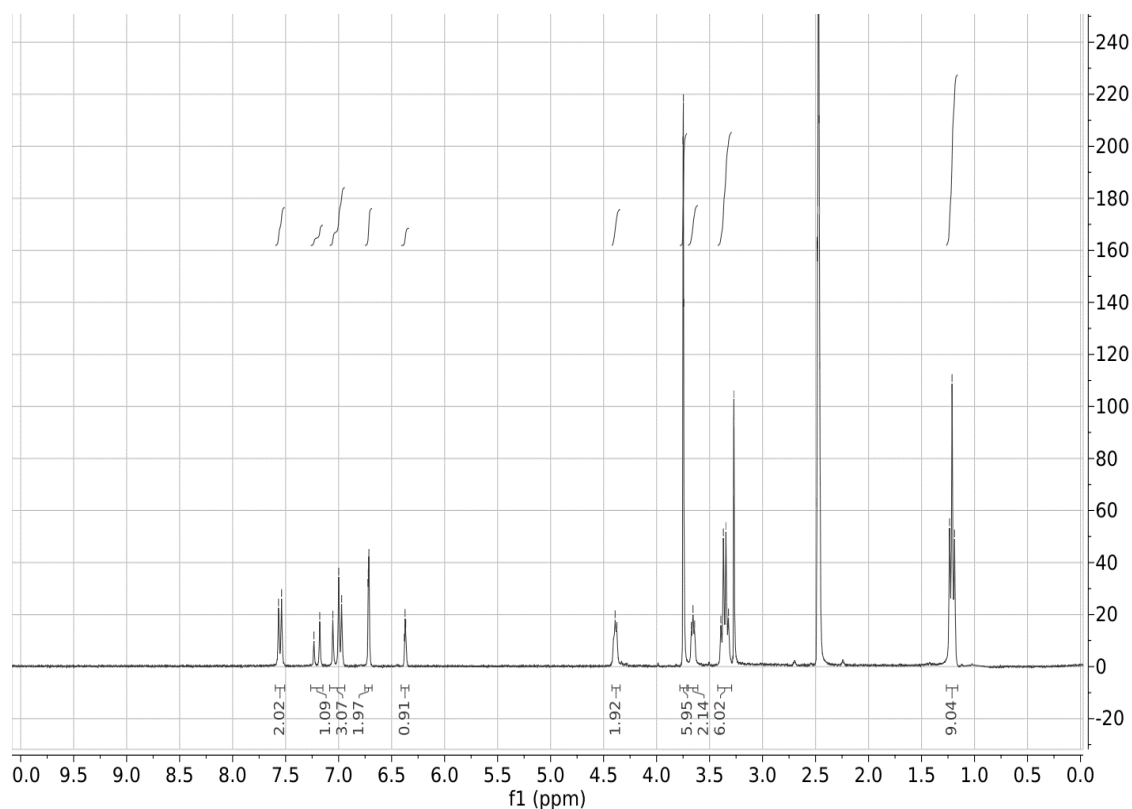
Synthesis of (*E*)-3,5-dimethoxy-4'-(2-triethylammoniummethoxy)stilbene iodide (**13**)

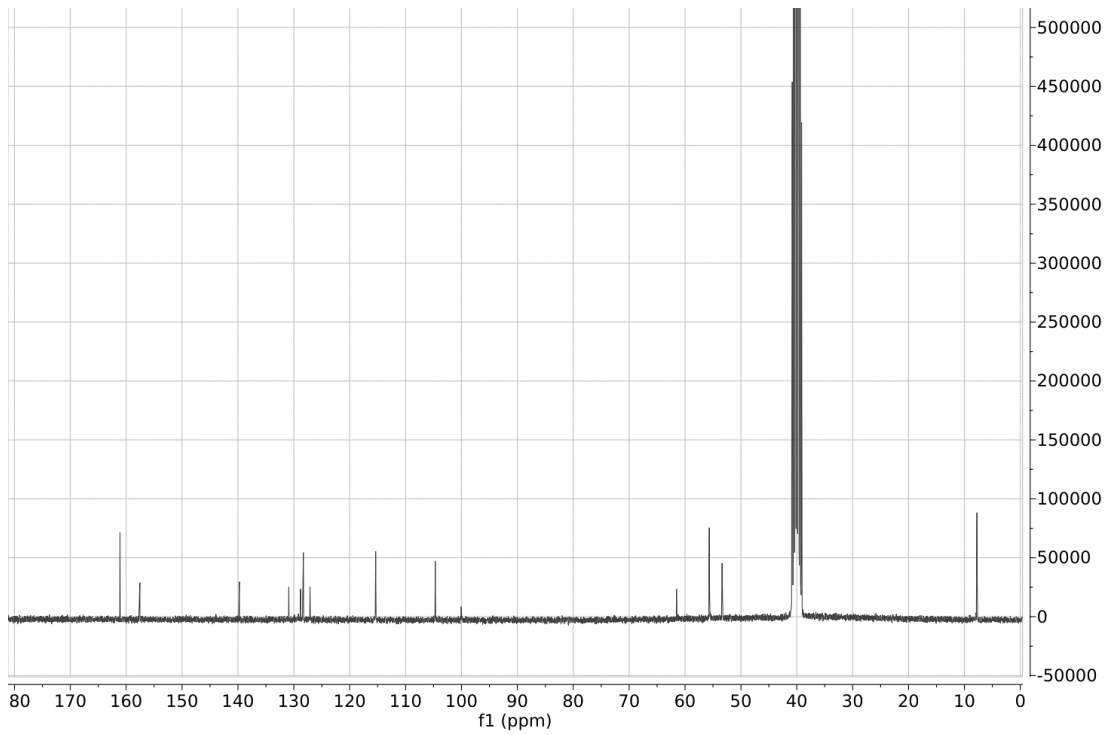


Molecular Weight: 511.44

The intermediate (*E*)-3,5-dimethoxy-4'-(2-iodoethoxy)stilbene (**117a**) (410 mg – 1 mmol) was dissolved in 3 ml of triethylamine and 3 ml of toluene and stirred at reflux temperature for 5 hours. Upon concentration under vacuum, the residue was diluted with diethyl ether and the obtained suspension was filtered, affording the desired product **13** as a solid (455 mg – 0.89 mmol, 89%). M.p. = 169 °C. ¹H NMR (300 MHz, DMSO): δ 7.56 (d, J = 8.7 Hz, 2H), 7.22 (d,

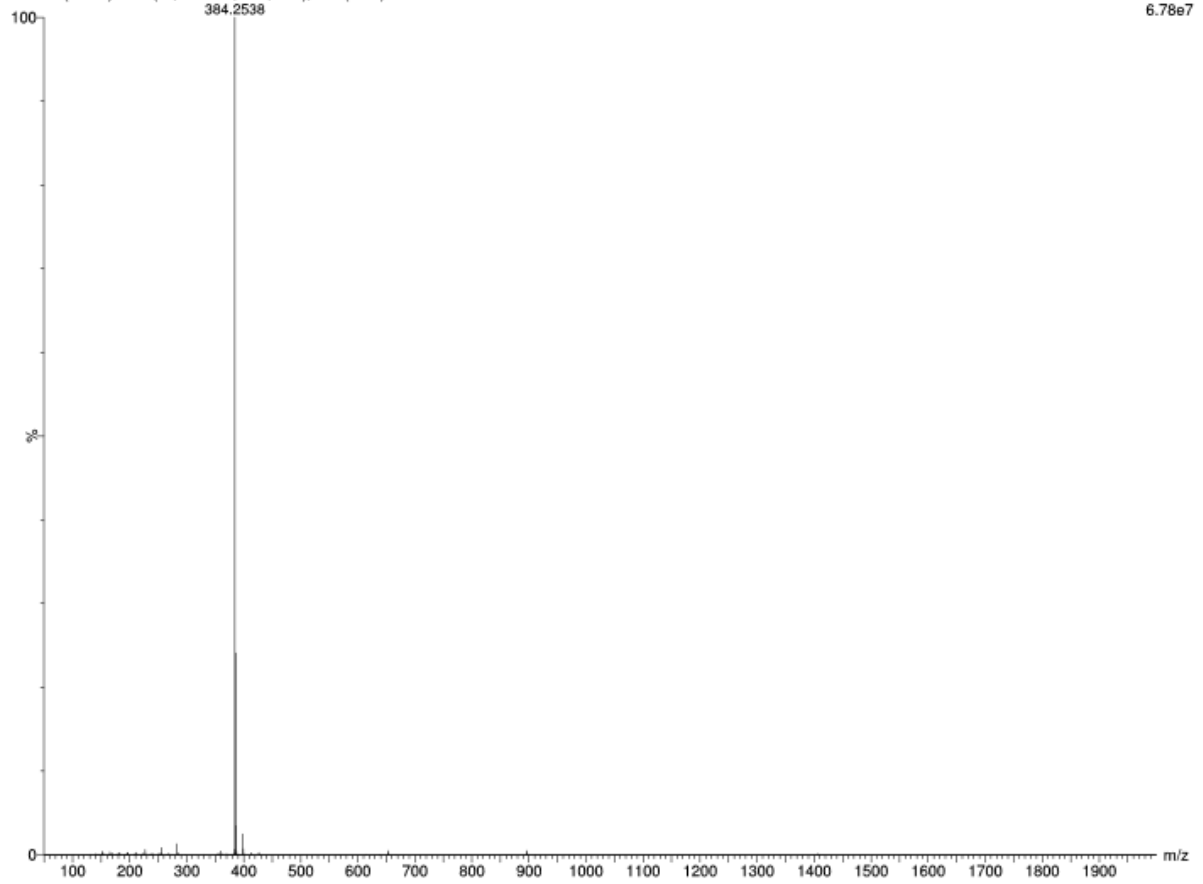
$J = 16.4$ Hz, 1H), 7.02 (m, 3H), 6.73 (d, $J = 2.2$ Hz, 2H), 6.38 (t, $J = 2.2$ Hz, 1H), 4.40 (t, $J = 4.6$ Hz, 2H), 3.76 (s, 6H), 3.67 (t, $J = 4.6$ Hz, 2H), 3.37 (q, $J = 7.1$ Hz, 6H), 1.22 (t, $J = 7.1$ Hz, 9H). ^{13}C NMR (75 MHz, DMSO): δ 161.11, 157.55, 139.75, 130.90, 128.79, 128.29, 127.11, 115.35, 104.69, 100.04, 61.51, 55.66, 53.37, 7.76. **Anal.** Calc. for $\text{C}_{24}\text{H}_{34}\text{INO}_3$: theor. C= 56.36; H= 6.70; N= 2.74; I= 24.81; found C= 56.20; H= 6.72; N= 2.73; I= 24.66. **HRMS (ESI⁺):** calc. for $\text{C}_{24}\text{H}_{34}\text{NO}_3$: theor. 384.2539; found $[\text{M}]^+$: 384.2538.





RS36 1 (0.053) AM2 (Ar,40000.0,0.00,0.00); Cm (1:52)

1: TOF MS ES+
6.78e7



Single Mass Analysis

Tolerance = 5.0 PPM / DBE: min = -1.5, max = 200.0

Element prediction: Off

Number of isotope peaks used for i-FIT = 5

Monoisotopic Mass, Even Electron Ions

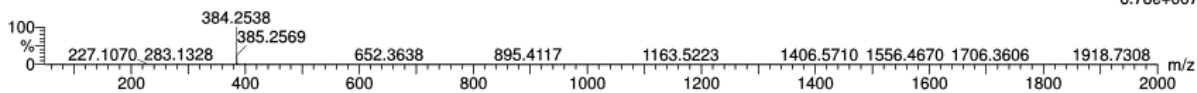
540 formula(e) evaluated with 1 results within limits (all results (up to 1000) for each mass)

Elements Used:

C: 24-24 H: 10-100 N: 0-20 O: 0-15 Na: 0-1

RS36 1 (0.053) AM2 (Ar,40000.0,0.00,0.00); Cm (1:52)

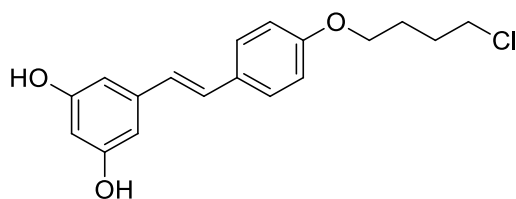
1: TOF MS ES+
6.78e+007



Minimum: -1.5
Maximum: 0.5 5.0 200.0

Mass	Calc. Mass	mDa	PPM	DBE	i-FIT	Norm	Conf (%)	Formula
384.2538	384.2539	-0.1	-0.3	8.5	2816.9	n/a	n/a	C24 H34 N O3

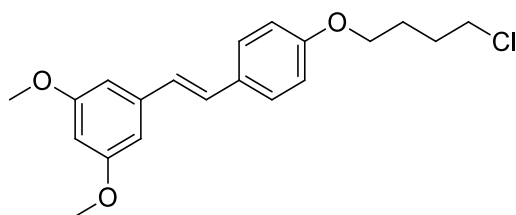
Synthesis of (*E*)-3,5-dihydroxy-4'-(4-chlorobutyloxy)stilbene (**115c**)



Molecular Weight: 318.79

Procedure adapted from literature.¹⁴⁰ K₂CO₃ (152 mg – 1.1 mmol) was added to a solution of resveratrol (228 mg – 1 mmol) in 1.2 ml of anhydrous DMF. After stirring for 20 minutes, 1-bromo-4-chlorobutane (257 mg – 1.5 mmol) was added dropwise and the reaction was stirred overnight at 60 °C. After an HCl/AcOEt extraction, the organic phase was dried over NaSO₄, filtered and evaporated under vacuum. The crude was then purified by flash column chromatography (gradient from dichloromethane to dichloromethane/methanol 9:1), affording the desired intermediate **115c** as a brownish solid (95 mg – 0.30 mmol, 30%). TLC (Dichloromethane / Methanol 9:1): R_f= 0.54. M.p.= 148 °C. ¹H NMR (300 MHz, DMSO): δ 9.18 (s, 2H, exchange with D₂O), 7.48 (d, *J* = 8.7 Hz, 2H), 6.91 (m, 4H), 6.38 (d, *J* = 2.0 Hz, 2H), 6.10 (t, *J* = 2.0 Hz, 1H), 4.00 (t, *J* = 5.9 Hz, 2H), 3.70 (t, *J* = 5.9 Hz, 2H), 1.97 – 1.70 (m, 4H).¹⁴⁰

Synthesis of (*E*)-3,5-dimethoxy-4'-(4-chlorobutyloxy)stilbene (**116c**)

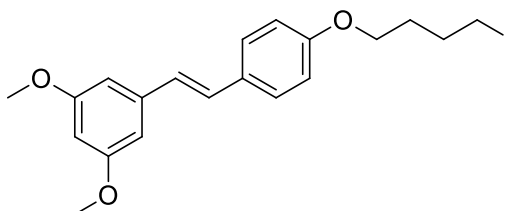


Molecular Weight: 346.85

Cs₂CO₃ (701 mg – 2.2 mmol) was added to a stirred solution of (*E*)-3,5-dihydroxy-4'-(4-chlorobutyloxy)stilbene (**115c**) (319 mg – 1 mmol) in anhydrous DMF (1.5 ml). The resultant mixture was stirred for 20 minutes. Afterward, MeI (312 mg – 2.2 mmol) was added dropwise and the reaction mixture was stirred overnight at room temperature. After HCl/EtOAc extraction, the organic phase was dried over NaSO₄, filtered and concentrated under vacuum. The crude residue was then purified by flash column chromatography (cyclohexane/ethyl acetate 95:5), affording the desired intermediate **116c** as a pale yellow solid (219 mg – 0.63 mmol, 63%). TLC (Cyclohexane / Ethyl acetate 95:5): R_f= 0.22. M.p.= 77 °C. ¹H NMR (300

MHz, CDCl₃): δ 7.43 (d, J = 8.6 Hz, 2H), 7.03 (d, J = 16.2 Hz, 1H), 6.95 – 6.81 (m, 3H), 6.65 (d, J = 1.9 Hz, 2H), 6.37 (t, J = 1.9 Hz, 1H), 4.03 (d, J = 5.8 Hz, 2H), 3.83 (s, 6H), 3.63 (t, J = 5.8 Hz, 2H), 1.97 (m, 4H).

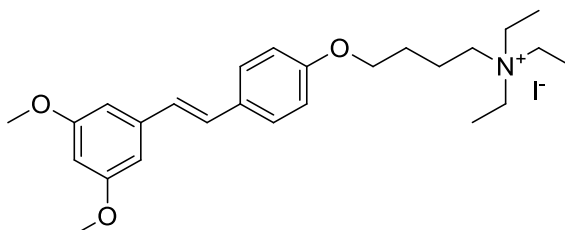
Synthesis of (*E*)-3,5-dimethoxy-4'--(4-iodobutyloxy)stilbene (**117c**)



Molecular Weight: 438.30

Procedure adapted from literature.¹⁴⁰ Intermediate (*E*)-3,5-dimethoxy-4'--(4-chlorobutyloxy)stilbene (**116c**) (347 mg – 1 mmol) was dissolved in a saturated solution of NaI in acetone (10 ml), which was then refluxed overnight. After concentrating under vacuum, the residue was diluted with diethyl ether and subsequently washed with 10% aqueous Na₂S₂O₅ and then with brine. The organic phase was dried over Na₂SO₄, filtered, and the solvent was evaporated under vacuum to give the desired intermediate **117c** as a white solid (421 mg – 0.96 mmol, 96%). TLC (Cyclohexane / Ethyl acetate 9:1): R_f = 0.36. M.p. = 87 °C. ¹H NMR (300 MHz, CDCl₃): δ 7.43 (d, J = 8.7 Hz, 2H), 7.03 (d, J = 16.3 Hz, 1H), 6.96 – 6.76 (m, 3H), 6.65 (d, J = 2.2 Hz, 2H), 6.38 (t, J = 2.2 Hz, 1H), 4.01 (t, J = 6.0 Hz, 2H), 3.83 (s, 6H), 3.27 (t, J = 6.8 Hz, 2H), 2.14 – 1.85 (m, 4H).

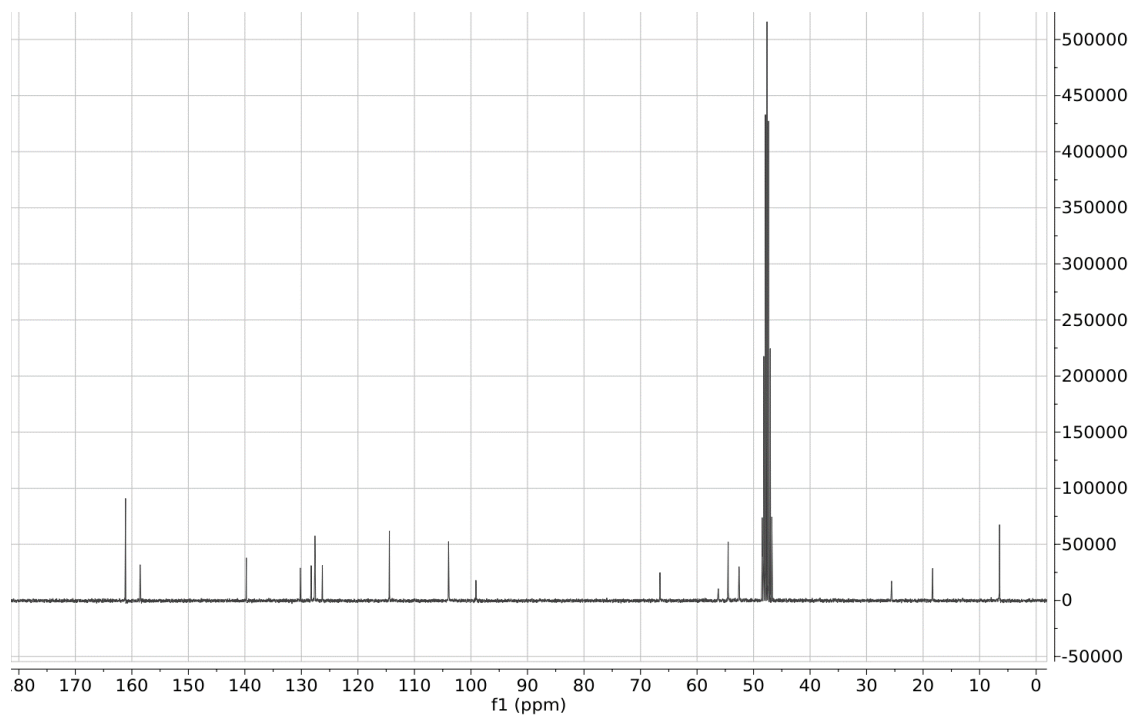
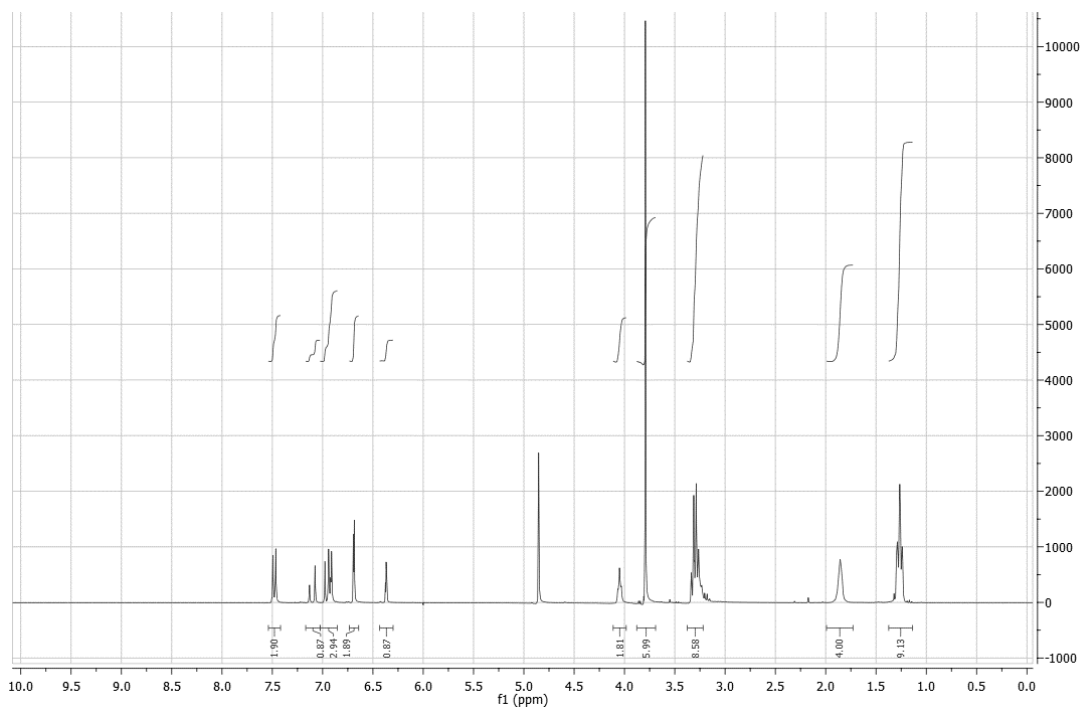
Synthesis of (*E*)-3,5-dimethoxy-4'--(4-triethylammoniumbutyloxy)stilbene iodide (**17**)

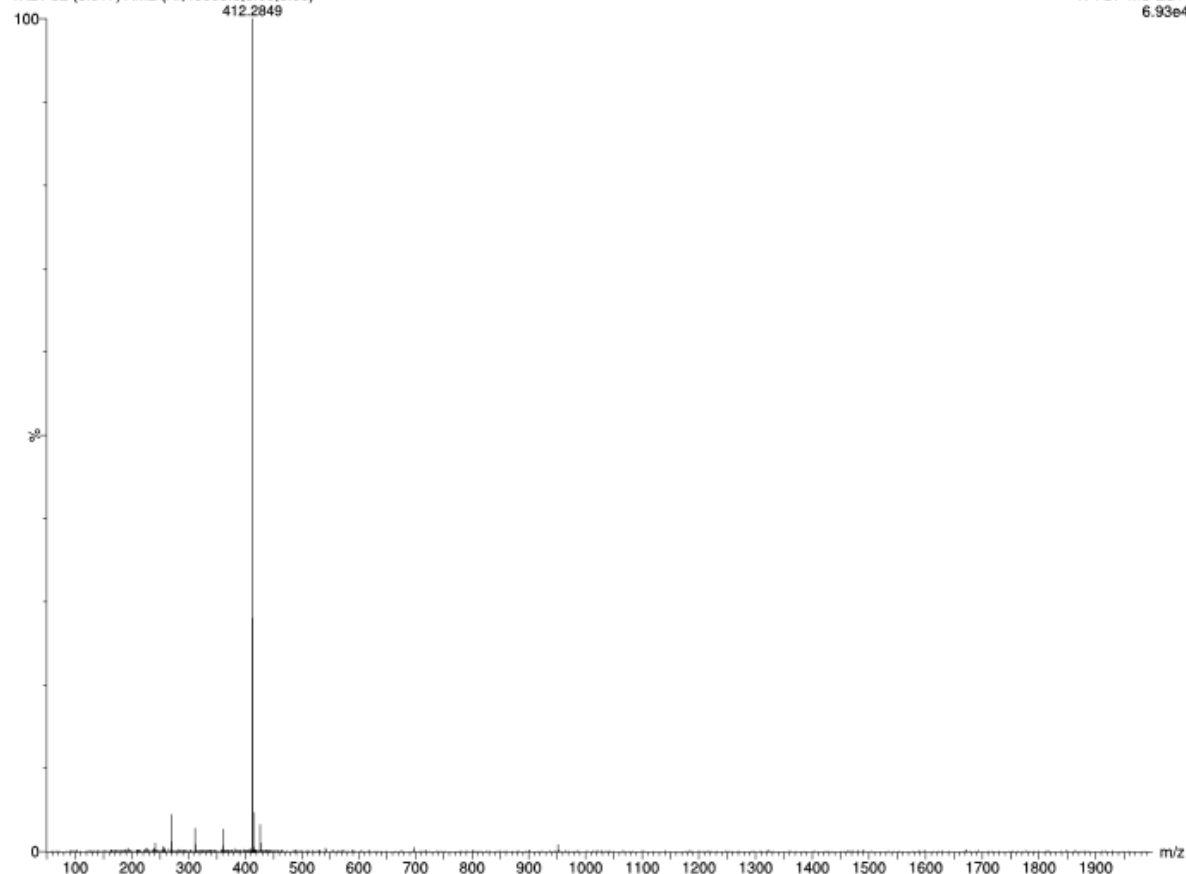


Molecular Weight: 539.49

The intermediate (*E*)-3,5-dimethoxy-4'--(4-iodobutyloxy)stilbene (**117c**) (438 mg – 1 mmol) was dissolved in 3 ml of triethylamine and 3 ml of toluene and stirred at reflux temperature for 5 hours. Upon concentration under vacuum, the residue was diluted with diethyl ether and the obtained suspension was filtered, affording the desired product **17** as a solid (496 mg – 0.92

mmol, 92%). **M.p.** = 138 °C. **¹H NMR** (300 MHz, MeOD): δ 7.54 – 7.43 (m, 2H), 7.10 (d, *J* = 16.3 Hz, 1H), 7.01 – 6.86 (m, 3H), 6.69 (d, *J* = 2.2 Hz, 2H), 6.37 (t, *J* = 2.2 Hz, 1H), 4.05 (t, *J* = 5.4 Hz, 2H), 3.79 (s, 6H), 3.37 – 3.25 (m, 8H), 1.85 (m, 4H), 1.26 (t, *J* = 7.4, 9H). **¹³C NMR** (75 MHz, MeOD): δ 161.12, 158.53, 139.74, 130.20, 128.27, 127.60, 126.29, 114.44, 103.96, 99.13, 66.56, 56.24, 54.49, 52.57, 25.59, 18.30, 6.47. **Anal.** Calc. for C₂₆H₃₈INO₃: theor. C = 57.88; H = 7.10; N = 2.60; I = 23.52; found C = 57.69; H = 7.10; N = 2.59; I = 23.58. **HRMS (ESI⁺)**: calc. for C₂₆H₃₈NO₃: theor. 412.2852; found [M]⁺: 412.2849.





Elemental Composition Report

Single Mass Analysis

Tolerance = 5.0 PPM / DBE: min = -1.5, max = 200.0
 Element prediction: Off
 Number of isotope peaks used for i-FIT = 5

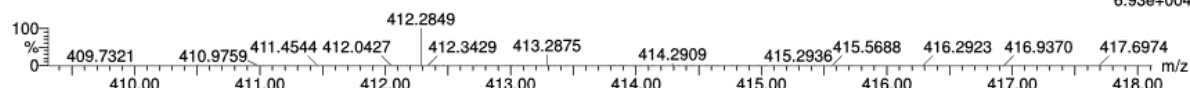
Monoisotopic Mass, Even Electron Ions

61 formula(e) evaluated with 1 results within limits (all results (up to 1000) for each mass)

Elements Used:

C: 26-26 H: 10-100 N: 0-5 O: 0-5 Na: 0-1

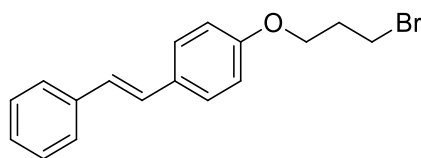
VA21 32 (0.617) AM2 (Ar,40000.0,0.00,0.00)



Minimum: -1.5
 Maximum: 0.5 5.0 200.0

Mass	Calc. Mass	mDa	PPM	DBE	i-FIT	Norm	Conf (%)	Formula
412.2849	412.2852	-0.3	-0.7	8.5	407.1	n/a	n/a	C26 H38 N O3

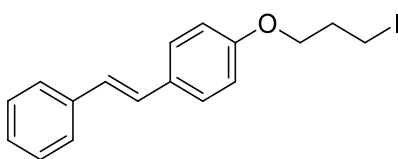
Synthesis of (*E*)-4-(3-bromopropoxy)stilbene (**118b**)



Molecular Weight: 317.22

Procedure adapted from literature.¹⁹² A solution of *trans*-4-hydroxystilbene (196 mg – 1 mmol) in DMSO (1.4 ml) was added to a stirred suspension of finely ground NaOH (85 mg – 2.1 mmol) in DMSO (5.6 ml). The mixture was stirred at room temperature for 30 minutes and then the 1,3-dibromopropane (403 mg – 2 mmol) was added dropwise. When stilbenol was reacted, the reaction mixture was filtered and 1M aqueous solution of HCl was added dropwise to the filtrate to reach pH 3. The crude product was precipitated by slowly adding cold water. The precipitate was isolated by filtration, dried under vacuum and recrystallized from ethanol affording a crude that was further purified through silica gel flash chromatography (gradient from hexane to hexane/acetonitrile 9:1). The pure product **118b** was obtained as a beige solid (165 mg – 0.52 mmol, 52%). TLC (cyclohexane/ethyl acetate 9:1): R_f = 0.61. M.p. = 109 °C; literature¹⁹²: M.p. = 108 – 109 °C. ¹H NMR (300 MHz, CDCl₃): δ 7.54 – 7.41 (m, 4H), 7.35 (t, *J* = 6.7 Hz, 2H), 7.26 – 7.19 (m, 1H), 7.08 (d, *J* = 15.5 Hz, 1H), 7.03 – 6.87 (m, 3H), 4.14 (t, *J* = 6.4 Hz, 2H), 3.62 (t, *J* = 7.0 Hz, 2H), 2.34 (m, 2H).¹⁹²

Synthesis of (*E*)-4-(3-iodopropoxy)stilbene (**119b**)

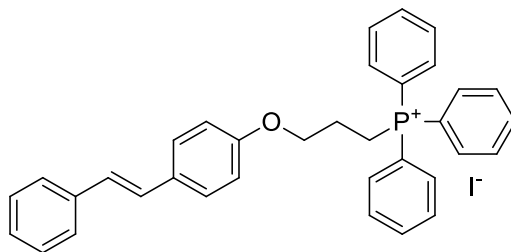


Molecular Weight: 364.22

Procedure adapted from literature.¹⁴⁰ Intermediate (*E*)-4-(3-bromopropoxy)stilbene (**118b**) (317 mg – 1 mmol) was dissolved in a saturated solution of NaI in acetone (10 ml), which was then refluxed overnight. After concentrating under vacuum, the residue was diluted with diethyl ether and subsequently washed with 10% aqueous Na₂S₂O₅ and then with brine. The organic phase was dried over Na₂SO₄, filtered, and the solvent was evaporated under vacuum to give the desired intermediates **119b** as a white solid (357 mg – 0.98 mmol, 98%). TLC (cyclohexane/ethyl acetate 9:1): R_f = 0.69. M.p. = 117 °C. ¹H NMR (300 MHz, CDCl₃): δ 7.47

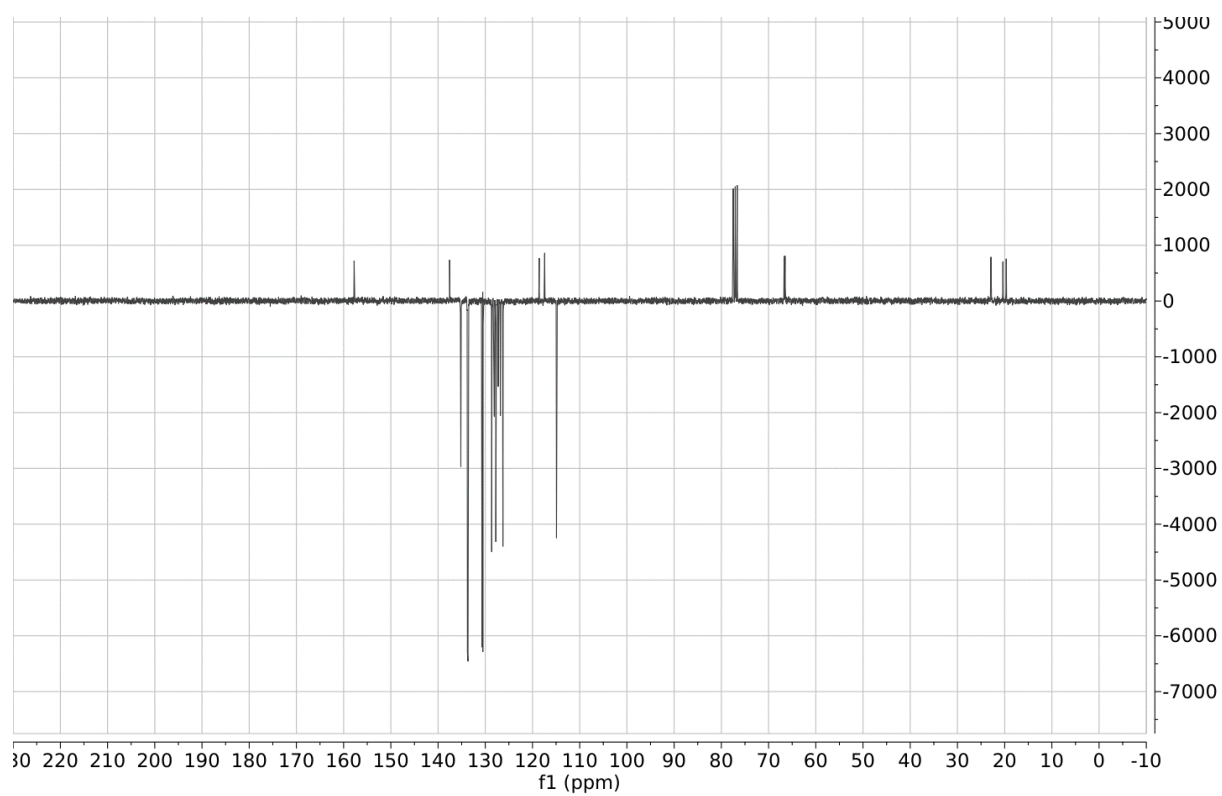
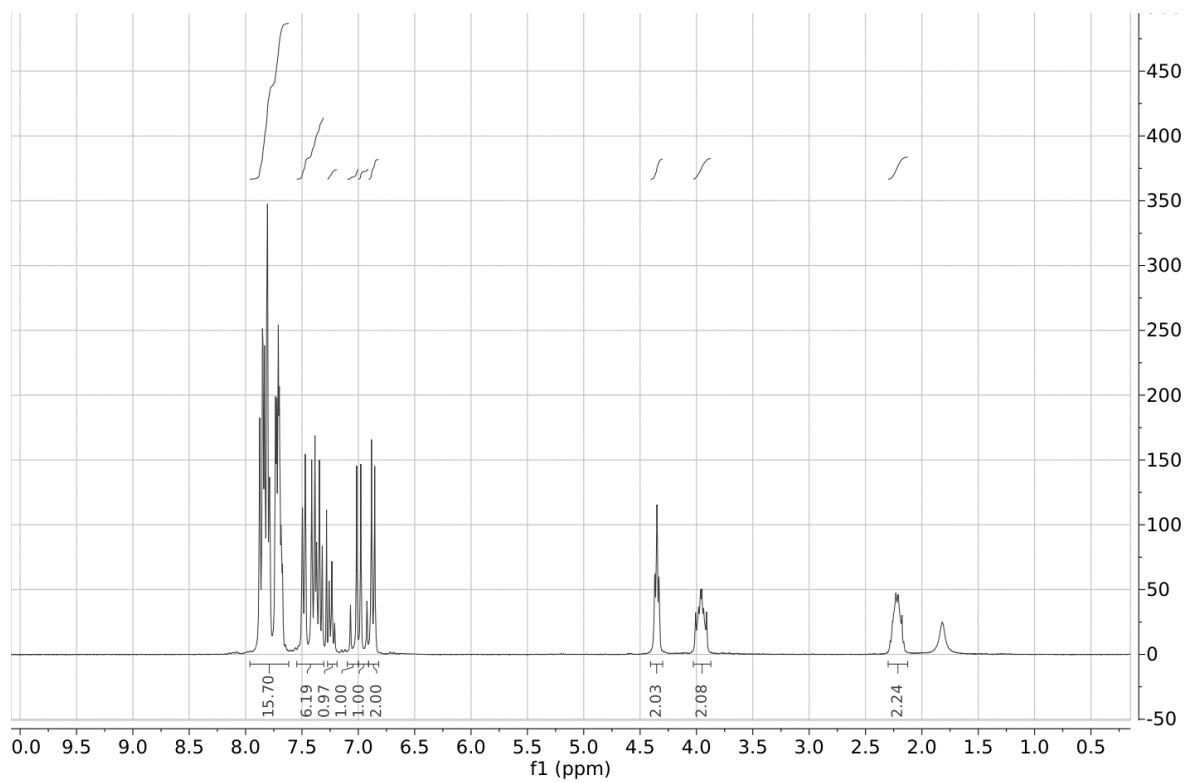
(m, 4H), 7.34 (t, $J = 7.4$ Hz, 2H), 7.23 (m, 1H), 7.07 (d, $J = 16.2$ Hz, 1H), 6.97 (d, $J = 16.2$ Hz, 1H), 6.89 (d, $J = 8.8$ Hz, 2H), 4.07 (t, $J = 5.4$ Hz, 2H), 3.38 (t, $J = 6.2$ Hz, 2H), 2.29 (m, 2H).

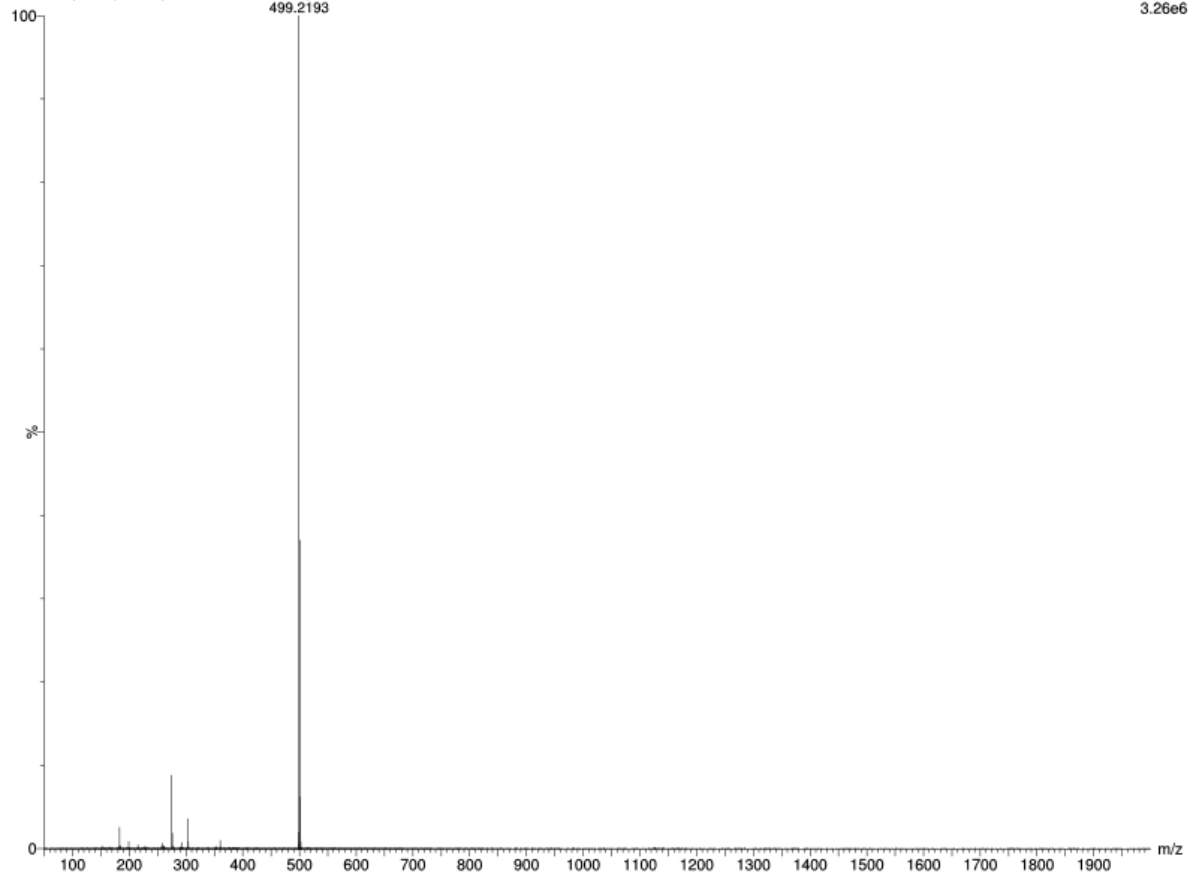
Synthesis of (*E*)-4-(3-triphenylphosphoniumpropoxy)stilbene iodide (**18**)



Molecular Weight: 626.51

Procedure adapted from literature.¹⁴⁰ A solid mixture of PPh₃ (5.25 g – 20 mmol) and intermediate (*E*)-4-(3-iodopropoxy)stilbene (**119b**) (364 mg – 1 mmol) was heated to 100 °C so as to obtain a solution of the starting material in molten PPh₃. The reaction mixture was slowly stirred at 100 °C for 3 hours and then cooled to room temperature without stirring any further. The re-solidified mixture was dissolved in the smallest possible volume of dichloromethane and diethyl ether was added dropwise under vigorous stirring. Afterwards, the solid precipitate was isolated by filtration affording the desired product **18** as a pale yellow solid (451 mg – 0.72 mmol, 72%). **M.p.** = 107 °C. **¹H NMR** (300 MHz, CDCl₃): δ 7.96 – 7.62 (m, 15H), 7.55 – 7.31 (m, 6H), 7.27 – 7.19 (m, 1H), 7.04 (d, $J = 16.3$ Hz, 1H), 6.95 (d, $J = 16.3$ Hz, 1H), 6.91 – 6.82 (m, 2H), 4.35 (t, $J = 5.7$ Hz, 2H), 4.03 – 3.87 (m, 2H), 2.30 – 2.13 (m, 2H). **¹³C NMR** (75 MHz, CDCl₃) δ 157.78, 137.55, 135.20, 135.17, 133.79, 133.69, 130.67, 130.50, 128.65, 128.09, 127.77, 127.26, 126.81, 126.26, 118.57, 117.42, 114.92, 66.71, 66.49, 22.90, 22.86, 20.37, 19.67. **Anal.** Calc. for C₃₅H₃₂IOP: theor. C= 67.10; H= 5.15; P= 4.94; I= 20.26; found C= 66.91; H= 5.15; P= 4.90; I= 20.20. **HRMS (ESI⁺)**: calc. for C₃₅H₃₂OP: theor. 499.2191; found [M]⁺: 499.2193.





Elemental Composition Report

Single Mass Analysis

Tolerance = 5.0 PPM / DBE: min = -1.5, max = 200.0
 Element prediction: Off
 Number of isotope peaks used for i-FIT = 5

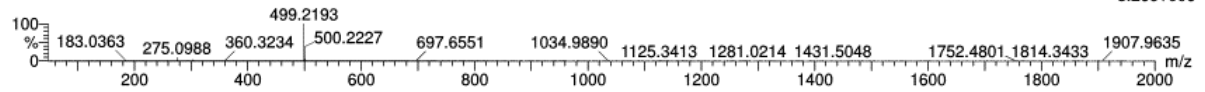
Monoisotopic Mass, Even Electron Ions

331 formula(e) evaluated with 1 results within limits (all results (up to 1000) for each mass)

Elements Used:

C: 35-35 H: 10-10 O: 0-15 Na: 0-1 P: 0-10

ST27 33 (0.634) AM2 (Ar,40000.0,0.00,0.00)



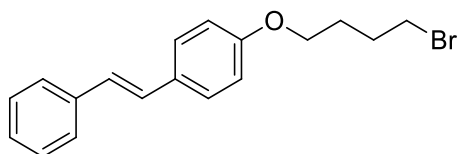
Minimum:

Maximum: 0.5 5.0 -1.5

Mass	Calc. Mass	mDa	PPM	DBE	i-FIT	Norm	Conf(%)	Formula
------	------------	-----	-----	-----	-------	------	---------	---------

499.2193	499.2191	0.2	0.4	20.5	1528.1	n/a	n/a	C35 H32 O P
----------	----------	-----	-----	------	--------	-----	-----	-------------

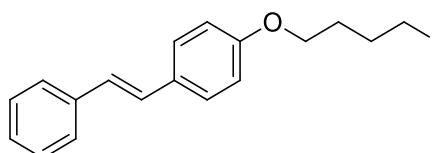
Synthesis of (*E*)-4-(4-bromobutyloxy)stilbene (**118c**)



Molecular Weight: 331.25

Procedure adapted from literature.¹⁹² A solution of *trans*-4-hydroxystilbene (196 mg – 1 mmol) in DMSO (1.4 ml) was added to a stirred suspension of finely ground NaOH (85 mg – 2.1 mmol) in DMSO (5.6 ml). The mixture was stirred at room temperature for 30 minutes and then the 1,4-dibromobutane (431 mg – 2 mmol) was added dropwise. When stilbenol was reacted, the reaction mixture was filtered and 1M aqueous solution of HCl was added dropwise to the filtrate to reach pH 3. The crude product was precipitated by slowly adding cold water. The precipitate was isolated by filtration, dried under vacuum and recrystallized from ethanol affording the pure compound **118c** as a white solid (123 mg – 0.37 mmol, 37%). **TLC** (cyclohexane/ethyl acetate 9:1): **R_f** = 0.61. **M.p.** = 115 °C; literature¹⁹²: **M.p.** = 108 – 110 °C. **¹H NMR** (300 MHz, CDCl₃): δ 7.50 – 7.43 (m, 4H), 7.34 (t, *J* = 7.7 Hz, 2H), 7.23 (m, 1H), 7.06 (d, *J* = 16.3 Hz, 1H), 6.97 (d, *J* = 16.3 Hz, 1H), 6.88 (d, *J* = 8.7 Hz, 2H), 4.02 (t, *J* = 5.9 Hz, 2H), 3.50 (t, *J* = 6.5 Hz, 2H), 2.16 – 2.02 (m, 2H), 2.00 – 1.93 (m, 2H).¹⁹²

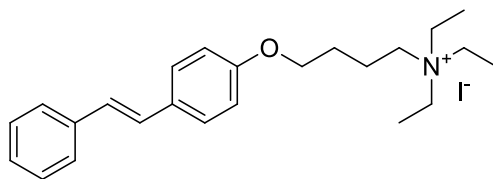
Synthesis of (*E*)-4-(4-iodobutyloxy)stilbene (**119c**)



Molecular Weight: 378.25

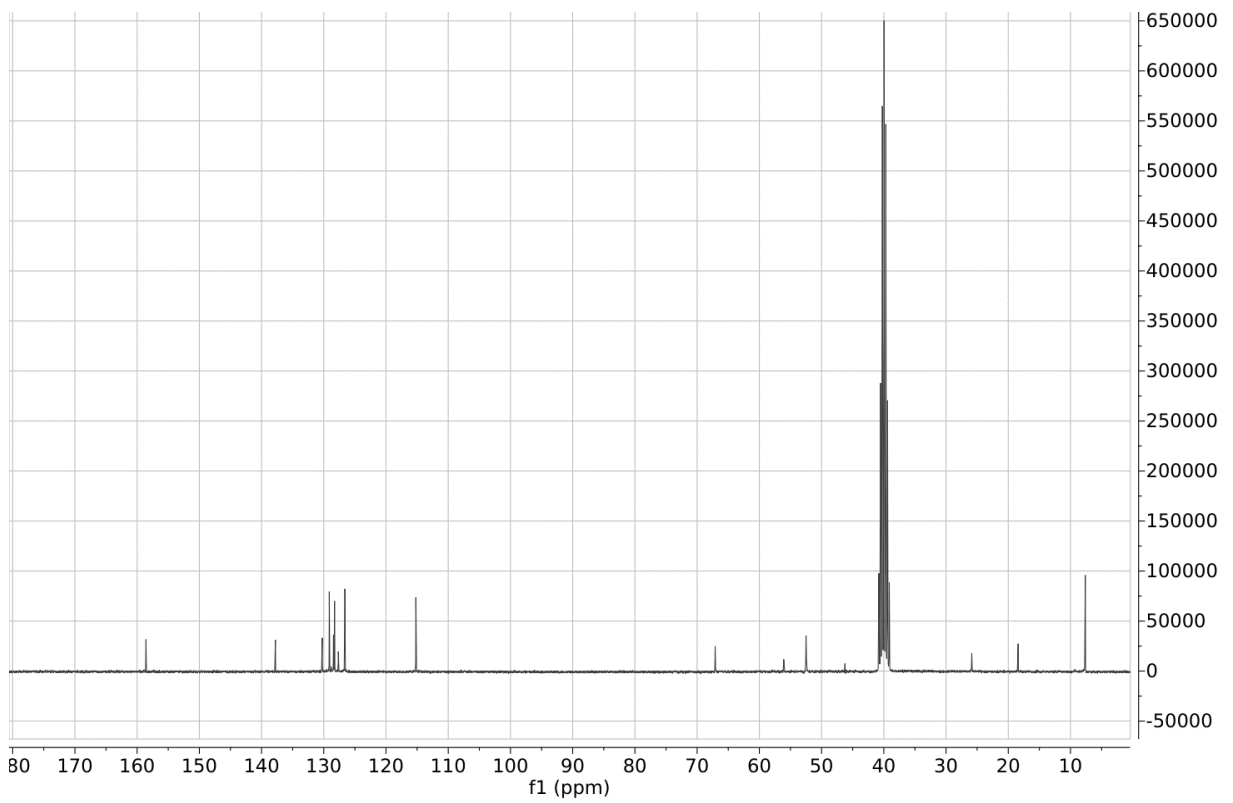
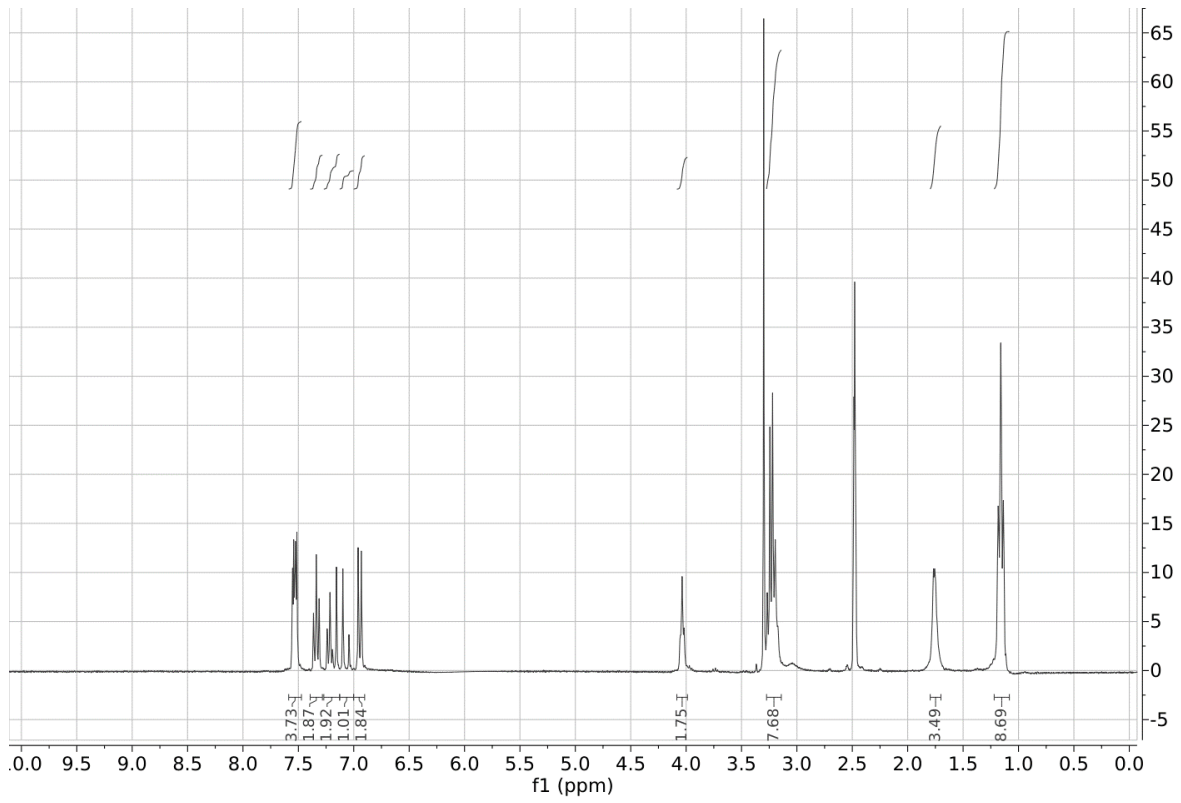
Intermediate (*E*)-4-(4-bromobutyloxy)stilbene (**118c**) (331 mg – 1 mmol) was dissolved in a saturated solution of NaI in acetone (10 ml), which was then refluxed overnight. After concentrating under vacuum, the residue was diluted with diethyl ether and subsequently washed with 10% aqueous Na₂S₂O₅ and then with brine. The organic phase was dried over Na₂SO₄, filtered, and the solvent was evaporated under vacuum to give the desired intermediate **119c** as a white solid (374 mg – 0.99 mmol, 99%). **TLC** (cyclohexane/ethyl acetate 9:1): **R_f** = 0.66. **M.p.** = 124 °C. **¹H NMR** (300 MHz, CDCl₃): δ 7.47 (m, 4H), 7.34 (t, *J* = 7.6 Hz, 2H), 7.23 (m, 1H), 7.06 (d, *J* = 16.3 Hz, 1H), 6.97 (d, *J* = 16.3 Hz, 1H), 6.88 (t, *J* = 8.7 Hz, 2H), 4.01 (t, *J* = 6.0 Hz, 2H), 3.27 (t, *J* = 6.8 Hz, 2H), 2.12 – 1.98 (m, 2H), 1.98-1.83 (m, 2H).

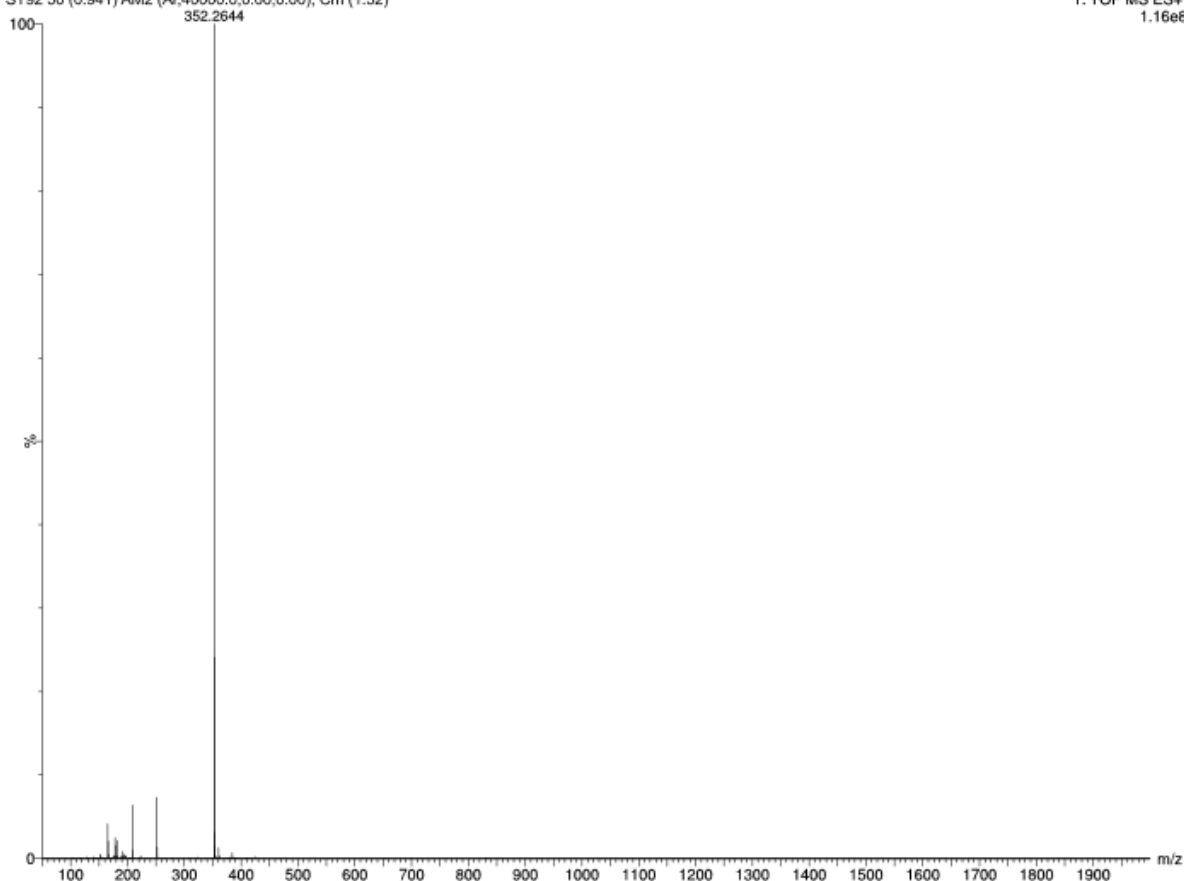
Synthesis of (*E*)-4-(4-(triethylammoniumbutyloxy)stilbene iodide (**15**)



Molecular Weight: 479.44

Intermediate (*E*)-4-(4-iodobutyloxy)stilbene (**119c**) (378 mg – 1 mmol) was dissolved in 3 ml of triethylamine and 3 ml of toluene for 5 hours. Upon concentration under vacuum, the residue was diluted with diethyl ether and the obtained suspension was filtered, affording the desired product **15** as a beige solid (441 mg – 0.92 mmol, 92%). **M.p.** = 159 °C. **¹H NMR** (300 MHz, DMSO): δ 7.57 – 7.49 (m, 4H), 7.34 (t, J = 7.6 Hz, 2H), 7.26 – 7.13 (m, 2H), 7.07 (d, J = 16.4 Hz, 1H), 6.95 (d, J = 8.7 Hz, 2H), 4.03 (m, 2H), 3.23 (m, 8H), 1.76 (m, 4H), 1.16 (t, J = 7.0 Hz, 9H). **¹³C NMR** (75 MHz, DMSO): δ 158.58, 137.78, 130.24, 129.12, 128.82, 128.44, 128.26, 127.67, 126.63, 126.61, 115.20, 67.10, 56.08, 52.53, 52.49, 52.45, 46.24, 25.86, 18.41, 7.62. **Anal.** Calc. for C₂₄H₃₄INO: theor. C = 60.12; H = 7.15; N = 2.92; I = 26.47; found C = 59.92; H = 7.18; N = 2.89; I = 26.58. **HRMS (ESI⁺)**: calc. for C₂₄H₃₄NO: theor. 352.2640; found [M]⁺: 352.2644.





Elemental Composition Report

Single Mass Analysis

Tolerance = 5.0 PPM / DBE: min = -1.5, max = 200.0
 Element prediction: Off
 Number of isotope peaks used for i-FIT = 5

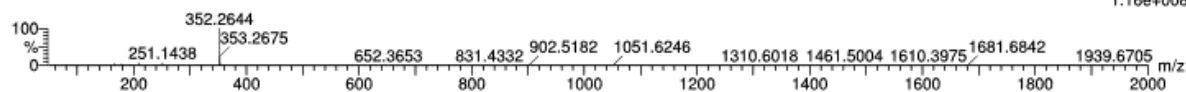
Monoisotopic Mass, Even Electron Ions

494 formula(e) evaluated with 1 results within limits (all results (up to 1000) for each mass)

Elements Used:

C: 24-24 H: 10-100 N: 0-20 O: 0-15 Na: 0-1

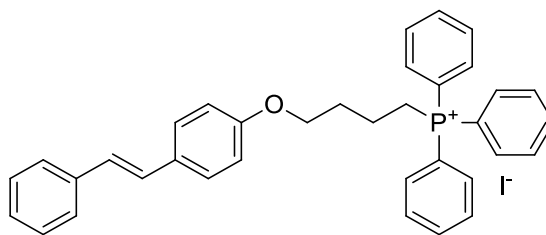
ST92 50 (0.941) AM2 (Ar,40000.0,0.00,0.00); Cm (1:52)



Minimum: -1.5
 Maximum: 0.5 5.0 200.0

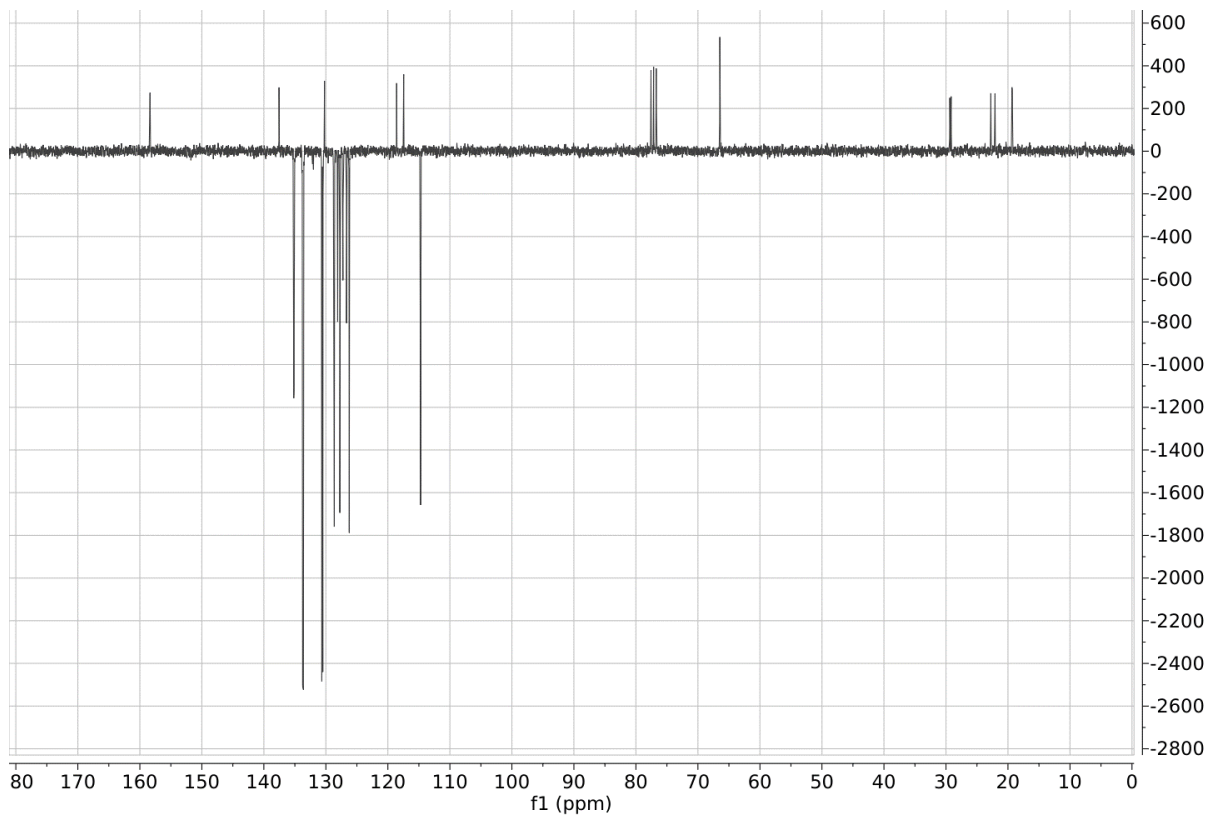
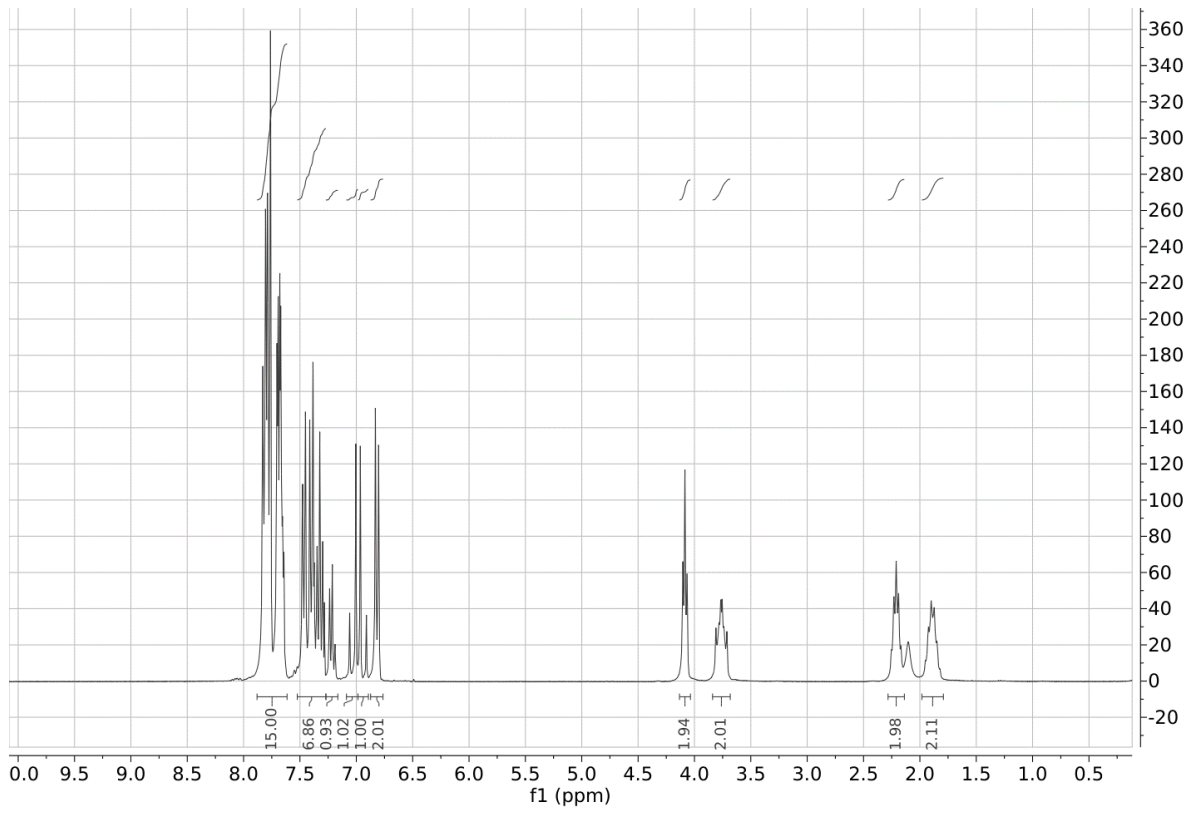
Mass	Calc. Mass	mDa	PPM	DBE	i-FIT	Norm	Conf (%)	Formula
352.2644	352.2640	0.4	1.1	8.5	3155.7	n/a	n/a	C24 H34 N O

Synthesis of (*E*)-4-(4-triphenylphosphoniumbutyloxy)stilbene iodide (**16**)



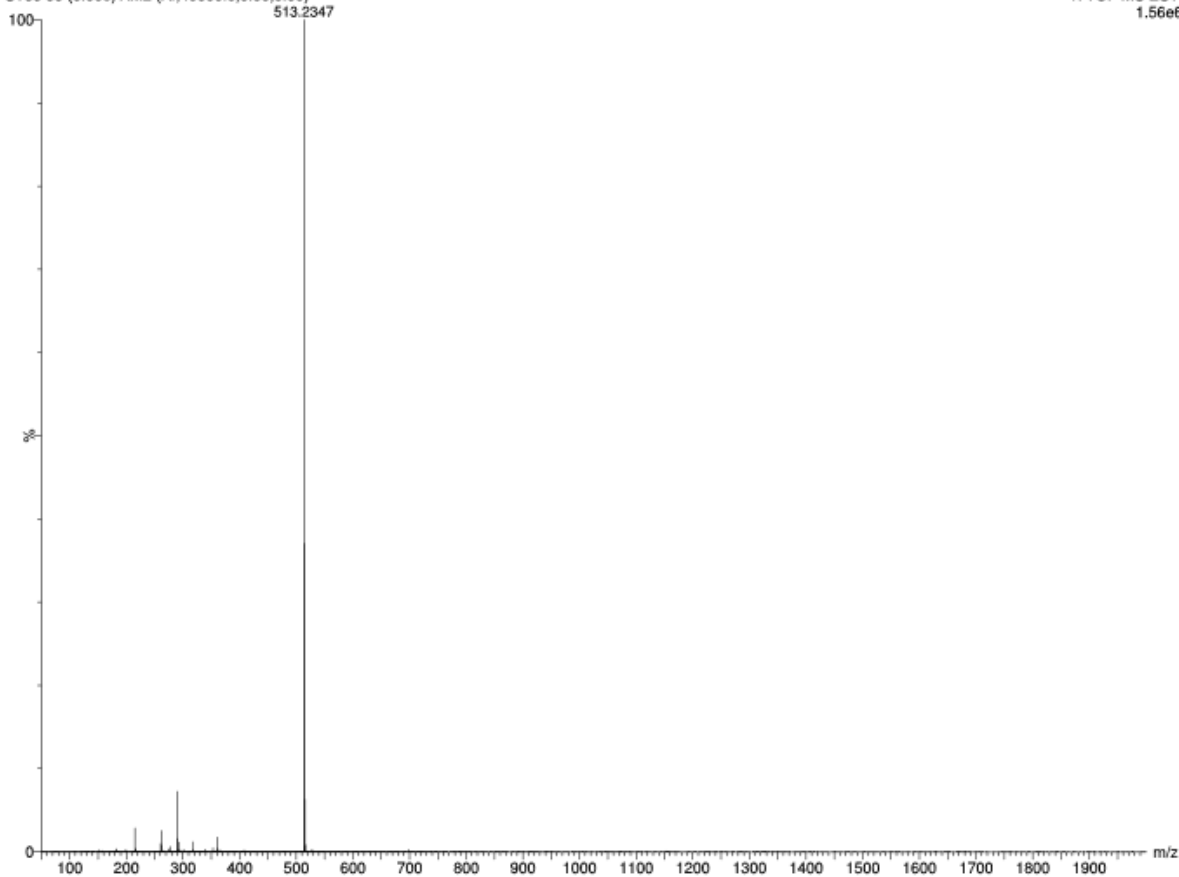
Molecular Weight: 640.53

Procedure adapted from literature.¹⁴⁰ A solid mixture of PPh₃ (5.25 g – 20 mmol) and intermediate (*E*)-4-(4-iodobutyloxy)stilbene (**119c**) (378 mg – 1 mmol) was heated to 100 °C so as to obtain a solution of the starting material in molten PPh₃. The reaction mixture was slowly stirred at 100 °C for 3 hours and then cooled to room temperature without stirring any further. The re-solidified mixture was dissolved in the smallest possible volume of dichloromethane and diethyl ether was added dropwise under vigorous stirring. Afterwards, the solid precipitate was isolated by filtration affording the desired product (**16**) as a white solid (512 mg – 0.80 mmol, 80%). **M.p.** = 109 °C. **¹H NMR** (300 MHz, CDCl₃): δ 7.91 – 7.60 (m, 15H), 7.54 – 7.27 (m, 6H), 7.27 – 7.17 (m, 1H), 7.03 (d, *J* = 16.3 Hz, 1H), 6.94 (d, *J* = 16.3 Hz, 1H), 6.87 – 6.76 (d, *J* = 8.7 Hz, 2H), 4.08 (t, *J* = 5.6 Hz, 2H), 3.84 – 3.68 (m, 2H), 2.21 (p, *J* = 6.4 Hz, 2H), 1.98 – 1.79 (m, 2H). **¹³C NMR** (75 MHz, CDCl₃) δ 158.36, 137.55, 135.18, 135.16, 135.14, 133.75, 130.65, 130.65, 130.49, 130.22, 128.10, 127.75, 127.25, 126.67, 126.23, 118.59, 117.45, 114.73, 66.47, 29.38, 29.16, 22.76, 22.09, 19.36, 19.31. **Anal.** Calc. for C₃₆H₃₄IOP: theor. C = 67.50; H = 5.35; P = 4.84; I = 19.81; found C = 67.32; H = 5.37; P = 4.81; I = 19.73. **HRMS (ESI⁺)**: calc. for C₃₆H₃₄OP: theor. 513.2347; found [M]⁺: 513.2348.



ST33 35 (0.668) AM2 (Ar,40000.0,0.00,0.00)

1: TOF MS ES+
1.56e6



Elemental Composition Report

Page 1

Single Mass Analysis

Tolerance = 5.0 PPM / DBE: min = -1.5, max = 200.0

Element prediction: Off

Number of isotope peaks used for i-FIT = 5

Monoisotopic Mass, Even Electron Ions

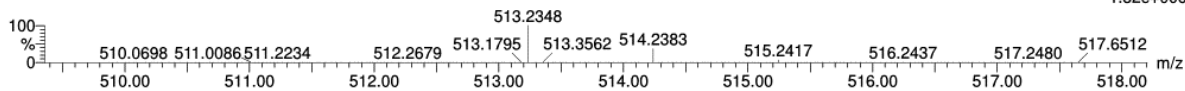
126 formula(e) evaluated with 1 results within limits (all results (up to 1000) for each mass)

Elements Used:

C: 36-36 H: 10-100 O: 0-5 Na: 0-1 P: 0-10

ST33 39 (0.735) AM2 (Ar,40000.0,0.00,0.00)

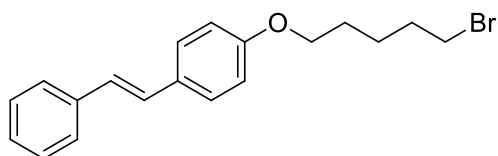
1: TOF MS ES+
1.32e+006



Minimum: -1.5
Maximum: 0.5 5.0 200.0

Mass	Calc. Mass	mDa	PPM	DBE	i-FIT	Norm	Conf (%)	Formula
513.2348	513.2347	0.1	0.2	20.5	1219.5	n/a	n/a	C36 H34 O P

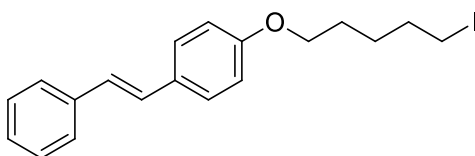
Synthesis of (*E*)-4-(5-bromopentyloxy)stilbene (**118d**)



Molecular Weight: 345.27

Procedure adapted from literature.¹⁹² A solution of *trans*-4-hydroxystilbene (196 mg – 1 mmol) in DMSO (1.4 ml) was added to a stirred suspension of finely ground NaOH (85 mg – 2.1 mmol) in DMSO (5.6 ml). The mixture was stirred at room temperature for 30 minutes and then the 1,5-dibromopentane (458 mg – 2 mmol) was added dropwise. When stilbenol was reacted, the reaction mixture was filtered and 1M aqueous solution of HCl was added dropwise to the filtrate to reach pH 3. The crude product was precipitated by slowly adding cold water. The precipitate was isolated by filtration, dried under vacuum and recrystallized from ethanol affording the pure compound **118d** as a white solid (97 mg – 0.28 mmol, 28%). **TLC** (cyclohexane/ethyl acetate 9:1): **R_f** = 0.62. **M.p.** = 98 °C; literature¹⁹²: **M.p.** = 83 – 85 °C. **¹H NMR** (300 MHz, CDCl₃): δ 7.46 (m, 4H), 7.34 (t, *J* = 7.6 Hz, 2H), 7.22 (m, 1H), 7.07 (d, *J* = 16.4 Hz, 1H), 6.97 (d, *J* = 16.4 Hz, 1H), 6.88 (d, *J* = 8.7 Hz, 2H), 3.99 (t, *J* = 6.3 Hz, 2H), 3.45 (t, *J* = 6.7 Hz, 2H), 2.02 – 1.89 (m, 2H), 1.89 – 1.77 (m, 2H), 1.65 (m, 2H).

Synthesis of (*E*)-4-(5-iodopentyloxy)stilbene (**119d**)

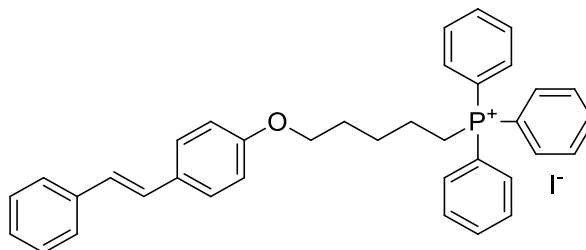


Molecular Weight: 392.27

Procedure adapted from literature.¹⁴⁰ Intermediate (*E*)-4-(5-bromopentyloxy)stilbene (**118d**) (345 mg – 1 mmol) was dissolved in a saturated solution of NaI in acetone (10 ml), which was then refluxed overnight. After concentrating under vacuum, the residue was diluted with diethyl ether and subsequently washed with 10% aqueous Na₂S₂O₅ and then with brine. The organic phase was dried over Na₂SO₄, filtered, and the solvent was evaporated under vacuum to give the desired intermediate **119d** as a white solid (392 mg – 1.00 mmol, 100%). **TLC** (cyclohexane/ethyl acetate 9:1): **R_f** = 0.68. **M.p.** = 102 °C. **¹H NMR** (300 MHz, CDCl₃): δ 7.47 (m, 4H), 7.34 (t, *J* = 7.5 Hz, 2H), 7.23 (m, 1H), 7.06 (d, *J* = 16.3 Hz, 1H), 6.96 (d, *J* = 16.3 Hz,

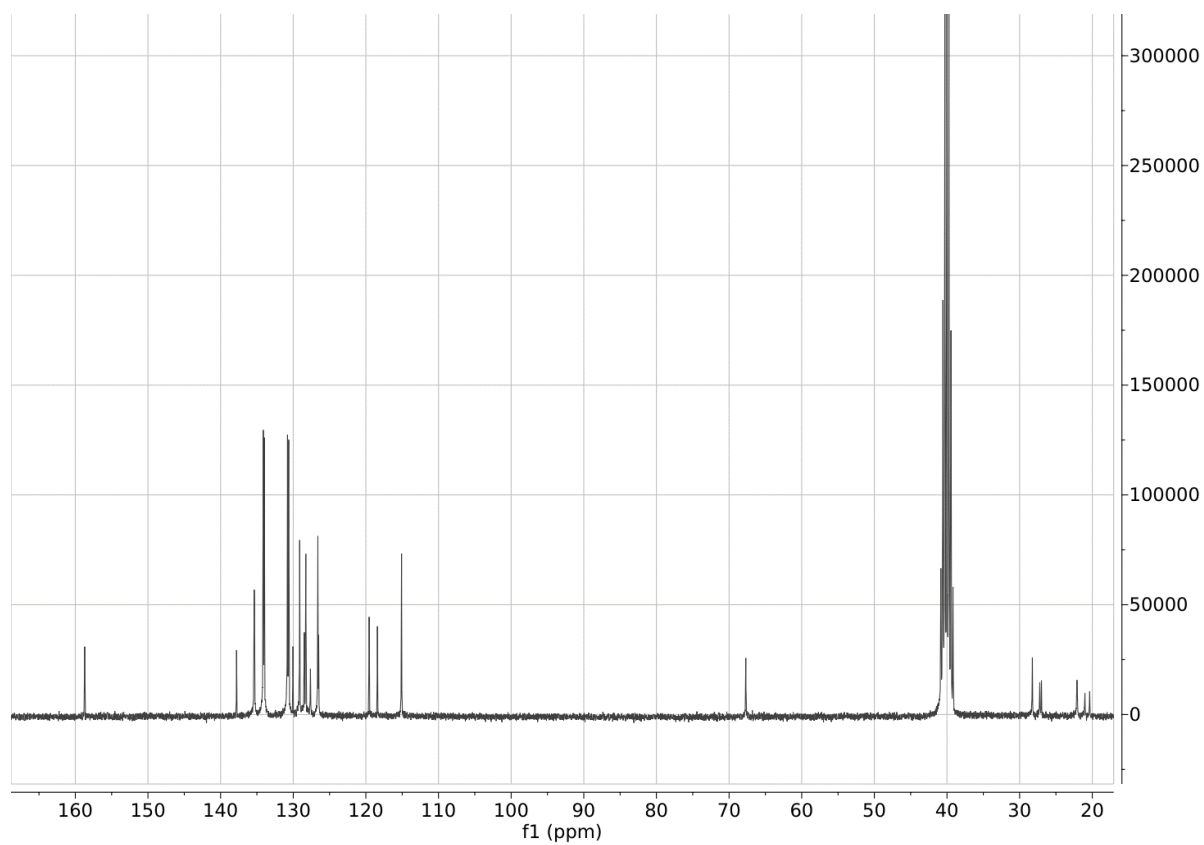
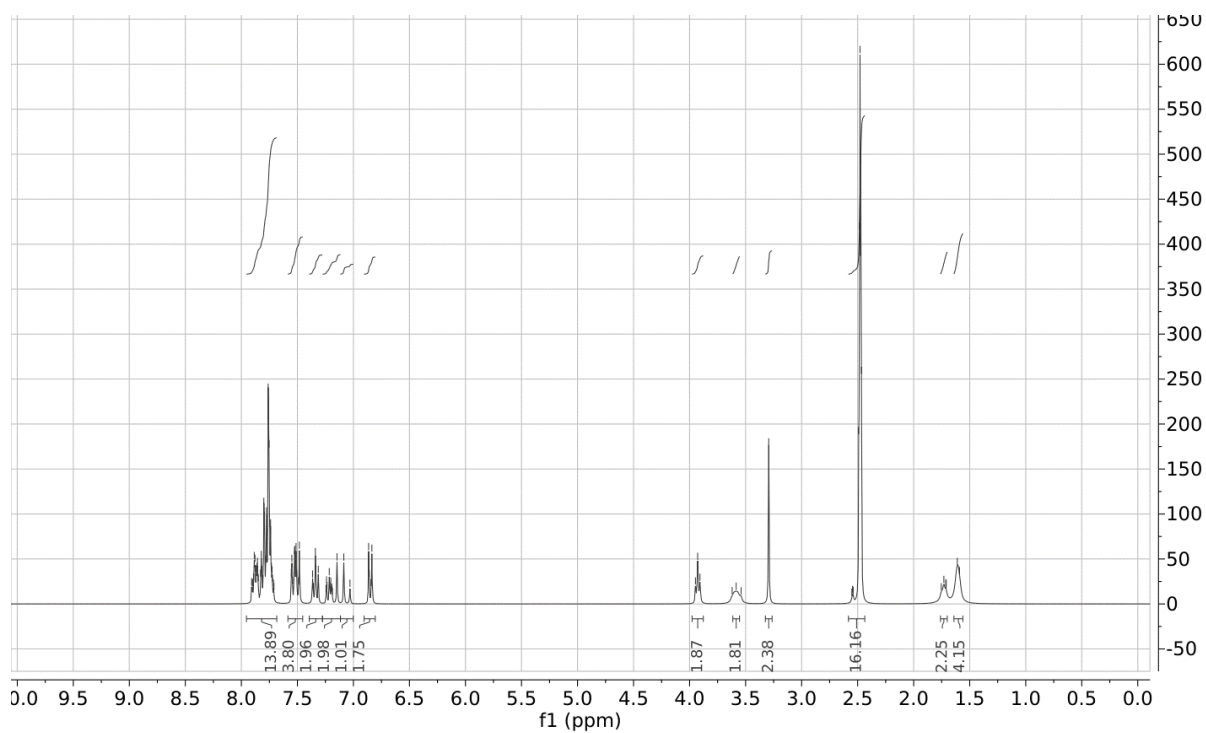
1H), 6.88 (d, $J = 8.7$ Hz, 2H), 3.99 (t, $J = 6.3$ Hz, 2H), 3.23 (t, $J = 7.0$ Hz, 2H), 1.99 – 1.74 (m, 4H), 1.68 – 1.56 (m, 2H).

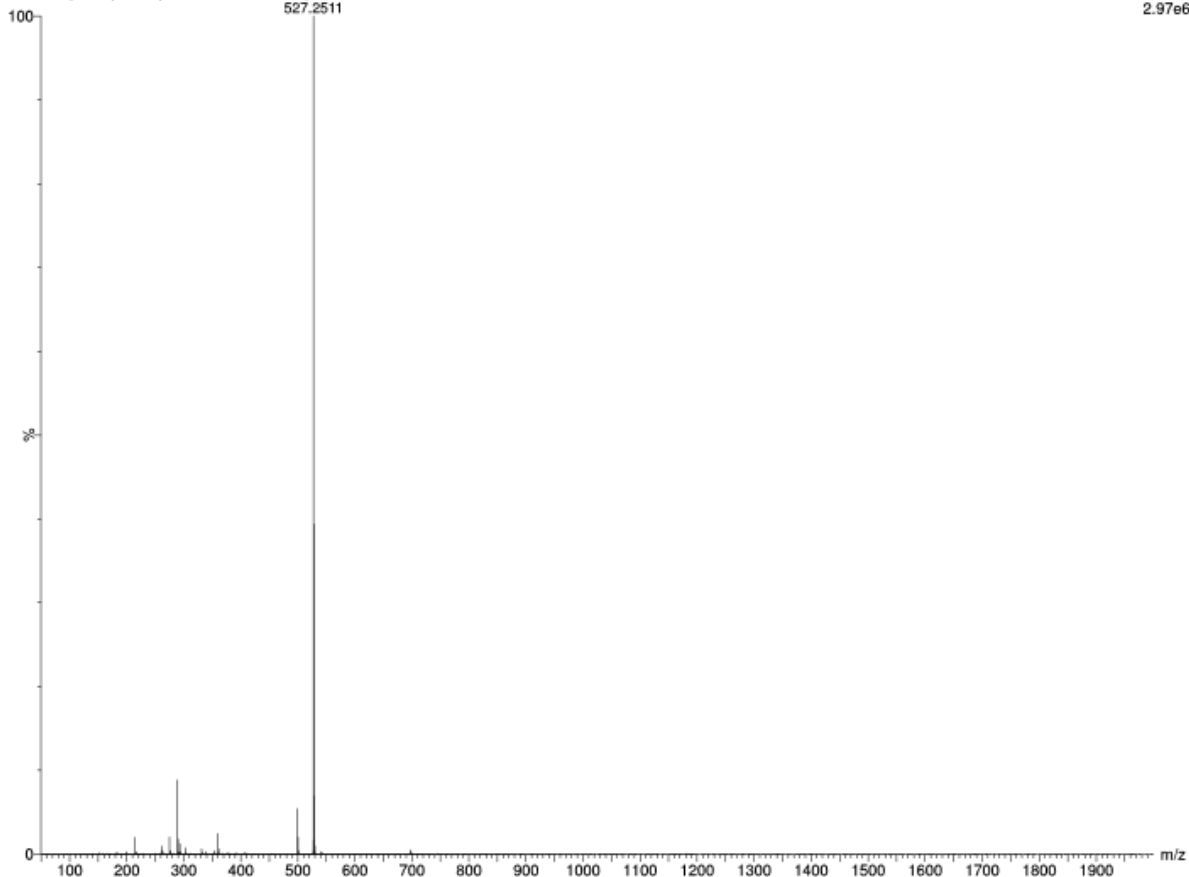
Synthesis of (*E*)-4-(5-triphenylphosphoniumpentyloxy)stilbene iodide (**19**)



Molecular Weight: 654.56

Procedure adapted from literature.¹⁴⁰ A solid mixture of PPh₃ (5.25 g – 20 mmol) and intermediate (*E*)-4-(5-iodopentyloxy)stilbene (392 mg – 1 mmol) was heated to 100 °C so as to obtain a solution of the starting material in molten PPh₃. The reaction mixture was slowly stirred at 100 °C for 3 hours and then cooled to room temperature without stirring any further. The re-solidified mixture was dissolved in the smallest possible volume of dichloromethane and diethyl ether was added dropwise under vigorous stirring. Afterwards, the solid precipitate was isolated by filtration affording the desired product **19** as a white solid (602 mg – 0.92 mmol, 92%). **M.p.** = 99 °C. **¹H NMR** (300 MHz, DMSO): δ 7.94 – 7.68 (m, 15H), 7.58 – 7.45 (m, 4H), 7.34 (t, $J = 7.6$ Hz, 2H), 7.27 – 7.12 (m, 2H), 7.06 (d, $J = 16.4$ Hz, 1H), 6.85 (d, $J = 8.7$ Hz, 2H), 3.93 (t, $J = 6.0$ Hz, 2H), 3.62 – 3.54 (m, 2H), 1.72 (m, 2H), 1.60 (m, 4H). **¹³C NMR** (75 MHz, DMSO): δ 158.71, 137.80, 135.37, 135.33, 134.12, 133.99, 130.79, 130.63, 130.04, 129.11, 128.47, 128.26, 127.63, 126.61, 126.50, 119.55, 118.42, 115.09, 67.69, 28.25, 27.22, 27.00, 22.09, 21.02, 20.36. **Anal.** Calc. for C₃₇H₃₆IOP: theor. C= 67.89; H= 5.54; P= 4.73; I= 19.39; found C= 67.61; H= 5.58; P= 4.67; I= 19.27. **HRMS (ESI⁺)**: calc. for C₃₇H₃₆OP: theor. 527.2504; found [M]⁺: 527.2511.





Elemental Composition Report

Single Mass Analysis

Tolerance = 5.0 PPM / DBE: min = -1.5, max = 200.0
 Element prediction: Off
 Number of isotope peaks used for i-FIT = 5

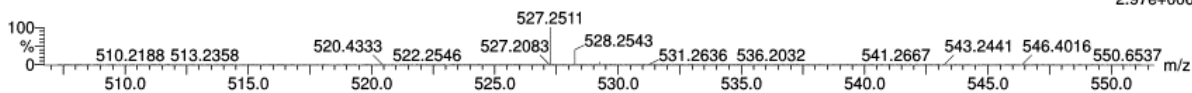
Monoisotopic Mass, Even Electron Ions

126 formula(e) evaluated with 1 results within limits (all results (up to 1000) for each mass)

Elements Used:

C: 37-37 H: 10-100 O: 0-5 Na: 0-1 P: 0-10

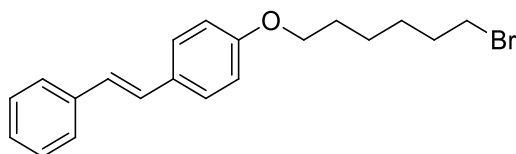
ST34 35 (0.668) AM2 (Ar,40000.0,0.00,0.00)



Minimum: -1.5
 Maximum: 0.5 5.0 200.0

Mass	Calc. Mass	mDa	PPM	DBE	i-FIT	Norm	Conf (%)	Formula
527.2511	527.2504	0.7	1.3	20.5	1585.5	n/a	n/a	C37 H36 O P

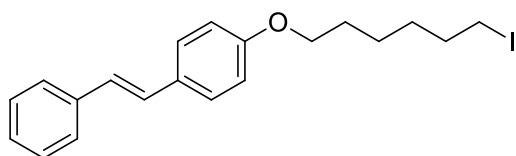
Synthesis of (*E*)-4-(6-bromohexyloxy)stilbene (**118e**)



Molecular Weight: 359.30

Procedure adapted from literature.¹⁹³ A solution of *trans*-4-hydroxystilbene (196 mg – 1 mmol) in DMSO (1.4 ml) was added to a stirred suspension of finely ground NaOH (85 mg – 2.1 mmol) in DMSO (5.6 ml). The mixture was stirred at room temperature for 30 minutes and then the 1,6-dibromohexane (488 mg – 2 mmol) was added dropwise. When stilbenol was reacted, the reaction mixture was filtered and 1M aqueous solution of HCl was added dropwise to the filtrate to reach pH 3. The crude product was precipitated by slowly adding cold water. The precipitate was isolated by filtration, dried under vacuum and recrystallized from ethanol affording the pure compound **118e** as a white solid (144 mg – 0.40 mmol, 40%). **TLC** (Cyclohexane / Ethyl acetate 9:1): **R_f** = 0.62. **M.p.** = 111 °C; literature¹⁹³: **M.p.** = 89 – 91 °C. **¹H NMR** (300 MHz, CDCl₃): δ 7.46 (m, 4H), 7.34 (t, *J* = 7.6 Hz, 2H), 7.25 – 7.18 (m, 1H), 7.06 (d, *J* = 16.4 Hz, 1H), 6.96 (d, *J* = 16.4 Hz, 1H), 6.88 (d, *J* = 7.9 Hz, 2H), 3.98 (t, *J* = 6.4 Hz, 2H), 3.42 (t, *J* = 6.7 Hz, 2H), 1.96 – 1.73 (m, 4H), 1.55 – 1.44 (m, 4H).

Synthesis of (*E*)-4-(6-iodohexyloxy)stilbene (**119e**)

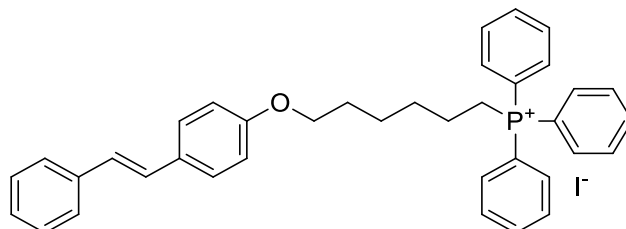


Molecular Weight: 406.30

Procedure adapted from literature.¹⁴⁰ Intermediate (*E*)-4-(6-bromohexyloxy)stilbene (**118e**) (359 mg – 1 mmol) was dissolved in a saturated solution of NaI in acetone (10 ml), which was then refluxed overnight. After concentrating under vacuum, the residue was diluted with diethyl ether and subsequently washed with 10% aqueous Na₂S₂O₅ and then with brine. The organic phase was dried over Na₂SO₄, filtered, and the solvent was evaporated under vacuum to give the desired intermediate **119e** as a white solid (406 mg – 1.00 mmol, 100%). **TLC** (cyclohexane/ethyl acetate 9:1): **R_f** = 0.76. **M.p.** = 126 °C. **¹H NMR** (300 MHz, CDCl₃): δ 7.47 (m, 4H), 7.34 (t, *J* = 7.6 Hz, 2H), 7.23 (m, 1H), 7.06 (d, *J* = 16.3 Hz, 1H), 6.96 (d, *J* = 16.3 Hz,

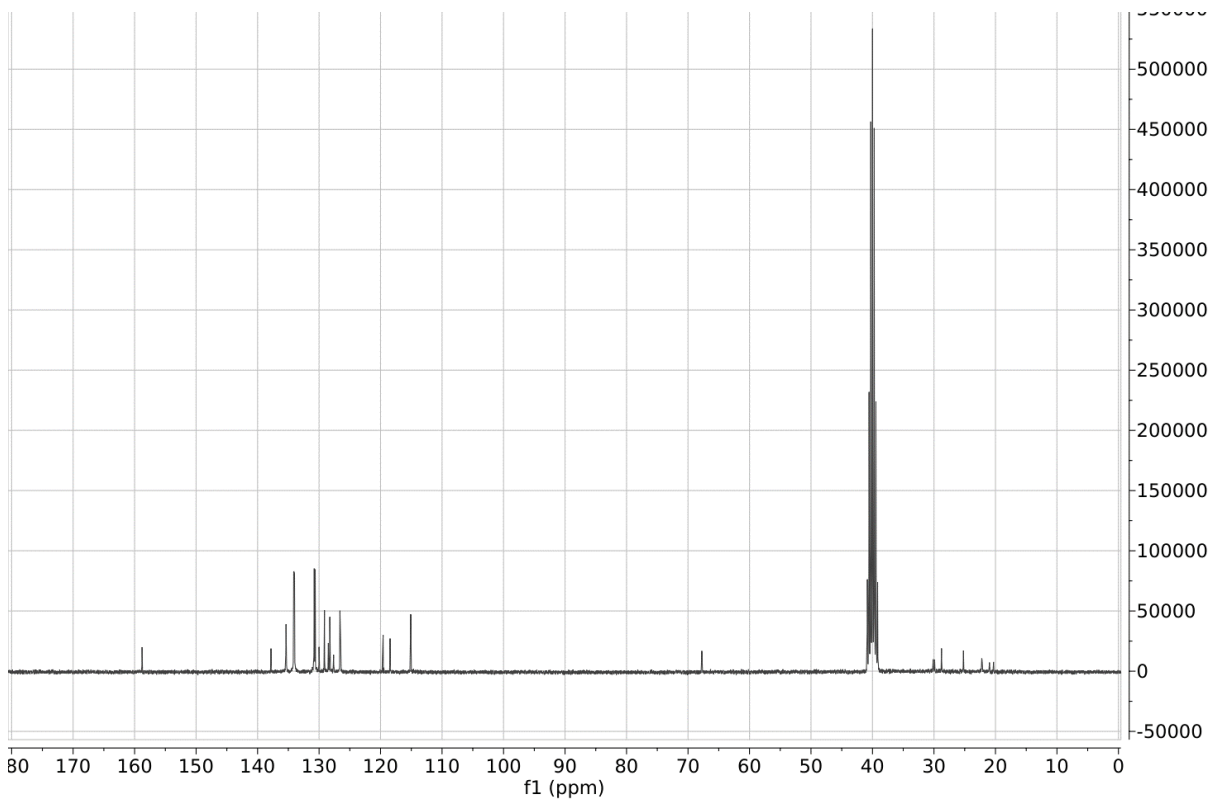
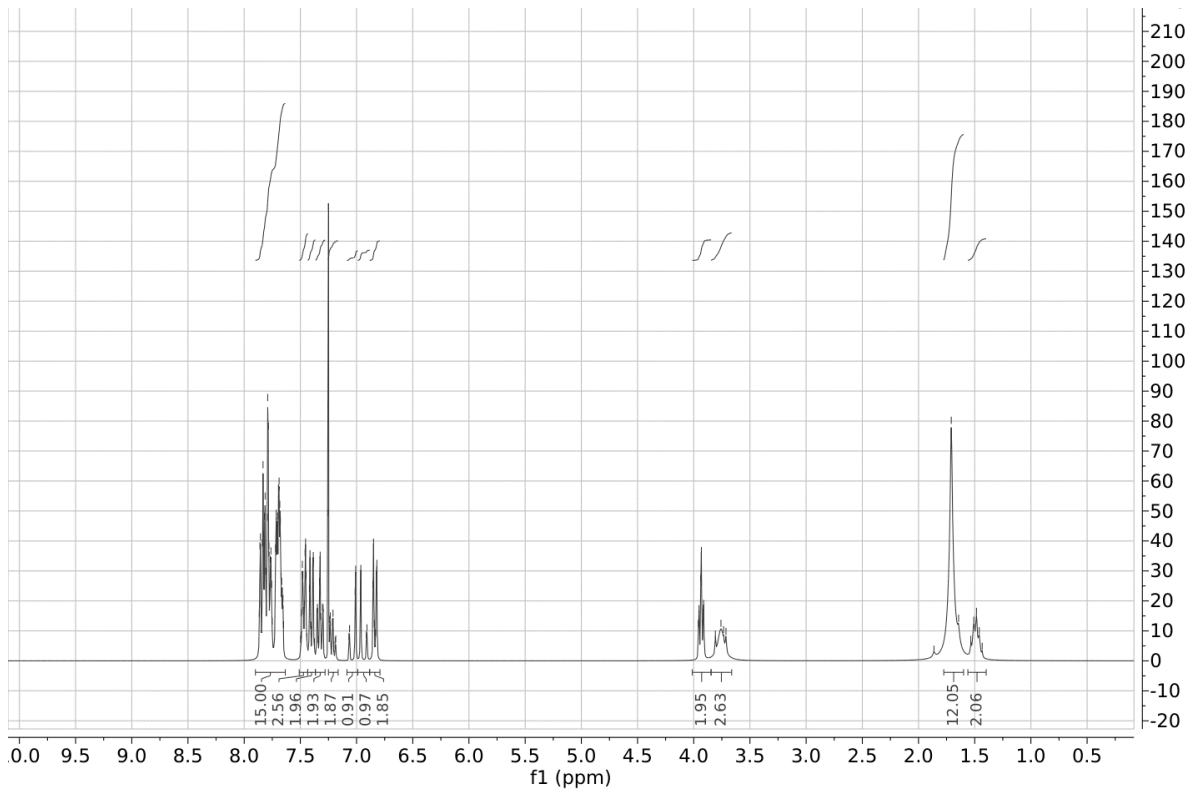
1H), 6.88 (d, $J = 8.6$ Hz, 2H), 3.98 (t, $J = 6.4$ Hz, 2H), 3.20 (t, $J = 6.7$ Hz, 2H), 1.93 – 1.72 (m, 4H), 1.50 – 1.37 (m, 4H).

Synthesis of (*E*)-4-(6-triphenylphosphoniumhexyloxy)stilbene iodide (**20**)



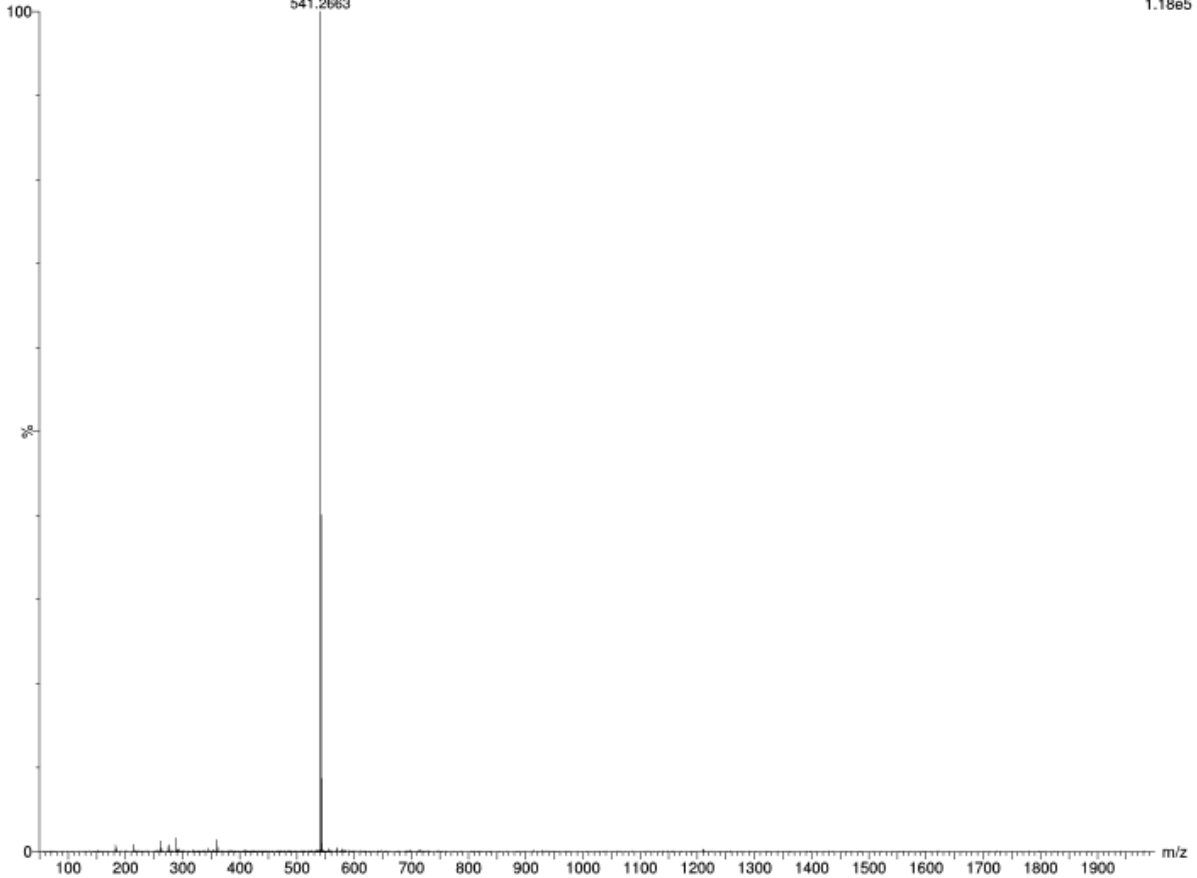
Molecular Weight: 668.59

Procedure adapted from literature.¹⁴⁰ A solid mixture of PPh₃ (5.25 g – 20 mmol) and intermediate (*E*)-4-(6-iodohexyloxy)stilbene (**119e**) (406 mg – 1 mmol) was heated to 100 °C so as to obtain a solution of the starting material in molten PPh₃. The reaction mixture was slowly stirred at 100 °C for 3 hours and then cooled to room temperature without stirring any further. The re-solidified mixture was dissolved in the smallest possible volume of dichloromethane and diethyl ether was added dropwise under vigorous stirring. Afterwards, the solid precipitate was isolated by filtration affording the desired product **20** as a white solid (595 mg – 0.89 mmol, 89%). **M.p.** = 88 °C. **¹H NMR** (300 MHz, CDCl₃): δ 7.90 – 7.63 (m, 15H), 7.50 – 7.36 (m, 4H), 7.33 (t, $J = 7.4$ Hz, 2H), 7.25 – 7.16 (m, 1H), 7.04 (d, $J = 16.4$ Hz, 1H), 6.94 (d, $J = 16.4$ Hz, 1H), 6.88 – 6.79 (d, $J = 8.8$ Hz, 2H), 3.93 (t, $J = 6.2$, 2H), 3.76 (m, 2H), 1.71 (m, 6H), 1.48 (m, 2H). **¹³C NMR** (75 MHz, DMSO) δ 158.79, 137.81, 135.38, 135.33, 134.13, 133.99, 130.79, 130.63, 130.00, 129.12, 128.49, 128.26, 127.64, 126.61, 126.49, 119.58, 118.45, 115.10, 67.76, 30.13, 29.90, 28.78, 25.21, 22.22, 20.97, 20.31. **Anal.** Calc. for C₃₈H₃₈IOP: theor. C = 68.26; H = 5.73; P = 4.63; I = 18.98; found C = 68.08; H = 5.76; P = 4.57; I = 18.81. **HRMS (ESI⁺)**: calc. for C₃₈H₃₈OP: theor. 541.2660; found [M]⁺: 541.2663.



ST152 28 (0.550) AM2 (Ar,40000.0,0.00,0.00)

1: TOF MS ES+
1.18e5



Elemental Composition Report

Single Mass Analysis

Tolerance = 5.0 PPM / DBE: min = -1.5, max = 200.0
 Element prediction: Off
 Number of isotope peaks used for i-FIT = 5

Monoisotopic Mass, Even Electron Ions

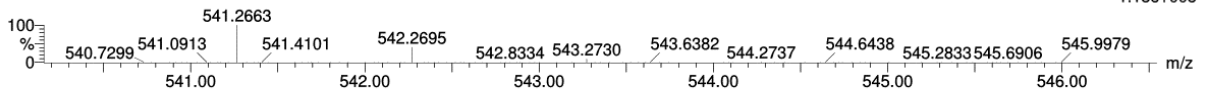
126 formula(e) evaluated with 1 results within limits (all results (up to 1000) for each mass)

Elements Used:

C: 38-38 H: 10-100 O: 0-5 Na: 0-1 P: 0-10

ST152 28 (0.550) AM2 (Ar,40000.0,0.00,0.00)

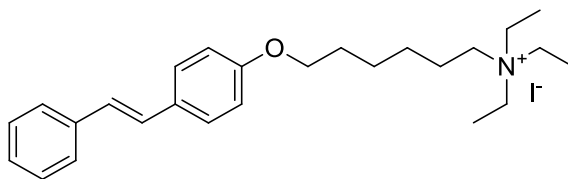
1: TOF MS ES+
1.18e+005



Minimum: -1.5
 Maximum: 0.5 5.0 200.0

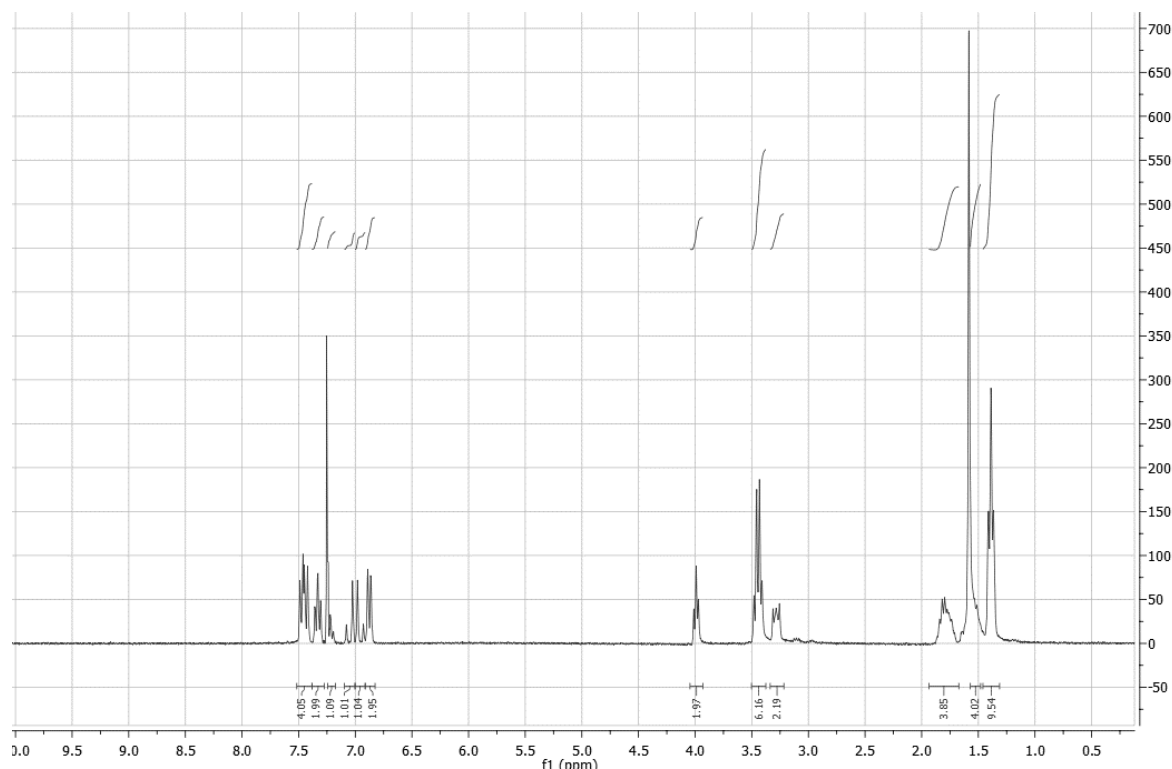
Mass	Calc. Mass	mDa	PPM	DBE	i-FIT	Norm	Conf (%)	Formula
541.2663	541.2660	0.3	0.6	20.5	531.4	n/a	n/a	C38 H38 O P

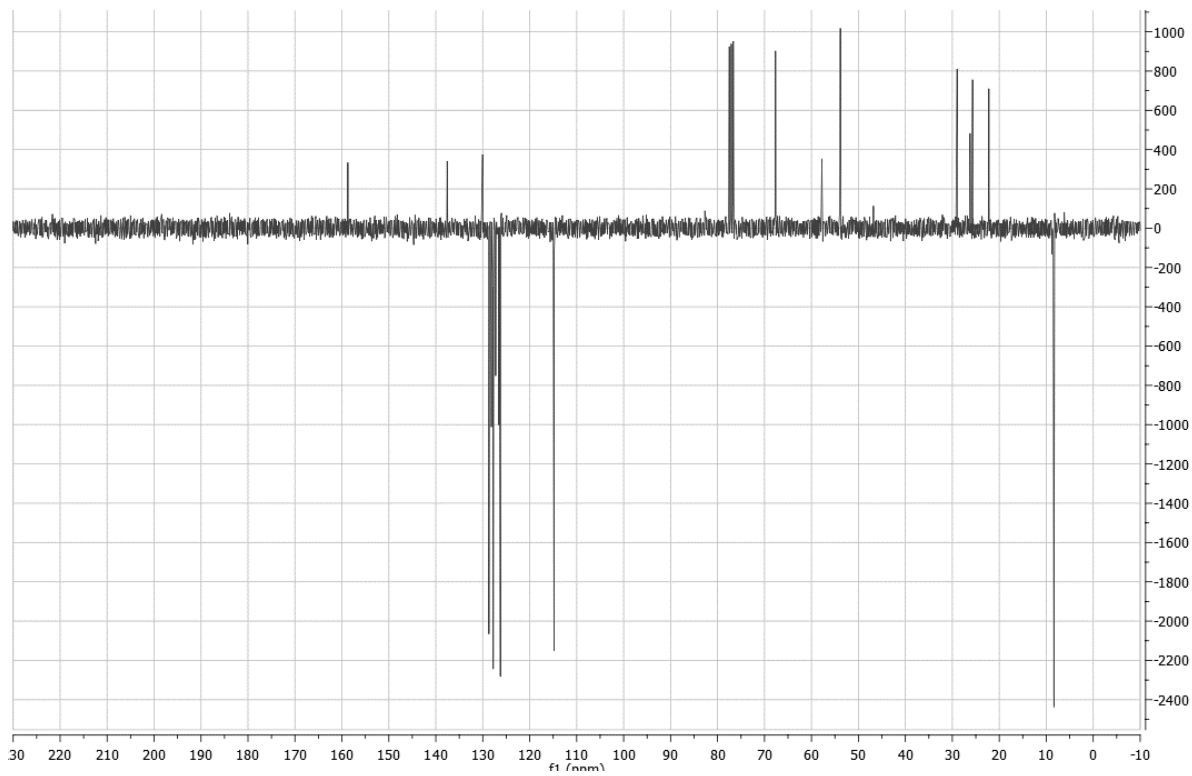
Synthesis of (*E*)-4-(6-triethylammoniumhexyloxy)stilbene iodide (**25**)



Molecular Weight: 507.49

Intermediate (*E*)-4-(6-iodohexyloxy)stilbene (**119e**) (406 mg – 1 mmol) was dissolved in 3 ml of triethylamine and 3 ml of toluene for 5 hours. Upon concentration under vacuum, the residue was diluted with diethyl ether and the obtained suspension was filtered, affording the desired product **25** as a beige solid (411 mg – 0.81 mmol, 81%). **M.p.** = 166 °C. **¹H NMR** (300 MHz, CDCl₃): δ 7.52 – 7.38 (m, 4H), 7.33 (t, *J* = 7.6 Hz, 2H), 7.24 – 7.18 (m, 1H), 7.05 (d, *J* = 16.5 Hz, 1H), 6.95 (d, *J* = 16.5 Hz, 1H), 6.88 (d, *J* = 7.3 Hz, 2H), 3.99 (t, *J* = 6.0 Hz, 2H), 3.44 (q, *J* = 7.0 Hz, 6H), 3.34 – 3.22 (m, 2H), 1.94 – 1.67 (m, 4H), 1.57 – 1.48 (m, 4H), 1.39 (t, *J* = 7.0 Hz, 9H). **¹³C NMR** (75 MHz, CDCl₃): δ 158.72, 137.58, 130.03, 128.67, 128.16, 127.77, 127.25, 126.57, 126.24, 114.82, 67.65, 57.77, 53.85, 28.98, 26.22, 25.69, 22.21, 8.36. **Anal.** Calc. for C₂₆H₃₈INO: theor. C = 61.53; H = 7.55; I = 25.01; N = 2.76; found C = 61.33; H = 7.57; I = 25.11; N = 2.74. **HRMS (ESI⁺)**: calc. for C₂₆H₃₈NO: theor. 380.2953; found [M]⁺: 380.2950.

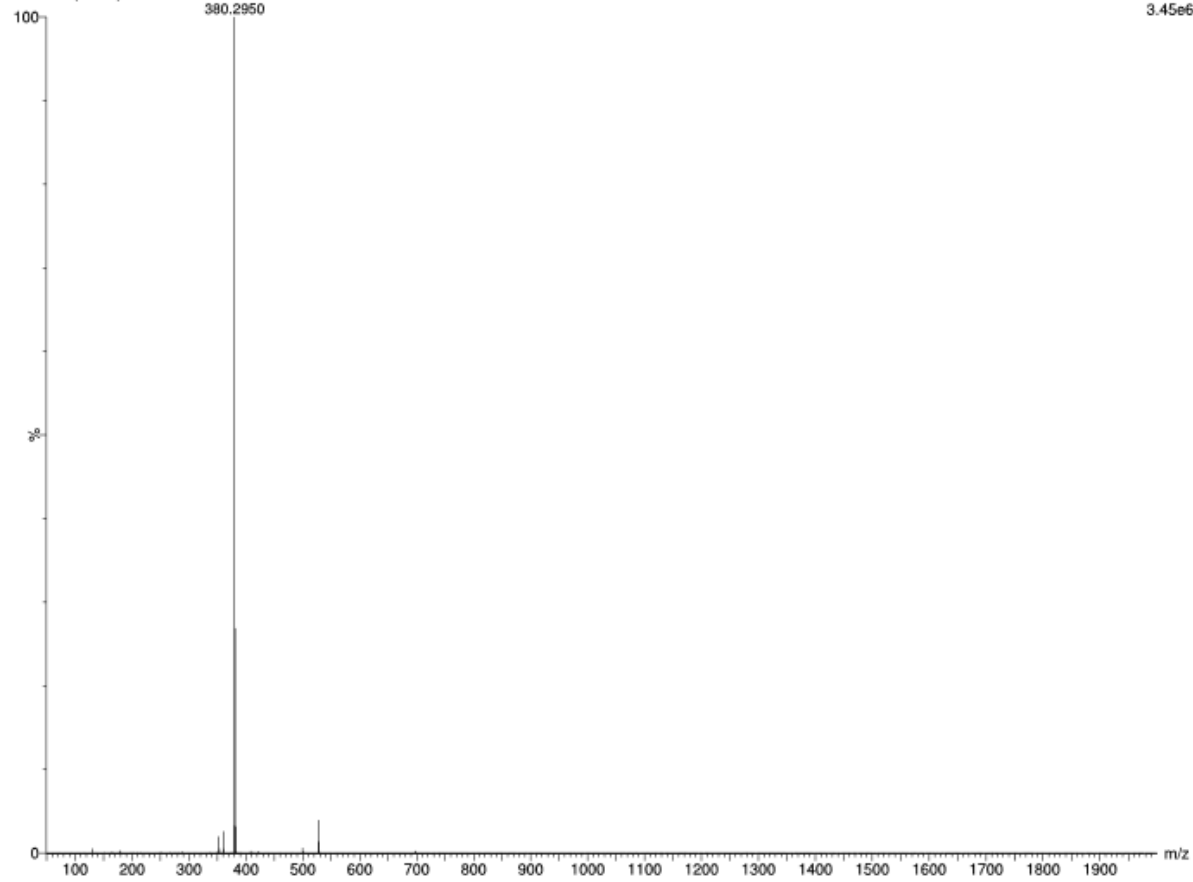




ST48 35 (0.668)

380.2950

1: TOF MS ES+
3.45e6



Single Mass Analysis

Tolerance = 5.0 PPM / DBE: min = -1.5, max = 200.0

Element prediction: Off

Number of isotope peaks used for i-FIT = 5

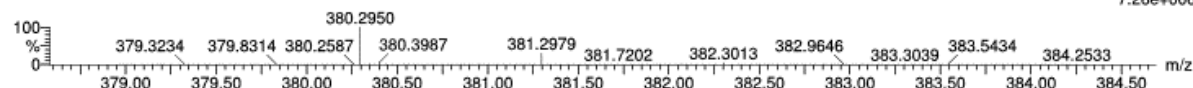
Monoisotopic Mass, Even Electron Ions

62 formula(e) evaluated with 1 results within limits (all results (up to 1000) for each mass)

Elements Used:

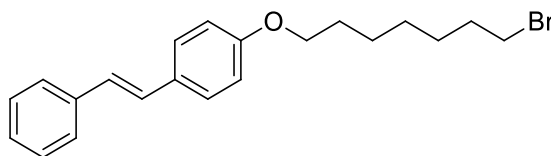
C: 26-26 H: 10-100 N: 0-5 O: 0-5 Na: 0-1

ST48 35 (0.668) AM2 (Ar,40000.0,0.00,0.00)

1: TOF MS ES+
7.26e+006

Minimum: -1.5
Maximum: 0.5 5.0 200.0

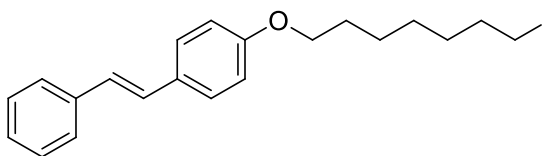
Mass	Calc. Mass	mDa	PPM	DBE	i-FIT	Norm	Conf (%)	Formula
380.2950	380.2953	-0.3	-0.8	8.5	1949.1	n/a	n/a	C ₂₆ H ₃₈ N O

Synthesis of (*E*)-4-(7-bromoheptyloxy)stilbene (**118f**)

Molecular Weight: 373.33

Procedure adapted from literature.¹⁹³ A solution of *trans*-4-hydroxystilbene (196 mg – 1 mmol) in DMSO (1.4 ml) was added to a stirred suspension of finely ground NaOH (85 mg – 2.1 mmol) in DMSO (5.6 ml). The mixture was stirred at room temperature for 30 minutes and then the 1,7-dibromoheptane (516 mg – 2 mmol) was added dropwise. When stilbenol was reacted, the reaction mixture was filtered and 1M aqueous solution of HCl was added dropwise to the filtrate to reach pH 3. The crude product was precipitated by slowly adding cold water. The precipitate was isolated by filtration, dried under vacuum and recrystallized from ethanol affording the pure compound **118f** as a white solid (153 mg – 0.41 mmol, 41%). TLC (cyclohexane/ethyl acetate 9:1): **R_f** = 0.62. **M.p.** = 111 °C. **¹H NMR** (300 MHz, CDCl₃): 7.45 (m, 4H), 7.33 (t, *J* = 7.3 Hz, 2H), 7.23 (m, 1H), 7.05 (d, *J* = 16.3 Hz, 1H), 6.95 (d, *J* = 16.3 Hz, 1H), 6.87 (d, *J* = 8.5 Hz, 2H), 3.96 (t, *J* = 6.2 Hz, 2H), 3.40 (t, *J* = 6.7 Hz, 2H), 1.95 – 1.70 (m, 4H), 1.47 (s, 6H).

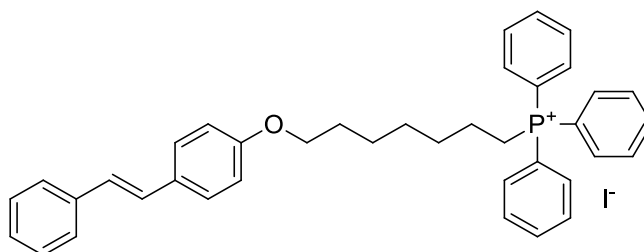
Synthesis of (*E*)-4-(7-iodoheptyloxy)stilbene (**119f**)



Molecular Weight: 420.33

Procedure adapted from literature.¹⁴⁰ Intermediate (*E*)-4-(7-bromoheptyloxy)stilbene (**118f**) (373 mg – 1 mmol) was dissolved in a saturated solution of NaI in acetone (10 ml), which was then refluxed overnight. After concentrating under vacuum, the residue was diluted with diethyl ether and subsequently washed with 10% aqueous Na₂S₂O₅ and then with brine. The organic phase was dried over Na₂SO₄, filtered, and the solvent was evaporated under vacuum to give the desired intermediate **119f** as a white solid (420 mg – 1.00 mmol, 100%). **TLC** (cyclohexane/ethyl acetate 9:1): **R_f**= 0.76. **M.p.**= 84 °C. **¹H NMR** (300 MHz, CDCl₃): δ 7.47 (m, 4H), 7.34 (t, *J* = 7.7 Hz, 2H), 7.22 (m, 1H), 7.06 (d, *J* = 16.3 Hz, 1H), 6.96 (d, *J* = 16.3 Hz, 1H), 6.88 (d, *J* = 8.6 Hz, 2H), 3.97 (t, *J* = 6.5 Hz, 2H), 3.19 (t, *J* = 6.0, *J* = 4.2 Hz, 2H), 1.89 – 1.72 (m, 4H), 1.44 (m, 6H).

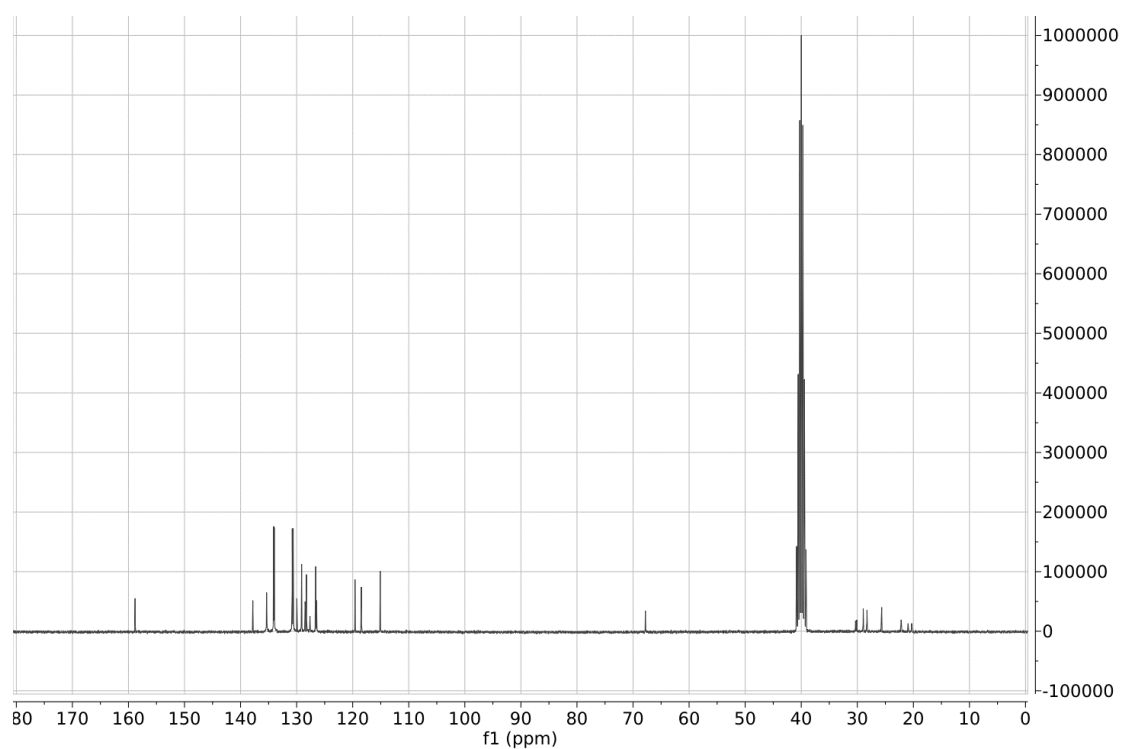
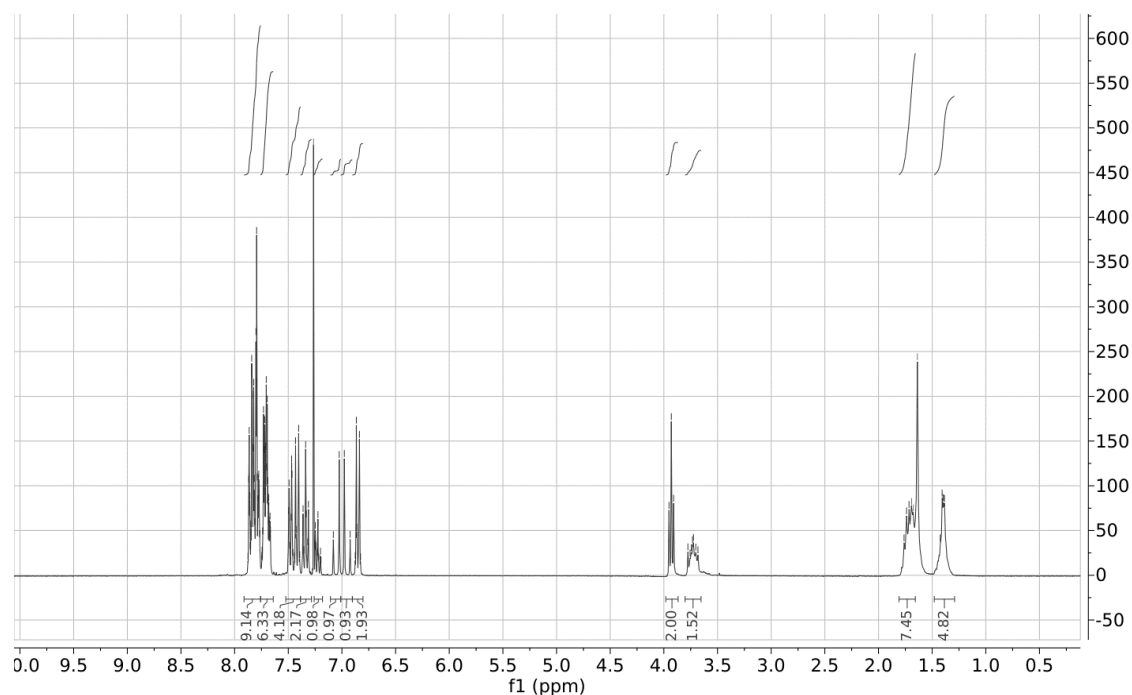
Synthesis of (*E*)-4-(7-triphenylphosphoniumheptyloxy)stilbene iodide (**21**)

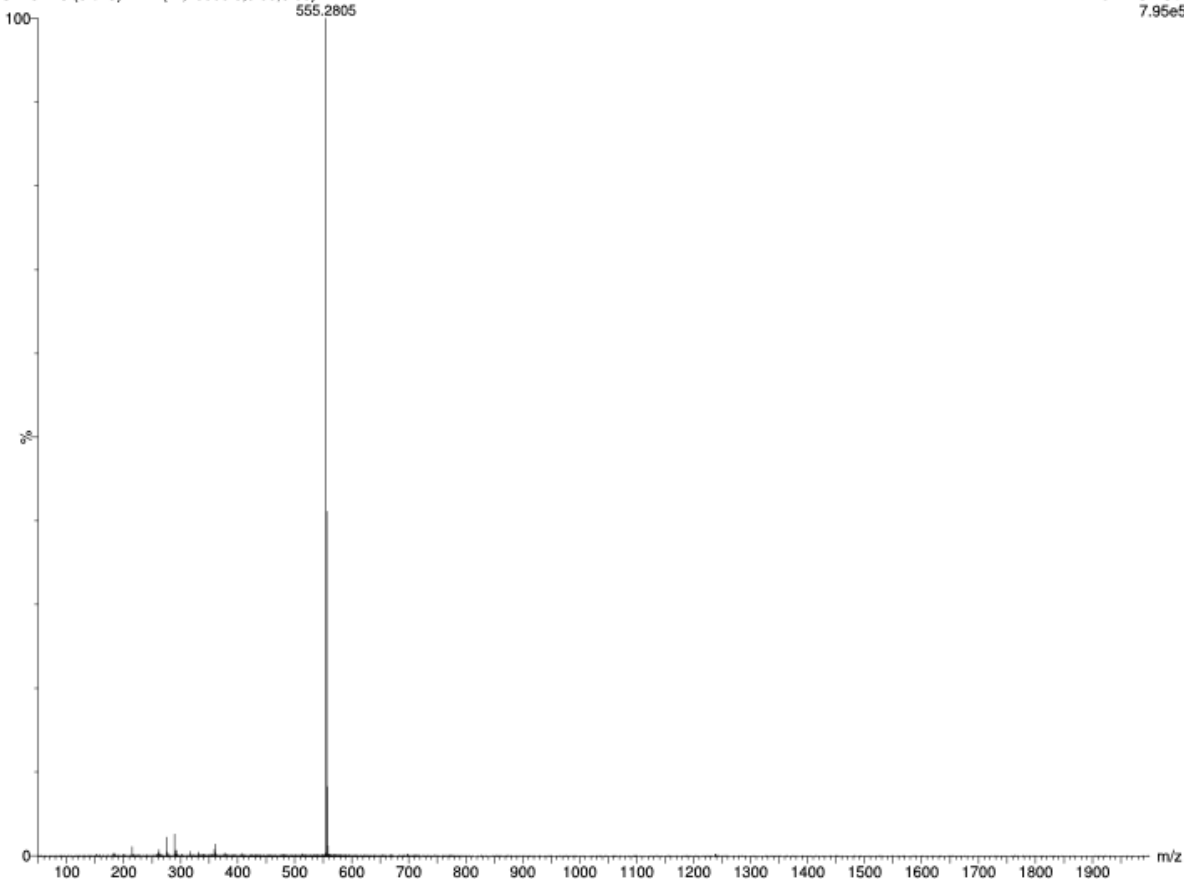


Molecular Weight: 682.61

Procedure adapted from literature.¹⁴⁰ A solid mixture of PPh₃ (5.25 g – 20 mmol) and intermediate (*E*)-4-(7-iodoheptyloxy)stilbene (**119f**) (420 mg – 1 mmol) was heated to 100 °C so as to obtain a solution of the starting material in molten PPh₃. The reaction mixture was slowly stirred at 100 °C for 3 hours and then cooled to room temperature without stirring any further. The re-solidified mixture was dissolved in the smallest possible volume of dichloromethane and diethyl ether was added dropwise under vigorous stirring. Afterwards, the solid precipitate was isolated by filtration affording the desired product **21** as a white solid (608 mg – 0.89 mmol, 89%). **M.p.**= 76 °C. **¹H NMR** (300 MHz, CDCl₃): δ 7.91 – 7.76 (m, 9H), 7.76 – 7.64 (m, 6H), 7.52 – 7.39 (m, 4H), 7.34 (t, *J* = 7.5 Hz, 2H), 7.26 – 7.18 (m, 1H), 7.05 (d, *J* =

16.3 Hz, 1H), 6.95 (d, $J = 16.3$ Hz, 1H), 6.85 (d, $J = 8.8$ Hz, 2H), 3.93 (t, $J = 6.4$ Hz, 2H), 3.80 – 3.65 (m, 2H), 1.81 – 1.66 (m, 6H), 1.48 – 1.29 (m, 4H). ^{13}C NMR (75 MHz, DMSO): δ 158.82, 137.81, 135.36, 135.32, 134.11, 133.98, 130.79, 130.62, 129.96, 129.28, 129.11, 128.49, 128.25, 127.62, 126.60, 126.45, 119.58, 118.45, 115.09, 67.80, 30.32, 30.10, 28.94, 28.27, 25.65, 22.18, 22.13, 20.95, 20.29. **Anal.** Calc. for $\text{C}_{39}\text{H}_{40}\text{IOP}$: theor. C= 68.62; H= 5.91; P= 4.54; I= 18.59; found C= 68.49; H= 5.92; P= 4.47; I= 18.53. **HRMS (ESI⁺)**: calc. for $\text{C}_{39}\text{H}_{40}\text{OP}$: theor. 555.2817; found $[\text{M}]^+$: 555.2805.





Elemental Composition Report

Single Mass Analysis

Tolerance = 5.0 PPM / DBE: min = -1.5, max = 200.0
 Element prediction: Off
 Number of isotope peaks used for i-FIT = 5

Monoisotopic Mass, Even Electron Ions

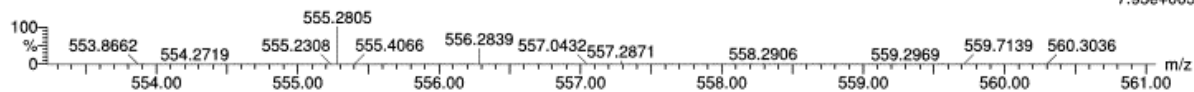
125 formula(e) evaluated with 1 results within limits (all results (up to 1000) for each mass)

Elements Used:

C: 39-39 H: 10-10 O: 0-5 Na: 0-1 P: 0-10

ST151 43 (0.823) AM2 (Ar,40000.0,0.00,0.00)

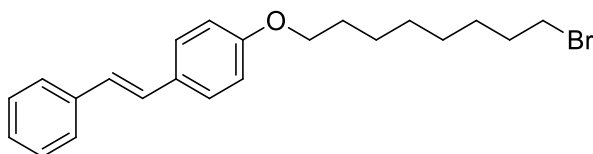
1: TOF MS ES+
7.95e+005



Minimum: -1.5
 Maximum: 0.5 5.0 200.0

Mass	Calc. Mass	mDa	PPM	DBE	i-FIT	Norm	Conf(%)	Formula
555.2805	555.2817	-1.2	-2.2	20.5	1147.5	n/a	n/a	C39 H40 O P

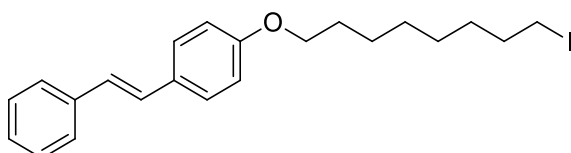
Synthesis of (*E*)-4-(8-bromooctyloxy)stilbene (**118g**)



Molecular Weight: 387.35

Procedure adapted from literature.¹⁹³ A solution of *trans*-4-hydroxystilbene (196 mg – 1 mmol) in DMSO (1.4 ml) was added to a stirred suspension of finely ground NaOH (85 mg – 2.1 mmol) in DMSO (5.6 ml). The mixture was stirred at room temperature for 30 minutes and then the 1,8-dibromooctane (544 mg – 2 mmol) was added dropwise. When stilbenol was reacted, the reaction mixture was filtered and 1M aqueous solution of HCl was added dropwise to the filtrate to reach pH 3. The crude product was precipitated by slowly adding cold water. The precipitate was isolated by filtration, dried under vacuum and recrystallized from ethanol affording the pure compound **118g** as a white solid (174 mg – 0.45 mmol, 45%). TLC (Cyclohexane / Ethyl acetate 9:1): R_f = 0.63. M.p. = 110 °C. ¹H NMR (300 MHz, CDCl₃): δ 7.46 (m, 4H), 7.34 (t, *J* = 7.5 Hz, 2H), 7.2 (m, 1H), 7.07 (d, *J* = 16.3 Hz, 1H), 6.96 (d, *J* = 16.3 Hz, 1H), 6.88 (d, *J* = 8.6 Hz, 2H), 3.97 (t, *J* = 6.5 Hz, 2H), 3.41 (t, *J* = 6.8 Hz, 2H), 1.92 – 1.72 (m, 4H), 1.52 – 1.27 (m, 8H).

Synthesis of (*E*)-4-(8-iodooctyloxy)stilbene (**119g**)

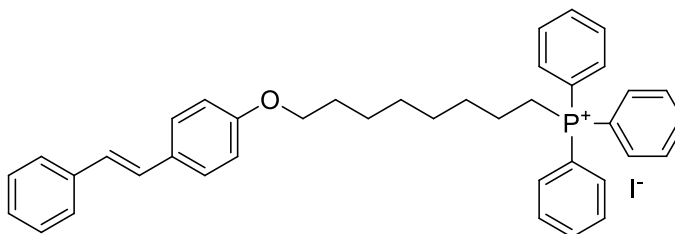


Molecular Weight: 434.35

Procedure adapted from literature.¹⁴⁰ Intermediate (*E*)-4-(8-bromooctyloxy)stilbene (**118g**) (387 mg – 1 mmol) was dissolved in a saturated solution of NaI in acetone (10 ml), which was then refluxed overnight. After concentrating under vacuum, the residue was diluted with diethyl ether and subsequently washed with 10% aqueous Na₂S₂O₅ and then with brine. The organic phase was dried over Na₂SO₄, filtered, and the solvent was evaporated under vacuum to give the desired intermediate **119g** as a white solid (430 mg – 0.99 mmol, 99%). TLC (Cyclohexane / Ethyl Acetate 9:1): R_f = 0.74. M.p. = 120 °C. ¹H NMR (300 MHz, CDCl₃): δ 7.46 (m, 4 H), 7.33 (t, *J* = 7.5 Hz, 2H), 7.22 (m, 1H), 7.06 (d, *J* = 16.3 Hz, 1H), 6.95 (d, *J* = 16.3 Hz, 1H), 6.88

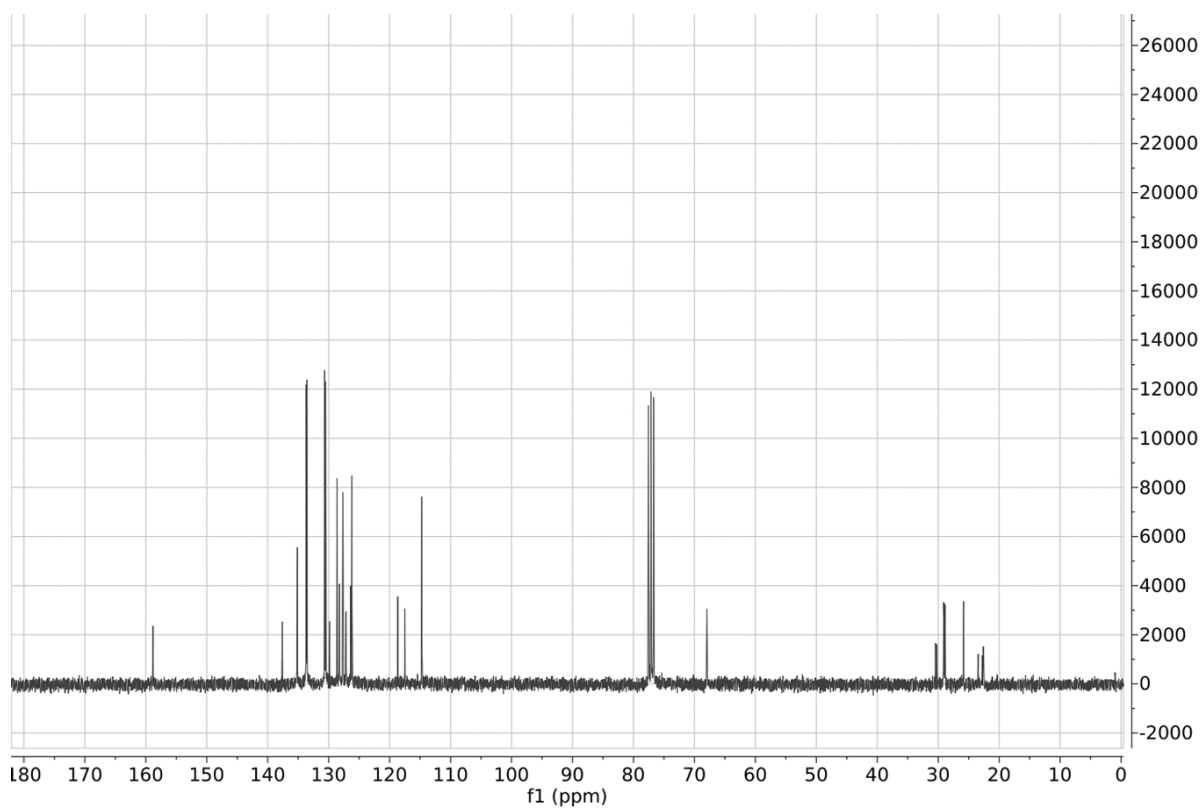
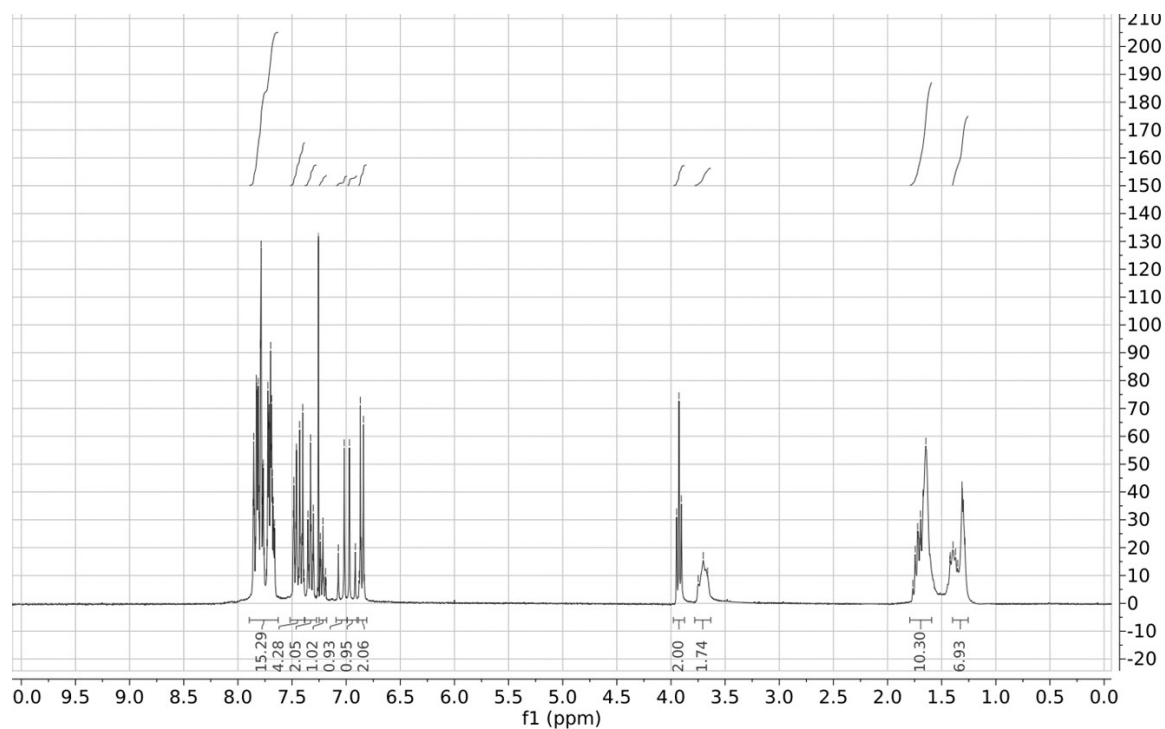
(d, $J = 8.7$ Hz, 2H), 3.97 (t, $J = 6.5$ Hz, 2H), 3.18 (t, $J = 7.0$ Hz, 2H), 1.79 (m, 4H), 1.43 - 1.31 (m, 8H).

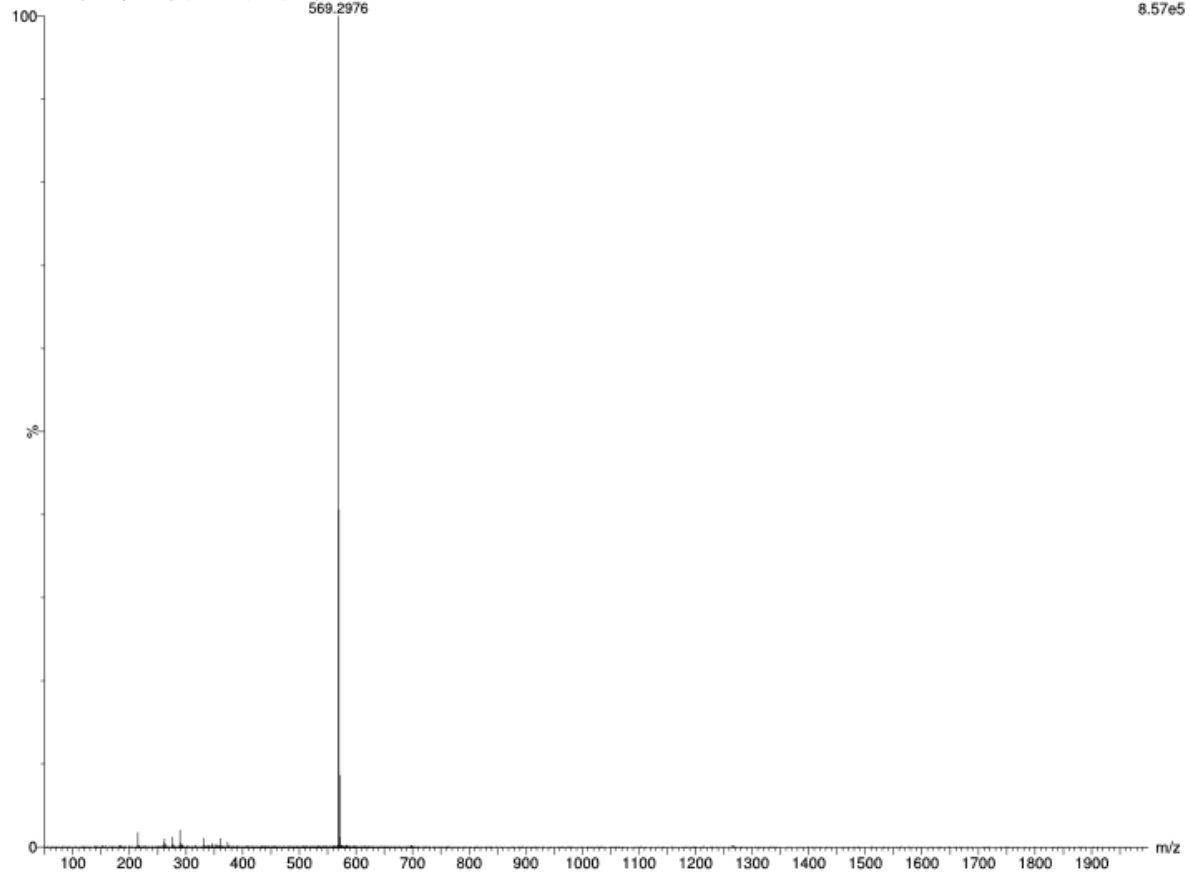
Synthesis of (*E*)-4-(8-triphenylphosphonioctyloxy)stilbene iodide (**22**)



Molecular Weight: 696.64

Procedure adapted from literature.¹⁴⁰ A solid mixture of PPh₃ (5.25 g – 20 mmol) and intermediate (*E*)-4-(8-iodooctyloxy)stilbene (**119g**) (434 mg – 1 mmol) was heated to 100 °C so as to obtain a solution of the starting material in molten PPh₃. The reaction mixture was slowly stirred at 100 °C for 3 hours and then cooled to room temperature without stirring any further. The re-solidified mixture was dissolved in the smallest possible volume of dichloromethane and diethyl ether was added dropwise under vigorous stirring. Afterwards, the solid precipitate was isolated by filtration affording the desired product **22** as a white solid (599 mg – 0.86 mmol, 86%). **M.p.** = 80 °C. **¹H NMR** (300 MHz, CDCl₃): δ 7.89 – 7.74 (m, 9H), 7.74 – 7.65 (m, 6H), 7.52 – 7.38 (m, 4H), 7.33 (t, $J = 7.5$ Hz, 2H), 7.27 – 7.16 (m, 1H), 7.05 (d, $J = 16.3$ Hz, 1H), 6.94 (d, $J = 16.3$ Hz, 1H), 6.85 (d, $J = 8.8$ Hz, 2H), 3.93 (t, $J = 6.5$ Hz, 2H), 3.78 – 3.63 (m, 2H), 1.78 – 1.66 (m, 6H), 1.47 – 1.25 (m, 6H). **¹³C NMR** (75 MHz, CDCl₃): δ 158.83, 137.63, 135.17, 135.13, 133.70, 133.57, 130.66, 130.50, 129.84, 128.61, 128.24, 127.66, 127.15, 126.39, 126.19, 118.65, 117.51, 114.71, 67.94, 30.43, 30.23, 29.09, 29.01, 28.87, 25.82, 23.44, 22.77, 22.60, 22.54. **Anal.** Calc. for C₄₀H₄₂IOP: theor. C= 68.96; H= 6.08; P= 4.45; I= 18.22; found C= 68.88; H= 6.08; P= 4.39; I= 18.16. **HRMS (ESI⁺)**: calc. for C₄₀H₄₂OP: theor. 569.2973; found [M]⁺: 569.2976.





Elemental Composition Report

Single Mass Analysis

Tolerance = 5.0 PPM / DBE: min = -1.5, max = 200.0
 Element prediction: Off
 Number of isotope peaks used for i-FIT = 5

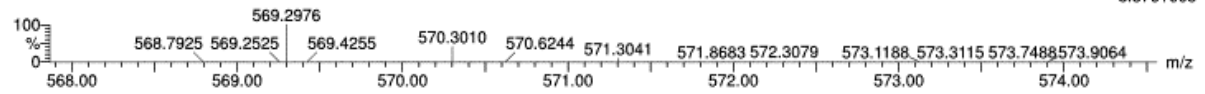
Monoisotopic Mass, Even Electron Ions

125 formula(e) evaluated with 1 results within limits (all results (up to 1000) for each mass)

Elements Used:

C: 40-40 H: 10-100 O: 0-5 Na: 0-1 P: 0-10

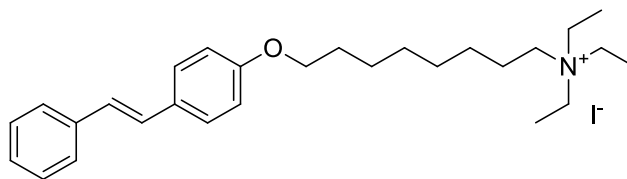
ST207 34 (0.651) AM2 (Ar,40000.0,0.00,0.00)



Minimum: -1.5
 Maximum: 0.5 5.0 200.0

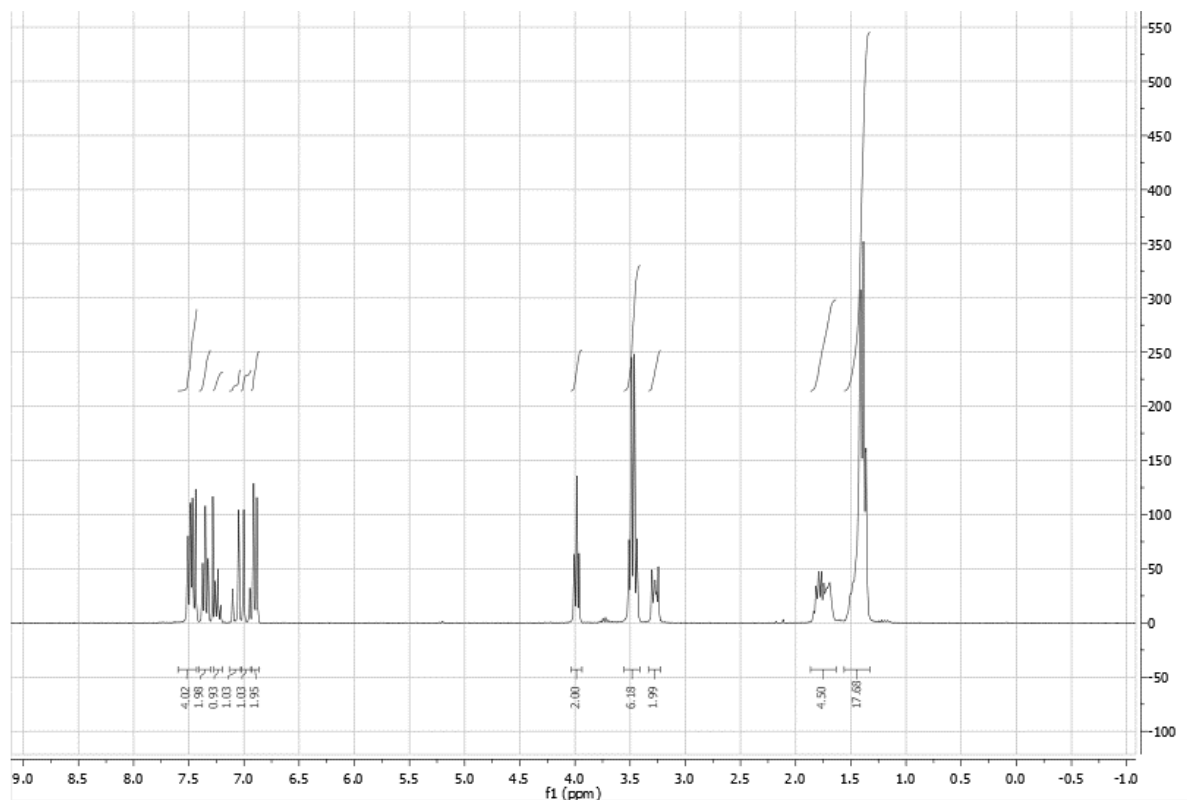
Mass	Calc. Mass	mDa	PPM	DBE	i-FIT	Norm	Conf (%)	Formula
569.2976	569.2973	0.3	0.5	20.5	1234.1	n/a	n/a	C40 H42 O P

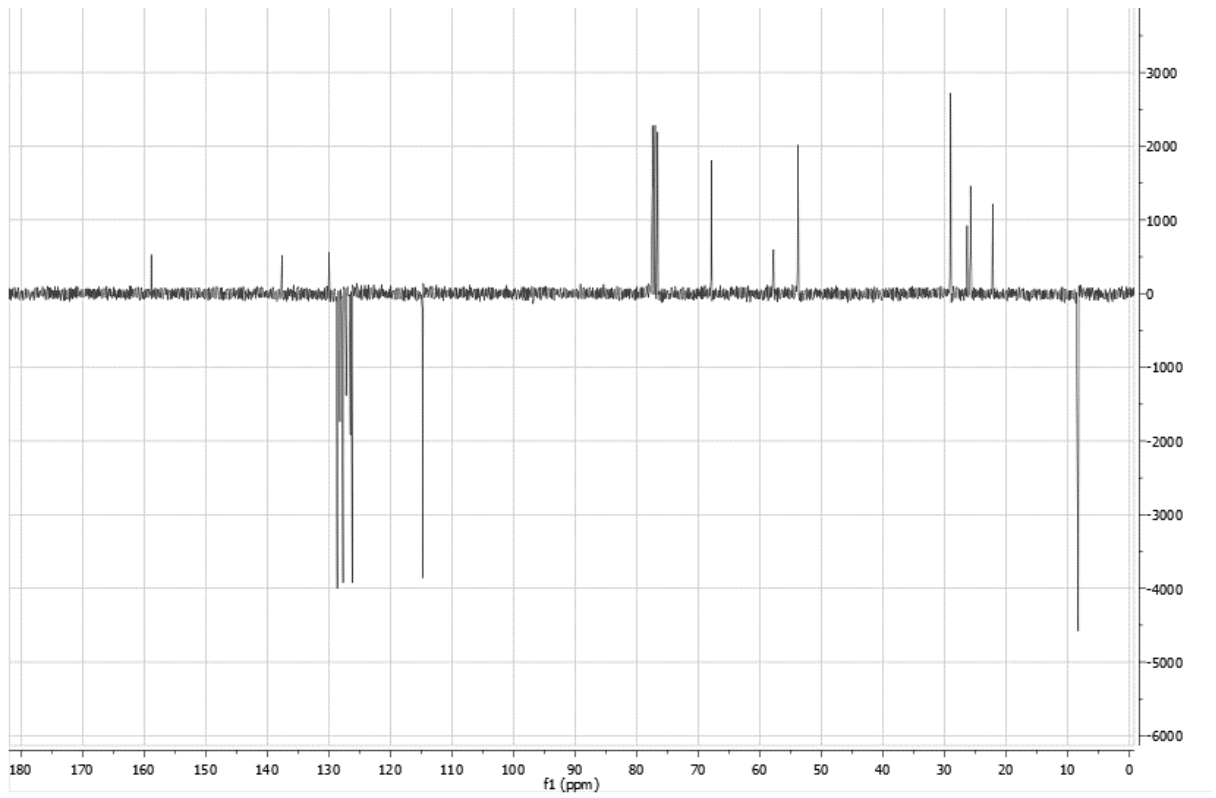
Synthesis of (*E*)-4-(8-triethylammoniooctyloxy)stilbene iodide (**26**)



Molecular Weight: 535.54

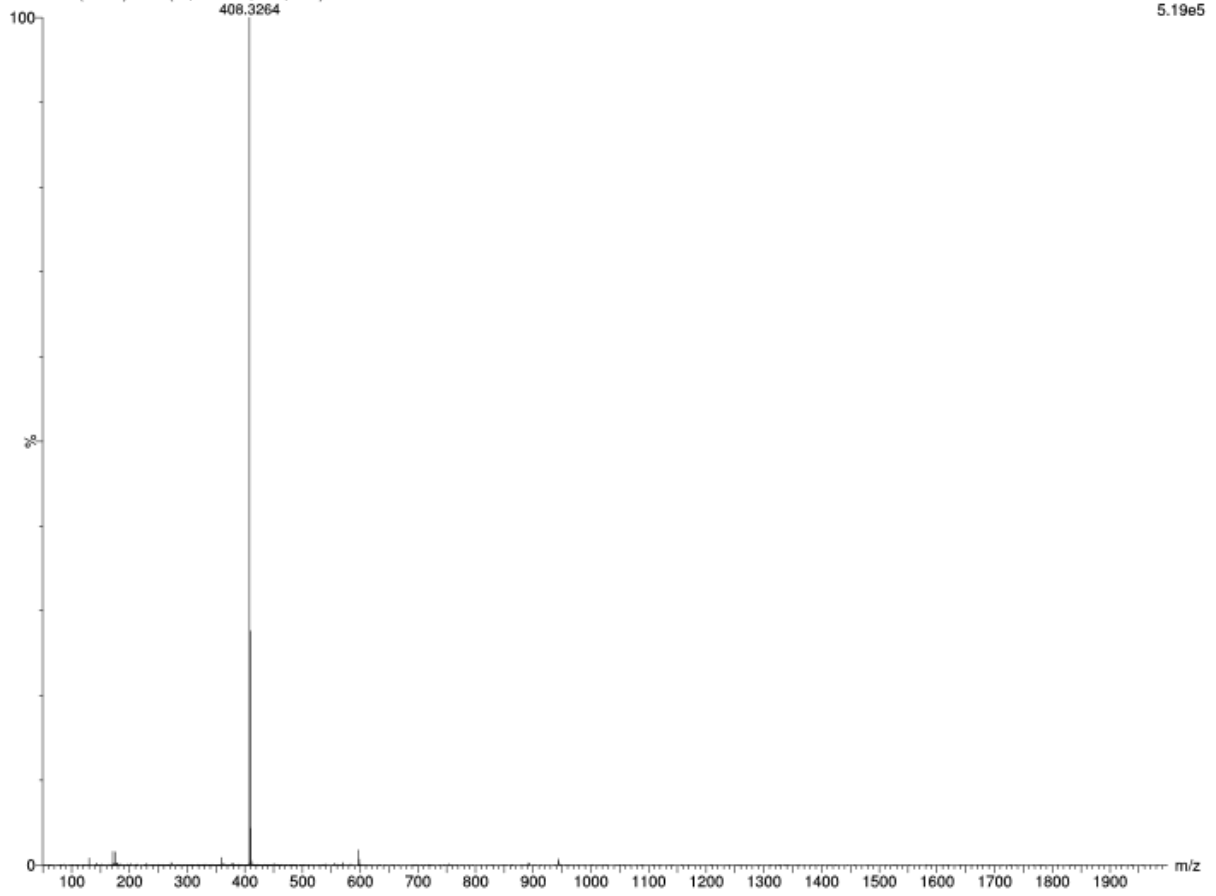
Intermediate (*E*)-4-(8-iodooctyloxy)stilbene (**119g**) (434 mg – 1 mmol) was dissolved in 3 ml of triethylamine and 3 ml of toluene for 5 hours. Upon concentration under vacuum, the residue was diluted with diethyl ether and the obtained suspension was filtered, affording the desired product **26** as a beige solid 402 mg – 0.75 mmol, 75%). **M.p.** = 163 °C. **¹H NMR** (300 MHz, CDCl₃): δ 7.53 – 7.38 (m, 4H), 7.33 (t, *J* = 7.6 Hz, 2H), 7.25 – 7.17 (m, 1H), 7.05 (d, *J* = 16.4 Hz, 1H), 6.95 (d, *J* = 16.4 Hz, 1H), 6.87 (d, *J* = 8.8 Hz, 2H), 3.95 (t, *J* = 6.4 Hz, 2H), 3.44 (q, *J* = 7.2 Hz, 6H), 3.31 – 3.19 (m, 2H), 1.84 – 1.58 (m, 4H), 1.53 – 1.27 (m, 17H). **¹³C NMR** (75 MHz, CDCl₃): δ 158.84, 137.62, 129.95, 128.64, 128.21, 127.70, 127.20, 126.50, 126.21, 114.76, 67.91, 57.80, 53.82, 29.12, 29.04, 26.37, 25.83, 22.21, 8.32. **Anal.** Calc. for C₂₈H₄₂INO: theor. C = 62.80; H = 7.90; I = 23.70; N = 2.62; found C = 62.58; H = 7.92; I = 23.80; N = 2.59. **HRMS (ESI⁺)**: calc. for C₂₈H₄₂NO: theor. 408.3266; found [M]⁺: 408.3264.





ST210 35 (0.668) AM2 (Ar,40000.0,0.00,0.00)

1: TOF MS ES+
5.19e5



Single Mass Analysis

Tolerance = 5.0 PPM / DBE: min = -1.5, max = 200.0

Element prediction: Off

Number of isotope peaks used for i-FIT = 5

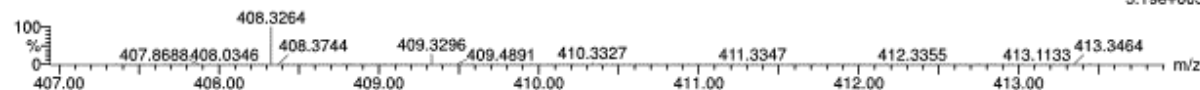
Monoisotopic Mass, Even Electron Ions

62 formula(e) evaluated with 1 results within limits (all results (up to 1000) for each mass)

Elements Used:

C: 28-28 H: 10-100 N: 0-5 O: 0-5 Na: 0-1

ST210 35 (0.668) AM2 (Ar,40000.0,0.00,0.00)

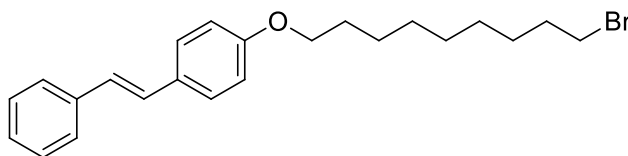
1: TOF MS ES+
5.19e+005

Minimum:

Maximum:

			-1.5
0.5	5.0		200.0

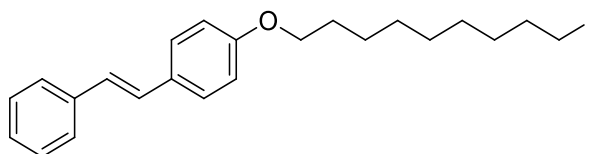
Mass	Calc. Mass	mDa	PPM	DBE	i-FIT	Norm	Conf(%)	Formula
408.3264	408.3266	-0.2	-0.5	8.5	1212.9	n/a	n/a	C28 H42 N O

Synthesis of (*E*)-4-(9-bromononyloxy)stilbene (**118h**)

Molecular Weight: 401.38

Procedure adapted from literature.¹⁹³ A solution of *trans*-4-hydroxystilbene (196 mg – 1 mmol) in DMSO (1.4 ml) was added to a stirred suspension of finely ground NaOH (85 mg – 2.1 mmol) in DMSO (5.6 ml). The mixture was stirred at room temperature for 30 minutes and then the 1,9-dibromononane (572 mg – 2 mmol) was added dropwise. When stilbenol was reacted, the reaction mixture was filtered and 1M aqueous solution of HCl was added dropwise to the filtrate to reach pH 3. The crude product was precipitated by slowly adding cold water. The precipitate was isolated by filtration, dried under vacuum and recrystallized from ethanol affording the pure compound **118h** as a white solid (337 mg – 0.84 mmol, 84%). TLC (Cyclohexane / Ethyl acetate 9:1): **R_f** = 0.63. **M.p.** = 111 °C. **¹H NMR** (300 MHz, CDCl₃): δ 7.46 (m, 4H), 7.34 (t, *J* = 7.5 Hz, 2H), 7.23 (m, 1H), 7.07 (d, *J* = 16.3 Hz, 1H), 6.96 (d, *J* = 16.3 Hz, 1H), 6.88 (d, *J* = 8.7 Hz, 2H), 3.97 (t, *J* = 6.5 Hz, 2H), 3.41 (t, *J* = 6.8 Hz, 2H), 1.95 – 1.68 (m, 4H), 1.49 – 1.24 (m, 10H).

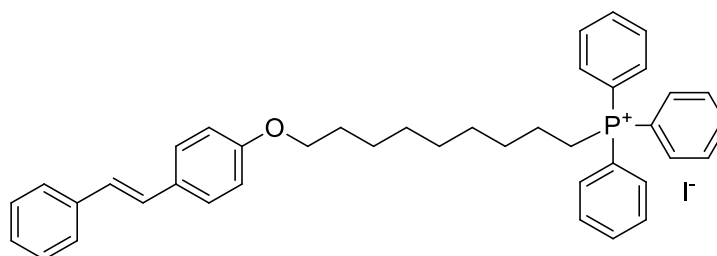
Synthesis of (*E*)-4-(9-iodononyloxy)stilbene (**119h**)



Molecular Weight: 448.38

Procedure adapted from literature.¹⁴⁰ Intermediate (*E*)-4-(9-bromononyloxy)stilbene (**118h**) (401 mg – 1 mmol) was dissolved in a saturated solution of NaI in acetone (10 ml), which was then refluxed overnight. After concentrating under vacuum, the residue was diluted with diethyl ether and subsequently washed with 10% aqueous Na₂S₂O₅ and then with brine. The organic phase was dried over Na₂SO₄, filtered, and the solvent was evaporated under vacuum to give the desired intermediate **119h** as a white solid (448 mg – 1.00 mmol, 100%). TLC (cyclohexane/ethyl acetate 9:1): R_f = 0.74. M.p. = 100 °C. ¹H NMR (300 MHz, CDCl₃): δ 7.46 (m, 4H), 7.34 (t, *J* = 7.5, 2H), 7.22 (m, 1H), 7.06 (d, *J* = 16.3 Hz, 1H), 6.96 (d, *J* = 16.3 Hz, 1H), 6.88 (d, *J* = 8.8 Hz, 2H), 3.97 (t, *J* = 6.5 Hz, 2H), 3.19 (t, *J* = 7.0 Hz, 2H), 1.92 – 1.68 (m, 4H), 1.49 – 1.18 (m, 10H).

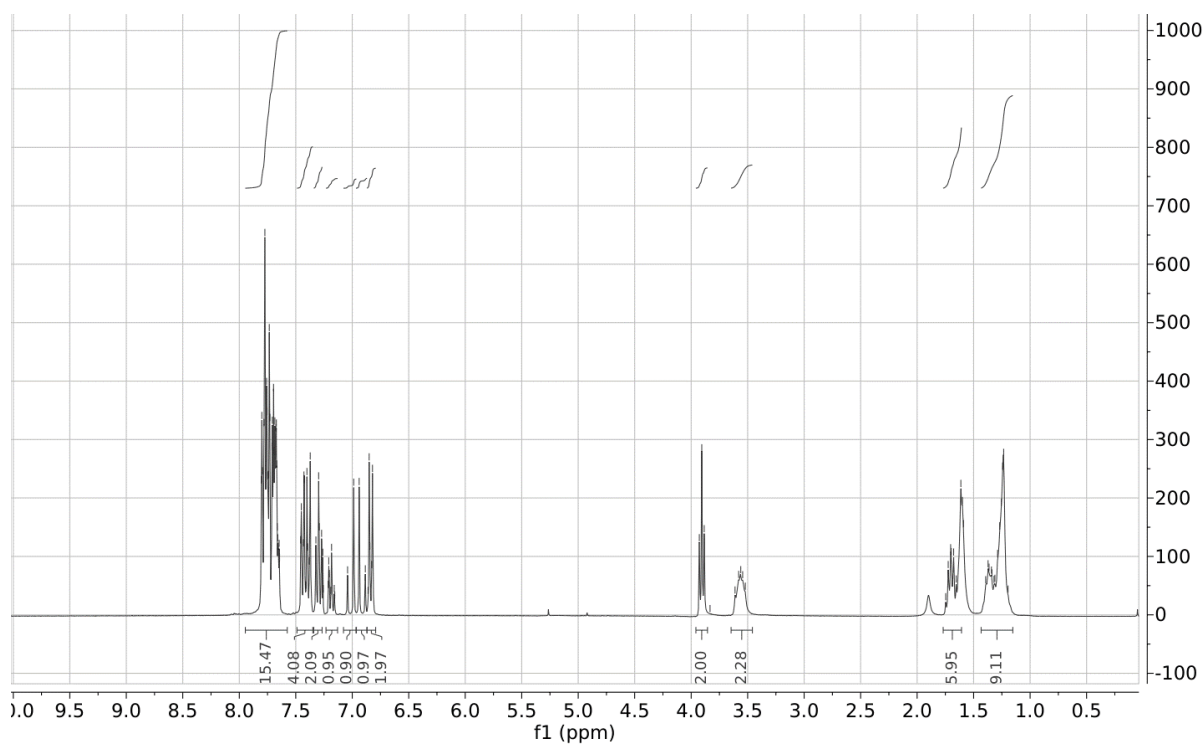
Synthesis of (*E*)-4-(9-triphenylphosphoniumnonyloxy)stilbene iodide (**23**)

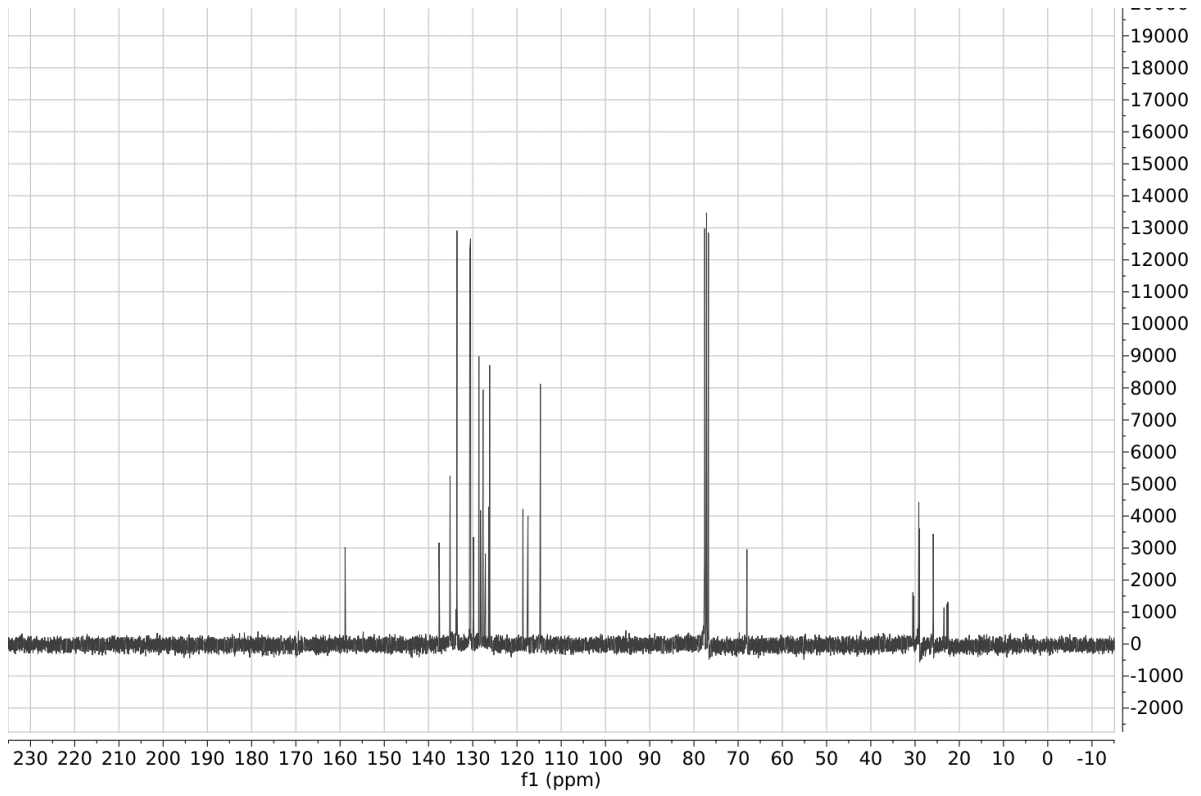


Molecular Weight: 710.67

A solid mixture of PPh₃ (5.25 g – 20 mmol) and intermediate (*E*)-4-(9-iodononyloxy)stilbene (**119h**) (448 mg – 1 mmol) was heated to 100 °C so as to obtain a solution of the starting material in molten PPh₃. The reaction mixture was slowly stirred at 100 °C for 3 hours and then cooled to room temperature without stirring any further. The re-solidified mixture was dissolved in the smallest possible volume of dichloromethane and diethyl ether was added dropwise under vigorous stirring. Afterwards, the solid precipitate was isolated by filtration affording the desired product **23** as a white solid (647 mg – 0.91 mmol, 91%). M.p. = 72 °C. ¹H NMR (300 MHz, CDCl₃): δ 7.83 – 7.72 (m, 9H), 7.72 – 7.62 (m, 6H), 7.48 – 7.34 (m, 4H), 7.30 (t, *J* = 7.5 Hz, 2H), 7.18 (m, 1H), 7.01 (d, *J* = 16.3 Hz, 1H), 6.91 (d, *J* = 16.3 Hz, 1H), 6.84 (d, *J* = 8.7 Hz,

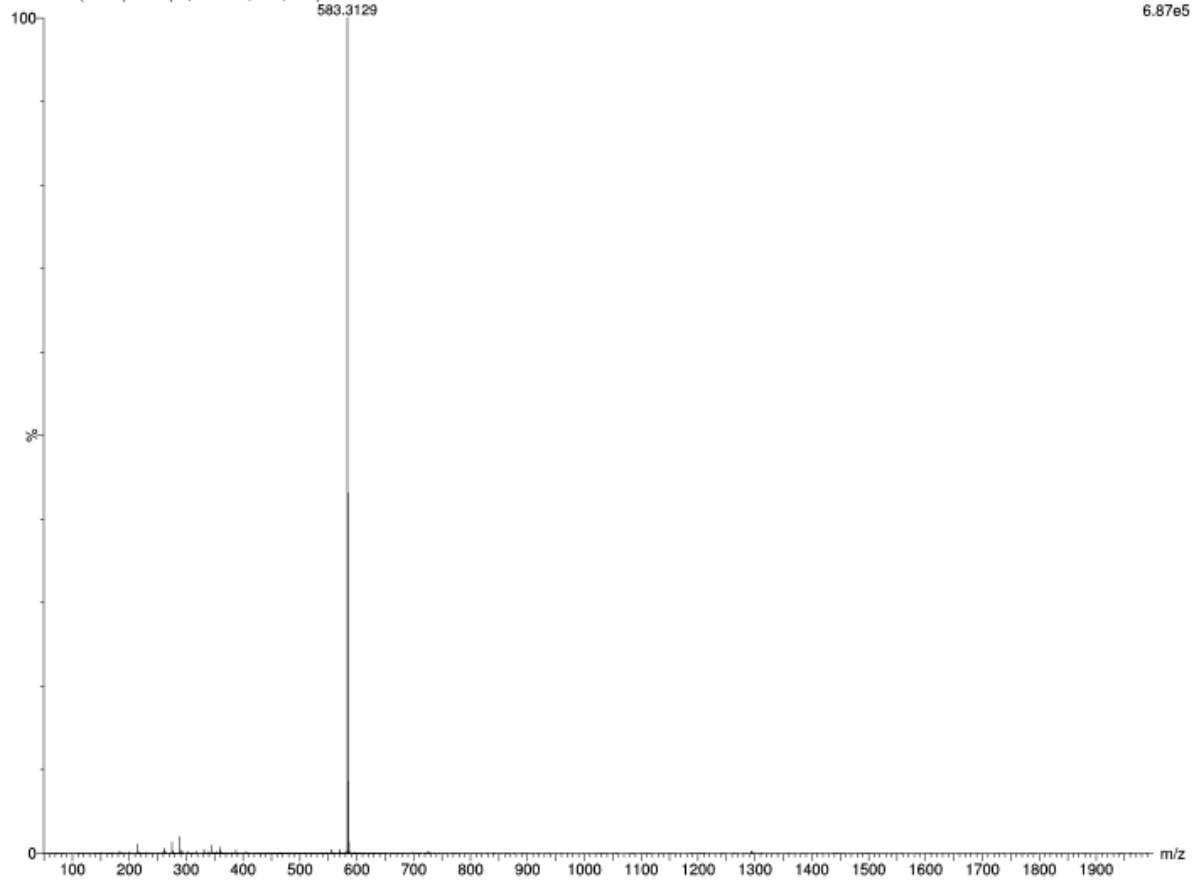
2H), 3.91 (t, $J = 6.5$ Hz, 2H), 3.59 (m, 2H), 1.79 – 1.51 (m, 6H), 1.45 – 1.12 (m, 8H). ^{13}C NMR (75 MHz, CDCl_3): δ 158.86, 137.63, 135.17, 135.13, 133.70, 133.57, 130.66, 130.50, 129.84, 128.61, 128.24, 127.67, 127.14, 126.38, 126.19, 118.65, 117.51, 114.71, 68.01, 30.48, 30.28, 29.15, 29.13, 29.04, 29.01, 25.89, 23.45, 22.79, 22.59, 22.53. **Anal.** Calc. for $\text{C}_{41}\text{H}_{44}\text{IOP}$: theor. C= 69.29; H= 6.24; P= 4.36; I= 17.86; found C= 69.02; H= 6.26; P= 4.30; I= 17.78. **HRMS (ESI⁺)**: calc. for $\text{C}_{41}\text{H}_{44}\text{OP}$: theor. 583.3130; found $[\text{M}]^+$: 583.3129.





ST208 36 (0.685) AM2 (Ar,40000.0,0.00,0.00)

1: TOF MS ES+
6.87e5



Single Mass Analysis

Tolerance = 5.0 PPM / DBE: min = -1.5, max = 200.0

Element prediction: Off

Number of isotope peaks used for i-FIT = 5

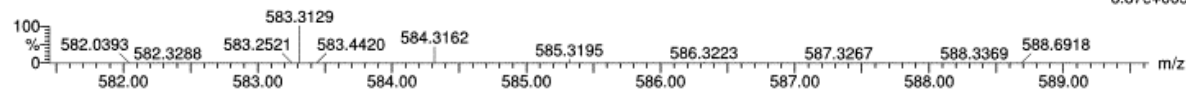
Monoisotopic Mass, Even Electron Ions

126 formula(e) evaluated with 1 results within limits (all results (up to 1000) for each mass)

Elements Used:

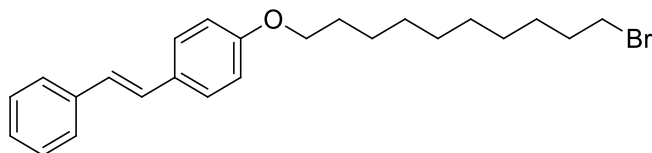
C: 41-41 H: 10-100 O: 0-5 Na: 0-1 P: 0-10

ST208 36 (0.685) AM2 (Ar,40000.0,0.00,0.00)

1: TOF MS ES+
6.87e+005

Minimum: -1.5
Maximum: 0.5 5.0 200.0

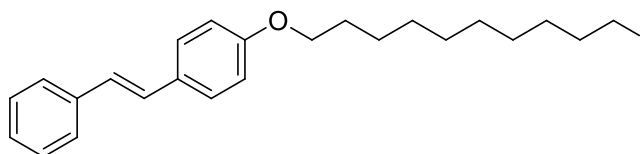
Mass	Calc. Mass	mDa	PPM	DBE	i-FIT	Norm	Conf(%)	Formula
583.3129	583.3130	-0.1	-0.2	20.5	1066.3	n/a	n/a	C41 H44 O P

Synthesis of (*E*)-4-(10-bromodecyloxy)stilbene (**118i**)

Molecular Weight: 415.41

Procedure adapted from literature.¹⁹³ A solution of *trans*-4-hydroxystilbene (196 mg – 1 mmol) in DMSO (1.4 ml) was added to a stirred suspension of finely ground NaOH (85 mg – 2.1 mmol) in DMSO (5.6 ml). The mixture was stirred at room temperature for 30 minutes and then the 1,4-dibromobutane (600 mg – 2 mmol) was added dropwise. When stilbenol was reacted, the reaction mixture was filtered and 1M aqueous solution of HCl was added dropwise to the filtrate to reach pH 3. The crude product was precipitated by slowly adding cold water. The precipitate was isolated by filtration, dried under vacuum and recrystallized from ethanol affording the pure compound **118i** as a white solid (153 mg – 0.37 mmol, 37%). **TLC** (Cyclohexane / Ethyl Acetate 9:1): **Rf**= 0.63. **M.p.**= 112 °C. **¹H NMR** (300 MHz, CDCl₃): δ 7.46 (m, 4H), 7.34 (t, *J* = 7.6 Hz, 2H), 7.23 (m, 1H), 7.06 (d, *J* = 16.3 Hz, 1H), 6.96 (d, *J* = 16.3 Hz, 1H), 6.89 (d, *J* = 8.7 Hz, 2H), 3.97 (t, *J* = 6.5 Hz, 2H), 3.41 (t, *J* = 6.9 Hz, 2H), 1.93 – 1.71 (m, 4H), 1.49 – 1.23 (m, 12H).

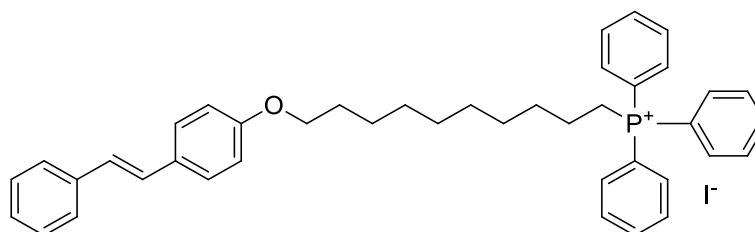
Synthesis of (*E*)-4-(10-iododecyloxy)stilbene (**119i**)



Molecular Weight: 462.41

Procedure adapted from literature.¹⁴⁰ Intermediate (*E*)-4-(10-bromodecyloxy)stilbene (**118i**) (415 mg – 1 mmol) was dissolved in a saturated solution of NaI in acetone (10 ml), which was then refluxed overnight. After concentrating under vacuum, the residue was diluted with diethyl ether and subsequently washed with 10% aqueous Na₂S₂O₅ and then with brine. The organic phase was dried over Na₂SO₄, filtered, and the solvent was evaporated under vacuum to give the desired intermediate **119i** as a white solid (462 mg – 1.00 mmol, 100%). TLC (Cyclohexane / Ethyl Acetate 9:1): R_f = 0.74. M.p. = 122 °C. ¹H NMR (300 MHz, CDCl₃): δ 7.46 (m, 4H), 7.34 (t, *J* = 7.5 Hz, 2H), 7.22 (m, 1H), 7.06 (d, *J* = 16.4 Hz, 1H), 6.96 (d, *J* = 16.4 Hz, 1H), 6.92 – 6.85 (m, 2H), 3.97 (t, *J* = 6.5 Hz, 2H), 3.19 (t, *J* = 7.0 Hz, 2H), 1.88 – 1.70 (m, 4H), 1.51 – 1.22 (m, 12H).

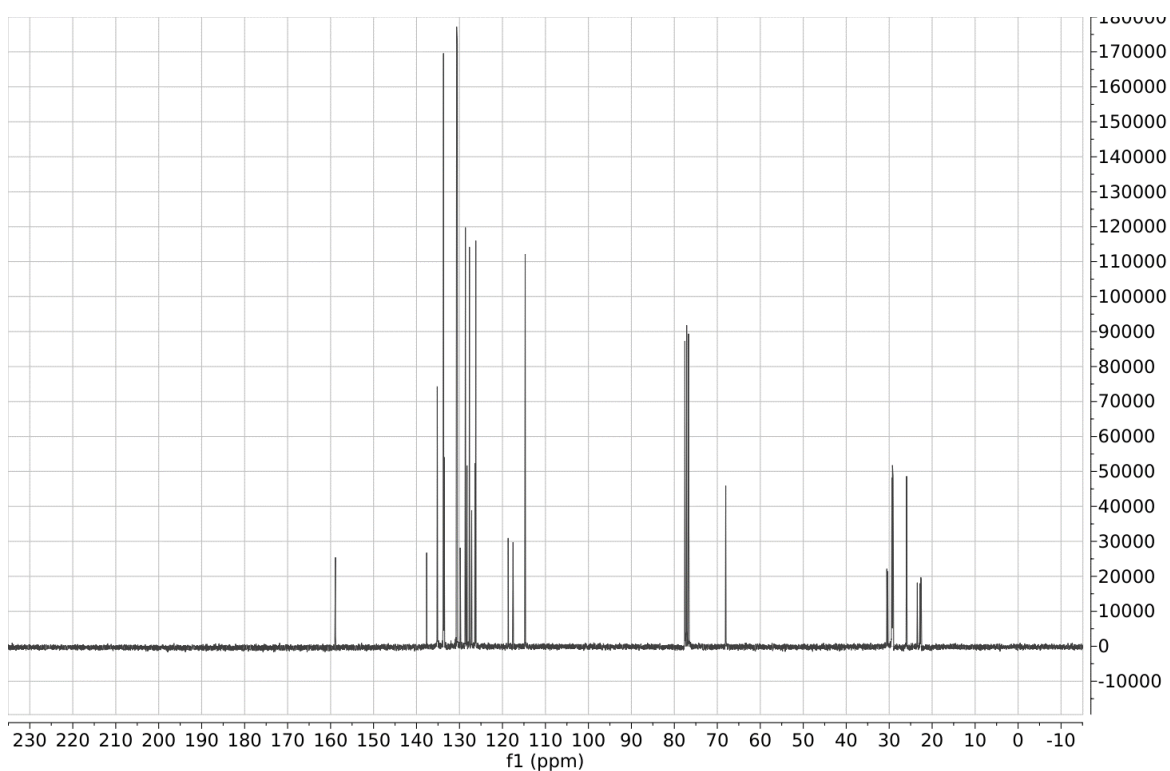
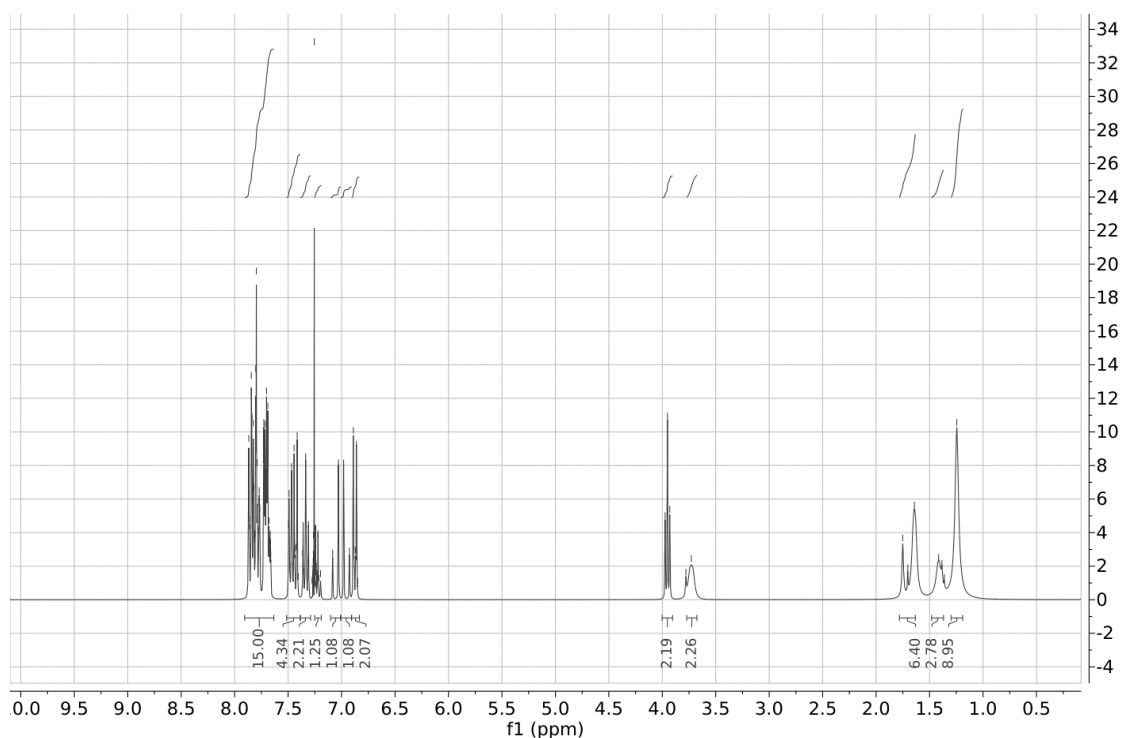
Synthesis of (*E*)-4-(10-triphenylphosphoniumdecyloxy)stilbene iodide (**24**)



Molecular Weight: 724.69

Procedure adapted from literature.¹⁴⁰ A solid mixture of PPh₃ (5.25 g – 20 mmol) and intermediate (*E*)-4-(10-bromodecyloxy)stilbene (**119i**) (448 mg – 1 mmol) was heated to 100 °C so as to obtain a solution of the starting material in molten PPh₃. The reaction mixture was slowly stirred at 100 °C for 3 hours and then cooled to room temperature without stirring any further. The re-solidified mixture was dissolved in the smallest possible volume of dichloromethane and diethyl ether was added dropwise under vigorous stirring. Afterwards, the solid precipitate was isolated by filtration affording the desired product **24** as a white solid (647 mg – 0.87 mmol, 87%). M.p. = 67 °C. ¹H NMR (300 MHz, CDCl₃): δ 7.90 – 7.74 (m, 9H), 7.79 – 7.63 (m, 6H), 7.53 – 7.38 (m, 4H), 7.33 (t, *J* = 7.5 Hz, 2H), 7.31 – 7.17 (m, 1H), 7.06 (d, *J* = 16.3 Hz, 1H), 6.95 (d, *J* = 16.3 Hz, 1H), 6.88 (d, *J* = 8.7 Hz, 2H), 3.95 (t, *J* = 6.5 Hz, 2H),

3.73 (m, 2H), 1.82 – 1.60 (m, 6H), 1.42 (m, 2H), 1.25 (m, 8H). ^{13}C NMR (75 MHz, CDCl_3): δ 158.87, 137.64, 135.18, 135.14, 133.72, 133.59, 130.67, 130.50, 129.84, 128.63, 128.53, 128.43, 128.25, 127.68, 127.16, 126.38, 126.20, 118.67, 117.53, 114.71, 68.03, 30.54, 30.34, 29.36, 29.24, 29.20, 29.13, 29.12, 29.09, 25.94, 23.46, 22.80, 22.62, 22.56. **Anal.** Calc. for $\text{C}_{42}\text{H}_{46}\text{IOP}$: theor. C= 69.61; H= 6.40; P= 4.27; I= 17.51; found C= 69.54; H= 6.39; P= 4.19; I= 17.39. **HRMS (ESI $^+$)**: calc. for $\text{C}_{42}\text{H}_{46}\text{OP}$: theor. 597.3286; found $[\text{M}]^+$: 597.3295.





Elemental Composition Report

Single Mass Analysis

Tolerance = 5.0 PPM / DBE: min = -1.5, max = 200.0
 Element prediction: Off
 Number of isotope peaks used for i-FIT = 5

Monoisotopic Mass, Even Electron Ions

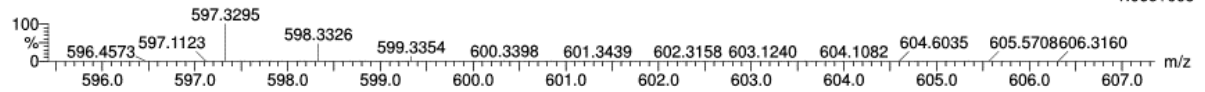
126 formula(e) evaluated with 1 results within limits (all results (up to 1000) for each mass)

Elements Used:

C: 42-42 H: 10-100 O: 0-5 Na: 0-1 P: 0-10

ST209 35 (0.668) AM2 (Ar,40000.0,0.00,0.00)

1: TOF MS ES+
1.06e+005



Minimum: -1.5
 Maximum: 0.5 5.0 200.0

Mass	Calc. Mass	mDa	PPM	DBE	i-FIT	Norm	Conf (%)	Formula
597.3295	597.3286	0.9	1.5	20.5	512.1	n/a	n/a	C42 H46 O P

Bibliography

- (1) Alexander, S. P. H.; Christopoulos, A.; Davenport, A. P.; Kelly, E.; Marrion, N. V.; Peters, J. A.; Faccenda, E.; Harding, S. D.; Pawson, A. J.; Sharman, J. L.; et al. The Concise Guide To Pharmacology 2017/18: G Protein-Coupled Receptors. *Br. J. Pharmacol.* **2017**, *174*, S17–S129.
- (2) Alexander, S. P. H.; Kelly, E.; Marrion, N. V.; Peters, J. A.; Faccenda, E.; Harding, S. D.; Pawson, A. J.; Sharman, J. L.; Southan, C.; Davies, J. A. The Concise Guide to Pharmacology 2017/18: Other Ion Channels. *Br. J. Pharmacol.* **2017**, *174*, S195–S207.
- (3) Albuquerque, E. X.; Pereira, E. F. R.; Alkondon, M.; Rogers, S. W. Mammalian Nicotinic Acetylcholine Receptors: From Structure to Function. *Physiol. Rev.* **2009**, *89* (1), 73–120.
- (4) Zoli, M.; Pistillo, F.; Gotti, C. Diversity of Native Nicotinic Receptor Subtypes in Mammalian Brain. *Neuropharmacology* **2015**, *96*, 302–311.
- (5) Gotti, C.; Clementi, F. Neuronal Nicotinic Receptors: From Structure to Pathology. *Prog. Neurobiol.* **2004**, *74* (6), 363–396.
- (6) Zoli, M.; Pucci, S.; Vilella, A.; Gotti, C. Neuronal and Extraneuronal Nicotinic Acetylcholine Receptors. *Curr. Neuropharmacol.* **2018**, *16* (4), 338–349.
- (7) Barlow, R. B.; Ing, H. R. Curare-like Action of Polymethylene Bis-Quaternary Ammonium Salts. *Br. J. Pharmacol. Chemother.* **1948**, *3* (4), 298–304.
- (8) Paton, W. D. M.; Zaimis, E. J. The Pharmacological Actions of Polymethylene Bistrimethylammonium Salts. *Br. J. Pharmacol. Chemother.* **1949**, *4*, 381–400.
- (9) Dani, J. A. Neuronal Nicotinic Acetylcholine Receptor Structure and Function and Response to Nicotine. *Int. Rev. Neurobiol.* **2015**, *124*, 3–19.
- (10) Corradi, J.; Bouzat, C. Understanding the Bases of Function and Modulation of A7 Nicotinic Receptors: Implications for Drug Discovery. *Mol. Pharmacol.* **2016**, *90* (3), 288–299.
- (11) Clarke, P. B. S.; Schwartz, R. D.; Paul, S. M.; Pert, C. B.; Pert, A. Nicotinic Binding in Rat Brain: Autoradiographic Comparison of [3H]Acetylcholine, [3H]Nicotine, and [125I]- α -Bungarotoxin. *J. Neurosci.* **1985**, *5* (5), 1307–1315.
- (12) Gotti, C.; Moretti, M.; Gaimarri, A.; Zanardi, A.; Clementi, F.; Zoli, M. Heterogeneity and Complexity of Native Brain Nicotinic Receptors. *Biochem. Pharmacol.* **2007**, *74* (8), 1102–1111.
- (13) Bateman, A.; Martin, M. J.; O'Donovan, C.; Magrane, M.; Alpi, E.; Antunes, R.; Bely, B.; Bingley, M.; Bonilla, C.; Britto, R.; et al. UniProt: The Universal Protein Knowledgebase. *Nucleic Acids Res.* **2017**, *45*, D158–D169.
- (14) Quick, M. W.; Lester, R. A. J. Desensitization of Nicotinic Receptors. *J. Neurobiol.* **2002**, *53* (4), 457–478.
- (15) Thesleff, S.; Katz, B. A Study of the “Desensitization” Produced by Acetylcholine at the Motor End-Plate. *J. Physiol.* **1957**, *138*, 63–80.
- (16) Changeux, J. P.; Devillers-Thiéry, A.; Chemouilli, P. Acetylcholine Receptor: An Allosteric Protein. *Science (80-.)*. **1984**, *225* (4668), 1335–1345.

- (17) Changeux, J.-P. Allostery and the Monod-Wyman-Changeux Model After 50 Years. *Annu. Rev. Biophys.* **2012**, *41* (1), 103–133.
- (18) Gotti, C.; Clementi, F.; Fornari, A.; Gaimarri, A.; Guiducci, S.; Manfredi, I.; Moretti, M.; Pedrazzi, P.; Pucci, L.; Zoli, M. Structural and Functional Diversity of Native Brain Neuronal Nicotinic Receptors. *Biochem. Pharmacol.* **2009**, *78* (7), 703–711.
- (19) Walsh, R. M.; Roh, S. H.; Gharpure, A.; Morales-Perez, C. L.; Teng, J.; Hibbs, R. E. Structural Principles of Distinct Assemblies of the Human A4 β 2 Nicotinic Receptor. *Nature* **2018**, *557*, 261–265.
- (20) Morales-Perez, C. L.; Noviello, C. M.; Hibbs, R. E. X-Ray Structure of the Human A4 β 2 Nicotinic Receptor. *Nature* **2016**, *538* (7625), 411–415.
- (21) Nelson, M. E.; Kuryatov, A.; Choi, C. H.; Zhou, Y.; Lindstrom, J. Alternate Stoichiometries of A4 β 2 Nicotinic Acetylcholine Receptors. *Mol. Pharmacol.* **2003**, *63* (2), 332–341.
- (22) Brisson, A.; Unwin, P. N. T. Tubular Crystals of Acetylcholine Receptor. *J. Cell Biol.* **1984**, *99*, 1202–1211.
- (23) Unwin, N. Nicotinic Acetylcholine Receptor at 9 Å Resolution. *J. Mol. Biol.* **1993**, *229*, 1101–1124.
- (24) Miyazawa, A.; Fujiyoshi, Y.; Stowell, M.; Unwin, N. Nicotinic Acetylcholine Receptor at 4.6 Å Resolution: Transverse Tunnels in the Channel Wall. *J. Mol. Biol.* **1999**, *288*, 765–786.
- (25) Brejc, K.; van Dijk, W. J.; Klaassen, R. V.; Schuurmans, M.; van der Oost, J.; Smit, A. B.; Sixma, T. K. Crystal Structure of an ACh-Binding Protein Reveals the Ligand-Binding Domain of Nicotinic Receptors. *Nature* **2001**, *411*, 269–276.
- (26) Smit, A. B.; Celie, P. H. N.; Kasheverov, I. E.; Mordvintsev, D. Y.; van Nierop, P.; Bertrand, D.; Tsetlin, V.; Sixma, T. K. Acetylcholine-Binding Proteins Functional and Structural Homologs of Nicotinic Acetylcholine Receptors August. *J. Mol. Neurosci.* **2006**, *30*, 9–10.
- (27) Wishart, D. S.; Feunang, Y. D.; Guo, A. C.; Lo, E. J.; Marcu, A.; Grant, J. R.; Sajed, T.; Johnson, D.; Li, C.; Sayeeda, Z.; et al. DrugBank 5.0: A Major Update to the DrugBank Database for 2018. *Nucleic Acids Res.* **2018**, *46* (D1), D1074–D1082.
- (28) Li, Y. H.; Yu, C. Y.; Li, X. X.; Zhang, P.; Tang, J.; Yang, Q.; Fu, T.; Zhang, X.; Cui, X.; Tu, G.; et al. Therapeutic Target Database Update 2018: Enriched Resource for Facilitating Bench-to-Clinic Research of Targeted Therapeutics. *Nucleic Acids Res.* **2018**, *46* (D1), D1121–D1127.
- (29) Picciotto, M. R.; Zoli, M.; Léna, C.; Bessis, A.; Lallemand, Y.; LeNovère, N.; Vincent, P.; Pinch, E. M.; Brulet, P.; Changeux, J.-P. Abnormal Avoidance Learning in Mice Lacking Functional High-Affinity Nicotine Receptor in the Brain. *Nature*. 1995, pp 65–67.
- (30) Steinlein, O. K. Genes and Mutations in Human Idiopathic Epilepsy. *Am. J. Med. Genet.* **2001**, *106*, 139–145.
- (31) Govind, A. P.; Vezina, P.; Green, W. N. Nicotine-Induced Upregulation of Nicotinic Receptors: Underlying Mechanisms and Relevance to Nicotine Addiction. *Biochem. Pharmacol.* **2009**, *78* (7), 756–765.

- (32) Dani, J. A.; Bertrand, D. Nicotinic Acetylcholine Receptors and Nicotinic Cholinergic Mechanisms of the Central Nervous System. *Annu. Rev. Pharmacol. Toxicol.* **2007**, *47* (1), 699–729.
- (33) Hurst, R.; Rollema, H.; Bertrand, D. Nicotinic Acetylcholine Receptors: From Basic Science to Therapeutics. *Pharmacol. Ther.* **2013**, *137* (1), 22–54.
- (34) Besson, M.; Granon, S.; Mameli-Engvall, M.; Cloëz-Tayarani, I.; Maubourguet, N.; Cormier, A.; Cazala, P.; David, V.; Changeux, J.-P.; Faure, P. Long-Term Effects of Chronic Nicotine Exposure on Brain Nicotinic Receptors. *Proc. Natl. Acad. Sci.* **2007**, *104* (19), 8155–8160.
- (35) NIDA. Tobacco , Nicotine , and E-Cigarettes Table of Contents. **2018**, No. January, 1–72.
- (36) Sanner, T.; Grimsrud, T. K. Nicotine: Carcinogenicity and Effects on Response to Cancer Treatment – a Review. *Front. Oncol.* **2015**, *5* (196), 1–10.
- (37) Mucchietto, V.; Fasoli, F.; Pucci, S.; Moretti, M.; Benfante, R.; Maroli, A.; Di Lascio, S.; Bolchi, C.; Pallavicini, M.; Dowell, C.; et al. A9- and A7-Containing Receptors Mediate the pro-Proliferative Effects of Nicotine in the A549 Adenocarcinoma Cell Line. *Br. J. Pharmacol.* **2018**, *175* (11), 1957–1972.
- (38) Markou, A. Neurobiology of Nicotine Dependence. *Philos. Trans. R. Soc. B Biol. Sci.* **2008**, *363* (1507), 3159–3168.
- (39) Mineur, Y. S.; Einstein, E. B.; Seymour, P. A.; Coe, J. W.; O’Neill, B. T.; Rollema, H.; Picciotto, M. R. A4 β 2 Nicotinic Acetylcholine Receptor Partial Agonists With Low Intrinsic Efficacy Have Antidepressant-Like Properties. *Behav. Pharmacol.* **2011**, *22* (4), 291–299.
- (40) Frolich, L.; Ashwoodb, T.; Nilssonc, J.; Eckerwallb, G. Effects of AZD3480 on Cognition in Patients with Mild-to-Moderate Alzheimer’s Disease: A Phase IIb Dose-Finding Study. *J. Alzheimer’s Dis.* **2011**, *24*, 363–374.
- (41) Yu, L. F.; Zhang, H. K.; Caldarone, B. J.; Eaton, J. B.; Lukas, R. J.; Kozikowski, A. P. Recent Developments in Novel Antidepressants Targeting A4 β 2-Nicotinic Acetylcholine Receptors. *J. Med. Chem.* **2014**, *57* (20), 8204–8223.
- (42) Rahman, S.; Engleman, E. A.; Bell, R. L. Nicotinic Receptor Modulation to Treat Alcohol and Drug Dependence. *Front. Neurosci.* **2015**, *9*, 1–11.
- (43) Rollema, H.; Hurst, R. S. The Contribution of Agonist and Antagonist Activities of A4 β 2* NACHR Ligands to Smoking Cessation Efficacy: A Quantitative Analysis of Literature Data. *Psychopharmacology (Berl)*. **2018**, *235* (9), 2479–2505.
- (44) Rose, J. E.; Levin, E. D. Concurrent Agonist-Antagonist Administration for the Analysis and Treatment of Drug Dependence. *Pharmacol. Biochem. Behav.* **1992**, *41* (1), 219–226.
- (45) Daly, J. W.; Garraffo, H. M.; Spande, T. F.; Decker, M. W.; Sullivan, J. P.; Williams, M. Alkaloids from Frog Skin: The Discovery of Epibatidine and the Potential for Developing Novel Non-Opioid Analgesics. *Nat. Prod. Rep.* **2000**, *17* (2), 131–135.
- (46) Traynor, J. R. Epibatidine and Pain. *Br. J. Anaesth.* **1998**, *81* (1), 69–76.
- (47) Pin, F.; Vercouillie, J.; Ouach, A.; Mavel, S.; Gulhan, Z.; Chicheri, G.; Jarry, C.; Massip, S.; Deloye, J. B.; Guilloteau, D.; et al. Design of ??? Nicotinic Acetylcholine Receptor

- Ligands in Quinuclidine, Tropane and Quinazoline Series. Chemistry, Molecular Modeling, Radiochemistry, in Vitro and in Rats Evaluations of a [18F] Quinuclidine Derivative. *Eur. J. Med. Chem.* **2014**, *82*, 214–224.
- (48) Radchenko, E. V.; Dravolina, O. A.; Beshpalov, A. Y. Agonist and Antagonist Effects of Cytisine in Vivo. *Neuropharmacology* **2015**, *95*, 206–214.
- (49) West, R.; Zatonski, W.; Cedzynska, M.; Lewandowska, D.; Pazik, J.; Aveyard, P.; Stapleton, J. Placebo-Controlled Trial of Cytisine for Smoking Cessation. *N. Engl. J. Med.* **2011**, *365* (13), 1193–1200.
- (50) Hajek, P.; McRobbie, H.; Myers, K. Efficacy of Cytisine in Helping Smokers Quit: Systematic Review and Meta-Analysis. *Thorax* **2013**, *68* (11), 1037–1042.
- (51) Rego Campello, H.; Del Villar, S. G.; Honraedt, A.; Minguez, T.; Oliveira, A. S. F.; Ranaghan, K. E.; Shoemark, D. K.; Bermudez, I.; Gotti, C.; Sessions, R. B.; et al. Unlocking Nicotinic Selectivity via Direct C–H Functionalization of (–)-Cytisine. *Chem* **2018**, *4*, 1710–1725.
- (52) Coe, J. W.; Brooks, P. R.; Vetelino, M. G.; Wirtz, M. C.; Arnold, E. P.; Huang, J.; Sands, S. B.; Davis, T. I.; Lebel, L. A.; Fox, C. B.; et al. Varenicline: An A4 β 2 Nicotinic Receptor Partial Agonist for Smoking Cessation. *J. Med. Chem.* **2005**, *48* (10), 3474–3477.
- (53) Mihalak, K. B.; Carroll, F. I.; Luetje, C. W. Varenicline Is a Partial Agonist at A4 β 2 and a Full Agonist at A7 Neuronal Nicotinic Receptors. *J. Pharmacol. Exp. Ther.* **2006**, *70* (3), 801–805.
- (54) Peng, C.; Stokes, C.; Mineur, Y. S.; Picciotto, M. R.; Tian, C.; Eibl, C.; Tomassoli, I.; Guendisch, D.; Papke, R. L. Differential Modulation of Brain Nicotinic Acetylcholine Receptor Function by Cytisine, Varenicline, and Two Novel Bispidine Compounds: Emergent Properties of a Hybrid Molecule. *J. Pharmacol. Exp. Ther.* **2013**, *347* (2), 424–437.
- (55) Banerjee, J.; Yongye, A. B.; Chang, Y. P.; Gyanda, R.; Medina-Franco, J. L.; Armishaw, C. J. Design and Synthesis of α -Conotoxin G1D Analogues as Selective A4 β 2 Nicotinic Acetylcholine Receptor Antagonists. *Biopolym. - Pept. Sci. Sect.* **2014**, *102* (1), 78–87.
- (56) Abdrakhmanova, G. R.; Damaj, M. I.; Carroll, F. I.; Martin, B. R. 2-Fluoro-3-(4-Nitro-Phenyl)Deschloroepibatidine Is a Novel Potent Competitive Antagonist of Human Neuronal A4 β 2 NACHRs. *Mol. Pharmacol.* **2006**, *69* (6), 1945–1952.
- (57) Faundez-Parraguez, M.; Farias-Rabelo, N.; Gonzalez-Gutierrez, J. P.; Etcheverry-Berrios, A.; Alzate-Morales, J.; Adasme-Carreño, F.; Varas, R.; Bermudez, I.; Iturriaga-Vasquez, P. Neonicotinic Analogues: Selective Antagonists for A4 β 2 Nicotinic Acetylcholine Receptors. *Bioorganic Med. Chem.* **2013**, *21* (10), 2687–2694.
- (58) Itier, V.; Schönbächler, R.; Tribollet, E.; Honer, M.; Prinz, K.; Marguerat, A.; Bertrand, S.; Bunnelle, W. H.; Schubiger, P. A.; Meyer, M. D.; et al. A-186253, a Specific Antagonist of the A4 β 2 NACHRs: Its Properties and Potential to Study Brain Nicotinic Acetylcholine Receptors. *Neuropharmacology* **2004**, *47* (4), 538–557.
- (59) Abreo, M. A.; Lin, N. H.; Garvey, D. S.; Gunn, D. E.; Hettlinger, A. M.; Wasicak, J. T.; Pavlik, P. A.; Martin, Y. C.; Donnelly-Roberts, D. L.; Anderson, D. J.; et al. Novel 3-Pyridyl Ethers with Subnanomolar Affinity for Central Neuronal Nicotinic Acetylcholine Receptors. *J. Med. Chem.* **1996**, *39* (4), 817–825.

- (60) Holladay, M. W.; Dart, M. J.; Lynch, J. K. Neuronal Nicotinic Acetylcholine Receptors as Targets for Drug Discovery. *J. Med. Chem.* **1997**, *40* (26), 4169–4193.
- (61) Wei, Z. L.; Xiao, Y.; Yuan, H.; Baydyuk, M.; Petukhov, P. A.; Musachio, J. L.; Kellar, K. J.; Kozikowski, A. P. Novel Pyridyl Ring C5 Substituted Analogues of Epibatidine and 3-(1-Methyl-2(S)-Pyrrolidinylmethoxy)Pyridine (A-84543) as Highly Selective Agents for Neuronal Nicotinic Acetylcholine Receptors Containing B2 Subunits. *J. Med. Chem.* **2005**, *48* (6), 1721–1724.
- (62) Xiao, Y.; Baydyuk, M.; Wang, H.; Davis, H. E.; Kellar, K. J. Pharmacology of the Agonist Binding Sites of Rat Neuronal Nicotinic Receptor Subtypes Expressed in HEK 293 Cells. *Bioorganic Med. Chem. Lett.* **2004**, *14* (8), 1845–1848.
- (63) Elliott, R. L.; Kopecka, H.; Gunn, D. E.; Lin, N. H.; Garvey, D. S.; Ryther, K. B.; Holladay, M. W.; Anderson, D. J.; Campbell, J. E.; Sullivan, J. P.; et al. 2-(Aryloxymethyl) Azacyclic Analogues as Novel Nicotinic Acetylcholine Receptor (NACHR) Ligands. *Bioorganic Med. Chem. Lett.* **1996**, *6* (19), 2283–2288.
- (64) Pabreza, L. A.; Dhawan, S.; Kellar, K. J. [3H]Cytisine Binding to Nicotinic Cholinergic Receptors in Brain. *Mol. Pharmacol.* **1991**, *39* (1), 9–12.
- (65) Xiao, Y.; Fan, H.; Musachio, J. L.; Wei, Z.-L.; Chellappan, S. K.; Kozikowski, A. P.; Kellar, K. J. Sazetidine-A, A Novel Ligand That Desensitizes A4 β 2 Nicotinic Acetylcholine Receptors without Activating Them. *Mol. Pharmacol.* **2006**, *70* (4), 1454–1460.
- (66) Zwart, R.; Carbone, A. L.; Moroni, M.; Bermudez, I.; Mogg, A. J.; Folly, E. A.; Broad, L. M.; Williams, A. C.; Zhang, D.; Ding, C.; et al. Sazetidine-A Is a Potent and Selective Agonist at Native and Recombinant α 2 Nicotinic Acetylcholine Receptors. *Mol. Pharmacol.* **2008**, *73* (6), 1838–1843.
- (67) Levin, E. D.; Rezvani, A. H.; Xiao, Y.; Slade, S.; Cauley, M.; Wells, C.; Hampton, D.; Petro, A.; Rose, J. E.; Brown, M. L.; et al. Sazetidine-A, a Selective A4 β 2 Nicotinic Receptor Desensitizing Agent and Partial Agonist, Reduces Nicotine Self-Administration in Rats. *J. Pharmacol. Exp. Ther.* **2010**, *332* (3), 933–939.
- (68) Rezvani, A. H.; Slade, S.; Wells, C.; Petro, A.; Lumeng, L.; Li, T. K.; Xiao, Y.; Brown, M. L.; Paige, M. A.; McDowell, B. E.; et al. Effects of Sazetidine-A, a Selective A4 β 2 Nicotinic Acetylcholine Receptor Desensitizing Agent on Alcohol and Nicotine Self-Administration in Selectively Bred Alcohol-Preferring (P) Rats. *Psychopharmacology (Berl)*. **2010**, *211* (2), 161–174.
- (69) Kozikowski, A. P.; Brek Eaton, J.; Bajjuri, K. M.; Chellappan, S. K.; Chen, Y.; Karadi, S.; He, R.; Caldarone, B.; Manzano, M.; Yuen, P. W.; et al. Chemistry and Pharmacology of Nicotinic Ligands Based on 6-[5-(Azetidin-2-Ylmethoxy)Pyridin-3-Yl]Hex-5-Yn-1-Ol (AMOP-H-OH) for Possible Use in Depression. *ChemMedChem* **2009**, *4* (8), 1279–1291.
- (70) Turner, J. R.; Castellano, L. M.; Blendy, J. A. Nicotinic Partial Agonists Varenicline and Sazetidine-A Have Differential Effects on Affective Behavior. *J. Pharmacol. Exp. Ther.* **2010**, *334* (2), 665–672.
- (71) Caldarone, B. J.; Wang, D.; Paterson, N. E.; Manzano, M.; Fedolak, A.; Cavino, K.; Kwan, M.; Hanania, T.; Chellappan, S. K.; Kozikowski, A. P.; et al. Dissociation between Duration of Action in the Forced Swim Test in Mice and Nicotinic Acetylcholine Receptor Occupancy with Sazetidine, Varenicline, and 5-I-A85380.

Psychopharmacology (Berl). **2011**, *217* (2), 199–210.

- (72) Pallavicini, M.; Moroni, B.; Bolchi, C.; Cilia, A.; Clementi, F.; Fumagalli, L.; Gotti, C.; Meneghetti, F.; Riganti, L.; Vistoli, G.; et al. Synthesis and A4 β 2 Nicotinic Affinity of Unichiral 5-(2-Pyrrolidinyl)Oxazolidinones and 2-(2-Pyrrolidinyl)Benzodioxanes. *Bioorg. Med. Chem. Lett.* **2006**, *16* (21), 5610–5615.
- (73) Pallavicini, M.; Bolchi, C.; Binda, M.; Cilia, A.; Clementi, F.; Ferrara, R.; Fumagalli, L.; Gotti, C.; Moretti, M.; Pedretti, A.; et al. 5-(2-Pyrrolidinyl)Oxazolidinones and 2-(2-Pyrrolidinyl)Benzodioxanes: Synthesis of All the Stereoisomers and A4 β 2 Nicotinic Affinity. *Bioorganic Med. Chem. Lett.* **2009**, *19* (3), 854–859.
- (74) Bolchi, C.; Gotti, C.; Binda, M.; Fumagalli, L.; Pucci, L.; Pistillo, F.; Vistoli, G.; Valoti, E.; Pallavicini, M. Unichiral 2-(2'-Pyrrolidinyl)-1,4-Benzodioxanes: The 2R,2'S Diastereomer of the N -Methyl-7-Hydroxy Analogue Is a Potent A4 β 2- and A6 β 2-Nicotinic Acetylcholine Receptor Partial Agonist. *J. Med. Chem.* **2011**, *54* (21), 7588–7601.
- (75) Bolchi, C.; Valoti, E.; Gotti, C.; Fasoli, F.; Ruggeri, P.; Fumagalli, L.; Binda, M.; Mucchietto, V.; Sciacaluga, M.; Budriesi, R.; et al. Chemistry and Pharmacology of a Series of Unichiral Analogues of 2-(2-Pyrrolidinyl)-1,4-Benzodioxane, Prolinol Phenyl Ether, and Prolinol 3-Pyridyl Ether Designed as A4 β 2-Nicotinic Acetylcholine Receptor Agonists. *J. Med. Chem.* **2015**, *58* (16), 6665–6677.
- (76) Yenugonda, V. M.; Xiao, Y.; Levin, E. D.; Rezvani, A. H.; Tran, T.; Al-Muhtasib, N.; Sahibzada, N.; Xie, T.; Wells, C.; Slade, S.; et al. Design, Synthesis and Discovery of Picomolar Selective A4 β 2 Nicotinic Acetylcholine Receptor Ligands. *J. Med. Chem.* **2013**, *56* (21), 8404–8421.
- (77) Bolchi, C.; Bavo, F.; Fumagalli, L.; Gotti, C.; Fasoli, F.; Moretti, M.; Pallavicini, M. Novel 5-Substituted 3-Hydroxyphenyl and 3-Nitrophenyl Ethers of S-Prolinol as A4 β 2-Nicotinic Acetylcholine Receptor Ligands. *Bioorganic Med. Chem. Lett.* **2016**, *26* (23), 5613–5617.
- (78) Bolchi, C.; Bavo, F.; Gotti, C.; Fumagalli, L.; Fasoli, F.; Binda, M.; Mucchietto, V.; Sciacaluga, M.; Plutino, S.; Fucile, S.; et al. From Pyrrolidinyl-Benzodioxane to Pyrrolidinyl-Pyridodioxanes, or from Unselective Antagonism to Selective Partial Agonism at A4 β 2 Nicotinic Acetylcholine Receptor. *Eur. J. Med. Chem.* **2017**, *125*, 1132–1144.
- (79) Lin, N. H.; Gunn, D. E.; Li, Y.; He, Y.; Bai, H.; Ryther, K. B.; Kuntzweiler, T.; Donnelly-Roberts, D. L.; Anderson, D. J.; Campbell, J. E.; et al. Synthesis and Structure-Activity Relationships of Pyridine-Modified Analogs of 3-[2-((S)-Pyrrolidinyl)Methoxy]Pyridine, A-84543, a Potent Nicotinic Acetylcholine Receptor Agonist. *Bioorganic Med. Chem. Lett.* **1998**, *8* (3), 249–254.
- (80) Gunn, D. E.; Elliott, R. L.; Lin, N.; Kopecka, H.; Holladay, M. W. US5472958A, 1995.
- (81) Bolchi, C.; Valoti, E.; Gotti, C.; Fasoli, F.; Ruggeri, P.; Fumagalli, L.; Binda, M.; Mucchietto, V.; Sciacaluga, M.; Budriesi, R.; et al. Chemistry and Pharmacology of a Series of Unichiral Analogues of 2-(2-Pyrrolidinyl)-1,4-Benzodioxane, Prolinol Phenyl Ether, and Prolinol 3-Pyridyl Ether Designed as A4 β 2-Nicotinic Acetylcholine Receptor Agonists. *J. Med. Chem.* **2015**, *58*, 6665–6677.
- (82) Yuan, H.; Petukhov, P. A. Computational Evidence for the Ligand Selectivity to the A4 β 2 and A3 β 4 Nicotinic Acetylcholine Receptors. *Bioorganic Med. Chem.* **2006**, *14*

- (23), 7936–7942.
- (83) Lin, N.; Abreo, M. A.; Gunn, D. E.; Lebold, S. A.; Lee, E. L.; Wasicak, J. T.; Hettinger, A.; Daanen, J. F.; Garvey, D. S.; Campbell, J. E.; et al. Structure-Activity Studies on a Novel Series of Cholinergic Channel Activators Based on a Heteroaryl Ether Framework. *Bioorg. Med. Chem. Lett.* **1999**, *9*, 2747–2752.
- (84) Ogunjirin, A. E.; Fortunak, J. M.; Brown, L. V. L.; Xiao, Y.; Dávila-García, M. I. Competition, Selectivity and Efficacy of Analogs of A-84543 for Nicotinic Acetylcholine Receptors with Repositioning of Pyridine Nitrogen. *Neurochem. Res.* **2015**, *40* (10), 2131–2142.
- (85) Elliott, R. L.; Ryther, K. B.; Anderson, D. J.; Piattoni-kaplan, M.; Kuntzweiler, T. A.; Donnelly-roberts, D.; Americ, S. P.; Holladay, M. W. Novel 2-(2'-Furo[3,2-b]Pyridinyl) Pyrrolidines: Potent Neuronal Nicotinic Acetylcholine Receptor Ligands. *Bioorg. Med. Chem. Lett.* **1997**, *7* (21), 2703–2708.
- (86) Dart, M. J.; Wasicak, J. T.; Ryther, K. B.; Schrimpf, M. R.; Kim, K. H.; Anderson, D. J.; Sullivan, J. P.; Meyer, M. D. Structural Aspects of High Affinity Ligands for the A4 β 2 Neuronal Nicotinic Receptor. *Pharm Acta Helv.* **2000**, *74* (2–3), 115–123.
- (87) Huber, R. G.; Margreiter, M. A.; Fuchs, J. E.; Von Grafenstein, S.; Tautermann, C. S.; Liedl, K. R.; Fox, T. Heteroaromatic π -Stacking Energy Landscapes. *J. Chem. Inf. Model.* **2014**, *54* (5), 1371–1379.
- (88) Sala, M.; Braidà, D.; Pucci, L.; Manfredi, I.; Marks, M. J.; Wageman, C. R.; Grady, S. R.; Loi, B.; Fucile, S.; Fasoli, F.; et al. CC4, a Dimer of Cytisine, Is a Selective Partial Agonist at A4 β 2/A6 β 2 NACHR with Improved Selectivity for Tobacco Smoking Cessation. *Br. J. Pharmacol.* **2013**, *168* (4), 835–849.
- (89) Bolchi, C.; Bavo, F.; Gotti, C.; Fumagalli, L.; Fasoli, F.; Binda, M.; Mucchietto, V.; Sciacaluga, M.; Plutino, S.; Fucile, S.; et al. From Pyrrolidinyl-Benzodioxane to Pyrrolidinyl-Pyridodioxanes, or from Unselective Antagonism to Selective Partial Agonism at A4 β 2 Nicotinic Acetylcholine Receptor. *Eur. J. Med. Chem.* **2017**, *125*.
- (90) Celie, P. H. N.; van Rossum-Fikker, S. E.; van Dijk, W. J.; Brejc, K.; Smit, A. B.; Sixma, T. K. Nicotine and Carbamylcholine Binding to Nicotinic Acetylcholine Receptors as Studied in AChBP Crystal Structures. **2004**, *41*, 907–914.
- (91) Blum, A. P.; Lester, H. A.; Dougherty, D. A. Nicotinic Pharmacophore: The Pyridine N of Nicotine and Carbonyl of Acetylcholine Hydrogen Bond across a Subunit Interface to a Backbone NH. *Proc. Natl. Acad. Sci.* **2010**, *107* (30), 13206–13211.
- (92) Michel, J.; Tirado-rives, J.; Jorgensen, W. L. Energetics of Displacing Water Molecules from Protein Binding Sites: Consequences for Ligand Optimization. *October* **2009**, *131* (42), 15403–15411.
- (93) Liu, Q.; Huang, Y.; Xue, F.; Simard, A.; DeChon, J.; Li, G.; Zhang, J.; Lucero, L.; Wang, M.; Sierks, M.; et al. A Novel Nicotinic Acetylcholine Receptor Subtype in Basal Forebrain Cholinergic Neurons with High Sensitivity to Amyloid Peptides. *J. Neurosci.* **2009**, *29* (4), 918–929.
- (94) Shen, J. X.; Yakel, J. L. Nicotinic Acetylcholine Receptor-Mediated Calcium Signaling in the Nervous System. *Acta Pharmacol. Sin.* **2009**, *30* (6), 673–680.
- (95) Cheng, H.; Fan, C.; Zhang, S. W.; Wu, Z. S.; Cui, Z. C.; Melcher, K.; Zhang, C. H.; Jiang, Y.; Cong, Y.; Xu, H. E. Crystallization Scale Purification of A7 Nicotinic

- Acetylcholine Receptor from Mammalian Cells Using a BacMam Expression System. *Acta Pharmacol. Sin.* **2015**, *36* (8), 1013–1023.
- (96) Li, S. X.; Huang, S.; Bren, N.; Noridomi, K.; Dellisanti, C. D.; Sine, S. M.; Chen, L. Ligand-Binding Domain of an A7-Nicotinic Receptor Chimera and Its Complex with Agonist. *Nat. Neurosci.* **2011**, *14* (10), 1253–1259.
- (97) Spurny, R.; Debaveye, S.; Farinha, A.; Veys, K.; Vos, A. M.; Gossas, T.; Atack, J.; Bertrand, S.; Bertrand, D.; Danielson, U. H.; et al. Molecular Blueprint of Allosteric Binding Sites in a Homologue of the Agonist-Binding Domain of the A7 Nicotinic Acetylcholine Receptor. *Proc. Natl. Acad. Sci.* **2015**, *112*, E2543–E2552.
- (98) Mowrey, D. D.; Liu, Q.; Bondarenko, V.; Chen, Q.; Seyoum, E.; Xu, Y.; Wu, J.; Tang, P. Insights into Distinct Modulation of A7 and A7 β 2 Nicotinic Acetylcholine Receptors by the Volatile Anesthetic. *J. Biol. Chem.* **2013**, *288* (50), 35793–35800.
- (99) Hibbs, R. E.; Gouaux, E. Principles of Activation and Permeation in an Anion-Selective Cys-Loop Receptor. *Nature* **2011**, *474* (7349), 54–60.
- (100) Miller, P. S.; Aricescu, A. R. Crystal Structure of a Human GABA Receptor. *Nature* **2014**, *512* (7514), 270–275.
- (101) Thompson, A. J.; Metzger, S.; Lochner, M.; Ruepp, M. D. The Binding Orientation of Epibatidine at A7 NACH Receptors. *Neuropharmacology* **2017**, *116*, 421–428.
- (102) Nemečz, Á.; Taylor, P. Creating an A7 Nicotinic Acetylcholine Recognition Domain from the Acetylcholine-Binding Protein: Crystallographic and Ligand Selectivity Analyses. *J. Biol. Chem.* **2011**, *286* (49), 42555–42565.
- (103) Hansen, S. B.; Sulzenbacher, G.; Huxford, T.; Marchot, P.; Taylor, P.; Bourne, Y. Structures of Aplysia AChBP Complexes with Nicotinic Agonists and Antagonists Reveal Distinctive Binding Interfaces and Conformations. *EMBO J.* **2005**, *24* (20), 3635–3646.
- (104) Krause, R. M.; Buisson, B.; Bertrand, S.; Corringer, P.; Galzi, J.; Changeux, J.; Bertrand, D.; Centre, U. R. A.; De, N. Ivermectin: A Positive Allosteric Effector of the α 7 Neuronal Nicotinic Acetylcholine Receptor. *Mol. Pharmacol.* **1998**, *53*, 283–294.
- (105) Zwart, R.; Filippi, G. De; Broad, L. M.; McPhie, G. I.; Pearson, K. H.; Baldwin, T.; Sher, E. 5-Hydroxyindole Potentiates Human A7 Nicotinic Receptor-Mediated Responses and Enhances Acetylcholine-Induced Glutamate Release in Cerebellar Slices. **2002**, *43*, 374–384.
- (106) Arias, H. R.; Gu, R. X.; Feuerbach, D.; Guo, B. B.; Ye, Y.; Wei, D. Q. Novel Positive Allosteric Modulators of the Human A7 Nicotinic Acetylcholine Receptor. *Biochemistry* **2011**, *50* (23), 5263–5278.
- (107) Targowska-Duda, K. M.; Kaczor, A. A.; Jozwiak, K.; Arias, H. R. Molecular Interactions of Type I and Type II Positive Allosteric Modulators with the Human A7 Nicotinic Acetylcholine Receptor: An in Silico Study. *J. Biomol. Struct. Dyn.* **2018**, *16*, 1–29.
- (108) Bertrand, D.; Lee, C.-H. L.; Flood, D.; Marger, F.; Donnelly-Roberts, D. Therapeutic Potential of A7 Nicotinic Acetylcholine Receptors. *Pharmacol. Rev.* **2015**, *67* (4), 1025–1073.
- (109) Gee, K. W.; Olincy, A.; Kanner, R.; Johnson, L.; Hogenkamp, D.; Harris, J.; Tran, M.; Edmonds, S. A.; Sauer, W.; Yoshimura, R.; et al. First in Human Trial of a Type i

- Positive Allosteric Modulator of A7-Nicotinic Acetylcholine Receptors: Pharmacokinetics, Safety, and Evidence for Neurocognitive Effect of AVL-3288. *J. Psychopharmacol.* **2017**, *31* (4), 434–441.
- (110) Delbart, F.; Brams, M.; Gruss, F.; Noppen, S.; Peigneur, S.; Boland, S.; Chaltin, P.; Brandao-Neto, J.; Von Delft, F.; Touw, W. G.; et al. An Allosteric Binding Site of the A7 Nicotinic Acetylcholine Receptor Revealed in a Humanized Acetylcholine-Binding Protein. *J. Biol. Chem.* **2018**, *293* (7), 2534–2545.
- (111) Pesti, K.; Szabo, A. K.; Mike, A.; Vizi, E. S. Kinetic Properties and Open Probability of A7 Nicotinic Acetylcholine Receptors. *Neuropharmacology* **2014**, *81*, 101–115.
- (112) Dineley, K. T.; Pandya, A. A.; Yakel, J. L. Nicotinic ACh Receptors as Therapeutic Targets in CNS Disorders. *Trends Pharmacol. Sci.* **2015**, *36* (2), 96–108.
- (113) Papke, R. L.; Meyer, E. M.; Lavieri, S.; Bollampally, S. R.; Papke, T. A. S.; Horenstein, N. A.; Itoh, Y.; Porter Papke, J. K. Effects at a Distance in A7 NACHR Selective Agonists: Benzylidene Substitutions That Regulate Potency and Efficacy. *Neuropharmacology* **2004**, *46* (7), 1023–1038.
- (114) Papke, R. L.; Kem, W. R.; Soti, F.; Lopez-Hernandez, G. Y.; Horenstein, N. A. Activation and Desensitization of Nicotinic A7-Type Acetylcholine Receptors by Benzylidene Anabaseines and Nicotine. *J. Pharmacol. Exp. Ther.* **2009**, *329* (2), 791–807.
- (115) Papke, R. L.; Chojnacka, K.; Horenstein, N. A. The Minimal Pharmacophore for Silent Agonism of the A7 Nicotinic Acetylcholine Receptor. *J. Pharmacol. Exp. Ther.* **2014**, *350* (3), 665–680.
- (116) Williams, D. K.; Peng, C.; Kimbrell, M. R.; Papke, R. L. Intrinsically Low Open Probability of A7 Nicotinic Acetylcholine Receptors Can Be Overcome by Positive Allosteric Modulation and Serum Factors Leading to the Generation of Excitotoxic Currents at Physiological Temperatures. *Mol. Pharmacol.* **2012**, *82* (4), 746–759.
- (117) Chojnacka, K.; Papke, R. L.; Horenstein, N. A. Synthesis and Evaluation of a Conditionally-Silent Agonist for the A7 Nicotinic Acetylcholine Receptor. *Bioorg. Med. Chem. Lett.* **2013**, *23* (14), 4145–4149.
- (118) Chiodo, L.; Malliavin, T. E.; Maragliano, L.; Cottone, G. A Possible Desensitized State Conformation of the Human A7 Nicotinic Receptor: A Molecular Dynamics Study. *Biophys. Chem.* **2017**, *229*, 99–109.
- (119) Levin, E. D.; McClernon, F. J.; Rezvani, A. H. Nicotinic Effects on Cognitive Function: Behavioral Characterization, Pharmacological Specification, and Anatomic Localization. *Psychopharmacology (Berl)*. **2006**, *184* (3–4), 523–539.
- (120) Gallowitsch-Puerta, M.; Tracey, K. J. Immunologic Role of the Cholinergic Anti-Inflammatory Pathway and the Nicotinic Acetylcholine A7 Receptor. *Ann. N. Y. Acad. Sci.* **2005**, *1062*, 209–219.
- (121) Dang, N.; Meng, X.; Song, H. Nicotinic Acetylcholine Receptors and Cancer. *Biomed. Reports* **2016**, *4* (5), 515–518.
- (122) Zhang, C.; Ding, X.-P.; Zhao, Q.-N.; Yang, X.-J.; An, S.-M.; Wang, H.; Xu, L.; Zhu, L.; Chen, H.-Z. Role of A7-Nicotinic Acetylcholine Receptor in Nicotine-Induced Invasion and Epithelial-to-Mesenchymal Transition in Human Non-Small Cell Lung Cancer Cells. *Oncotarget* **2016**, *7* (37), 59199–59208.

- (123) Burns, D. M. Tobacco-Related Diseases. *Semin. Oncol. Nurs.* **2003**, *19* (4), 244–249.
- (124) Siegel, R. L.; Miller, K. D.; Jemal, A. Cancer Statistics, 2017. *CA. Cancer J. Clin.* **2017**, *67* (1), 7–30.
- (125) Wang, S.; Hu, Y. A7 Nicotinic Acetylcholine Receptors in Lung Cancer (Review). *Oncol. Lett.* **2018**, *16* (2), 1375–1382.
- (126) Dallanoce, C.; Magrone, P.; Matera, C.; Frigerio, F.; Grazioso, G.; DeAmici, M.; Fucile, S.; Piccari, V.; Frydenvang, K.; Pucci, L.; et al. Design, Synthesis, and Pharmacological Characterization of Novel Spirocyclic Quinuclidinyl- Δ^2 -Isoxazoline Derivatives as Potent and Selective Agonists of A7 Nicotinic Acetylcholine Receptors. *ChemMedChem* **2011**, *6* (5), 889–903.
- (127) Schuller, H. M. Is Cancer Triggered by Altered Signalling of Nicotinic Acetylcholine Receptors? *Nat. Rev. Cancer* **2009**, *9* (3), 195–205.
- (128) Momi, N.; Ponnusamy, M. P.; Kaur, S.; Rachagani, S.; Kunigal, S. S.; Chellappan, S.; Ouellette, M. M.; Batra, S. K. Nicotine/Cigarette Smoke Promotes Metastasis of Pancreatic Cancer through A7nAChR-Mediated MUC4 Upregulation. *Oncogene* **2013**, *32* (11), 1384–1395.
- (129) Tu, C.-C.; Huang, C.-Y.; Cheng, W.-L.; Hung, C.-S.; Uyanga, B.; Wei, P.-L.; Chang, Y.-J. The A7-Nicotinic Acetylcholine Receptor Mediates the Sensitivity of Gastric Cancer Cells to Taxanes. *Tumor Biol.* **2016**, *37* (4), 4421–4428.
- (130) Kem, W.; Soti, F.; Wildeboer, K.; LeFrancois, S.; MacDougall, K.; Wei, D. Q.; Chou, K. C.; Arias, H. R. The Nemertine Toxin Anabaseine and Its Derivative DMXBA (GTS-21): Chemical and Pharmacological Properties. *Mar. Drugs* **2006**, *4* (3), 255–273.
- (131) Mullen, G.; Napier, J.; Balestra, M.; Decory, T.; Hale, G.; Macor, J.; Mack, R.; Loch, J.; Wu, E.; Kover, A.; et al. (-)-Spiro[1-Azabicyclo[2.2.2]Octane-3,5'-Oxazolidin-2-One], a Conformationally Restricted Analogue of Acetylcholine, Is a Highly Selective Full Agonist at the A7 Nicotinic Acetylcholine Receptor. *J. Med. Chem.* **2000**, *43* (22), 4045–4050.
- (132) Briggs, C. A.; Anderson, D. J.; Brioni, J. D.; Buccafusco, J. J.; Buckley, M. J.; Campbell, J. E.; Decker, M. W.; Donnelly-Roberts, D.; Elliott, R. L.; Gopalakrishnan, M.; et al. Functional Characterization of the Novel Neuronal Nicotinic Acetylcholine Receptor Ligand GTS-21 in Vitro and in Vivo. *Pharmacol. Biochem. Behav.* **1997**, *57* (1–2), 231–241.
- (133) Romero, H. K.; Christensen, S. B.; Di Cesare Mannelli, L.; Gajewiak, J.; Ramachandra, R.; Elmslie, K. S.; Vetter, D. E.; Ghelardini, C.; Iadonato, S. P.; Mercado, J. L.; et al. Inhibition of A9 α 10 Nicotinic Acetylcholine Receptors Prevents Chemotherapy-Induced Neuropathic Pain. *Proc. Natl. Acad. Sci.* **2017**, *114* (10), E1825–E1832.
- (134) Ellison, M.; Haberlandt, C.; Gomez-Casati, M. E.; Watkins, M.; Elgoyhen, A. B.; McIntosh, J. M.; Olivera, B. M. α -RgIA: A Novel Conotoxin That Specifically and Potently Blocks the A9 α 10 NACHR. *Biochemistry* **2006**, *45* (5), 1511–1517.
- (135) Christensen, S. B.; Hone, A. J.; Roux, I.; Kniazeff, J.; Pin, J.-P.; Upert, G.; Servent, D.; Glowatzki, E.; McIntosh, J. M. RgIA4 Potently Blocks Mouse A9 α 10 NACHRs and Provides Long Lasting Protection against Oxaliplatin-Induced Cold Allodynia. *Front. Cell. Neurosci.* **2017**, *11* (July), 1–12.
- (136) Tu, A. T.; Hong, B. S. Purification and Chemical Studies of a Toxin from the Venom of

- Lapemis Hardwickii (Hardwick's Sea Snake). *J. Biol. Chem.* **1971**, *246* (9), 2772–2779.
- (137) Cavallini, G.; Mantegazza, P.; Massarini, E.; Tommasini, R. Sull'attività Ganglioplegica Di Alcuni Derivati Alchilaminici Dello Stilbene e Del Difenile. *Farm.* **1953**, *6*, 317–331.
- (138) Gotti, C.; Balestra, B.; Moretti, M.; Rovati, G. E.; Maggi, L.; Rossoni, G.; Berti, F.; Villa, L.; Pallavicini, M.; Clementi, F. 4-Oxystilbene Compounds Are Selective Ligands for Neuronal Nicotinic α -Bungarotoxin Receptors. *Br J Pharmacol* **1998**, *124* (6), 1197–1206.
- (139) Maggi, L.; Palma, E.; Eusebi, F.; Moretti, M.; Balcstra, B.; Clementi, F.; Gotti, C. Selective Effects of a 4-Oxystilbene Derivative on Wild and Mutant Neuronal Chick A1 Nicotinic Receptor. *Br. J. Pharmacol.* **1999**, *126* (1), 285–295.
- (140) Biasutto, L.; Mattarei, A.; Marotta, E.; Bradaschia, A.; Sassi, N.; Garbisa, S.; Zoratti, M.; Paradisi, C. Development of Mitochondria-Targeted Derivatives of Resveratrol. *Bioorganic Med. Chem. Lett.* **2008**, *18* (20), 5594–5597.
- (141) Schneider, Y.; Vincent, F.; Duranton, B.; Badolo, L.; Gossé, F.; Bergmann, C.; Seiler, N.; Raul, F. Anti-Proliferative Effect of Resveratrol, a Natural Component of Grapes and Wine, on Human Colonic Cancer Cells. *Cancer Lett.* **2000**, *158* (1), 85–91.
- (142) Kumar, S.; Stokes, J.; Singh, U. P.; Scisum-Gunn, K.; Singh, R.; Manne, U.; Mishra, M. K. Prolonged Exposure of Resveratrol Induces Reactive Superoxide Species-independent Apoptosis in Murine Prostate Cells. *Tumor Biol.* **2017**, *39* (10), 1–10.
- (143) Pelicano, H.; Carney, D.; Huang, P. ROS Stress in Cancer Cells and Therapeutic Implications. *Drug Resist. Updat.* **2004**, *7* (2), 97–110.
- (144) Juan, M. E.; Wenzel, U.; Daniel, H.; Planas, J. M. Resveratrol Induces Apoptosis through ROS-Dependent Mitochondria Pathway in HT-29 Human Colorectal Carcinoma Cells. *J. Agric. Food Chem.* **2008**, *56* (12), 4813–4818.
- (145) Hoye, A.; Davoren, J.; Wipf, P.; Fink, M.; Kagan, V. Targeting Mitochondria. *Acc. Chem. Res* **2007**, *41* (1).
- (146) Fantin, V. R.; Leder, P. Mitochondriotoxic Compounds for Cancer Therapy. *Oncogene* **2006**, *25* (34), 4787–4797.
- (147) Sassi, N.; Mattarei, A.; Azzolini, M.; Bernardi, P.; Szabo', I.; Paradisi, C.; Zoratti, M.; Biasutto, L. Mitochondria-Targeted Resveratrol Derivatives Act as Cytotoxic Pro-Oxidants. *Curr. Pharm. Des.* **2014**, *20* (2), 172–179.
- (148) Sassi, N.; Mattarei, A.; Azzolini, M.; Szabo', I.; Paradisi, C.; Zoratti, M.; Biasutto, L. Cytotoxicity of Mitochondria-Targeted Resveratrol Derivatives: Interactions with Respiratory Chain Complexes and ATP Synthase. *Biochim. Biophys. Acta - Bioenerg.* **2014**, *1837* (10), 1781–1789.
- (149) Rohlena, J.; Dong, L.-F.; Kluckova, K.; Zabalova, R.; Goodwin, J.; Tilly, D.; Stursa, J.; Pecinova, A.; Philimonenko, A.; Hozak, P.; et al. Mitochondrially Targeted α -Tocopheryl Succinate Is Antiangiogenic: Potential Benefit Against Tumor Angiogenesis but Caution Against Wound Healing. *Antioxid. Redox Signal.* **2011**, *15* (12), 2923–2935.
- (150) Weber, G. F. Time and Circumstances: Cancer Cell Metabolism at Various Stages of Disease Progression. *Front. Oncol.* **2016**, *6* (December), 1–9.
- (151) Widiandi, T.; Hiraga, Y.; Kojima, S.; Abe, M. Novel Cyclic β -Aminophosphonate Derivatives as Efficient Organocatalysts for the Asymmetric Michael Addition

- Reactions of Ketones to Nitrostyrenes. *Tetrahedron Asymmetry* **2010**, *21* (15), 1861–1868.
- (152) Belokon', Y. N.; Kochetkov, K. A.; Churkina, T. D.; Ikonnikov, N. S.; Orlova, S. A.; Kuz'mina, N. A.; Bodrov, D. E. Asymmetric Addition of Methyl Nitroacetate to Crotonaldehyde Catalyzed by Chiral Amines. *Russ. Chem. Bull.* **1993**, *42* (9), 1525–1529.
- (153) Nouch, R.; Cini, M.; Magre, M.; Abid, M.; Diéguez, M.; Pàmies, O.; Woodward, S.; Lewis, W. Enantioselective Synthesis of 6,6-Disubstituted Pentafulvenes Containing a Chiral Pendant Hydroxy Group. *Chem. - A Eur. J.* **2017**, *23* (68), 17195–17198.
- (154) Wu, Z.; Laffoon, S. D.; Nguyen, T. T.; McAlpin, J. D.; Hull, K. L. Rhodium-Catalyzed Asymmetric Synthesis of β -Branched Amides. *Angew. Chemie Int. Ed.* **2017**, *56* (5), 1371–1375.
- (155) Molnár, I. G.; Holland, M. C.; Daniliuc, C.; Houk, K. N.; Gilmour, R. Organocatalysis Intermediates as Platforms to Study Noncovalent Interactions: Integrating Fluorine Gauche Effects in Iminium Systems to Facilitate Acyclic Conformational Control. *Synlett* **2016**, *27* (7), 1051–1055.
- (156) Kaga, A.; Hayashi, H.; Hakamata, H.; Oi, M.; Uchiyama, M.; Takita, R.; Chiba, S. Nucleophilic Amination of Methoxy Arenes Promoted by a Sodium Hydride/Iodide Composite. *Angew. Chemie - Int. Ed.* **2017**, *56* (39), 11807–11811.
- (157) Chaudhuri, D.; Sigmund, E.; Meyer, A.; Röck, L.; Klemm, P.; Lautenschlager, S.; Schmid, A.; Yost, S. R.; Vanvoorhis, T.; Bange, S.; et al. Metal-Free OLED Triplet Emitters by Side-Stepping Kasha's Rule. *Angew. Chemie - Int. Ed.* **2013**, *52* (50), 13449–13452.
- (158) Axford, L. C.; Agarwal, P. K.; Anderson, K. H.; Andrau, L. N.; Atherall, J.; Barker, S.; Bennett, J. M.; Blair, M.; Collins, I.; Czaplewski, L. G.; et al. Design, Synthesis and Biological Evaluation of α -Substituted Isonipetric Acid Benzothiazole Analogues as Potent Bacterial Type II Topoisomerase Inhibitors. *Bioorganic Med. Chem. Lett.* **2013**, *23* (24), 6598–6603.
- (159) Haydon, D. R.; Czaplewski, L. G.; Palmer, N. J.; Mitchell, D. R.; Atherall, J. F.; Steele, C. R.; Ladduwahetty, T. WO2007/148093 A1.Pdf, 2007.
- (160) Lee, M.; Ikejiri, M.; Chag, M.; Fridman, R.; Mobashery, S. WO2006/125208 A1.Pdf, 2006.
- (161) Khalfina, I. A.; Beregovaya, I. V.; Vlasov, V. M. Structure of Potassium Carbonate Complexes with Phenols and Thiophenols in Aprotic Dipolar Solvents. *Russ. J. Org. Chem.* **2003**, *39* (8), 1104–1115.
- (162) Guzl, T. J.; Paruch, K.; Dwyer, M. P.; Parry, D. A.; Zhao, L.; Curran, P. J.; Belanger, D. B.; Hamann, B.; Reddy, P. A. P.; Siddiqui, M. A.; et al. US2007/105864 A1.Pdf, 2007.
- (163) Matveeva, E. D.; Podrugina, T. A.; Morozkin, I. G.; Tkachenko, S. E.; Zefirov, N. S. Synthesis and Neuroprotective Properties of Isosteric Analogs of Nicotine. *Chem. Heterocycl. Compd.* **2000**, *36* (10), 1149–1153.
- (164) Sundalam, S. K.; Stuart, D. R. Base Mediated Synthesis of Alkyl-Aryl Ethers from the Reaction of Aliphatic Alcohols and Unsymmetric Diaryliodonium Salts. *J. Org. Chem.* **2015**, *80* (12), 6456–6466.

- (165) Takeuchi, Y.; Yamada, A.; Suzuki, T.; Koizumi, T. Synthetic Studies towards Proline Amide Isosteres, Potentially Useful Molecules for Biological Investigations. *Tetrahedron* **1996**, *52* (1), 225–232.
- (166) De Luca, L.; Giacomelli, G.; Masala, S.; Porcheddu, A. Trichloroisocyanuric/TEMPO Oxidation of Alcohols under Mild Conditions: A Close Investigation. *J. Org. Chem.* **2003**, *68* (12), 4999–5001.
- (167) Aitken, R. A.; Karodia, N.; Massil, T.; Young, R. J. Flash Vacuum Pyrolysis of Stabilised Phosphorus Ylides. Part 17. Preparation of Aliphatic Amino Acid Derived γ -Alkoxy-carbonylamino- β -Oxo Ylides and Pyrolysis to Give α,β -Acetylenic γ -Amino Acid and GABA Analogues. *J. Chem. Soc. Perkin 1* **2002**, *2* (4), 533–541.
- (168) Subhas Bose, D.; Idrees, M.; Todewale, I. K.; Jakka, N. M.; Venkateswara Rao, J. Hybrids of Privileged Structures Benzothiazoles and Pyrrolo[2,1-c][1,4]Benzodiazepin-5-One, and Diversity-Oriented Synthesis of Benzothiazoles. *Eur. J. Med. Chem.* **2012**, *50*, 27–38.
- (169) Hanessian, S.; Sharma, R. The Synthesis of Bicyclic Piperazine-2-Carboxylic Acids from L-Proline. Pdf. *Heterocycles* **2000**, *52* (3), 1231–1239.
- (170) Fournier, A. M.; Brown, R. A.; Farnaby, W.; Miyatake-ondoabal, H.; Clayden, J. Synthesis of (-)-(S,S)-Clemastine by Invertive N f C Aryl Migration in a Lithiated Carbamate. *Org. Lett.* **2010**, *12* (10), 2222–2225.
- (171) Rueeger, H.; Benn, M. The Synthesis of (-)-Isoretronecanol, (-)-Trachelanthamidine, and (-)-Supinidine from (S)-Proline. *Heterocycles* **1982**, *19* (9), 1677–1680.
- (172) Bureš, F.; Kulhánek, J. Chiral Imidazole Derivatives Synthesis from Enantiopure N-Protected α -Amino Acids. *Tetrahedron Asymmetry* **2005**, *16* (7), 1347–1354.
- (173) Furukawa, K.; Shibuya, M.; Yamamoto, Y. Chemoselective Catalytic Oxidation of 1,2-Diols to α -Hydroxy Acids Controlled by TEMPO-CIO₂ Charge-Transfer Complex. *Org. Lett.* **2015**, *17* (9), 2282–2285.
- (174) Genin, M. J.; Poel, T. J.; Yagi, Y.; Biles, C.; Althaus, I.; Keiser, B. J.; Kopta, L. A.; Friis, J. M.; Reusser, F.; Adams, W. J.; et al. Synthesis and Bioactivity of Novel Bis(Heteroaryl)Piperazine (BHAP) Reverse Transcriptase Inhibitors: Structure-Activity Relationships and Increased Metabolic Stability of Novel Substituted Pyridine Analogs. *J. Med. Chem.* **1996**, *39* (96), 5267–5275.
- (175) Rommel, M.; Ernst, A.; Koert, U. Synthetic Routes to Three Novel Scaffolds for Potential Glycosidase Inhibitors. *European J. Org. Chem.* **2007**, No. 26, 4408–4430.
- (176) Shimano, M.; Kamei, N.; Shibata, T.; Inoguchi, K.; Itoh, N.; Ikari, T.; Senda, H. Total Synthesis of the Antifungal Dilactones UK-2A and UK-3A: The Determination of Their Relative and Absolute COnfigurations, Analog Synthesis and Antifungal Activities. **1998**, *54*, 12745–12774.
- (177) Yoshitomo, T.; Yuzuru, S. US6537948 B1. Pdf, 2003.
- (178) Holladay, M. W.; Bai, H.; Li, Y.; Lin, N. H.; Daanen, J. F.; Ryther, K. B.; Wasicak, J. T.; Kincaid, J. F.; He, Y.; Hettinger, A. M.; et al. Structure-Activity Studies Related to ABT-594, a Potent Nonopioid Analgesic Agent: Effect of Pyridine and Azetidine Ring Substitutions on Nicotinic Acetylcholine Receptor Binding Affinity and Analgesic Activity in Mice. *Bioorganic Med. Chem. Lett.* **1998**, *8* (19), 2797–2802.

- (179) Knight, B. J.; Stache, E. E.; Ferreira, E. M. Complementary Stereochemical Outcomes in Proline-Based Self-Regenerations of Stereocenters. *Org. Lett.* **2014**, *16* (2), 432–435.
- (180) Maheswara Rao, B. L.; Nowshuddin, S.; Jha, A.; Divi, M. K.; Rao, M. N. A. New Reagent for the Introduction of Boc Protecting Group to Amines: Boc-OASUD. *Synth. Commun.* **2017**, *47* (22), 2127–2132.
- (181) Al-Azemi, T. F.; Mohamod, A. A.; Vinodh, M. Ring-Closing Metathesis Approach for the Synthesis of Optically Active L-Proline-Based Macrocycles. *Tetrahedron* **2015**, *71* (10), 1523–1528.
- (182) Schjøth-Eskesen, C.; Jensen, H. H. Efficient Arndt-Eistert Synthesis of Selective 5-HT₇receptor Antagonist SB-269970. *Synth. Commun.* **2009**, *39* (18), 3243–3253.
- (183) Abele, S.; Vöggtli, K.; Seebach, D. Oligomers of B₂- and of B₃-Homoproline: What Are the Secondary Structures of β -Peptides Lacking H-Bonds? *Helv. Chim. Acta* **1999**, *82* (10), 1539–1558.
- (184) Vasanthakumar, G. R.; Patil, B. S.; Suresh Babu, V. V. Homologation of α -Amino Acids to β -Amino Acids Using Boc₂O. *J. Chem. Soc. Perkin 1* **2002**, *2* (18), 2087–2089.
- (185) Schuster, T.; Gobel, M. W. Synthesis of a Chiral Receptor Molecule with Converging Amidinium and Hydroxy Groups. *Synlett* **1999**, No. S1, 966–968.
- (186) Li, P.; Alenezi, K.; Ibrahim, S. K.; Wright, J. A.; Hughes, D. L.; Pickett, C. J. Towards Alternatives to Anodic Water Oxidation: Basket-Handle Thiolate Fe^{III} Porphyrins for Electrocatalytic Hydrocarbon Oxidation. *ChemSusChem* **2012**, *5* (12), 2361–2375.
- (187) Grimmond, B. J.; Rishel, M. J.; Roberts, J. C. US2014/086846 A1.Pdf, 2014.
- (188) Schepartz, A.; Breslow, R. Hydrolysis of an Amide in a Carboxypeptidase Model Using Co(III) and Bifunctional Catalysts. *J. Am. Chem. Soc.* **1987**, *109* (6), 1814–1826.
- (189) Bolchi, C.; Bavo, F.; Pallavicini, M. Preparation and Unequivocal Identification of the Regioisomers of Nitrocatechol Monobenzyl Ether. *Synth. Commun.* **2017**, *47* (16), 1507–1513.
- (190) Berkessel, A.; Günther, T.; Wang, Q.; Neudörfl, J. M. Titanium Salalen Catalysts Based on Cis-1,2-Diaminocyclohexane: Enantioselective Epoxidation of Terminal Non-Conjugated Olefins with H₂O₂. *Angew. Chemie - Int. Ed.* **2013**, *52* (32), 8467–8471.
- (191) Verner, E.; Katz, B. A.; Spencer, J. R.; Allen, D.; Hataye, J.; Hruzewicz, W.; Hui, H. C.; Kolesnikov, A.; Li, Y.; Luong, C.; et al. Development of Serine Protease Inhibitors Displaying a Multicentered Short (<2.3 Å) Hydrogen Bond Binding Mode: Inhibitors of Urokinase-Type Plasminogen Activator and Factor Xa. *J. Med. Chem.* **2001**, *44* (17), 2753–2771.
- (192) Wyrzykiewicz, E.; Wendzonka, M. Synthesis and Physicochemical Characterization of Fluorescent (E)-2-Stilbenyloxyalkylthiouracils and Isomer Differentiation Using EIMS. *J. Heterocycl. Chem.* **2004**, *41* (2), 177–186.
- (193) Wyrzykiewicz, E.; Wybieralska, J.; Grzesiak, J.; Prukala, W. New Fluorescent Uracil Derivatives. *Pol. J. Chem.* **1990**, *64*, 323–331.